

**NEW THERMOSETTING RESINS BASED ON  
SOME BISPHENOLS**

A thesis submitted to the

**UNIVERSITY OF PUNE**

for the degree of

**DOCTOR OF PHILOSOPHY**

in

**CHEMISTRY**

By

**Arun D. Kulkarni**

Polymer Science and Engineering Division  
National Chemical Laboratory  
PUNE 411 008

**March 2010**

*To,*

*My Family*

*&*

*Late Mr. R. K. Shegunashi  
(uncle)*

---



राष्ट्रीय रासायनिक प्रयोगशाला  
(वैज्ञानिक तथा औद्योगिक अनुसंधान परिषद)  
डॉ. होमी भाभा मार्ग पुणे - 411 008. भारत  
**NATIONAL CHEMICAL LABORATORY**  
(Council of Scientific & Industrial Research)  
Dr. Homi Bhabha Road, Pune - 411 008. India.



**Certificate of the Guide**

**Certified** that the work incorporated in the thesis entitled: “**New Thermosetting Resins Based on Some Bisphenols**”, submitted by **Mr. Arun D. Kulkarni** was carried out under my supervision / guidance. Such material as obtained from other sources has been duly acknowledged in the thesis.

**March 2010**

**Pune**

**Prakash P. Wadgaonkar**

(Research Guide)

**Communication  
Channels**

 NCL Level DID : 2590  
NCL Board No. : +91-20-25902000  
EPABX : +91-20-25893300  
+91-20-25893400

**FAX**

Director's Office : +91-20-25902601  
COA's Office : +91-20-25902660  
COS&P's Office : +91-20-25902664

**WEBSITE**

[www.ncl-india.org](http://www.ncl-india.org)

## DECLARATION

I hereby declare that all the experiments embodied in this thesis entitled “**New Thermosetting Resins Based on Some Bisphenols**”, submitted for the degree of Doctor of Philosophy in Chemistry, to the University of Pune has been carried out by me at the Polymer Science and Engineering Division, National Chemical Laboratory, Pune, 411008, India, under the supervision of Dr. Prakash P. Wadgaonkar. The work is original and has not been submitted in part or full by me, for any degree or diploma to this or to any other University.

March 2010

Pune



Arun D. Kulkarni

Senior Research Fellow  
Polymer Science and Engineering Division  
National Chemical Laboratory  
Pune – 411 008

## **Acknowledgement**

*Pursuing the Ph.D. degree is both a painful and an enjoyable journey. The pain could mainly be due to the frustration at different stages, the time period, isolation, loneliness, the feeling of losing the track, etc. The joy of freedom, the extension of student life, the delight of learning process, the intoxication of working, the trust and encouragement makes the process very much enjoyable. This is an opportunity to express my gratitude for all the people who helped to drive the work towards completion.*

*My sincere thanks to my mentor, Dr. Prakash P. Wadgaonkar for his enthusiastic involvement, patient supervision with friendly and sporty spirit. Throughout the process, he has been a great philosopher and a friend. Many times he went out of the way to take care of me. He took tremendous efforts to inculcate the habit of thinking for “designing”, though it is a God given. He never forced to perform experiments simply because he is saying, but explained in detail the necessity of that. He was never a task master with hunter in one hand. His integrity, humanity, tenderness and foresight have made a deep impression on me. He encouraged me not only to grow as an experimentalist but as an independent researcher.*

*For everything you have done for me, Dr. Wadgaonkar, I will be highly obliged up to my last breath.*

*I am deeply indebted to my promoter Dr. C.P.Reghunadhan Nair, Head, PSCG, VSSC, Trivandrum, India, for his stimulating and untiring suggestions and constant encouragement. I could not have finished this work successfully without his help. His doors were always open to me for discussion. He taught me the chemistry of cyanate ester resins and kinetics of curing without expecting anything in return. I am really touched upon by his unconditional scientific inputs and humanity. Plain “Thanks” cannot express my gratitude for him.*

*My special thanks to Dr. C. V. Avadhani, PSE division, NCL, by holding whose hand, I started this journey, who then allowed me to fly freely after making sure to have gathered enough strength in the wings. He not only taught me how to perform the experiments safely, but also essential etiquettes. I could learn the importance of maintenance and proper documentation from him. Dear Sir, thank you very much for all your efforts.*

*My sincere thanks to Dr. S. Sivaram, Director, N.C.L. and Dr. M. G. Kulkarni, Head, Polymer Science and Engineering Division, for allowing me to work in this prestigious Institute and for providing access to the facilities in the division.*

*I owe special thanks to Dr. J.P. Jog and Mrs. D.A. Dhoble for allowing me to use the instruments without questioning. I am very much grateful to Dr. A.K. Lele, Dr. M.V. Badiger, Dr. N.P. Argade, Dr. K. Guruswamy, Dr. S. Radhakrishnan, Dr. K.V. Pandhare and Dr. A. S. Jadhav for their valuable suggestions and advice during this journey. I am very much thankful to Mr. K. G. Raut, Mr. A. S. Patil, Dr. R.A. Kulkarni, Dr. B.D. Sarwade, Dr. B.B. Idage, Dr. S. B. Idage, Dr. N.N. Chavan, Dr. V. Garnaik, Dr. S. K. Asha, Dr. C. Ramesh, Dr. T.P. Mohandas, Mr. S.K. Menon, and Dr. R. P. Singh for their co-operation.*

*I am thankful to the NMR group, Glass blowing group, DIRC group and Workshop group for their timely help. I also wish to thank Library, Administrative and other supporting staff for their co-operation. I am grateful to Siddheshwar, Mahesh Rote, Vikram, Jine, Kakade, Jadhav, More and Shelar for their co-operation. I am also thankful to Mrs. Shevade and other staff at University of Pune.*

*My sincere thanks to Dr. Ramesh Ghatge and Mr. Jadhav for their helpful suggestions. I am thankful to Mr. Nabin Chandra (ABR Organics, Hyderabad) and Dr. Pramod Kumbhar (M/s Herdillia Chemicals, Mumbai) for generously gifting chemicals.*

*My friends made the process very much enjoyable. Many thanks to Vijay, Pandurang, and Ganapathi (alias gana, balaji, brad, pittoba.) for chaay, weekend (sometimes weekdays too) movies, the battles of non-scientific discussions, su-dokus, long drives, Ram and Neeta for*

*maintaining friendly atmosphere in 107, Arvind for nice company throughout the journey and nana songs, Raghunadh for his nice words and company for late-night teas. Pamyra, Satya, Girya, Ajya and Dhanubhau; thanks for being with me, always. R.Gnaneshwar was always ready to give a company for movies of Rahul Bose.*

*One of the reasons for being in the lab was collection of data and the task was feasible because of PPW group-mates, Anjana, Sony, Bapu, Dyaneshwar, Pandurang, Arvind, Vijay, Vaibhav-Nilakshi, Lav., Ranjeet, Prakash, Mahesh, Nagendra, Anil, Shivkumar, Sandip, Mahadev, Savita, Divya, Vidya, Mugdha, Parimal, Kishor, Sharad, Shraddha, Deepshikha, Bhausheb and Indravadan. Thanks for all the parties, celebrations, fun and pleasant atmosphere. I could really work peacefully because of the support from you all. I extend my thanks to Nilakshi and Nagendra for helping me in HPLC and synthesis, respectively.*

*I am also thankful to Mallikarjun, Bhoje, Smitha, Sulatha, Sandhya, Mahesh, Ravi, Sandeep, Jiten, Hemant, Suresh, Ramesh, Vivek, Rajeshwari, Santosh Mhaske, Santosh Hire, Santosh Wanjale, Chetan, Abhijeet, Prashant, Poorvi, Sarojkumar, Ghanashyam, Nagesh, Shailesh, Vipin, Chandrashekhar, Mohanraj, Venkat, Sudhakar, Bhaskar, Sudhir, Bapu Shingate Vivek and Sajjid for the help.*

*My stay at Trivandrum (of course for work) wouldn't have been enjoyable and fruitful without the help of Dr. Girish Galgali, Dr. Mathew, Santhosh, Deepakvishnu, Amol, Vinayakan, and Bibin. Thanks friends for the efforts. I am also thankful to Dilip Kulkarni Sir (Wadia College, Pune).*

*I do not know where I would have been if Mr. Shirish Kawathekar and Dr. Pravin Puranik hadn't shown me the path. Thank you very much from the bottom of heart. The stay in Pune was pleasant due to the support of the Naiks, Torgattis, Sadanandans, Kulkarnis (Pashan), Kulkarnis (Kothrud), and Wadgaonkars. Plain words are not enough to express my feelings towards them. My sincere thanks to Shri. Prashant Puranik and Shri. Sudhir Peshwe for the encouragement. I am deeply indebted to my dear friends Santosh and Jayant for the nice company.*

*It is my mother who taught me the value of hard work by her own example. I bow my head in respect for all she has done for me. I share this happy moment with my brother and Vahinee. They rendered me enormous support during the whole tenure of my research. My soul-mate, my wife Suju (Sujata) came into my life at a proper time to energize me to keep on going. Being very much understanding, she never questioned about the time-frame. She allowed me to fully concentrate on research with no complaints. Innocent smile of an angel, my daughter "Swara" provided me an enormous energy, enthusiasm and encouragement. My in-laws, Kulkarni (2), Pande and Deshpande, cooperated patiently in many aspects. I am more than thankful to God for placing me in such a healthy environment.*

*Finally, I would like to thank the Council of Scientific and Industrial Research for the award of Senior Research Fellowship.*

***Arun D. Kulkarni***

***March 2010.***

## Table of Contents

Description	Page No.
◆ Abstract	i
◆ Glossary	vi
◆ List of Tables	vii
◆ List of Schemes	ix
◆ List of Figures	xi

---

### Chapter 1 Introduction and Literature Survey

---

1.1	Introduction	1
1.2	Cyanate ester resins	2
1.2.1	Synthesis of cyanate esters	2
1.2.1.1	Synthesis of cyanate esters from phenol / alcohol and cyanogen halide	3
1.2.1.2	Synthesis of cyanate esters by thermolysis of thiazotriazoles	4
1.2.1.3	Synthesis of cyanate esters by dehydration of alkyl thiocarbamates	4
1.2.1.4	Synthesis of cyanate esters from alkyl- <i>N</i> -hydroxythiocarbamates	5
1.2.2	Cyanate ester monomers	5
1.2.3	Spectroscopic characterization of cyanate ester monomers	6
1.2.4	Mechanism of cyanate ester polymerization	7
1.2.5	Cure catalysis and cure kinetics	9
1.2.5.1	Catalysts for cyanate ester cure	10
1.2.5.2	Cure kinetics	11
1.2.6	Structure-property relationship	14
1.2.6.1	Glass transition temperature	14
1.2.6.2	Dielectric constant	15
1.2.6.3	Moisture absorption	16
1.3	Epoxy resins	16
1.3.1	Synthesis of epoxy resins	16
1.3.1.1	Synthesis of epoxy resins by coupling reaction	17
1.3.1.2	Synthesis of epoxy resins by epoxidation reaction	18
1.3.2	Commercial types of basic epoxies	19
1.3.3	Characterization of uncured epoxies	19
1.3.4	Curing of epoxy resins	21

1.3.4.1	Curing agents for epoxy curing	21
1.3.4.2	Epoxy curing kinetics	24
1.3.5	Structure-property relationship in epoxy resins	26
1.4	Bismaleimides	26
1.4.1	Synthesis of bismaleimides	27
1.4.1.1	Synthesis of bismaleimides from diamines	27
1.4.1.2	Synthesis of bismaleimides from acid / acid chloride	29
1.4.2	Curing of bismaleimides	29
1.4.3	Cure kinetics	32
1.4.4	Thermal properties of bismaleimides	33
1.5	Propargyl-terminated resins	34
1.5.1	Synthesis of bispropargyl ethers	35
1.5.2	Curing of propargyl-terminated resins	36
1.5.3	Kinetics of bispropargyl ether curing	37
1.6	Applications of cyanate ester resins, epoxy resins and bismaleimides	38
1.7	Outlook	40
	References	41

---



---

## **Chapter 2**                      **Scope and Objectives**

---



---

2.1	Scope and objectives	48
	References	52

---



---

## **Chapter 3**                      **Synthesis and Characterization of Cyanate Ester Monomers**

---



---

3.1	Introduction	53
3.2	Experimental	57
3.2.1	Materials	57
3.2.2	Characterization	57
3.3	Preparations	57
3.3.1	Synthesis of 1,1-bis(4-cyanatophenyl)-3-pentadecylcyclohexane	57
3.3.1.1	Synthesis of 3-pentadecyl cyclohexanol from 3-pentadecyl phenol	57
3.3.1.2	Synthesis of 3-pentadecyl cyclohexanone from 3-pentadecyl cyclohexanol	58
3.3.1.3	Synthesis of 1,1-bis(4-hydroxyphenyl)-3-pentadecyl cyclohexane from 3-pentadecyl cyclohexanone and phenol	58
3.3.1.4	Synthesis of 1,1-bis(4-cyanatophenyl)-3-pentadecylcyclohexane	59
3.3.2	Synthesis of 1,1- bis-(4-cyanatophenyl)decahydronaphthalene	59
3.3.2.1	Synthesis of decahydro-2-naphthol from $\beta$ -naphthol	59



3.3.2.2	Synthesis of 2-decalone from decahydro-2-naphthol	60
3.3.2.3	Synthesis of 1,1- bis-(4-hydroxyphenyl)decahydronaphthalene from 2-decalone and phenol	60
3.3.2.4	Synthesis of 1,1- bis-(4-cyanatophenyl)decahydronaphthalene	61
3.3.3	Synthesis of 1,1- bis-(4-cyanato-3-methylphenyl) decahydronaphthalene	61
3.3.3.1	Synthesis of 1,1- bis-(4-hydroxy-3-methylphenyl) decahydronaphthalene	61
3.3.3.2	Synthesis of 1,1- bis-(4-cyanato-3-methylphenyl) decahydronaphthalene	62
3.3.4	Synthesis of 1,1- bis-(4-cyanato-3,5-dimethylphenyl)decahydronaphthalene	62
3.3.4.1	Synthesis of 1,1- bis-(4-hydroxy-3,5-dimethylphenyl)decahydronaphthalene	62
3.3.4.2	Synthesis of 1,1- bis-(4-cyanato-3,5-dimethylphenyl)decahydronaphthalene	63
3.3.5	Synthesis of 1,1- bis-(4-cyanatophenyl)-4-perhydrocumylcyclohexane	63
3.3.5.1	Synthesis of 4-perhydrocumyl cyclohexanol from <i>p</i> -cumyl phenol	63
3.3.5.2	Synthesis of 4-perhydrocumyl cyclohexanone from 4-perhydrocumyl cyclohexanol	64
3.3.5.3	Synthesis of 1,1-bis(4-hydroxyphenyl)-4-perhydrocumylcyclohexane from 4-perhydrocumyl cyclohexanone and phenol	64
3.3.5.4	Synthesis of 1,1- bis-(4-cyanatophenyl)-4-perhydrocumylcyclohexane	65
3.3.6	Synthesis of 1,1- bis-(4-cyanato-3-methylphenyl) -4-perhydrocumylcyclohexane	65
3.3.6.1	Synthesis of 1,1- bis-(4-hydroxy-3-methylphenyl) -4-perhydrocumyl cyclohexane from 4-perhydrocumyl cyclohexanone and <i>o</i> -cresol	65
3.3.6.2	Synthesis of 1,1- bis-(4-cyanato-3-methylphenyl) -4-perhydrocumyl cyclohexane	66
3.3.7	Synthesis of 1,1- bis-(4-cyanato-3,5-dimethylphenyl) -4-perhydrocumyl cyclohexane	66
3.3.7.1	Synthesis of 1,1- bis-(4-hydroxy-3,5-dimethylphenyl) -4-perhydrocumyl cyclohexane from 4-perhydrocumyl cyclohexanone and 2,6-dimethylphenol	66
3.3.7.2	Synthesis of 1,1- bis-(4-cyanato-3,5-dimethylphenyl) -4-perhydrocumyl cyclohexane	67
3.3.8	Synthesis of 1,1- bis-(4-cyanatophenyl) cyclohexane	67
3.3.8.1	Synthesis of 1,1- bis-(4-hydroxyphenyl) cyclohexane from cyclohexanone and phenol	67
3.3.8.2	Synthesis of 1,1- bis-(4-cyanatophenyl) cyclohexane	68
3.3.9	Synthesis of 2,7-bis(4-cyanatophenyl)-2,7-dimethyloctane	69
3.3.9.1	Synthesis of dimethyl adipate from adipic acid	69
3.3.9.2	Synthesis of 2,7-bishydroxy-2,7-dimethyloctane from dimethyl adipate	69
3.3.9.3	Synthesis of 2,7-bis(4-hydroxy phenyl)-2,7-dimethyloctane from 2,7-bis hydroxy-2,7-dimethyloctane	69
3.3.9.4	Synthesis of 2,7-bis(4-cyanatophenyl)-2,7-dimethyloctane	70
3.4	Results and Discussion	70
3.4.1	Synthesis and characterization of cyanate ester monomers containing cycloaliphatic “cardo” group	70

3.4.1.1	Synthesis and characterization of cyanate ester monomer starting from 3-pentadecylphenol	70
3.4.1.2	Synthesis and characterization of cyanate ester monomers starting from $\beta$ -naphthol	76
3.4.1.3	Synthesis and characterization of cyanate ester monomers starting from <i>p</i> -cumylphenol	85
3.4.2	Synthesis and characterization of cyanate ester monomers containing alkylene spacer	94
3.5	Conclusions	99
	References	100

---

## **Chapter 4 Curing Kinetics and Processing of Cyanate Esters**

---

### **Chapter 4 A Curing Kinetics of Cyanate Ester Monomers**

---

4A.1	Introduction	101
4A.2	Experimental	103
4A.2.1	Materials	103
4A.2.2	Sample preparation	103
4A.2.3	DSC analysis	103
4A.3	Results and Discussion	104
4A.3.1	Non-isothermal curing kinetics	104
4A.3.1.1	Kinetics of cure	110
4A.3.2	Isothermal curing kinetics	113
4A.4	Conclusions	120
	References	121

---

### **Chapter 4 B Processing of Cyanate Ester Monomers**

---

4B.1	Introduction	122
4B.2	Experimental	123
4B.2.1	Materials	123
4B.2.2	Characterization	123
4B.2.3	Curing	124
4B.3	Results and Discussion	124
4B.3.1	Dynamic mechanical thermal analysis	127
4B.3.2	Thermal properties	129
4B.3.3	Moisture absorption	132
4B.4	Conclusions	133
	References	134

---

---

**Chapter 5                    Synthesis, Characterization and Curing of Epoxy Resins**

---

---

5.1	Introduction	135
5.2	Experimental	138
5.2.1	Materials	138
5.2.2	Characterization	138
5.2.3	Synthesis of epoxies	139
5.2.3.1	Synthesis of diglycidyl ether of 1,1-bis(4-hydroxyphenyl)-3-pentadecyl cyclohexane	139
5.2.3.2	Synthesis of diglycidyl ether of 1,1-bis(4-hydroxyphenyl)cyclohexane	140
5.2.4	Curing	140
5.3	Results and Discussion	141
5.3.1	Synthesis of epoxies	141
5.3.2	Non-isothermal curing kinetics of epoxy resins	147
5.3.2.1	Kinetics of curing	148
5.3.3	Characterization of cured network	150
5.3.3.1	Dynamic mechanical thermal analysis	151
5.3.3.2	Thermal properties	152
5.3.3.3	Moisture absorption	154
5.4	Conclusions	155
	References	156

---

---

**Chapter 6                    Synthesis, Characterization and Curing Studies of Bismaleimides**

---

---

6.1	Introduction	157
6.2	Experimental	160
6.2.1	Materials	160
6.2.2	Characterization	161
6.3	Preparations	161
6.3.1	Synthesis of 1,1-bis[4-(4- maleimidophenoxy)phenyl] -3-pentadecylcyclohexane	161
6.3.1.1	Synthesis of 1,1-bis-[4-(4-nitrophenoxy)phenyl] -3-pentadecylcyclohexane	161
6.3.1.2	Synthesis of 1,1-bis-[4-(4-aminophenoxy)phenyl] -3-pentadecylcyclohexane	162
6.3.1.3	Synthesis of 1,1-bis[4-(4-maleimidophenoxy)phenyl] -3-pentadecyl cyclohexane	162
6.3.2	Synthesis of 4,4'-bis(maleimido)-3-pentadecyldiphenylether	162
6.3.2.1	Synthesis of 4-amino-3-pentadecyl phenol	162
6.3.2.2	Synthesis of 4-(4'-nitrophenoxy)-2-pentadecylbenzenamine	163

6.3.2.3	Synthesis of 4-(4'-aminophenoxy)-2-pentadecylbenzenamine	164
6.3.2.4	Synthesis of 4,4'-bis(maleimido)-3-pentadecyldiphenylether	164
6.3.3	Synthesis of 1,3-bis(maleimido)-4-pentadecylbenzene	164
6.3.3.1	Synthesis of 1-methane sulfonyloxy-3-pentadecyl benzene	164
6.3.3.2	Synthesis of pentadecyl benzene	165
6.3.3.3	Synthesis of 1,3-dinitro-4-pentadecylbenzene	165
6.3.3.4	Synthesis of 4-pentadecylbenzene-1,3-diamine	166
6.3.3.5	Synthesis of 1,3-bis(maleimido)-4-pentadecylbenzene	166
6.3.4	Synthesis of 1,1-bis[4-(4- maleimidophenoxy)phenyl] cyclohexane	167
6.3.4.1	Synthesis of 1,1-bis-[4-(4-nitrophenoxy)phenyl] cyclohexane	167
6.3.4.2	Synthesis of 1,1-bis-[4-(4-aminophenoxy)phenyl] cyclohexane	167
6.3.4.3	Synthesis of 1,1-bis[4-(4-maleimidophenoxy)phenyl] cyclohexane	168
6.3.5	Synthesis of 4,4'-bis(maleimido)diphenylether	168
6.4	Results and Discussion	168
6.4.1	Synthesis of 1,1-bis[4-(4- maleimidophenoxy)phenyl]-3-pentadecylcyclohexane	168
6.4.2	Synthesis of 4,4'-bis(maleimido)-3-pentadecyldiphenylether	177
6.4.3	Synthesis of 1,3-bis(maleimido)-4 -pentadecylbenzene	182
6.4.4	Synthesis of 1,1-bis[4-(4- maleimidophenoxy)phenyl]cyclohexane	187
6.4.5	Synthesis of 4, 4'-bis(maleimido)diphenylether	189
6.4.6	Solubility of bismaleimides	191
6.4.7	Kinetics of curing	192
6.4.7.1	Nonisothermal cure kinetics	196
6.4.8	Thermal stability of cured network	198
6.5	Conclusions	200
	References	201

---

## **Chapter 7      Synthesis, Characterization and Curing Studies of Bispropargyl Ethers**

---

7.1	Introduction	203
7.2	Experimental	206
7.2.1	Materials	206
7.2.2	Characterization	206
7.3	Preparations	207
7.4	Results and Discussion	207
7.4.1	Synthesis and characterization of 1,1-bis[4-(2-propynyloxy)phenyl]cyclohexane	208
7.4.2	Synthesis and characterization of 1,1-bis[4-(2-propynyloxy)phenyl]-3-pentadecyl cyclohexane	211

7.4.3	Synthesis and characterization of 1,1-bis[4-(2-propynyloxy)phenyl]decahydronaphthalene	214
7.4.4	Synthesis and characterization of 1,1-bis[4-(2-propynyloxy)phenyl]-4-perhydrocumylcyclohexane	216
7.4.5	Synthesis and characterization of 2,2-bis[4-(2-propynyloxy)phenyl]propane	220
7.4.6	Cure kinetics of bispropargyl ethers	221
	7.4.6.1 Activation parameters using Kissinger method	222
	7.4.6.2 Activation parameters using Coats-Redfern method	225
7.4.7	Thermal stability of cured network	227
7.5	Conclusions	229
	References	230

---



---

## **Chapter 8                      Summary and Conclusions**

---

8.1	Summary and Conclusions	231
8.2	Perspectives	235
	♦ Synopsis	237
	♦ List of Publications	247

---



---

## Abstract

---

Thermosetting resins find applications in many industries including transportation, communication, construction and leisure goods. An area that has immensely benefited by the advancement of thermosetting resins is aerospace. The current developments in composite materials finding applications in aerospace industry are centered on the advanced thermosetting resins *viz*; epoxy resins, bismaleimides, cyanate ester resins, polybenzoxazines, propargyl-terminated resins, etc,. The properties such as excellent mechanical strength, high glass transition temperature, low dielectric constant, excellent metal adhesion, and compatibility with carbon fiber reinforcements make these thermosets the material of choice. Furthermore, the ability to tune the properties *via* tailoring / proper selection of the precursor bisphenol functions as an additional asset. A variety of bisphenols have been synthesized till date in order to enrich the applications of these types thermosetting resins.

Cyanate esters (CEs) form a family of new generation thermosetting resins. The chemistry and technology of CEs is relatively new and continue to evolve and enthuse researchers.

The major goal the current research was to design and synthesize new CE monomers containing cycloaliphatic “cardo” group based on corresponding bisphenols and to study thermal, thermomechanical and moisture absorption behavior of polycyanurates derived therefrom. The driving force for the designing of new CE monomers was the development of corresponding polycyanurate with lower moisture absorption and therefore, the synthetic efforts were directed towards structural modifications by introducing i) cycloaliphatic moiety, ii) methyl groups *ortho* to cyanate functionality, and iii) alkylene spacer.

One of the approaches for pursuing the goal involved making use of 3-pentadecyl phenol, which in turn is obtainable from cashew nut shell liquid (CNSL) –a renewable resource material. The dual phenolic/ alkenyl nature of CNSL makes it an ideal renewable raw material for the synthesis of water-resistant resins and polymers. The other approaches involved i) the use of commercially available *p*-cumyl phenol and  $\beta$ -naphthol as a starting materials to introduce cycloaliphatic “cardo” group and ii) the use of adipic acid as a starting material to incorporate alkylene spacer.

Another objective of the study was to explore bisphenols containing cycloaliphatic “cardo” group to synthesize other types of thermosetting resins *viz*; epoxy resins, bismaleimides and propargyl ether resins (propargyl-terminated resins).

The thesis has been divided into the following eight chapters.

**Chapter 1** deals with comprehensive review of literature on thermosetting resins with particular emphasis on cyanate ester resins, epoxy resins, bismaleimides and propargyl-terminated resins covering methods of synthesis, curing/processing, structure-property relationship, etc.

**Chapter 2** discusses scope and objectives of the present thesis.

**Chapter 3** describes the synthesis of a variety of new CE monomers containing cycloaliphatic “cardo” group (**Table 1, Sr. No. 2-9**) and alkylene spacer (**Table 1, Sr. No. 10**) viz;

- 1,1-Bis(4-cyanatophenyl)cyclohexane (BPZCN),
- 1,1-Bis(4-cyanatophenyl)-3-pentadecylcyclohexane (BPC15CN),
- 1,1-Bis(4-cyanatophenyl)decahydronaphthalene (BPDCCN),
- 1,1-Bis(4-cyanato-3-methylphenyl)decahydronaphthalene (DMBPDCCN),
- 1,1-Bis(4-cyanato-3,5-dimethylphenyl) decahydronaphthalene (TMBPDCCN),
- 1,1-Bis(4-cyanatophenyl)-4-perhydrocumylcyclohexane (BPPCPCN),
- 1,1-Bis(4-cyanato-3-methylphenyl)-4-perhydrocumylcyclohexane (DMBPPCPCN),
- 1,1-Bis(4-cyanato-3,5-dimethylphenyl)-4-perhydrocumylcyclohexane (TMBPPCPCN), and
- 2,7-Bis(4-cyanatophenyl)-2,7-dimethyloctane (BPC6CN).

The CE monomers and the intermediates involved in their synthesis were characterized by IR, <sup>1</sup>H-NMR, and <sup>13</sup>C-NMR spectroscopy.

**Chapter 4** describes curing kinetics and processing of cyanate ester monomes. This chapter is divided into two sections; chapter 4A and chapter 4B.

**Chapter 4A** focuses on the curing kinetics studies of selected CE monomers. The kinetics of curing of five cyanate esters viz; BPZCN, BPC15CN, BPDCCN, BPPCPCN and BPC6CN was studied under nonisothermal and isothermal mode employing copper acetylacetonate-nonylphenol catalytic system using DSC. The results obtained were compared with the cure kinetics of commercially available CE monomer- 2,2-bis(4-cyanatophenyl)propane (BPACN). The heat of catalyzed cure reaction of cyanate ester monomers under study was observed in the range 190 – 230 kJ/mol which is in accordance with the reported values for BPACN (195 – 238 kJ/mol). The activation energy of catalyzed curing of cyanate ester monomers containing “cardo” group viz; BPZCN, BPC15CN, BPDCCN, and BPPCPCN under nonisothermal mode was lower (65 – 85 kJ/mol) than that of BPC6CN (119 kJ/mol) and BPACN (116 kJ/mol) while the activation energy for catalyzed cure of CE monomers under isothermal mode was in the range 55 – 60 kJ/mol.

In **Chapter 4B**, processing of CE monomers and characterization of polycyanurates derived therefrom is discussed. The storage modulus of cured BPZCN, BPC15CN and BPACN was  $1.59 \times 10^9$ ,  $1.07 \times 10^9$  and  $1.39 \times 10^9$  Pa, respectively. The glass transition temperature, as analyzed by DMTA, of cured resins followed the order BPZCN > BPACN > BPC15CN (302, 288 and 160 °C, respectively). The T<sub>g</sub> of cured BPDCCN, BPPCPCN and BPC6CN was in the order BPDCCN > BPPCPCN > BPC6CN. The T<sub>10</sub> values, as analyzed by TGA, of cured network of cyanate ester monomers under study were in the range 410 – 435 °C indicating their good thermal stability. The percentage moisture absorption of polycyanurates followed the order BPC15CN < BPZCN < BPACN (0.7, 1.1, 1.5 %, respectively).

**Chapter 5** describes the synthesis of epoxy resins starting from bisphenols containing cycloaliphatic “cardo” group *viz*; diglycidyl ether of 1,1-bis(4-hydroxyphenyl)cyclohexane (DGE BPZ) and diglycidyl ether of 1,1-bis(4-hydroxyphenyl)-3-pentadecylcyclohexane (DGE BPC15). (**Table 1, Sr. No. 11, 12**) The epoxy equivalent weights of DGE BPZ and DGE BPC15, as determined by pyridine-HCl method, were 221 and 333 g/equiv., respectively. The activation energy of epoxy curing calculated by Coats-Redfern method under nonisothermal mode employing 4,4'-methylenedianiline as a curing agent was in the range 48-52 kJ/mol. The storage modulus and the T<sub>g</sub> of cured epoxy resins followed the order DGE BPZ > DGE BPA > DGE BPC15. The thermal degradation of cured epoxy resins under study when analyzed by TGA showed a single step degradation with T<sub>10</sub> values in the range 340 – 375 °C. The percentage moisture absorption of cured epoxy resins followed the order DGE BPC15 < DGE BPZ < DGE BPA (1.8, 2.6, and 3.2 %, respectively).

**Chapter 6** deals with the synthesis of three new BMI monomers containing pendent flexible pentadecyl chain *viz*; 1,1-bis[4-(4-maleimidophenoxy)phenyl]-3-pentadecylcyclohexane, (BPC15 BMI), 4,4'-bis(maleimido)-3-pentadecyldiphenylether (ODAC15BMI) and 1,3-bis(maleimido)-4-pentadecylbenzene (MPDAC15BMI), (**Table 1, Sr. No. 14-16**), characterization of BMI monomers by FTIR, and NMR (<sup>1</sup>H and <sup>13</sup>C-NMR) spectroscopic techniques, curing kinetics by DSC and thermal properties of cured resins by TGA. The melting points of new BMIs *viz*; 4,4'-bis(maleimido)-3-pentadecyldiphenylether (69-70 °C) and 1,3-bis(maleimido)-4-pentadecylbenzene (96-98 °C) were lower than that of 4,4'-bis(maleimido)diphenylether (177 °C) and 1,3-bis(maleimido)benzene (MPDABMI) (205 °C), respectively. The new BMIs *viz*; BPZBMI, (**Table 1, Sr. No. 13**), BPC15BMI, ODAC15BMI, and MPDAC15BMI were soluble in common organic solvents such as chloroform, dichloromethane, while ODABMI was insoluble in chloroform, and dichloromethane at 5 wt % solution. The curing kinetics of new BMIs was studied by using DSC under nonisothermal mode using Coats-Redfern method. The BMIs *viz*; BPZBMI, BPC15BMI and MPDAC15BMI exhibited comparatively a broader processing window (> 100 °C) than that of ODABMI and MPDABMI (~ 40 °C). The activation energy of BMI curing was observed in the range 103 – 131 kJ/mol for BPZBMI, ODAC15BMI, ODABMI and MPDAC15BMI. The cured network of all the BMIs under study showed a single stage decomposition with T<sub>10</sub> values in the range 390 – 485 °C indicating their good thermal stability.

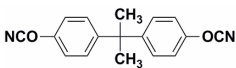
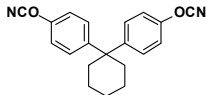
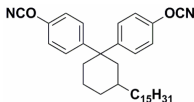
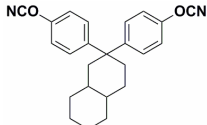
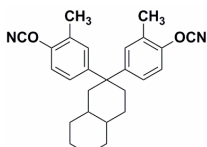
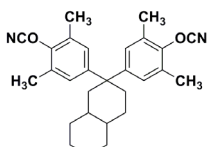
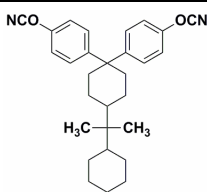
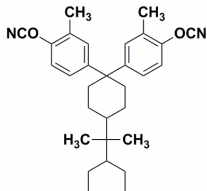
**Chapter 7** describes synthesis of bispropargyl ethers *viz*; 1,1-bis[4-(2-propynyloxy) phenyl] cyclohexane (BPZPT), 1,1-bis[4-(2-propynyloxy) phenyl]-3-pentadecylcyclohexane (BPC15PT), 1,1-bis[4-(2-propynyloxy) phenyl]decahydronaphthalene, (BPDCPT), 1,1-bis[4-(2-propynyloxy) phenyl]-4-perhydrocumylcyclohexane (BPPCPPT) and 2,2-bis[4-(2-propynyloxy) phenyl]propane (BPAPT). (**Table 1, Sr. No. 17-20**). The activation energy of the curing reaction studied in uncatalysed nonisothermal mode using DSC was in the range of 141-154 kJ/mol by Kissinger method and 171-182 kJ/mol by Coats-Redfern method for all bispropargyl ethers under study. The



study indicated that the bispropargyl ether monomers possessing cycloaliphatic “cardo” group follows similar cure kinetics as that of bisphenol-A based bispropargyl ether. The  $T_{10}$  values of cured bispropargyl ethers containing “cardo” group were in the range 410 - 435 °C indicating good thermal stability of the cured network. However, the weight residue at 800 °C of cured bispropargyl ethers containing “cardo” group was lower (3-12 %) than that of cured network of BPAPT (32 %).

**Chapter 8** summarizes the results and describes salient conclusions of the investigations reported in the present thesis.

**Table 1 : Structure of various monomers synthesized in the present work.**

Sr.No.	Category	Name	Structure
1	Cyanate Ester Resins	2,2-Bis(4-cyanatophenyl)propane (BPACN)	
2		1,1-Bis(4-cyanatophenyl)cyclohexane (BPZCN)	
3		1,1-Bis(4-cyanatophenyl)-3-pentadecylcyclohexane (BPC15CN)	
4		1,1-Bis(4-cyanatophenyl)decahydronaphthalene (BPDCCN)	
5		1,1-Bis(4-cyano-3-methylphenyl)decahydronaphthalene (DMBPDCCN)	
6		1,1-Bis(4-cyano-3,5-dimethylphenyl)decahydronaphthalene (TMBPDCCN)	
7		1,1-Bis(4-cyanatophenyl)-4-perhydrocumylcyclohexane (BPPCCPN)	
8		1,1-Bis(4-cyano-3-methylphenyl)-4-perhydrocumylcyclohexane (DMBPPCCPN)	

9		1,1-Bis(4-cyanato-3,5-dimethylphenyl)-4-perhydrocumyl cyclohexane (TMBPPCPCN)	
10		2,7-Bis(4-cyanatophenyl)-2,7-dimethyloctane (BPC6CN)	
11	Epoxy Resins	Diglycidyl ether of 1,1-bis(4-hydroxyphenyl)cyclohexane (DGEBPZ)	
12		Diglycidyl ether of 1,1-bis(4-hydroxyphenyl)-3-pentadecylcyclohexane (DGEBPC15)	
13	Bismaleimides	1,1-Bis[4-(4-maleimidophenoxy)phenyl] cyclohexane (BPZBMI)	
14		1,1-Bis[4-(4-maleimidophenoxy)phenyl]-3-pentadecyl cyclohexane (BPC15BMI)	
15		4,4'-Bis(maleimido)-3-pentadecyl diphenylether (ODAC15BMI)	
16		1,3-Bis(maleimido)-4-pentadecylbenzene (MPDAC15BMI)	
17	Bispropargyl Ethers	2,2-Bis[4-(2-propynyloxy)phenyl]propane (BPAPT)	
18		1,1-Bis[4-(2-propynyloxy)phenyl] cyclohexane (BPZPT)	
19		1,1-Bis[4-(2-propynyloxy)phenyl]-3-pentadecylcyclohexane (BPC15PT)	
20		1,1-Bis[4-(2-propynyloxy)phenyl] decahydronaphthalene (BPDCPT)	
21		1,1-Bis[4-(2-propynyloxy)phenyl]-4-perhydrocumyl cyclohexane (BPPCPPT)	

## Glossary

<b>BMI</b>	Bismaleimide
<b>BPA</b>	Bisphenol-A
<b>BPACN</b>	Dicyanate of bisphenol-A
<b>CE</b>	Cyanate ester
<b>CNSL</b>	Cashew nut shell liquid
<b>DABA</b>	o,o'-Diallylbisphenol-A
<b>DCM</b>	Dichloromethane
<b>DEPT</b>	Distortionless enhancement by polarization transfer
<b>DGEBA</b>	Diglycidyl ether of bisphenol-A
<b>DMF</b>	<i>N,N</i> -Dimethyl formamide
<b>DMSO</b>	Dimethylsulphoxide
<b>DMTA</b>	Dynamic mechanical thermal analysis
<b>DSC</b>	Differential scanning calorimetry
<b>EEW</b>	Epoxy equivalent weight
<b>GPC</b>	Gel permeation chromatography
<b>MDA</b>	4,4'-Methylenedianiline
<b>MPDABMI</b>	1,3-Bis(maleimido)benzene
<b>NMP</b>	1-Methyl-2-pyrrolidinone
<b>ODABMI</b>	4,4'-Bis(maleimido)diphenylether
<b>PCC</b>	Pyridinium chlorochromate
<b>TGA</b>	Thermogravimetric analysis
<b>THF</b>	Tetrahydrofuran

## List of Tables

Table No.	Description	Page No.
Table 1.1	List of commercial cyanate ester monomers with their trade names	6
Table 1.2	Characteristic <sup>13</sup> C and <sup>15</sup> N NMR chemical shifts of functionalities associated with cyanate ester curing	7
Table 1.3	Activation energies for various cyanate ester monomers calculated by neat/catalysed isothermal curing kinetics.	13
Table 1.4	Relationship between dicyanate structural units and characteristics of resulting polycyanurate network	14
Table 1.5	Properties of polycyanurates based on commercial CE monomers	15
Table 1.6	Commercial amine functional curing agents used for epoxy curing	22
Table 1.7	Anhydride functional curing agents used for epoxy curing	23
Table 1.8	Activation energies of curing of commercially available BMI monomers	33
Table 1.9	Glass transition temperature of cured bismaleimides	34
Table 1.10	Activation energies of curing of bispropargyl ethers.	38
Table 1.11	Applications of thermosetting resins	39
Table 3.1	Literature examples of selected CE monomers containing “cardo” with / or cycloaliphatic moiety	54
Table 3.2	Literature examples of selected CE monomers containing flexible spacers	55
Table 3.3	List of CE monomers synthesized in the present study	56
Table 4A.1	List of CE monomers used for curing study	101
Table 4A.2	DSC characteristics of CE monomers (neat)	107
Table 4A.3	Cure characteristics of CE monomers (catalysed)	110
Table 4A.4	Activation parameters of CE monomers by Coats-Redfern method	113
Table 4A.5	Activation parameters of CE monomers by isothermal method	119
Table 4B.1	Cure schedule of CE monomers.	126
Table 4B.2	Dynamic mechanical analysis of cured CE resins	129
Table 4B.3	Thermal characterization of CE resins	131
Table 4B.4	Percentage moisture absorption of polycyanurates	132
Table 5.1	Epoxy resins containing “cycloaliphatic / cardo” moiety.	136
Table 5.2	Curing characteristics of epoxy resins	148
Table 5.3	Activation parameters of epoxy curing by Coats-Redfern method	150
Table 5.4	Dynamic mechanical properties of cured epoxy resins	152
Table 5.5	Thermal properties of cured epoxy resins	153
Table 5.6	Percentage moisture absorption of cured epoxy resins	154
Table 6.1	List of bismaleimide monomers containing alkylene chain / ether units	158
Table 6.2	List of bismaleimide monomers synthesized in the present study	160
Table 6.3	Solubility of bismaleimide monomers at 5 wt % concentration	191

Table 6.4	Cure profile of bismaleimides	195
Table 6.5	Kinetic parameters of bismaleimide curing	198
Table 6.6	Thermal properties of cured bismaleimides	199
Table 7.1	Literature examples of bispropargyl ethers	204
Table 7.2	Bispropargyl ether monomers synthesized in the present work.	205
Table 7.3	Melting point and cure profile of bispropargyl ethers	222
Table 7.4	Peak temperatures of curing of bispropargyl ethers under study	224
Table 7.5	Kinetic parameters of bispropargyl ether curing	227
Table 7.6	Thermal characterization of propargyl-terminated resins	228

## List of Schemes

Scheme No.	Description	Page No.
Scheme 1.1	Synthesis of cyanate esters from phenol / alcohol and cyanogen halide	3
Scheme 1.2	Von Braun reaction	3
Scheme 1.3	Synthesis of cyanate esters by thermolysis of thiazotriazoles	4
Scheme 1.4	Synthesis of cyanate esters by dehydration of alkyl thiocarbamates.	4
Scheme 1.5	Synthesis of cyanate esters by dehydration of alkyl- <i>N</i> -thiocarbamates	5
Scheme 1.6	Mechanism of cyanate ester polymerization ( Brownhill <i>et.al.</i> )	8
Scheme 1.7	Mechanism of cyanate ester polymerization (Loustalot <i>et.al.</i> )	9
Scheme 1.8	Synthesis of bisphenol-A based epoxy resin	17
Scheme 1.9	Hydrolysis of epoxide ring	17
Scheme 1.10	Abnormal addition of epichlorohydrin	18
Scheme 1.11	Reaction of epichlorohydrin with hydroxyl groups	18
Scheme 1.12	Synthesis of epoxy resins by epoxidation reaction	18
Scheme 1.13	Synthesis of diglycidyl ether of bisphenol-A	19
Scheme 1.14	Reaction of epoxy group with amine functionality	25
Scheme 1.15	Various reaction pathways for the reaction of epoxy and amine	25
Scheme 1.16	Synthesis of bismaleimides from diamines	27
Scheme 1.17	Base -catalysed cyclodehydration of <i>N,N'</i> -bismaleamic acid	28
Scheme 1.18	Synthesis of bismaleimide by acid chloride route	29
Scheme 1.19	Homopolymerization of bismaleimides <i>via</i> addition reaction	30
Scheme 1.20	Mechanism of bismaleimide curing	31
Scheme 1.21	Donor-acceptor type mechanism	31
Scheme 1.22	Synthesis of bispropargyl ethers	35
Scheme 1.23	Chromene formation <i>via</i> Claisen rearrangement	36
Scheme 1.24	Curing reaction of bispropargyl ethers	37
Scheme 3.1	Synthesis of 1,1-bis(4-cyanatophenyl)-3-pentadecylcyclohexane	72
Scheme 3.2	Synthesis of cyanate ester monomers starting from $\beta$ -naphthol	76
Scheme 3.3	Synthesis of cyanate ester monomers starting from <i>p</i> -cumylphenol	85
Scheme 3.4	Synthesis of 2,7-bis(4-cyanatophenyl)-2,7-dimethyloctane	94
Scheme 5.1	Synthesis of diglycidyl ether of 1,1-bis(4-hydroxyphenyl)-3-pentadecyl cyclohexane	141
Scheme 5.2	Synthesis of diglycidyl ether of 1,1-bis(4-hydroxyphenyl) cyclohexane	145

Scheme 6.1	Synthesis of 1,1-bis[4-(4- maleimidophenoxy)phenyl]-3-pentadecylcyclohexane	169
Scheme 6.2	Synthesis of 4,4'-bis(maleimido)-3-pentadecyldiphenylether	178
Scheme 6.3	Synthesis of 1,3-bis(maleimido)-4 -pentadecylbenzene	183
Scheme 6.4	Synthesis of 1,1-bis[4-(4- maleimidophenoxy)phenyl]cyclohexane	187
Scheme 6.5	Synthesis of 4, 4'-bis(maleimido)diphenylether	190
Scheme 7.1	Polymerization of bispropargyl ethers	203
Scheme 7.2	General scheme for the synthesis of bispropargyl ethers	208

## List of Figures

Figure No.	Description	Page No.
Figure 1.1	General structure of cyanate ester monomers	2
Figure 1.2	Structure of oxirane ring	16
Figure 1.3	Incomplete dehydrochlorination	18
Figure 1.4	Commercial types of basic epoxies	20
Figure 1.5	General structure of bismaleimides	26
Figure 1.6	Structure of 1,1-bis(4-maleimidophenyl)methane	27
Figure 1.7	General structure of bispropargyl ethers	35
Figure 1.8	Structures of side products formed by Claisen rearrangement	35
Figure 3.1	IR spectrum of 1,1-bis(4-cyanatophenyl)-3-pentadecylcyclohexane	73
Figure 3.2	<sup>1</sup> H-NMR spectrum of 1,1-bis(4-cyanatophenyl)-3-pentadecylcyclohexane (CDCl <sub>3</sub> )	74
Figure 3.3	<sup>13</sup> C-NMR spectrum of 1,1-bis(4-cyanatophenyl)-3-pentadecylcyclohexane (CDCl <sub>3</sub> )	75
Figure 3.4	<sup>13</sup> C-DEPT NMR spectrum of 1,1-bis(4-cyanatophenyl)-3-pentadecylcyclohexane. (CDCl <sub>3</sub> )	75
Figure 3.5	IR spectrum of 1,1-bis(4-cyanatophenyl)decahydronaphthalene	77
Figure 3.6	<sup>1</sup> H-NMR spectrum of 1,1-bis(4-cyanatophenyl)decahydronaphthalene(CDCl <sub>3</sub> )	78
Figure 3.7	<sup>13</sup> C-NMR spectrum of 1,1-bis(4-cyanatophenyl)decahydronaphthalene (CDCl <sub>3</sub> )	78
Figure 3.8	<sup>13</sup> C-DEPT NMR spectrum of 1,1-bis(4-cyanatophenyl)decahydronaphthalene (CDCl <sub>3</sub> ).	79
Figure 3.9	IR spectrum of 1,1-bis(4-cyano-3-methylphenyl) decahydronaphthalene	80
Figure 3.10	<sup>1</sup> H-NMR spectrum of 1,1-bis(4-cyano-3-methylphenyl) decahydronaphthalene (CDCl <sub>3</sub> ).	80
Figure 3.11	<sup>13</sup> C-NMR spectrum of 1,1-bis(4-cyano-3-methylphenyl) decahydronaphthalene (CDCl <sub>3</sub> ).	81
Figure 3.12	<sup>13</sup> C-DEPT NMR spectrum of 1,1-bis(4-cyano-3-methylphenyl) decahydro naphthalene (CDCl <sub>3</sub> ).	82
Figure 3.13	IR spectrum of 1,1-bis(4-cyano-3,5-dimethylphenyl)decahydronaphthalene	82
Figure 3.14	<sup>1</sup> H-NMR spectrum of 1,1-bis(4-cyano-3,5-dimethylphenyl)decahydronaphthalene (CDCl <sub>3</sub> ).	83
Figure 3.15	<sup>13</sup> C-NMR spectrum of 1,1-bis(4-cyano-3,5-dimethylphenyl)decahydronaphthalene (CDCl <sub>3</sub> ).	84
Figure 3.16	<sup>13</sup> C-DEPT NMR spectrum of 1,1-bis(4-cyano-3,5-dimethylphenyl) decahydro naphthalene (CDCl <sub>3</sub> ).	84
Figure 3.17	IR spectrum of 1,1-bis(4-cyanatophenyl)-4-perhydrocumylcyclohexane	86
Figure 3.18	<sup>1</sup> H-NMR spectrum of 1,1-bis(4-cyanatophenyl)-4-perhydrocumylcyclohexane (CDCl <sub>3</sub> ).	87
Figure 3.19	<sup>13</sup> C-NMR spectrum of 1,1-bis(4-cyanatophenyl)-4-perhydrocumylcyclohexane (CDCl <sub>3</sub> ).	88
Figure 3.20	<sup>13</sup> C- DEPT NMR spectrum of 1,1-bis(4-cyanatophenyl)-4-perhydrocumylcyclohexane (CDCl <sub>3</sub> ).	88
Figure 3.21	IR spectrum of 1,1-bis(4-cyano-3-methylphenyl)-4-perhydrocumylcyclohexane	89



Figure 3.22	<sup>1</sup> H-NMR spectrum of 1,1-bis(4-cyanato-3-methylphenyl)-4-perhydrocumyl cyclohexane (CDCl <sub>3</sub> )	89
Figure 3.23	<sup>13</sup> C-NMR spectrum of 1,1-bis(4-cyanato-3-methylphenyl)-4-perhydrocumyl cyclohexane (CDCl <sub>3</sub> )	90
Figure 3.24	<sup>13</sup> C-DEPT NMR spectrum of 1,1-bis(4-cyanato-3-methylphenyl)-4-perhydrocumyl cyclohexane (CDCl <sub>3</sub> )	91
Figure 3.25	IR spectrum of 1,1-bis(4-cyanato-3,5-dimethylphenyl)-4-perhydrocumylcyclohexane	91
Figure 3.26	<sup>1</sup> H-NMR spectrum of 1,1-bis(4-cyanato-3,5-dimethylphenyl)-4-perhydrocumyl cyclohexane (CDCl <sub>3</sub> ).	92
Figure 3.27	<sup>13</sup> C-NMR spectrum of 1,1-bis(4-cyanato-3,5-dimethylphenyl)-4-perhydrocumyl cyclohexane (CDCl <sub>3</sub> ).	93
Figure 3.28	<sup>13</sup> C-DEPT NMR spectrum of 1,1-bis(4-cyanato-3,5-dimethylphenyl)-4-perhydro cumylcyclohexane (CDCl <sub>3</sub> ).	93
Figure 3.29	IR spectrum of 2,7-bis(4-hydroxyphenyl)-2,7-dimethyloctane	95
Figure 3.30	<sup>1</sup> H-NMR spectrum of 2,7-bis(4-hydroxyphenyl)-2,7-dimethyloctane (CDCl <sub>3</sub> )	95
Figure 3.31	<sup>13</sup> C-NMR spectrum of 2,7-bis(4-hydroxyphenyl)-2,7-dimethyloctane (CDCl <sub>3</sub> + DMSO-d <sub>6</sub> )	96
Figure 3.32	IR spectrum of 2,7-bis(4-cyanatophenyl)-2,7-dimethyloctane.	96
Figure 3.33	<sup>1</sup> H-NMR spectrum of 2,7-bis(4-cyanatophenyl)-2,7-dimethyloctane (CDCl <sub>3</sub> )	97
Figure 3.34	<sup>13</sup> C-NMR spectrum of 2,7-bis(4-cyanatophenyl)-2,7-dimethyloctane (CDCl <sub>3</sub> )	98
Figure 3.35	<sup>13</sup> C-DEPT NMR spectrum of 2,7-bis(4-cyanatophenyl)-2,7-dimethyloctane (CDCl <sub>3</sub> )	98
Figure 4A.1	DSC thermogram illustrating the cure onset temperature	103
Figure 4A.2	Illustrative DSC thermograms of isothermal cure study	104
Figure 4A.3	DSC curves of neat CE monomers A) BPACN, B) BPZCN and C) BPC15CN	105
Figure 4A.4	DSC curves of neat CE monomers A) BPDCCN, B) DMBPDCCN and C) TMBPDCCN	105
Figure 4A.5	DSC curves of neat CE monomers A) BPPCPCN, B) DMBPPCPCN and C) TMBPPCPCN	106
Figure 4A.6	DSC curve of neat BPC6CN.	106
Figure 4A.7	DSC curves of catalyzed CE monomers A) BPACN, B) BPZCN, C) BPC15CN, D) BPDCCN, E) BPPCPCN and F) BPC6CN.	109
Figure 4A.8	Coats-Redfern plot for determination of <i>n</i> A) BPACN, B) BPZCN, C) BPC15CN, D) BPDCCN, E) BPPCPCN and F) BPC6CN.	112
Figure 4A.9	DSC isothermal curves of CE monomers at different temperatures; a) BPACN, b) BPZCN, c) BPC15CN, d) BPDCCN, e) BPPCPCN and f) BPC6CN.	115
Figure 4A.10	Fractional conversion ( $\alpha$ ) vs ln Time at various temperatures for CE monomers ; A) BPACN B) BPZCN, C) BPC15CN, D) BPDCCN, E) BPPCPCN and F) BPC6CN.	116
Figure 4A.11	Fractional conversion ( $\alpha$ ) vs Shift Factor + ln Time at various temperatures for CE monomers ; A) BPACN B) BPZCN, C) BPC15CN, D) BPDCCN, E) BPPCPCN and F) BPC6CN	117
Figure 4A.12	Arrhenius plots of Shift Factor vs Reciprocal Temperature for catalysed CE monomers; A) BPACN B) BPZCN, C) BPC15CN, D) BPDCCN, E) BPPCPCN and F) BPC6CN.	118
Figure 4B.1	Formation of polycyanurate network	122
Figure 4B.2	Slabs of cured BPACN, BPZCN and BPC15CN network.	125

Figure 4B.3	IR spectra of polycyanurate network	127
Figure 4B.4	Storage modulus of polycyanurate network	128
Figure 4B.5	Tan $\delta$ of polycyanurate network	128
Figure 4B.6	TG curves of polycyanurates	130
Figure 4B.7	TG curve of BPC6CN polycyanurate	130
Figure 4B.8	DSC curves of cured BPPCPCN, BPDCCN and BPC6CN network	132
Figure 5.1	Epoxy resins (a) diglycidyl ether of 1,1-bis(4-hydroxyphenyl)-3-pentadecyl cyclohexane (b) diglycidyl ether of 1,1-bis(4-hydroxyphenyl)cyclohexane	138
Figure 5.2	IR spectrum of diglycidyl ether of 1,1-bis(4-hydroxyphenyl)-3-pentadecyl cyclohexane	142
Figure 5.3	$^1\text{H}$ -NMR spectrum of diglycidyl ether of 1,1-bis(4-hydroxyphenyl)-3-pentadecyl cyclohexane ( $\text{CDCl}_3$ )	143
Figure 5.4	$^{13}\text{C}$ -NMR spectrum of diglycidyl ether of 1,1-bis(4-hydroxyphenyl)-3-pentadecylcyclohexane ( $\text{CDCl}_3$ )	144
Figure 5.5	$^{13}\text{C}$ -DEPT NMR spectrum of diglycidyl ether of 1,1-bis(4-hydroxyphenyl)-3-pentadecylcyclohexane ( $\text{CDCl}_3$ )	144
Figure 5.6	IR spectrum of diglycidyl ether of 1,1-bis(4-hydroxyphenyl) cyclohexane	145
Figure 5.7	$^1\text{H}$ -NMR spectrum of diglycidyl ether of 1,1-bis(4-hydroxyphenyl)cyclohexane ( $\text{CDCl}_3$ )	146
Figure 5.8	$^{13}\text{C}$ -NMR spectrum of diglycidyl ether of 1,1-bis(4-hydroxyphenyl)cyclohexane ( $\text{CDCl}_3$ )	146
Figure 5.9	$^{13}\text{C}$ -DEPT NMR spectrum of diglycidyl ether of 1,1-bis(4-hydroxyphenyl)cyclohexane ( $\text{CDCl}_3$ )	147
Figure 5.10	DSC thermograms of epoxy resins (curing agent 4,4'-methylenedianiline)	147
Figure 5.11	Coats-Redfern plot for determination of order of reaction for A) DGEBA-MDA B) DGEBA-MDA	149
Figure 5.12	IR spectra of cured epoxy resins; A) DGEBA resin, B) DGEBA resin C) DGEBA resin	150
Figure 5.13	Storage modulus of cured epoxy resins	151
Figure 5.14	Tan $\delta$ curves of cured epoxy resins	152
Figure 5.15	TG curves of cured epoxy resins	153
Figure 6.1	IR spectrum of 1,1-bis-[4-(4-nitrophenoxy)phenyl]-3-pentadecylcyclohexane	170
Figure 6.2	$^1\text{H}$ -NMR spectrum of 1,1-bis-[4-(4-nitrophenoxy) phenyl]-3-pentadecyl cyclohexane ( $\text{CDCl}_3$ ).	171
Figure 6.3	$^{13}\text{C}$ -NMR spectrum of 1,1-bis-[4-(4-nitrophenoxy) phenyl]-3-pentadecyl cyclohexane ( $\text{CDCl}_3$ )	171
Figure 6.4	IR spectrum of 1,1-bis-[4-(4-aminophenoxy)phenyl]-3-pentadecylcyclohexane	172
Figure 6.5	$^1\text{H}$ -NMR spectrum of 1,1-bis-[4-(4-aminophenoxy)phenyl]-3-pentadecylcyclohexane ( $\text{CDCl}_3$ ).	173
Figure 6.6	$^{13}\text{C}$ -NMR spectrum of 1,1-bis-[4-(4-aminophenoxy)phenyl]-3-pentadecylcyclohexane ( $\text{CDCl}_3$ ).	173
Figure 6.7	IR spectrum of 1,1-bis[4-(4- maleimidophenoxy)phenyl]-3-pentadecylcyclohexane.	174
Figure 6.8	$^1\text{H}$ -NMR spectrum of 1,1-bis[4-(4- maleimidophenoxy)phenyl]-3-pentadecyl cyclohexane ( $\text{CDCl}_3$ )	175

Figure 6.9	$^{13}\text{C}$ -NMR spectrum of 1,1-bis[4-(4- maleimidophenoxy)phenyl]-3-pentadecyl cyclohexane ( $\text{CDCl}_3$ )	176
Figure 6.10	Stacked partial $^{13}\text{C}$ and $^{13}\text{C}$ -DEPT NMR spectrum of 1,1-bis[4-(4-maleimidophenoxy) phenyl]-3-pentadecylcyclohexane (Aromatic region)	176
Figure 6.11	$^{13}\text{C}$ -DEPT NMR spectrum of 1,1-bis[4-(4- maleimidophenoxy) phenyl]-3- pentadecyl cyclohexane ( $\text{CDCl}_3$ )	177
Figure 6.12	IR spectrum of 4,4'-bis(maleimido)-3-pentadecyldiphenylether	179
Figure 6.13	$^1\text{H}$ -NMR spectrum of 4,4'-bis(maleimido)-3-pentadecyldiphenylether ( $\text{CDCl}_3$ )	179
Figure 6.14	$^{13}\text{C}$ -NMR spectrum of 4,4'-bis(maleimido)-3-pentadecyldiphenylether ( $\text{CDCl}_3$ )	180
Figure 6.15	Stacked partial $^{13}\text{C}$ and $^{13}\text{C}$ -DEPT NMR spectrum of 4, 4'-bis(maleimido)-3-pentadecyldiphenylether (Aromatic region).	181
Figure 6.16	$^{13}\text{C}$ -DEPT spectrum of 4,4'-bis(maleimido)-3-pentadecyldiphenylether ( $\text{CDCl}_3$ )	181
Figure 6.17	IR spectrum of 1,3-bis(maleimido)-4 -pentadecylbenzene.	184
Figure 6.18	$^1\text{H}$ -NMR spectrum of 1,3-bis(maleimido)-4 -pentadecylbenzene ( $\text{CDCl}_3$ )	184
Figure 6.19	$^{13}\text{C}$ -NMR spectrum of 1,3-bis(maleimido)-4 -pentadecylbenzene ( $\text{CDCl}_3$ )	185
Figure 6.20	Stacked partial $^{13}\text{C}$ and $^{13}\text{C}$ DEPT NMR spectrum of 1,3-bis(maleimido)-4 – pentadecylbenzene (Aromatic region)	186
Figure 6.21	$^{13}\text{C}$ -DEPT NMR spectrum of 1,3-bis(maleimido)-4–pentadecylbenzene ( $\text{CDCl}_3$ )	186
Figure 6.22	IR spectrum of 1,1-bis[4-(4- maleimidophenoxy)phenyl]cyclohexane	188
Figure 6.23	$^1\text{H}$ -NMR spectrum of 1,1-bis[4-(4- maleimidophenoxy)phenyl] cyclohexane ( $\text{CDCl}_3$ )	188
Figure 6.24	$^{13}\text{C}$ -NMR spectrum of 1,1-bis[4-(4- maleimidophenoxy)phenyl] cyclohexane( $\text{CDCl}_3$ )	189
Figure 6.25	$^{13}\text{C}$ - DEPT NMR spectrum of 1,1-bis[4-(4- maleimidophenoxy)phenyl] cyclohexane ( $\text{CDCl}_3$ ).	189
Figure 6.26	IR spectrum of 4, 4'-bis(maleimido)diphenylether	190
Figure 6.27	$^1\text{H}$ -NMR spectrum of 4, 4'-bis(maleimido)diphenylether ( $\text{CDCl}_3$ )	190
Figure 6.28	$^{13}\text{C}$ -NMR spectrum of 4, 4'-bis(maleimido)diphenylether ( $\text{DMSO-d}_6$ )	191
Figure 6. 29	DSC thermograms of bismaleimides. (A) ODABMI (B) BPZBMI (C) BPC15BMI (D) ODAC15BMI (E) MPDAC15BMI	193
Figure 6. 30	DSC thermograms of ODAC15BMI (A) 0 – 240 $^\circ\text{C}$ @ 10 $^\circ\text{C}/\text{min}$ , (B) quenched A and rescanned from 40 – 385 $^\circ\text{C}$ @ 10 $^\circ\text{C}/\text{min}$ , (C) quenched B and rescanned from 40 – 385 $^\circ\text{C}$ @ 10 $^\circ\text{C}/\text{min}$	194
Figure 6. 31	Determination of order of bismaleimide curing reaction by Coats- Redfern equation.	197
Figure 6.32	TG curves of bismaleimides	199
Figure 7.1	IR spectrum of 1,1-bis[4-(2-propynyloxy)phenyl] cyclohexane	208
Figure 7.2	$^1\text{H}$ -NMR spectrum of 1,1-bis[4-(2-propynyloxy)phenyl]cyclohexane ( $\text{CDCl}_3$ )	209
Figure 7.3	$^{13}\text{C}$ -NMR spectrum of 1,1-bis[4-(2-propynyloxy)phenyl] cyclohexane ( $\text{CDCl}_3$ )	210
Figure 7.4	$^{13}\text{C}$ -DEPT NMR spectrum of 1,1-bis[4-(2-propynyloxy)phenyl] cyclohexane ( $\text{CDCl}_3$ )	210
Figure 7.5	IR spectrum of 1,1-bis[4-(2-propynyloxy)phenyl]-3-pentadecylcyclohexane	211
Figure 7.6	$^1\text{H}$ -NMR spectrum of 1,1-bis[4-(2-propynyloxy)phenyl]-3-pentadecylcyclohexane ( $\text{CDCl}_3$ )	212
Figure 7.7	$^{13}\text{C}$ -NMR spectrum of 1,1-bis[4-(2-propynyloxy)phenyl]-3-pentadecylcyclohexane ( $\text{CDCl}_3$ )	213

---

Figure 7.8	$^{13}\text{C}$ -DEPT NMR spectrum of 1,1-bis[4-(2-propynyloxy)phenyl]-3-pentadecyl cyclohexane ( $\text{CDCl}_3$ )	213
Figure 7.9	IR spectrum of 1,1-bis[4-(2-propynyloxy)phenyl] decahydronaphthalene	214
Figure 7.10	$^1\text{H}$ -NMR spectrum of 1,1-bis[4-(2-propynyloxy)phenyl] decahydro naphthalene ( $\text{CDCl}_3$ )	215
Figure 7.11	$^{13}\text{C}$ -NMR spectrum of 1,1-bis[4-(2-propynyloxy)phenyl]decahydronaphthalene ( $\text{CDCl}_3$ )	216
Figure 7.12	$^{13}\text{C}$ -DEPT spectrum of 1,1-bis[4-(2-propynyloxy)phenyl]decahydronaphthalene ( $\text{CDCl}_3$ )	216
Figure 7.13	IR spectrum of 1,1-bis[4-(2-propynyloxy)phenyl]-4-perhydrocumylcyclohexane	217
Figure 7.14	$^1\text{H}$ -NMR spectrum of 1,1-bis[4-(2-propynyloxy)phenyl]-4-perhydrocumyl cyclohexane ( $\text{CDCl}_3$ )	218
Figure 7.15	$^{13}\text{C}$ -NMR spectrum of 1,1-bis[4-(2-propynyloxy)phenyl] -4-perhydrocumyl cyclohexane ( $\text{CDCl}_3$ )	219
Figure 7.16	$^{13}\text{C}$ -DEPT NMR spectrum of 1,1-bis[4-(2-propynyloxy)phenyl] -4-perhydrocumyl cyclohexane ( $\text{CDCl}_3$ )	219
Figure 7.17	IR spectrum of 2,2-bis[4-(2-propynyloxy) phenyl]propane	220
Figure 7.18	$^1\text{H}$ -NMR spectrum of 2,2-bis[4-(2-propynyloxy) phenyl]propane ( $\text{CDCl}_3$ )	220
Figure 7.19	$^{13}\text{C}$ -NMR spectrum of 2,2-bis[4-(2-propynyloxy) phenyl]propane ( $\text{CDCl}_3$ )	221
Figure 7.20	DSC thermograms of bispropargyl ethers containing cardo /(cyclo) aliphatic moiety	221
Figure 7.21	DSC thermograms of bispropargyl ethers BPAPT, BPZPT, BPC15PT, BPDCPT and BPPCPPT at different heating rates.	223
Figure 7.22	Kissinger plots for determination of kinetic constants	225
Figure 7.23	Determination of order of curing reaction of bispropargyl ethers by Coats-Redfern equation.	226
Figure 7.24	TG curves of propargyl terminated resins	228

# Chapter **1**

Introduction and Literature Survey

## 1.1 Introduction

The human life has been enriched by long and persevering studies from a host of motivated material scientists and engineers. The rapid pace of advances in polymers, which are an important class of advanced materials, has been remarkable. Polymers are so well integrated into the fabric of society that we take a little notice of our dependence on them. This is truly the “polymer age”! The society benefits across the board- in health, medicine, clothing, transportation, housing, defense, energy, electronics, and so on. There is no doubt that synthetic polymers have large impacts on our daily lives.

Goodyear’s (and Hancock in England) discovery of the vulcanization of natural rubber in 1839 could be construed as the first successful commercial product of polymer research. The plastic industry dates the beginning of synthetic polymers to the invention of thermosetting phenol-formaldehyde resin called Bakelite by Leo Baekeland in 1909. The wide variety of thermoset products *viz*; phenolic resins, amino resins, epoxy resins, unsaturated polyester resins, allyl resins, bismaleimides, cyanate ester resins, etc. were subsequently invented and commercialized using various reactive monomers and prepolymers (or polymers).

Thermosets, unlike thermoplastics, are permanently cross-linked networks which can not be reformed upon further application of heat and/or pressure. The curing (polymerization) is often activated thermally or by radiations. Uncured thermosets is a mixture of small reactive molecules; monomers. They may contain additives such as catalysts to promote or accelerate cure.

The crosslinked network of thermosets can be formed in a number of ways, including:

1. Condensation type polymerization by systems in which at least one of the monomers or oligomer precursors has functionality higher than two. The examples of this type of materials include silicone resins, aminoplastics, phenolics, cyanate ester resins, etc.
2. The use of crosslinking species to form crosslinks between polymer molecules. The examples of this type of materials include epoxy resins where the crosslinking system includes a difunctional amine, anhydride, etc.,
3. The addition polymerization of monomers containing two double (or triple) bonds. A few examples of this type of materials are allyl resins, acrylic resins, bismaleimides, benzoxazines, propargyl-terminated resins, etc.,

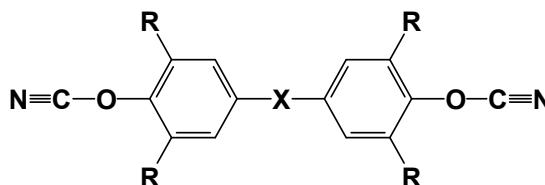
Thermosets, in general, possess good dimensional stability, thermal stability, chemical resistance and electrical properties. They find a widespread use in several applications such as adhesives; primary and secondary structures in aerospace; countertops and floors for manufacturing facilities and homes; printed circuit boards, conductive polymer elements and encapsulation materials for electronic applications; and recreational products such as tennis

racquets, bicycle frames, golf clubs, fishing rods, etc.,. The growing need for high use-temperature matrix resins in fibre-reinforced composites in the aerospace industry has encouraged intensive research. Epoxy resins are currently by far the largest segment of thermosetting polymers which are used to make structural composites in the aerospace industry. Epoxies owe their wide usage to the ease of handling and processability. In circumstances where epoxies can not be used, higher temperature performance resins are needed and several other candidates *e.g.* bismaleimides, cyanate ester resins, polybenzoxazines, etc., are currently being investigated.

The present chapter briefly summarizes the literature on thermosetting resins with particular emphasis on cyanate ester resins, epoxy resins, bismaleimides and propargyl-terminated resins covering methods of synthesis, curing/processing, structure-property relationship, applications, etc.

## 1.2 Cyanate ester resins

The term ‘cyanate ester resins’ is used to describe both prepolymers and cured resins; the former containing reactive ring-forming cyanate functional groups<sup>1, 2</sup>. This family of thermosetting monomers and their prepolymers are esters of bisphenol and cyanic acid. Commercial monomers may be represented by the general structure illustrated in **Figure 1.1** where “R” may be a range of functional groups *e.g.* hydrogen atoms, methyl or allyl groups and the bridging group “X” may be simply an isopropylidene moiety or an extended aromatic or cycloaliphatic moiety, etc.



**Figure 1.1** General structure of cyanate ester monomers

### 1.2.1 Synthesis of cyanate esters

Though practical synthetic route to manufacturing cyanate esters was invented and developed at Bayer AG in the 1960s<sup>3</sup>, efforts were initialized in 1857 when Cloez<sup>4</sup> attempted the synthesis of alkyl cyanates by reacting sodium alkoxides with cyanogen chloride. However, the products obtained by Cloez were mixtures containing mainly trialkyl cyanurates and dialkyl imidocarbonates. Theoretically, cyanate esters would be directly synthesized from cyanic acid (HOCN). However, as cyanic acid exists predominantly in the *iso* form, HNCO, the major product was an isocyanate<sup>5</sup>. Because of many discouraging results, the esters of cyanic acid were for many years considered to be ‘non-existent compounds’.

The following methods have been listed as the most reasonable for the synthesis of cyanate esters.<sup>6</sup>

- (1) Reaction of phenol or alcohol with cyanogen halide
- (2) Thermolysis of thiazoles
- (3) Dehydration of alkyl thiocarbamates, and
- (4) Acylation and decomposition of alkyl-*N*-hydroxythiocarbamates

Of these, the first two methods are practical and the remaining two are of historical importance. The reaction of cyanogen halide with an alcohol or phenol is by far the most widely used and successfully employed for the synthesis of aryl, alkyl and fluoroalkyl cyanate monomers.

### 1.2.1.1 Synthesis of cyanate esters from phenol / alcohol and cyanogen halide

Grigat and Putter (Bayer AG)<sup>3, 7-9</sup> reported the practically viable route for the synthesis of cyanate esters. The reaction involves the addition of a base, generally triethylamine to phenol-cyanogen halide mixture at -30 to 10 °C. (**Scheme 1.1**)



X = Cl, Br

#### **Scheme 1.1 : Synthesis of cyanate esters from phenol / alcohol and cyanogen halide**

A large number of aryl cyanates were synthesized in excellent yields and were found to be remarkably stable. Triethylamine functions as a base of appropriate strength with solubility in organic solvents. At higher temperatures, Von Braun reaction<sup>10</sup> competes with cyanate forming reaction producing diethylcyanamide; an undesirable by-product. In Von Braun reaction, a tertiary amine reacts with cyanogen bromide to form a disubstituted cyanamide and an alkyl bromide (**Scheme 1.2**).



#### **Scheme 1.2: Von Braun reaction**

For aliphatic amines, Van Braun reaction is reported to be vigorous and requires dilution and cooling. Diethylcyanamide is undesirable because, as a low volatile liquid contaminant in a cyanate prepolymer, it can cause voids by out-gassing under curing conditions. The reports of Von Braun reaction<sup>10, 11</sup> indicate no examples for diethylcyanamide formation using cyanogen chloride.

A large variety of solvents *e.g.* benzene, chloroform, dichloromethane, carbon tetrachloride, diethyl ether, acetone, methyl ethyl ketone, tetrahydrofuran, ethyl acetate, acetonitrile, etc., have been used for cyanate ester synthesis but there is some strategy to the



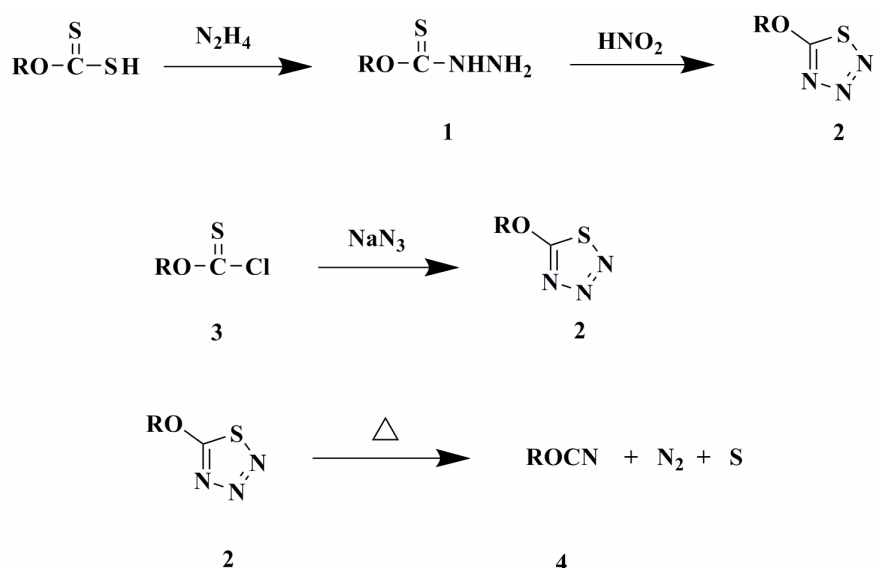
selection. When triethylamine base is being used, the triethyl ammonium halide salt will precipitate as the reaction progresses in the solvents such as benzene, diethyl ether, carbon tetrachloride and acetone. The purification may be conducted by distillation, crystallization or with a silica gel column chromatography.

The method is not suitable for alkyl cyanates unless they are stabilized by halo substituents or by steric hindrance<sup>12</sup>.

### 1.2.1.2 Synthesis of cyanate esters by thermolysis of thiazotriazoles

This route to synthesize organic cyanate esters was discovered independently and nearly simultaneously by Jensen and Holm<sup>13</sup> and by Martin<sup>14</sup> and was reported in 1960.

The method involved decomposition of thiazotriazoles (2) in ether solution at 20 °C leading to the formation of alkyl cyanates or aryl cyanates (4) in high yields. The thiazotriazoles were prepared by thiocarbonylhydrazines (1) or chlorothioformates (3) route. (**Scheme 1.3**).



**Scheme 1.3 : Synthesis of cyanate esters by thermolysis of thiazotriazoles**

### 1.2.1.3 Synthesis of cyanate esters by dehydration of alkyl thiocarbamates

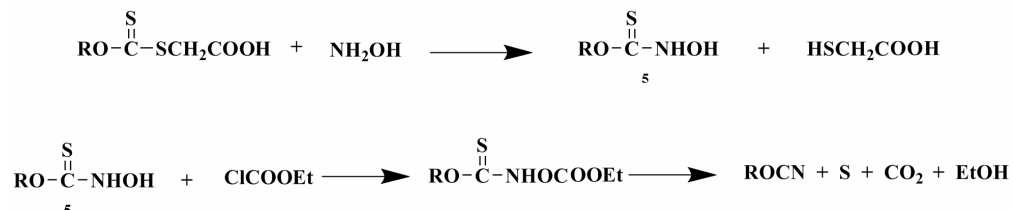
Alkyl cyanates were obtained by treatment of alkyl thiocarbamates with heavy metal oxides such as, HgO, Ag<sub>2</sub>O, etc., in ether solution at 0 °C (**Scheme 1.4**)<sup>15</sup>. However, the yield of alkyl cyanates was reported to be very poor (5%) and hence, the method is not of practical choice.



**Scheme 1.4 : Synthesis of cyanate esters by dehydration of alkyl thiocarbamates.**

### 1.2.1.4 Synthesis of cyanate esters from alkyl-*N*-hydroxythiocarbamates

Alkyl-*N*-hydroxythiocarbamates (5) on acylation undergo Lossen rearrangement to yield alkyl cyanates at room temperature <sup>16</sup> (**Scheme 1.5**). The yields are good and the preparation of alkyl cyanates by this method is considerably faster than that of thiazotriazole route.



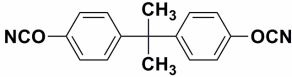

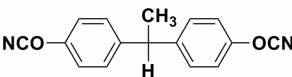
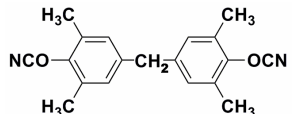
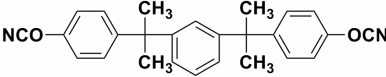
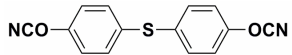
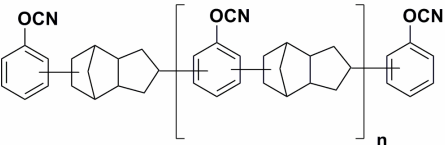
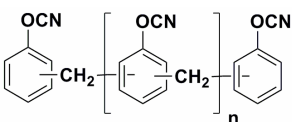
**Scheme 1.5 : Synthesis of cyanate esters by dehydration of alkyl-*N*-thiocarbamates**

### 1.2.2 Cyanate ester monomers

The research efforts initiated by Celanese Corp. (Ciba-Geigy)<sup>17, 18</sup>, Dow Chemicals<sup>19, 20</sup> and Allied-Signal<sup>21</sup>, utilizing chemically tailored bisphenols and polyphenols expanded the family of CE monomers. An excellent review on these has been provided by Shimp<sup>22</sup> and Snow<sup>23</sup>. **Table 1.1** presents a list of CE monomers of commercial importance with their trade names.

Bisphenol A dicyanate (AroCy B-10, BPACN) was the first CE monomer to be commercialized. The cured resins of dicyanates AroCy F-10 (Fluorinated analogue of BPACN), RTX-366 and XU 71787 have remarkably low dielectric constant ( 2.66, 2.64 and 2.80, respectively) and moisture absorption (1.8, 0.7 and 1.4, respectively). A trifunctional CE monomer REX-371/Primaset derived from low molecular weight novolacs, on curing results in a network with high Tg (320-350 °C).<sup>22,23</sup>

**Table 1.1 : List of commercial cyanate ester monomers with their trade names.**

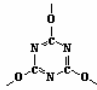
Sr. No	Cyanate Ester Monomers	Trade Name
1		AroCy B-10 (Ciba)
2		AroCy F-10 (Ciba)
3		AroCy L-10 (Ciba)
4		AroCy M-10 (Ciba)
5		RTX-366 (Ciba)
6		AroCy T-10 (Ciba)
7		XU71787 (Dow)
8		REX-371 (Ciba) Primaset (Allied-Signal)

### 1.2.3 Spectroscopic characterization of cyanate ester monomers

The issue of purity and understanding the nature of impurity(ies) by spectroscopic investigations is important because some impurities (e.g. phenol, triethylamine, carbamate, diethylcyanamide, and residual solvent) either accelerate the polymerization exotherm or generate voids during processing. The methods that are found useful for identification / quantification of impurities are nuclear magnetic resonance spectroscopy<sup>24-27</sup> (both <sup>13</sup>C and <sup>15</sup>N NMR), infrared spectroscopy<sup>28-30</sup> (IR), differential scanning calorimetry<sup>31-33</sup> (DSC), refractive index<sup>34, 35</sup> (RI), high performance liquid chromatography<sup>36, 37</sup> (HPLC), and gel permeation chromatography<sup>27, 36, 38</sup> (GPC).

$^{13}\text{C}$  and  $^{15}\text{N}$ -NMR spectra were studied by many researchers<sup>24-27</sup>, and the appropriate assignments were made. The impurities derived (i.e. carbamate, imidocarbonate and cyanurate) from reaction of the cyanate group may be identified from the corresponding  $^{13}\text{C}$  and  $^{15}\text{N}$  chemical resonance shifts as indicated in **Table 1.2**.

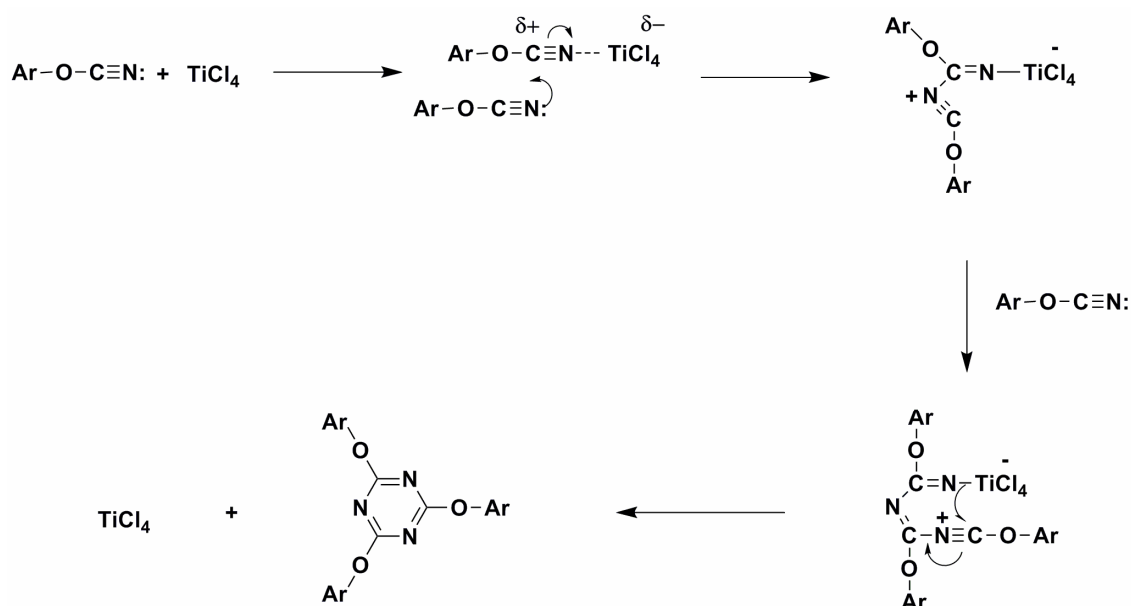
**Table 1.2 : Characteristic  $^{13}\text{C}$  and  $^{15}\text{N}$  NMR chemical shifts of functionalities associated with cyanate ester curing.**

Functionality	$^{13}\text{C}$ Chemical Shift ( TMS , $\delta$ ppm)	$^{15}\text{N}$ Chemical Shift ( Formamide, $\delta$ ppm)
Ar-OCN	109	52
Ar-O-CO-NH <sub>2</sub>	156	- 40
Ar-O-C(OR)=NH	159.5	43
 Ar-O-Triazine	174	87

IR spectroscopy has been very important tool for CE monomer identification, measurement of conversion to polymer and identification of hydrolysis products and impurities. The cyanate functional group is identified by a strong  $\text{C}\equiv\text{N}$  stretching band in the range 2200-2300  $\text{cm}^{-1}$  and a strong C-O-C stretch in the range 1160-1240  $\text{cm}^{-1}$ . The  $\text{C}\equiv\text{N}$  stretching is of considerable importance as it is used to quantify the conversion to prepolymer and cured polymer.

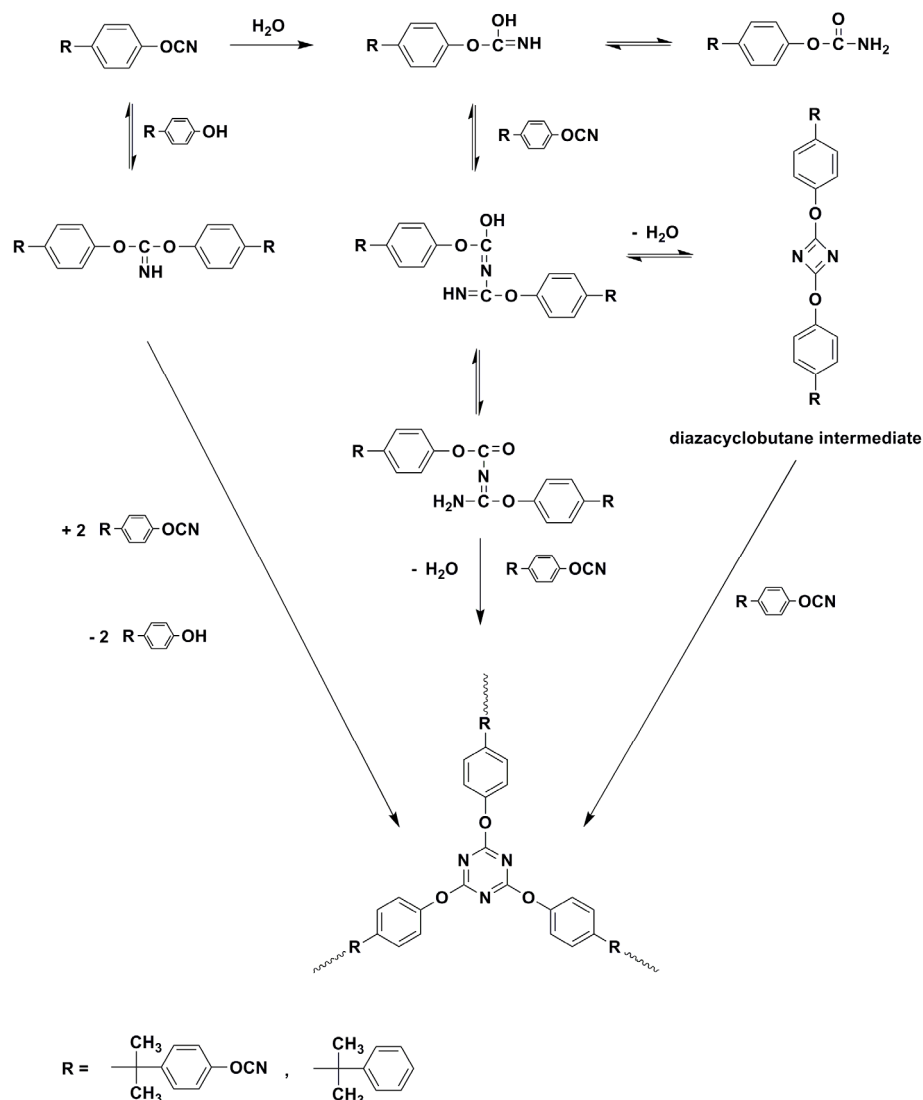
#### 1.2.4 Mechanism of cyanate ester polymerization

Cyanate esters undergo thermal or catalytic polycyclotrimerization to give polycyanurates *via* typical step-growth network building process. Starting from low molecular weight monomers with at least two cyanate groups, the reacting system passes through a pregel state with a broad distribution of oligomers to reach the gel point at a certain value of the functional groups' conversion. Finally, when nearly all functional groups have reacted, the system consists of one giant macromolecule. Generally, cyanate esters are cured with a transition metal catalyst or chelate catalyst in the presence of a hydrogen donor such as nonyl phenol (described in section 1.2.5). The cyanate groups are believed to be coordinated through the metal ion to allow ring closure.<sup>39</sup> Brownhill *et al.*<sup>40</sup> reported that transition metal (e.g. Ti) co-ordinates with the nitrogen, enhancing the electrophilicity of the nitrile group for addition of another cyanate group to it (**Scheme 1.6**).



**Scheme 1.6 : Mechanism of cyanate ester polymerization ( Brownhill *et.al.*<sup>40</sup> ).**

Grener-Loustalot *et al.*<sup>41,42</sup> investigated the mechanism of polymerization of mono- and dicyanates by HPLC and spectroscopic methods (**Scheme 1.7**). It was found that in catalysed systems, iminocarbonates, diazacyclobutane intermediate (dimer) and carbamates were present in considerable proportions. The key product during cyclotrimerization of cyanates without adding a catalyst is an intermediate iminocarbonate.



**Scheme 1.7 : Mechanism of cyanate ester polymerization (Loustalot *et.al.*<sup>42</sup>).**

### 1.2.5 Cure catalysis and cure kinetics

Cyanate esters cure *via* cyclotrimerization reaction leading to the formation of highly stable, six membered triazine rings. The cyclization reaction can be induced thermally, but this reaction is slow and usually difficult to drive to high levels of conversion. The cure reaction is highly susceptible to catalysis. A small amount of impurities (e. g. H<sub>2</sub>O, ArOH, metal ions) (stemmed from monomer synthesis) catalyze the curing reaction. In fact, no reaction takes place if completely purified cyanate esters are heated<sup>36</sup>. For common aryl dicyanates, a wide variety of catalysts including transition metal carboxylates, acetyl acetonates, phenols, metal carbonyls, adventitious moisture, etc. have been found to be effective.<sup>43 - 45</sup> The selection of catalyst system is governed by a number of factors, including the monomer type, the required pot-life and the type of processing method selected.

### 1.2.5.1 Catalysts for cyanate ester cure

The rate of the cyclotrimerization reaction is catalyst dependent. By judicious choice of catalyst type and addition level, the rate of cure of cyanate esters may be varied.<sup>46</sup> By far, the most common types of catalyst used for the aryl dicyanates are carboxylate salts and chelates of transition metal ions<sup>43-45</sup>. The role of transition metal ions in the polymerization reaction is to facilitate the cyclization reaction of three cyanate monomer functionalities by formation of coordination complexes<sup>39</sup>. Used alone, the transition metal salts and chelates do not dissolve readily in molten cyanate ester monomer. This can result in the need for high temperatures and/or long cure times for complete curing. The presence of catalyst residue particles in the cured resins is also undesirable. For this reason, a co-catalyst is also added. The co-catalyst serves a dual purpose of acting as a solvent for the transition metal catalyst and completing ring closure of the triazine ring *via* hydrogen transfer.<sup>47</sup> The most commonly used co-catalyst is alkyl phenol such as nonyl phenol. The other active hydrogen sources *e.g.* other alkyl phenols, bisphenols, alcohols, imidazoles or aromatic amines may be used, but nonyl phenol seems to be adequate for most purposes<sup>44, 46, 47</sup>.

The pot-life, gel time and total cure time of cyanate ester composition typically depends on the type and concentration of catalytic system employed. In general, the carboxylates show higher activity than the chelates. The choice of transition metals is very wide, but certain types of metal should be avoided. Tin, lead, antimony and titanium, can promote transesterification and hydrolysis reactions and are best avoided<sup>48, 49</sup>. Shimp<sup>48</sup> compared the effect of six different metal acetylacetonates on cyanate ester cure and the properties of the cured resins. The preferred metal ions were ranked in the order  $\text{Cu}^{2+} = \text{Co}^{2+} > \text{Zn}^{2+} > \text{Mn}^{2+} > \text{Fe}^{3+} > \text{Al}^{3+}$ . It was also shown that the choice of metal ions has a relatively minor effect on the degree of conversion.

Urea compounds have also been reported to be effective cure catalysts for cyanate ester resins<sup>43, 44</sup>. The formulations have a good pot-life at room temperature and can be cured to a high conversion. Epoxy resins can also catalyse the cure of cyanate ester resins, wherein the catalytic effect is provided by hydroxyl groups<sup>43, 44</sup>.

The presence of alkyl phenol; a source of active hydrogen, not only improves mixing of catalyst with the resin but also has an advantageous effect on properties. With the optimum concentration of nonyl phenol co-catalyst, cured cyanate esters achieve higher levels of conversion than would otherwise be obtained. The cure rate is dependent on the mobility and concentration of active hydrogen species present. The majority of cured resin properties are not compromised by this increase, although the maximum glass transition temperature (T<sub>g</sub>) and heat distortion temperature (HDT) are reduced as a result of the plasticization effect of

nonylphenol<sup>50, 51</sup>. Although nonyl phenol is effective as a co-catalyst for the transition metal catalysts, it is relatively ineffective on its own<sup>39</sup>.

### 1.2.5.2 Cure kinetics

The kinetics of cyanate ester trimerization was investigated by several researchers<sup>52-77</sup> so as to understand the processing of CE resins. Most of the work was carried out on the reaction of BPACN<sup>50-57, 59, 64, 67-69, 74</sup>. The reactions were carried out in bulk<sup>55-62</sup> or in solution<sup>52-54</sup>, neat<sup>55-64, 71, 72, 75, 77</sup> or in the presence of a catalyst<sup>50-54, 63, 65, 67-70, 74</sup>.

The quantitative detection of cyanate concentrations in the resin system facilitates monitoring the progress of curing. Various techniques (e.g. spectroscopic, calorimetric, etc) were employed to understand curing kinetics of CE monomers.

Simon *et.al*<sup>30</sup> described the details of the IR technique, including the initial peak height perturbation of the 2270 cm<sup>-1</sup> peak. The characteristic C≡N stretching doublets at 2270 and 2235 cm<sup>-1</sup> of cyanate were compared with the side chain methyl C-H stretching at 2970 cm<sup>-1</sup>.

The application of NMR spectroscopy to probe the cyanate –triazine reaction was first reported by Fang<sup>24</sup> in 1990. NMR spectroscopy is the only method that provides both the conversion as well as the molecular weight data in single experiment without using internal standard. <sup>15</sup>N-NMR spectroscopy is a reliable tool for cure monitoring of cyanate esters as the signals due to the OCN and triazine appear as two isolated signals.<sup>24-27</sup>

Both Kohn *et.al*<sup>78</sup> and Bauer and coworkers<sup>79</sup> proposed simultaneously colorimetric procedure to detect nanomolar quantities of cyanates in solution. In DSC, the methods based on residual heat ( $\Delta H$ ) and Tg were used to monitor cyanate conversions. The conversion was calculated based on the ratio of enthalpy consumed to the total enthalpy available in the cyanate ester system for the residual heat method, whereas a predetermined Tg-conversion chart was used in Tg method<sup>32, 33</sup>.

Torsional braid analysis (TBA) is a dynamic mechanical method that monitors the progress of polymerization by measuring the damping and frequency of a monomer-impregnated braid.<sup>80, 81</sup> The technique allows a wide temperature-range to be studied from which various transitions of non-volatile monomers can be monitored.

Dynamic mechanical analysis (DMA) is normally performed in a dynamic rheometer using a parallel plate configuration. A sinusoidal strain is applied to the sample disc and the resulting stress amplitudes and phase angles are measured by a strain-gauge transducer from which the shear elastic modulus, shear viscous modulus and complex viscosity are obtained which can be used to monitor the cure process.<sup>82, 83</sup>

The cure monitoring of cyanates by conventional dielectrometry using a parallel conducting plates cell or microdielectrometry has been reported.<sup>84, 85</sup> The microdielectrometry is



capable of measuring the dielectric loss factor rather than the loss tangent measured by conventional dielectrometry.

Snow and Armistead<sup>86</sup> published a detailed description on a dilatometer used for measuring the change in volume during the cure of BPACN. Measuring the change in refractive index with time at a constant temperature can provide kinetic data for the cyclotrimerization curing reaction. This technique is useful for assessing and controlling polymerization hazards associated with heating cyanate esters for dissolving polymeric components or applying catalysed formulations at elevated temperatures<sup>87</sup>.

The progress of polymerization of cyanate resins can also be monitored turbidimetrically. The gradual addition of poor solvent into a solution of cyanate polymer will generate a turbid solution. The amount of poor solvent added to produce a constant turbidity is a sensitive function of conversion and molecular weight<sup>43</sup>.

Apart from these, techniques like HPLC, UV, and dispersive fiber optic Raman Spectroscopy, were also reported to monitor cure conversion<sup>43-45</sup>.

Although the mechanisms for the several catalysts and reaction conditions are different, Bauer *et.al.* stated some common facts<sup>44</sup>:

- The reaction of cyanate ester groups into cyanurates is almost completely selective with an enthalpic effect of  $\Delta H \approx -105$  kJ/mol –OCN group.
- Nearly full conversion of the functional groups can be achieved when working at sufficiently high temperatures.
- A catalytically active species are formed during the process that gives the reaction an autocatalytic character.
- The reaction rate is very sensitive to small impurities in the monomer or the added catalyst.
- The overall kinetics can be described by simple equations regardless of the catalyst.

On these lines, Bauer *et. al.* developed two different approaches.<sup>29,36,55</sup> Simon and Gillham<sup>58,61</sup> modified the kinetic scheme of Bauer *et. al.*<sup>29,36,55</sup> and obtained:

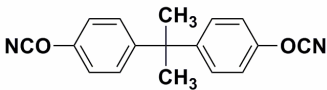
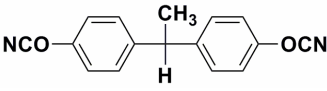
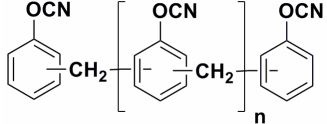
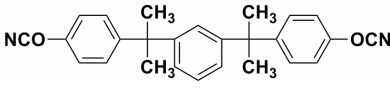
$$\frac{d\alpha}{dt} = k_1(1-\alpha)^2 + k_2\alpha(1-\alpha)^2 \quad (1)$$

where  $\alpha$  is a fractional conversion of –OCN groups and  $k_1$  and  $k_2$  are rate constants for a second-order and a second-order autocatalytic reaction. With the help of this equation the reaction kinetics was described including the very early stages of the reaction. At higher temperature or higher catalyst concentration, a simple  $n^{\text{th}}$  order kinetic equation (equation 2) was used to get a satisfactory description of the kinetics:

$$\frac{d\alpha}{dt} = k(1-\alpha)^n \quad (2)$$

A first-order behavior was obtained for both the uncatalysed and the catalysed reaction. The rate constant  $k$  also includes the effects of catalysts and was found for the uncatalysed case to be proportional to the concentration of initial phenolic –OH groups<sup>29, 36, 55, 57</sup>. **Table 1.3** summarizes activation energies for different CE monomers calculated under isothermal curing mode (neat or catalyzed).

**Table 1.3: Activation energies for various cyanate ester monomers calculated by neat/catalysed isothermal curing kinetics.**

Sr. No	Monomer	Catalysed / Neat	Activation Energy (kJ/mol)	Reference
1		Manganese octoate	76	50, 51
		Zinc octoate	80	50, 51
		Cobalt acetylacetonate	104	50, 51
		Neat *	35[Ea <sub>1</sub> ], 88 [Ea <sub>2</sub> ]	64
		Neat #	42[Ea <sub>1</sub> ], 89[Ea <sub>2</sub> ]	64
		Copper acetylacetonate	65[Ea <sub>1</sub> ], 74[Ea <sub>2</sub> ]	68
		Dibutyl tin dilaurate	69	73
		Cobalt acetylacetonate	69-71	74
2		Zinc naphthanate	59[Ea <sub>1</sub> ], 69[Ea <sub>2</sub> ]	66
		Dibutyl tin dilaurate	66	73
		Neat	18[Ea <sub>1</sub> ], 24[Ea <sub>2</sub> ]	72
		Neat	60	77
3		Neat	81[Ea <sub>1</sub> ], 82[Ea <sub>2</sub> ]	71
		Neat	88[Ea <sub>1</sub> ], 114[Ea <sub>2</sub> ]	75
4		Neat	92	63
		Copper naphthanate	54	63

\* Air medium ,

# Argon medium,

[Ea<sub>1</sub>] Activation energy for rate constant  $k_1$

[Ea<sub>2</sub>] Activation energy for rate constant  $k_2$

### 1.2.6 Structure-property relationship

The common characteristics associated with aryldicyanate monomers, their prepolymers and polycyanurates are summarized in **Table 1.4**.

**Table 1.4: Relationship between dicyanate structural units and characteristics of resulting polycyanurate network**

Structural Unit	Characteristic
Cyanate functionality	Low toxicity Easy to process Reacts with epoxides Blends with thermoplastics
Ring forming	High service temperature
-O- linkages	Toughness
Low crosslink density	Toughness
Low polarity	Low dielectric loss Low moisture absorption

The unique chemistry of –OCN functionality and the aryl polycyanurate network formed after cure creates distinctive features which can be further enhanced by altering the polyphenol backbone structures.<sup>43, 88</sup> The properties like Tg, dielectric constant, moisture absorption, fracture toughness, etc., can be altered by changing backbone structure. In the present section, the dependence of Tg, dielectric constant and moisture absorption on CE monomer structure is discussed.

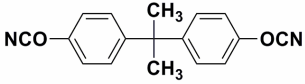
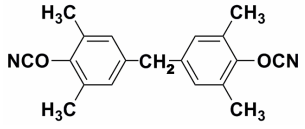
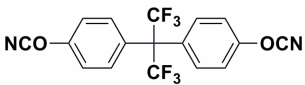
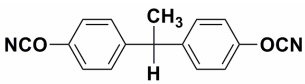
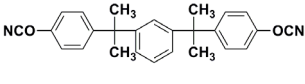
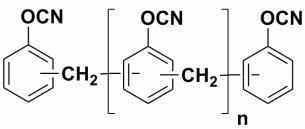
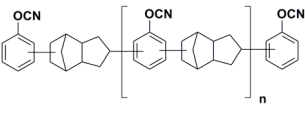
#### 1.2.6.1 Glass transition temperature

The glass transition temperature of cured network of commercial monomers varies in the range 190-290 °C. **Table 1.5** summarizes properties (Tg, dielectric constant and moisture absorption) of polycyanurates based on commercial CE monomers.

Through many studies, it has been observed that spacers play a major role in altering Tg of polycyanurate system. The introduction of aliphatic/flexible spacers is reported to act as effective diluent thereby reducing crosslink density (branching density) which reflects in decrease in Tg.<sup>23</sup> The free volume of polycyanurate system also governs Tg. *Ortho*-methylation is reported to increase free volume, providing enough space rotation, results in lowering the Tg of polycyanurate network.<sup>23</sup> The Tg of polycyanurates based on *para*-substituted CE monomers is reported to be higher than that of *meta*-substituted counterparts.<sup>89</sup>

Apart from monomer structure, Tg of polycyanurate is also governed by conversion<sup>63,90</sup>. Gillham *et.al.*<sup>63,90</sup> revealed one-to-one relation between conversion and Tg.

**Table 1.5: Properties of polycyanurates based on commercial CE monomers \*.**

Sr. No.	Monomer Structure	Trade Name	Homopolymer properties		
			Tg (°C)	Dielectric constant (Dk at 1 MHz)	Moisture absorption (%)
1		AroCy B-10	289	2.91	2.5
2		AroCy M-10	252	2.75	1.4
3		AroCy F-10	270	2.66	1.8
4		AroCy L-10	258	2.98	2.4
5		RTX-366	192	2.64	0.7
6		Primaset PT	270- >350	3.08	3.8
7		XU-71787	244	2.80	1.4

\* Data taken from reference 88.

### 1.2.6.2 Dielectric constant

A symmetrical arrangement of electronegative oxygen and nitrogen atoms around a central electropositive carbon atom in a polycyanurate network contributes to lower dielectric loss properties. Furthermore, the presence of structural units which lower polarizability per unit volume lowers the dielectric constant of polycyanurate network<sup>91</sup>. As can be inferred from the data presented in **Table 1.5**, dielectric constant progressively decreased as the cyanurate structure is diluted with the hydrocarbon linking unit by increasing number of rings : Primaset PT (3.08) > AroCy B-10 (2.91) > RTX-366 (2.64). The fluorine substitution reduces polarizability, and this effect is reflected in lower dielectric constants if dipoles are not generated. The polycyanurate of hexafluorobisphenol A dicyanate (Arocy F-10) therefore

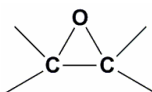
shows lower dielectric constant as compared to biphenol A dicyanate (Arocy B-10 )<sup>91</sup>. Molecular packing is one of the deciding factors for dielectric constant. The increase in free volume assists lowering dielectric constant. The *ortho*-substitution of methyl groups (Arocy M-10) inhibits close ordered packing causing significant reduction in dielectric constant when compared with Arocy B-10. *Ortho*-Methylation of RTX-366 is also reported in lowering dielectric constant from 2.64 to 2.59 at 1 GHz<sup>92</sup>.

### 1.2.6.3 Moisture absorption

The cyanurate ester linkage is very resistant to hydrolysis, withstanding hundreds of hours' immersion in boiling water. As a class, cyanate ester homopolymers absorb less water at saturation than competing resins such as epoxies, BMIs, etc. From the data summarized in **Table 1.5**, it can be understood that hydrophobicity within the cyanate ester family can be increased by fluorination, *ortho*-methylation and by the incorporation of bulky hydrocarbon units within the bisphenol structure.

## 1.3 Epoxy resins

Epoxy resins are an important class of polymeric materials, characterized by the presence of more than one three-membered ring known as the epoxy, epoxide, oxirane, or ethoxyline group (**Figure 1.2**).



**Figure 1.2 : Structure of oxirane ring**

The word “epoxy” is derived from the Greek prefix “ep,” which means over and between, and “oxy,” the combining form of oxygen<sup>93, 94</sup>. By strict definition, epoxy resins refer only to uncross-linked monomers or oligomers containing epoxy groups. However, in practice, the term “*epoxy resins*” is loosely used to include cured epoxy systems. The capability of the highly strained epoxy ring to react with a wide variety of curing agents under diverse conditions and temperatures imparts additional versatility to the epoxies. Recently, many research articles reflecting chemical versatility of the oxirane group and the range of applications of epoxy resins have been published<sup>95</sup>.

### 1.3.1 Synthesis of epoxy resins

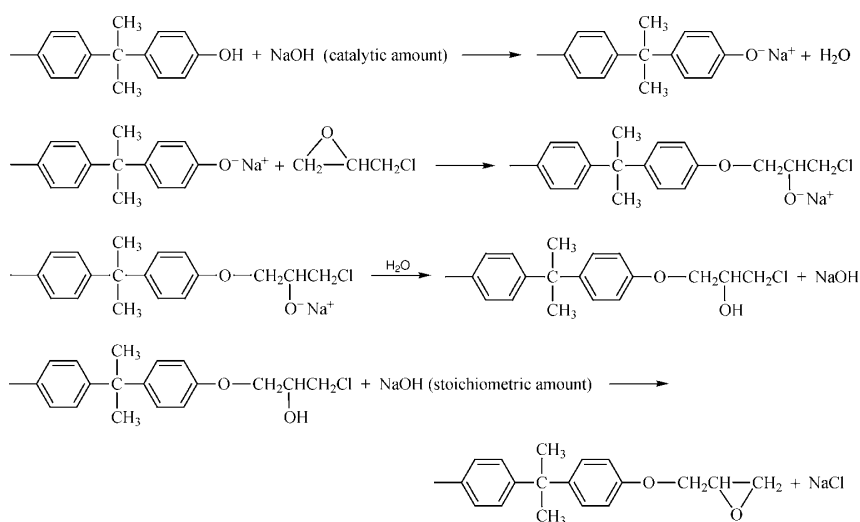
The patent literature indicates that the synthesis of epoxy compounds was discovered as early as the late 1890s<sup>93</sup>. However, the commercial possibilities for epoxy resins were only recognized a few years later, simultaneously and independently, by the DeTrey Freres Co. in Switzerland<sup>96</sup> and by the DeVoe and Reynolds Co.<sup>97</sup> The significant development of the

electronics and computer industries demanded higher performance epoxy resins and new epoxy resins were developed to satisfy the needs.

### 1.3.1.1 Synthesis of epoxy resins by coupling reaction

Most commercially important epoxy resins are prepared by the coupling reaction<sup>98-99</sup> of compounds containing at least two active hydrogen atoms with epichlorohydrin followed by dehydrohalogenation (**Scheme 1.8**). A source of active hydrogen includes polyphenolic compounds, mono and diamines, amino phenols, heterocyclic imides and amides, aliphatic diols and polyols, and dimeric fatty acids.

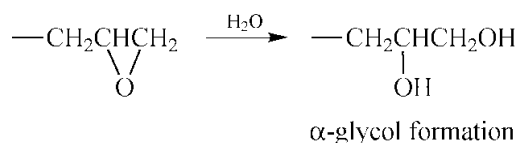
The most important intermediate in epoxy resin technology is the bisphenol A based liquid epoxy resins. These are prepared in a two-step reaction sequence starting from bisphenol A and epichlorohydrin. The first step is the base-catalysed coupling of bisphenol A and epichlorohydrin to yield a chlorohydrin. The dehydrohalogenation of the chlorohydrin intermediate with a stoichiometric amount of base affords the epoxy resin (glycidyl ether). The coupling is generally achieved employing caustic and phase transfer catalysts<sup>100-107</sup>.



**Scheme 1.8: Synthesis of bisphenol A based epoxy resin.**

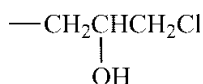
The coupling process is often accompanied with side reactions. The five common side reactions<sup>108-111</sup> are as follows:

The unavoidable hydrolysis of the oxirane ring (**Scheme 1.9**) gives a small amount (0.1–5%) of monohydrolyzed resin (MHR) or  $\alpha$ -glycol. It has been reported that rates of epoxy resin curing with diamines can be dramatically increased by higher levels of MHR<sup>109</sup>.



**Scheme 1.9: Hydrolysis of epoxide ring**

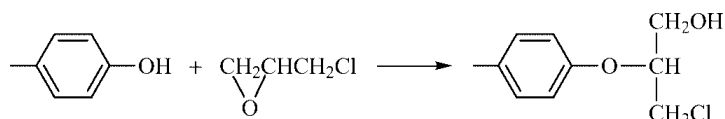
The incomplete dehydrochlorination (**Figure 1.3**) results in residual saponifiable or hydrolysable chloride:



**Figure 1.3: Incomplete dehydrochlorination**

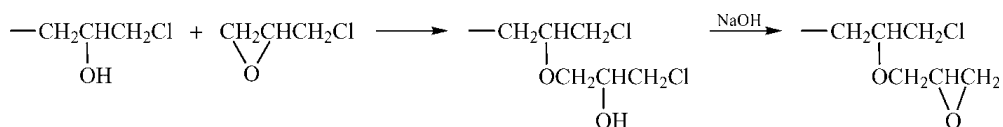
The incomplete dehydrochlorination increases the level of hydrolyzable chloride in the resin, which affects the suitability for applications requiring superior electrical properties. In addition, hydrolyzable chlorides can affect reactivity by neutralizing basic catalysts such as tertiary amines.

The abnormal addition of epichlorohydrin, i.e., abnormal phenoxide attack at the central carbon of epichlorohydrin (**Scheme 1.10**) results in an end group that is more difficult to dehydrochlorinate:



**Scheme 1.10 : Abnormal addition of epichlorohydrin**

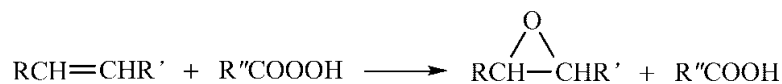
The formation of bound chlorides by the reaction of epichlorohydrin with hydroxyl groups in the polymer backbone (**Scheme 1.11**) is one of the side reactions.



**Scheme 1.11 Reaction of epichlorohydrin with hydroxyl groups.**

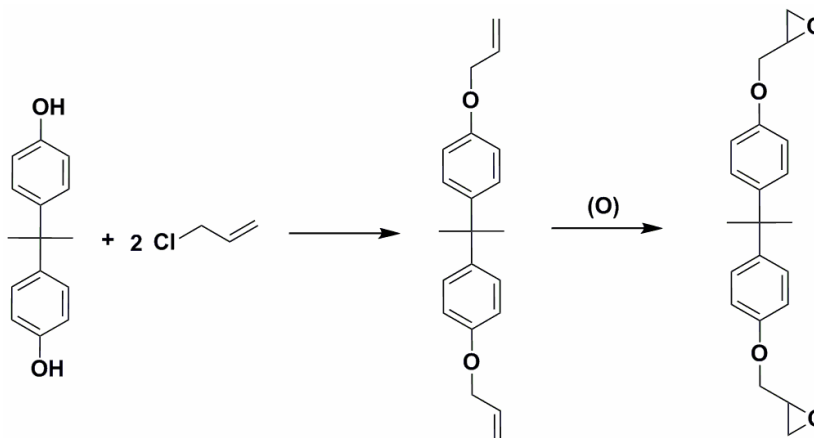
### 1.3.1.2 Synthesis of epoxy resins by epoxidation reaction

Epoxy resins based on epoxidized aliphatic or cycloaliphatic alkenes are produced by direct epoxidation of olefins by peracids<sup>112</sup> (**Scheme 1.12**)



**Scheme 1.12: Synthesis of epoxy resins by epoxidation reaction**

The advantage of the method lies in the synthesis of pure epoxies (n=0). Pure diglycidyl ether of bisphenol A (**Scheme 1.13**) is a solid melting at 43 °C.



Scheme 1.13 : Synthesis of diglycidyl ether of bisphenol-A

### 1.3.2 Commercial types of basic epoxies

Today, the most widely used epoxy resin is produced from bisphenol A, and epichlorohydrin, known as conventional or DGEBA resin (structure A, Figure 1.4). These diglycidyl ethers of bisphenol A (and their higher molecular weight homologues) account for about 80-85 % of the total worldwide epoxy consumption. The other types of basic epoxies are brominated resins (structure B), cycloaliphatic resins (structure C), novolac resins (structure D) and phenoxy resins (structure E).

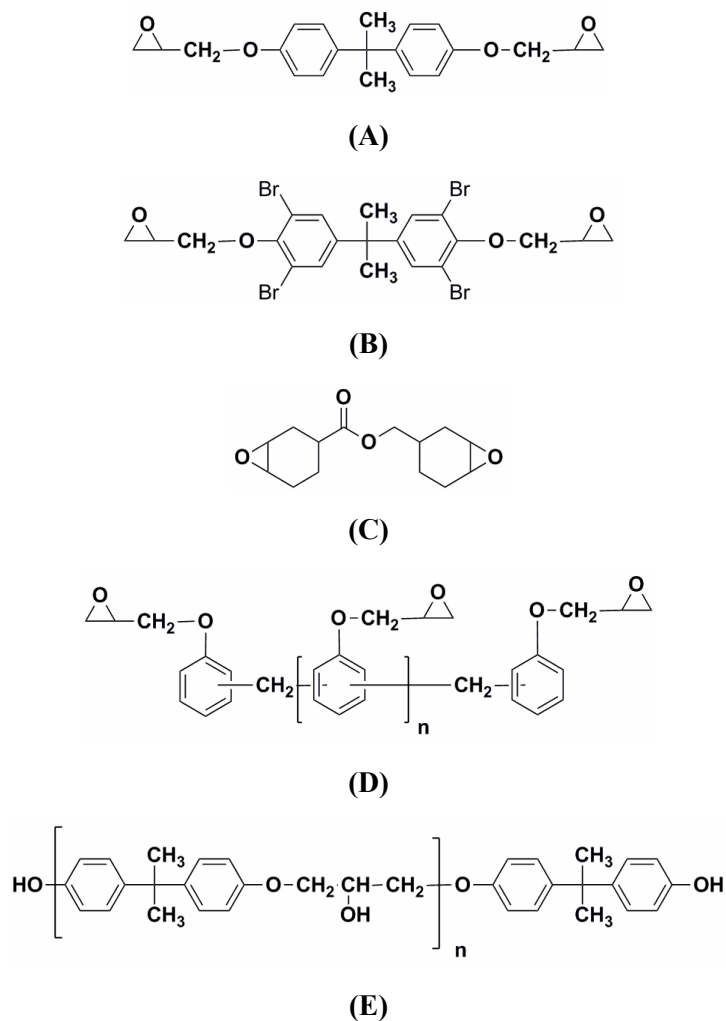
Brominated epoxies are ignition-resistant compounds and are used extensively in the production of laminates for printed circuit boards. Novolac epoxies include primarily polyglycidyl ethers of phenol-formaldehyde or cresol-formaldehyde resins. When cured, these epoxies have better high temperature properties than conventional epoxy resins. Cycloaliphatic epoxy resins are usually non-glycidyl ethers which exhibit higher heat distortion temperatures, lower dielectric constants, and excellent weatherability. Phenoxy resins are higher-molecular-weight polymers derived from epichlorohydrin and bisphenol A lacking terminal epoxy groups.

### 1.3.3 Characterization of uncured epoxies

Epoxies often contain isomers, oligomers, and other minor constituents. Liquid/solid epoxy resins are mainly characterized by epoxy content, viscosity, color, density, hydrolyzable chloride, and volatile content<sup>93,98,113</sup>. In addition, GPC, HPLC<sup>98,114-116</sup>, IR<sup>117</sup>, NMR<sup>118</sup>, etc., are performed to determine molecular weight, oligomer composition, functional groups, and impurities.

The epoxy content of liquid resins is frequently expressed as *epoxide equivalent weight (EEW)* or *weight per epoxide (WPE)*, which is defined as the weight in grams that contains 1 g equivalent of epoxide. A common chemical method of analysis for epoxy content is the titration of the epoxide ring by hydrochloric acid-pyridine in methanol<sup>93, 119, 120</sup>.





**Figure 1.4 : Commercial types of basic epoxies.**

The viscosity of epoxy resins is another important characteristic affecting handling, processing, and application of formulations. For example, high viscosity epoxy resins impede good mixing with curing agents, resulting in inhomogeneous mixtures, incomplete network formation, and poor performance. On the other hand, too low viscosity would affect application characteristics such as coverage and appearance. The viscosity of epoxy resins is typically determined using Cannon-Fenske capillary viscometer or a Brookfield viscometer.

The presence of ionic hydrolyzable chlorides (HyCl) and total chlorides has been observed to affect electrical properties of epoxy molding compounds used in semiconductor encapsulation. These are determined by dehydrochlorination with potassium hydroxide solution under reflux conditions and potentiometric titration of the chloride liberated by silver nitrate. The solvent(s) employed and reflux conditions can influence the extent of dehydrochlorination and give different results.<sup>93, 98</sup>

### 1.3.4 Curing of epoxy resins

With the exception of the very high molecular weight phenoxy resins and epoxy-based thermoplastic resins, almost all epoxy resins are converted into solid, infusible, and insoluble three-dimensional thermoset networks by curing with appropriate cross-linkers (also called as hardeners or curing agents). The selection of appropriate curing agent depends on the requirements of the application process techniques, pot-life, cure conditions, and ultimate physical properties. Epoxy resins contain two chemically reactive functional groups: epoxy and hydroxyl. Low molecular weight epoxy resins are considered difunctional epoxy monomers or prepolymers and are mostly cured *via* the epoxy group. However, as the molecular weight of epoxy resins increases, the epoxy content decreases, whereas the hydroxyl content increases. High molecular weight epoxy resins can cross-link *via* reactions with both the epoxy and hydroxyl functionalities, depending on the choice of curing agent and curing conditions.

The reaction of the epoxy group involves the opening of the oxirane ring and formation of linear C-O bonds. This feature accounts for the low shrinkage and good dimensional stability of cured epoxies. It is the unique ability of the strained epoxy ring to react with a wide variety of reactants under many diverse conditions that gives epoxies their versatility<sup>121</sup>. It has been postulated that the highly strained bond angles, along with the polarization of the C-C and C-O bonds account for the high reactivity of the epoxide. Detailed discussions on the probable electronic configurations, molecular orbitals, bond angles, and reactivity of the epoxy ring are available in the literature<sup>122</sup>. The electron-deficient carbon can undergo nucleophilic reactions, whereas the electron-rich oxygen can react with electrophiles.

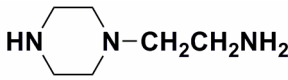
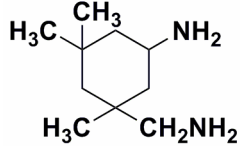
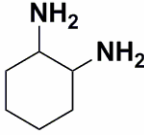
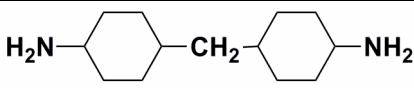
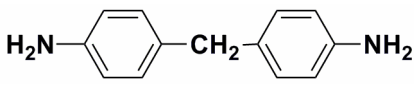
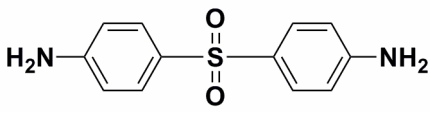
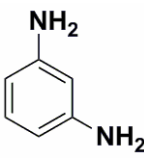
#### 1.3.4.1 Curing agents for epoxy curing

Besides affecting viscosity and reactivity of the formulation, curing agents determine both the types of chemical bonds formed and the degree of crosslinking that will occur. These, in turn, affect the chemical resistance, electrical properties, mechanical properties, and heat resistance of the cured thermosets. Curing agents are either catalytic or coreactive. A catalytic curing agent functions as an initiator for epoxy resin homopolymerization or as an accelerator for other curing agents, whereas the coreactive curing agent acts as a comonomer in the polymerization process. The majority of epoxy curing occurs by nucleophilic mechanisms. The most important groups of coreactive curing agents are those with active hydrogen atoms, *e.g.*, primary and secondary amines, anhydrides, phenols, thiols, etc., Lewis acids, *e.g.*, boron trihalides, and Lewis bases, *e.g.*, tertiary amines, ionic liquids initiate catalytic cure.

Primary and secondary amines and their adducts are the most widely used curing agents. **Table 1.6** lists some commercial curing agents bearing amine functionality. It has been reported that primary amines react much faster than secondary amines. In general, the reactivity

of amines towards aromatic glycidyl ethers follows nucleophilicity order; aliphatic amines > cycloaliphatic amines > aromatic amines.<sup>123</sup> Aliphatic amines cure aromatic glycidyl ethers at room temperature without accelerators, whereas aromatic amines require elevated temperature.<sup>124</sup>

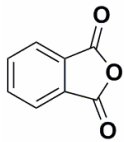
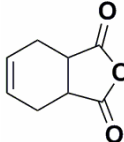
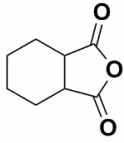
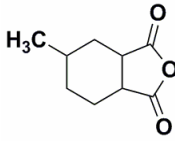
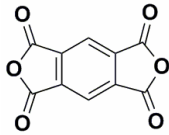
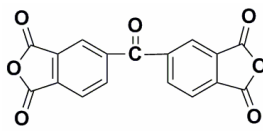
**Table 1.6: Commercial amine functional curing agents used for epoxy curing**

Structure	Name
$\text{NH}_2\text{CH}_2\text{CH}_2\text{NHCH}_2\text{CH}_2\text{NH}_2$	Diethylenetriamine (DETA)
$\text{NH}_2\text{CH}_2\text{CH}_2\text{NHCH}_2\text{CH}_2\text{NHCH}_2\text{CH}_2\text{NH}_2$	Triethylenetetraamine (TETA)
$\begin{array}{c} \text{CH}_3 \qquad \qquad \text{CH}_3 \\   \qquad \qquad \qquad   \\ \text{NH}_2\text{CHCH}_2(\text{OCH}_2\text{CH})_n\text{NH}_2 \end{array}$	Poly(oxypropylene diamine)
	Aminoethylpiperazine (AEP)
	Isophorone diamine (IPDA)
	1,2-Diaminocyclohexane (DACH)
	Bis(4-aminocyclohexyl)methane (PACM)
	4,4'-Diaminodiphenylmethane (MDA, DDM)
	4,4'-Diaminodiphenylsulfone (DDS)
	<i>meta</i> -Phenylenediamine (MPD)

Anhydrides are some of the very first epoxy curing agents used, and remain a major class of curing agents used in heat-cured structural composites and electrical encapsulation. Epoxy-anhydride systems exhibit low viscosity and long pot-life, low exothermic heats of reaction, and little shrinkage when cured at elevated temperatures<sup>125</sup>. The low exothermic heat

generation is a unique attribute of anhydrides, making suitable for uses in large mass epoxy cures. Curing is slow at temperatures below 200 °C and is often catalysed by Lewis bases or acids. Post-cure is often needed to develop optimum properties. Cured epoxy–anhydride systems exhibit excellent thermal, mechanical, and electrical properties. Anhydrides are the widely employed curing agents for cycloaliphatic and epoxidized olefin resins. Numerous structurally different anhydrides can be used as epoxy curing agents. The most important commercial anhydrides are listed in **Table 1.7**.

**Table 1.7: Anhydride functional curing agents used for epoxy curing**

Structure	Name	Structure	Name
	Phthalic anhydride (PA)		Tetrahydrophthalic anhydride (THPA)
	Hexahydrophthalic anhydride (HHPA)		Methylhexahydrophthalic anhydride (MHHPA)
	Pyromellitic dianhydride (PMDA)		Benzophenone-3,3',4,4'-tetracarboxylic dianhydride (BTDA)

Melamine–formaldehyde, urea–formaldehyde, and phenol–formaldehyde resins react with hydroxyl groups of high molecular weight epoxy resins to afford cross-linked networks.<sup>126</sup>

Polysulfide and polymercaptan compounds which contain terminal thiols react very slowly with epoxy resins at ambient temperature. However, when converted by a tertiary amine to a mercaptide ion, they are extremely reactive<sup>127</sup>.

Cyclic amidine curing agents are typically used in epoxy powder coating formulations and in decorative epoxy–polyester hybrid powder coatings.<sup>111</sup>

Isocyanates react with epoxy resins *via* epoxy group to produce an oxazolidone structure<sup>128,129</sup> or with a hydroxyl group to yield a urethane linkage.

Cyanate esters can be used to cure epoxy resins to produce highly cross-linked thermosets with high modulus and excellent thermal, electrical, and chemical resistance properties. Cure involves oxazoline formation catalysed by metal carboxylates in addition to homopolymerization of both cyanate ester and epoxy<sup>44</sup>.

The catalytic curing agents are a group of compounds that promote epoxy reactions without being consumed in the process. The frequently employed catalysts for epoxy homopolymerization are imidazoles<sup>130</sup>, substituted ureas<sup>131,132</sup>, tertiary amines<sup>133</sup>, quaternary phosphonium salts<sup>134</sup>, boron trihalide<sup>135</sup>, etc., Photoinitiators used for epoxy curing include aryldiazonium salts ( $\text{ArN}_2^+\text{X}^-$ ), diaryliodonium salts ( $\text{Ar}_2\text{I}^+\text{X}^-$ ), and onium salts of Group VIA elements, especially salts of positively charged sulfur ( $\text{Ar}_3\text{S}^+\text{X}^-$ )<sup>136,137</sup>.

#### 1.3.4.2 Epoxy curing kinetics

The epoxy curing process is an important factor deciding performance of cured epoxy network. Consequently, it is imperative to understand the curing process and its kinetics to design the proper cure schedule to obtain optimum network structure and performance. A number of articles and reports on curing kinetics of epoxies are available in the literature<sup>112,123, 138-157</sup>.

In the early stages of cure prior to gelation or vitrification, the epoxy curing reactions are kinetically controlled. In the region between gelation and vitrification (rubber region) the reaction can range from kinetic to diffusion controlled.<sup>143, 144, 147</sup> As curing proceeds, the viscosity of the system increases as a result of increasing molecular weight, and the reaction becomes diffusion-controlled and eventually is quenched as the material vitrifies<sup>144</sup>. After quenching, the cure conversion can be increased by raising the temperature. The time-temperature-transformation (TTT) diagram is useful in understanding the cure kinetics, conversion, gelation, and vitrification of the curing thermoset<sup>144, 147, 152</sup>. Understanding the gelation and vitrification characteristics of an epoxy/curing agent system is critical in developing the proper cure schedule / process to achieve optimum performance.

Curing of epoxy resins using aromatic and aliphatic amines as curing agents proceeds with fairly low activation energy of 50–60 kJ/mol.<sup>151-157</sup>

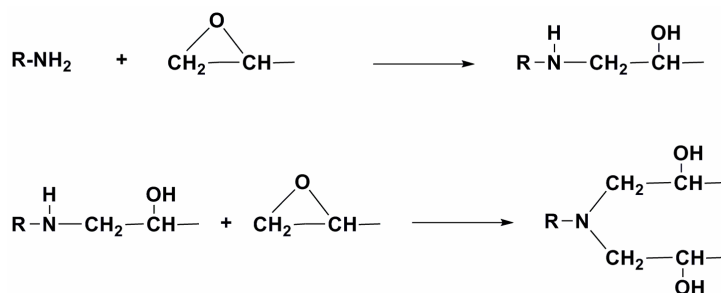
In the literature, thermal curing kinetics of epoxy-amine system has been explained by two main forms; empirical and mechanistic model. Kamal *et. al.*,<sup>142</sup> suggested the semi-empirical equation by considering autocatalytic feature of epoxy-amine reaction:

$$\frac{dx}{dt} = (k_1 + k_2x^m)(1-x)^n \quad (3)$$

where ‘m’ and ‘n’ exponents represent the order of reaction. The reaction rate constants  $k_1$  and  $k_2$  depend on the temperature according to Arrhenius behaviour.

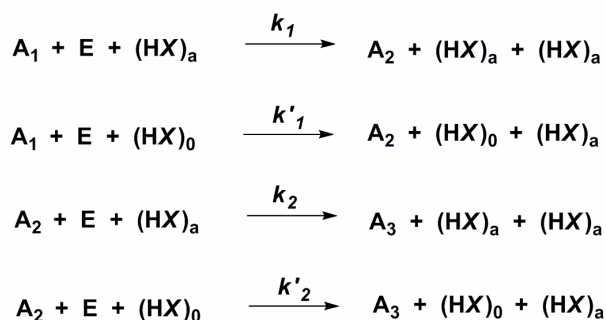
The second form; mechanistic model is based on mechanistic considerations and has been reviewed by several investigators<sup>123,149,152,154,155</sup>. The curing of epoxy with primary amine involves two principal reactions; the reaction between primary amine hydrogen and epoxy to form secondary amine, and the reaction between secondary amine hydrogen and epoxy to form

tertiary amine<sup>123</sup>(**Scheme 1.14**). Both reactions are found to be catalysed by the hydroxyl groups formed during the reaction.



**Scheme 1.14 : Reaction of epoxy group with amine functionality**

Horie *et. al.*<sup>123</sup>. derived the following scheme (**Scheme 1.15**) to describe the overall kinetics of the epoxide reaction with primary amine, taking into account the autocatalytic action of the hydroxyl groups generated during the reaction and assuming that some catalyst or impurity is initially present in the system:



**Scheme 1.15 : Various reaction pathways for the reaction of epoxy and amine**

where  $\text{A}_1$ ,  $\text{A}_2$  and  $\text{A}_3$  are primary, secondary and tertiary amine, respectively; E is the epoxy group;  $(\text{HX})_a$  is the pendant hydroxyl groups on the backbone of the reaction products; and  $(\text{HX})_0$  is the initial catalyst or impurities. The rate constants for the individual reactions are defined in the scheme.  $(\text{HX})_a$  and  $(\text{HX})_0$  are assumed to act as catalysts with no net consumption by side reactions.

Considering these reactions, Gillham *et. al.*<sup>149</sup> derived an equation expressing the reaction rate for an initial stoichiometric mixture of epoxy and amine assuming equal reactivity of all amine hydrogens.

$$\frac{dx}{dt} = k(1-x)^2(x+B) \quad (4)$$

where  $k = k_1 e_0^2 / 2$ ,  $B = k'_1 c_0 / k_1 e_0$ , and  $e_0$ ,  $c_0$  are the initial concentrations of epoxide groups and  $(\text{HX})_0$ , respectively. Using the relation (4), the authors described reaction kinetics of epoxy-amine system.<sup>149</sup>

### 1.3.5 Structure-property relationship in epoxy resins.

The cured epoxy system derives its properties mostly from a combination of cross-link density, monomer/hardener structure and the curing process. The factors determining the structure of cured resins and affecting the physical and mechanical properties are:

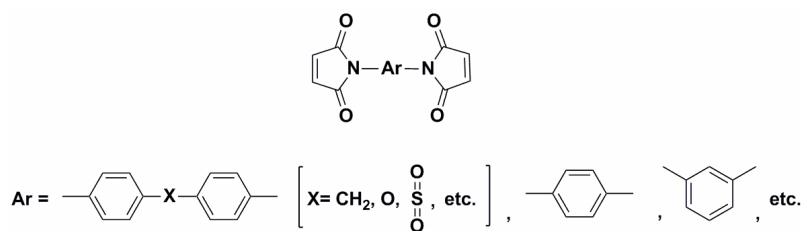
1. Curing mechanism: type of functional groups of hardeners.
2. Number of functional groups in resins and hardeners: density of crosslinking.
3. Molar ratio of resin and hardener: density of crosslinking.
4. Molecular structure of bridges between functional groups in resins and hardeners.
5. Degree of curing, or curing conditions.

There is a large body of specific structure/property relationship knowledge in the epoxy industry and literature, but only a few systematic treatments are available<sup>158-167</sup>. Most of the epoxy resin prepolymers in industrial use are diglycidyl ethers having two epoxy groups per molecule; a few tens of other epoxy resin prepolymers are also available in the market. On the other hand, more than one hundred hardeners are known. Therefore, the number of combinations of resins and hardeners is very high and, accordingly, it is hardly possible to describe all the properties (thermal properties, electrical properties, moisture absorption, mechanical properties, etc) of the cured resins with many different structures. The curing temperature and process strongly influence cross-link density, molecular architecture, network morphology, residual stress, and the ultimate performance<sup>149, 152, 157, 168</sup>.

### 1.4 Bismaleimides

Bismaleimide (BMI) resins are addition type polyimide resins produced from bismaleimide bearing reactive end cappers<sup>169</sup>.

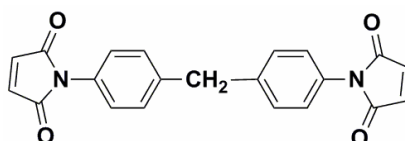
Rhone Poulenc deserves the honour of having recognized the potential of bismaleimides as building blocks for temperature resistant addition polyimides. Within a period of only ten years between 1964 and 1974, the research in the area of curable imide oligomers produced cure concepts through maleimide-, nadimide- and ethynyl-terminal groups. The general structure of a bismaleimide building block is shown in **Figure 1.5**.



**Figure 1.5: General structure of bismaleimides.**

Bismaleimides cure thermally through addition reaction to produce thermoset resins exhibiting high thermal and oxidative stability, good physical and mechanical properties, and low moisture absorption<sup>170-172</sup>. They have become one of the important high-performance thermosetting engineering plastics in various applications, such as multilayer printed circuit boards<sup>173-176</sup>, advanced composites for aerospace industries<sup>177,178</sup>, structural adhesives and potting resins.

The bismaleimide prepared from 4,4'-diaminodiphenylmethane (**Figure 1.6**) has been the most widely used because of its high melt flow, relatively low curing temperature, and especially because of the commercial availability at low cost.



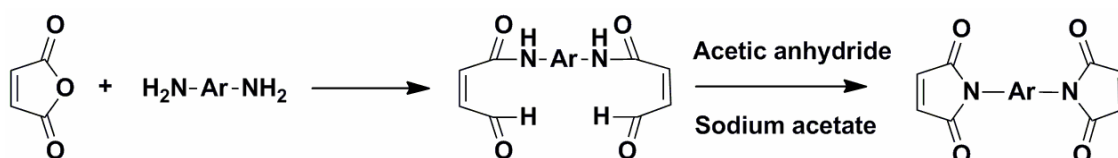
**Figure 1.6: Structure of 1,1-bis(4-maleimidophenyl)methane**

#### 1.4.1 Synthesis of bismaleimides.

The preparation of maleimide monomers was reported way back in 1948 by Searle<sup>179,180</sup>. In 1964, a patent was granted to Rhone Poulenc, France, for crosslinked polyimides obtained through the homo- and/or co-polymerization of bismaleimides<sup>181</sup>. A number of bismaleimide resins based on this chemical concept became commercially available through Rhone Poulenc and were promoted for their application in printed circuit boards and molding compounds.

##### 1.4.1.1 Synthesis of bismaleimides from diamines.

A standard synthesis for *N,N'*-arylene bismaleimides is the cyclodehydration of diamine and maleic anhydride in the presence of a catalyst<sup>182</sup> (**Scheme 1.16**)

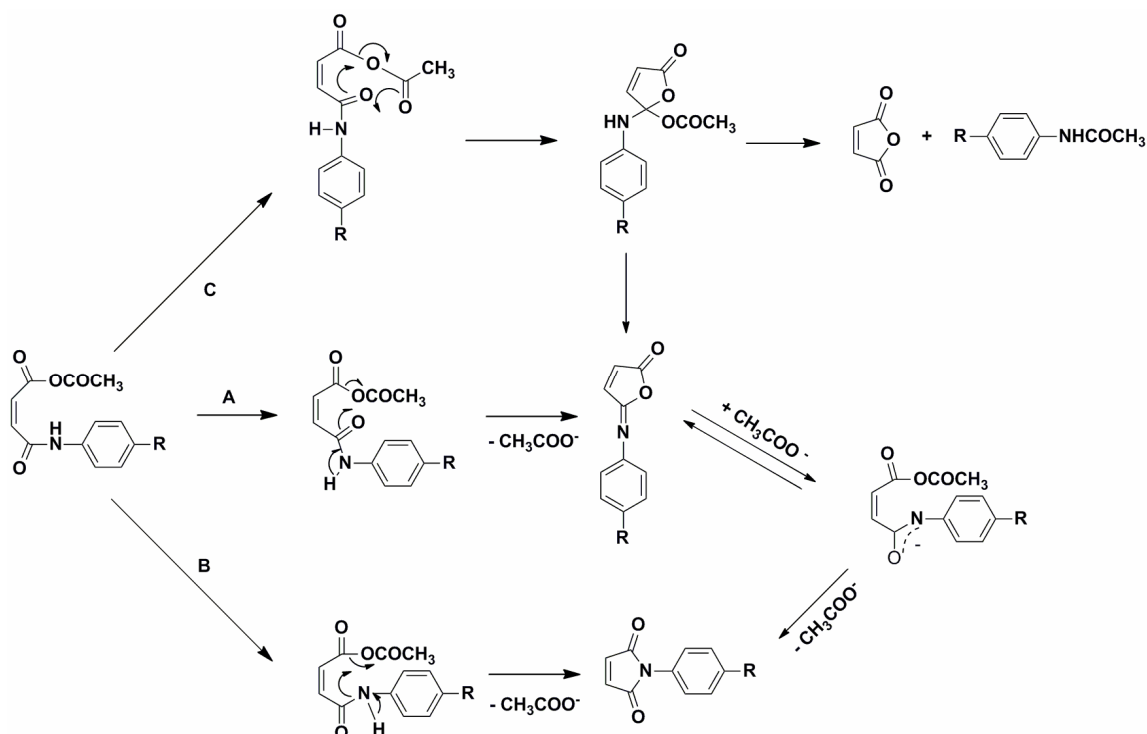


**Scheme 1.16: Synthesis of bismaleimides from diamines**

The yield of pure recrystallized BMI is usually 65-75 % when sodium acetate is employed as a catalyst. The side reactions which lead to the formation of isoimides, acetanilides, maleimide-acetic acid adducts and products with mixed functionalities are responsible for the relatively low yield of pure bismaleimide (**Scheme 1.17**). The cyclodehydration conditions such as temperature, type and concentration of catalyst and solvent influence the yield of these by-products<sup>183</sup>. It is well documented that the isoimide is the kinetically favoured product and that isomerization yields the thermodynamically stable imide



when sodium acetate is used as the catalyst. High catalyst concentrations provide maleimides with low isoimide impurity. The mechanism by which the chemical imidization is thought to occur is shown in **Scheme 1.17**.



**Scheme 1.17: Base -catalysed cyclodehydration of *N,N'*-bismaleamic acid**

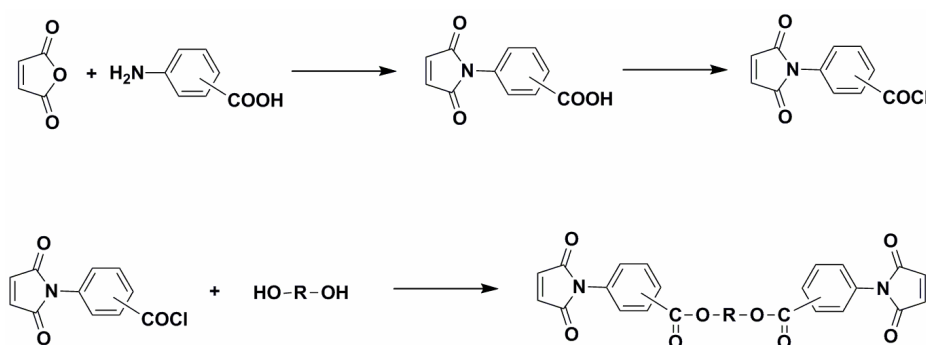
The first step in the dehydration reaction may be formation of the acetic acid-maleamic acid mixed anhydride. This species could lose acetic acid in one of the two ways. Path A involves participation by the neighboring amide carbonyl oxygen to eject acetate ion with simultaneous or subsequent loss of proton on nitrogen to form the isoimide. Path B involves loss of acetate ion assisted by the attack of nitrogen with simultaneous or subsequent loss of the proton on nitrogen to form the imide. If the cyclodehydration is executed in acetic anhydride in the absence of the base catalyst, isoimide is the main reaction product. At high temperatures with low catalyst concentration the formation of acetanilides is favored. Maleic anhydride and acetanilides may be formed directly from the mixed anhydride by an initial attack of the nitrogen on the acetate carbonyl, but this process would involve a seven membered ring transition state. Another base catalyzed side reaction is the formation of Michael adducts between the maleimide and the acetic acid present in the reaction mixture. In general, both the acetanilides and the Michael adducts are favored when high catalyst concentrations and high temperatures are used for the synthesis.

It has always been the target to optimize the synthetic conditions in order to maximize the yield of pure bismaleimide by minimizing the side reactions. Low cyclization temperatures

were found to be advantageous and could be achieved with catalysts such as tertiary amines<sup>184</sup> (in combination with metal salts), cobalt acetate<sup>185</sup>, triethyl amine<sup>186</sup>, and sodium carbonate<sup>187</sup>. Because of the various side reactions of the cyclodehydration, high cost for solvents, catalyst and cyclodehydration agent, researchers have been looking at more economic ways to manufacture bismaleimides. Efforts have been directed towards a catalytic cyclodehydration process *via* azeotropic distillation to avoid undesirable byproducts and to achieve improved yield of pure bismaleimide. The use of Lewis acid/base salts based on *para*-toluene sulfonic acid, sulfuric acid or trifluoroacetic acid and dimethylformamide (DMF), 1-methyl-2-pyrrolidinone (NMP), etc., as bases provided high yields of high purity bismaleimide<sup>188</sup>. Dimethyldialkylammoniummethane sulfonate is also claimed as a useful catalyst<sup>189</sup>. Japanese workers have developed a process for N-substituted maleimides which comprises heating maleic anhydride and aromatic or aliphatic primary diamine in the presence of an ion exchange resin in an organic solvent at 50-160°C to effect cyclodehydration<sup>190</sup>.

#### 1.4.1.2 Synthesis of bismaleimides from acid / acid chloride

This method of bismaleimide synthesis is based on the reaction of a functionalized monomaleimide such as maleimido benzoic acid or its acid halide with a polyfunctional monomer (dihydroxy compounds) or oligomer<sup>191-194</sup> (**Scheme 1.18**).



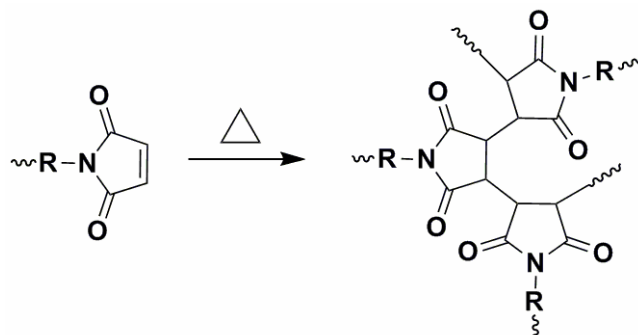
**Scheme 1.18 : Synthesis of bismaleimide by acid chloride route.**

The method is of choice for synthesizing bismaleimides with long flexible / rigid / polymeric backbone.

#### 1.4.2 Curing of bismaleimides

The maleimido group can undergo a variety of chemical reactions. The reactivity of the double bond is a consequence of the electron withdrawing nature of the two adjacent carbonyl groups. The double bond is susceptible to homo- and co-polymerizations. The homopolymerization (curing) may be induced thermally or by free radicals or anions to give a network with high cross-link density *via* addition reaction<sup>195,196</sup> (**Scheme 1.19**).

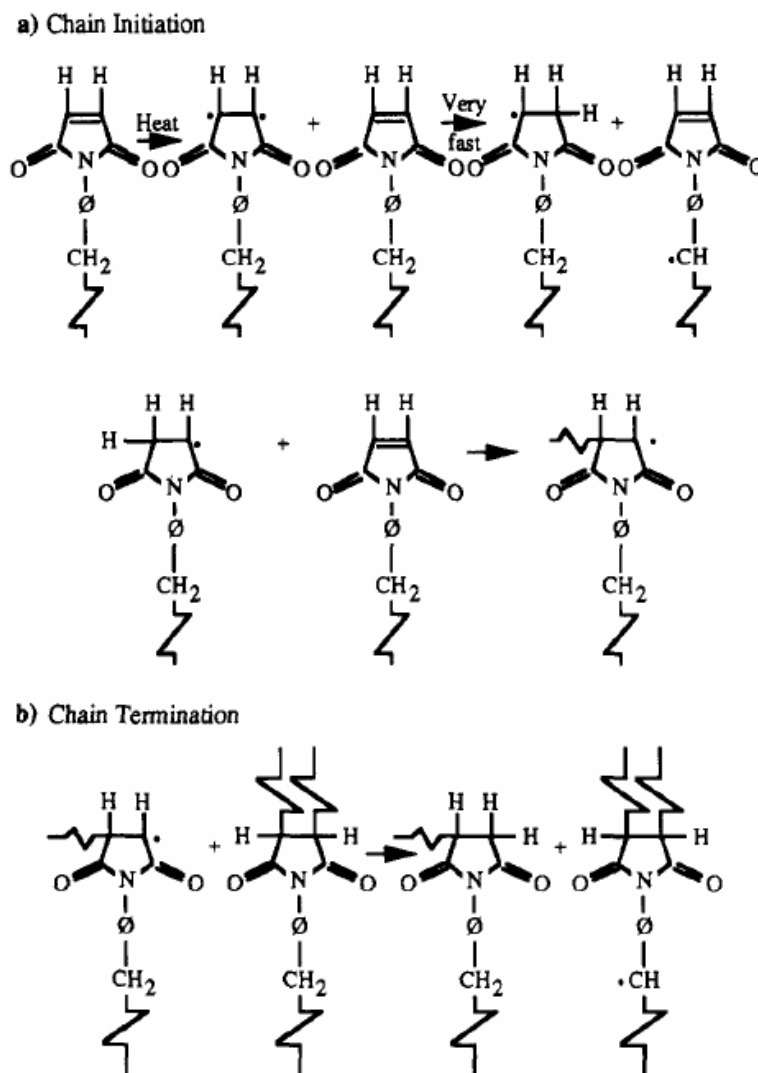
The nucleophiles such as primary and secondary amines, aminobenzoic hydrazides, phenates, thiophenates, carboxylates, etc. can be copolymerized *via* classical Michael addition mechanism<sup>197,198</sup>. Bismaleimides undergo rapid and exothermic polymerization with hydrogen sulphide and polythiols<sup>199,200</sup>.



**Scheme 1.19: Homopolymerization of bismaleimides *via* addition reaction**

An important chemical reaction of the maleimide group is the “ENE” reaction with allylphenyl compounds<sup>201</sup>. The most attractive comonomer of this family is *o,o'*-diallyl bisphenol-A (DABA) particularly when tough bismaleimide resins are desired<sup>202</sup>. In the following section, homopolymerization of BMIs will mainly be discussed.

Brown *et. al.*<sup>203-205</sup> proposed a detailed mechanism for the polymerization of maleimides. The homopolymerization involves first an initiation or priming step in which there is thermally induced rupture of the double bond with the formation of biradical (**Scheme 1.20**). The biradical then rapidly adds to another monomer, furnishing two additional radicals, one active and the other inactive. The active radical adds to another monomer molecule, playing the role of reaction intermediate in the formation and growth of the network by radical polymerization.



Scheme 1.20 : Mechanism of bismaleimide curing

The maleimide group contains both donor and acceptor groups in the form of carbonyl and electrophilic double bond, respectively. Based on this, Hill *et.al.*<sup>206</sup> suggested a donor-acceptor mechanism for BMI curing. Initiation is much more likely to occur *via* a donor-acceptor complex with the resulting formation of two separate radicals (Scheme 1.21) that can then undergo propagation reactions.



Scheme 1.21: Donor-acceptor type mechanism

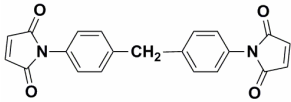
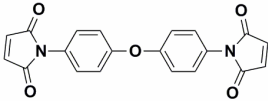
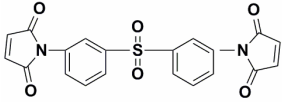
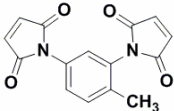
The curing of BMI depends essentially on the cure temperature and the duration of heat treatment. The cure of BMI is generally accompanied by higher cure onset temperature (>150°C). High temperature (> 250 °C) is needed to bring about effective cross-linking. The use of radical initiators is reported to reduce cure temperature<sup>207-210</sup>. Use of eutectic mixture of BMIs considerably lowers cure onset temperature<sup>211</sup>. The purity of BMI monomer has marked effects on curing. It has been shown that impurities (inhibitors) in bismaleimides considerably increase cure onset temperature<sup>212-214</sup>. It was observed that the chemical structure of the skeleton between the two terminal maleimide functionalities affects zones of reactivity of BMI systems. The presence of electron withdrawing groups along the backbone decreases the reactivity<sup>215</sup> while the presence of long chain doesn't exert a significant influence on the polymerization rate<sup>216</sup>. The steric effects also play a vital role in the cure rate. The presence of alkyl group (s) at *ortho* to reactive maleimide functionality reduces the reactivity mainly due to steric hindrance thereby resulting into increase in the cure onset temperature<sup>217, 218</sup>.

### 1.4.3 Cure Kinetics

Various spectroscopic techniques and model monomer systems have been used to study the cure of BMI system. Much of this research is aimed at investigating the single overall rate constant for the cure process. These investigations have utilized techniques like IR<sup>195,219</sup>, NMR<sup>217,218</sup> spectroscopy, DSC<sup>212-216,220-224</sup>, etc., to investigate kinetics of the cure process. The overall reaction rate of the polymerization is governed by (1) the reactivity of the maleic double bond and (2) by the mobility of the reactive sites in the system. The mobility of the reactive sites in the system is highly influenced by the viscosity of the medium and, finally, by the degree of cross-linking. In the beginning of the polymerization, the viscosity is low. With increasing conversions: the viscosity of the system increases rapidly and the mobility of the monomer molecules (and mobility of the reactive sites in the polymer) also will be hindered<sup>170,195</sup>.

The cure process of bismaleimides follows autocatalytic first order kinetics. **Table 1.8** summarizes activation energies for curing of some commercially available BMI monomers.

**Table 1.8 : Activation energies of curing of commercially available BMI monomers**

Bismaleimide	Activation Energy (kJ/mol)	Reference
	152	215
	77	221
	288 (Purity of BMI 95%)	223
	123 (Purity of BMI 99.6 %)	223
	137	215
	120	221
	104	221
	82	223

#### 1.4.4 Thermal properties of bismaleimides

The high crosslink density and the presence of rigid structures impart high Tg (>400 °C) to BMI resins<sup>195,207</sup>. The spacers play a major role in altering Tg of cured BMI resin. The introduction of aliphatic/flexible spacers is reported to act as effective diluent thereby reducing crosslink density (branching density) which reflects in decrease in Tg<sup>225</sup>. The Tg is also governed by cure conditions<sup>226</sup>. **Table 1.9** summarizes Tg of some cured BMIs.

**Table 1.9 : Glass transition temperature of cured bismaleimides**

Sr. No.	Bismaleimide	Tg (°C)	Reference
1		479	227
2		409 <sup>#</sup> 478 <sup>†</sup>	227 228
3		> 400 (n = 1) 395 (n = 2) 390 (n = 3) 375 (n = 4)	225
4		406 (n = 3) 402 (n = 5) 388 (n = 7)	229
5		435	227
6		283	227
7		445	227

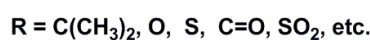
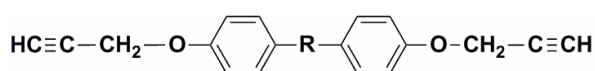
# Cured at 250 °C / 10 h.

† Cured at 300 °C / 3 h.

### 1.5 Propargyl-terminated resins

Acetylene-terminated monomers and polymers are gaining importance in view of the increased need for easily processable thermally stable polymers possessing improved performance under hot-wet conditions<sup>230</sup>. Their good attributes include; good thermal stability, low water absorption, good dielectric properties, low monomer sensitivity to boiling water, good solvent resistance and excellent physical and mechanical properties<sup>231</sup>. Such polymers with a properly designed backbone could potentially serve as matrices in carbon-carbon composites, electronics

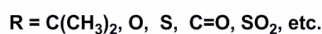
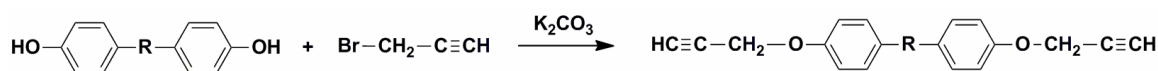
and optoelectronics and in various high-performance polymer composite structures for space applications<sup>232</sup>. Acetylene-terminated polymers were intensively studied as polymers offering promising applications in electronics and optoelectronics<sup>233,234</sup>. Acetylene-terminated monomers and polymers fall into two main categories, those terminated by arylacetylene and those by arylpropargyl-ether groups. Propargyl terminated resins (**Figure 1.7**) were proposed and evaluated as matrices for advanced polymeric composites. One of the key features of these systems is their ability to undergo curing through addition reaction of the acetylene groups, either linearly or *via* cyclization.



**Figure 1.7 : General structure of bispropargyl ethers**

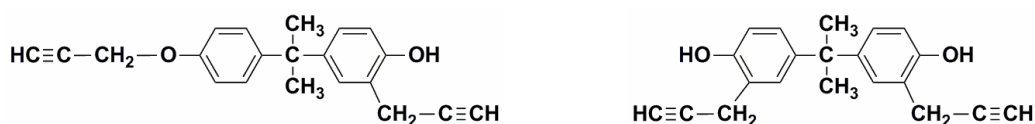
### 1.5.1 Synthesis of bispropargyl ethers

Hay *et. al.*<sup>235,236</sup> reported the synthesis of bispropargyl ethers of dihydric phenols using propargyl halides (e.g. propargyl bromide). (**Scheme 1.22**)



**Scheme 1.22 : Synthesis of bispropargyl ethers**

The use of aqueous sodium hydroxide is reported to reduce reaction time from 72 h to 2 h and the formation of side products, 3- and 3', 3'-propargylbisphenols *via* Claisen rearrangement<sup>237</sup> (**Figure 1.8**). The presence of these side products decrease the thermal stability and increase moisture absorption of the final thermoset. The use of phase transfer catalysts such as tetrabutylammonium bromide yields the product with high purity (> 99%) without side reactions<sup>238</sup>.

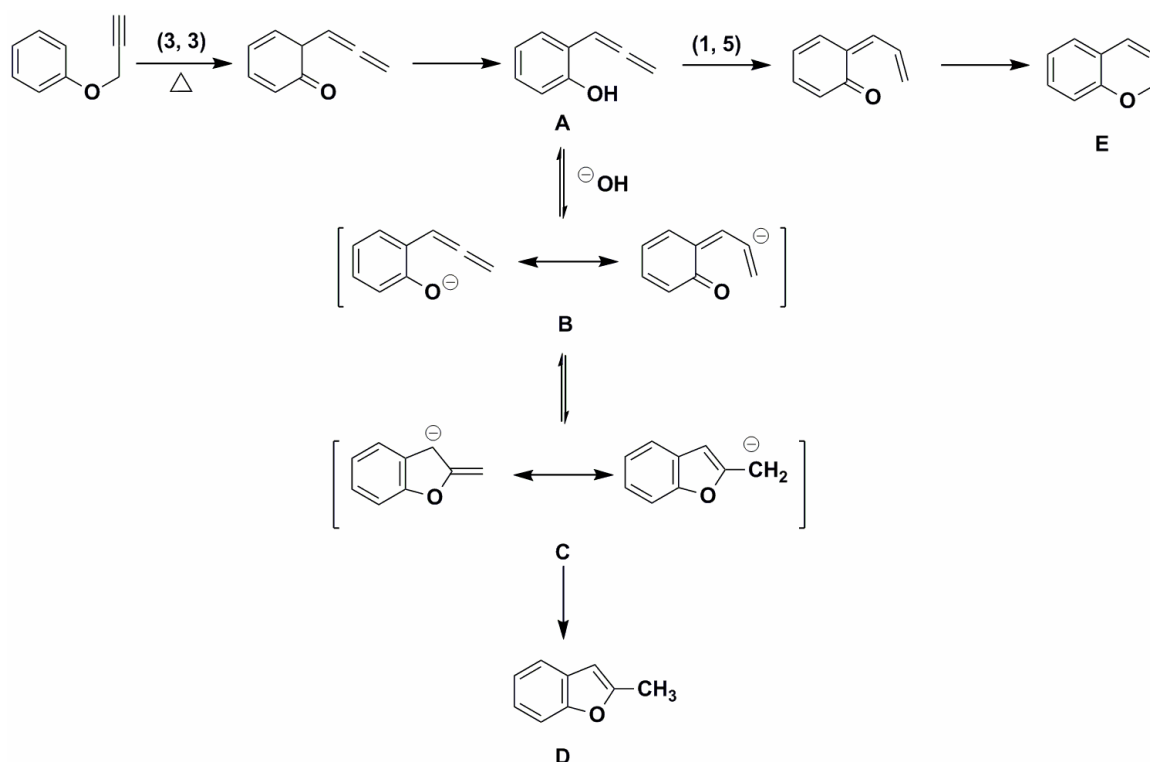


**Figure 1.8 : Structures of side products formed by Claisen rearrangement.**



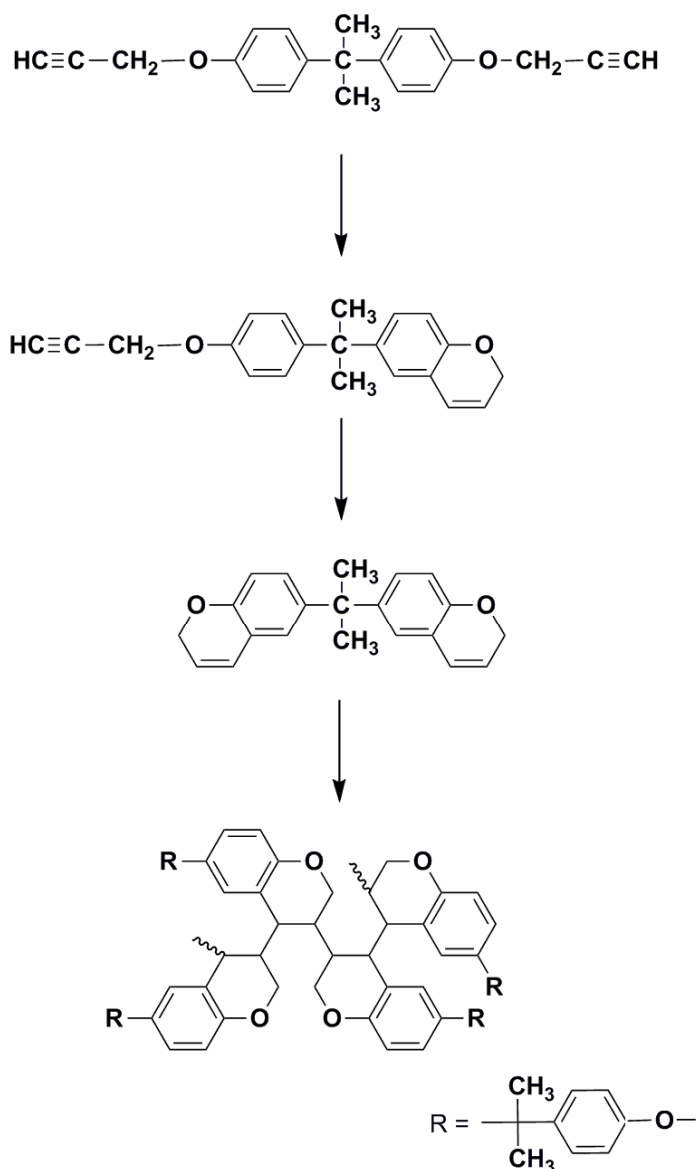
### 1.5.2 Curing of propargyl terminated resins

Polymerization of bispropargyl ethers involve initial Claisen rearrangement to 2-*H*-1-benzopyran (chromene) groups which subsequently polymerize<sup>239-242</sup>. Depending on the curing conditions, bispropargyl ethers yield either linear polymer or cured network *via* cyclotrimerization<sup>231,235,236,243-245</sup>. For conferring thermal stability, cyclotrimerization is preferred to linear polymerization. Tungsten- and molybdenum-based metathesis catalyst systems (*viz*;  $\text{WoCl}_4/\text{Me}_4\text{Sn}$ ,  $\text{MoOCl}_4/\text{Me}_4\text{Sn}$  and  $\text{MoCl}_5/\text{EtAlCl}_2$ ) are found to promote linear polymerization while cyclotrimerization is favored using cyclopentyl cobalt dicarbonyl catalyst<sup>246-248</sup>.



**Scheme 1.23 : Chromene formation *via* Claisen rearrangement**

The rearrangement carried out in solution gives rise to a mixture of chromene (E) and its polymer and some amount of methyl benzofuran (D *via* B and C) as a secondary product. Thus, bispropargyl ethers on uncatalysed thermal polymerization in bulk give crosslinked bichromenes. The mechanism of polymerization (**Scheme 1.24**), was established by NMR spectroscopic studies<sup>240</sup>.



**Scheme 1.24 : Curing reaction of bispropargyl ethers.**

The Claisen rearrangement and the subsequent polymerization are so exothermic that curing has to be carried out under controlled conditions, with a slow phase. B-staging of the resin is possible at 185 °C. B-staging also helps to avoid the otherwise excessive cure shrinkage (10–12%). The shrinkage of the B-staged material to the final network is below 1%. The final curing of propargyl resin is normally carried out at high temperature (typical case >200 °C/4 h). The post curing is carried out at > 260 °C<sup>230</sup>.

### 1.5.3 Kinetics of bispropargyl ether curing

Nair *et.al.*,<sup>249-251</sup> studied the kinetics of uncatalysed curing of various bispropargyl ethers (Table 1.10) using DSC.

The non-isothermal kinetic analysis of the cure reaction using four integral methods revealed that the presence of an electron-withdrawing group did not favor the cyclization reaction leading to formation of chromene, which precedes the polymerization, and is in agreement with the proposed polymerization mechanism. The higher activation energy of bispropargyl ethers (**Table 1.10, Sr. No. 2 and 3**) was co-related with the electron withdrawing nature of carbonyl and sulfone groups, respectively.

**Table 1.10: Activation energies of curing of bispropargyl ethers.**

Sr.No.	Bispropargyl ethers	Activation Energy (kJ/mol)	Reference
1.		153	249
2.		171	249
3.		213	249

### 1.6 Applications of cyanate ester resins, epoxy resins and bismaleimides.

Cyanate ester resins, epoxy resin, bismaleimides, propargyl-terminated resins possess high thermal and oxidative stability, good physical and mechanical properties, good dielectric properties with lower moisture absorption. The set of such properties make these a resin of choice for various applications. These applications are broadly categorized in **Table 1.11**.

**Table 1.11 : Applications of thermosetting resins**

<b>Thermoset</b>	<b>Applications</b>		<b>Reference</b>
<b>Cyanate Ester Resins</b>	<b>Aerospace</b>	Primary and secondary structures in military aircraft, radome applications, and satellite applications.	43 - 45, 252-254
	<b>Electronics</b>	In the microelectronics industry for manufacturing high density, high speed multi-layer boards. In photonics, as optical wave guides, and in nonlinear optics	43,45, 88, 91, 255, 256
	<b>Adhesion</b>	In various formulations for adhesion, structural film adhesives for microwave applications.	88, 257,258
	<b>Miscellaneous</b>	As heat resistant photoresists , in thin films, foams, friction materials with improved antifade properties as binder for rare earth magnetic powders, wave guides	259-264
<b>Epoxy Resins</b>	<b>Coatings</b>	Automotive primers in marine and industrial maintenance coatings, and metal container interior coatings.	112, 265- 267
	<b>Structural</b>	As electrical laminates for printed circuit boards, fiber-reinforced composites; manufacturing of automotive, aerospace, electrical, industrial, sports/recreation equipments. Engineering/structural adhesive in many industries including aerospace, automotive, construction, electrical/electronic, transportation, dental, and consumer	98, 99160, 161, 268- 276.
	<b>Civil Engineering, Flooring, and Construction</b>	Flooring for walk-in freezers, coolers, kitchens, and restaurants, electronics manufacturing plants, bridge expansion joints and to repair concrete cracks	277-279
	<b>Inks and Resists</b>	lithographic and flexographic inks followed by electronic inks and resists.	280
<b>Bismaleimides</b>	Multilayer printed circuit boards, advanced composites for aerospace industries, structural adhesives.		173-178

## 1.7 Outlook

Cyanate ester system has emerged as a new generation of thermosetting polymer, encompassing several characteristics required of an ideal high performance matrix. The salient feature of addition curing through cyclotrimerization without any volatile evolution is highly desired for their use in void-free composites. A literature survey revealed that CEs have the added advantages of attractive physical, electrical and mechanical properties. This system also shows much lower out-gassing and exhibit higher heat tolerance. Amongst various CEs, BPACN has penetrated well into the market due to its ease of synthesis, purification and storage. The attractive physical, mechanical and processing characteristics of cyanate systems predict that the coming years will witness their expansion as the matrix of choice in many critical engineering areas as this single system answers the majority of the serious problems faced by many of the other polymer matrices.

Epoxy resins due to their unique features like excellent mechanical strength and toughness; outstanding chemical, moisture, and corrosion resistance; good thermal, adhesive, and electrical properties; no volatiles emission and low shrinkage upon cure; and dimensional stability have been servicing many areas since more than a century. The capability of the highly strained epoxy ring to react with a wide variety of curing agents under diverse conditions and temperatures adds additional versatility. With a massive list of available epoxies and number of possible new monomers, the system is expected to satisfy the need for better and better performance for many more years to come.

Bismaleimides, as a class of addition-type polyimides were extensively investigated in late 1960s to furnish the increasing need of materials for high performance, high temperature resistant aerospace structural composite applications. Because of their easy availability, low price and outstanding thermomechanical and flammability behavior at elevated temperatures in the finally cured state, BMIs turned out to be a popular system. The resin formulations of bismaleimides derived from aromatic diamino compounds were used for castings, for prepregging and glass-fabric laminate fabrication for filament winding operations. However toughness and processing improvement needs more attention.

Propargyl terminated resins would be potential competitors for epoxy resins for composites, adhesives and coatings and electronic applications after overcoming the problems associated with processing.

## References:

1. Shimp, D.A.; Christenson, J.R.; Ising, S.J. *Int. SAMPE Symp. Exhibit.* **1989**, 34, 222.
2. Graver, R.B. In *International Encyclopedia of Composites*. Lee, S.M. ED **1990**, VCH, Glasgow. Vol. 1, p. 548.
3. Grigat, E.; Putter, R. (Bayer AG) *German Patent* 1,195,764 **1963**.
4. Cloez, S. *Acad. Sci.* **1857**, 44, 482.
5. Groving, N.; Holm, A. *Acta. Chem. Scand.* **1965**, 19, 1768.
6. Pankratov, V.A.; Vinogradova, S.V.; Korshak, V.V. *Russ. Chem. Rev.* **1977**, 46, 278.
7. Grigat, E.; Putter, R. *Chem.Ber.* **1964**, 97, 3012.
8. Grigat, E.; Putter, R. *Angew.Chem.Int.Ed.* **1967**, 6, 206.
9. Grigat, E.; Putter, R. (Bayer AG) *U.S.Patent* 4,028,393, **1977**.
10. Hageman, H.A. *Org. React.* **1953**, 7, 198.
11. Cooley, J.H.; Evain, E.J. *Synthesis*, **1989**, 1.
12. Kauer, J.C.; Henderson, W. W. *J. Am. Chem. Soc.*, **1964**, 86, 4732.
13. Jensen, K.A.; Holm, A. *Acta. Chem. Scand.* **1964**, 18, 826.
14. Martin, D. *Angew. Chem.* **1964**, 76, 303.
15. Jensen, K.A.; Holm, A. *Acta. Chem. Scand.* **1964**, 18, 2417
16. Holm, A. *Acta. Chem. Scand.* **1968**, 22, 2019.
17. Craig Jr, W. M.; (Ciba-Geigy) *U.S.Patent*, 4,839,442, **1989**.
18. Shimp, D. A.; Vanderlip, J.T. (Ciba-Geigy) *U.S.Patent*, 5, 068,309, **1991**.
19. Woo, E.P.; Dellar, D.V. (Dow Chemicals) *U.S.Patent* 4,528,336, **1985**.
20. Woo, E.P.; Murray, D.J. (Dow Chemicals) *U.S.Patent* 4,713,442, **1987**.
21. Das, S.; Prevorsek, D.; Debona, B. *21st Int. SAMPE Tech. Conf.* **1989**, 972.
22. Shimp, D.A.; Christenson, J.R.; Ising, S.J. *Cyanate Ester Resins-Chemistry, Properties and Applications*, **1991**, Technical Bulletin, Ciba, Ardsley, New York.
23. Snow, AW. In *Chemistry and Technology of Cyanate Ester Resins*. Hamerton, I. ED **1994**, Chapman and Hall, Glasgow, Chap 2.
24. Fang, T. *Macromolecules*, **1990**, 23, 4553.
25. Barton, J.M.; Greenfield, D.C.L.; Hamerton, I.; Jones, J.R. *Polym. Bull.* **1991**, 25,475.
26. Fyfe, C.A.; Niu, J.; Rettig, S.J.; Burlinson, N.E.; Reidsema, C.M.; Wang, D.W.; Poliks, M. *Macromolecules* **1992**, 25, 6289.
27. Gupta, A.M.; Macosko, C.W. *Macromolecules*, **1993**, 26, 2455.
28. Heckle, W.A.; Ory, H.A.; Talber, J.M. *Spectrochim Acta.* **1961**, 17, 600
29. Bauer, M.; Bauer, J. Kuhn, G. *Acta. Polym.* **1986**, 37, 715.
30. Simon, S.L.; Gillham, J.K. *J. Appl. Polym. Sci.* **1993**, 47, 461
31. ASTM E 928-83. *Mol Percent Impurity by Differential Scanning Calorimetry*
32. Couchman, P.R. *Macromolecules*, **1987**, 20, 1712.
33. Pascult J.P.; Williams J.J. *J. Polym. Sci. Phys. Ed.* **1990**, 28, 85
34. Meyer, K.-H.; Burkhardt, C.; Bottenbruch, L. (Bayer AG) *U.S.Patent*, 3,994,949, **1976**.
35. Craig, Jr W. M.; (Ciba-Geigy) *U.S.Patent*, 5,162,574, **1992**.
36. Bauer, M.; Bauer, J. Much, H. *Acta. Polym.* **1986**, 37, 221.
37. Bauer, M.; Bauer, J. *Makromol. Chem. Symp.* **1989**, 30, 1
38. Micro, V.; Cao, Z, Q; Mechin, F.; Pascualt, J.P. *Proc. ACS. Div. Polym. Mat. Sci. Eng.* **1992**, 66, 451.
39. Shimp D.A.; *Proc. Am. Chem. Soc. Div. Polym. Mater. Sci. Eng.* **1986**, 54, 107.
40. Cunningham, I.D.; Brownhill, A.; Hamerton, I.; Howlin, B.J. *J.Chem. Soc. Perkin Trans.* **1994**, 2, 1937.

41. Grenier-Loustalot M.F.; Lartigau, C.; Grenier, P. *Eur. Polym. J.* **1995**, 31, 1139
42. Grenier-Loustalot M.F.; Lartigau, C.; metras, F.; Grenier, P. *J.Polym. Sci. Polym. Chem.* **1996**, 34, 2955
43. Fang, T.; Shimp, D.A. *Prog. Polym. Sci.* **1995**, 20, 61.
44. Hamerton, I. Ed. *Chemistry and Technology of Cyanate Ester Resins.* **1994**, Chapman and Hall, Glasgow.
45. Nair, C.P.R.; Mathew, D; Ninan, K.N. *Adv. Polym. Sci.* **2001**, 155, 1.
46. Shimp, D.A. In *Engineered Materials Handbook*, **1988**, vol 2, ASM International, Metals Park, Ohio, pp.232-239.
47. Hi-Tek Polymers Inc. *U.S.Patent*, 4,847,233 , **1989**.
48. Shimp, D. A. *32<sup>nd</sup> Int. SAMPE Symp.*, **1987**, 32, 1063.
49. Shimp, D. A.; Craig, W.M. Jr. *34<sup>th</sup> Int. SAMPE Symp.*, **1989**, 34, 1336.
50. Owusu, O.A.; Martin, G.C.; Gottro, J.T. *Polym. Engg. Sci.* **1991**, 31, 1604.
51. Owusu, O.A.; Martin, G.C.; Gottro, J.T. *Polym. Engg. Sci.* **1992**, 32, 535.
52. Bonezkaya, A.K.; Kravtschenko, M.A.; Korshak, V.V.; Frankel, Z.M.; Pankratov, V.A.; Vinogradova, S. V. *Vysokomol. Soed.* **1975**, B17, 282.
53. Frankel, Z.M.; Korshak, V.V.; Bonezkaya, A.K.; Pankratov, V.A.; Vinogradova, S. V.; Kravtschenko, M.A. *J. Prakt. Chem.* **1976**, 318, 923.
54. Bonezkaya, A.K.; Ivanov, V.V.; Kravtschenko, M.A.; Pankratov, V.A.; Frankel, Z.M.; Korshak, V.V.; Vinogradova, S. V. *Vysokomol. Soed.* **1980**, A22,766.
55. Bauer, M.; Bauer, J. Garske, B. *Acta. Polym.* **1986**, 37, 604.
56. Khanna, Y. P.; Kumar, R.; Das, S. *Polym. Eng. Sci.* **1990**, 30, 1171.
57. Bauer, J. Thesis, B. Academy of Sciences of the GDR, Berlin, **1990**.
58. Simon, S.L.; Gillham, J.K. *Proc.Am Chem.Soc., Div. Polym. Chem.*, **1991**, 32, 182.
59. Gupta, A.M.; Macosko, C.W. *Makromol.Chem.,Macromol.Symp.*, **1991**, 45, 105.
60. Mirco, V.; Cao, Z.Q.; Mechin, F.; Pascult, J.P. *Proc. Am Chem.Soc., Div. Polym.Mat. Sci. Eng.* **1992**, 66, 451.
61. Simon, S.L.; Gillham, J.K. *Proc. Am Chem.Soc., Div. Polym .Mat. Sci Eng.* **1992**, 66, 453.
62. Lin, R.H.; Hong, J.L.; Su, A.C. *Proc. Am Chem.Soc., Div. Polym.Mat. Sci. Eng.* **1992**, 66, 464.
63. Simon, S.L.; Gillham, J.K. *J.Appl. Polym.Sci.* **1993**, 47, 461.
64. Georjon, O.; Galy, J.; Pascult, J.P. *J. Appl. Polym. Sci.* **1993**, 49, 1441.
65. Liu, H.; George, G.A. *Polymer*, **1996**, 37, 3675
66. Chen, Y-T.; Macosko, C.W. *J.Appl. Polym.Sci.* **1996**, 62, 576.
67. Mathew, D.; Nair, C.P.R.; Krishnan, K.; Ninan, K.N.; *J.Polym.Sci., Part A: Polym. Chem.* **1999**, 37,1103
68. Harismendy, I.; Gomez, C.M.; Rio, M.D. Mondragon, I. *Polym. Int.* **2000**, 49, 735.
69. Nair, C.P.R., Gopalkrishnan, C.; Ninan, K.N. *Polym. Polym. Compos.* **2001**, 9, 531.
70. Yan, H.Q.; Ji, L.; Qi, G.R. *J. Appl. Polym. Sci.* **2004**, 91, 3927.
71. Chen, C.C.; Don, T. M.; Lin, T.H.; Cheng, L.P. *J. Appl. Polym. Sci.* **2004**, 92, 3067.
72. Hong, B.T.; Roh, S.S.; Kim, D.S. *Polym. Int.* **2004**, 53, 640.
73. Li, W.; Liang, G.; Xin, W. *Polym. Int.* **2004**, 53, 869.
74. Recalde, H.B.; Recalde, G.; Garcia-Lopera, R. Gomez, C. M. *Eur. Polym.J.* **2005**, 41, 2635.
75. Wu, S.J.; Mi, F. L. *Polym. Int.* **2006**, 55, 1296.
76. Zhao, L.; Hu, X. *Polymer*, **2007**, 48, 6125.
77. Sheng, X.; Akinc, M. Kessler, M.R. *J. Therm. Anal. Cal.*, **2008**, 93, 77
78. Kohn, J.; Albert, E.C.; Wilchek, M.; Langer, R. *Anal. Chem.* **1986**, 58, 3184.
79. Bauer, M.; Rodekirch, G. *Acta. Polym.* **1986**, 37, 654.

80. Gillham, J.K. In *Developments in Polymer Characterization*, Dawkins, J.V. ED, **1982**, Elsevier Applied Science, London.
81. Simon, S.L.; Gillham, J.K. *J. Appl. Polym. Sci.*, **1994**, 51, 1741
82. Khanna, Y.P.; Kumar, R.; Das, S. *Polym. Engg. Sci.* **1989**, 29, 1488.
83. Ferry, J. *Viscoelastic Properties of Polymers*, 3<sup>rd</sup> Edn, **1982**, Wiley, New York.
84. Senturia, S.; Sheppard, N.; Lee, H.L.; Day, D.R. *J.Adhes.*, **1982**, 15, 69.
85. Senturia, S.; Sheppard, N. *Adv. Polym. Sci.*, **1986**, 80, 1.
86. Snow, A.W., Armistead, J.P. In *Dilatometry on Thermoset Resins*, **1991**, NRL Memorandum Report, 6848.
87. Shimp, D.A. *AroCy Cyanate Ester Safety and Handling Bulletin*, **1992**, Ciba-Geigy publication.
88. Shimp, D.A. In *Chemistry and Technology of Cyanate Ester Resins*. Hamerton, I. ED **1994**, Chapman and Hall, Glasgow, Chap 10.
89. Marcos-Fernandez, A; Posadas, P; Rodriguez, A; Gonzalez, L. *J. Polym. Sci. Part. A: Polym. Chem.* **1999**, 37, 3155.
90. Simon, S.L.; Gillham, J.K. In *Chemistry and Technology of Cyanate Ester Resins*. Hamerton, I. ED **1994**, Chapman and Hall, Glasgow, Chap 4.
91. Snow, A.W.; Buckley L.J. In *Handbook of Low and High Dielectric Constant Materials and Their Applications*. Nalwa, H.S. ED **1999**, Academic Press; New York, Vol. 1, Chap 4.
92. Maya, E.M.; Snow, A.W.; Buckley, L.J. *J.Polym.Sci., Part A:Polym.Chem.* **2003**, 41, 60.
93. Lee, H.; Neville, K. *Handbook of Epoxy Resins*, **1967**, McGraw-Hill, Inc., New York,
94. Hartman, S. J. *The Epoxy Resin Formulators Training Manual*, The Society of the Plastics Industry, Inc., New York, 1984, p. 1.
95. Issue, 9. *Polym. Int.* **2009**, 58, 969.
96. Castan, P. (Ciba-Geigy) *U.S. Patent*. 2,324,483, **1943**.
97. Greenlee, S.O. (DeVoe & Raynolds) *U.S. Patent*. 2,456,408 **1948**.
98. May, C; Tanaka, Y. Eds. *Epoxy Resins: Chemistry and Technology*, **1988**, 2<sup>nd</sup> Ed, Marcel Dekker, Inc, New York.
99. Pascult, J.P.; Williams, R. J. J. Ed. *Epoxy Polymers: New Materials and Innovations* **2010**, Wiley-VCH, New York.
100. Potter, W. G. *Epoxide Resins*, **1970**, Springer-Verlag, New York.
101. Newley, H.A.; Shokal, E. C. (Shell Oil Co.) *U.S. Patent* 2,575,558 **1951**.
- 102 Reinking, N. H. (Union Carbide Corp.) *U.S. Patent* 2,943,095 **1960**.
103. Griffin, L.H.; Long, J.H. (Shell Development) *U.S. Patent* 2,848,435 **1958**.
104. Moroson, H. L. (Reichhold Chemicals, Inc.) *U.S. Patent* 2,921,049 **1960**.
105. Spence, S. P.; Grover, A. R.; Klosek, F. P.; Nicolson, R. E. (Union Carbide Corp.) *U.S.Patent* 3,069,434 **1962**.
106. Wang, C. S.; Pham, H. Q.; Bertram J. L. (Dow Chemical Co.) *U.S.Patent* 4,499,255 **1985**.
107. Ogata, T.; Nakanishi, H.; Aritomi M. (Tohto Kasei K. K.) *Jpn. Patent* 61/195111A **1986**.
108. Bowen, D. O.; Whiteside, R. C. In *Epoxy Resins*, Gould R. F. Ed., Advances Chemistry Series 92, **1970**, American Chemical Society, Washington, D.C., p. 48.
109. Bowen, D. O.; Whiteside, R. C. In *Epoxy Resins*, Gould R. F. Ed., Advances Chemistry Series 92, **1970**, American Chemical Society, Washington, D.C., p. 48.
110. Enikolopyan, N. S.; Markevitch, M. A.; Sakhonenko, L. S.; Rogovina, S. Z.; Oshmyan, V. G. *J. Polym. Sci., Chem. Ed.* **1982**, 20, 1231.
111. Pham, H; Marks, M. *Epoxy Resins*, In *Encyclopedia of Polymer Science and Technology*, **2004**, 3<sup>rd</sup> Ed, Wiley Interscience, New Jersey, Vol 9, p 678.
112. Ellis, B. Ed. *Chemistry and Technology of Epoxy Resins*, **1993**, 1<sup>st</sup> Ed. Blackie Academic



- and Professional, Glasgow, U.K.
113. Annu. Book ASTM Stand. Section 8 (Plastics). Web site: <http://www.astm.org>.
114. Sheih, D. P.; Benton, D. E., *Analysis of Paints and Related Materials: Current Techniques for Solving Coatings Problems*, ASTM Special Technical Publication STP 1119, **1992**, pp. 41.
115. Pasch, H.; Unvericht, R.; Resch, M. *Angew. Makromol. Chem.* **1993**, 212, 191.
116. Pasch, H.; Adrian, J.; Braun, D. *GIT Spezial Separation* **2001**, 21, 104.
117. Crozier, D.; Morse, G.; Tajima, Y. *SAMPE J.* **1982**, 18, 17.
118. Fuchslueger, U.; Stephan, H.; Grether, H.-J.; Grasserbauer, M. *Polymer*, **1999**, 40, 661.
119. Jay, R. *Anal. Chem.* **1964**, 36, 667.
120. Dobinson, B.; Hofmann, W.; Stark, B. *The Determination of Epoxide Groups*, **1969**, Pergamon Press, Elmsford, New York.
121. Lwowski, W. In *Comprehensive Heterocyclic Chemistry* Katritzky, A. R.; Rees, C. W. Ed., **1984**, Pergamon Press, Oxford, Vol. 7, pp. 1.
122. Parker R. E.; Isaacs, N. S. *Chem. Rev.* **1959**, 59, 737.
123. Horie, K.; Hiura, H.; Sawada, M.; Mita, I.; Kambe, H. *J. Polym. Sci., A-1* **1970**, 8, 1357
124. Bosch, A. *Epoxy Resins*, In *Polymeric Materials Encyclopedia*, Salamone J.C. Ed., **1996**, CRC Press, Boca Raton vol 3, p 2246.
125. Shechter, L.; Wynstra, J.; Kurkijy, R. P. *Ind. Eng. Chem.* **1956** 48, 94.
126. Ording, P. K. T. *Waterborne and Solvent Based Epoxies and Their End User Applications*, **1996**, John Wiley & Sons Inc., New York, p. 57.
127. Rees, T. M. *J. Oil Color Chem. Assoc.* **1988**, 71, 39.
128. Speranza, G. P. (Jefferson Chemical) *U.S. Patent* 3,020,262, **1962**.
129. Marks, M. J.; Plepys, R. A. (Dow Chemical Co.) *U.S. Patent* 4,658,007, **1987**.
130. Hamterton, I. *Recent Developments in Epoxy Resins*, Rapra Review Reports, **1996**, vol 8 report 91.
131. Ricciardi, F.; Romanchick, W. A.; Joullie, M. M. *J. Polym. Sci., Polym. Chem. Ed.* **1983**, 21, 1475.
132. Heise, M. S.; Martin, G. C. *Macromolecules* **1989**, 22, 99.
133. Three Bond Technical News, **1990**, Issue 32. Website <http://www.threebond.co.jp>
134. Smith, J. D. B.; *Org. Coat. Plast. Chem.* **1978**, 39, 42.
135. Morgan, R.J. In *Epoxy Resins and Composites I*. Cantow, H-J.Ed. *Adv. Polym. Sci.* **1985**, **72**, **7**.
136. Crivello, J. V.; Lam, J. H. W. *Macromolecules* **1977**, 10, 1307.
137. Crivello, J. V.; Lam, J. H. W. *ACS Symp. Ser.*, **1979**, 114, 1.
138. Smith, I.T. *Polymer*, **1961**, 2, 95.
139. Gordon, M.; Simpson, W. *Polymer*, **1961**, 2, 383.
140. Aciteli, M.A.; Prime, R. B.; Sacher, E. *Polymer*, **1971**, 12, 333.
141. Kamal, M.R. *Polym. Eng. Sci.*, **1974**, 14, 231.
142. Lunak, S.; Vladyka, J.; Dusek, K. *Polymer*, **1978**, 19, 931.
143. Dutta, A; Ryan, M.E. *J.Appl.Polym.Sci.*, **1979**, 24, 635.
144. Enns, J.B.; Gillham, J.K. *J. Appl. Polym. Sci.*, **1983**, 28, 2567.
145. Barton, J.M. *Adv. Polym. Sci.*, **1985**, 72, 111.
146. Choy, I.C.; Plazek, D.J. *J. Polym. Sci. Polym. Phys. Ed.*, **1986**, 24, 1303.
147. Pang, K.P.; Gillham, J.K. *J. Appl. Polym. Sci.*, **1989**, 37, 1969.
148. Pang, K.P.; Gillham, J.K. *J. Appl. Polym. Sci.*, **1990**, 39, 909.
149. Wisanrakkit, G.; Gillham, J.K. *J. Appl. Polym. Sci.*, **1990**, 41, 2885.
150. Min, B.G.; Stachurski, Z.H.; Hodgkin, J.H. *Polymer*, **1993**, 34, 4908.
151. Min, B.G.; Stachurski, Z.H.; Hodgkin, J.H. *Polymer*, **1993**, 34, 4488.
152. Venditti, R.A.; Gillham, J.K. *J. Appl. Polym. Sci.*, **1995**, 56, 1687.

153. Vyazovkin, S.; Sbirrazzuoli, N. *Macromolecules*, **1996**, 29, 1867.
154. Pichaud, S.; Duteurtre, X.; Fit, A.; Stephan, F.; Maazouz, A.; Pascault, J.P. *Polym. Int.* **1999**, 48, 1205.
155. Perrin, F., -X.; Nguyen, T.M.H; Vernet, J.-L. *Macromol. Chem. Phys.*, **2007**, 208, 718.
156. Dai, Z.; Li, Y.; Yang, S.; Zhao, N.; Zhang, X.; Xu, J. *Eur. Polym. J.*, **2009**, 45, 1941.
157. Marks, M.J.; Snelgrove, R.V. *ACS Appl. Mater. Interaces.*, **2009**, 1, 921.
158. Erich, W.; Bonder, M.J. *J. Appl. Polym. Sci.*, **1960**, 3, 296.
159. Kline, D.E. *J. Polym. Sci.*, **1960**, 47, 237.
160. Lin, S.C.; Pearce, E.M. *J. Polym. Sci. Polym.Chem. Ed.*, **1979**, 17, 3095.
161. Chen, C.S.; Bulkin, B.J.; Pearce, E.M. *J. Appl. Polym.Sci.*, **1982**, 27, 1177.
162. Chen, C.S.; Bulkin, B.J.; Pearce, E.M. *J. Appl. Polym.Sci.*, **1982**, 27, 3289.
163. Kamon, T. ; Furukawa, H. In *Epoxy Resins and Composites IV*, Advances in Polymer Science 80 , Dusek, K. Ed., **1986**, Springer-Verlag, Berlin.
164. Bellenger, V.; Morel, E.; Verdu, J. *J. Mater. Sci.*, **1988**, 23, 4244.
165. Bellenger, V.; Verdu, J.; Morel, E. *J. Mater. Sci.*, **1989**, 24, 63.
166. Morel, E.; Bellenger, V.; Bocquet, M.; *J. Mater. Sci.*, **1989**, 24, 69.
167. Amdouni, N.; Sautereau, H.; Gerard, J-F, ; Pascault, J-P. *Polymer*, **1990**, 31, 1245.
168. Thompson, Z. J.; Hillmyer, M.A.; Liu, J.; Sue, H.J.; Dettloff, M.; Bates, F.S. *Macromolecules*, **2009**, 42, 2333.
169. Crivello, J. V. *J. Polym. Sci.* **1973**, 11, 1185.
170. Stenzenberger, H.D. *Appl. Polym. Symp.* **1973**, 22, 77.
171. Nagai, A.; Takahashi, A.; Wajima, M.; Tsukanishi, K. *Polym. J.* **1988**, 20, 125.
172. Wilson, D.; Stenzenberger, H. D.; Hergenrother, P. M. Eds., *Polyimides*, **1990**, Blackie, Glasgow and London.
173. Pappalardo, L.T. *J. Appl. Polym. Sci.*, **1977**, 21, 809.
174. Gotro, J.T.; Appelt, B.K. *IBM J. Res. Dev.*, **1988**, 32, 616.
175. Takahasshi, A.; Nagai, A.; Mukoh, A.; Tsukanishi, K. *IEEE Trans. Comp. Hybrids Manuf. Technol.*, **1990**, 13, 1115.
176. Stenzenberger, H. D. *Adv. Polym. Sci.*, **1994**, 117, 165.
177. Brown, A. S. *Aerospace Am.*, **1989**, 27, 18.
178. Xiang, Z.D.; Jomes, F. R. *Composites Sci. Technol.*, **1993**, 47, 209.
179. Searle, N.E. (Du pont) *U.S. Patent*, 2444536, **1948**.
180. Searle, N.E. *Chem. Abstr.* **1948**, 42, 7340.
181. Grundschober, F.; Sambeth, J. *U.S. Patent* 3,380,964 **1968**.
182. Cole, N.; Gruber, W. F. *U.S. Patent* 3,127,414 **1964**.
183. Sauers, C.K. *J. Org. Chem.* **1969**, 34, 2275.
184. Orphanides, G. *Germ. Offen.* 27 19 903 **1977**.
185. Orphanides, G. *U.S. Patent* 4,154,737 **1979**.
186. Haug, T.; Kiefer, J.; Renner, A. *Ger. Patent* DE 2,715,503 C2 **1985**.
187. Lancaster, M. *Europ. Pat. Appl.* 367,599 **1990**.
188. Abblard, J. Boudin, M. *Germ. Offen.* 27 51 901 **1978**.
189. Boudin, M.; Abblard, J. *Germ. Offen.* 28 34 919 **1979**.
190. Shumichi, D.; Yasuyuki, T. *Europ. Pat. Appl.* 0 177,031 **1985**.
191. Bergmann, F.; Schapiro, D. *J. Org. Chem.*, **1941**, 6, 774.
192. Houlub, F. F.; Evans L. M. *Germ. Offen.* 20 31 573 and 20 31 574 **1971**.
193. Kawahara, H.; Maikuma, T. *Jpn. Kokai.* 74,35397 **1974**.
194. Kawahara, H.; Maikuma, T. *Chem. Abstr.*, **1974**, 81, 170240t.
195. Hummel, D. O.; Heinenen, K.-U. Stenzenberger, H.; Siesler, H. *J. Appl. Polym. Sci.*, **1974**, 18, 2015.
196. Stenzenberger, H.D. *Chemistry and Properties of Addition Polyimides* In; *Polyimides*, Wilson D.; Stenzenberger, H.D.; Hergenrother, P. M. Ed. **1990**, Chapman and Hall, New York.
197. Crivello, J. V. *J. Polym. Sci. Polym. Chem. Ed.*, **1973**, 11, 1185.
198. Varma, I.K.; Fohlen, G.M.; Parker, J. A. *J. Polym. Sci. Polym. Chem. Ed.*, **1983**, 28, 191.

199. Crivello, J. V. *J. Polym. Sci. Polym. Chem. Ed.*, **1976**,14, 159.
200. Ghatge, N.D. Murthy, R.A.N *Polymer* **1981**, 22, 1250.
201. Wagner-Jauregg, T. *Tetrahedron Lett.*, **1967**, 13, 1175.
202. White, J.E.; *Ind. Eng. Chem. Pro. Res. Dev.* **1986**, 26, 395.
203. Brown, I.M.; Sandreczki, T.C. *Macromolecules* **1990**, 23, 94.
204. Sandreczki, T.C.; Brown, I.M. *Macromolecules* **1990**, 23, 1979.
205. Brown, I.M.; Sandreczki, T.C. *Macromolecules* **1990**, 23, 4918.
206. Hopewell, J.L.; Hill, D.J.T.; Pomery, P. *J. Polymer* **1998**, 39, 5601
207. Kwiatkowski, G.T.; Robeson, L.M.; Brode, G.L.; Bedwin, A. W. *J. Polym.Sci.Polym. Chem. Edn.*, **1975**, 13, 961.
208. Stenzenberger, H. D. In *Structural Adhesives* Kinloch, A.J. Ed., **1986**, Elsevier, London.
209. Varma, I. K.; Gupta, S. P.; Varma, D. S. *J. Appl. Polym. Sci.*, **1987**, 33, 151.
210. Acevedo, M.; de la Campa J. G.; de Abajo, J. *J. Appl. Polym. Sci.*, **1989**, 38, 1745.
211. Grenier-Loustalot, M-F.; Cunha L.D. *Polymer* **1997**, 38, 6303.
212. Barton, J.M; Hamerton, I.; Rose, J. B.; Warner, D. *Polymer*, **1991**, 32, 358.
213. Barton, J.M; Hamerton, I.; Rose, J. B.; Warner, D. *Polymer*, **1991**, 32, 2482.
214. Barton, J.M; Hamerton, I.; Jones, J. R.; Stedman, J. C. *Polym. Bull.*, **1991**,27, 163.
215. Varma, I.K.; Sharma, S. *Polymer* **1985**, 26, 1561.
216. Acevedo, M.; de Abajo, J.; de la Campa J. G. *Polymer* **1990**, 31, 1955.
217. Grenier-Loustalot, M-F.; Cunha L.D. *Eur. Polym. J.*, **1998**, 34, 95.
218. Grenier-Loustalot, M-F.; Cunha L.D. *Polymer* **1998**, 39, 1833.
219. Tungare, A.V. ; Martin, C.G. *J. Appl. Polym. Sci.*, **1992**, 46, 1125.
220. Galanti, A. V. *J. Appl. Polym. Sci.*, **1984**, 29, 1611.
221. Ninan, K.N.; Krishnan, K.; Mathew, J. *J. Appl. Polym. Sci.*, **1986**, 32,6033.
222. Nagai, A.; Takahashi, A.; Suzuki, M.; Katagiri, J.; Mukoh, A. *J. Appl. Polym. Sci.*, **1990**, 41, 2241.
223. Series, A.; Mechin, F.; Pascult, J.P. *J. Appl. Polym. Sci.*, **1993**, 48, 257.
224. Chun-Shan, W.; Tsu-Shang, L. *Polymer* **1999**, 40, 5407.
225. Goldfarb, I.J.; Feld, W.A.; Saikumar, J. *Polymer* **1993**, 34, 813.
226. Di Giulio, C.; Gautier, M.; Jasse, B. *J.Appl. Polym. Sci.*, **1984**, 29, 1771.
227. Hsiao, S-H.; Chang, C-F. *J. Polym. Res.*, **1996**, 3, 31
228. Hsiao, S-H.; Yang, C-P.; Chen, S-H. *J. Polym. Res.*, **1999**, 6, 141.
229. Feng, J.L.; Yue, C.Y.; Chian, K.S. *e-Polymers* **2006**, 044.
230. Nair, C.P.R. *Prog. Polym. Sci.*, **2004**, 29, 401.
231. Dirlikov, S.K. *High Perform. Polym.*, **1990**, 2, 67.
232. Baklouti, M.; Chaagouni, R.; Fontanille, M.; Villenave, J-J. *Eur. Polym. J.*, **1995**, 31, 215..
233. Herenrother, P.M.; Mark, H.F.; Bikales, N.M.; Overberger, C.G.; Menges, G.; Kroshwitz, J.J. Eds. *Encyclopedia of Polymer Science and Engineering* **1985**, 2<sup>nd</sup> Ed., Wiley, New York, Vol. 1, p 61.
234. Lee, CY-C.; Pritchard, G. Eds. *Developments in Reinforced Plastics* **1986**, Elsevier, Barking, Vol. 5, p 121.
235. Hay, A.S.; Bolon, D.A.; Leimer, K.R.; Clark, R.F. *Polym. Lett.*, **1970**, 8, 97.
236. Hay, A. S. *U.S.Patent* 3,594,175 **1971**.
237. Picklesimer, L.G. *U.S.Patent* 4,226,800 **1980**.
238. Inbasekaran, M.N.; Dirlikov, S.K. *U.S.Patent* 4,885,403 **1989**.
239. Douglas, W.E.; Overend, A.S. *31<sup>st</sup> IUPAC Macromolecular Symposium, 1987 (June/July)*, Paper I/SL/46, Merseburg, Germany.
240. Douglas, W.E.; Overend, A.S. *Eur. Polym. J.* **1991**, 27, 1279.
241. Dirlikov, S.K.; Feng, Y. *Polym. Prepr.*, **1991**, 32, 363.
242. Grenier-Loustalot, M.F.; Sanglar, C. *High Perform. Polym.* **1996**, 8, 341.
243. Wu, X.; Feng, Y.; Dirlikov, S.K. *Proc. ACS. Div. Polym. Mater. Sci. Eng.*, **1989**, 60, 103.
244. Wu, X.; Dirlikov, S.K. *Mod. Paint Coat.*, **1989**, 79, 54.
245. Wu, X.; Feng, Y.; Dirlikov, S.K. *ACS Symp. Series*, **1990**, 417, 194.
246. Douglas, W.E.; Overend, A. S. *Polymer* **1993**, 34, 1544.
247. Grenier-Loustalot, M.F.; Sanglar, C. *Eur. Polym. J.* **1997**, 33, 1125.
248. Balcar, H.; Kalisz, T.; Sedlacek, J.; Blechta, V.; Matejka, P. *Polymer* **1998**, 39, 4443.
249. Nair, C.P.R.; Bindu, R.L.; Krishnan, K.; Ninan, K.N. *Eur. Polym. J.* **1999**, 35, 235.
250. Bindu, R. L.; Nair, C.P.R.; Ninan, K.N. *Polym. Int.* **2001**, 50, 651.

251. Nair, C.P.R.; Bindu, R.L.; Ninan, K.N. *J. Mat. Sci.* **2001**, 36, 4151.
252. Harvey, J.A. In *Process Fabr Appl Adv Compos Proc Conf*, Updadhaya Kamleswar ED **1993**, ASM, Materials Park, Ohio, p 199.
253. Mehrkam, P.; Cochran, R. *26<sup>th</sup> Int. SAMPE Tech. Conf.*, **1994**, p 215.
254. Epstein, G.; Ruth, S. *SAMPE J.*, **1996**, 32, 1.
255. *High Performance Plastics*, **July 1994**, p 10.
256. Deutsch, A. *IEEE Trans. Comp. Packag. Manuf. Technol.* **1996**, B19, 331.
257. Shimp, D.A. *Adhesion Soc. Meet.*, Clearwater, **1991**, Feb, p 16.
258. Possart, W.; Dieckhoff, S. *Int. J. Adh. Adhes.* **1999**, 19, 425.
259. Burack, J.J.; Fang, T.; LaGrange, J.D. *U.S. Patents* 5,165,959 & 5,208,892, **1992**.
260. Ikeguchi, N. *Japan Kokai Tokkyo Koho JP 10 142,797*, **1998**.
261. Ikeguchi, N. *Japan Kokai Tokkyo Koho JP 10 212,431*, **1998**.
262. Ohya, K.; Sayama, N. *Eur Pat Appl EP 554,902*, **1993**.
263. Ooya, K.; Sayama, N.; Kamioka, N.; Shibuya, S.; Nagakawa, T.; Yamashita, M. *Jpn Kokai Tokkyo Koho JP 07,277,844*, **1995**.
264. Shimp, D.A.; Southcott, M. *38<sup>th</sup> Int. SAMPE Symp. Exhib.*, **1993**, p 370.
265. Steele, D. L. *Surface Coat. Aus.* **1992**, 6, 12.
266. Wood, W. J. *Protective Coat. Linings*, **1987**, 32, 38.
267. Bauer, R. S. Ed., *Epoxy Resin Chemistry 2*, **1983**, American Chemical Society, Washington, D.C.
268. Christiansen, W.; Shirrell, D.; Aguirre, B.; Wilkins, J. In *Proceedings of the Technical Conference*, IPC Printed Circuits Expo 2001, Anaheim, Calif., pp. SO3-1-1, SO3-1-7.
269. Sharma, J.; Choate, M.; Peters, S. In *Proceedings of the Technical Conference*, IPC Printed Circuits Expo 2002, Long Beach, Calif., pp. SO5-1-1, SO5-1-8.
270. Ehrler, S.; *PC Fab Apr.* **2002**, 32, 38.
271. Ehrler, S.; *PC Fab May.* **2002**, 32, 36.
272. Ishihara, K., Sato, T., Aida, K. Hoshono, T. (Tohto Kasei K.K.) *Jpn. Patent* 08198949 A , **1996**.
273. Helrold, U.; Mason, J.; Verghese, N.; Chen, H.; Reddy, H.; In *Proceedings of NACE Corossion 2003 Conference*, **March 2003**, Houston, Tex.
274. Tzou, M. J. (Nan Ya Plastics Corp.). *U.S. Patent* 6,512,075, **2003**.
275. Sheehan, J. *The Epoxy Resin Formulators Training Manual*, **1984**, The Society of the Plastics Industry, Inc., New York, Chap. XV.
276. Goulding, T. M. In *Handbook of Adhesive Technology*, Pizzi, A.; Mittal, K. L. Eds, **2003**, 2<sup>nd</sup> ed., Marcel Dekker, Inc., New York, pp. 823.
277. Kriegh, D. Ed., *Epoxies with Concrete*, **1968**, American Concrete Institute, Detroit, Mich.
278. McGown, R. L. In *Proceedings of the 1991 Steel, Structures, Painting Council (SSPC) National Conference and Exhibition*, **1991**, Long Beach, Calif.
279. Mihashi, H.; Kaneko, Y. *Transactions Mater. Res. Soc. Japan*, **2000**, 25, 557.
280. Green, G. E.; Stark, B. P.; Zahir, S. A. *J. Macromol. Sci. Revs. Macromol. Chem.* **1981 / 1982**, 21, 187.

# Chapter **2**

## Scope and Objectives

## 2.1 Scope and Objectives

From the time of Baekeland to the present, the chemistry of polymers has been constantly dominated by the synthetic organic chemist's viewpoint, whose focus is the synthesis of new polymeric materials. The synthesis of bisphenol-A, which is one of the darling monomers of polymer chemists, by the condensation reaction of acetone and phenol in 1891 by Danin<sup>1</sup> could be considered as one of the major contributions of synthetic chemists towards polymer science. Since then, several bisphenols were introduced which formed the basis to synthesize a wide range of thermoplastics such as polyarylates, polycarbonates, polyethersulfones, polyetherketones, polyetherimides, and thermosetting resins *viz*: epoxy resins, cyanate ester resins, polybenzoxazines, phenolic resins, propargyl-terminated resins enriching the applications of these polymers.

The application of thermosetting resins has helped to boost many industries including transportation, communication, construction and leisure goods. An area that has immensely benefited from the advancement in thermosetting resins is aerospace, where the impact of these materials can be seen in the space programs, rocket motors, stealth military aircraft, commercial transport, and so on. Composites for the specific applications with desired properties are realizable through appropriate choice of the resin, reinforcement, and their perfect processing. The bulk of the research in aerospace composite materials centers on epoxy resins, bismaleimides, cyanate ester resins, propargyl-terminated resins, polybenzoxazines, etc.

**A) Cyanate ester resins:** Cyanate ester (CE) resins, which were introduced in early 80's have received considerable attention because of their outstanding performance with respect to resistance to fire and moisture, good mechanical strength, high glass transition temperature, low dielectric constant, radiation resistance, excellent metal adhesion, and compatibility with carbon fiber reinforcements.<sup>2-4</sup> These highly desirable properties make CEs the preferred candidates as structural materials for high temperature applications in aerospace, insulation, microelectronics and adhesive industries.<sup>5-8</sup> The versatility of their synthetic method made it possible to incorporate different structural moieties into CE monomer *via* appropriate selection of precursor bisphenols offering a good control over the physical, thermal and mechanical properties of the resins.

The major limitations of most of the current CE resins are the necessity for B-stage processing, and the formation of inherently brittle polymers resulting from the highly crosslinked system. The quest for the development of improved polycyanurate system has been the driving force for the research in new monomers. The key properties that serve as a basis for identifying 'improved' polycyanurate system include (1) ease of processing (2) high glass transition temperature (3) excellent mechanical properties such as elastic modulus and impact strength (4) low moisture absorption and (5) low dielectric constant.<sup>2-9</sup>

It has been reported that the introduction of alkylene spacers / cycloaliphatic moiety into CE monomer helps in lowering of moisture absorption<sup>10</sup>, albeit compromising thermal stability to some extent. Our synthetic efforts were thus directed towards structural modifications of CEs designed to introduce-

- i) (substituted) hydrophobic cycloaliphatic moiety,
- ii) methyl groups *ortho* to cyanate functionality.

The major objective of the current research was to design and synthesize new cyanate ester monomers containing flexible alkyl chain and/or cycloaliphatic “cardo” group based on corresponding bisphenols which were in turn prepared from cheap and commercially available raw materials using simple organic transformations. Another objective was to study thermal, thermomechanical and moisture absorption behavior of polycyanurates derived therefrom.

One of the approaches for pursuing the goal involved making use of 3-pentadecyl phenol, which in turn obtainable from cashew nut shell liquid (CNSL); –a renewable resource material. The dual phenolic/ alkenyl nature of CNSL makes it an ideal renewable raw material for the synthesis of water-resistant resins and polymers.<sup>11</sup> The other approaches included the use of commercially available *p*-cumyl phenol and  $\beta$ -naphthol as the starting materials for introducing hydrophobic cycloaliphatic “cardo” group into CE monomer. The new CE monomers containing cycloaliphatic “cardo” group were expected to result into polycyanurate system with lower moisture absorption.

**B) Epoxy resins:** Epoxy resins in combination with graphite/glass and to a limited extent with organic reinforcements like aramids dominate in aerospace applications, printed circuit boards, semiconductor encapsulants, and adhesives.<sup>12-15</sup> The attractive features of epoxies include ease of processing and handling convenience, good mechanical properties due to excellent adhesion to a variety of reinforcements, toughness, outstanding corrosion resistance, no volatiles emission and low shrinkage upon cure and low cost - a unique combination of properties generally not found in many plastic materials.

However, the use of a conventional epoxy system has drawbacks due to excessive water absorption and residual stress, resulting in the propensity to microcrack when thermally cycled. The absorbed moisture acts as a plasticizer, deteriorating the thermal, mechanical and dielectric properties of cured resins.<sup>16,17</sup> The moisture absorption causes lowering of  $T_g$  of a laminate material and may also cause ‘popcorn phenomenon’ when in contact with solder at a high temperature. Therefore, low moisture absorption is necessary for laminate materials.<sup>18</sup> A search for an alternate epoxy resin system with lower dielectric properties, reduced moisture absorption and improved toughness has been one of the active areas of research in the recent past.

The objective of the study was to synthesize new epoxy resin(s) containing cycloaliphatic “cardo” group by the judicious selection of bisphenol(s) and to study thermal, thermomechanical and moisture absorption behavior of cured network derived therefrom.

**C) Bismaleimides:** The addition-type polyimide systems are used as matrix resins, adhesives, and coatings for high performance applications in the aerospace and electronics industries.<sup>19-21</sup> These are low molar mass, multifunctional monomers or prepolymers that carry additional curable terminal functions and imide functions in their backbone. Bismaleimides (BMIs), bisitaconimides, and bisnadimides are the versatile ones in this category. Of these, bismaleimides dominate the high temperature polymer scenario for aerospace applications.

The brittleness of cured BMIs has been one of the problems. The introduction of flexible units such as siloxane, ether linkages, etc., as spacers is reported to reduce the crosslinking density of cured BMIs offering better toughening property.<sup>22-24</sup> However, the melting temperature ( $T_m$ ) of BMI monomers tends to increase with increasing molecular weight because the cohesive energy between molecules in the crystal state is large. This increase in melting point (greater than 150 °C) close to the onset temperature of curing induces a short gel time or short pot-life of the melt making the processing difficult.<sup>25</sup>

It has been reported that the introduction of alkylene chain / spacers lowers the melting point of BMIs and improves solubility in common organic solvents.<sup>22,25-27</sup> It was of interest to explore the use of 3-pentadecyl phenol as a starting material towards the synthesis of new BMI monomers with lower melting points and improved solubility in common organic solvents.

**D) Propargyl-terminated resins:** Propargyl ether functional resins (also popularly known as propargyl-terminated resins) were developed as a potential hydrophobic substitute for epoxies in advanced composites, electronics, adhesives and coatings.<sup>28-30</sup> The synthetic method of bispropargyl ethers makes it possible to tailor the properties by varying the monomer structure.

It was of interest to synthesize new bispropargyl ethers based on bisphenols containing cycloaliphatic “cardo” group and to study the effect of incorporation of cycloaliphatic “cardo” group on the cure kinetics of bispropargyl ethers.



**Objectives of the present thesis:**

- ◆ Design and synthesis of new cyanate ester monomers containing cycloaliphatic “cardo” group or alkylene chain with systematic variation in the structure starting from corresponding bisphenols.
- ◆ To investigate cure kinetics of selected cyanate ester monomers under nonisothermal and isothermal mode using DSC technique.
- ◆ The processing of CE monomers and to study thermo-mechanical behavior and moisture absorption characteristics of cured polycyanurate network.
- ◆ Synthesis and characterization of epoxies containing cycloaliphatic “cardo” group starting from corresponding bisphenols.
- ◆ The curing of epoxies using 4,4'-methylenedianiline (MDA) curing agent and to study the thermal, thermo-mechanical and moisture absorption behavior of cured epoxy resins in order to study the effect of incorporation of cycloaliphatic “cardo” group into epoxy resins.
- ◆ Synthesis and characterization of new bismaleimides starting from 3-pentadecylphenol and to study the kinetics of curing of bismaleimides
- ◆ Synthesis and characterization of bispropargyl ethers based on bisphenols containing cycloaliphatic “cardo” group and to study the effect of incorporation of cycloaliphatic “cardo” group on i) cure kinetics of bispropargyl ethers and ii) thermal properties of cured network.

**References:**

1. Dianin, A. P. *Zhurnal russkogo fiziko-khimicheskogo obshchestva*. **1891**, 23, 492.
2. Shimp, D.A.; Christenson, J.R.; Ising, S.J. *Cyanate Ester Resins-Chemistry, Properties and Applications*, **1991**, Technical Bulletin, Ciba, Ardsley, New York.
3. Hamerton, I. Ed *Chemistry and Technology of Cyanate Ester Resins*. **1994**, Chapman and Hall, Glasgow.
4. Nair, C.P.R.; Mathew, D.; Ninan, K.N. *Adv. Polym. Sci.* **2001**, 155, 1.
5. Harvey, J.A. In *Process Fabr Appl Adv Compos Proc Conf*, Updadhaya Kamleswar ED **1993**, ASM, Materials Park, Ohio, p 199.
6. Epstein, G.; Ruth, S. *SAMPE J.*, **1996**, 32, 1.
7. Ikeguchi, N. *Japan Kokai Tokkyo Koho JP 10 212,431*, **1998**.
8. Possart, W.; Dieckhoff, S. *Int. J. Adh. Adhes.* **1999**, 19, 425.
9. Guenther, AJ; Yandek, GR; Wright, ME, Petteys, BJ; Quintana, R; Connor, D; Gilardi, RD; Marchant, D. *Macromolecules*, **2006**, 39, 6046.
10. Snow, A.W.; Buckley L.J. In *Handbook of Low and High Dielectric Constant Materials and Their Applications*. Nalwa, H.S. Ed **1999**, Academic Press; New York, Vol. 1, Chap 4.
11. Talbiersky, J.; Polaczek, J.; Ramamoorthy, R.; Shishlov, O. *European Magazine* **2009**, 35, OG33
12. Pascult, J.P.; Williams, R. J. J. Ed. *Epoxy Polymers: New Materials and Innovations* **2010**, Wiley-VCH, New York.
13. Pham, H; Marks, M. *Epoxy Resins*, In *Encyclopedia of Polymer Science and Technology*, **2004**, 3<sup>rd</sup> Ed, Wiley Interscience, New Jersey, Vol 9, p 678.
14. May, C; Tanaka, Y. Eds. *Epoxy Resins: Chemistry and Technology*, **1988**, 2<sup>nd</sup> Ed, Marcel Dekker, Inc, New York.
15. Goulding, T. M. In *Handbook of Adhesive Technology*, Pizzi, A.; Mittal, K. L. Eds, **2003**, 2<sup>nd</sup> ed., Marcel Dekker, Inc., New York, p. 823.
16. Mokienko, R.L.; Cherkasova, N.G.; Mikhailova, O.I.; Protasenya, A. V. *Fibre Chemistry*, **1996**, 28, 175.
17. Lieux, R.L.; La, B.R. (Dow Chemical Company) *U.S. Patent 5274013* **1993**.
18. Hamerton, I.; Herman, H.; Rees, K.T; Chaplin, A.; Shaw, S.J. *Polym. Int.* **2001**, 50, 475.
19. Gotro, J.T.; Appelt, B.K. *IBM J. Res. Dev.*, **1988**, 32, 616.
20. Brown, A. S. *Aerospace Am.*, **1989**, 27, 18.
21. Stenzenberger, H. D. *Adv. Polym. Sci.*, **1994**, 117, 165.
22. Hsiao, S-H.; Yang, C-P.; Chen, S-H. *J. Polym. Res.*, **1999**, 6, 141.
23. Wang, C-S.; Leu, T.-S. *J. Appl. Polym. Sci.* **1999**, 73, 833.
24. Davidson, G.; Soutar, I.; Preston, P.N.; Shah, V.K.; Simpson, S.W.; Stewart, N.J. *Polymer*, **1994**, 35, 653.
25. Barton, J.M; Hamerton, I.; Rose, J. B.; Warner, D. *Polymer*, **1991**, 32, 358.
26. Dumont, F.; Visseaus, M.; Barbier-Baudry, D.; Dormond, A. *Polymer* **2000**, 41, 6043.
27. Feng, J.L.; Yue, C.Y.; Chian, K.S. *e-Polymers* **2006**, 044.
28. Dirlikov, S.K. *High Perform. Polym.*, **1990**, 2, 67.
29. Douglas, W.E.; Overend, A. S. *Polymer* **1993**, 34, 1544.
30. Nair, C.P.R. *Prog. Polym. Sci.*, **2004**, 29, 401.

# Chapter **3**

## Synthesis and Characterization of Cyanate Ester Monomers

### 3.1 Introduction

One of the most important criteria that decide the final properties of a polycyanurate is the structure of cyanate ester (CE) monomer. By the appropriate selection of monomers, the properties of a polycyanurate could be tailored. The synthetic method introduced by Grigat *et. al.*<sup>1</sup> for the synthesis of cyanate ester (CE) monomers made it possible to synthesize CE monomers with different structures. Since then, CE monomers containing different moieties *viz*; aliphatic, cycloaliphatic, fluoroaliphatic, ether linkage, siloxane, sulfone, sulfoxide, phosphine oxide, phosphazene, etc., were synthesized.<sup>2-13</sup>

There are a plethora of CE monomers with structural variations that have been synthesized to date, and too large to be catalogued here. The CE monomers having relevance with the present work are summarized in **Table 3.1** and **Table 3.2**. **Table 3.1** summarizes CE monomers containing “cardo” group with/or cycloaliphatic moiety. CE monomers containing cycloaliphatic moiety results into polycyanurate with low moisture absorption, and low dielectric constant.<sup>12-15</sup> CE monomers with flexible spacers are catalogued in **Table 3.2**. The incorporation of aliphatic spacer into CE monomer is known to result into polycyanurate network with lower crosslink density and improved mechanical properties.<sup>5,16</sup>

In the present work, CE monomers containing cycloaliphatic “cardo” group and/or flexible linkage were designed and synthesized. For a new monomer synthesis, it was needed that the synthetic steps used were i) high yielding, ii) affording product with high purity and iii) using inexpensive starting materials. By taking these factors into account, starting from cheap, commercially available raw materials *viz*; 3-pentadecylphenol,  $\beta$ -naphthol, *p*-cumylphenol and adipic acid, a variety of new CE monomers (**Table 3.3**) were designed and synthesized. The new CE monomers containing cycloaliphatic “cardo” group were designed to result into polycyanurate system with lower moisture absorption. These synthesized CE monomers were characterized using FT-IR, <sup>1</sup>H-NMR and <sup>13</sup>C-NMR spectroscopy.

**Table 3.1: Literature examples of selected CE monomers containing “cardo” group with / or cycloaliphatic moiety**

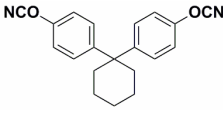
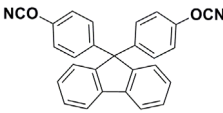
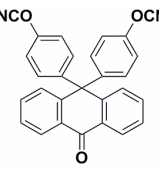
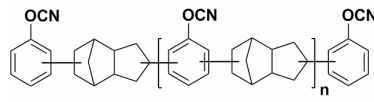
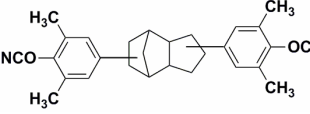
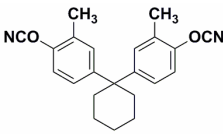
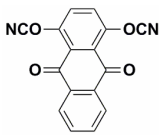
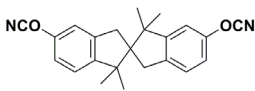
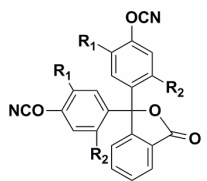
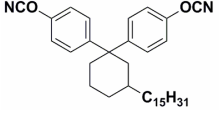
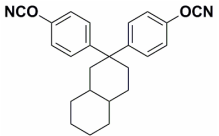
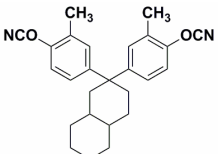
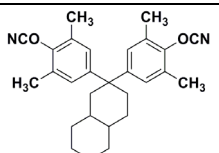
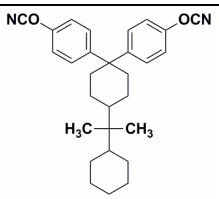
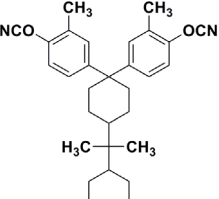
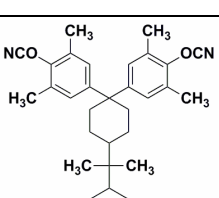
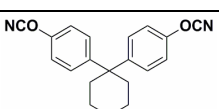
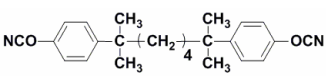
Sr. No	CE Monomer	Reference
1		2, 3
2		2, 3
3		3
4		14
5		12, 15
6		17
7		18
8		19
9	 <p data-bbox="678 1892 853 1960"> <math>R_1 = \text{H, CH}_3, \text{CH}(\text{CH}_3)_2</math>  <math>R_2 = \text{H, CH}_3, \text{CH}(\text{CH}_3)_2</math> </p>	3, 20

Table 3.2: Literature examples of selected CE monomers containing flexible spacers

Sr. No	CE Monomer	Reference
1	$\text{NCO}-\text{CH}_2-(\text{CF}_2)_2-\text{O}-(\text{CF}_2)_4-\text{O}-(\text{CF}_2)_2-\text{CH}_2-\text{OCN}$	21
2	$\text{NCO}-\text{CH}_2-\text{CF}_2-\overset{\text{C}_2\text{F}_5}{\text{CF}}-\text{CF}_2-\text{CF}_2-\text{CH}_2-\text{OCN}$	21
3	$\text{NCO}-\text{CH}_2-(\text{CF}_2)_n-\text{CH}_2-\text{OCN}$ $n = 3, 4, 6, 8, 10$	21 (n= 3,4), 5 (n = 3,4,6,8,10)
4	$\text{NCO}-\text{CH}_2-(\text{CF}_2)_2-\text{O}-(\text{CF}_2)_2-\text{CH}_2-\text{OCN}$	21
5	$\text{NCO}-\overset{\text{CF}_3}{\underset{\text{CF}_3}{\text{C}}}-(\text{CH}_2)_n-\overset{\text{CF}_3}{\underset{\text{CF}_3}{\text{C}}}-\text{OCN}$ $n = 6, 9$	22
6	$\text{NCO}-\text{C}_6\text{H}_4-(\text{CF}_2)_6-\text{C}_6\text{H}_4-\text{OCN}$	23
7	$\text{NCO}-\text{C}_6\text{H}_4-\text{N}=\text{CH}-\text{C}_6\text{H}_4-\text{O}-\text{R}-\text{O}-\text{C}_6\text{H}_4-\text{CH}=\text{N}-\text{C}_6\text{H}_4-\text{OCN}$ $\text{R} = -(\text{CH}_2\text{CH}_2\text{O})_n-\text{CH}_2\text{CH}_2-$ $n = 1, 2$	24
8	$\text{N}\equiv\text{C}-\text{O}-\text{C}_6\text{H}_4-\text{O}-(\text{C}_6\text{H}_4-\text{O})_n-\text{C}\equiv\text{N}$ $n = 1, 3$	25
9	$\text{NCO}-\text{C}_6\text{H}_3(\text{H}_3\text{CO})-\text{CH}_2\text{CH}_2\text{CH}_2-\text{C}_6\text{H}_3(\text{R}_1, \text{R}_2)-\text{OCN}$ $\text{R}_1 = \text{R}_2 = -\text{H}, -\text{CH}_3, -\text{OCH}_3$	26
10	$\text{NCO}-\text{C}_6\text{H}_4-\overset{\text{CH}_3}{\underset{\text{CH}_3}{\text{C}}}-\text{C}_6\text{H}_4-\text{O}-\text{CH}_2\text{CH}_2-\text{O}-\text{C}_6\text{H}_4-\overset{\text{CH}_3}{\underset{\text{CH}_3}{\text{C}}}-\text{C}_6\text{H}_4-\text{OCN}$	27
11	$\text{NCO}-\text{C}_6\text{H}_4-\text{O}-(\text{CH}_2-\text{CH}_2-\text{O})_n-\text{C}_6\text{H}_4-\text{OCN}$ $n = 1, 2, 3$	28

Table 3.3 : List of CE monomers synthesized in the present study.

Sr. No	CE Monomer	Name
1		1,1-Bis(4-cyanatophenyl)-3-pentadecylcyclohexane (BPC15CN)
2		1,1-Bis(4-cyanatophenyl)decahydronaphthalene (BPDCCN)
3		1,1-Bis(4-cyano-3-methylphenyl)decahydronaphthalene (DMBPDCCN)
4		1,1-Bis(4-cyano-3,5-dimethylphenyl) decahydronaphthalene (TMBPDCCN)
5		1,1-Bis(4-cyanatophenyl)-4-perhydrocumylcyclohexane (BPPCPCN)
6		1,1-Bis(4-cyano-3-methylphenyl)-4-perhydrocumylcyclohexane (DMBPPCPCN)
7		1,1-Bis(4-cyano-3,5-dimethylphenyl)-4-perhydrocumylcyclohexane (TMBPPCPCN)
8		1,1-Bis(4-cyanatophenyl)cyclohexane (BPZCN)
9		2,7-Bis(4-cyanatophenyl)-2,7-dimethyloctane (BPC6CN)

## 3.2 Experimental

### 3.2.1 Materials

3-Pentadecyl phenol, ruthenium-on-carbon (Ru/C) (5 wt.%) and 3-mercaptopropionic acid were purchased from Sigma-Aldrich Inc. USA. Acetone, chloroform, cyclohexane, cyclohexanone, dichloromethane, ethylacetate, isopropanol, toluene, phenol, *o*-cresol, 2,6-dimethyl phenol,  $\beta$ -naphthol, acetic acid, hydrochloric acid, triethylamine, potassium hydroxide, sodium bicarbonate, sodium chloride, sodium sulfate, celite and silica gel were procured from Merck India. Cyanogen bromide was purchased from SRL, India. *p*-Cumyl phenol was obtained from M/s Herdillia Chemicals, Mumbai.

Pyridiniumchlorochromate (PCC) was prepared according to the procedure reported in the literature.<sup>29</sup>

### 3.2.2 Characterization

Melting points were determined by open capillary method and are uncorrected.

Infrared spectra were recorded on Perkin-Elmer spectrum GX model at a resolution of  $4\text{ cm}^{-1}$ . The spectra were recorded by depositing samples as solvent-cast thin films on sodium chloride cells.

NMR spectra were recorded on Bruker NMR spectrophotometer (200 or 400 MHz) using  $\text{CDCl}_3$  or  $\text{DMSO-d}_6$  solvent.

## 3.3 Preparations

### 3.3.1 Synthesis of 1,1-bis(4-cyanatophenyl)-3-pentadecylcyclohexane

#### 3.3.1.1 Synthesis of 3-pentadecyl cyclohexanol from 3-pentadecyl phenol

3-Pentadecylphenol (40.35 g, 0.13 mol) was placed in a Parr reactor (300 mL capacity) and dissolved in isopropanol (150 mL). Ru/C (0.8 g, 2 wt%) was added. Hydrogenation was carried out at  $120\text{ }^\circ\text{C}$  / 700 psi hydrogen pressure. The reaction was continued until there was no further absorption of hydrogen (1.5 h). The catalyst was separated by filtering the reaction mixture through Whatman filter paper. Isopropyl alcohol was stripped off and the product was dried under reduced pressure.

Yield: 40.6 g (98 %).

MP:  $44 - 46\text{ }^\circ\text{C}$ . (Lit.:  $45 - 48\text{ }^\circ\text{C}$ ).<sup>30</sup>

IR ( $\text{CHCl}_3$ ,  $\text{cm}^{-1}$ ) : 3345 (-OH stretching).



<sup>1</sup>H-NMR (CDCl<sub>3</sub>): δ (ppm), 3.98 - 4.11 (m, H (e) CH attached to OH), 3.49 – 3.63 (m, H (a) CH attached to OH), 1.25 – 1.69 (m, 37 H, CH<sub>2</sub> and CH), 0.88 (t, 3 H, CH<sub>3</sub>).

### 3.3.1.2 Synthesis of 3-pentadecyl cyclohexanone from 3-pentadecyl cyclohexanol

Into a 2 L two-necked round bottom flask equipped with an overhead stirrer were added a finely ground mixture of pyridinium chlorochromate (32.25 g, 0.15 mol)-silica gel (32.25 g) and chloroform (300 mL). To the mixture, 3-pentadecyl cyclohexanol (31 g, 0.1 mol) dissolved in chloroform (300 mL) was added at 0 °C. The reaction mixture was stirred at 0 °C for 4 h and then filtered through a sintered funnel. The residue was washed several times with chloroform. All the washings were combined and concentrated to around 500 mL. The solution was then passed through a bed of celite-silica gel. Chloroform solution was washed with saturated solution of aqueous sodium bicarbonate (2 x 75 mL) followed by brine water (2 x 75 mL) and finally with water (75 mL), dried over sodium sulfate, filtered and the solvent was removed on a rotary evaporator to yield a white waxy solid. The product was purified by distillation at 60 - 62 °C /0.02 mm Hg.

Yield: 28.3 g (92 %).

MP: 41 °C. (Lit.: 41 °C).<sup>31</sup>

IR (CHCl<sub>3</sub>, cm<sup>-1</sup>) : 1705 (C=O stretching).

<sup>1</sup>H-NMR (CDCl<sub>3</sub>): δ (ppm), 2.32 - 2.45 (m, 4H, CH<sub>2</sub> α to C=O), 1.26 - 2.0 (m, 33 H, CH<sub>2</sub> and CH), 0.88 (t, 3 H, CH<sub>3</sub>).

### 3.3.1.3 Synthesis of 1,1-bis(4-hydroxyphenyl)-3-pentadecyl cyclohexane from 3-pentadecyl cyclohexanone and phenol

Into a 250 mL three-necked round bottom flask equipped with an overhead stirrer and a gas inlet and outlet were added 3-pentadecyl cyclohexanone (21.56 g, 0.07 mol), phenol (39.48 g, 0.42 mol) and 3-mercaptopropionic acid (0.6 mL, 7 mmol). The reaction mixture was stirred at room temperature for 15 minutes. Anhydrous hydrogen chloride was bubbled through the reaction mixture. After 1 h, the reaction mixture solidified. The reaction mixture was dissolved in ethyl acetate (500 mL) and neutralized by washing with saturated solution of aqueous sodium bicarbonate (3 x 75 mL) followed by washing with brine (3 x 75 mL) and finally with water (75 mL). The ethyl acetate solution was dried over sodium sulfate and filtered. Ethyl acetate was removed under reduced pressure on a rotary evaporator and finally at pump to obtain a pink solid which was washed with pet ether to remove excess phenol. The crude bisphenol was recrystallized using pet ether to afford a white crystalline solid.

Yield: 33.45 g (70 %).

MP: 104 °C. (Lit. 104 °C).<sup>31, 32</sup>

IR (CHCl<sub>3</sub>, cm<sup>-1</sup>) : 3290 (-OH stretching).

<sup>1</sup>H-NMR (CDCl<sub>3</sub>): δ (ppm), 7.11 (d, 2 H(e), Ar-H *meta*-to OH), 6.92 (d, 2 H(a), Ar-H *meta*-to OH), 6.70 (d, 2 H(e), Ar-H *ortho*- to OH), 6.58 (d, 2 H(a), Ar-H *ortho*-to OH), 4.77 (s, 1 H, OH), 4.70 (s, 1 H, OH), 1.13 – 2.48 (m, 37 H, CH<sub>2</sub> and CH), 0.80 (t, 3 H, CH<sub>3</sub>).

#### 3.3.1.4 Synthesis of 1,1-bis(4-cyanatophenyl)-3-pentadecyl cyclohexane

Into a 250 mL three-necked round bottom flask equipped with a magnetic stirring bar, a pressure equalizing dropping funnel and a thermowell were added cyanogen bromide (4.77 g, 0.05 mol) and 1,1-bis(4-hydroxyphenyl)-3-pentadecylcyclohexane (9.56 g, 0.02 mol). The reactants were dissolved in acetone (100 mL). To the reaction mixture, freshly distilled triethylamine (stored over KOH) (6.0 mL, 0.05 mol) diluted with acetone (10 mL) was added at -15 °C over a period of 30 minutes with a constant stirring. After the completion of addition, the reaction mixture was stirred at -15 °C for 3 h and then filtered through a sintered funnel. The residue was washed with acetone ( 2 x 15 mL). The filtrate was concentrated under reduced pressure at room temperature and then dissolved in dichloromethane (150 mL). The product was washed successively with 4% aqueous sodium chloride solution (3 x 25 mL) and water (2 x 25 mL). The dichloromethane solution was dried over sodium sulfate, filtered and concentrated on a rotary evaporator at room temperature under reduced pressure to yield a colorless viscous liquid which was purified by passing through a bed of silica gel-celite. The product solidified on freezing for 24 h.

Yield: 8.76 g (83 %).

MP: 46 - 48 °C.

#### 3.3.2 Synthesis of 1,1- bis-(4-cyanatophenyl)decahydronaphthalene

##### 3.3.2.1 Synthesis of decahydro-2-naphthol from β-naphthol

β-Naphthol (40.0 g, 0.28 mol) was placed in a Parr reactor (300 mL capacity) and dissolved in isopropanol (120 mL). Ru/C (1.2 g, 3 wt %) was added. Hydrogenation was carried out at 125 °C/ 700 psi hydrogen pressure. The reaction was continued until there was no further absorption of hydrogen (3 h). The reaction mixture was filtered through a Whatman filter paper. Isopropyl alcohol was stripped off and the compound was dried under reduced pressure to yield decahydro-2-naphthol as a semisolid compound.

Yield: 36.4 g (85 %).

IR (CHCl<sub>3</sub>, cm<sup>-1</sup>) : 3340 (-OH stretching).

$^1\text{H-NMR}$  ( $\text{CDCl}_3$ ):  $\delta$  (ppm), 1.21 – 4.08 (m,  $\text{CH}_2$  and CH).

### 3.3.2.2 Synthesis of 2-decalone from decahydro-2-naphthol

Into a 5-L two-necked round bottom flask equipped with an overhead stirrer were added finely ground mixture of pyridinium chlorochromate (75.6 g, 0.35 mol)-silica gel (75.6 g) and chloroform (1 L). To the reaction mixture, decahydro-2-naphthol (35 g, 0.23 mol) dissolved in chloroform (1 L) was added at 0 °C. The reaction mixture was stirred at 0 °C for 4 h and then filtered through a sintered funnel. The residue was washed several times with chloroform. All the washings were combined and the solution was concentrated up to around 1 L. The solution was then passed through a bed of celite-silica gel. Chloroform solution was washed successively with aqueous sodium bicarbonate solution (3 x 250 mL), brine (2 x 250 mL) and water (2 x 250 mL) and dried over sodium sulfate and filtered. Chloroform was removed on a rotary evaporator to yield a colorless liquid. The product was purified by distillation at 63-65 °C / 0.03 mm Hg.

Yield: 60.8 g (88 %).

IR ( $\text{CHCl}_3$ ,  $\text{cm}^{-1}$ ) : 1716 (C=O stretching),

$^1\text{H-NMR}$  ( $\text{CDCl}_3$ ),  $\delta$  (ppm) : 1.21 – 2.33 (m,  $\text{CH}_2$  and CH).

### 3.3.2.3 Synthesis of 1,1- bis-(4-hydroxyphenyl)decahydronaphthalene from 2-decalone and phenol

Into a 500 mL round bottom flask equipped with a magnetic stirring bar were added, 2-decalone (10.7 g, 0.07 mol), phenol (26.3 g, 0.28 mol), 3-mercaptopropionic acid (0.6 mL, 7 mmol), glacial acetic acid (20 mL) and hydrochloric acid (36%), (40 mL). The reaction mixture was stirred at room temperature for 5 days. The reaction was quenched by adding water (100 mL). The solid obtained was filtered, and the residue was washed several times with water. The solid was dissolved in ethyl acetate (200 mL) and washed sequentially with an aqueous sodium bicarbonate solution (4 x 75 mL), brine (3 x 50 mL), and water (3 x 50 mL). Ethyl acetate solution was dried over sodium sulfate and filtered. Ethyl acetate was removed under reduced pressure on a rotary evaporator and finally at pump to obtain a brown solid. The crude bisphenol was recrystallized using acetic acid to afford a white solid.

Yield: 13.2 g (65 %).

MP: 230 °C. (Lit. 230 °C).<sup>33</sup>

IR ( $\text{CHCl}_3$ ,  $\text{cm}^{-1}$ ) : 3280 (-OH stretching).

$^1\text{H-NMR}$  ( $\text{DMSO-d}_6$ ),  $\delta$  (ppm) : 9.13 (s, 1 H, OH), 9.07 (s, 1 H, OH), 7.12 (d, 2 H(e), Ar-H *meta*-to OH), 6.98 (d, 2 H(a), Ar-H *meta*-to OH), 6.69 (d, 2 H (e), Ar-H *ortho*- to OH), 6.59 (d, 2 H (a), Ar-H *ortho*-to OH), 1.17 - 2.33 (m, 16 H,  $\text{CH}_2$  and CH).

#### 3.3.2.4 Synthesis of 1,1- bis-(4-cyanatophenyl)decahydronaphthalene

Into a 100 mL three-necked round bottom flask equipped with a magnetic stirring bar, a pressure equalizing dropping funnel and a thermowell were added cyanogen bromide (8.5 g, 0.08 mol) and 1,1- bis-(4-hydroxyphenyl)decahydronaphthalene (12.9 g, 0.04 mol). The reactants were dissolved in acetone (100 mL). To the reaction mixture, freshly distilled triethylamine (stored over KOH) (10.6 mL, 0.08 mol) diluted with acetone (10 mL) was added at  $-15\text{ }^\circ\text{C}$  over a period of 20 minutes with a constant stirring. After the completion of addition, the reaction mixture was stirred for 3 h maintaining the temperature at  $-15\text{ }^\circ\text{C}$  and then filtered through a sintered funnel. The residue was washed with acetone (3 x 25 mL). The filtrate was concentrated under reduced pressure at room temperature and then dissolved in 150 mL of dichloromethane. Dichloromethane solution was washed with 4% aqueous sodium chloride solution (3 x 50 mL) followed by washing with water (2 x 50 mL). The dichloromethane solution was dried over sodium sulfate, filtered and concentrated at room temperature under reduced pressure to yield a white powder. The product was recrystallized using cyclohexane.

Yield: 18.9 g (93 %).

MP: 120 - 121  $^\circ\text{C}$ .

#### 3.3.3 Synthesis of 1,1- bis-(4-cyano-3-methylphenyl)decahydronaphthalene

##### 3.3.3.1 Synthesis of 1,1- bis-(4-hydroxy-3-methylphenyl)decahydronaphthalene

Into a 500 mL round bottom flask equipped with a magnetic stirring bar were charged 2-decalone (7.6 g, 0.05 mol), *o*-cresol (32 g, 0.3 mol), 3-mercaptopropionic acid (0.4 mL, 5 mmol) and a mixture of hydrochloric acid (36%) (30 mL) and glacial acetic acid (15 mL). The reaction mixture was stirred at room temperature for 48 h. The solid obtained was dissolved in ethyl acetate (250 mL) and washed successively with aqueous sodium bicarbonate solution (3 x 100 mL), brine (2 x 100 mL) and water (2 x 100 mL). Ethyl acetate layer was dried over sodium sulfate and filtered. Ethyl acetate was removed on a rotary evaporator under reduced pressure. Excess *o*-cresol was removed by distillation under reduced pressure and the crude product was purified by recrystallization using toluene.

Yield: 8.5 g (50 %).

MP: 170  $^\circ\text{C}$ . (Lit.:170  $^\circ\text{C}$ ).<sup>33</sup>

IR ( $\text{CHCl}_3$ ,  $\text{cm}^{-1}$ ) : 3320 (-OH stretching).

<sup>1</sup>H-NMR (DMSO-d<sub>6</sub>), δ (ppm): 6.91(d, 1 H(e), Ar-H *ortho* to CH<sub>3</sub>), 6.84 (d, 1 H(a), Ar-H *ortho* to CH<sub>3</sub>), 6.72 (d, 1 H, Ar-H *para* to CH<sub>3</sub>), 6.68 (d, 1 H, Ar-H *para* to CH<sub>3</sub>), 6.57(d, 2 H, Ar-H *ortho*- to OH), 2.10 (s, 3H (e), Ar-CH<sub>3</sub>), 2.06 (s, 3 H(a), Ar-CH<sub>3</sub>), 1.14 – 2.04 (m, 16 H, CH<sub>2</sub> and CH).

### 3.3.3.2 Synthesis of 1,1- bis-(4-cyanato-3-methylphenyl)decahydronaphthalene

Into a 100 mL three-necked round bottom flask equipped with a magnetic stirring bar, a pressure equalizing dropping funnel and a thermowell were added cyanogen bromide (4.46 g, 0.04 mol) and 1,1- bis-(4-hydroxy-3-methylphenyl)decahydronaphthalene (7.0 g, 0.02 mol). The reactants were dissolved in acetone (50 mL). To the reaction mixture, freshly distilled triethylamine (stored over KOH) (5.4 mL, 0.04 mol) diluted with acetone (10 mL) was added at –15 °C over a period of 20 minutes with a constant stirring. After the completion of addition, the reaction mixture was stirred for 3 h maintaining the temperature at –15 °C and then filtered through a sintered funnel. The residue was washed with acetone (3 x 10 mL). The filtrate was concentrated under reduced pressure at room temperature and then dissolved in dichloromethane (100 mL). Dichloromethane solution was successively washed with 4% aqueous sodium chloride solution (2 x 25 mL) and water (3 x 25 mL). The dichloromethane solution was dried over sodium sulfate, filtered and concentrated on a rotary evaporator at room temperature under reduced pressure to yield a white powder. The product was recrystallized using cyclohexane.

Yield: 7.2 g (90 %).

MP: 130-132 °C.

### 3.3.4 Synthesis of 1,1- bis-(4-cyanato-3,5-dimethylphenyl)decahydronaphthalene

#### 3.3.4.1 Synthesis of 1,1- bis-(4-hydroxy-3,5-dimethylphenyl)decahydronaphthalene

Into a 500 mL round bottom flask equipped with a magnetic stirring bar were charged 2-decalone (7.6 g, 0.05 mol), 2,6-dimethylphenol (13.42 g, 0.11 mol), 3-mercaptopropionic acid (0.4 mL, 5 mmol) and a mixture of hydrochloric acid (36%) (30 mL) and glacial acetic acid (15 mL). The reaction mixture was stirred at room temperature for 48 h. The solid obtained was dissolved in ethyl acetate (250 mL) and washed successively with aqueous sodium bicarbonate solution (3 x 100 mL), brine (2 x 100 mL) and water (2 x 100 mL). Ethyl acetate layer was dried over sodium sulfate and filtered. Ethyl acetate was removed on a rotary evaporator under reduced pressure. The crude product was purified by recrystallization using toluene.

Yield: 11 g (60 %).

MP: 222 °C. (Lit.: 222 °C).<sup>33</sup>

IR (CHCl<sub>3</sub>, cm<sup>-1</sup>) : 3335 (-OH stretching).

<sup>1</sup>H-NMR (DMSO-d<sub>6</sub>), δ (ppm): 6.94 (d, 2 H(e), *meta* to -OH), 6.84 (d, 2 H(a), Ar-H *meta* to -OH), 4.43 (s, 2H, -OH), 2.23 (s, 6 H(e), Ar-CH<sub>3</sub>), 2.18 (s, 6 H(a), Ar-CH<sub>3</sub>), 1.25 – 2.11(m, 16 H, CH<sub>2</sub> and CH).

#### 3.3.4.2 Synthesis of 1,1- bis-(4-cyanato-3,5-dimethylphenyl)decahydronaphthalene

Into a 100 mL three-necked round bottom flask equipped with a magnetic stirring bar, a pressure equalizing dropping funnel and a thermowell were added cyanogen bromide (4.46 g, 0.04 mol) and 1,1- bis-(4-hydroxy-3,5-dimethylphenyl)decahydronaphthalene (7.56 g, 0.02 mol). The reactants were dissolved in acetone (50 mL). To the reaction mixture, freshly distilled triethylamine (stored over KOH) (5.4 mL, 0.04 mol) diluted with acetone (10 mL) was added at -15 °C over a period of 20 minutes with a constant stirring. After the completion of addition, the reaction mixture was stirred for 3 h maintaining the temperature at -15 °C and then filtered through a sintered funnel. The residue was washed with acetone (3 x 10 mL). The filtrate was concentrated under reduced pressure at room temperature and then dissolved in dichloromethane (100 mL). Dichloromethane solution was washed with 4% aqueous sodium chloride solution (2 x 25 mL) followed by water (3 x 25 mL). The dichloromethane solution was dried over sodium sulfate, filtered and concentrated on a rotary evaporator at room temperature under reduced pressure to yield a white powder. The product was recrystallized using cyclohexane.

Yield: 7.7 g (90 %).

MP: 145 - 146 °C.

#### 3.3.5 Synthesis of 1,1-bis(4-cyanatophenyl)-4-perhydrocumyl cyclohexane

##### 3.3.5.1 Synthesis of 4-perhydrocumyl cyclohexanol from *p*-cumyl phenol

*p*-Cumyl phenol (40.0 g, 0.19 mol) was placed in a Parr reactor (300 mL capacity) and dissolved in isopropanol (120 mL). Ru/C (0.8 g, 2 wt %) was added. Hydrogenation was carried out at 120 °C / 700 psi hydrogen pressure. The reaction was continued until there was no further absorption of hydrogen (2 h). The catalyst was separated by filtering the reaction mixture through Whatman filter paper. Isopropyl alcohol was stripped off and the product was dried under reduced pressure to afford a white solid.

Yield: 41.3 g (97 %),

MP: 63 - 64 °C. (Lit.:63 - 64 °C).<sup>31,34</sup>

IR (CHCl<sub>3</sub>, cm<sup>-1</sup>) : 3275 (-OH stretching).

<sup>1</sup>H-NMR (CDCl<sub>3</sub>): δ (ppm), 3.96 – 4.08 (m, H (e), CH), 3.47 - 3.57 (m, H (a) CH), 0.77 – 2.38 (m, 20 H, CH<sub>2</sub> and CH of cyclohexyl ring), 0.71 (s, 6 H, CH<sub>3</sub>).

### 3.3.5.2 Synthesis of 4-perhydrocumyl cyclohexanone from 4-perhydrocumyl cyclohexanol

Into a 2-L two-necked round bottom flask equipped with an overhead stirrer were added a finely ground mixture of pyridinium chlorochromate (57.86 g, 0.27 mol) and silica gel (57.86 g) and chloroform (500 mL). To the reaction mixture, 4-perhydrocumyl cyclohexanol (40 g, 0.18 mol) dissolved in chloroform (500 mL), was added at 0 °C. The reaction mixture was stirred at 0 °C for 4 h and then filtered through a sintered funnel. The residue was washed several times with chloroform. All the washings were combined and concentrated to around 1 L. The solution was then passed through a bed of celite-silica gel. Chloroform solution was successively washed with aqueous sodium bicarbonate solution (2 x 100 mL), brine (2 x 100 mL) and water (2 x 100 mL) and dried over sodium sulfate and filtered. The solvent was removed by distillation to yield a white solid. The product was purified by distillation at 135 °C / 0.02 mm Hg.

Yield: 36.4 g (92 %).

IR (CHCl<sub>3</sub>, cm<sup>-1</sup>) : 1720 (C=O stretching).

MP: 88 - 89 °C. (Lit.: 88 - 89 °C).<sup>31,34</sup>

<sup>1</sup>H-NMR (CDCl<sub>3</sub>): δ (ppm), 2.28 – 2.48 (m, 4H, CH<sub>2</sub> α to C=O), 0.91 – 2.11 (m, 16 H, CH<sub>2</sub> and CH of cyclohexyl ring), 0.77 (s, 6 H, CH<sub>3</sub>).

### 3.3.5.3 Synthesis of 1,1-bis(4-hydroxyphenyl)-4-perhydrocumylcyclohexane from 4-perhydrocumyl cyclohexanone and phenol

Into a 250 mL three-necked round bottom flask equipped with a magnetic stirring bar and a gas inlet and outlet were added 4 -perhydrocumyl cyclohexanone (11.1 g, 0.05 mol), phenol (23.5 g, 0.25 mol) and 3-mercaptopropionic acid (0.4 mL, 5 mmol). The reaction mixture was stirred at 40°C for 12 h. Anhydrous hydrogen chloride gas was bubbled through the reaction mixture. After 12 h, the reaction mixture solidified. The reaction mixture was dissolved in ethyl acetate (500 mL) and successively washed with an aqueous sodium bicarbonate solution (3 x 100 mL), brine (3 x 100 mL) and water ( 2 x 100 mL). The ethyl acetate solution was dried over sodium sulfate, and filtered. Ethyl acetate was removed by distillation under reduced pressure to obtain a brown viscous liquid which was washed with pet ether to remove phenol. The crude bisphenol was recrystallized using a mixture of toluene and pet ether (70/30, v/v) to afford a white, crystalline solid.

Yield: 12.8 g (65 %).

MP: 185 °C. (Lit.: 185 °C).<sup>31,34</sup>

IR (CHCl<sub>3</sub>, cm<sup>-1</sup>) : 3295 (-OH stretching).

<sup>1</sup>H-NMR (CDCl<sub>3</sub>): δ (ppm), 7.06 (d, 2 H (e), Ar-H *meta*-to OH), 6.83 (d, 2 H (a), Ar-H *meta*-to OH), 6.71 (d, 2 H(e), Ar-H *ortho*- to OH), 6.59 (d, 2 H (a), Ar-H *ortho*-to OH), 4.55 (s, 1 H(e), OH), 4.49 (s, 1 H(a), OH), 0.90 - 2.64 (m, 20 H, CH<sub>2</sub> and CH), 0.60 (s, 6 H, CH<sub>3</sub>).

#### 3.3.5.4 Synthesis of 1,1-bis(4-cyanatophenyl)-4-perhydrocumyl cyclohexane

Into a 500 mL three-necked round bottom flask equipped with a magnetic stirring bar, a pressure equalizing dropping funnel and a thermowell were added cyanogen bromide (7.15 g, 0.07 mol) and 1,1-bis(4-hydroxyphenyl)-4-perhydrocumylcyclohexane (12 g, 0.03 mol). The reagents were dissolved in acetone (150 mL). To the reaction mixture, freshly distilled triethylamine (stored over KOH) (9.3 mL, 0.07 mol) diluted with acetone (50 mL) was added at -15 °C over a period of 30 minutes with a constant stirring. After the completion of addition, the reaction mixture was stirred at -15 °C for 3 h and then filtered through a sintered funnel. The residue was washed with acetone (3 x 20 mL). The filtrate was concentrated on a rotary evaporator under reduced pressure at room temperature and then dissolved in dichloromethane (150 mL). The product was washed with 4% aqueous sodium chloride solution (3 x 50 mL) followed by water (2 x 50 mL). Dichloromethane solution was dried over sodium sulfate, filtered and concentrated on a rotary evaporator at room temperature under reduced pressure to yield a white powder. The product was recrystallized using cyclohexane.

Yield: 11.3 g (85 %).

MP: 109-111 °C.

#### 3.3.6 Synthesis of 1,1-bis-(4-cyanato-3-methylphenyl)-4-perhydrocumyl cyclohexane

##### 3.3.6.1 Synthesis of 1,1-bis-(4-hydroxy-3-methylphenyl)-4-perhydrocumyl cyclohexane from 4-perhydrocumyl cyclohexanone and *o*-cresol

Into a 250 mL three-necked round bottom flask equipped with a magnetic stirring bar and a gas inlet and outlet were added 4-perhydrocumyl cyclohexanone (11.1 g, 0.05 mol), *o*-cresol (21.6 g, 0.2 mol) and 3-mercaptopropionic acid (0.4 mL, 5 mol). The reaction mixture was stirred at 40 °C for 12 h. Anhydrous hydrogen chloride gas was bubbled through the reaction mixture. After 12 h, the reaction mixture solidified. The reaction mixture was dissolved in ethyl acetate (250 mL) and washed successively with an aqueous sodium bicarbonate solution (3 x 75 mL), brine (3 x 75 mL) and water (3 x 75 mL). The ethyl acetate solution was dried over sodium sulfate and filtered. Ethyl acetate was removed on a rotary evaporator under reduced pressure and finally at pump to obtain a brown viscous liquid which was washed with pet ether to



remove *o*-cresol. The crude bisphenol was recrystallized using toluene to afford a white crystalline solid.

Yield: 16.2 g (77 %).

MP: 189 °C. (Lit.: 189 °C).<sup>31</sup>

IR (CHCl<sub>3</sub>, cm<sup>-1</sup>) : 3390 (-OH stretching).

<sup>1</sup>H-NMR (CDCl<sub>3</sub>): δ (ppm), 7.05 (d, 2H, Ar-H), 6.93 (d, 1H, Ar-H), 6.83 (d, 1H, Ar-H), 6.72 (d, 1H(e), Ar-H *ortho*- to OH), 6.60 (d, 1H(a), Ar-H *ortho*-to OH), 4.55 (s, 1H, OH), 4.49 (s, 1H, OH), 2.22 (s, 3 H(e), Ar-CH<sub>3</sub>), 2.17 (s, 3 H(a), Ar-CH<sub>3</sub>), 0.93 – 2.64 (m, 20 H, CH<sub>2</sub> and CH), 0.60 (s, 6 H, CH<sub>3</sub>).

### 3.3.6.2 Synthesis of 1,1-bis-(4-cyanato-3-methylphenyl)-4-perhydrocumylcyclohexane

Into a 250 mL three-necked round bottom flask equipped with a magnetic stirring bar, a pressure equalizing dropping funnel and a thermowell, were added cyanogen bromide (2.12 g, 0.02 mol) and 1,1-bis-(4-hydroxyphenyl-3-methyl)-4-perhydrocumylcyclohexane (4.2 g, 0.01 mol). The reactants were dissolved in acetone (50 mL). To the reaction mixture, freshly distilled triethylamine (stored over KOH) (2.8 mL, 0.02 mol) diluted with acetone (10 mL) was added at -15 °C over a period of 15 minutes with a constant stirring. After the completion of addition, the reaction mixture was stirred at -15 °C for 3 h and then filtered through a sintered funnel. The residue was washed with acetone (2 x 10 mL). The filtrate was concentrated on a rotary evaporator under reduced pressure at room temperature. The product was dissolved in dichloromethane (50 mL). Dichloromethane solution was washed with 4% aqueous sodium chloride solution (2 x 10 mL) followed by washing with water (3 x 10 mL). Dichloromethane solution was dried over sodium sulfate, filtered and concentrated on a rotary evaporator at room temperature under reduced pressure to yield a white powder. The product was recrystallized using cyclohexane.

Yield: 4.2 g (90 %).

MP: 144 - 146 °C.

### 3.3.7 Synthesis of 1,1- bis-(4-cyanato-3,5-dimethylphenyl) -4-perhydrocumylcyclohexane

#### 3.3.7.1 Synthesis of 1,1- bis-(4-hydroxy-3,5-dimethylphenyl)-4-perhydrocumylcyclohexane from 4-perhydrocumylcyclohexanone and 2,6-dimethylphenol

Into a 500 mL round bottom flask equipped with a magnetic stirring bar were charged 4-perhydrocumyl cyclohexanone (11.1 g, 0.05 mol), 2,6-dimethylphenol (13.42 g, 0.11 mol), 3-mercaptopropionic acid (0.4 mL, 5 mmol) and a mixture of hydrochloric acid (35-36%) (30

mL) and glacial acetic acid (15 mL). The reaction mixture was stirred at room temperature for 48 h. The solid obtained was dissolved in ethyl acetate (250 mL) and washed successively with aqueous sodium bicarbonate solution (3 x 100 mL), brine (2 x 100 mL) and water (2 x 100 mL). Ethyl acetate layer was dried over sodium sulfate and filtered. Ethyl acetate was removed on a rotary evaporator under reduced pressure. The crude product was purified by recrystallization using toluene.

Yield: 17.2 g (77 %).

MP: 213 °C. (Lit.: 213 °C).<sup>34</sup>

IR (CHCl<sub>3</sub>, cm<sup>-1</sup>) : 3390 (-OH stretching).

<sup>1</sup>H-NMR (CDCl<sub>3</sub>): δ (ppm), 6.92 (d, 2 H(e), Ar-H *meta* to -OH), 6.77 (d, 2 H(a), Ar-H *meta* to OH) 4.47 (s, 1H, OH), 4.41 (s, 1 H, OH), 2.22 (s, 6H(e), Ar-CH<sub>3</sub>), 2.15 (s, 3 H(a), Ar-CH<sub>3</sub>) 0.74 – 2.66 (m, 20 H, CH<sub>2</sub> and CH), 0.60 (s, 6 H, CH<sub>3</sub>).

### 3.3.7.2 Synthesis of 1,1- bis-(4-cyanato-3,5-dimethylphenyl)-4-perhydrocumylcyclohexane

Into a 250 mL three-necked round bottom flask equipped with a magnetic stirring bar, a pressure equalizing dropping funnel and a thermowell were added cyanogen bromide (2.12 g, 0.02 mol) and 1,1-bis-(4-hydroxyphenyl,3,5-dimethyl)-4-perhydrocumylcyclohexane (4.48 g, 0.01 mol). The reactants were dissolved in acetone (50 mL). To the reaction mixture, freshly distilled triethylamine (stored over KOH) (2.8 mL, 0.02 mol) diluted with acetone (10 mL) was added at -15 °C over a period of 15 minutes with a constant stirring. After the completion of addition, the reaction mixture was stirred at -15 °C for 3 h. To the reaction mixture, water (25 mL) was added and the precipitate was filtered. The residue was dissolved in dichloromethane (50 mL). Dichloromethane solution was washed with 4% aqueous sodium chloride solution (3 x 10 mL) followed by washing with water (3 x 10 mL). Dichloromethane solution was dried over sodium sulfate, filtered and dichloromethane was evaporated on a rotary evaporator at room temperature under reduced pressure to yield a white powder. The product was recrystallized using acetone.

Yield: 4.2 g (85 %).

MP: 210 - 211 °C.

### 3.3.8 Synthesis of 1,1-bis(4-cyanatophenyl)cyclohexane

#### 3.3.8.1 Synthesis of 1,1-bis(4-hydroxyphenyl)cyclohexane from cyclohexanone and phenol

Into a 500 mL three-necked round bottom flask equipped with an overhead stirrer and a gas inlet and outlet were added cyclohexanone (40 g, 0.4 mol), phenol (150.4 g, 1.6 mol) and 3-

mercaptopropionic acid (3.3 mL, 0.04 mol). Anhydrous hydrogen chloride was bubbled through the reaction mixture at room temperature. After 1/2 h, the reaction mixture solidified. The reaction mixture was dissolved in ethyl acetate (500 mL) and washed successively with an aqueous sodium bicarbonate solution (4 x 100 mL), brine (2 x 100 mL) and water (2 x 100 mL) and ethyl acetate solution was dried over sodium sulfate and filtered. Evaporation of ethyl acetate on a rotary evaporator under reduced pressure yielded a pink solid. The product was washed with pet ether to remove phenol and the crude product was recrystallized using a mixture of toluene and pet ether (80/20, v/v) to afford a white solid.

Yield: 75 g (70 %)

MP: 190 - 191 °C. (Lit. 190-192 °C).<sup>35</sup>

IR (CHCl<sub>3</sub>, cm<sup>-1</sup>): 3280 (-OH stretching).

<sup>1</sup>H-NMR (DMSO-d<sub>6</sub>): δ (ppm) 7.03 (d, 4 H, Ar-H *meta* to -OH), 6.72 (d, 4 H, Ar-H *ortho* to -OH), 1.49 – 2.16 (m, 10 H, CH<sub>2</sub>).

### 3.3.8.2 Synthesis of 1,1-bis(4-cyanatophenyl)cyclohexane

Into a 1-L three-necked round bottom flask equipped with an overhead stirrer, a pressure equalizing dropping funnel and a thermowell were added cyanogen bromide (22.57 g, 0.22 mol) and 1,1-bis(4-hydroxyphenyl)cyclohexane (26.8 g, 0.1 mol). The reactants were dissolved in acetone (500 mL). To the reaction mixture, freshly distilled triethylamine (stored over KOH) (29.7 mL, 0.22 mol) diluted with acetone (100 mL) was added at -15 °C over a period of 30 minutes with a constant stirring. After the completion of addition, the reaction mixture was stirred at -15 °C for 3 h and then filtered through a sintered funnel. The residue was washed with acetone (100 mL). The filtrate was concentrated under reduced pressure at room temperature and then dissolved in dichloromethane (500 mL), washed with 4% aqueous sodium chloride solution (3 x 100 mL) followed by washing with water (2 x 75 mL) and dried over sodium sulfate and filtered. Dichloromethane solution was passed through a bed of silica gel-celite and concentrated on a rotary evaporator at room temperature under reduced pressure to yield a white powder.

Yield: 25 g (80 %).

MP: 57 - 58 °C. (Lit. 58.5 - 59.5 °C).<sup>2</sup>

IR (CHCl<sub>3</sub>, cm<sup>-1</sup>): 2269 and 2240 (-OCN stretching).

<sup>1</sup>H-NMR (CDCl<sub>3</sub>): δ (ppm) 7.31 (d, 4 H, Ar-H *meta* to -OH), 7.20(d, 4 H, Ar-H *ortho* to -OH), 1.45 – 2.30 (m, 10 H, CH<sub>2</sub>).

### 3.3.9 Synthesis of 2,7-bis(4-cyanatophenyl)-2,7-dimethyloctane

#### 3.3.9.1 Synthesis of dimethyl adipate from adipic acid

Into a single-necked 500 mL round bottom flask equipped with a reflux condenser and a magnetic stirring bar were added adipic acid (20 g, 0.14 mol), methanol (200 mL, molar excess), and concentrated sulphuric acid (1.0 g, 5 wt% based on adipic acid) and the reaction mixture was refluxed for 24 h. The excess methanol was distilled off and the reaction mixture was dissolved in ethyl acetate (100 mL). The ethyl acetate layer was washed successively with saturated aqueous solution of sodium bicarbonate (3 x 25 mL), brine (3 x 25 mL) and water (2 x 25 mL). The ethyl acetate layer was dried over sodium sulfate, filtered and concentrated on rotary evaporator to afford a white product.

Yield: 15 g (60%).

MP : 174 °C. (Lit. 174 °C).<sup>36</sup>

IR : 1740 (C=O), 1260 (-C-O-C-).

#### 3.3.9.2 Synthesis of 2,7-bishydroxy-2,7-dimethyloctane from dimethyl adipate

Into a three-necked 250 mL round bottom flask equipped with a reflux condenser, a dropping funnel, a nitrogen-filled balloon, and a magnetic stirring bar were added dimethyl adipate (8.7 g, 0.05 mol) and diethyl ether (20 mL). To the reaction mixture was added 2 M Grignard reagent [which was prepared from magnesium turnings (9.6 g, 0.2 mol), and methyl iodide (28.4 g or 5.75 mL, 0.2 mol) in dry diethyl ether (100 mL) at 0°C] very slowly ensuring that the temperature remains at 0°C. The reaction was continued for 12 h. After 12 h, the reaction mixture was refluxed for 1h, cooled and then poured into aqueous ammonium chloride solution (80 mL). The mixture was stirred for 30 minutes and then extracted with diethyl ether. Diethyl ether solution was dried over sodium sulfate, filtered, and concentrated on rotary evaporator. The crude compound was recrystallized using pet ether.

Yield: 6.96 g (80 %).

MP: 87°C. (Lit. 87 °C).<sup>36</sup>

IR : 3360 (-OH).

#### 3.3.9.3 Synthesis of 2,7-bis(4-hydroxyphenyl)-2,7-dimethyloctane from 2,7-bishydroxy-2,7-dimethyloctane

Into a 100 mL three-necked round bottom flask equipped with a magnetic stirring bar and a gas inlet-outlet were added 2,7-bishydroxy-2,7-dimethyloctane (3.48 g, 0.02 mol), phenol (11.28 g, 0.12 mol) and 3-mercaptopropionic acid (0.2 mL, 2 mmol). Anhydrous hydrogen chloride was

bubbled through the reaction mixture at 50 °C. After 12 h, the reaction mixture was dissolved in ethyl acetate (75 mL) and washed successively with an aqueous sodium bicarbonate solution (4 x 25 mL), brine (2 x 25 mL) and water (2 x 25 mL) and ethyl acetate solution was dried over sodium sulfate and filtered. Evaporation of ethyl acetate on a rotary evaporator under reduced pressure yielded a pink solid. The product was washed with pet ether to remove phenol and the crude product was recrystallized using a mixture of toluene and pet ether (80/20, v/v) to afford a white solid.

Yield: 4.33 g (66 %)

MP: 137-138 °C. (Lit. 137-138 °C)<sup>36, 37</sup>.

#### **3.3.9.4 Synthesis of 2,7-bis(4-cyanatophenyl)-2,7-dimethyloctane**

Into a 250 mL three-necked round bottom flask equipped with a magnetic stirring bar, a pressure equalizing dropping funnel and a thermowell were added cyanogen bromide (2.39 g, 0.02 mol) and 2,7-bis(4-hydroxyphenyl)-2,7-dimethyloctane (3.28 g, 0.01 mol). The reactants were dissolved in acetone (50 mL). To the reaction mixture, freshly distilled triethylamine (stored over KOH) (3.0 mL, 0.2 mol) diluted with acetone (10 mL) was added at -15 °C over a period of 15 minutes with a constant stirring. After the completion of addition, the reaction mixture was stirred at -15 °C for 3 h and then filtered through a sintered funnel. The residue was washed with acetone (2 x 10 mL). The filtrate was concentrated on a rotary evaporator under reduced pressure at room temperature and then dissolved in dichloromethane (50 mL), washed with 4% aqueous sodium chloride solution (3 x 20 mL) followed by washing with water (2 x 20 mL) and dried over sodium sulfate and filtered. Dichloromethane solution was passed through a bed of silica gel-celite and concentrated on a rotary evaporator at room temperature under reduced pressure to yield a white powder.

Yield: 3.1 g (80 %).

MP: 52 - 53 °C.

### **3.4 Results and Discussion**

#### **3.4.1 Synthesis and characterization of cyanate ester monomers containing cycloaliphatic “cardo” group.**

##### **3.4.1.1 Synthesis and characterization of cyanate ester monomer starting from 3-pentadecylphenol.**

A new CE monomer *viz*; 1,1-bis(4-cyanatophenyl)-3-pentadecylcyclohexane, containing pendent flexible pentadecyl chain was synthesized starting from 3-pentadecylphenol which in turn was obtained from cashew nut shell liquid making use of simple organic transformations

like hydrogenation, oxidation, acid-catalyzed condensation with phenol and cyanation. **Scheme 3.1** depicts the route followed for the synthesis of 1,1-bis(4-cyanatophenyl)-3-pentadecyl cyclohexane.

3-Pentadecylphenol was hydrogenated using 5 % Ru/C in a Parr reactor. The reduction of 3-pentadecyl phenol gives a mixture of *cis*- and *trans*-3-pentadecylcyclohexanol.<sup>30</sup> 3-Pentadecylcyclohexanol was characterized by FT-IR, and <sup>1</sup>H-NMR spectroscopy. The disappearance of the band corresponding to aromatic C=C stretching ( $\approx 1600\text{ cm}^{-1}$ ) in FT-IR spectrum indicated the reduction of aromatic ring. The O-H stretching vibration was observed at  $3335\text{ cm}^{-1}$ . The complete reduction of aromatic ring was further indicated by the disappearance of peaks corresponding to aromatic protons (in the region 6.65 - 7.18 ppm) in <sup>1</sup>H-NMR spectrum of 3-pentadecylcyclohexanol.

Various reagents *viz*; high valent chromium, and manganese compounds, hypervalent iodine compounds, peracids or sodium hypochlorite, H<sub>2</sub>O<sub>2</sub>, O<sub>2</sub>, and/air etc., have been reported to be efficient for the oxidation of alcohols to aldehydes and ketones.<sup>38</sup> In the present study, pyridinium chlorochromate (PCC) was used for oxidation of 3-pentadecylcyclohexanol because of its easy and safe preparation as well as its utility for moderate to large scale oxidations.

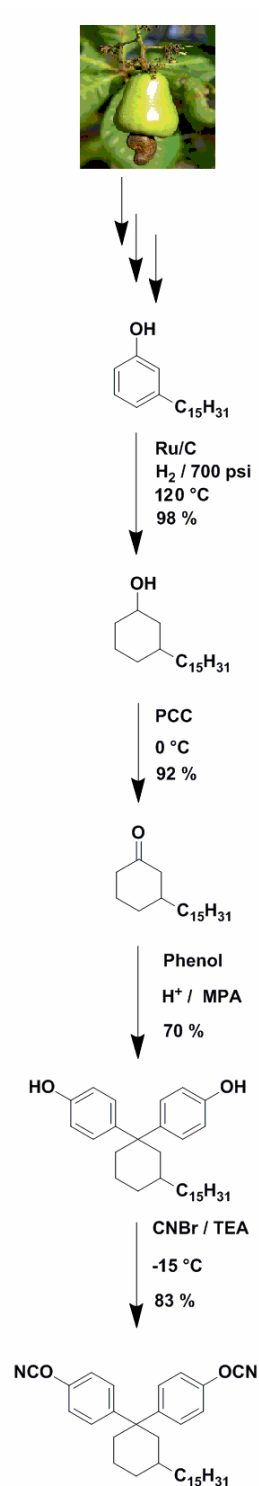
The oxidation of 3-pentadecylcyclohexanol to 3-pentadecylcyclohexanone was confirmed by the absence of hydroxyl band at  $3335\text{ cm}^{-1}$  and by the appearance of characteristic carbonyl stretching at  $1705\text{ cm}^{-1}$  in IR spectrum. 3-Pentadecylcyclohexanone was purified by distillation ( $60 - 62\text{ }^{\circ}\text{C} / 0.02\text{ mm Hg}$ ) so as to get rid of metal impurities like chromium; the presence of which in ppm level would affect curing reaction of cyanate ester.

3-Pentadecylcyclohexanone was condensed with phenol using hydrogen chloride/3-mercaptopropionic acid catalyst system to obtain 1,1-bis(4-hydroxyphenyl)-3-pentadecyl cyclohexane (BPC15). The role of 3-mercaptopropionic acid for this reaction has been investigated in detail by various researchers<sup>39,40</sup>. When 3-mercaptopropionic acid is used in combination with other strong acids for the condensation, the rate and the selectivity for the formation of desired bisphenol (*p,p'*-isomer) increases. The formation of bisphenol BPC15 was confirmed by IR and <sup>1</sup>H-NMR spectroscopy. IR spectrum showed a broad band at  $3290\text{ cm}^{-1}$  corresponding to hydroxyl stretching.

The cyanation of bisphenol was carried out by following the protocol developed by Grigat and Putter<sup>1,2</sup>. The reaction involved the addition of triethylamine to bisphenol-cyanogen bromide mixture at  $-15\text{ }^{\circ}\text{C}$ . The triethyl ammonium halide salt precipitated in acetone as the reaction progressed. The reaction temperature plays a crucial role since at higher temperatures,

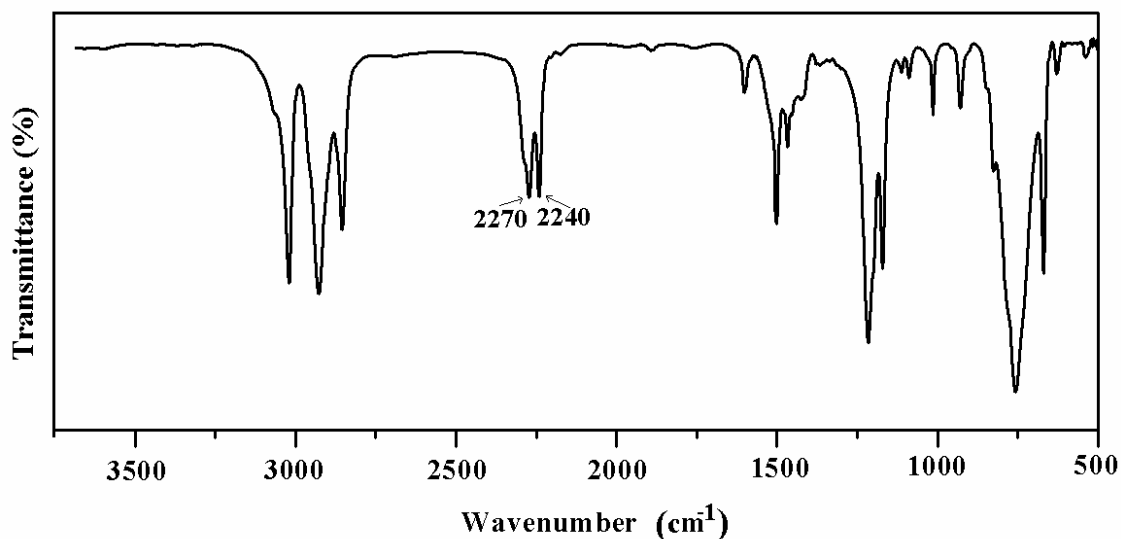
Von Braun reaction is reported to compete with cyanate forming reaction producing diethylcyanamide; an undesirable by-product.

1,1-Bis(4-cyanatophenyl)-3-pentadecylcyclohexane (BPC15CN) was characterized by FTIR,  $^1\text{H-NMR}$ , and  $^{13}\text{C-NMR}$  spectroscopy.



Scheme 3.1 : Synthesis of 1,1-bis(4-cyanatophenyl)-3-pentadecylcyclohexane

**Figure 3.1** represents IR spectrum of BPC15CN. IR spectrum indicated complete conversion of bisphenol as the hydroxyl O-H stretching band at  $3290\text{ cm}^{-1}$  was absent. The characteristic triple bond stretching in -OCN group was observed at  $2270\text{ cm}^{-1}$  and  $2240\text{ cm}^{-1}$ .

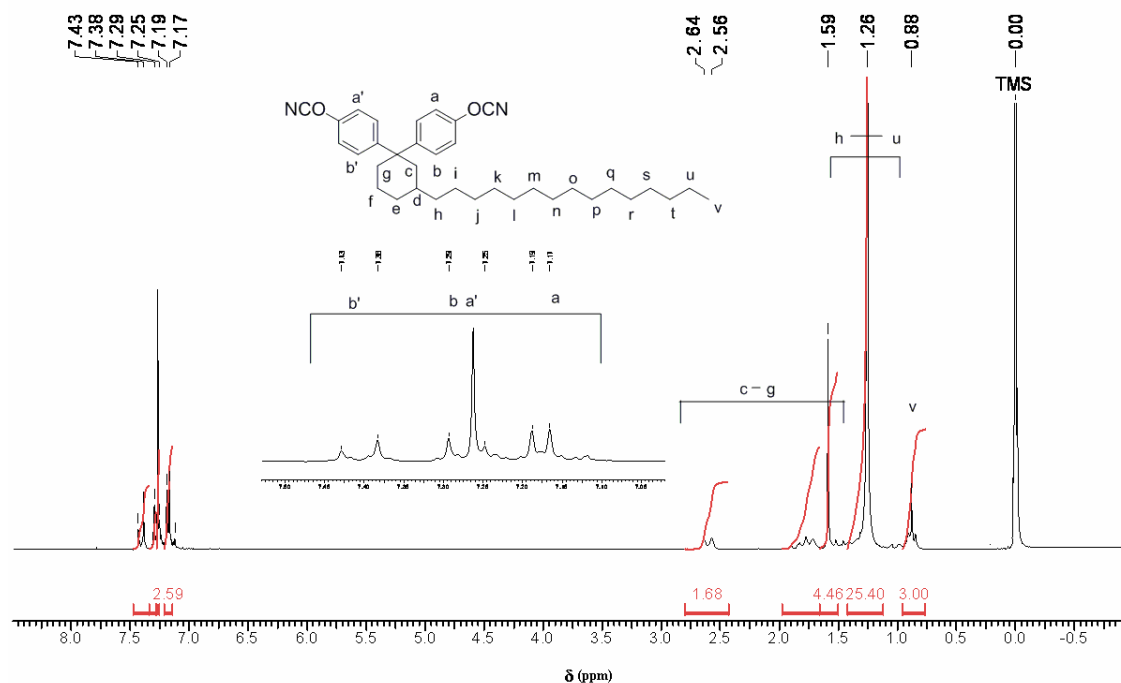


**Figure 3.1 :** IR spectrum of 1,1-bis(4-cyanatophenyl)-3-pentadecylcyclohexane

**Figure 3.2** illustrates  $^1\text{H-NMR}$  spectrum of BPC15CN. The monomer BPC15CN is not symmetrical about  $\text{C}_2$  axis between the two phenyl rings and this asymmetry results in different environment for the two phenyl rings. The pentadecyl chain substituent at cyclohexyl ring prevents ring inversion making thereby distinction between axial and equatorial phenyl rings possible. Aromatic protons a, a' and b, b' therefore showed separate sets of doublets. Generally, the protons of equatorial ring appear at lower field compared to the corresponding protons of axial ring. Aromatic proton labeled as a (*ortho* to -OCN group of axial phenyl ring) showed a doublet at 7.18 ppm while the proton b' (*meta* to -OCN group of equatorial phenyl ring) appeared as a doublet at 7.41 ppm. The proton a' (*ortho* to -OCN group of equatorial phenyl ring) and b (*meta* to -OCN group of axial phenyl ring) appeared in the region 7.19 - 7.29 ppm as closely placed two doublets. The signals observed in the range 1.26 - 2.37 ppm could be attributed to the protons of methylene and methine groups of cyclohexyl ring and pentadecyl side chain. A triplet appeared at 0.88 ppm could be assigned to the protons of terminal methyl group.

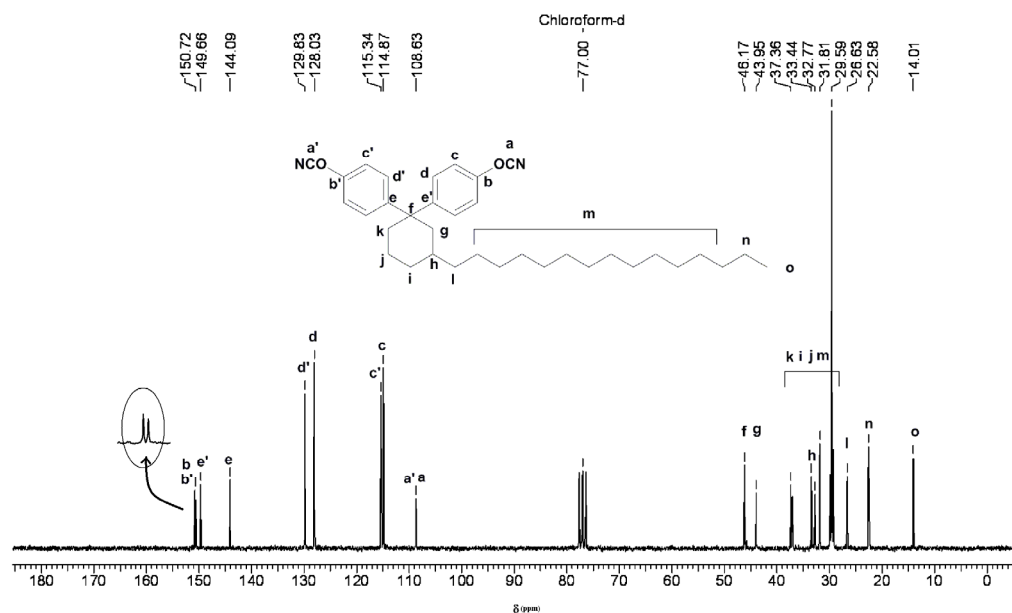
The aryl protons of BPC15CN were observed to have shifted downfield by ca. 0.3 - 0.4 ppm as compared to the aryl protons of the precursor bisphenol BPC15 as a result of the incorporation of cyanate group. This is consistent with the observations in the literature.<sup>28, 41, 42.</sup>





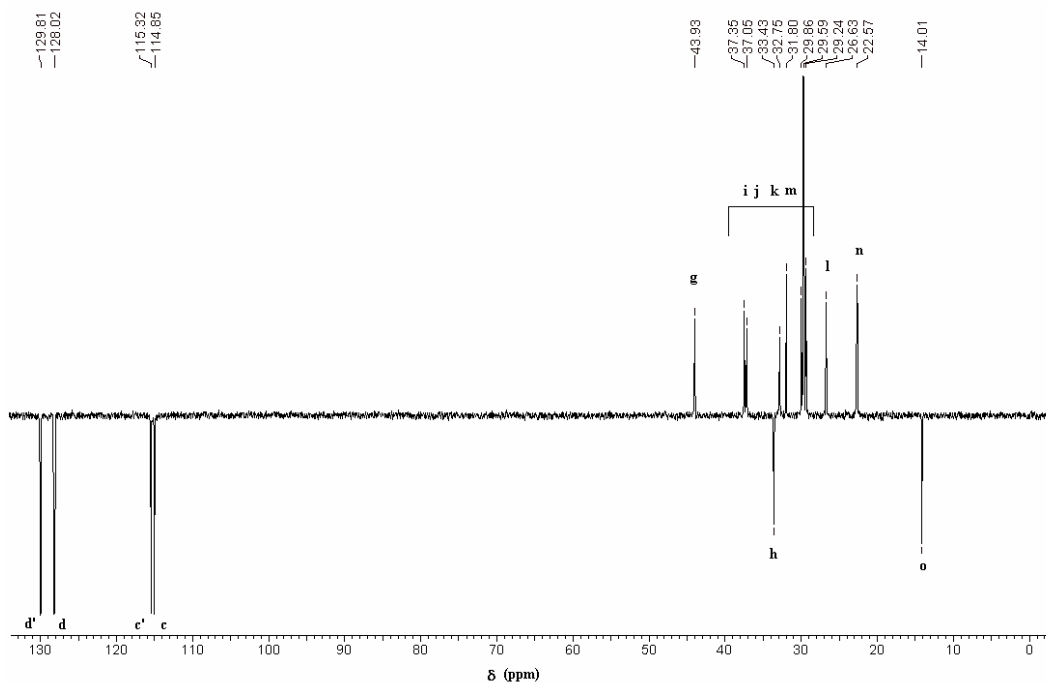
**Figure 3.2:**  $^1\text{H-NMR}$  spectrum of 1,1-bis(4-cyanatophenyl)-3-pentadecylcyclohexane ( $\text{CDCl}_3$ ).

**Figure 3.3** represents  $^{13}\text{C-NMR}$  of spectrum of BPC15CN. The peak appeared at 108.63 ppm corresponding to cyanate carbon confirmed the formation of BPC15CN. Aromatic carbons (b, b', c, c', d, d', e, and e') appeared in two sets confirming the presence of axial and equatorial phenyl rings. Aromatic carbons b, b' (attached to cyanate group) appeared at 150.58 (axial) and 150.72 (equatorial) ppm. The signals corresponding to aromatic carbons c, c' (*ortho* to cyanate group) were observed at 114.87 (axial) and 115.34 (equatorial) ppm. The peaks due to aromatic carbons d, d' (*meta* to cyanate group) appeared at 128.03 (axial) and 129.83 (equatorial) ppm. Aromatic carbons e, e' (*para* to cyanate group) showed signals at 144.09 (axial) and 149.66 (equatorial) ppm. The spectroscopic data of BPC15 has been thoroughly discussed in the literature<sup>31</sup>. The precursor bisphenol; BPC15 also showed the presence of distereotopic phenyl rings, which are magnetically non-equivalent.



**Figure 3.3:**  $^{13}\text{C}$ -NMR spectrum of 1,1-bis(4-cyanatophenyl)-3-pentadecylcyclohexane ( $\text{CDCl}_3$ )

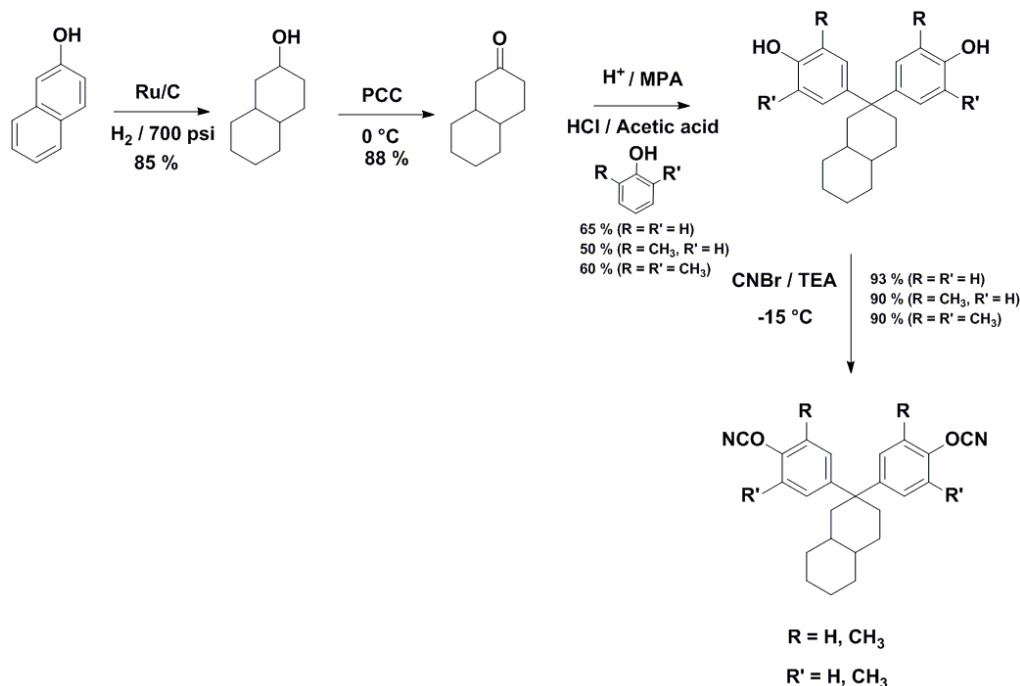
The assignments were further confirmed by  $^{13}\text{C}$ -DEPT spectrum (Figure 3.4). The peaks due to methine carbons (c, c', d, d' and h) and methyl carbon (o) were observed in negative phase while the signals due to methylene carbons g, i, j, k, l, m and n were observed in positive phase. The peaks due to quaternary carbons (a, a', b, b', e, e', and f) were absent.



**Figure 3.4:**  $^{13}\text{C}$ -DEPT NMR spectrum of 1,1-bis(4-cyanatophenyl)-3-pentadecylcyclohexane. ( $\text{CDCl}_3$ )

### 3.4.1.2 Synthesis and characterization of cyanate ester monomers starting from $\beta$ -naphthol

Three new CE monomers containing decahydronaphthalene moiety with systematic variation in the structure *viz.*: 1,1-bis(4-cyanato phenyl)decahydronaphthalene (BPDCCN), 1,1-bis(4-cyanato-3-methylphenyl)decahydronaphthalene (DMBPDCCN) and 1,1-bis(4-cyanato-3-5-dimethylphenyl) decahydronaphthalene (TMBPDCCN) were synthesized starting from  $\beta$ -naphthol as shown in **Scheme 3.2**.



**Scheme 3.2** : Synthesis of cyanate ester monomers starting from  $\beta$ -naphthol

The precursor bisphenols *viz.*; 1,1-bis(4-hydroxyphenyl) decahydronaphthalene (BPDC), 1,1-bis(4-hydroxy-3-methylphenyl)decahydronaphthalene (DMBPDC) and 1,1-bis(4-hydroxy-3-5-dimethylphenyl) decahydronaphthalene (TMBPDC) were synthesized according to the reported procedure.<sup>33</sup>

In the first step,  $\beta$ -naphthol was hydrogenated using 5 % Ru/C in a Parr reactor to afford decahydro-2-naphthol which was characterized by FTIR, and <sup>1</sup>H-NMR spectroscopy. The absence of band corresponding to aromatic C=C stretching ( $\approx 1600 \text{ cm}^{-1}$ ) in FTIR spectrum indicated the complete reduction of aromatic ring. The O-H stretching vibration was observed at  $3340 \text{ cm}^{-1}$ . The absence of peaks corresponding to aromatic protons in <sup>1</sup>H-NMR spectrum also confirmed the complete reduction of  $\beta$ -naphthol into decahydro-2-naphthol.

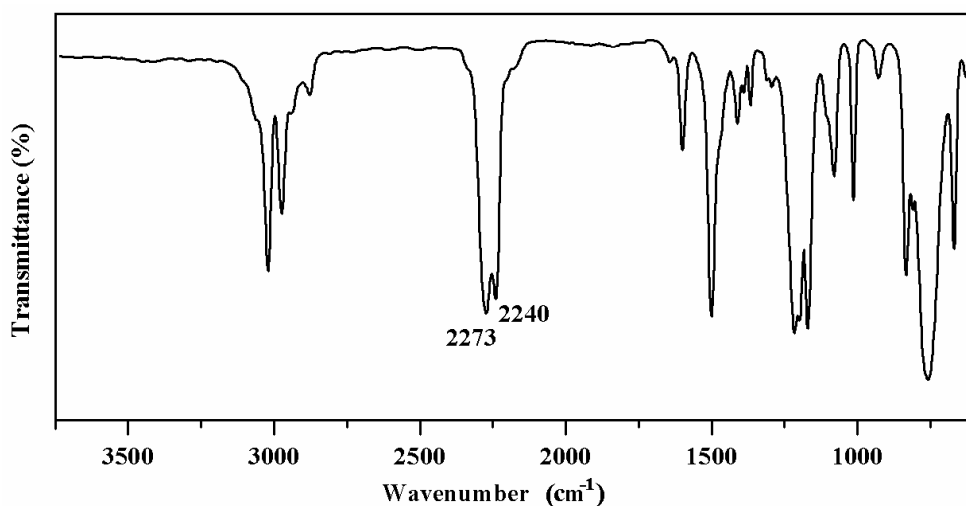
In the next step, decahydro-2-naphthol was oxidized to 2-decalone using PCC. The conversion was confirmed by the absence of hydroxyl band ( $3340 \text{ cm}^{-1}$ ) and by the presence of

characteristic carbonyl stretching at  $1716\text{ cm}^{-1}$  in FT-IR spectrum. 2-Decalone was purified by distillation ( $62 - 65\text{ }^{\circ}\text{C} / 0.03\text{ mm Hg}$ ).

2-Decalone was then condensed with phenol, *o*-cresol and 2,6-dimethylphenol to obtain BPDC, DMBPDC and TMBPDC, respectively. The formation of these bisphenols was confirmed by IR and  $^1\text{H-NMR}$  spectroscopy.

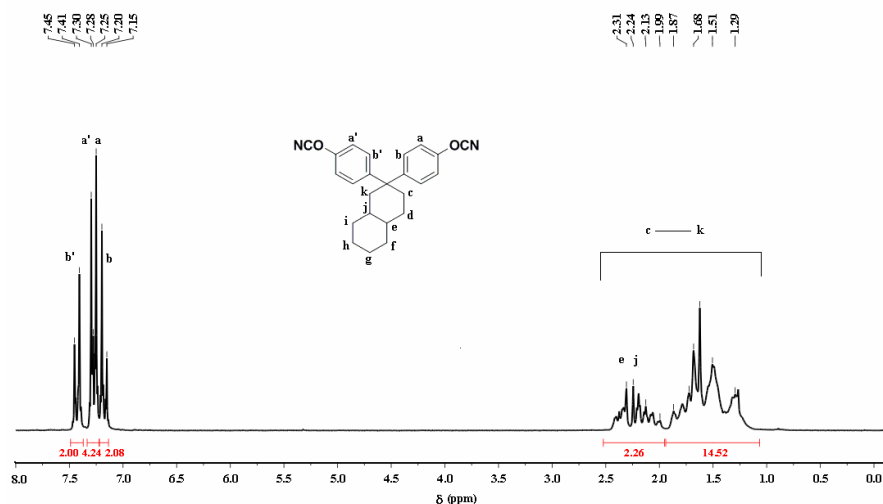
These bisphenols were then converted into corresponding cyanate esters BPDCCN, DMBPDCCN and TMBPDCCN using triethyl amine and cyanogen bromide (section 3.3.2 – 3.3.4).

BPDCCN was characterized by FT-IR,  $^1\text{H-NMR}$  and  $^{13}\text{C-NMR}$  spectroscopy. **Figure 3.5** shows FT-IR spectrum of BPDCCN. The characteristic  $\text{C}\equiv\text{N}$  stretchings were observed at  $2273\text{ cm}^{-1}$  and  $2240\text{ cm}^{-1}$ .



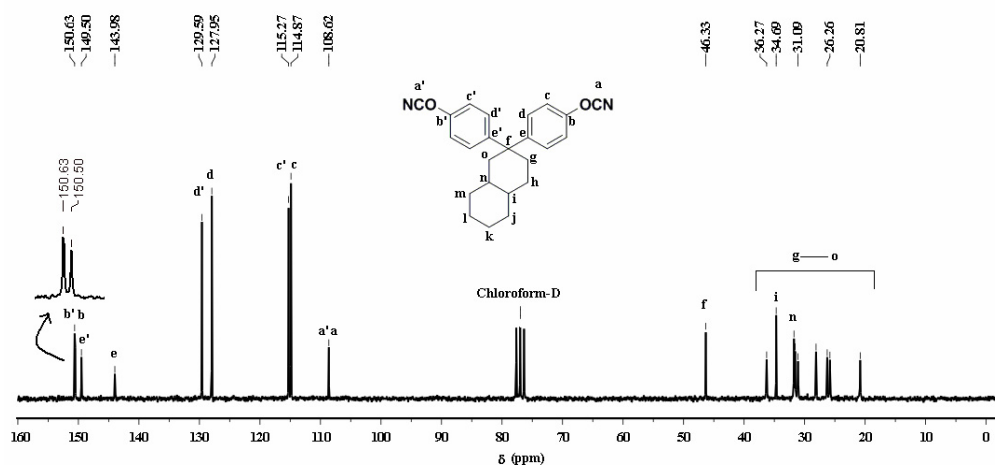
**Figure 3.5 : IR spectrum of 1,1-bis(4-cyanatophenyl)decahydronaphthalene.**

**Figure 3.6** displays  $^1\text{H-NMR}$  spectrum of BPDCCN. As observed for the precursor bisphenol, the two phenyl rings are magnetically non-equivalent in case of BPDCCN. The aromatic protons (a, a' b, and b') therefore appeared as four sets of doublets. Aromatic proton; a (*ortho* to  $-\text{OCN}$  group and axial phenyl ring) appeared as doublet at  $7.25\text{ ppm}$  while a' (*ortho* to  $-\text{OCN}$  group group and equatorial phenyl ring) displayed a doublet at  $7.30\text{ ppm}$ . A doublet observed at  $7.17\text{ ppm}$  could be assigned to aromatic proton b (*meta* to  $-\text{OCN}$  group and axial phenyl ring) while the doublet appeared at  $7.43\text{ ppm}$  could be due to aromatic proton b' (*meta* to  $-\text{OCN}$  group and equatorial phenyl ring). The peaks observed in the range  $1.29 - 2.31\text{ ppm}$  could be due to methylene and methine protons of decahydronaphthalene ring.



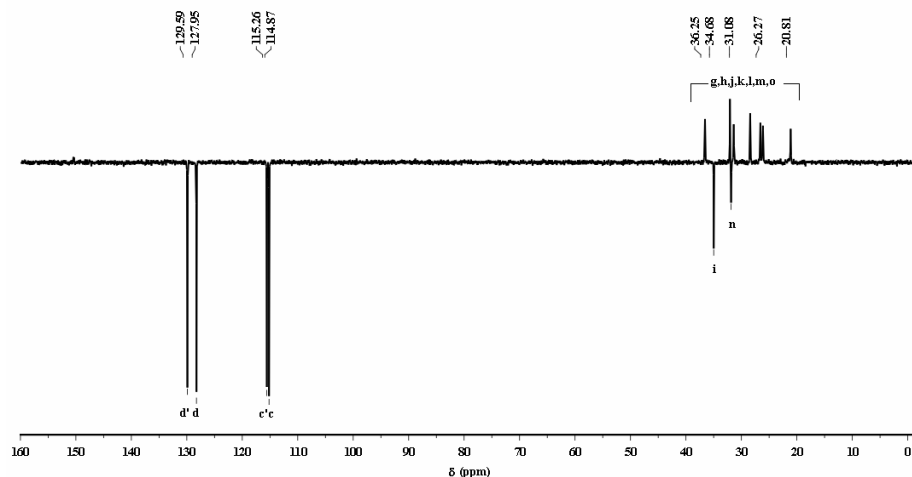
**Figure 3.6 :**  $^1\text{H-NMR}$  spectrum of 1,1-bis(4-cyanatophenyl)decahydronaphthalene ( $\text{CDCl}_3$ ).

**Figure 3.7** represents  $^{13}\text{C-NMR}$  spectrum of BPDCCN along with peak assignments. The peak corresponding to the carbon of cyanate functionality appeared at 108.62 ppm. Aromatic carbons b, b' (attached to cyanate group) showed peaks at 150.50 (axial phenyl ring) and 150.60 (equatorial phenyl ring) ppm. The peaks due to aromatic carbons c, c' (*ortho* to cyanate group) were observed at 115.20 (axial phenyl ring) and 115.27 (equatorial phenyl ring) ppm. Aromatic carbons d, d' (*meta* to cyanate group) showed a signal at 127.95 (axial phenyl ring) and 129.59 (equatorial phenyl ring) ppm. The peaks observed at 143.98 and 149.50 ppm could be attributed to carbons *para* to cyanate group (labeled as e and e') of axial and equatorial phenyl rings, respectively. The peaks appeared in the range 20.81 – 46.33 ppm could be due to aliphatic carbons of decahydronaphthalene moiety. The peak observed at 46.33 ppm could be due to the quaternary carbon f. The methine carbons labeled as i and n displayed peaks at 31.06 and 34.69 ppm, respectively. The peaks at 20.81, 25.81, 26.26, 28.11, 31.57, 31.76 and 36.27 ppm could be due to methylene carbons marked as g, h, j, k, l, m, and o.



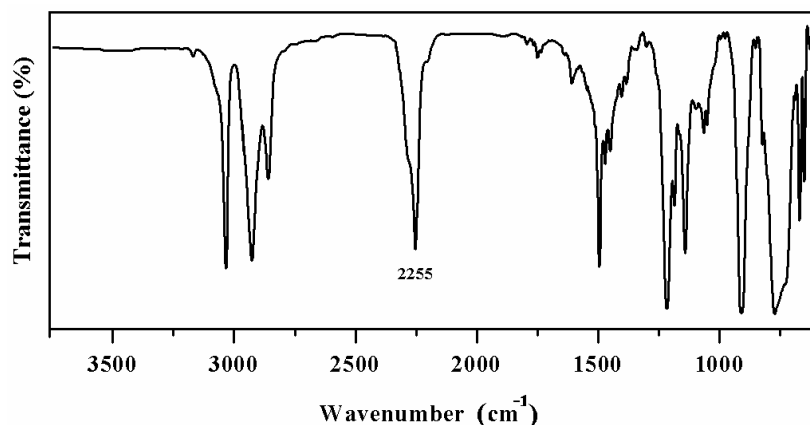
**Figure 3.7 :**  $^{13}\text{C-NMR}$  spectrum of 1,1-bis(4-cyanatophenyl)decahydronaphthalene ( $\text{CDCl}_3$ )

The assignments were supported by  $^{13}\text{C}$ - DEPT NMR spectrum (**Figure 3.8**). The peaks due to quaternary carbons labeled as a, b, e, and f were absent. The peaks appeared in negative phase confirmed the assignments for methine carbons c, c', d, d', i, and n. The peaks due to methylene carbons g, h, j, k, l, m, and o observed in positive phase.



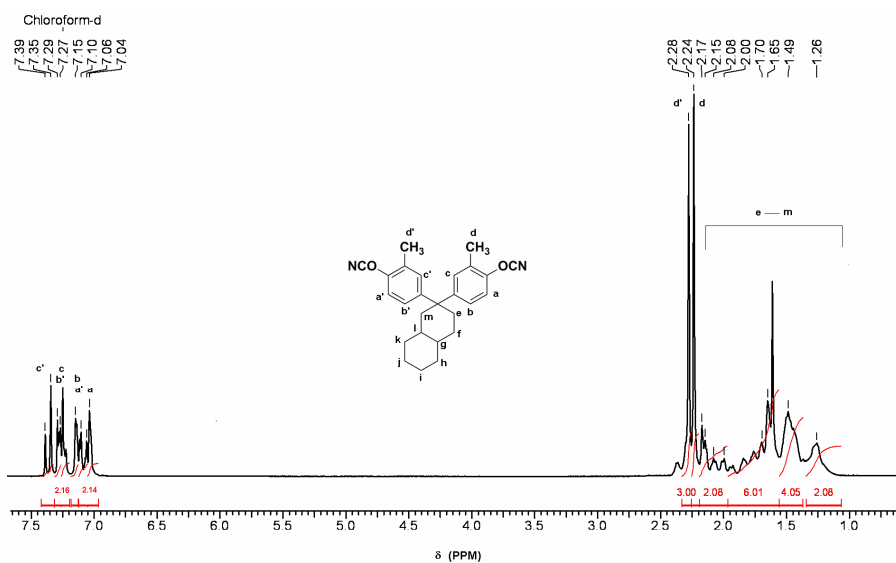
**Figure 3.8:**  $^{13}\text{C}$ - DEPT spectrum of 1,1-bis(4-cyanatophenyl)decahydronaphthalene ( $\text{CDCl}_3$ ).

DMBPDCCN was characterized by FT-IR,  $^1\text{H}$ -NMR and  $^{13}\text{C}$ -NMR spectroscopy. **Figure 3.9** represents FT-IR spectrum of DMBPDCCN. The characteristic  $\text{C}\equiv\text{N}$  stretching was observed at  $2255\text{ cm}^{-1}$ . The  $\text{C}\equiv\text{N}$  stretching peak in case of DMBPDCCN is not splitted into two well resolved peaks as was observed in BPDCCN (Figure 3.5), but appeared as two peaks merged together. Although, the splitting had been attributed to dimer complex formation<sup>43</sup>, the exact mechanism is not yet clearly understood. In case of alkyl cyanates, the splitting has been reported to be caused by a Fermi resonance between the  $2240\text{ cm}^{-1}$  stretching and the first overtone of the C-O-C asymmetric stretching mode<sup>4,43</sup>. In case of aryl cyanates, the splitting is less well understood however, the lack of splitting in case of *ortho*-substituted (mono- and di-) aromatic cyanates, has been correlated to comparatively lower degree of freedom due to substitution.<sup>9,10</sup>



**Figure 3.9 :** IR spectrum of 1,1-bis(4-cyanato-3-methylphenyl)decahydronaphthalene

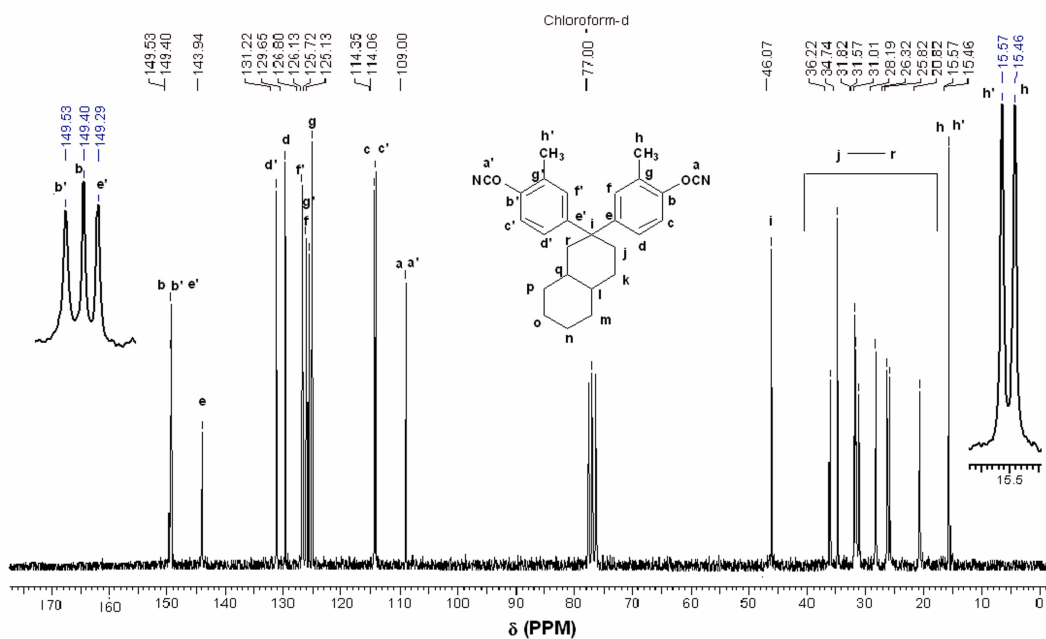
$^1\text{H-NMR}$  spectrum of DMBPDCCN with assignments is presented in **Figure 3.10**. The signals corresponding to aromatic protons were observed in the range 7.04 – 7.39 ppm. The protons of methyl group attached to phenyl ring appeared as two singlets at 2.24 and 2.28 ppm. The peaks observed in the range 1.26 – 2.17 ppm could be assigned to  $-\text{CH}$  and  $-\text{CH}_2$  of decahydronaphthalene ring.



**Figure 3.10 :**  $^1\text{H-NMR}$  spectrum of 1,1-bis(4-cyanato-3-methylphenyl)decahydronaphthalene ( $\text{CDCl}_3$ )

**Figure 3.11** shows  $^{13}\text{C-NMR}$  spectrum of DMBPDCCN with assignments. The signal corresponding to the carbon of cyanate functionality was observed at 109.0 ppm. The peaks due to aromatic carbons b, b' (attached to cyanate group) could be observed at 149.40 (axial phenyl ring) and 149.53 (equatorial phenyl ring) ppm while the carbons g, g' (attached to aromatic methyl group) showed a peak at 125.13 (axial phenyl ring) and 125.72 (equatorial phenyl ring) ppm. Aromatic carbons c, c' (*ortho* to cyanate group) displayed signals at 114.06 (axial phenyl ring) and 114.35 (equatorial phenyl ring) ppm. Aromatic carbons d, d' (*meta* to cyanate group

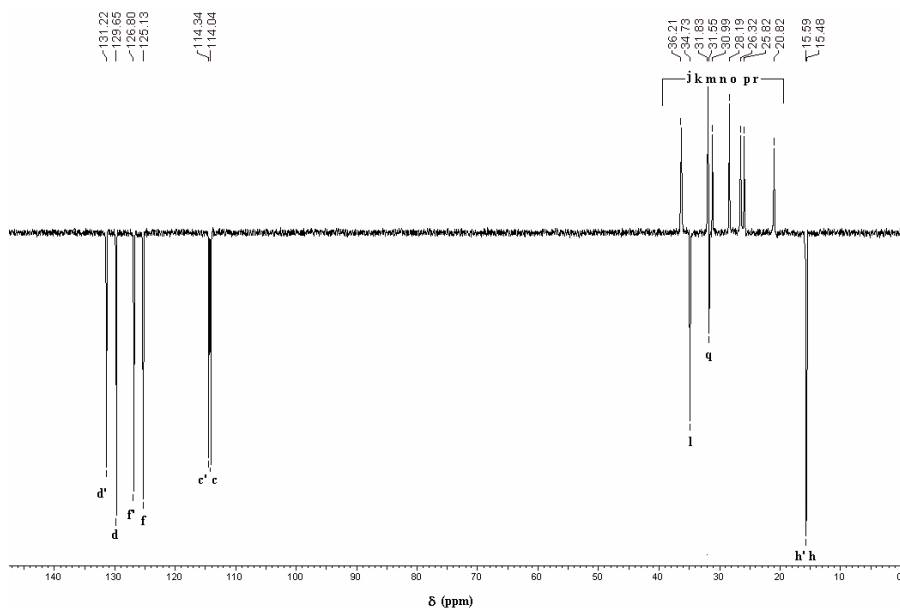
and *para* to  $-\text{CH}_3$ ) exhibited peaks at 129.65 (axial phenyl ring) and 131.22 (equatorial phenyl ring) ppm while aromatic carbons f, f' (*meta* to cyanate group and *ortho* to  $-\text{CH}_3$ ) displayed peaks at 126.13 (axial phenyl ring) and 126.80 (equatorial phenyl ring) ppm. The peaks observed at 143.94 and 149.29 ppm could be attributed to aromatic carbons *para* to cyanate group (marked as e and e') from axial and equatorial phenyl rings, respectively. The peaks appeared in the range 20.80 – 46.06 ppm could be due to aliphatic carbons of decahydronaphthalene ring. The peaks corresponding to carbons of methyl groups labeled as h, h' (attached to phenyl ring) being magnetically non-equivalent appeared separately at 15.46 (axial phenyl ring) and 15.57 (equatorial phenyl ring) ppm.



**Figure 3.11 :**  $^{13}\text{C}$ -NMR spectrum of 1,1-bis(4-cyanato-3-methylphenyl)decahydronaphthalene ( $\text{CDCl}_3$ )

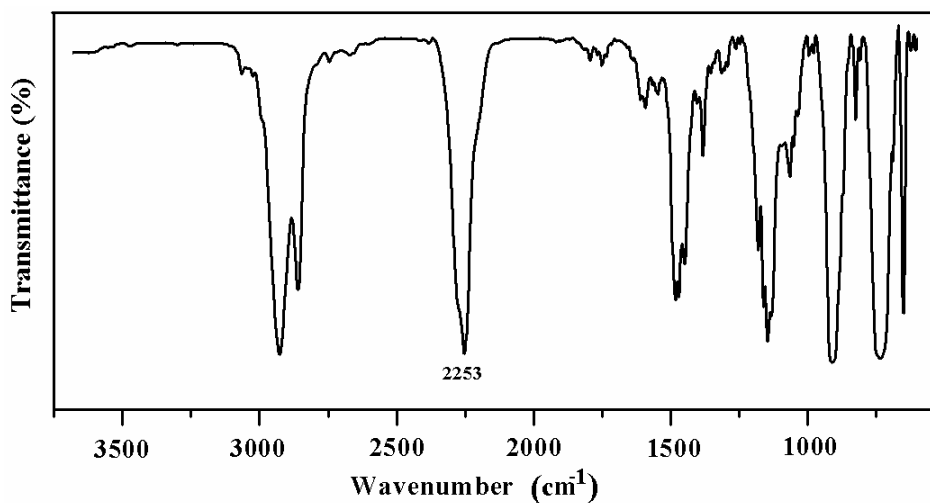
The assignments were also supported by  $^{13}\text{C}$ -DEPT spectrum. (**Figure 3.12**) The peaks due to quaternary carbons labeled as a, b, e, g, and i, were absent. The peaks appeared in negative phase confirmed assignments for methine carbons c, d, f, l, q, and methyl carbon h. The peaks due to methylene carbons j, k, m, n, o, p and r observed in positive phase.





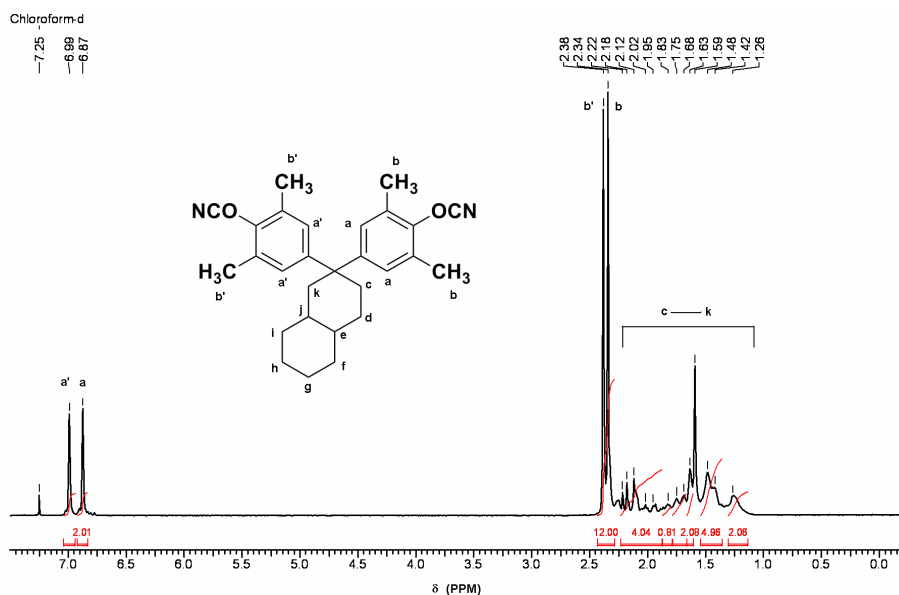
**Figure 3.12 :**  $^{13}\text{C}$ -DEPT NMR spectrum of 1,1-bis(4-cyanato-3-methylphenyl)decahydronaphthalene ( $\text{CDCl}_3$ )

TMBPDCCN was characterized by FT-IR,  $^1\text{H}$ -NMR and  $^{13}\text{C}$ -NMR spectroscopy. **Figure 3.13** illustrates FT-IR spectrum of TMBPDCCN. The characteristic  $\text{C}\equiv\text{N}$  stretching was observed as a broad peak at  $2253\text{ cm}^{-1}$ .



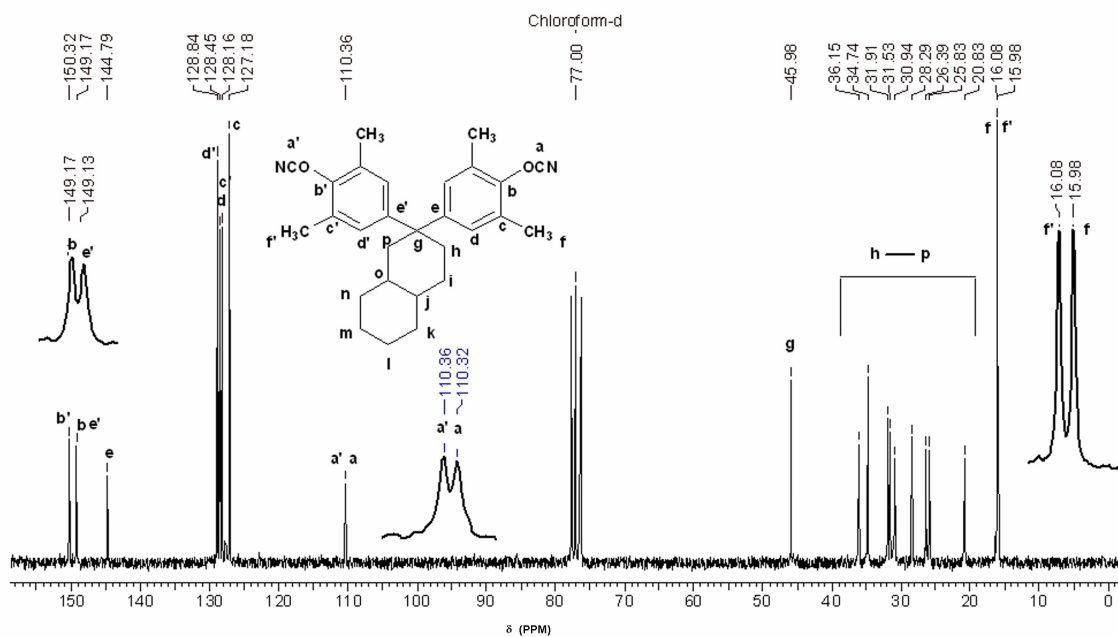
**Figure 3.13:** IR spectrum of 1,1-bis(4-cyanato-3,5-dimethylphenyl)decahydronaphthalene

$^1\text{H}$ -NMR spectrum of TMBPDCCN alongwith peak assignments is reproduced in **Figure 3.14**. The protons of methyl groups attached to phenyl ring appeared as two singlets at 2.34 and 2.38 ppm. Aromatic protons (a and a') (*meta* to cyanate group) displayed peaks at 6.87 (axial phenyl ring) and 6.99 (equatorial phenyl ring) ppm. The signals corresponding to methine and methylene protons of decahydronaphthalene moiety appeared in the range 1.28 - 2.22 ppm.



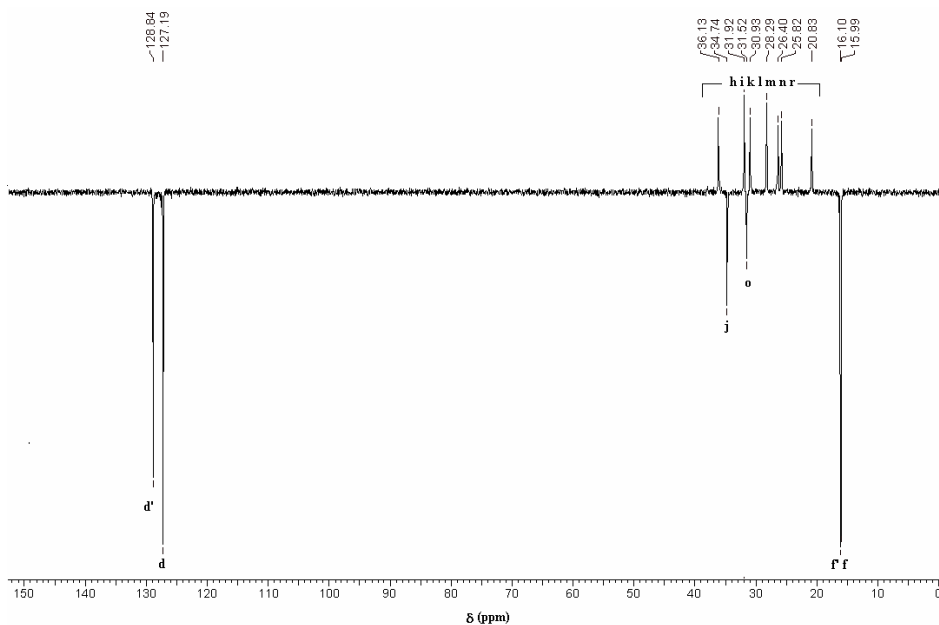
**Figure 3.14 :**  $^1\text{H}$ -NMR spectrum of 1,1-bis(4-cyano-3,5-dimethylphenyl)decahydronaphthalene ( $\text{CDCl}_3$ )

**Figure 3.15** represents  $^{13}\text{C}$ -NMR spectrum of TMBPDCCN with peaks assignments. The peaks due to carbon of cyanate group appeared separately at 110.32 (axial phenyl ring) and 110.36 (equatorial phenyl ring) ppm. In case of BPDCCN and DMBPDCCN, the distinction of peaks for a and a' was not clear. In case of TMBPDCCN, the di-substitution on phenyl ring restricts ring flipping to comparatively more extent and therefore, the carbon a, a' of  $-\text{OCN}$  group appeared separately. The peaks due to quaternary carbons labeled as b, b', were observed at 149.17 (axial phenyl ring), and 150.32 ppm (equatorial phenyl ring), while the quaternary carbon marked as e and e' exhibited peaks at 144.79 (axial phenyl ring), and 149.13 ppm (equatorial phenyl ring). The quaternary carbons designated as c and c' exhibited peaks at 127.18 (axial phenyl ring) and 128.16 ppm (equatorial phenyl ring). The signals observed at 128.16 and 128.82 ppm could be due to the aromatic carbons d (*meta* to cyanate group, axial phenyl ring), and d' (*meta* to cyanate group, equatorial phenyl ring), respectively. The aliphatic carbons of decahydronaphthalene ring showed peaks in the range 20.83 – 45.98 ppm. The peak appeared at 45.98 ppm could be assigned to the quaternary carbon marked as g. The signal corresponding to methine carbons (labeled as j and o) appeared at 34.74 and 31.53 ppm. The signals observed at 20.83, 25.83, 26.39, 28.29, 30.94, 31.91 and 36.15 ppm could be due to methylene carbons (h, i, k, l, m, n, and p,) of decahydronaphthalene ring. The carbons of methyl groups labeled as f, and f' (attached to phenyl ring) appeared separately (being magnetically non-equivalent) at 15.98 (axial phenyl ring) and 16.08 (equatorial phenyl ring) ppm.



**Figure 3.15 :**  $^{13}\text{C}$ -NMR spectrum of 1,1-bis(4-cyano-3,5-dimethylphenyl)decahydronaphthalene ( $\text{CDCl}_3$ ).

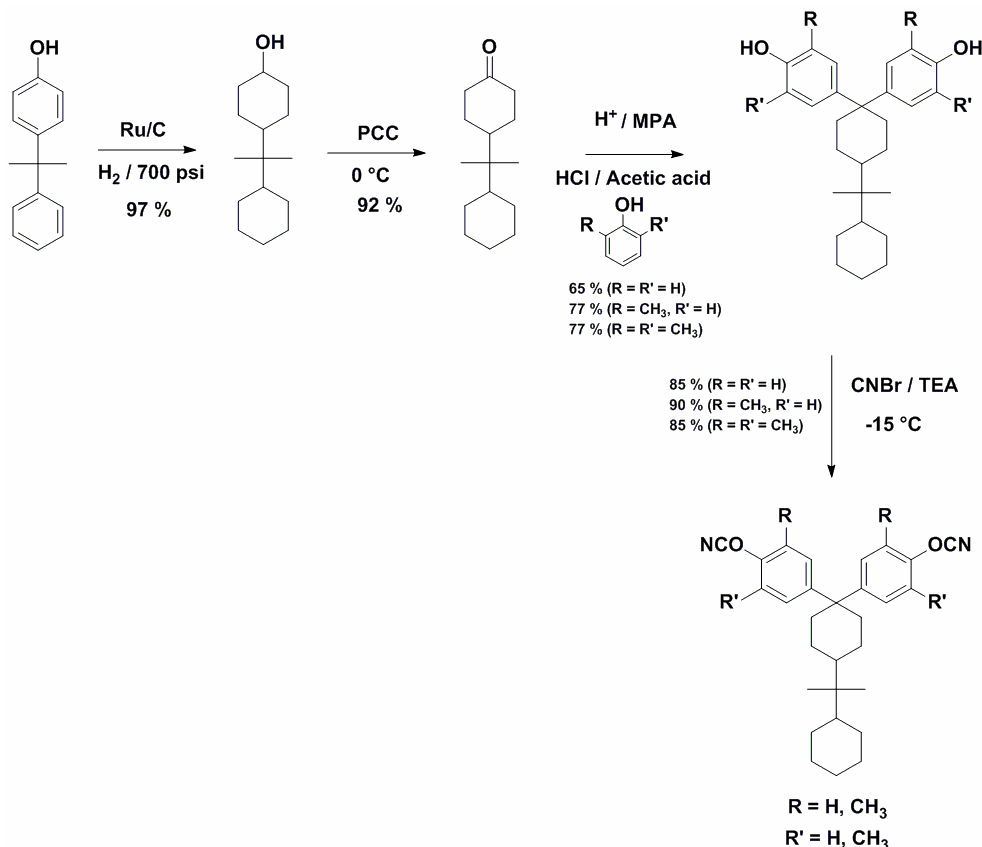
The assignments were further confirmed by  $^{13}\text{C}$ -DEPT NMR spectrum (**Figure 3.16**). The peaks due to quaternary carbons labeled as a, b, c, e, and g, were absent. The peaks appeared in negative phase confirmed assignments for methine carbons j and o, and methyl carbon f. The peaks due to methylene carbons h, i, k, l, m, n, and r were observed in positive phase.



**Figure 3.16 :**  $^{13}\text{C}$ -DEPT NMR spectrum of 1,1-bis(4-cyano-3,5-dimethylphenyl)decahydronaphthalene ( $\text{CDCl}_3$ ).

### 3.4.1.3 Synthesis and characterization of cyanate ester monomers starting from *p*-cumylphenol

Starting from *p*-cumylphenol, three new CE monomers with the systematic variation in the structure *viz*; 1,1-bis(4-cyanatophenyl)-4-perhydrocumylcyclohexane (BPPCCPN), 1,1-bis(4-cyanato-3-methylphenyl)-4-perhydrocumylcyclohexane (DMBPPCCPN) and 1,1-bis(4-cyanato-3,5-dimethylphenyl)-4-perhydrocumylcyclohexane (TMBPPCCPN) were synthesized. The route followed for the synthesis of these monomers is depicted in **Scheme 3.3**.



**Scheme 3.3:** Synthesis of cyanate ester monomers starting from *p*-cumylphenol

The precursor bisphenols were derived starting from *p*-cumyl phenol by following the reported procedure.<sup>31,34</sup>

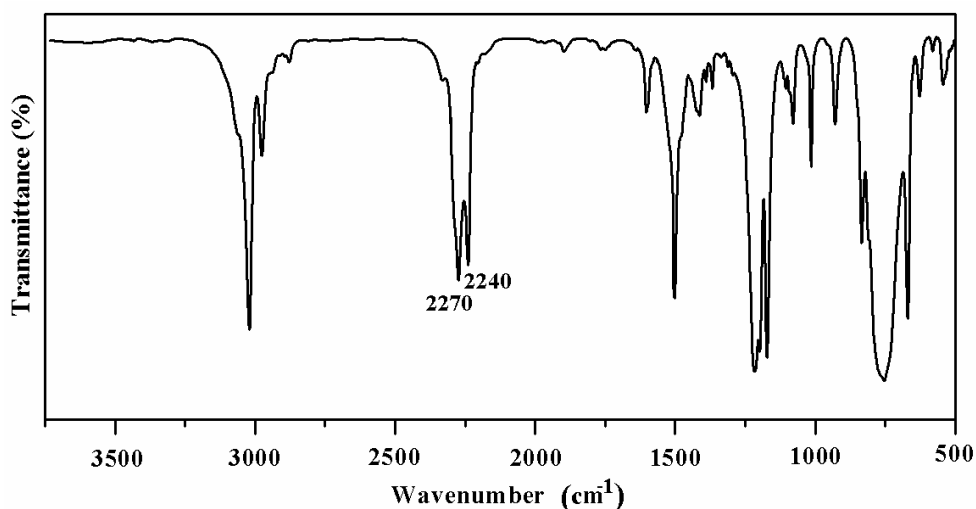
In the first step, *p*-cumylphenol was hydrogenated using 5 % Ru/C in a Parr reactor. 4-Perhydrocumyl cyclohexanol was characterized by FTIR, and <sup>1</sup>H-NMR spectroscopy. IR spectrum showed the absence of the band corresponding to aromatic C=C stretching ( $\approx 1600$   $\text{cm}^{-1}$ ) indicating the complete reduction of aromatic ring. The O-H stretching vibration was observed at  $3275$   $\text{cm}^{-1}$ . Furthermore, the absence of peaks corresponding to aromatic protons in <sup>1</sup>H-NMR spectrum indicated the complete reduction.

The oxidation of 4-perhydrocumyl cyclohexanol to 4-perhydrocumyl cyclohexanone was achieved using PCC. IR spectrum of 4-perhydrocumylcyclohexanone showed the absence of hydroxyl band at  $3275\text{ cm}^{-1}$  and the presence of characteristic carbonyl stretching at  $1720\text{ cm}^{-1}$ . 4-Perhydrocumylcyclohexanone was purified by distillation ( $135\text{ }^{\circ}\text{C} / 0.02\text{ mm Hg}$ ).

4-Perhydrocumylcyclohexanone was condensed with phenol and *o*-cresol and in the presence of hydrogen chloride / 3-mercaptopropionic acid to afford 1,1-bis(4-hydroxyphenyl)-4-perhydrocumylcyclohexane (BPPCP) and 1,1-bis(4-hydroxy-3-methylphenyl)-4-perhydrocumylcyclohexane (DMBPPCP), respectively. For the synthesis of 1,1-bis(4-hydroxy-3,5-dimethylphenyl)-4-perhydrocumylcyclohexane (TMBPPCP), 4-perhydrocumylcyclohexanone was condensed with 2,6-dimethylphenol in the presence of hydrochloric acid-acetic acid mixture. The formation of these bisphenols: BPPCP, DMBPPCP and TMBPPCP was confirmed by IR and  $^1\text{H-NMR}$  spectroscopy.

These bisphenols were then converted into corresponding cyanate esters BPPCPCN, DMBPPCPCN and TMBPPCPCN as described in section 3.4.1.1.

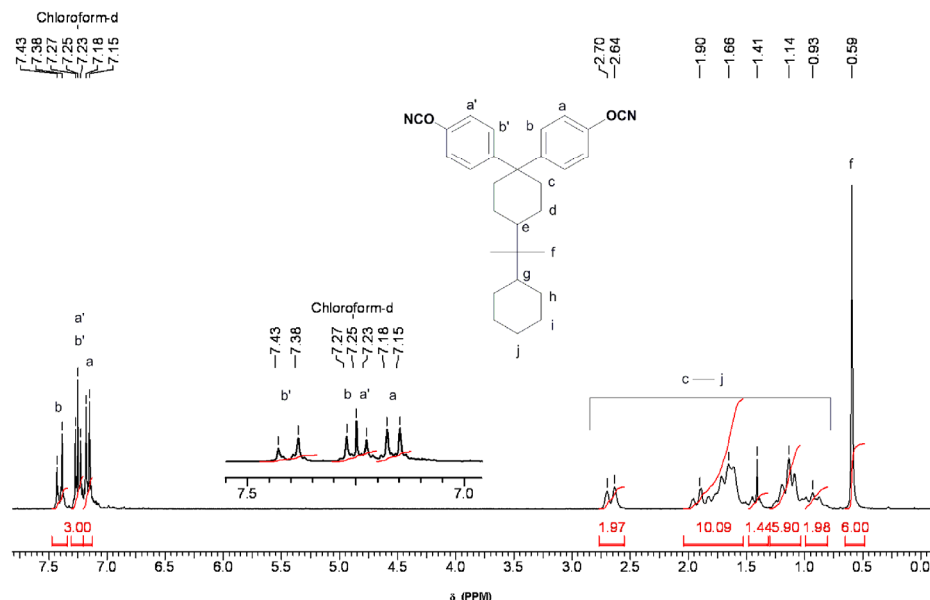
BPPCPCN was characterized by FT-IR,  $^1\text{H-NMR}$  and  $^{13}\text{C-NMR}$  spectroscopy. IR spectrum of BPPCPCN is reproduced in **Figure 3.17**. The stretching of  $\text{C}\equiv\text{N}$  was observed at  $2270\text{ cm}^{-1}$  and  $2240\text{ cm}^{-1}$  as two well resolved peaks.



**Figure 3.17** : IR spectrum of 1,1-bis(4-cyanatophenyl)-4-perhydrocumylcyclohexane

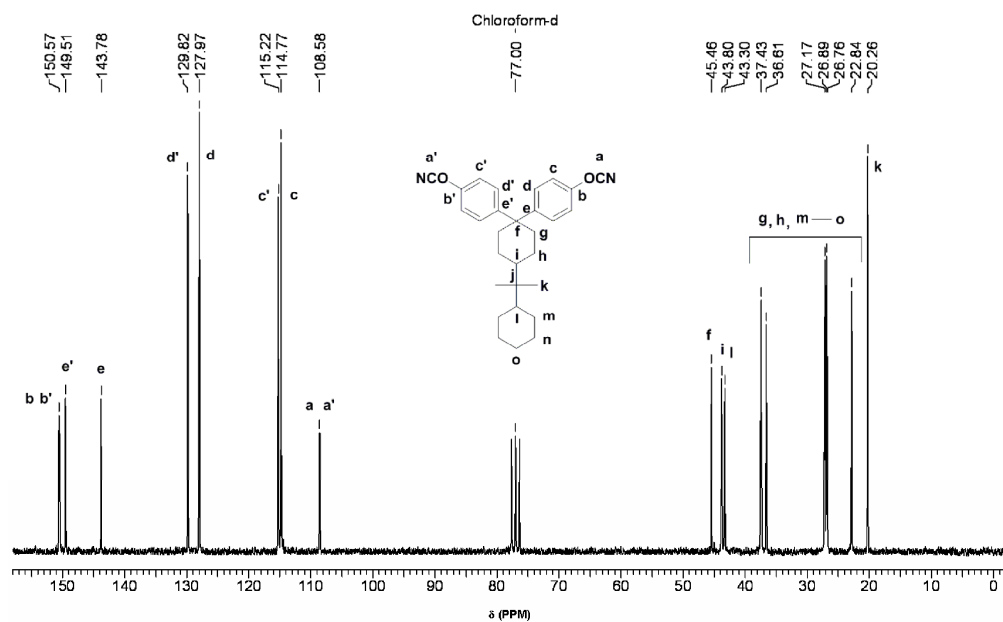
**Figure 3.18** represents  $^1\text{H-NMR}$  of BPPCPCN. As observed for the precursor bisphenol, the two phenyl rings are magnetically non-equivalent in case of BPPCPCN. The aromatic protons a, a' b, and b' therefore showed a separate set of doublets. The doublet corresponding to the aromatic proton 'a' (*ortho* to  $-\text{OCN}$  group of axial phenyl ring) observed at 7.17 ppm while b' (*meta* to  $-\text{OCN}$  group of equatorial phenyl ring) showed a doublet at 7.41

ppm. The peaks observed in the range 7.23-7.27 ppm could be assigned to aromatic protons a' (ortho to -OCN group, equatorial) and b (meta to -OCN group, axial). The peaks due to methylene and methine protons were observed in the range 0.93 – 2.70 ppm. The methyl protons displayed a singlet at 0.59 ppm.



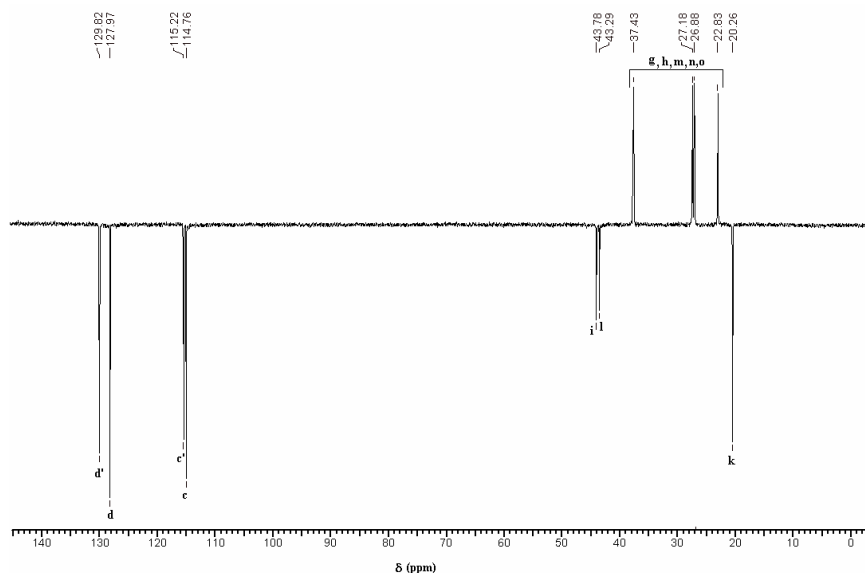
**Figure 3.18 :** <sup>1</sup>H-NMR spectrum of 1,1-bis(4-cyanatophenyl)-4-perhydrocumyl cyclohexane

**Figure 3.19** illustrates <sup>13</sup>C-NMR spectrum of BPPPCPN alongwith peak assignments. The peak due to carbon of cyanate functionality was observed at 108.58 ppm. The presence of magnetically non-equivalent phenyl rings was confirmed by the appearance of peaks due to aromatic carbons in two sets. Aromatic carbons labeled as b, b' (attached to cyanate group) showed signals at 150.47 (axial phenyl ring) and 150.57 ppm (equatorial phenyl ring). The peaks due to aromatic carbons c, c' (ortho to cyanate group) were observed at 114.77 (axial phenyl ring) and 115.22 ppm (equatorial phenyl ring). Aromatic carbons marked as d, d' (meta to cyanate group) displayed peaks at 127.97 (axial phenyl ring) and 129.82 ppm (equatorial phenyl ring). The peaks observed at 143.78 and 149.51 ppm could be attributed to aromatic carbons para to cyanate group (marked as e and e') of axial and equatorial phenyl rings, respectively. The peaks appeared in the range 20.26 – 45.46 ppm could be due to aliphatic carbons of cyclohexyl ring. The peaks due to quaternary carbons f and j could be observed at 45.46 and 36.81 ppm, respectively. The methine carbons labeled as i and l exhibited peaks at 43.80 and 43.30 ppm, respectively. The peaks appeared at 22.84, 26.76, 26.89, 27.17, and 37.43 ppm could be due to methylene carbons marked as g, h, m, n and o. The peak corresponding to the methyl carbon marked as k appeared at 20.26 ppm.



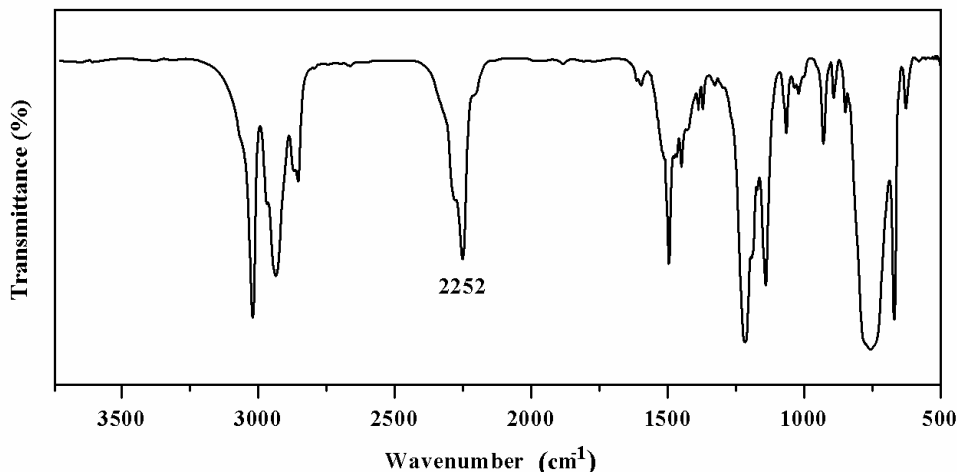
**Figure 3.19 :**  $^{13}\text{C}$ -NMR spectrum of 1,1-bis(4-cyanatophenyl)-4-perhydrocumyl-cyclohexane ( $\text{CDCl}_3$ ).

The assignments were further confirmed by  $^{13}\text{C}$ -DEPT spectrum (**Figure 3.20**). The peaks due to quaternary carbons labeled as a, b, e, f, and j were absent. The peaks appeared in negative phase confirmed assignments for methine carbons c, d, i, l and methyl carbon k. The peaks due to methylene carbons g, h, m, n and o were observed in positive phase.



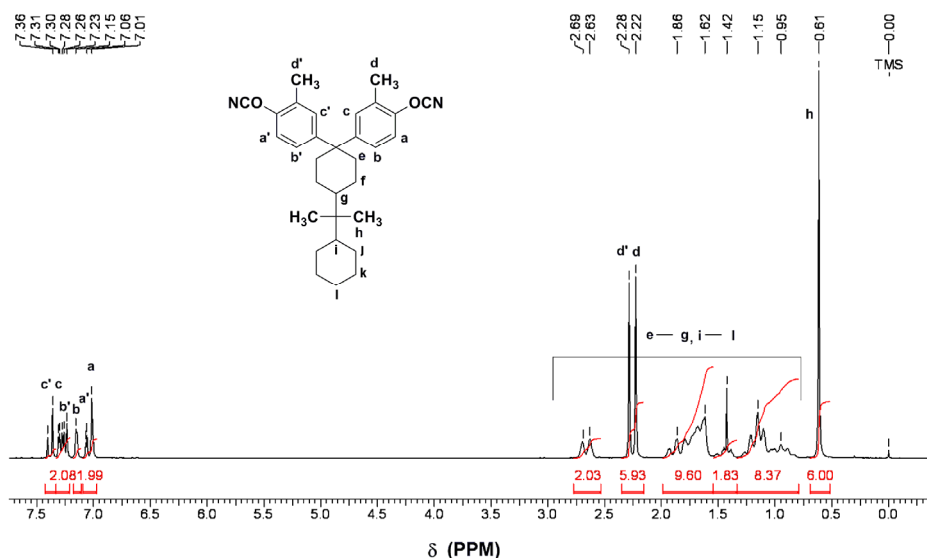
**Figure 3.20 :**  $^{13}\text{C}$ -DEPT NMR spectrum of 1,1-bis(4-cyanatophenyl)-4-perhydrocumyl-cyclohexane ( $\text{CDCl}_3$ ).

DMBPPCPCN was characterized by FT-IR,  $^1\text{H-NMR}$  and  $^{13}\text{C-NMR}$  spectroscopy. **Figure 3.21** represents FTIR spectrum of DMBPPCPCN. The cyanate stretching band ( $2252\text{ cm}^{-1}$ ) was not splitted into two well resolved modes as observed in case of BPPCPCN (**Figure 3.17**) but appeared with a shoulder peak due to substitution at *ortho* position to cyanate group.



**Figure 3.21** : IR spectrum of 1,1-bis(4-cyanato-3-methylphenyl)-4-perhydrocumyl cyclohexane

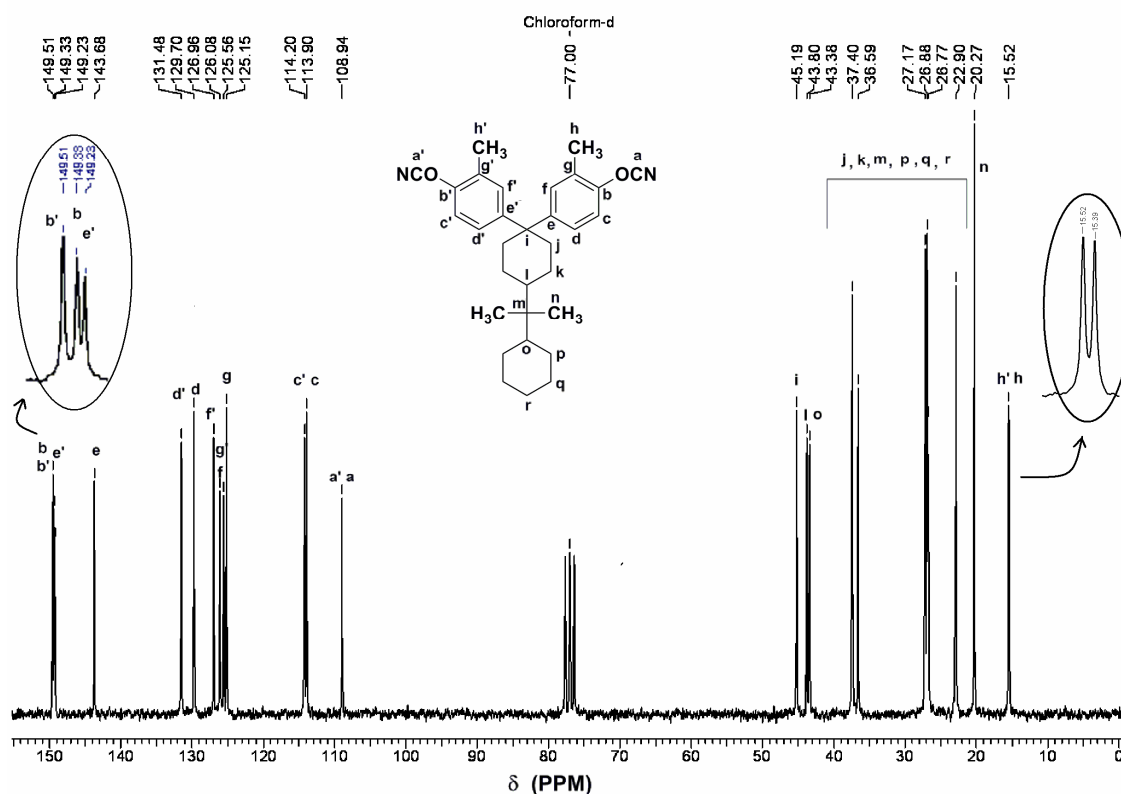
$^1\text{H-NMR}$  spectrum of DMBPPCPCN with peak assignments is presented in **Figure 3.22**. The protons of methyl group (labeled as d, d') attached to phenyl ring showed two singlets at 2.22 (axial phenyl ring) and 2.28 (equatorial phenyl ring) ppm. The peaks corresponding to aromatic protons marked as a, a', b, b', and c, c' appeared in the range 7.01 – 7.36 ppm. The peaks appeared in the range 0.95 – 2.69 ppm could be due to methylene and methine protons of cyclohexyl rings. The singlet observed at 0.61 ppm could be attributed to methyl protons.



**Figure 3.22** :  $^1\text{H-NMR}$  spectrum of 1,1-bis(4-cyanato-3-methylphenyl)-4-perhydrocumyl cyclohexane ( $\text{CDCl}_3$ )

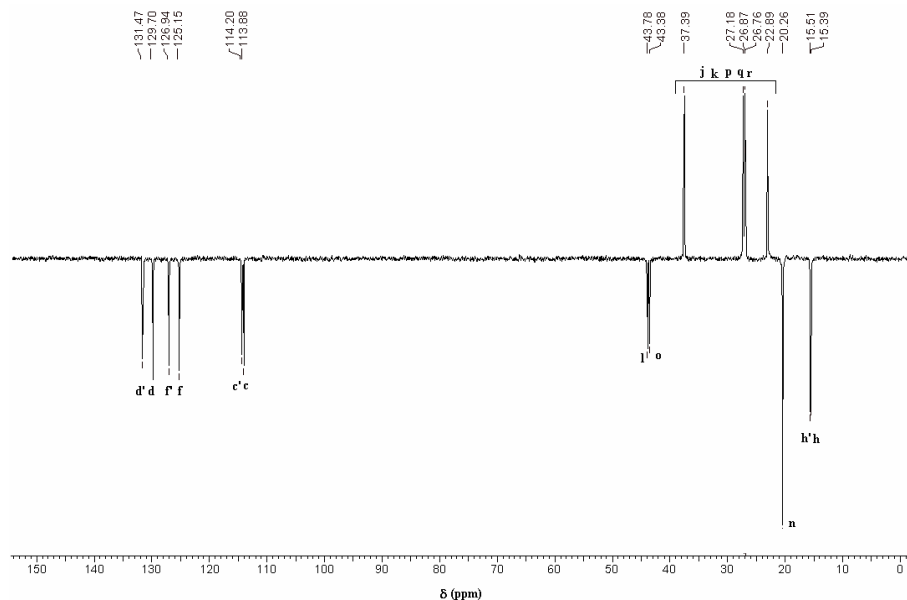


**Figure 3.23** represents  $^{13}\text{C}$ -NMR spectrum of DMBPPCPCN along with peak assignments. The signal corresponding to the carbon of cyanate functionality appeared at 108.94 ppm. The peaks due to aromatic carbons b, b' (attached to cyanate group) could be observed at 149.33 (axial phenyl ring) and 149.51 ppm (equatorial phenyl ring) while the peaks due to carbons g, g' (attached to aromatic methyl group) were observed at 125.15 (axial phenyl ring) and 125.56 ppm (equatorial phenyl ring). Aromatic carbons c, c' (*ortho* to cyanate group) displayed peaks at 113.90 (axial phenyl ring) and 114.20 ppm (equatorial phenyl ring). Aromatic carbons d, d' (*meta* to cyanate group and *para* to  $-\text{CH}_3$ ) exhibited peaks at 129.70 (axial phenyl ring) and 131.48 ppm (equatorial phenyl ring) while aromatic carbons f, f' (*meta* to cyanate group and *ortho* to  $-\text{CH}_3$ ) displayed peaks at 126.08 (axial phenyl ring) and 126.96 ppm (equatorial phenyl ring). The peaks observed at 143.68 and 149.23 ppm could be attributed to aromatic carbons *para* to cyanate group (labeled as e and e') of axial and equatorial phenyl rings, respectively. The peaks appeared in the range 22.90 – 45.19 ppm could be due to aliphatic carbons of perhydrocumyl ring. The methyl carbon marked as n showed a signal at 20.26 ppm while carbons of methyl groups labeled as h, h' (attached to phenyl ring) appeared separately at 15.39 (axial) and 15.52 (equatorial) ppm.



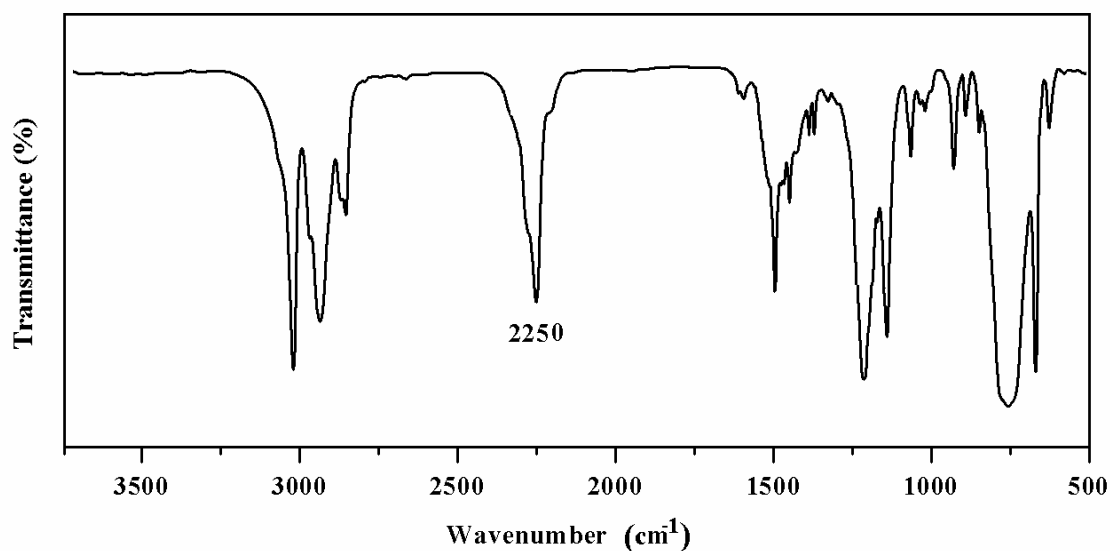
**Figure 3.23 :**  $^{13}\text{C}$ -NMR spectrum of 1,1-bis(4-cyanato-3-methylphenyl)-4-perhydrocumyl cyclohexane ( $\text{CDCl}_3$ )

The assignments were also supported by  $^{13}\text{C}$ -DEPT spectrum. (**Figure 3.24**) The peaks due to quaternary carbons labeled as a, b, g, e, i, and m were absent. The peaks appeared in negative phase confirmed assignments for methine carbons c, d, l, o, and methyl carbon h and n. The peaks due to methylene carbons j, k, p, q and r were observed in positive phase.



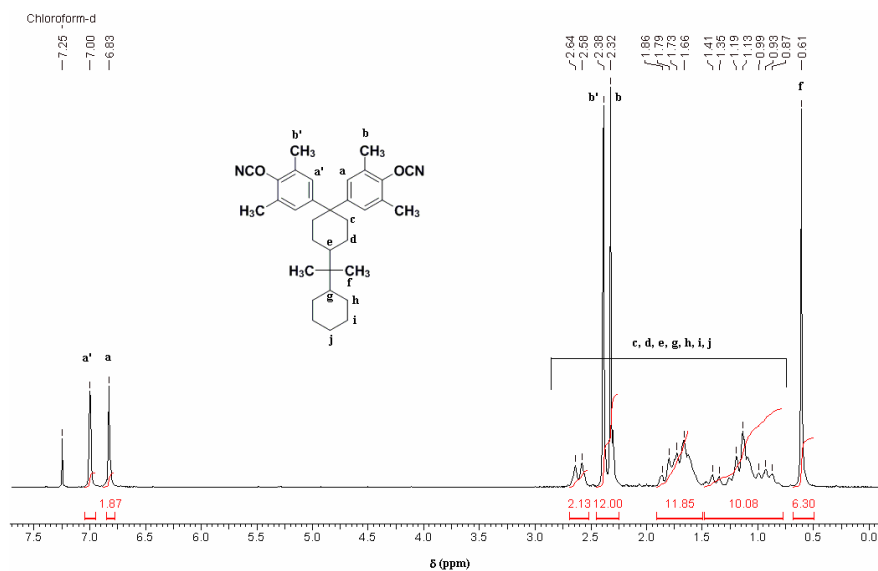
**Figure 3.24:**  $^{13}\text{C}$ -DEPT NMR spectrum of 1,1-bis(4-cyano-3-methylphenyl)-4-perhydrocumylcyclohexane ( $\text{CDCl}_3$ )

TMBPPPCN was characterized by FT-IR,  $^1\text{H}$ -NMR and  $^{13}\text{C}$ -NMR spectroscopy. **Figure 3.25** represents FTIR spectrum of TMBPPPCN. The cyanate stretching band ( $2250\text{ cm}^{-1}$ ) was not splitted into two well resolved peaks as observed in BPPPCN (**Figure 3.17**).



**Figure 3.25 :** IR spectrum of 1,1-bis(4-cyano-3,5-dimethylphenyl)-4-perhydrocumylcyclohexane

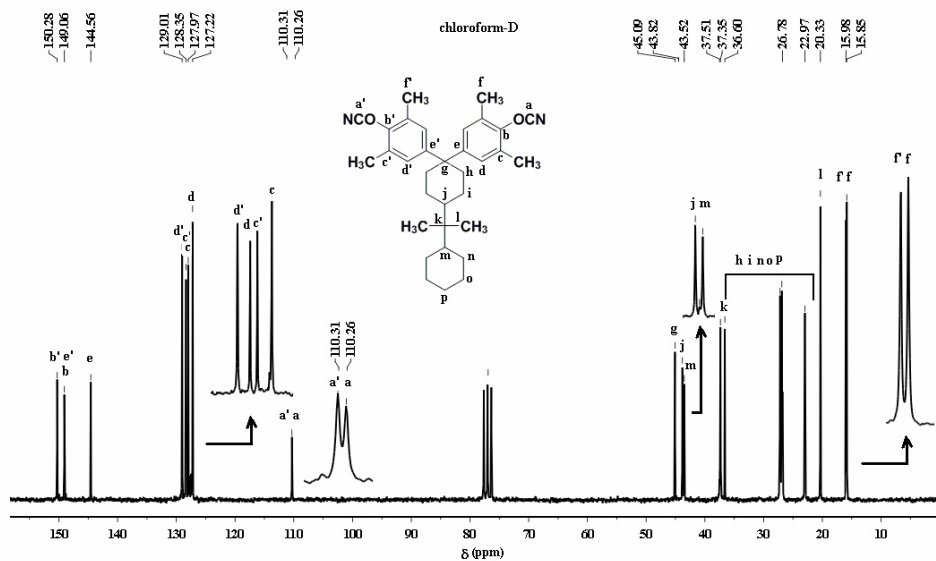
**Figure 3.26** represents  $^1\text{H-NMR}$  spectrum of TMBPPPCPN along with peak assignments. The protons of methyl group attached to phenyl ring (labeled as b, b') appeared as two separate singlets (being magnetically non-equivalent) at 2.38 and 2.32 ppm. The peaks corresponding to aromatic protons marked as a, a', appeared at 6.83 (axial phenyl ring) and 7.0 (equatorial phenyl ring) ppm. The singlet observed at 0.61 ppm could be attributed to methyl protons. The protons of perhydrocumyl ring appeared in the range 0.87 – 2.64 ppm. The methyl protons labeled as f exhibited a singlet at 0.61 ppm.



**Figure 3.26 :**  $^1\text{H-NMR}$  spectrum of 1,1-bis(4-cyanato-3,5-dimethylphenyl)-4-perhydrocumylcyclohexane ( $\text{CDCl}_3$ )

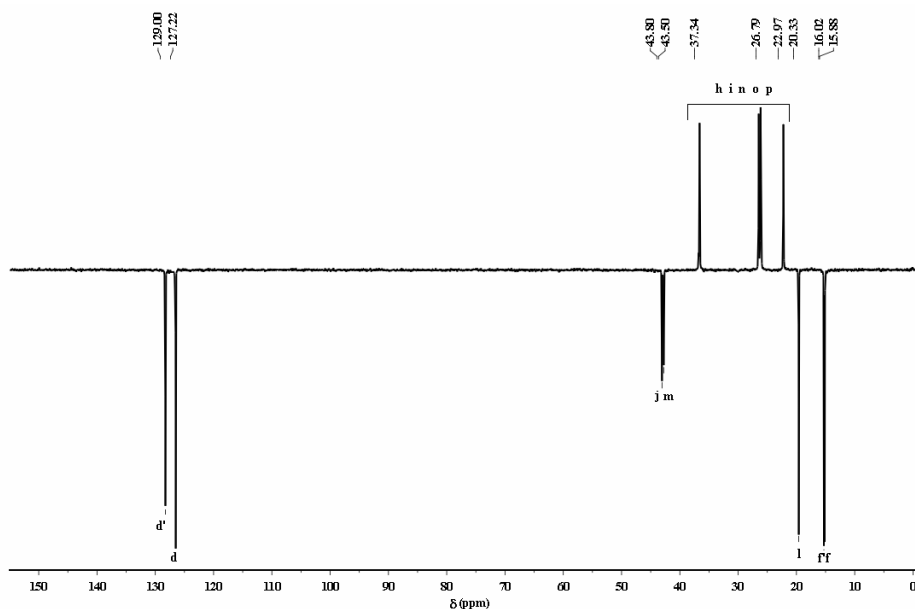
$^{13}\text{C-NMR}$  spectrum of TMBPPPCPN is shown in **Figure 3.27** along with peak assignments. The di-substitution on phenyl ring restricts ring flipping to comparatively more extent than BPPPCPN (no substitution) and DMBPPPCPN (mono substitution). The peaks due to carbon of cyanate functionality therefore appeared at 110.26 (axial phenyl ring) and 110.31 (equatorial phenyl ring) ppm. The peaks due to quaternary carbons b, b', e and e' could be observed in the range 144.56 – 150.28 ppm while the quaternary carbon c and c' exhibited signals at 127.97 (axial phenyl ring) and 128.35 (equatorial phenyl ring) ppm. The signals observed at 127.22 and 129.01 ppm could be due to aromatic carbons d (*meta* to cyanate group, axial phenyl ring), and d' (*meta* to cyanate group, equatorial phenyl ring), respectively. The aliphatic carbons of perhydrocumyl ring showed peaks in the range 20.33 – 45.09 ppm. The quaternary carbons marked as g and k appeared respectively at 45.09 and 37.35 ppm. The signal corresponding to methine carbons labeled as j and m appeared at 43.52 and 43.82 ppm. The signals observed at 22.97, 26.78, 26.89, 27.20, and 37.35 ppm could be due to methylene carbons (h, i, n, o and p) of cyclohexyl ring. The methyl carbons marked as l displayed a signal at 20.33 ppm while carbons of methyl groups labeled as f, and f' (attached to phenyl ring)

appeared separately (being magnetically non-equivalent) at 15.85 (axial phenyl ring) and 15.98 (equatorial phenyl ring) ppm.



**Figure 3.27 :**  $^{13}\text{C}$ -NMR spectrum of 1,1-bis(4-cyanato-3,5-dimethylphenyl)-4-perhydrocumylcyclohexane ( $\text{CDCl}_3$ )

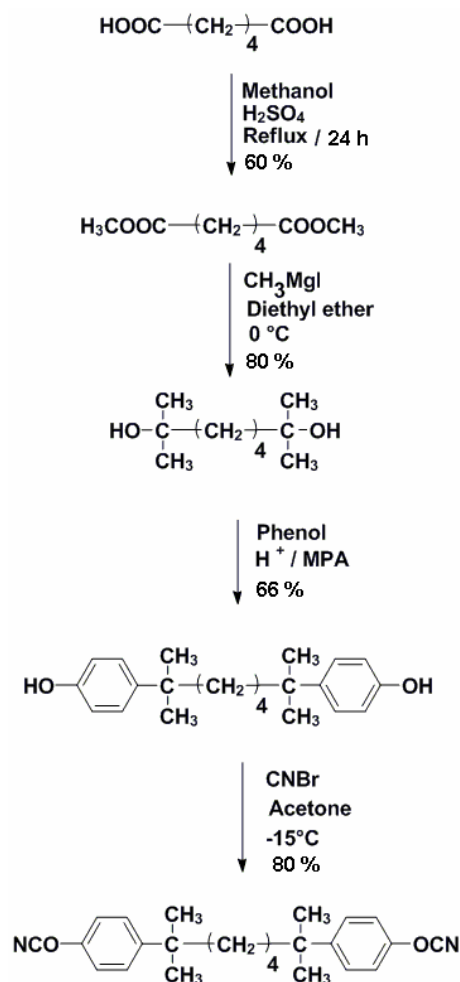
The assignments were further confirmed by  $^{13}\text{C}$ -DEPT NMR spectrum (Figure 3.28). The peaks due to quaternary carbons labeled as a, b, c, e, g, and k were absent. The peaks appeared in negative phase confirmed assignments for methine carbons d, j, and m, and methyl carbons l and f. The peaks due to methylene carbons h, i, n, o, and p observed in positive phase.



**Figure 3.28 :**  $^{13}\text{C}$ -DEPT NMR spectrum of 1,1-bis(4-cyanato-3,5-dimethylphenyl)-4-perhydrocumylcyclohexane ( $\text{CDCl}_3$ )

### 3.4.2 Synthesis and characterization of cyanate ester monomer containing alkylene spacer.

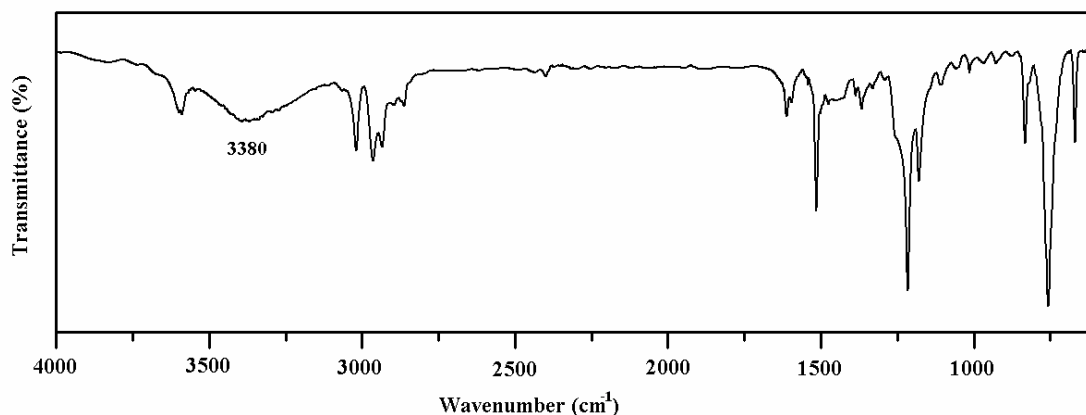
Starting from adipic acid, a new CE monomer containing alkylene spacer viz; 2,7-bis(4-cyanatophenyl)-2,7-dimethyloctane (BPC6CN) was synthesized by following the route as outlined in Scheme 3.4.



Scheme 3.4: Synthesis of 2,7-bis(4-cyanatophenyl)-2,7-dimethyloctane

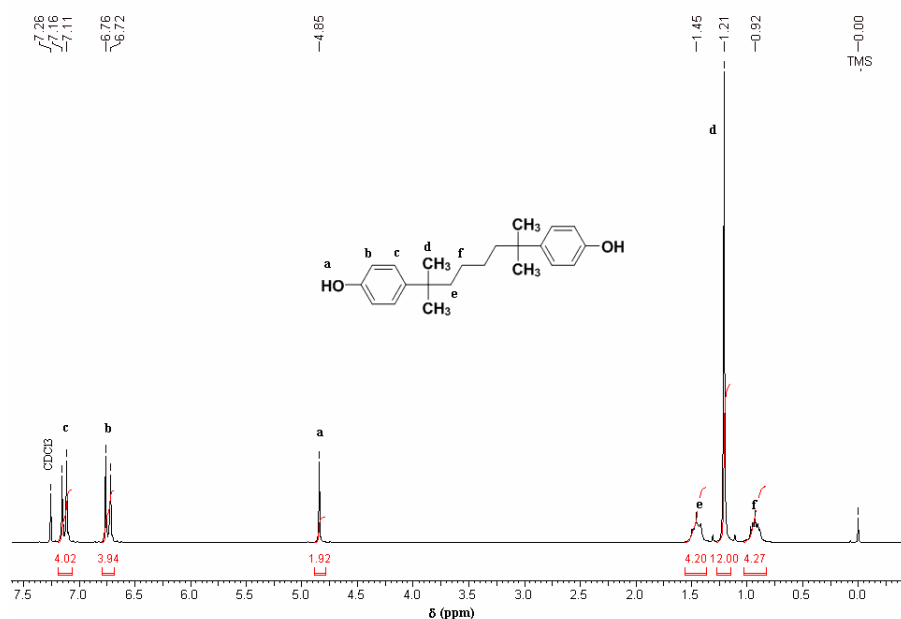
Adipic acid, in the first step was esterified to obtain dimethyl adipate using sulfuric acid as a catalyst. The product dimethyl adipate was characterized by IR and  $^1\text{H-NMR}$  spectroscopy. The conversion of ester into tertiary alcohol can be best achieved by Grignard reaction. Dimethyl adipate was then converted into 2,7-bishydroxy-2,7-dimethyloctane using a Grignard reagent (methylmagnesium iodide) by following the procedure reported in the literature.<sup>44</sup> The obtained crude product was recrystallized using pet ether. 2,7-Bishydroxy-2,7-dimethyloctane was characterized by FTIR and  $^1\text{H-NMR}$  spectroscopy. The tertiary diol viz; 2,7-bishydroxy-2,7-dimethyloctane was condensed with phenol in the presence of anhydrous hydrogen chloride and 3-mercaptopropionic acid to yield 2,7-bis(4-hydroxyphenyl)-2,7-

dimethyloctane (BPC6). BPC6 was characterized by IR and NMR spectroscopy. **Figure 3.29** represents IR spectrum of BPC6. The vibration due to hydroxyl stretching was observed at  $3380\text{ cm}^{-1}$ .



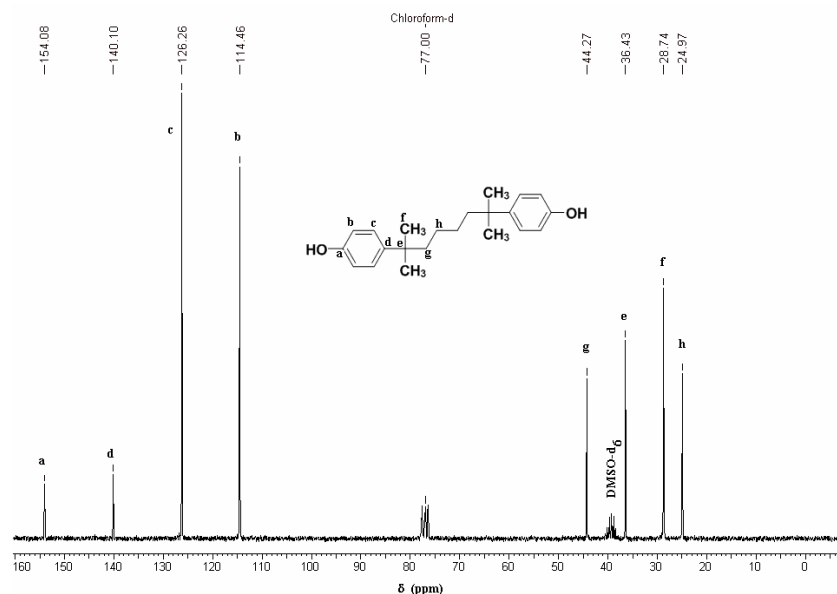
**Figure 3.29** : IR spectrum of 2,7-bis(4-hydroxyphenyl)-2,7-dimethyloctane

**Figure 3.30** represents  $^1\text{H-NMR}$  spectrum of BPC6 along with peak assignments. Aromatic protons labeled as b (*ortho* to  $-\text{OH}$ ) exhibited a doublet at 6.74 ppm while aromatic protons marked as c (*meta* to  $-\text{OH}$ ) displayed a doublet at 7.14 ppm. The signal at 4.85 ppm is due to protons of phenolic  $-\text{OH}$  group. A triplet centered at 1.45 ppm is assignable to methylene protons labeled as e while a multiplet in the range 0.86 – 0.98 ppm is due to methylene protons marked as f. The methyl protons designated as d displayed a singlet at 1.21 ppm.



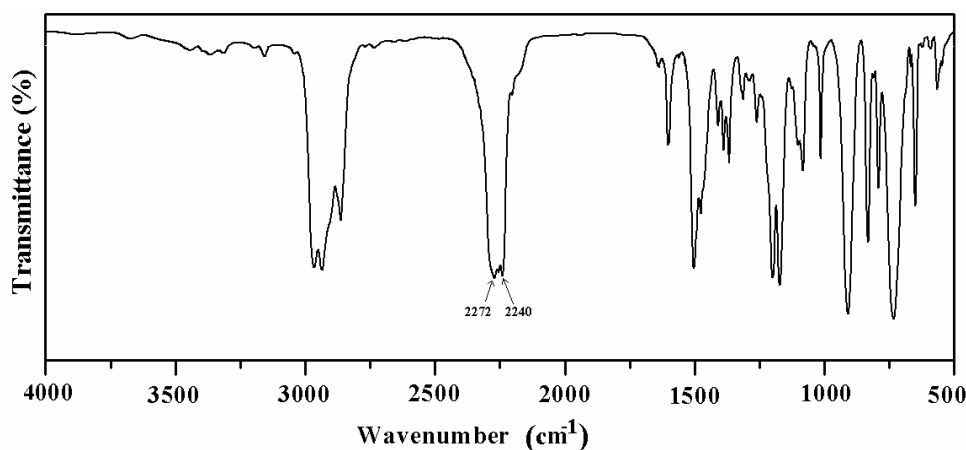
**Figure 3.30** :  $^1\text{H-NMR}$  spectrum of 2,7-bis(4-hydroxyphenyl)-2,7-dimethyloctane ( $\text{CDCl}_3$ )

$^{13}\text{C}$ -NMR spectrum of BPC6 is reproduced in **Figure 3.31**. The peaks corresponding to the quaternary aromatic carbons labeled as a and d appeared at 154.08 and 140.10 ppm, respectively. The aromatic carbon *ortho* to hydroxyl group (labeled as b) displayed a peak at 114.46 ppm while the carbon *meta* to hydroxyl group (labeled as c) exhibited a peak at 126.26 ppm. The peaks observed at 44.27 and 24.97 ppm could be assigned to methylene carbons labeled as g and h, respectively. The quaternary carbon marked as e exhibited a peak at 36.43 ppm. The peak appeared at 28.74 is due to methyl carbons designated as f.



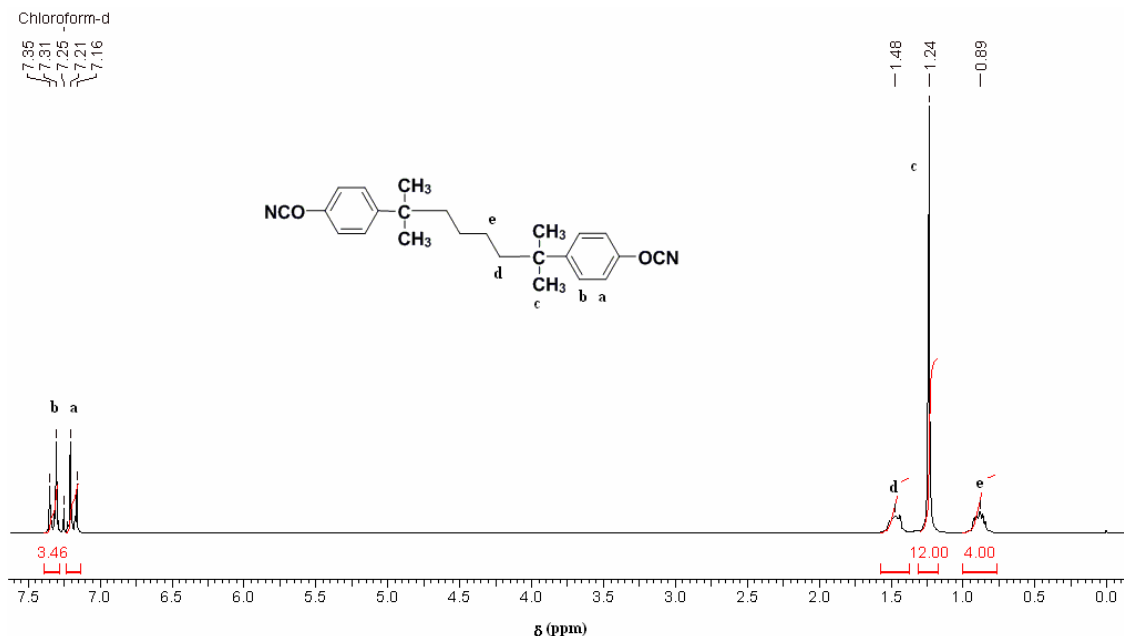
**Figure 3.31 :**  $^{13}\text{C}$ -NMR spectrum of 2,7-bis(4-hydroxyphenyl)-2,7-dimethyloctane ( $\text{CDCl}_3 + \text{DMSO-d}_6$ ).

BPC6 was converted into corresponding cyanate ester monomer BPC6CN by following the protocol developed by Grigat and Putter.<sup>1,2</sup> The crude product obtained was purified by filtration column chromatography using dichloromethane. BPC6CN was characterized by IR and NMR spectroscopy. The characteristic  $\text{-C}\equiv\text{N}$  stretchings were observed at 2272 and 2240  $\text{cm}^{-1}$  in IR spectrum (**Figure 3.32**).



**Figure 3.32 :** IR spectrum of 2,7-bis(4-cyanatophenyl)-2,7-dimethyloctane

$^1\text{H-NMR}$  spectrum of BPC6CN alongwith peak assignments is illustrated in **Figure 3.33**. Aromatic protons designated as a (*ortho* to cyanate group) exhibited a doublet at 7.19 ppm while the protons *meta* to cyanate groups (marked as b) displayed a doublet at 7.33 ppm. The multiplets appeared in the range 0.76 – 0.98 and 1.4 – 1.6 ppm could be due to protons of methylene groups labeled as e and d, respectively. The singlet observed at 1.24 ppm could be assigned to protons of methyl groups.



**Figure 3.33:**  $^1\text{H-NMR}$  spectrum of 2,7-bis(4-cyanatophenyl)-2,7-dimethyloctane ( $\text{CDCl}_3$ )

**Figure 3.34** represents  $^{13}\text{C-NMR}$  of spectrum of BPC6CN alongwith peak assignments. The peak corresponding to the carbon of cyanate functionality appeared at 108.92 ppm. The peaks due to quaternary aromatic carbon b, (attached to cyanate group) and e (*para* to cyanate group) appeared at 150.52 ppm and 148.47 ppm, respectively. The signals due to aromatic carbons c, (*ortho* to cyanate group) and d, (*meta* to cyanate group) were observed at 114.58 ppm and 127.69 ppm, respectively. The peak observed at 44.36 ppm could be assigned to the quaternary carbon labeled as f (attached to phenyl ring). The carbons of methyl groups showed signal at 28.76 ppm. The methylene carbons labeled as h and i displayed peaks at 37.43 and 25.11 ppm, respectively.



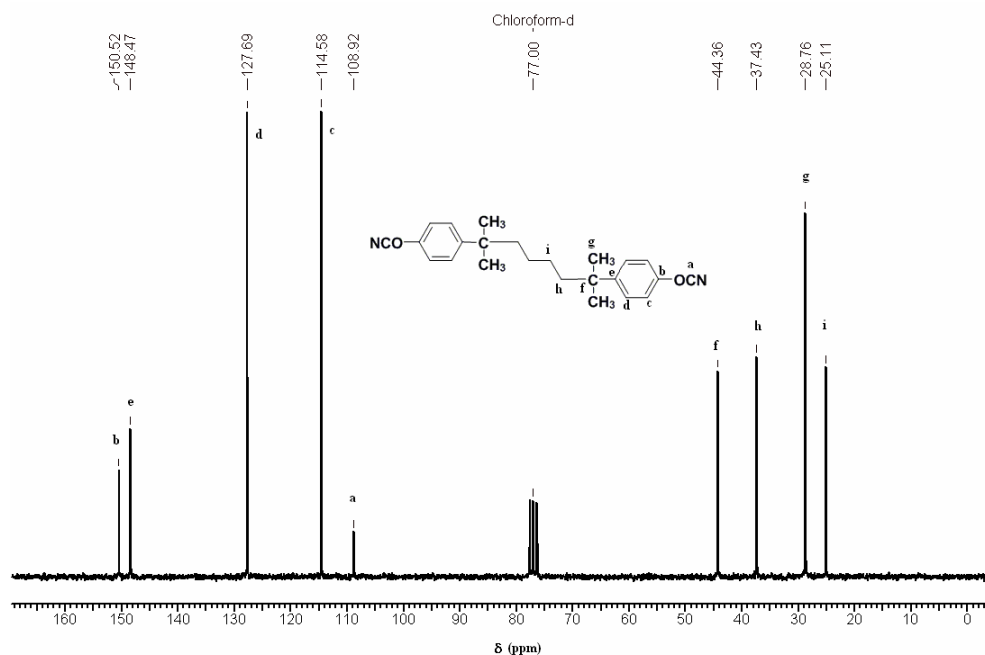


Figure 3.34 :  $^{13}\text{C}$ -NMR spectrum of 2,7-bis(4-cyanatophenyl)-2,7-dimethyloctane ( $\text{CDCl}_3$ )

The assignments were further confirmed by  $^{13}\text{C}$ -DEPT NMR spectrum (Figure 3.35). The peaks due to quaternary carbons labeled as a, b, e, and f were absent. The peak appeared in negative phase confirmed assignment for methyl carbons (g). The peaks due to methylene carbons h, and i, were observed in positive phase.

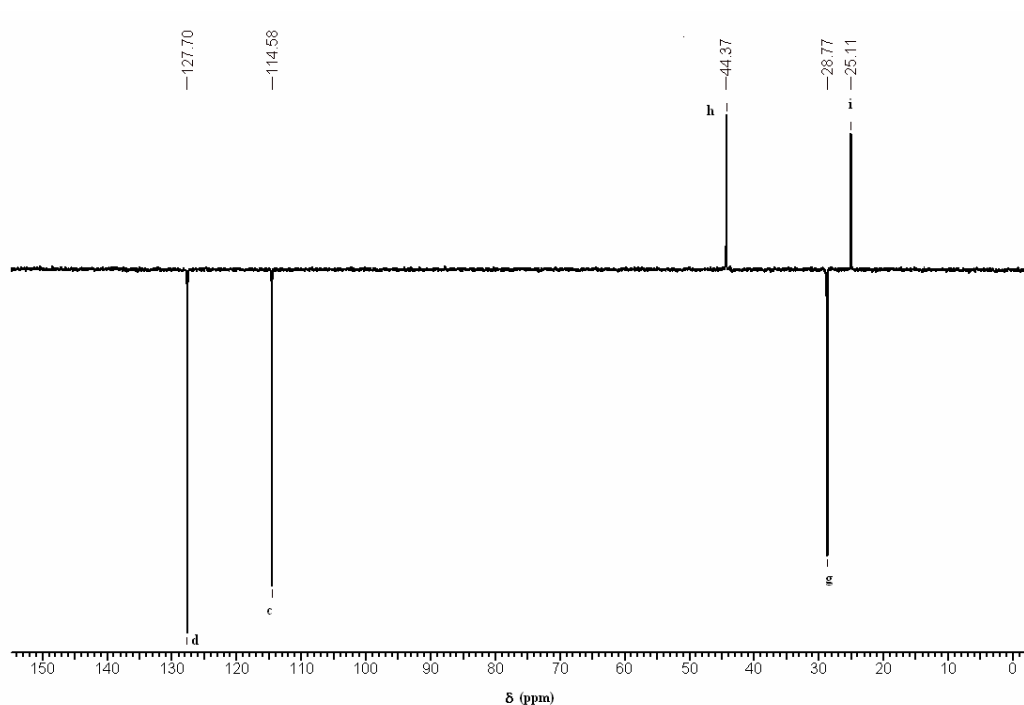


Figure 3.35 :  $^{13}\text{C}$ -DEPT NMR spectrum of 2,7-bis(4-cyanatophenyl)-2,7-dimethyloctane ( $\text{CDCl}_3$ )

### 3.5 Conclusions

1. Seven new cyanate ester monomers containing cycloaliphatic “cardo” group *viz*; 1,1-bis(4-cyanatophenyl)-3-pentadecylcyclohexane, 1,1-bis(4-cyanatophenyl)decahydronaphthalene, 1,1-bis(4-cyanato-3-methylphenyl)decahydronaphthalene, 1,1-bis(4-cyanato-3,5-dimethylphenyl)decahydronaphthalene, 1,1-bis(4-cyanatophenyl)-4-perhydrocumylcyclohexane, 1,1-bis(4-cyanato-3-methylphenyl)-4-perhydrocumylcyclohexane, 1,1-bis(4-cyanato-3,5-dimethylphenyl)-4-perhydrocumylcyclohexane were synthesized starting from commercially available raw materials.
2. The melting points of cyanate ester monomers containing cycloaliphatic “cardo” group increased with the substitution of methyl group(s) at *ortho* position to cyanate functionality.
3. A new cyanate ester monomer containing alkylene spacer *viz*; 2,7-bis(4-cyanato phenyl)-2,7-dimethyloctane was synthesized.
4. The cyanate ester monomers containing (substituted) cycloaliphatic “cardo” group showed the presence of magnetically non-equivalent distereotopic phenyl rings in the NMR spectra.

## References:

1. Grigat, E.; Putter, R. *Angew.Chem.Int.Ed.* **1967**, 6, 606
2. Grigat, E.; Putter, R. (Bayer AG) *U.S.Patent* 4,028,393, **1977**.
3. Pankratov, V.A.; Vinogradova, S.V.; Korshak, V.V. *Russ. Chem. Rev.* **1977**, 46, 278.
4. Snow, A.W. In *Chemistry and Technology of Cyanate Ester Resins*. Hamerton, I. Ed, **1994**, Chapman and Hall, Glasgow, Chap 2.
5. Snow, A.W.; Buckely, L.J. *Macromolecules* **1997**, 30, 394.
6. Abed, J.; Mercier, R.; McGrath, J.E. *J.Polym.Sci., Part A:Polym.Chem.* **1997**, 35, 977.
7. Marcos-Fernandez, A; Posadas, P; Rodriguez, A; Gonzalez, L. *J. Polym. Sci. Part. A: Polym. Chem.* **1999**, 37, 3155.
8. Mathew, D.; Nair, C.P.R.; Ninan K.N. *Polym. Int.* **2000**, 49, 48
9. Maya, E.M.; Snow, A.W.; Buckely, L.J. *Macromolecules* **2002**, 35, 460.
10. Maya, E.M.; Snow, A.W.; Buckely, L.J. *J.Polym.Sci., Part A:Polym.Chem.* **2003**, 41, 60.
11. Yan H.; Chen, S.; Qi, G. *Polymer* **2003**, 44, 7861
12. Hwang, H.J.; Li, C.H.; Wang, C.S. *J. Appl. Polym. Sci.* **2005**, 96, 2079.
13. Nair, CPR; Mathew, D; Ninan, KN. *Adv. Polym. Sci.* 2001, 155, 1.
14. Woo, EP; Dellar, DV. (Dow Chemicals) *U.S.Patent* 4,528,336, **1985**.
15. Lin, C.H.; Jiang, Z.R.; Wang, C.S. *J. Polym. Sci. Part A: Polym. Chem.* **2002**, 40, 4084.
16. Snow, A.W.; Buckley, L.J.; Armistead, J.P. *J. Polym. Sci. Part A: Polym. Chem.* **1999**, 37, 135.
17. Dinakaran, K.; Alagar, M. *Polym. Adv. Technol.* **2003**, 14, 544.
18. Grigat, E.; Putter, R. *Chem.Ber.* **1964**, 97, 3012
19. Wang, F. L.; Hong, J. L. *Polymer* **1998**, 39, 4319.
20. Zhang, B.; Wang, Z.; Zhang, X. *Polymer*, **2009**, 50, 817
21. Loudas, B.L.; Vogel, H.A. *U.S. Patent* 3,733,349, **1973**.
22. Snow, A. W.; Griffith, J.R. *J. Fluorine Chem.* **1980**, 15, 471.
23. Snow, A. W.; Griffith, J.R.; Soulen, R.L.; Greathouse, J.A.; Lodge, J.K. *Am. Chem..Soc.: Poly. Mat. Sci. Eng. Preprints* **1992**, 66, 466.
24. Wang, Y.H.; Hong, V.Y.L; Hong, J.L. *J. Polym.* **1993**, 34, 1970
25. Laskoski, M.; Dominguez, D. D.; Keller, T. M. *J. Polym. Sci. Part A: Polym Chem* **2006**, 44, 4559.
26. Anuradha, G.; Sarojadevi, M. *J. Appl. Polym. Sci.* **2008**, 110, 938.
27. Anuradha, G.; Sarojadevi, M. *J. Polym. Res.* **2008**, 15, 507.
28. Hamerton, I.; Howlin, B.J.; Klewpatinond, P.; Takeda, S. *Macromolecules* **2009**, 42, 7718.
29. Corey, E.J.; Sugges, J.W. *Tetrahedron Lett.* **1975**, 16, 2647.
30. Sethi, S.C.; Subbarao, B.C. *Ind.. J. Chem.* **1964**, 2, 178.
31. Shingte, R.D. *Synthesis of Processable High Performance Polymers*, PhD Dissertation, University of Pune, India, **2006**.
32. Avadhani, C.V.; Wadgaonkar, P. P.; Sivaram, S. S. *U.S. Patent* 6,255,439, **2001**.
33. Honkhambe, P.N. *Synthesis, Characterization and Applications of High Performance Polymers*, PhD Dissertation, Mumbai University, India, **2006**.
34. Bapat S.P. *Processable High Performance Polymers: Synthesis, Characterization and Application*, PhD Dissertation, University of Pune, India, **2007**.
35. Rao, M.V.; Rojivadiya, A.J.; Parsania, P.H.; Parekh, H.H. *J. Indian Chem. Soc.* **1987**, 758.
36. Avadhani, C.V.; Wadgaonkar, P. P.; Sivaram, S. S. *Internal report*, Unpublished data, **2001**.
37. Davis A.C.; Hunter, R.F. *J. Chem. Soc.* **1959**, 3081.
38. Tojo, G.; Fernández, M. In *Oxidation of alcohols to aldehydes and ketones* **2006**, 1<sup>st</sup> Ed. Springer, New York.
39. Yamada, M.; Sun, J.; Suda, Y.; Nakaya, T. *Chem. Lett.* **1998**, 1055.
40. Wehmeyer, R.; Walters, M.; Tasset, E.; Brewster, S.(Dow Chemicals) *US Patent* 5,463,140, **1995**.
41. Barton, J.M.; Hamerton, I.; Jones, J.R. *Polym. Int.* **1992**, 29, 145.
42. Chaplin, A.; Hamerton, I.; Howlin, B.J.; Barton, J.M. *Macromolecules* **1994**, 27, 4927.
43. Cercena, J.L., Ph.D. Dissertation, University of Connecticut, USA, 1984.
44. Furniss, B.S.; Hannford, A.J.; Smith, P.W.G.; Tatchell A. R. revised *Vogel's Textbook of Practical Organic Chemistry*, **1989**, 5<sup>th</sup> Ed, Longman, UK.

# Chapter **4**

## Curing Kinetics and Processing of Cyanate Esters

# Chapter **4A**

## Curing Kinetics of Cyanate Ester Monomers

### 4A.1 Introduction

Cyanate ester (CE) resins are an important class of thermosets that have grown rapidly in the past few years due to their unique combination of properties such as low dielectric constant, radar transparency, low moisture absorption, and superior adhesive properties. Relatively low curing temperatures and high thermal stability give CEs a distinct advantage over other resin systems such as phenolic resins, epoxy resin, bismaleimides, etc.<sup>1</sup> The cure reaction of CE monomers leading to the formation of polycyanurate networks is known to be catalyzed by a wide range of catalysts including transition metal carboxylates, acetyl acetonates, phenols, metal carbonyls, adventitious moisture, etc.<sup>2</sup> Several studies have been devoted to the reaction catalysis and kinetics wherein the main focus has been on the evaluation of activation parameters for different CE monomers using various catalysts.<sup>3-12</sup> The processability of the resin depends critically on the rate and extent of polymerization under the processing conditions.<sup>13</sup> The performance of cured resin depends on the network structure which in turn depends on its sensitivity to the curing conditions. A comprehensive understanding of the mechanism and kinetics of curing can lead to optimal curing process.<sup>13</sup> Different techniques based on DSC<sup>14-17</sup>, FTIR<sup>18</sup>, NMR<sup>19-21</sup>, HPLC<sup>22</sup>, dynamic dielectric analysis<sup>23</sup>, dispersive fibre optical Raman Spectroscopy, etc.<sup>24</sup> have been employed to follow cure reaction of cyanate ester resins.

In order to obtain protocol to predict the cure profile for optimizing processing conditions of newly developed cyanate esters containing cycloaliphatic “cardo” group or alkylene spacer (section 3.4, chapter 3), it was considered of importance to study the cure kinetics.

The present work deals with the curing study of following CE monomers (**Table 4A.1**) in dynamic as well as isothermal mode using DSC.

**Table 4A.1 : List of CE monomers used for curing study**

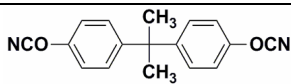
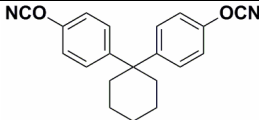
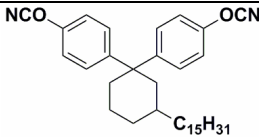
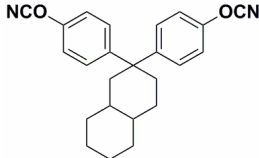
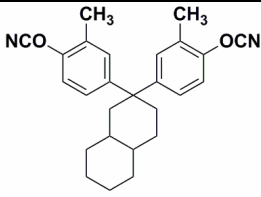
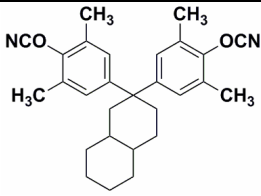
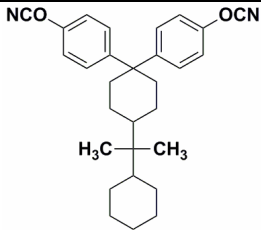
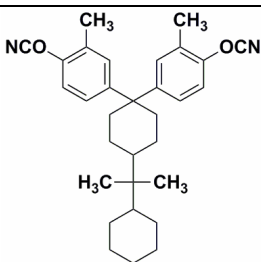
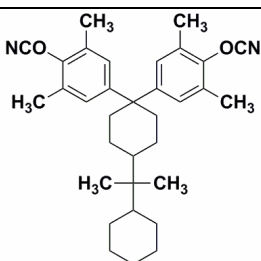
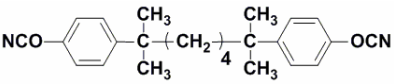
Sr. No.	Structure	Name
1		2,2-Bis(4-cyanatophenyl)propane (BPACN)
2		1,1-Bis(4-cyanatophenyl)cyclohexane (BPZCN)
3		1,1-Bis(4-cyanatophenyl)-3-pentadecyl cyclohexane (BPC15CN)
4		1,1-Bis(4-cyanatophenyl)decahydronaphthalene (BPDCCN)

Table 4A.1 continued...

5		1,1-Bis(4-cyanato-3-methylphenyl)decahydronaphthalene (DMBPDCCN)
6		1,1-Bis(4-cyanato-3,5-dimethylphenyl)decahydronaphthalene (TMBPDCCN)
7		1,1-Bis(4-cyanatophenyl)-4-perhydrocumylcyclohexane (BPPCPCN)
8		1,1-Bis(4-cyanato-3-methylphenyl)-4-perhydrocumylcyclohexane (DMBPCPCN)
9		1,1-Bis(4-cyanato-3,5-dimethylphenyl)-4-perhydrocumylcyclohexane (TMBPCPCN)
10		2,7-Bis(4-cyanatophenyl)-2,7-dimethyloctane (BPC6CN)

## 4A.2 Experimental

### 4A.2.1 Materials

Copper acetylacetonate, was purchased from Sigma-Aldrich Inc.USA. Nonyl phenol was obtained from M/s Herdillia Chemicals, Mumbai. The commercial monomer 2,2-bis(4-cyanatophenyl)propane (BPACN) was received as a gift sample from Vikram Sarabhai Space Centre, Trivandrum, India. The CE monomers viz; 1,1-bis(4-cyanatophenyl)cyclohexane (BPZCN), 1,1-bis(4-cyanatophenyl)-3-pentadecylcyclohexane (BPC15CN), 1,1-bis(4-cyanatophenyl)decahydronaphthalene (BPDCCN), 1,1-bis(4-cyanato-3-methylphenyl) decahydronaphthalene (DMBPDCCN), 1,1-bis(4-cyanato-3,5-dimethylphenyl) decahydronaphthalene (TMBPDCCN), 1,1-bis(4-cyanatophenyl)-4-perhydrocumylcyclohexane (BPPCPCN), 1,1-bis(4-cyanatophenyl-3-methyl)-4-perhydrocumylcyclohexane (DMBPPCPCN), 1,1-bis(4-cyanatophenyl-3,5-dimethyl)-4-perhydrocumylcyclohexane (TMBPPCPCN), and 2,7-bis(4-cyanatophenyl)-2,7-dimethyloctane were synthesized as described in chapter 3. Dichloromethane was of reagent grade quality and distilled over  $\text{CaH}_2$  before use.

### 4A.2.2 Sample preparation

From a standard stock solution of copper acetylacetonate (in dichloromethane), the required amount (0.11 mmol / mol CE monomer) was pipetted out and added to CE monomer. To the mixture, nonyl phenol (3 wt % based on CE monomer) was added and dichloromethane was evaporated on a rotary evaporator at room temperature under vacuum.

### 4A.2.3 DSC analysis

DSC measurements were performed on TA Instruments (Q10) supported by TA Universal Analysis software for data acquisition. Samples (5-7 milligrams) were sealed in hermetic aluminum pans and experiments were performed under a nitrogen flow of 50 mL / min. In nonisothermal studies, all the samples were subjected to a dynamic DSC scan at the heating rate of 10 °C/min. The total enthalpy of curing ( $\Delta H_T$ ) was determined from the area under the exothermic curve. The cure onset temperature ( $T_o$ ) was considered as the intersect of slope of baseline and tangent of curve leading to peak of transition (Figure 4A.1).

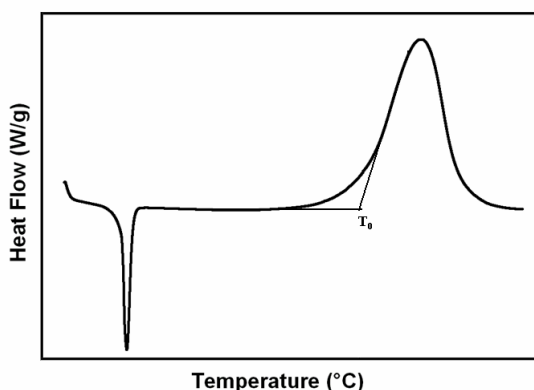


Figure 4A.1: DSC thermogram illustrating the cure onset temperature



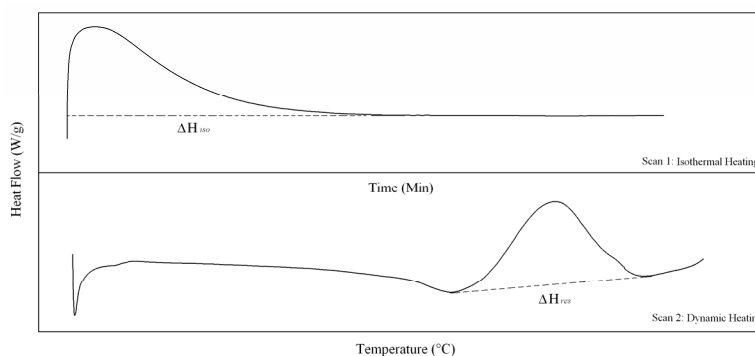
The fractional conversion ( $\alpha$ ) of each sample at a given temperature in nonisothermal study was calculated from the relation<sup>25</sup>:

$$\alpha_T = \Delta H_f / \Delta H_T \quad (1)$$

where  $\Delta H_f$  is the fractional enthalpy at a given temperature and  $\Delta H_T$ , the total heat of reaction. Isothermal curing was carried out by holding samples at 170 °C, 180 °C, 190 °C, 200 °C, 210 °C and 220 °C for 45 - 60 minutes and then subjecting to dynamic scan from 50 °C to 375 °C at 10 °C / min to determine the residual heat of reaction ( $\Delta H_{res}$ ) (**Figure 4A.2**). The fractional conversion of each sample ( $\alpha$ ) under isothermal mode was calculated from the relation<sup>5</sup>:

$$\alpha = (\Delta H_{iso}) / (\Delta H_{iso} + \Delta H_{res}) \quad (2)$$

where ( $\Delta H_{iso}$ ) is the enthalpy of reaction at time “t” and ( $\Delta H_{iso} + \Delta H_{res}$ ) is the total enthalpy of the reaction.



**Figure 4A.2 : Illustrative DSC thermograms of isothermal cure study.**

### 4A.3 Results and Discussion

A series of new CE monomers (**Table 4A.1**) containing cycloaliphatic “cardo” moiety was synthesized as detailed in chapter 3. The curing kinetics of these monomers was studied in non-isothermal and isothermal mode. A large number of qualitative studies have been reported on cure kinetics of BPACN and other CE monomers.<sup>3-12</sup> However, to the best of our knowledge, no information on the curing and curing kinetics of BPZCN is available in the literature.

#### 4A.3.1 Non-isothermal curing kinetics

**Figures 4A.3 - 4A.6** show DSC curves (neat) of CE monomers under study. The data regarding onset temperature ( $T_o$ ), peak temperature ( $T_p$ ) and final temperature ( $T_f$ ) of uncatalyzed curing from DSC curves are collected in **Table 4A.2**.

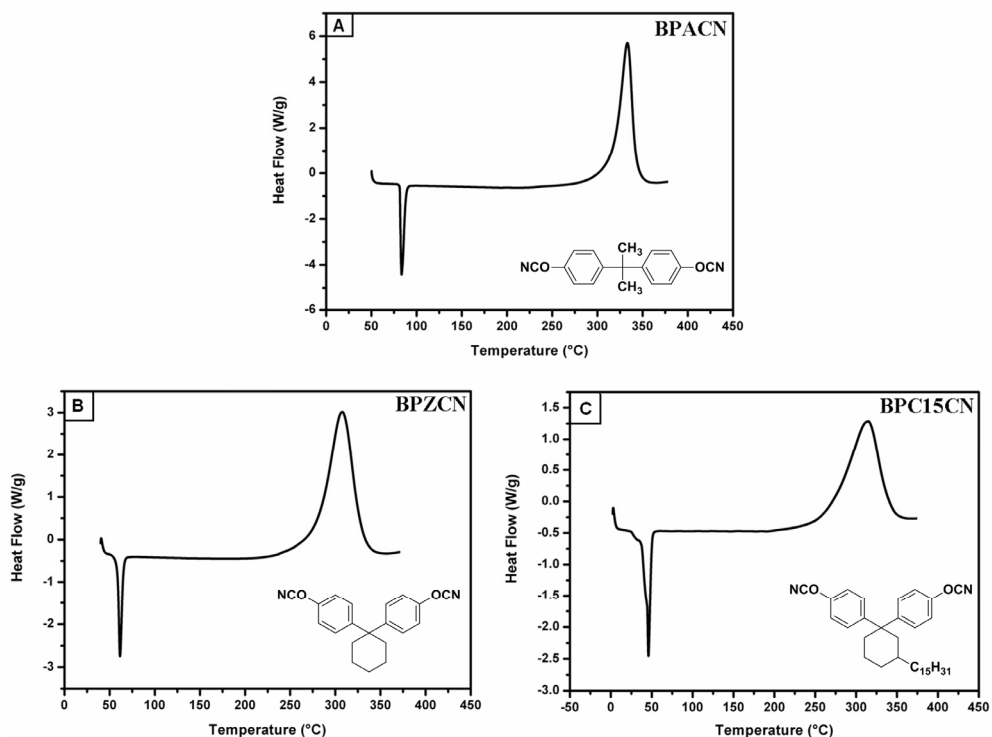


Figure 4A.3 : DSC curves of neat CE monomers A) BPACN, B) BPZCN and C) BPC15CN

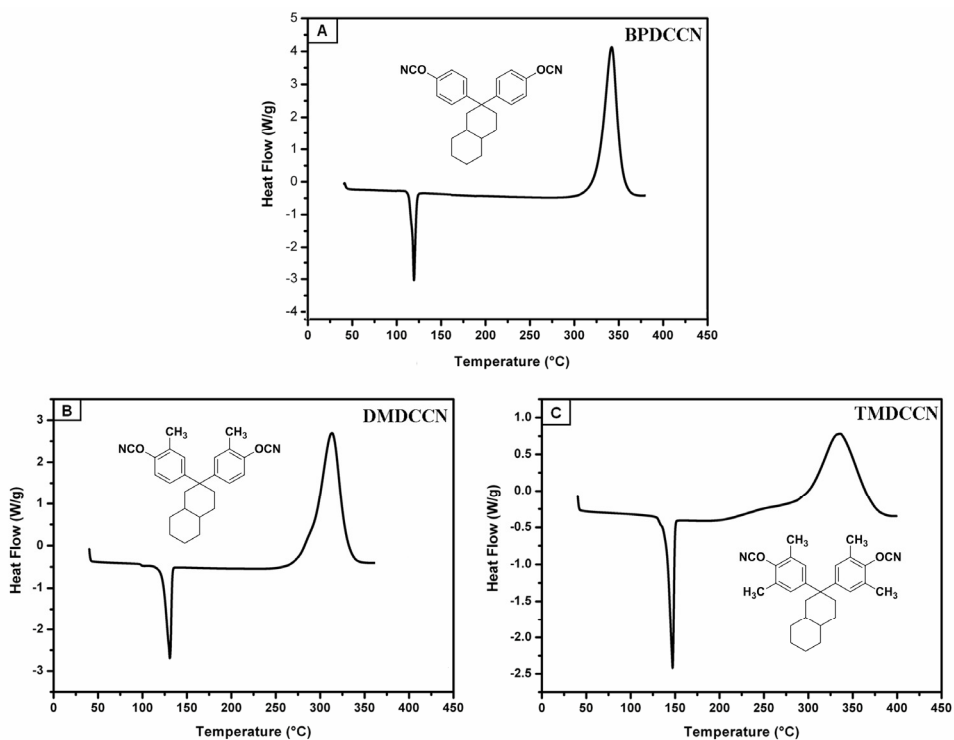


Figure 4A.4: DSC curves of neat CE monomers A) BPDCCN, B) DMBDCCN and C) TMBDCCN

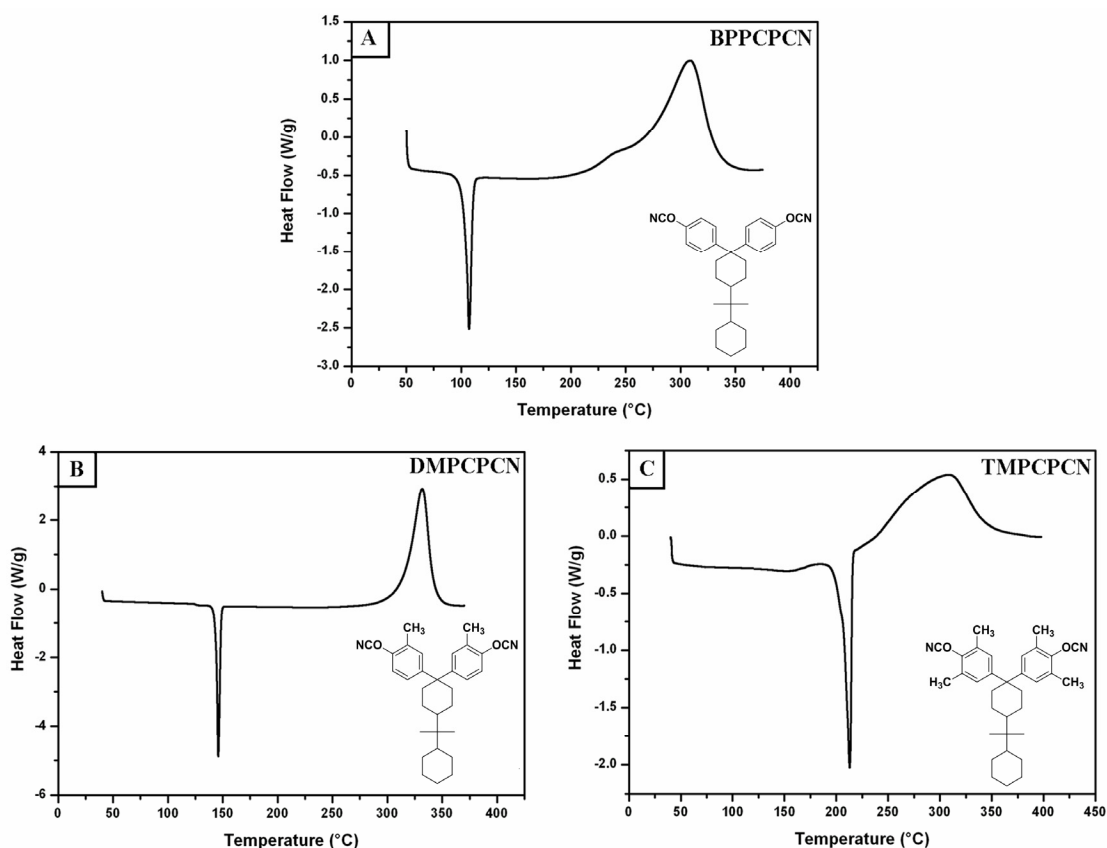


Figure 4A.5: DSC curves of neat CE monomers A) BPPCPCN, B) DMBPPCPCN and C) TMBPPCPCN.

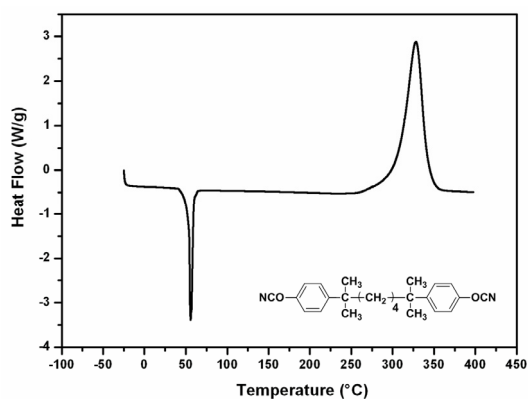


Figure 4A.6: DSC curve of neat BPC6CN.

Table 4A.2 summarizes cure characteristics of CE monomers under study. From the results presented in Table 4A.2, the change of melting point of CE monomer with the introduction of pendent flexible pentadecyl chain or methyl group can be observed. The melting point of BPC15CN (47 °C) is lower than that of BPZCN (61 °C). This could be due to interference caused by C15 chain for the close packing of molecules. In case of BPDCCN, DMBPDCCN and TMBPDCCN the melting point increased with the subsequent addition of methyl group(s) at *ortho* to cyanate functionality.

Table 4A.2: DSC characteristics of cyanate ester monomers (neat).

Sr. No.	CE Monomer	Structure	Melting Point (°C) <sup>1</sup>	Cure Characteristics			$\Delta H$ (kJ/mol)
				T <sub>o</sub> (°C)	T <sub>p</sub> (°C)	T <sub>f</sub> (°C)	
1.	BPACN		84	316	333	365	211
2.	BPZCN		61	278	308	353	235
3.	BPC15CN		47	268	315	370	249
4.	BPDCCN		121	298	318	360	242
5.	DMBPDCN		131	288	314	355	220
6.	TMBPDCCN		147	292	336	398	176
7.	BPPPCN		107	260	306	365	204
8.	DMBPPPCN		146	314	331	370	203
9.	TMBPPPCN		213	230	308	391	144
10.	BPC6CN		56	295	328	372	198

1 – From DSC melting endotherm

T<sub>o</sub> – Cure Onset TemperatureT<sub>p</sub> – Peak TemperatureT<sub>f</sub> – Final Cure Temperature

Similarly, in case of BPPCPCN, DMBPPCPCN and TMBPPCPCN, the melting point increased with subsequent addition of methyl group(s) at *ortho* to cyanate functionality. The melting point of BPC6CN (56 °C) is lower than that of BPACN (84 °C) due to the incorporation of flexible alkylene spacer between the reactive cyanate end groups.

The enthalpy data for the most studied CE monomer; BPACN is reported in the range of 195 - 238 kJ/mol by various researchers.<sup>26</sup> Therefore, in the present study, no attempt was made to correlate the variation of  $\Delta H$  with structure of dicyanate monomer.

**Figure 4A.3 (curve A)** shows a melting endotherm at 84 °C and the uncatalysed monomer exhibits a cure onset ( $T_o$ ) at 316 °C. It is known that no reaction occurs if absolutely pure BPACN is heated<sup>15</sup>. Therefore, in the absence of externally added catalyst, the reaction is believed to be catalyzed by residual hydrogen-donating impurities like phenols, moisture, etc. present in the sample. Since such trace impurities catalyze the curing reaction, in uncatalysed curing mode, the correlation of structure-based reactivity of the monomer becomes difficult. To swamp the effect of impurities, the kinetics of cure was studied under catalytic mode as is routinely done<sup>1, 8</sup>. A wide variety of different catalysts and catalyst types including transition metal carboxylates, acetyl acetonates, phenols, carbonyls, adventitious water, etc., have been found to be effective for curing of CE monomers.<sup>1,2,13</sup> (detailed in section 1.2.5, chapter 1).

The present study was carried out employing copper acetylacetonate/ nonylphenol catalytic system since the percentage conversion with this system has been reported to be higher than other catalytic systems.<sup>13</sup> The kinetics of curing was studied for BPACN, BPZCN, BPC15CN, BPDCCN, BPPCPCN and BPC6CN. The monomer was mixed with the catalyst by co-solvent (dichloromethane) technique. Evaporation of the co-solvent although caused phase separation of the catalyst, it dissolved in molten monomer prior to polymerization.

**Figure 4A.7** illustrates DSC curves of catalyzed curing of CE monomers. The curves for catalyzed monomers are not perfectly monomodal indicating inhomogeneity of the samples. Since the apparent activation energy of the overall reaction is considered to be averages of the various reaction steps, this inhomogeneity has no bearing on the overall kinetics of reaction to a large extent. The data on cure characteristics and the enthalpy of cure reaction ( $\Delta H$ ) for different monomers at the heating rate of 10 °C/min are collected in **Table 4A.3**.

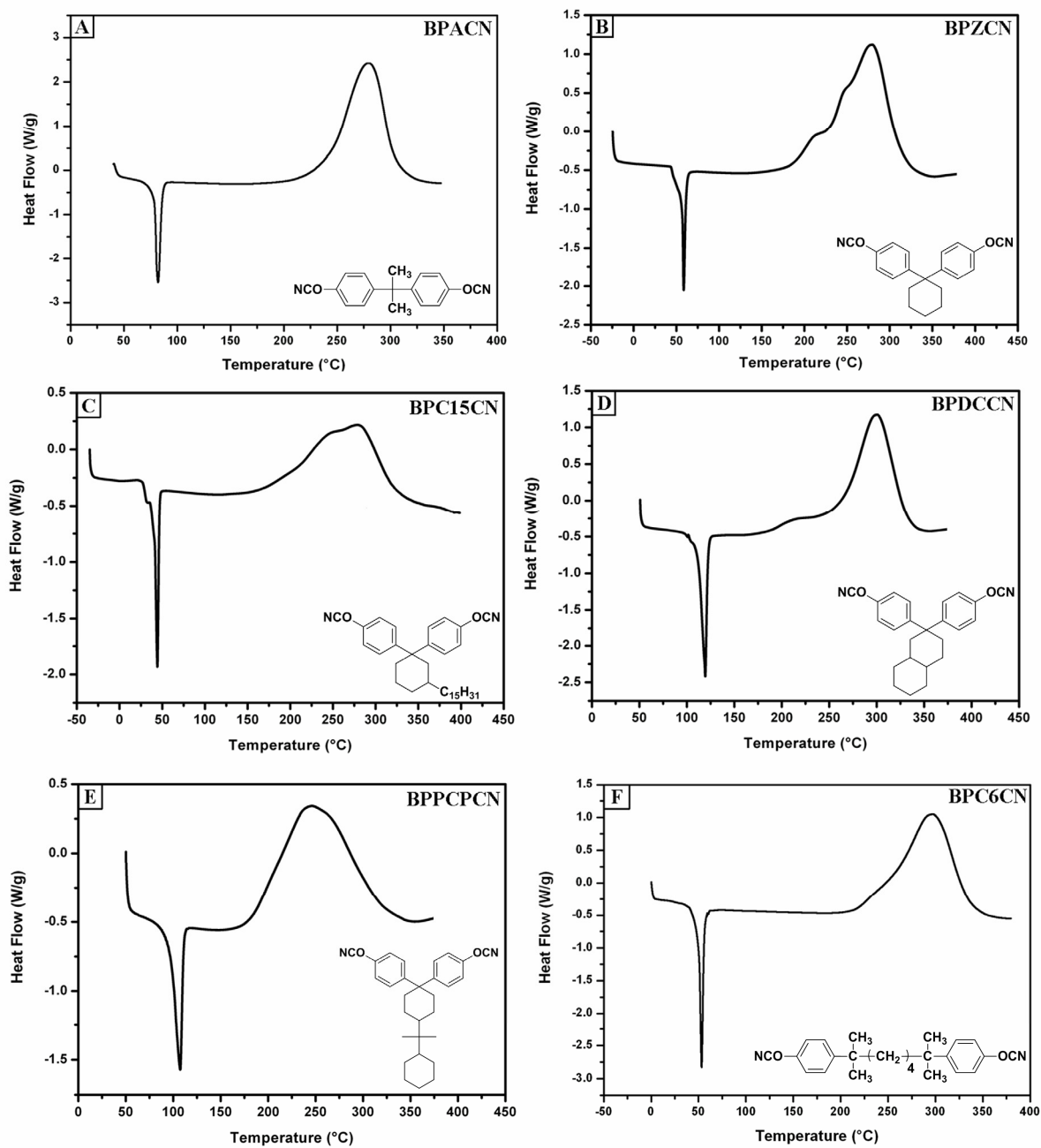
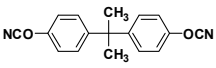
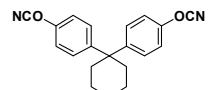
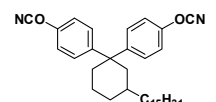
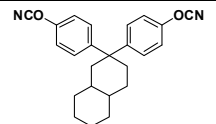
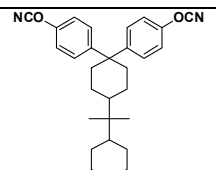
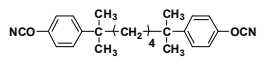


Figure 4A.7 : DSC curves of catalyzed CE monomers A) BPACN, B)BPZCN, C)BPC15CN, D) BPDCCN, E) BPPCCPN and F) BPC6CN.

Table 4A.3: Cure characteristics of CE monomers (catalysed)

Sr. No.	CE Monomer	Structure	T <sub>0</sub> (°C)	T <sub>p</sub> (°C)	T <sub>f</sub> (°C)	α <sub>p</sub> (%)	T <sub>60</sub> (°C)	ΔH (kJ/mol)
1.	BPACN		238	272	336	53	272	217
2.	BPZCN		217	279	340	66	274	226
3.	BPC15CN		175	279	358	69	271	212
4.	BPDCCN		258	301	355	65	298	197
5.	BPPCCN		180	246	356	44	260	202
6.	BPC6CN		223	296	370	62	295	191

α<sub>p</sub> – Conversion at Peak Temperature

T<sub>60</sub> – Temperature at 60 % Conversion

#### 4A.3.1.1 Kinetics of cure

The kinetics of catalyzed cure reaction of cyanate ester has been established to follow a classical n<sup>th</sup> order model as<sup>8</sup>:

$$d\alpha/dt = k_f(1-\alpha)^n \quad (3)$$

Under nonisothermal conditions, this rate expression takes the form:

$$d\alpha/dT = (A/\phi)e^{-E/RT} (1-\alpha)^n \quad (4)$$

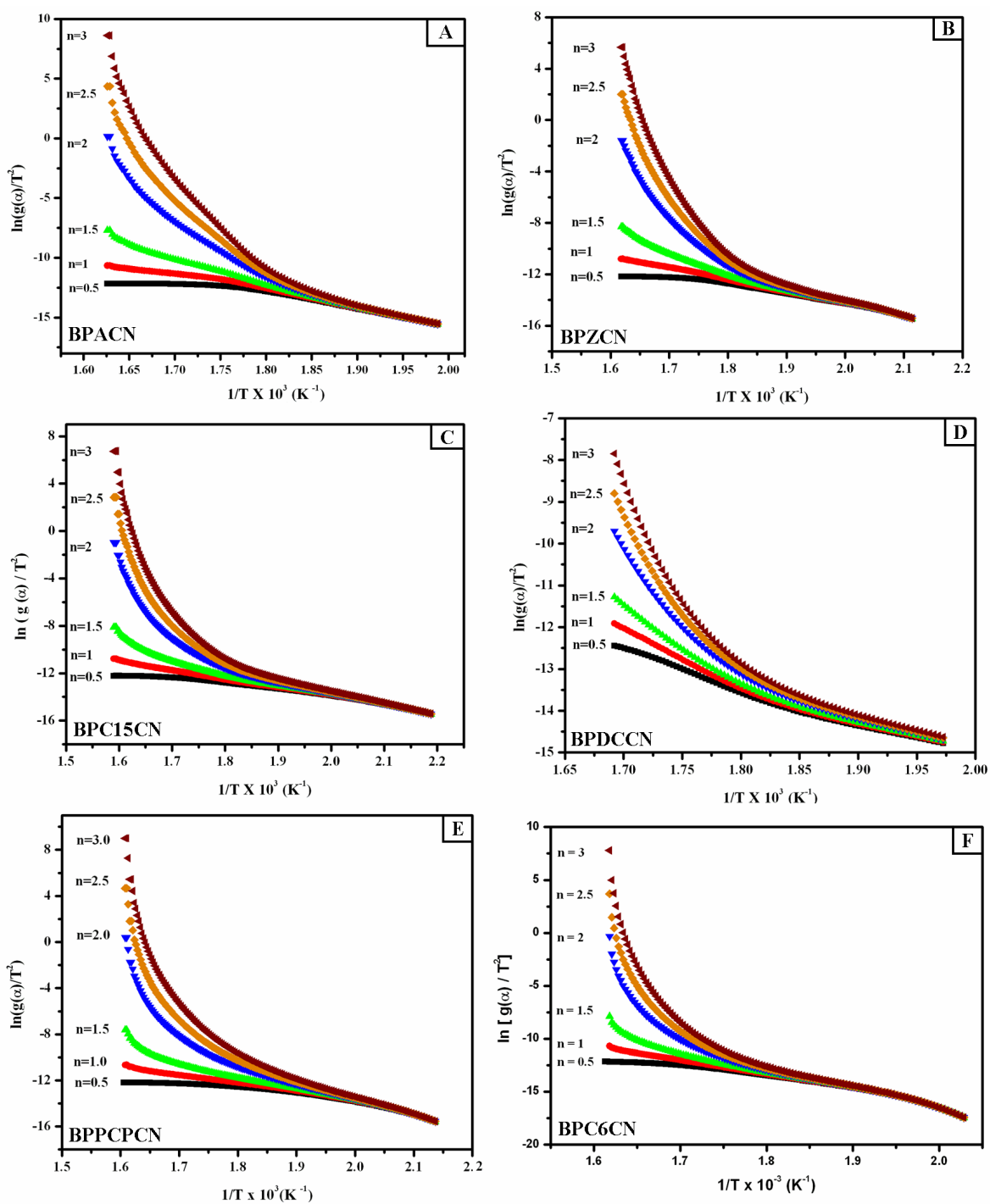
where,  $\alpha$  is the fractional conversion at temperature  $T$ , following a heating rate  $\phi$ .  $E$  is the activation energy and  $A$  the Arrhenius frequency factor. The order of reaction is  $n$ . Several authors have integrated the above equation using different approximations leading to integral equations. Some widely used methods include; Kissinger method<sup>27</sup>, Borchardt-Daniels method<sup>28</sup>, Ozawa method<sup>29</sup>, Coat-Redfern method<sup>30</sup>, Rogers method<sup>31</sup> etc. Kissinger and Ozawa methods are independent of reaction order and make use of variation of temperature corresponding to maximum of DSC exotherm at different heating rates. Since the nature of catalyzed DSC curves (**Figure 4A.7**) of CE monomers under present study is not perfectly monomodal, the results obtained by Kissinger, Ozawa methods would have been erroneous. Therefore, activation parameters were calculated using Coats-Redfern equation<sup>30</sup> (Equation 5):

$$\ln\{g(\alpha)/T^2\} = \ln\{AR/\phi E(1-2RT/E)\} - E/RT \quad (5)$$

where  $g(\alpha) = [1-(1-\alpha)^{1-n}] / (1-n)$ ; for  $n = 1$ ,  $g(\alpha) = -\ln(1-\alpha)$ ;  $R$  is the gas constant.

The order of the reaction was found from the best fit plots of  $\ln(g(\alpha)/T^2)$  vs  $1/T$  for different values of  $n$ . The kinetic plots for the determination of  $n$  for all the monomers under study are represented in **Figure 4A.8**.

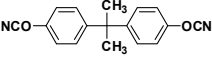
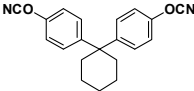
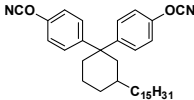
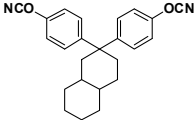
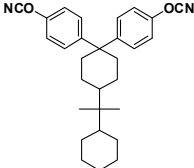
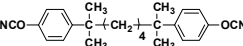




**Figure 4A.8 :** Coats-Redfern plot for determination of  $n$  A) BPACN, B)BPZCN, C)BPC15CN, D) BPDCCN, E) BPPCPCN and F) BPC6CN.

The value of  $n$  for all monomers was found to be close to 1 over most of the conversion range. The kinetic parameters ( $E$  and  $A$ ) were determined from the linear plots of  $\ln(g(\alpha)/T^2)$  vs.  $1/T$  (for  $n = 1$ ). The calculated activation parameters are collected in **Table 4A.4**.

Table 4A.4 : Activation parameters of CE monomers by Coats-Redfern method

Sr. No.	CE Monomer	Structure	Activation Energy Ea (kJ/mol)	Frequency Factor ln A (s <sup>-1</sup> )
1.	BPACN		116	12.3
2.	BPZCN		77	2.59
3.	BPC15CN		85	5.49
4.	BDCCN		68	2.41
5.	BPPCPCN		66	1.93
6.	BPC6CN		119	12.3

The activation energy of cyanate ester monomers containing cycloaliphatic “cardo” group *viz*; BPZCN, BPC15CN, BDCCN and BPPCPCN as calculated by Coats-Redfern method in nonisothermal mode was in the range of 66 – 85 kJ/mol which is lower as compared to activation energy of BPACN. At this point of time, no explanation can be put forth for the observed higher activation energy and frequency factor of BPC15CN amongst the CE monomers containing cycloaliphatic “cardo” group. The activation energy and frequency factor of BPC6CN and BPACN are almost in the same range. The introduction of alkylene spacer shows practically no influence on the cure kinetics of BPACN.

#### 4A.3.2 Isothermal curing kinetics

Isothermal DSC is a precise method for computing cure kinetics. The apparent activation energy of the reaction was obtained by Arrhenius plot of the shift factors used in the time-temperature superposition *vs.* reciprocal temperature as explained by Gillham *et.al.*<sup>5</sup> No knowledge of the form

of the rate expression is needed to obtain the apparent activation energy, which is assumed to be that of the overall reaction:

$$\frac{d\alpha}{dt} = k_0 e^{-E/RT_c} f(\alpha) \quad (6)$$

where  $k_0$  is the preexponential frequency factor and  $E$  is the apparent activation energy for the overall reaction. The above equation 6 on integrating and rearranging can be represented as :

$$\text{Ln} \int_0^\alpha \frac{d\alpha}{f(\alpha)} = \text{Ln} k_0 + \text{Ln} t - \left( \frac{E}{RT_c} \right) \quad (7)$$

Since the left hand side of the equation 7 is considered to be only a function of conversion, some function of conversion  $\alpha$ ,  $F(\alpha)$  can be substituted for the left hand side of the equation:

$$F(\alpha) = \text{Ln} k_0 + \text{Ln} t - \left( \frac{E}{RT_c} \right) \quad (8)$$

To construct a kinetically controlled curve,  $F(\alpha)$  vs.  $\text{Ln} t$  were superimposed at low conversion, to ensure being kinetically controlled regime with one of the curves being a reference curve at an arbitrary reference temperature. The horizontal shift factor,  $S(T_c)$  refers to the difference in  $\text{Ln} t$  between two curves shifted at constant conversion:

$$S(T_c) = \text{Ln} t_r - \text{Ln} t = \frac{-E}{R} \left( \frac{1}{T_c} - \frac{1}{T_r} \right) \quad (9)$$

where the subscript  $r$  pertains to the reference curve.

**Figure 4A.9** represents DSC isothermal curves (catalytic) of CE monomers at different temperatures ranging from 170 °C – 220 °C. **Figure 4A.10** represents curves for fractional conversion ( $\alpha$ ) vs  $\text{Ln} t$  at different temperatures for CE monomers.

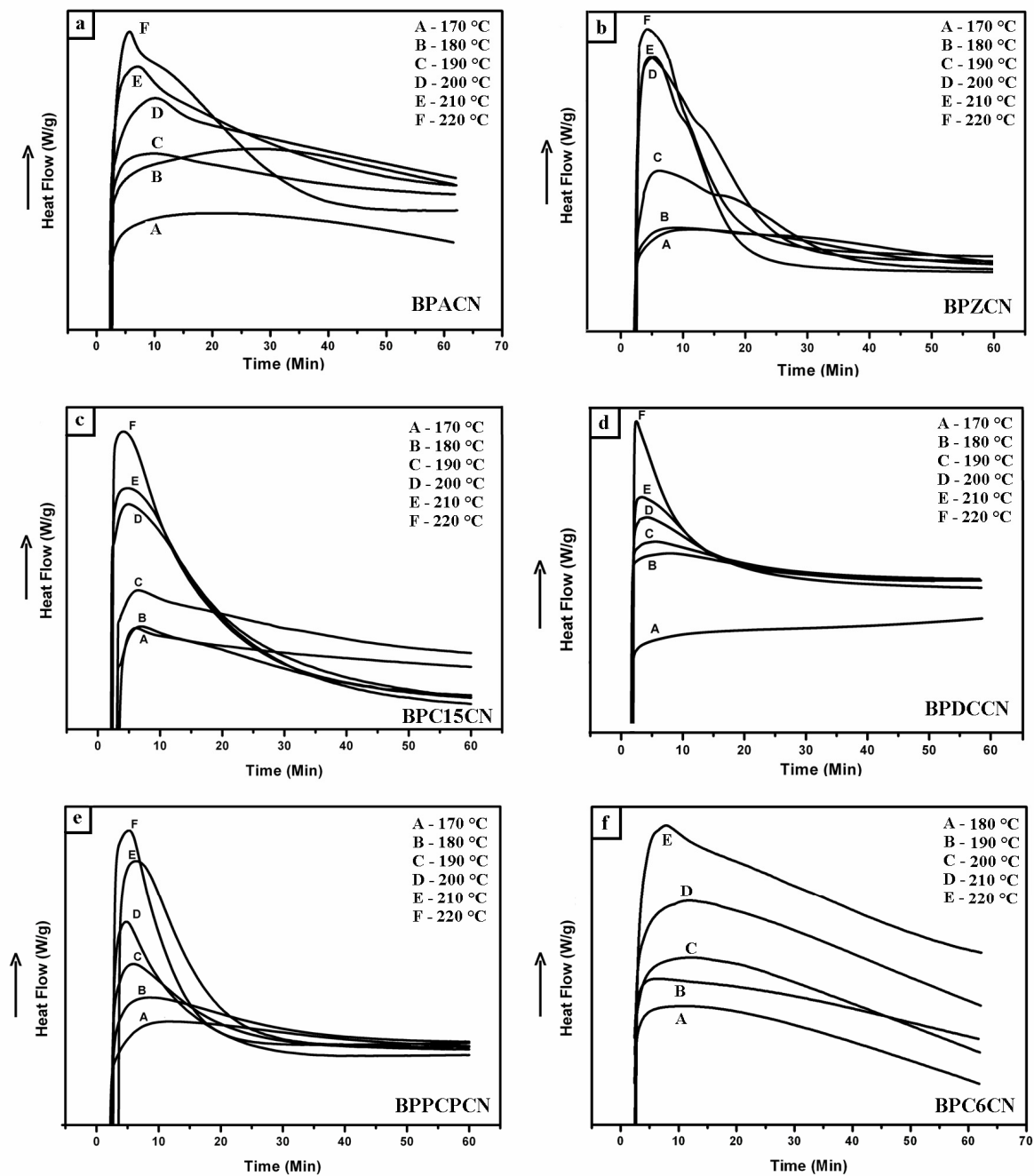
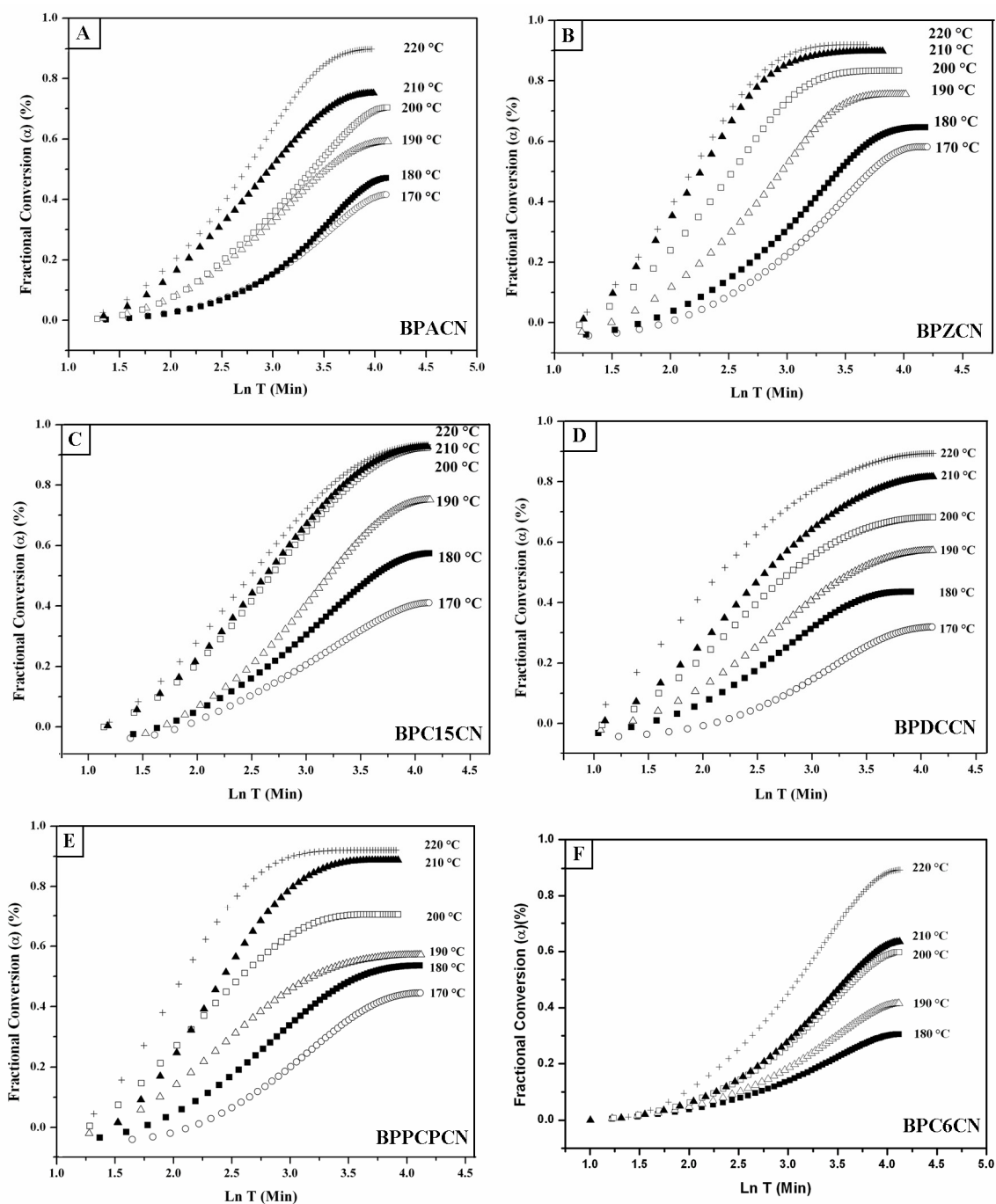


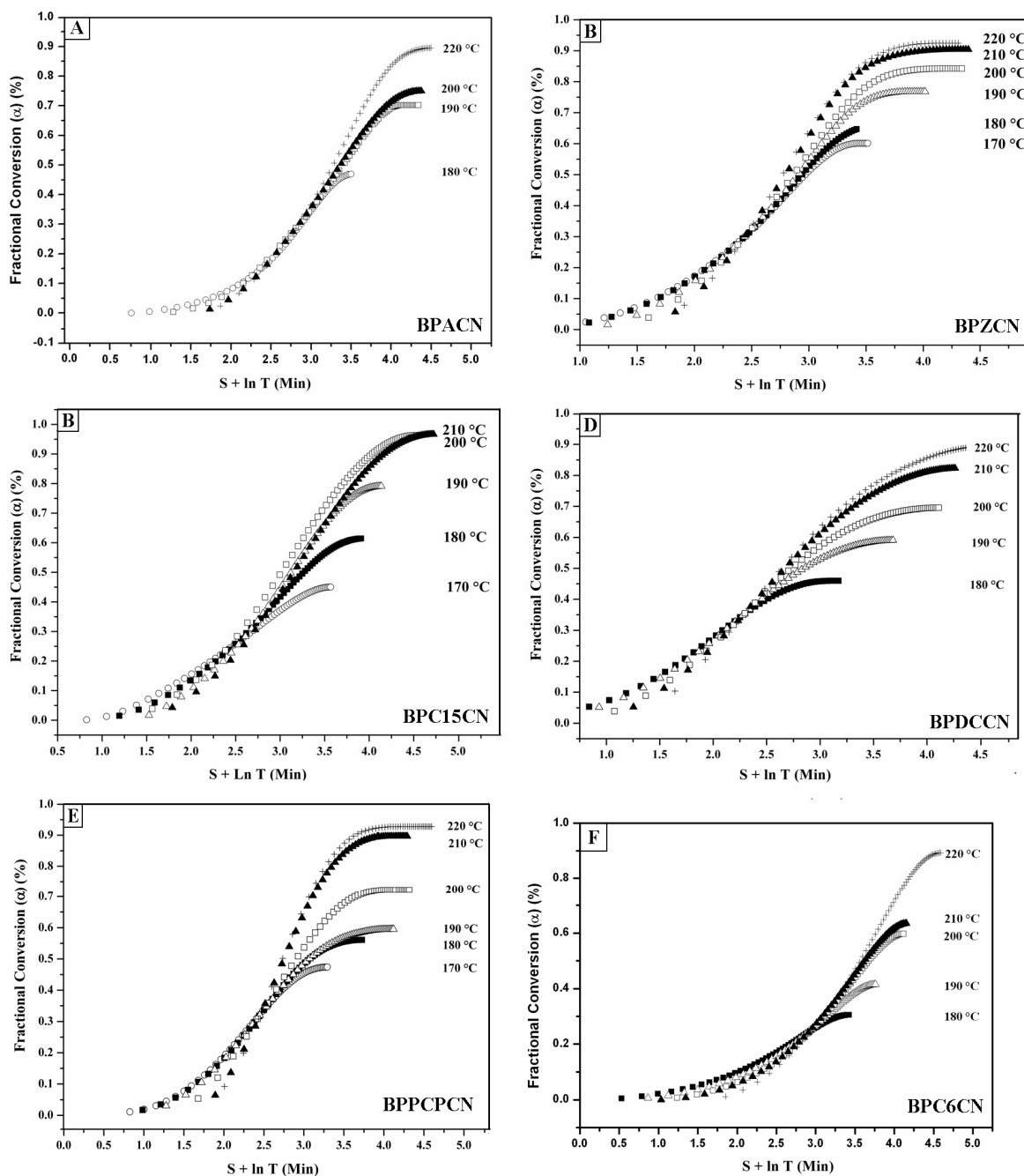
Figure 4A.9: DSC isothermal curves of CE monomers at different temperatures;  
a) BPACN, b) BPZCN, c) BPC15CN, d) BPDCCN, e) BPPCPCN and f) BPC6CN.



**Figure 4A.10 : Fractional conversion ( $\alpha$ ) vs  $\ln$  Time at various temperatures for CE monomers A) BPACN, B) BPZCN, C) BPC15CN, D) BPDCCN, E) BPPCPCN and F) BPC6CN.**

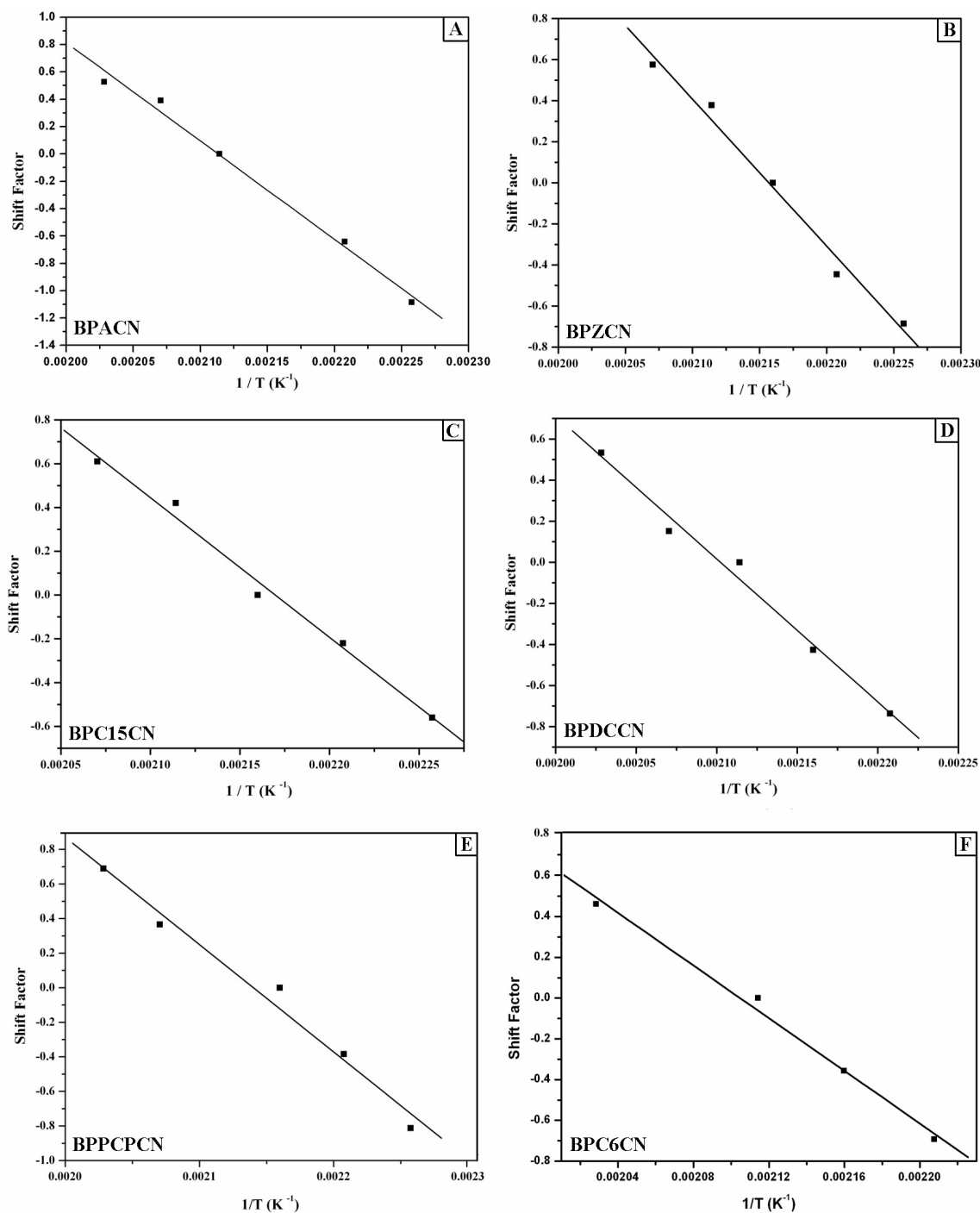
Figure 4A.11 represents superimposition of conversion curves by selecting a horizontal shift factor for each CE monomer. The basis for such a shift is the assumptions that i) the reaction is kinetically controlled in the shifted regime and ii) the reactions can be described by one activation energy<sup>5</sup>. Figure 4A.11 indicates that the reaction becomes diffusion controlled after around 50 % conversion. Below this conversion the experimental data for all cure temperature form a single

curve, whereas above this conversion, the curve starts to diverge and the conversion distinctly increases as the curing temperature increases.



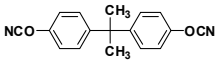
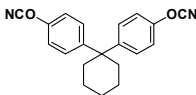
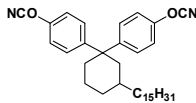
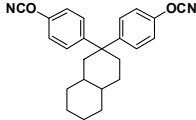
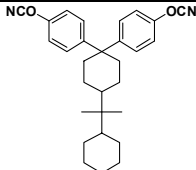
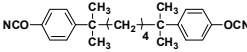
**Figure 4A.11 : Fractional conversion ( $\alpha$ ) vs Shift factor + ln Time at various temperatures for CE monomers ; A) BPACN, B) BPZCN, C) BPC15CN, D) BPDCCN, E) BPPPCN and F) BPC6CN.**

The activation parameters were calculated from a plot of shift factor vs reciprocal temperature (Figure 4A.12) and the data is collected in Table 4A.5.



**Figure 4A.12 :** Arrhenius plots of Shift factor vs Reciprocal temperature for catalysed CE monomers; A) BPACN B) BPZCN, C) BPC15CN, D) BPDCCN, E) BPPCPCN and F) BPC6CN.

**Table 4A.5 : Activation parameters of CE monomers by isothermal method**

Sr. No.	CE Monomer	Structure	Activation Energy Ea (kJ/mol)	Frequency Factor ln A (s <sup>-1</sup> )
1.	BPACN		60	15.2
2.	BPZCN		60	15.5
3.	BPC15CN		58	14.6
4.	BPDCCN		53	13.6
5.	BPPCCN		53	13.8
6.	BPC6CN		54	13.6

The activation energy calculated using Coats-Redfern equation in nonisothermal mode is normally higher than isothermal value due to variance in the assumptions in both the methods. The activation energy of curing of all the cyanate ester monomers under study as obtained in isothermal mode are in the range of 53 – 60 kJ/mol. The observed narrow range of activation energy and frequency factor of CE monomers under study indicate that the structural features such as incorporation of cycloaliphatic “cardo” group and introduction of alkylene spacer has practically no influence on the catalytic cure kinetics in isothermal mode.



#### 4A.4 Conclusions:

1. The kinetics of catalytic curing of five cyanate esters containing (substituted)(cyclo)aliphatic moiety viz; 1,1-bis(4-cyanatophenyl)cyclohexane, 1,1-bis(4-cyanatophenyl)-3-pentadecylcyclohexane, 1,1-bis(4-cyanatophenyl)decahydronaphthalene, 1,1-bis(4-cyanatophenyl)-4-perhydrocumylcyclohexane, and 2,7-bis(4-cyanatophenyl)- 2,7-dimethyloctane was studied in non-isothermal and isothermal mode using DSC and the results were compared with the curing kinetics data of 2,2-bis (4-cyanatophenyl)propane.
2. The heat of catalyzed cure reaction of cyanate ester monomers under study was observed in the range 190 – 230 kJ/mol which is in accordance with the reported values for 2,2-bis(4-cyanatophenyl) propane (195 – 238 kJ/mol)
3. The activation energy for catalyzed cure of cyanate ester monomers containing cycloaliphatic “cardo” group in nonisothermal mode was lower (65 – 85 kJ/mol) than that of 2,7-bis(4-cyanatophenyl)- 2,7-dimethyloctane (119 kJ/mol) and 2,2-bis(4-cyanatophenyl)propane ( 116 kJ/mol).
4. The activation energy for catalyzed cure of cyanate ester monomers under study under isothermal mode was in the range 53 – 60 kJ/mol.
5. The present cure kinetics study provided a protocol for the processing of synthesized cyanate ester monomers.

## References:

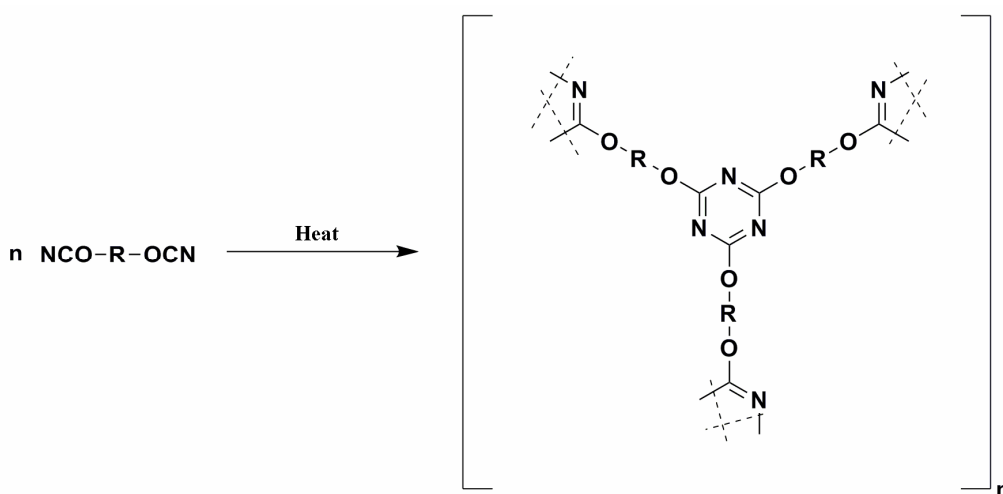
1. Nair, C.P.R.; Mathew, D.; Ninan, K.N. *Adv. Polym. Sci.*, **2001**, 155, 1.
2. Fang, T.; Shimp, D.A. *Prog. Polym. Sci.*, **1995**, 20, 61.
3. Owusu, O.A.; Martin, G.C.; Gottro, J.T. *Polym. Engg. Sci.* **1991**, 31, 1604.
4. Owusu, O.A.; Martin, G.C.; Gottro, J.T. *Polym. Engg. Sci.* **1992**, 32, 535.
5. Simon, S.L.; Gillham, J.K. *J. Appl. Polym. Sci.* **1993**, 47, 461.
6. Georjon, O.; Galy, J.; Pascult, J.P. *J. Appl. Polym. Sci.* **1993**, 49, 1441
7. Chen, Y-T.; Macosko, C.W. *J. Appl. Polym. Sci.* **1996**, 62, 576
8. Mathew, D.; Nair, C.P.R.; Krishnan, K.; Ninan, K.N.; *J. Polym. Sci., Part A: Polym. Chem.* **1999**, 37, 1103
9. Harismendy, I.; Gomez, C.M.; Rio, M.D. Mondragon, I. *Polym. Int.* **2000**, 49, 735.
10. Li, W.; Liang, G.; Xin, W. *Polym. Int.* **2004**, 53, 869.
11. Recalde, H.B.; Recalde, G.; Garcia-Lopera, R. Gomez, C. M. *Eur. Polym. J.* **2005**, 41, 2635.
12. Zhao, L.; Hu, X. *Polymer*, **2007**, 48, 6125.
13. Hay, J.N. In *Chemistry and Technology of Cyanate Ester Resins*. Hamerton, I. Ed. **1994**, Chapman and Hall, Glasgow, Chap 6, p 151-192.
14. Kohn, J.; Albert, E.C.; Wilchek, M.; Langer, R. *Anal. Chem.* **1986**, 58, 3184.
15. Bauer, M.; Rodekirch, G. *Acta. Polym.* **1986**, 37, 654.
16. Couchman, P.R. *Macromolecules*, **1987**, 20, 1712.
17. Pascult J.P.; Williams J.J. *J. Polym. Sci. Phys. Ed.* **1990**, 28, 85
18. Simon, S.L.; Gillham, J.K. *J. Appl. Polym. Sci.* **1993**, 47, 461.
19. Fang, T. *Macromolecules*, **1990**, 23, 4553
20. Fyfe, C.A.; Niu, J.; Rettig, S.J.; Burlinson, N.E.; Reidsema, C.M.; Wang, D.W.; Poliks, M. *Macromolecules* **1992**, 25, 6289.
21. Gupta, A.M.; Macosko, C.W. *Macromolecules*, **1993**, 26, 2455.
22. Grenier-Loustalot M.F.; Lartigau, C. *J. Polym. Sci. Polym. Chem.* **1997**, 35, 3101.
23. Deng, Y.; Martin, G.C. *Polymer*, **1996**, 37, 3593.
24. Cooper, J.B.; Vess, T.M.; Campbell, L.A.; Jensen, B.J. *J. Appl. Polym. Sci.* **1996**, 62, 135.
25. Prime R. B. In *Thermal Characterization of Polymeric Materials*. Turi, E.A. Ed. **1981**, Academic, New York, p 435.
26. Snow, AW. In *Chemistry and Technology of Cyanate Ester Resins*. Hamerton, I. Ed. **1994**, Chapman and Hall, Glasgow, Chap 2, p 7-57.
27. Kissinger, H.E. *Anal. Chem.* **1957**, 29, 1702.
28. Borchardt, H.J.; Daniels, F. *J. Amer. Chem. Soc.*, **1957**, 78, 41.
29. T. Ozawa *Bull. Chem. Soc. Jpn.* **1965**, 38, 1881. and T. Ozawa *J. Thermal Anal.*, **1970**, 2, 301.
30. Coats, A.W.; Redfern, J.P. *Nature* **1964**, 201, 68.
31. Rogers, R. N.; Morries, E.D. *Anal. Chem.*, **1992**, 32, 412.

# Chapter **4B**

## Processing of Cyanate Ester Monomers

### 4B.1 Introduction

Cyanate esters are amenable to processing by a large variety of conventional techniques such as by heating without any need for pressure leading to the formation of highly stable, six membered triazine rings (**Figure 4B.1**).<sup>1</sup> The cyclization reaction can be induced thermally or catalytically. As thermally induced reaction is slow and usually difficult to drive to high levels of conversion, catalysts are commonly used. For common aryl dicyanates, a wide variety of catalysts have been employed. The selection of appropriate catalyst system is governed by a number of factors, including the monomer type, the required pot life and the type of processing method selected (section 1.2.5 chapter 1).



**Figure 4B.1: Formation of polycyanurate network**

The conversion of cyanate ester resins has important effects on a number of properties. It directly affects the physical and mechanical properties of cured resin. As expected, the cure temperature directly influences the degree of conversion. The cure temperature and post-cure conditions have an effect on properties other than just the  $T_g$  of the cured resin. The post-cure significantly increases the hot-wet flexural strength, although the moisture absorption is also increased.<sup>1</sup> Apart from the degree of conversion, the above mentioned properties also vary with monomer structure. CE monomers (and polycyanurate network) with phenyl phosphine oxide, sulfone, carbonyl, ether and ether ketone, fluoromethylene, silicon, cycloaliphatic, cardo, etc., moieties into the CE backbone were synthesized to understand the effect of incorporation of these moieties on various properties such as thermal, mechanical, dielectric, hydrolytic, etc., of polycyanurate network.<sup>2-15</sup>

Aiming towards polycyanurates exhibiting lower moisture absorption, various new cyanate esters containing cycloaliphatic “cardo” group or alkylene spacer were designed and synthesized (as described in section 3.4, chapter 3). It was therefore of interest to study the properties of polycyanurates of these monomers. The present work describes processing of CE monomers

containing i) cycloaliphatic “cardo” group and ii) alkylene spacer and characterization of cured network by DMTA, DSC, TGA and moisture absorption.

## 4B.2 Experimental

### 4B.2.1 Materials

The CE monomers *viz*; 1,1-bis(4-cyanatophenyl)cyclohexane (BPZCN), 1,1-bis(4-cyanato phenyl)-3-pentadecylcyclohexane (BPC15CN), 1,1-bis(4-cyanatophenyl)-4-perhydrocumylcyclohexane (BPPCCN), 1,1-bis(4-cyanatophenyl)decahydronaphthalene (BPDCCN), and 2,7-bis(4-cyanatophenyl)-2,7-dimethyloctane (BPC6CN) were synthesized and purified as described in chapter 3 (section 3.3 and 3.4). The commercial CE monomer 2,2-bis(4-cyanatophenyl)propane (BPACN) was received as a gift sample from Vikram Sarabhai Space Centre, Trivandrum, India. Copper acetylacetonate, was purchased from Sigma-Aldrich Inc.USA. Nonyl phenol was obtained from M/s Herdillia Chemicals, Mumbai. Dichloromethane was of reagent grade quality (Merck, India) and was distilled over CaH<sub>2</sub> before use.

### 4B.2.2 Characterization

Infrared spectra were recorded on Perkin-Elmer, Spectrum GX model at a resolution of 4 cm<sup>-1</sup>. The spectra were recorded by depositing samples as fine particulates dispersed in KBr.

Differential scanning calorimetry (DSC) was conducted on a TA instrument (model Q 10) at the heating rate of 10 °C / min with nitrogen flow of 50 mL / min.

Thermogravimetric analysis (TGA) data were obtained using a TA instrument, (model Q 5000) at the heating rate of 10°C / min under nitrogen.

Dynamic mechanical thermal analysis (DMTA) was conducted on Rheometrics Scientific (model Mark IV) (UK) at the frequency of 1.0 Hz and the heating rate of 10°C /min in bending mode.

Percentage moisture absorption was calculated by placing vacuum dried, pre-weighed samples in boiling water for 24 hours and calculating the percentage weight gain by equation:

$$\% \text{ Moisture absorption} = [(W/W_0) - 1] \times 100 \quad (1)$$

where W is the weight of the sample after dipping in boiling water for 24 h and W<sub>0</sub> is the initial weight of the sample which was dried in vacuum for 12 h at 100 °C.

### 4B.2.3 Curing

The CE monomers were cured by employing copper acetylacetonate-nonylphenol catalyst system. The calculated amount of copper acetylacetonate (0.11 mmol / mol CE monomer) and nonyl phenol (3 wt % based on CE monomer) were added to CE monomer and the reaction mixture was degassed at 10 °C above the melting point of CE monomer for 10 minutes so as to remove entrapped air / moisture / solvent (if any). The molten mixture was transferred to a preheated mold and cured according to the curing schedule (**Table 4B.1**). The cured resins were slowly cooled (in order to avoid cracking due to sudden change in temperature) to ambient temperature, ejected from the mold and cut/polished wherever necessary for a uniform surface and thickness.

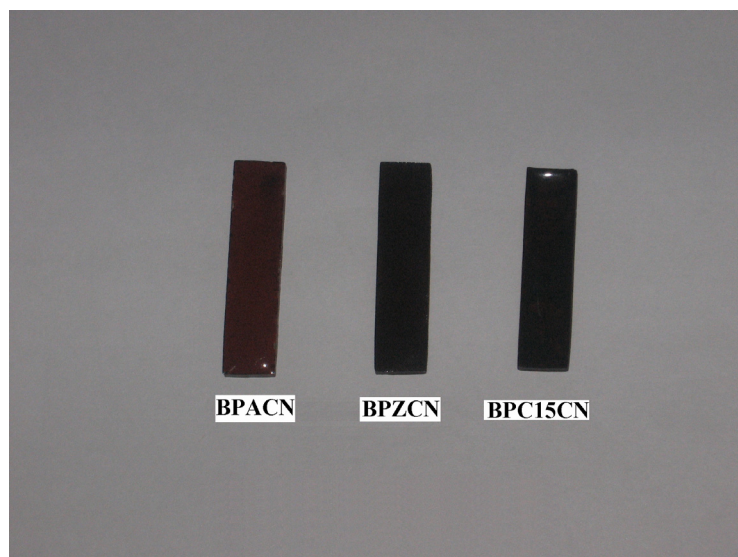
### 4B.3 Results and Discussion

It is well known that cyanate ester monomers are converted to a cured network by cyanate cyclotrimerization. The reaction occurs uncatalyzed at elevated temperatures and at lower temperatures with transition-metal/nonylphenol catalysts. Catalysts dissolved in nonylphenol significantly reduce the time and temperature needed for high cyanate conversions. The cure cycle depends on the catalyst level. However, it is generally accepted that catalysts are useful for inducing early gelation only.<sup>1</sup> In the present study, copper acetylacetonate/ nonylphenol catalytic system was employed.

As mentioned earlier in chapter 4A, higher melting points of CE monomers *viz*; 1,1-bis(4-cyanato-3-methylphenyl)decahydronaphthalene (DMBPDCCN), 1,1-bis(4-cyanato-3,5-dimethylphenyl)decahydronaphthalene (TMBPDCCN), 1,1-bis(4-cyanato-3-methylphenyl)-4-perhydrocumyl cyclohexane (DMBPPCPCN) and 1,1-bis(4-cyanato-3,5-dimethylphenyl)-4-perhydrocumyl cyclohexane (TMBPPCPCN) (131, 147, 146 and 213 °C, respectively) imposed difficulties for processing. In order to form a void free network, removing of entrapped air / moisture from molten CE monomer is necessary.<sup>1</sup> The cyanate ester resins having higher melting points may undergo gelation during B-staging under catalytic conditions. The short gel time makes the processing difficult. Therefore, curing studies of CE monomers DMBPDCCN, TMBPDCCN, DMBPPCPCN and TMBPPCPCN were not pursued. However, Wang *et.al.*<sup>15</sup> reported the curing of phenolphthalein-based CE monomers with higher melting points (>125 °C). The curing in that case was executed in neat conditions. In the present study, the monomers BPZCN, BPC15CN, BPDCCN, BPPCPCN and BPC6CN (**Table 4B.1**) were cured and characterized. The properties of cured network were compared with that of BPACN resin.

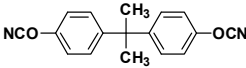
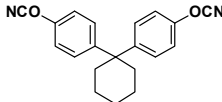
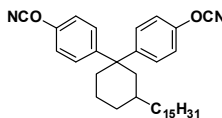
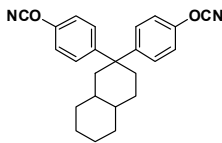
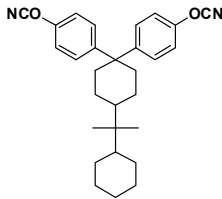
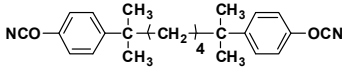
Since most of the cyanate esters are crystalline materials, in the majority of the cases the resins are B-staged so that they develop good tackiness. Since cyanate polymerization is accompanied by high heat of reaction, use of B-staged resin helps reduce the risk of highly exothermic, autocatalytic, and violent polymerization. The prepolymerization also reduces the risk

of melt flow during processing at higher processing temperatures.<sup>16</sup> Hence, for CE monomers under study, prepolymerization was executed during early stage of curing. As with other thermosets, as a rule of thumb, high temperature cure for high conversion is applicable to cyanate esters as well. High conversion obligatorily warrants heating to high temperature (220-250 °C) irrespective of the catalyst level. In the present study, the post curing was carried out at 220 - 250 °C. **Table 4B.1** summarizes the cure schedule followed for the curing of CE monomers. The CE monomer BPACN, BPZCN and BPC15CN formed amber castings as represented in **Figure 4B.2**.



**Figure 4B.2 : Slabs of cured BPACN, BPZCN and BPC15CN network.**

Table 4B.1 : Cure schedule of CE monomers.

Sr. No.	Monomer	Structure	Curing Schedule		
			B-staging [temp (°C)/ time (min)]	Curing [temp (°C)/ time (min)]	Postcuring [temp (°C)/ time (min)]
1.	BPACN		100 / 120	125 / 30 150 / 30 175 / 30 200 / 60	250 / 120
2.	BPZCN		80 / 120	125 / 30 150 / 30 175 / 30 200 / 60	225 / 120
3.	BPC15CN		80 / 120	110 / 60 140 / 60 180 / 60	225 / 120
4.	BPDCCN		125 / 120	150 / 60 175 / 30 200 / 60	250 / 120
5.	BPPCPCN		125 / 120	150 / 60 175 / 30 200 / 60	250 / 120
6.	BPC6CN		80 / 120	125 / 30 150 / 30 175 / 30 200 / 60	250 / 120

Qualitatively, the conversion can be checked by infrared spectroscopy.<sup>17</sup> The peaks at 2270-2240  $\text{cm}^{-1}$  corresponding to  $-\text{C}\equiv\text{N}$  stretching were not detected in IR spectrum (**Figure 4B.3**) of cured network confirming the conversion of cyanate monomer into polycyanurate. The appearance of broad band around 3300  $\text{cm}^{-1}$  (corresponding to  $-\text{OH}$  stretching) is due to nonyl phenol which was added as a co-solvent for copper acetylacetonate.



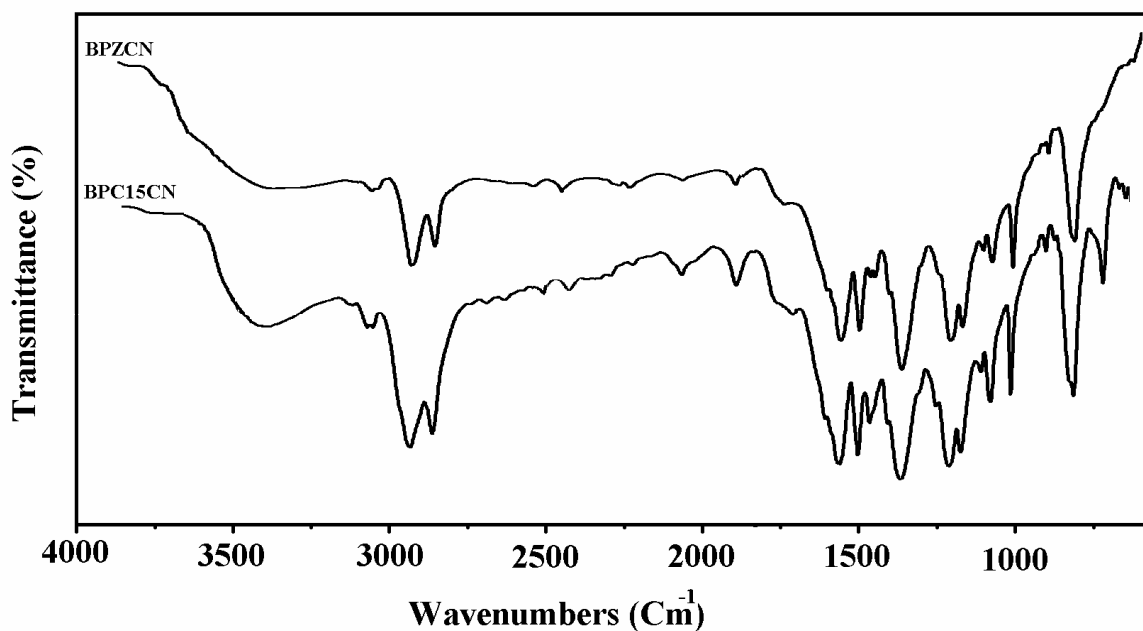


Figure 4B.3 : IR spectra of polycyanurate network.

#### 4B.3.1 Dynamic mechanical thermal analysis

DMTA is very useful tool to study the temperature profile of mechanical properties of neat resins. By this technique,  $T_g$  and other secondary transitions of the matrix which go undetected in other techniques like DSC can be clearly distinguished. The cured resins of BPACN, BPZCN and BPC15CN were subjected to DMTA analysis.

As can be seen from **Figure 4B.4**, the storage modulus of BPZCN resin at 35 °C ( $1.59 \times 10^9$  Pa) is higher than that of BPACN resin ( $1.39 \times 10^9$  Pa). The storage modulus ( $E'$ ) of a solid material at room temperature provides a measure of material stiffness under shear deformation. The cycloaliphatic moiety appears more able to resist segmental motion and thus is capable of storing elastic energy resulting in a higher glassy modulus. In the glassy state, stiffness is related to changes in the stored elastic energy upon small deformation as the molecular segments resist motion. The higher storage modulus of BPZCN resin as compared with BPACN resin in glassy state could be due to more rigid network.

As can be observed from **Figure 4B.5**, the height of the  $\tan \delta$  peak which is a measure of crosslinking density, is lower in case of BPZCN resin as compared to BPACN resin. As  $\tan \delta$  is a ratio of viscous to elastic components, it can be surmised that the decreased height is associated with a lower segmental mobility and fewer relaxing species and thus is indicative of rigidity of network. Furthermore, from the narrow peak width at half height of cured BPZCN network it can be concluded that the range of temperatures at which different segments of network gain mobility have decreased. This implies more tighter packing of segments with decreased free volume in cured BPZCN resin. This explains observed higher  $T_g$  of BPZCN polycyanurate network. In case of

BPC15CN resin, the long C-15 alkyl chain impedes tight packing thereby increasing free volume. Due to higher segmental mobility and more number of relaxing species, the cured network of BPC15CN exhibits lower  $T_g$  than BPZCN and BPACN network. **Table 4B.2** summarizes storage modulus ( $E'$ ), and  $T_g$  (from  $\tan \delta$  curve) of cured cyanate ester resins under investigations.

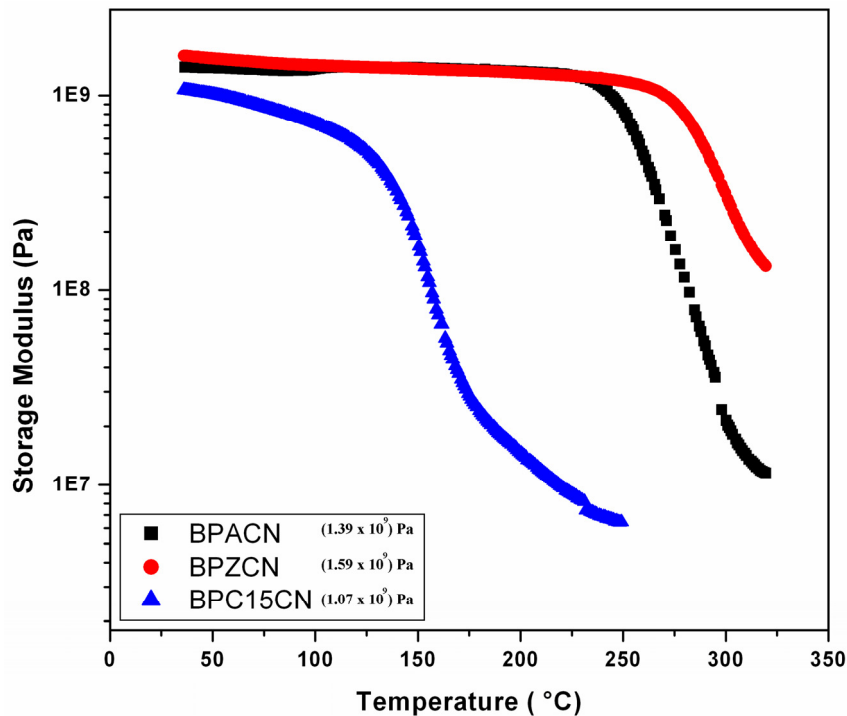


Figure 4B.4 : Storage modulus of polycyanurate network

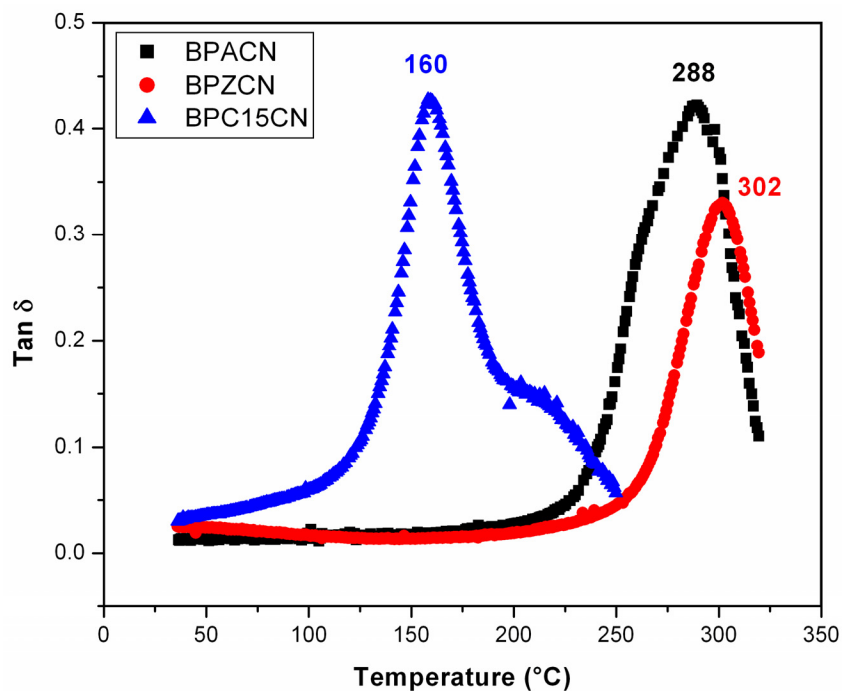
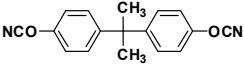
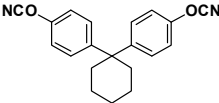
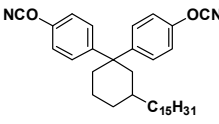


Figure 4B.5 :  $\tan \delta$  curves of polycyanurate network.

**Table 4B.2: Dynamic mechanical analysis of cured CE resins.**

Sr. No.	Sample	Monomer Structure	Storage Modulus E' (@ 35 °C) (Pa)	Tg (°C) (Tan δ)
1	BPACN		$1.39 \times 10^9$	288
2	BPZCN		$1.59 \times 10^9$	302
3	BPC15CN		$1.07 \times 10^9$	160

### 4B.3.2 Thermal properties

Thermogravimetric analysis is the most favored technique for the evaluation of the thermal stability of polymeric materials. It is especially useful in comparing the relative thermal stabilities of various polymers to establish structure-property relation.

Cyanate ester resins exhibit enhanced thermal stability due to the aromatic nature of s-triazine ring. Nakamura *et al.*<sup>18</sup> investigated a series of 40 substituted cyanate esters to demonstrate the effect of both molecular weight and the terminal functional groups on thermo-oxidative stability. The degradation products of unsubstituted polycyanurates consist mainly of carbon monoxide, carbon dioxide, hydrogen, compounds containing triazine moiety (cyanuric acid and its phenyl esters), phenol and bisphenols.<sup>3,18-20</sup>

**Figure 4B.6** illustrates the weight loss curves of polycyanurates when heated at 10 °C / min in nitrogen. The relative thermal stabilities of the cured resins were compared by the temperature of 10 % weight loss and char yield at 800 °C.

All cyanate ester resins showed a single stage decomposition. The temperature at 10% weight loss was in the range 410 - 435 °C indicating their good thermal stability. Amongst the series, cured BPC15CN performs substantially worse with higher weight loss rates at temperatures from 400 °C to around 500 °C. The char yield at 800 °C in case of cured BPC15CN was observed to be 14 % which is lower than other resins in the series. The decreased thermal stability of cured BPC15CN can be correlated to the higher aliphatic content. The data showed that thermal stability of resins gets hampered by incorporation of cycloaliphatic “cardo” group.

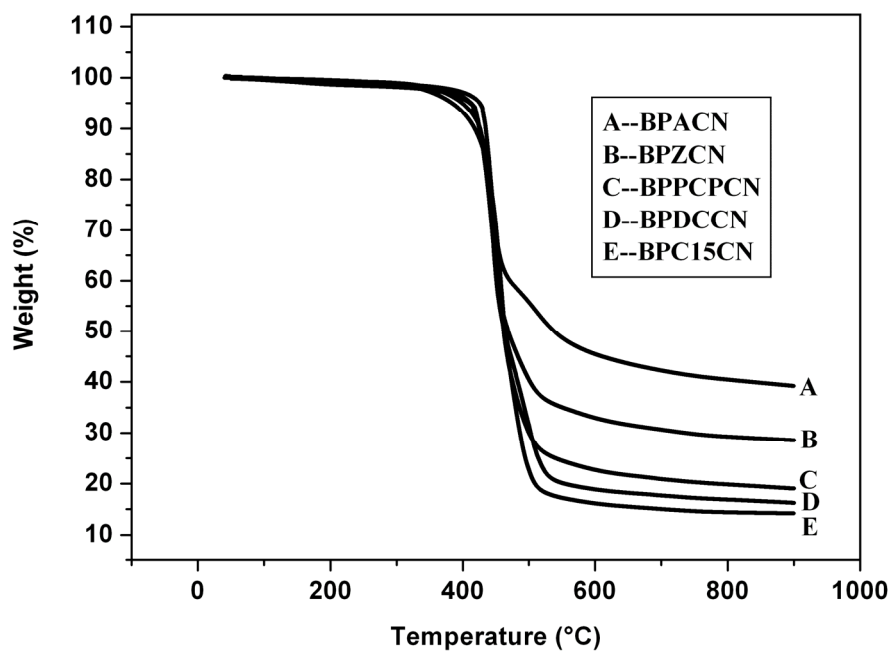


Figure 4B.6: TG curves of polycyanurates

Figure 4B.7 represents weight loss of cured BPC6CN resin. The temperature of 10% loss of the cured BPC6CN (435 °) is practically same as that of cured BPACN (434 °C) indicating good thermal stability. However, the char yield at 800 °C for cured BPC6CN (17 %) is lower than that of cured BPACN (40 %). The decreased char yield value is due to higher aliphatic content of cured BPC6CN.

The temperature of 10 % weight loss and the char yield at 800 °C are summarized in Table 4B.3.

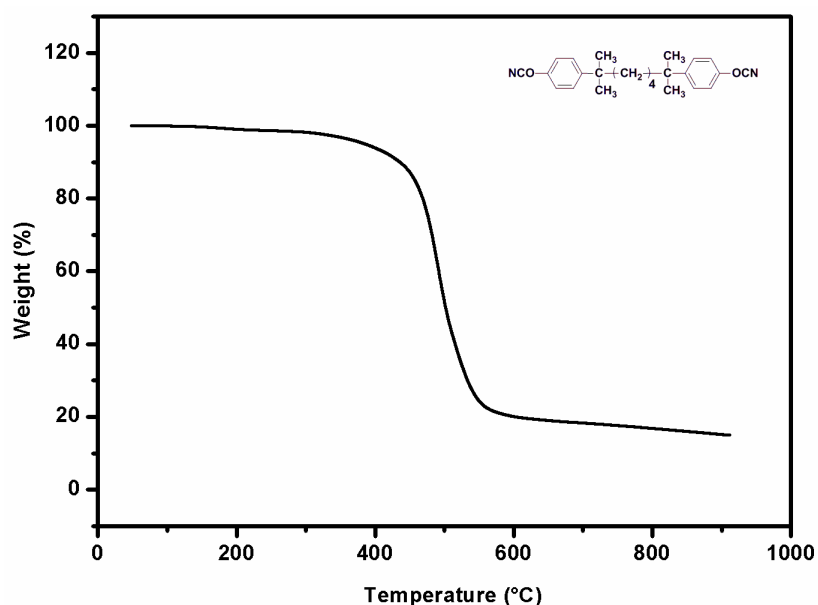
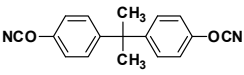
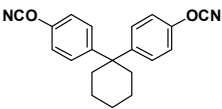
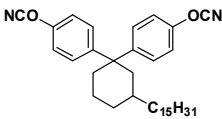
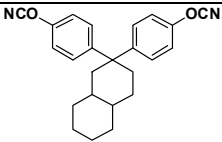
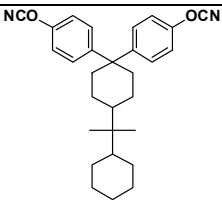
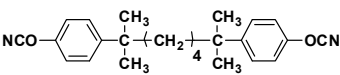


Figure 4B.7: TG curve of BPC6CN polycyanurate.

**Table 4B.3 : Thermal characterization of CE resins**

Sr. No	CE Resin	Monomer Structure	T <sub>g</sub> (°C)	T <sub>10</sub> (°C)	Char Yield at 800 °C (%)
1.	BPACN		288 <sup>a</sup>	434	40
2.	BPZCN		302 <sup>a</sup>	425	29
3.	BPC15CN		160 <sup>a</sup>	413	14
4.	BPDCCN		260 <sup>b</sup>	425	17
5.	BPPCPCN		252 <sup>b</sup>	426	20
6.	BPC6CN		149 <sup>b</sup>	435	17

a – from Tan δ curve by DMTA

b – by DSC

**Figure 4B.8** represents DSC curves (showing glass transition temperature) of cured BPPCPCN, BPDCCN and BPC6CN network. Due to the presence of alkylene spacer, the cured resin of BPC6CN exhibits comparatively lower T<sub>g</sub> ( 149 °C) than that of polycyanurates of cardo containing CE monomers BPPCPCN ( 252 °C) and BPDCCN (260 °C). The T<sub>g</sub> of cured BPACN and BPZCN could not be detected by DSC. The T<sub>g</sub> data of cured BPPCPCN, BPDCCN and BPC6CN are summarized in **Table 4B.3**.

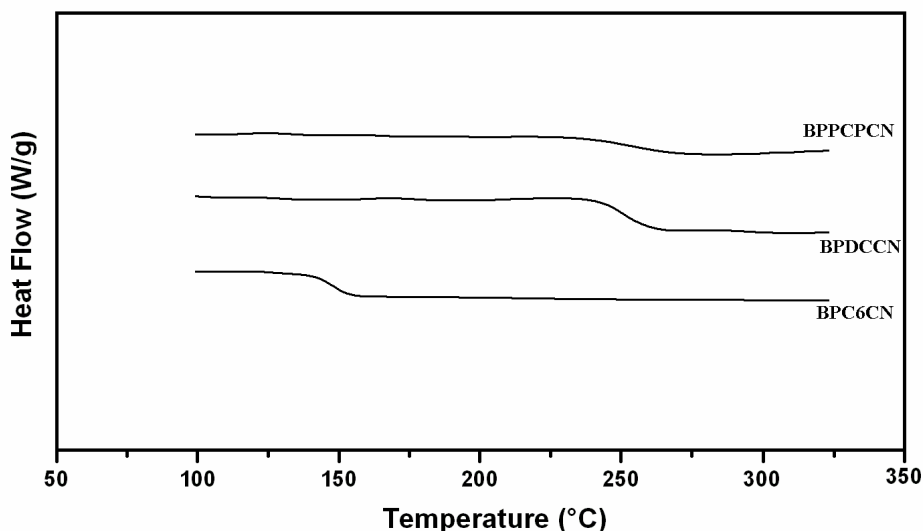


Figure 4B.8: DSC curves of cured BPPCCN, BPDCCN and BPC6CN network

### 4B.3.3 Moisture absorption

The absorbed moisture acts as a plasticizer, damaging mechanical and dielectric properties of cured resins by the contribution of water molecules to polarization and energy dissipation. It may also cause ‘popcorn phenomenon’ when in contact with solder at a high temperature.<sup>20,21</sup> The moisture absorption ionizes the ionic impurities (e.g.  $\text{Cl}^-$ ) and, therefore, corrodes the integrated circuits. Therefore, low moisture absorption is necessary for laminate materials.

Table 4B.4 summarizes percentage moisture absorption of BPACN, BPZCN and BPC15CN polycyanurates after 24 h exposure to boiling water. The weight gain during exposure for cured BPC15CN is only about 50 % of that observed in BPACN resin. The incorporation of hydrophobic cycloaliphatic moiety into a cyanate ester backbone decreased moisture absorption.

Table 4B.4: Percentage moisture absorption of polycyanurates

CE Resin	Monomer Structure	Moisture Absorption (%)
BPACN		1.5
BPZCN		1.1
BPC15CN		0.7

#### 4B. 4 Conclusions:

1. The cyanate ester monomers *viz*: 2,2-bis(4-cyanatophenyl)propane, 1,1-bis(4-cyanatophenyl)cyclohexane, 1,1-bis(4-cyanatophenyl)-3-pentadecylcyclohexane, 1,1-bis(4-cyanatophenyl)decahydronaphthalene, 1,1-bis(4-cyanatophenyl)-4-perhydrocumylcyclohexane and 2,7-bis(4-cyanatophenyl)-2,7-dimethyloctane were cured by employing copper acetylacetonate-nonyl phenol catalyst.
2. The storage modulus of cured network of 1,1-bis(4-cyanatophenyl) cyclohexane was higher than that of cured network of 2,2-bis(4-cyanato phenyl) propane and 1,1-bis(4-cyanatophenyl)-3-pentadecylcyclohexane due to the presence of rigid cycloaliphatic “cardo”group.
3. The  $T_{10}$  values of cured network of cyanate ester monomers under study were in the range 410 – 435 °C indicating their good thermal stability.
4. The percentage moisture absorption of polycyanurate of 1,1-bis(4-cyanatophenyl)-3-pentadecyl cyclohexane was lower than that of polycyanurate of 1,1-bis(4-cyanatophenyl)cyclohexane and 2,2-bis(4-cyanato phenyl) propane due to comparatively higher hydrophobic content of the network.

**References:**

1. Hay, J.N. In *Chemistry and Technology of Cyanate Ester Resins*. Hamerton, I. Ed. **1994**, Chapman and Hall, Glasgow, Chap 6, p 151-192.
2. Grigat, E.; Putter, R. (Bayer AG) *U.S.Patent* 4,028,393, **1977**.
3. Pankratov, V.A.; Vinogradova, S.V.; Korshak, V.V. *Russ. Chem. Rev.* **1977**, 46, 278.
4. Snow, A.W. In *Chemistry and Technology of Cyanate Ester Resins*. Hamerton, I. Ed. **1994**, Chapman and Hall, Glasgow, Chap 2, p 7-57.
5. Snow, A.W.; Buckely, L.J. *Macromolecules* **1997**, 30, 394.
6. Abed, J.; Mercier, R.; McGrath, J.E. *J.Polym.Sci., Part A:Polym.Chem.* **1997**, 35, 977.
7. Marcos-Fernandez, A; Posadas, P; Rodriguez, A; Gonzalez, L. *J. Polym. Sci. Part. A: Polym. Chem.* **1999**, 37, 3155.
8. Mathew, D.; Nair, C.P.R.; Ninan K.N. *Polym. Int.* **2000**, 49, 48.
9. Maya, E.M.; Snow, A.W.; Buckely, L.J. *Macromolecules* **2002**, 35, 460.
10. Maya, E.M.; Snow, A.W.; Buckely, L.J. *J.Polym.Sci., Part A:Polym.Chem.* **2003**, 41, 60.
11. Yan H.; Chen, S.; Qi, G. *Polymer* **2003**, 44, 7861.
12. Hwang, HJ; Li, CH; Wang, CS. *J. Appl. Polym. Sci.* **2005**, 96, 2079.
13. Woo, EP; Dellar, DV. (Dow Chemicals) *U.S.Patent* 4,528,336, **1985**.
14. Lin, C.H.; Jiang, Z.R.; Wang, C.S. *J. Polym. Sci. Part A: Polym. Chem.* **2002**, 40, 4084.
15. Zhang, B.; Wang, Z.; Zhang, X. *Polymer*, **2009**, 50, 817.
16. Nair, C.P.R.; Mathew, D; Ninan, K.N. *Adv. Polym. Sci.* **2001**, 155, 1.
17. Simon, S.L.; Gillham, J.K. *J. Appl. Polym. Sci.* **1993**, 47, 461.
18. Nakamura, Y.; Mori, K.; Tamura, K.; Saito, Y. *J. Polym. Sci. Part A-1*, **1969**, 7, 3089.
19. Korshak, V.V.; Gribkova, P.N.; Dmitrienko, A.V.; Puchin, A.G.; Pankrtov, V.A.; Vinogradova, S.V. *Vysokomol. Soed.*, **1974**, A 16, 15.
20. Hamerton, I. In *Chemistry and Technology of Cyanate Ester Resins*. Hamerton, I. Ed. **1994**, Chapman and Hall, Glasgow, Chap 7, p 193-229.
21. Snow A.W.; Buckley, L.J. In *Handbook of Low and High Dielectric Constant Materials and Their Applications*. Nalwa, H.S. Ed **1999** Academic, New York, Volume 1, Chapter 4, p 189-212.



# Chapter **5**

## Synthesis, Characterization and Curing of Epoxy Resins

## 5.1 Introduction

Epoxy resins have been useful in the aerospace and electronics industries in the form of structural adhesives, advanced composite matrices, and packaging materials since their introduction in 1938 by Pierre Castern;<sup>1-4</sup> thanks to the combination of good thermal and dimensional stability, excellent chemical and corrosion resistance, high tensile strength and modulus, and ease of handling and processability. Depending upon the end application, a variety of epoxy resins with different properties are in use. The structure of the epoxy resin is one of the factors that dictate properties of the cured resin. The synthesis of new epoxies allows enormous diversity in the structure and essentially allows the structure to be customized at the molecular level. The availability of new epoxies thus provides a basis for the systematic design of the improved epoxy resins.

The scientific endeavor has witnessed the development of novel epoxy resins that enhance the thermal, electrical and hydrolytic properties of epoxy thermosets finding applications in electrical and microelectronic devices<sup>5-8</sup>. Epoxy resins based on cycloaliphatic moiety have been one of the suitable epoxy systems for these applications. Cycloaliphatic epoxides<sup>9</sup> in which the oxirane rings are fused to the rings of cycloaliphatic hydrocarbon are the most common epoxies in this category. Characterized by the saturated cycloaliphatic ring structure with no aromatic unsaturation, they have lower viscosity before curing; their cured resin exhibits the advantages of good dielectric properties and durable performance for outdoor use. However, some inherent features of the resin such as the relatively low glass transition temperature (T<sub>g</sub>), inferior cracking-resistance when subjected to severe temperature and moisture environment, and low reactivity towards amine curing agents, may cause limitation to their application.

A wide variety of epoxies with structural variations have been synthesized to date, and the examples are too large to present here. The epoxies bearing relevance with the present work are summarized here. **Table 5.1** lists epoxies containing “cycloaliphatic / cardo” moiety.

Erich and Bodnar<sup>10</sup> studied the effect of cycloalkyl ring on the mechanical properties of epoxy resins. Diglycidyl ethers (**Table 5.1**) were cured using diethylene triamine (DETA) as a curing agent. Diglycidyl ether of 9,9-bis(4-hydroxyphenyl)fluorene (DGEBF) was first synthesized by Korshak *et al.*<sup>11</sup> The authors found that the cured resin (employing trimellitic anhydride or *meta*-phenylenediamine as a curing agent) possessed good heat resistance and high thermal stability with high T<sub>g</sub>. Further, Pearce *et al.*<sup>12-15</sup> reported a series of epoxy resins to study structure-property relation with respect to glass transition temperature, and thermal stability. The cured resins possessing “cardo” moiety exhibited higher T<sub>g</sub>, higher thermal stability, higher char yield and higher oxygen index than that of epoxy resin based on diglycidyl ether of bisphenol A. A similar trend was also observed by Xu *et al.*<sup>16</sup> where the authors reported the study on DGEBF epoxy resin using diaminodiphenylmethane (DDM) as a curing agent. Epoxy resins based on alkyl substituted

cycloalkyl moieties were reported by Muller and Franke<sup>17</sup>. Naphthyl moiety and cycloaliphatic based epoxy resin reported by Xu *et al.*<sup>18</sup> exhibited higher Tg, lower thermal expansion coefficient, lower dielectric constant, and lower moisture absorption than DGEBA. Su and Jing<sup>19</sup> reported adamantane containing epoxy resin which resulted into a cured network with enhanced moisture resistance and dielectric properties. Recently, dicyclopentadiene-cresol containing epoxy resin was reported by Wang *et al.*<sup>20</sup>.

**Table 5.1: Epoxy resins containing “cycloaliphatic / cardo” moiety.**

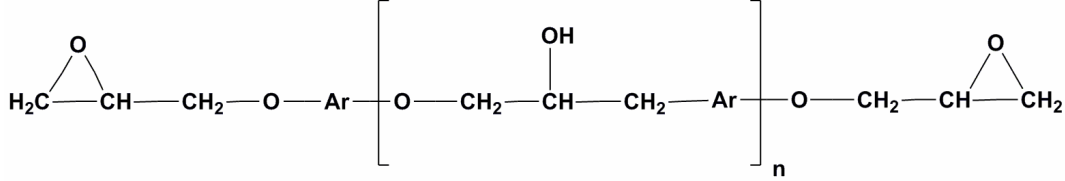
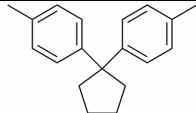
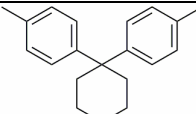
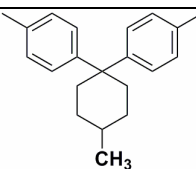
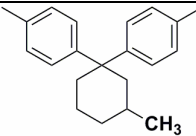
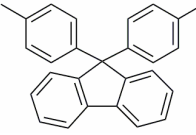
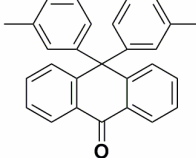
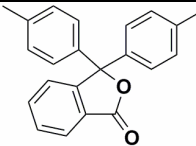
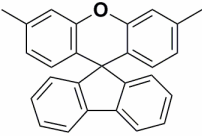
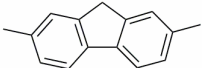
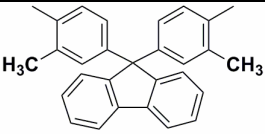
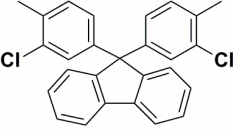
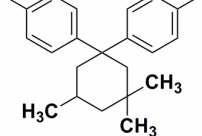
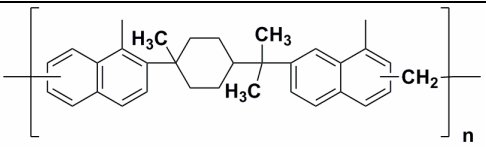
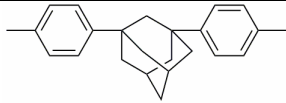
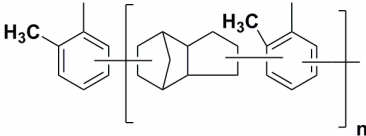
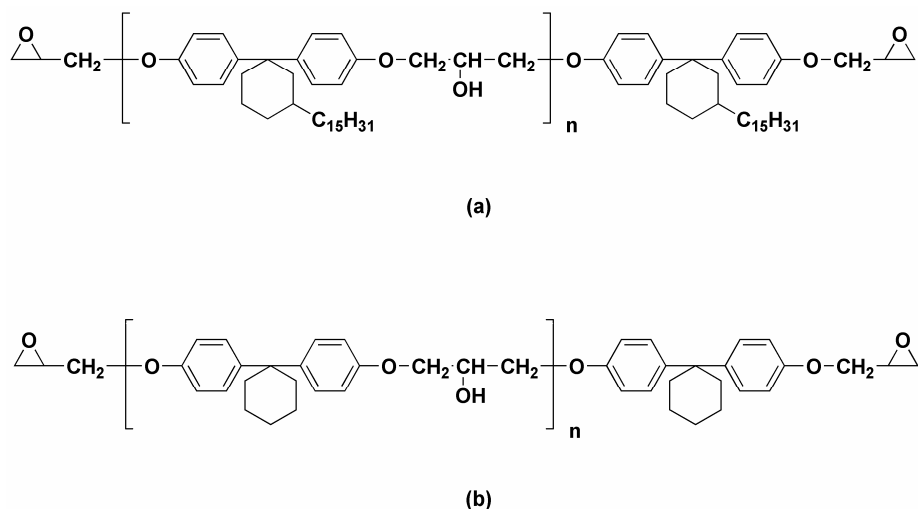
		
Sr. No.	Ar	Reference
1		10
2		10
3		10
4		10
5		11-16
6		12-15
7		12-15

Table 5.1 continued...

8		12-15
9		12-15
10		12-15
11		12-15
12		17
13		18
14		19
15		20

The present work discusses the synthesis and characterization of epoxy resins (**Figure 5.1**) starting from bisphenols containing cycloaliphatic “cardo” group *viz*; 1,1-bis(4-hydroxyphenyl)-3-pentadecylcyclohexane and 1,1-bis(4-hydroxyphenyl)cyclohexane. The results of curing studies of these epoxies employing 4,4-methylenedianiline as a curing agent and characterization of cured epoxy resins by IR, DMTA, DSC, and TGA are also discussed to decipher the effect of pendent flexible pentadecyl chain on the properties of cured epoxy network.



**Figure 5.1: Epoxy resins (a) diglycidyl ether of 1,1-bis(4-hydroxyphenyl)-3-pentadecyl cyclohexane (b) diglycidyl ether of 1,1-bis(4-hydroxyphenyl)cyclohexane**

## 5.2 Experimental

### 5.2.1 Materials

Epichlorohydrin was purchased from Loba Chemie Pvt Ltd, India. Pyridine and hydrochloric acid (36-38%) were procured from Merck India. Phenolphthalein was purchased from S.D. Fine-Chem Ltd, India. 4,4'-Methylenedianiline (MDA) was generously gifted by M/s ABR Organics, Hyderabad, India. The diglycidyl ether of bisphenol A (DEGBPA) with epoxy equivalent weight 185 g/equiv. was obtained from Ciba-Geigy. 1,1-Bis(4-hydroxyphenyl)cyclohexane (BPZ) and 1,1-bis(4-hydroxyphenyl)-3-pentadecylcyclohexane (BPC15) were synthesized as discussed in chapter 3 (section 3.3). The solvents were of reagent grade quality and were used as received.

### 5.2.2 Characterization

Infrared spectra were recorded on Perkin-Elmer, spectrum GX model at a resolution of  $4\text{ cm}^{-1}$ . For monomers, the spectra were recorded by depositing samples as solvent-cast thin films on sodium chloride cells and resins as fine particulates dispersed in KBr.

NMR spectra ( $^1\text{H}$  and  $^{13}\text{C}$ ) were recorded on Bruker NMR spectrophotometer (200 or 400 MHz).

Epoxy equivalent weight of epoxy resin was determined by pyridine-HCl method as reported in the literature<sup>21</sup>. The resin (1 g) was dissolved in HCl (20 mL, 6 N solution in pyridine), refluxed for 25 minute, cooled and titrated against standard (0.05 N) solution of NaOH in methanol. Epoxy equivalent weight (EEW) was calculated by relation;

$$\text{EEW} = W \times 1000 / [(A-B) \times N] \quad (1)$$

Where W = Weight of epoxy resin (g)

(A-B) = Difference of blank and sample reading (mL)

N = Normality of NaOH

DSC measurements were performed on TA Instruments (Q10) supported by TA Universal Analysis software for data acquisition. To understand the kinetics of curing under nonisothermal mode, samples (5-7 mg) were sealed in hermetic aluminum pans and experiments were performed under a nitrogen flow of 50 mL/ min. All the samples were subjected to a dynamic DSC scan at the heating rate of 10 °C/min. The enthalpy of curing  $\Delta H$  was determined from the area under the exothermic curve. Cure onset temperature ( $T_o$ ) was considered as the intersect of slope of baseline and tangent of curve leading to peak of transition. The fractional conversion ( $\alpha$ ) of each sample at a given temperature under nonisothermal condition was calculated from the relation:

$$\alpha_T = \Delta H_f / \Delta H_T \quad (2)$$

where  $\Delta H_f$  is the fractional enthalpy at that temperature and  $\Delta H_T$ , the total heat of reaction under nonisothermal mode.

Thermogravimetric analysis (TGA) data was obtained using a TA instrument, (model Q 5000) at the heating rate of 10°C / min under nitrogen.

Dynamic mechanical thermal analysis (DMTA) was conducted on Rheometrics Scientific (model Mark IV) (UK) at a frequency of 1.0 Hz and the heating rate of 10°C /min in a bending mode.

Percentage moisture absorption was tested by placing vacuum dried, pre-weighed samples in boiling water for 24 hours and calculating the % weight gain:

$$\% \text{ Moisture absorption} = [(W/W_o) - 1] \times 100 \quad (3)$$

where W is the weight of the sample after dipping in boiling water for 24 h and  $W_o$  is the initial weight of the sample after drying in vacuum for 12 h at room temperature.

### 5.2.3 Synthesis of epoxies.

#### 5.2.3.1 Synthesis of diglycidyl ether of 1,1-bis(4-hydroxyphenyl)-3-pentadecylcyclohexane

Into a 250 mL three-necked round bottom flask equipped with an overhead stirrer, a reflux condenser and a thermometer were added 1,1-bis(4-hydroxyphenyl)-3-pentadecylcyclohexane (9.56 g, 0.02 mol), epichlorohydrin (15.7 mL, 0.2 mol) and water (0.1 mL). To the reaction mixture, sodium hydroxide pellets (1.64 g, 0.04 mol) were added in portions. The first portion of sodium hydroxide (0.8 g) was added at room temperature and the reaction mixture was heated to 90 °C. When the reaction temperature was reached to 90 °C, another portion (0.84 g) of sodium hydroxide was added slowly so that the temperature does not exceed 100 °C. After the completion of addition,

the reaction mixture was heated at 90 °C for 30 minutes. Excess epichlorohydrin was distilled under reduced pressure. After the complete removal of epichlorohydrin, toluene (10 mL) was added to precipitate the salt formed and the solution was filtered under vacuum. The residue was washed with toluene (3 x 5 mL). All the washings were combined and toluene was distilled off under vacuum. Thus obtained viscous mass after heating at 150 °C under vacuum for 30 minutes, resulted into a slight yellow viscous resin.

Yield: 12.5 g

Epoxy equivalent weight: Experimental; 333 g/ equiv.

### 5.2.3.2 Synthesis of diglycidyl ether of 1,1-bis(4-hydroxyphenyl)cyclohexane

Into a 500 mL three-necked round bottom flask equipped with an overhead stirrer, a reflux condenser and a thermowell fitted with a thermometer were added 1,1-bis(4-hydroxyphenyl)cyclohexane (26.8 g, 0.1 mol), epichlorohydrin (78.4 mL, 1 mol) and water (0.5 mL). To the reaction mixture, sodium hydroxide pellets (8.2 g, 0.21 mol) were added in portions. The first portion of sodium hydroxide (1.3 g) was added at room temperature and the reaction mixture was heated to 90 °C. When the reaction temperature was reached to 90 °C, another portion (1.3 g) of sodium hydroxide was added slowly so that the temperature does not exceed 100 °C. The process was repeated till the complete addition of sodium hydroxide in portions (4 x 1.4 g). After the last portion was added, the reaction mixture was heated at 90 °C for 30 minutes. Excess epichlorohydrin was distilled under reduced pressure. After the complete removal of epichlorohydrin, toluene (25 mL) was added to precipitate the salt formed and the solution was filtered under vacuum. The residue was washed with toluene (3 x 10 mL). All the washings were combined and toluene was distilled off under vacuum. Thus obtained viscous mass after heating at 150 °C under vacuum for 30 minutes, resulted into a slight yellow viscous resin.

Yield: 43.5 g

Epoxy equivalent weight: Experimental; 221 g/ equiv.

### 5.2.4 Curing

Epoxies *viz*; diglycidyl ether of bisphenol-A (DGEBA), diglycidyl ether of BPZ (DGEBPZ) and diglycidyl ether of BPC15 (DGEBPC15) were cured using 4, 4'-methylenedianiline (MDA) as a curing agent. The calculated amount of epoxy resin and MDA were added and the mixture was stirred till homogenous. The mixture was then heated at 40 °C under vacuum for 10 minutes to remove entrapped air. In case of DGEBPC15, the mixture was heated at 80 °C for 20 minutes to form a homogenous mixture. This could be because of comparatively lower solubility of MDA in DGEBPC15. Thus obtained homogeneous samples were stored in a refrigerator before the DSC was performed so as to avoid any curing reaction. The curing of samples was carried out at 80 °C / 4 h

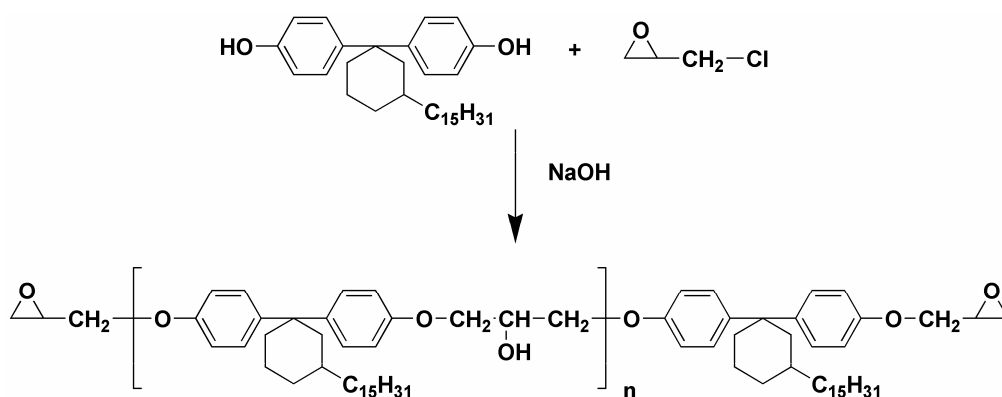
followed by postcuring at 150 °C / 2 h. The cured samples were slowly cooled to the ambient temperature to avoid cracking. The cured resin castings were ejected from the mold and cut/polished wherever necessary for a uniform surface and thickness.

## 5.3 Results and Discussion

### 5.3.1 Synthesis of epoxies

The synthesis of new monomers provides one of the promising approaches towards polymer backbone modification in order to achieve the desired properties. As an example, introduction of “cardo / cycloaliphatic” moiety has been reported to improve thermal, dielectric, and hydrolytic behavior of epoxy resins.<sup>12-20</sup>

In case of cyanate ester resins, it was observed that the introduction of cycloaliphatic “cardo” group results into polycyanurates with lower moisture absorption (chapter 4B section 4B.3.3). It was therefore of interest to understand the effect of introduction of cycloaliphatic “cardo” group into epoxy resins. For this purpose, a new epoxy resin containing cycloaliphatic “cardo” group possessing pendent flexible pentadecyl chain was synthesized by a conventional one step procedure starting from corresponding bisphenol *viz*; 1,1-bis(4-hydroxyphenyl)-3-pentadecylcyclohexane and epichlorohydrin as depicted in **Scheme 5.1**.

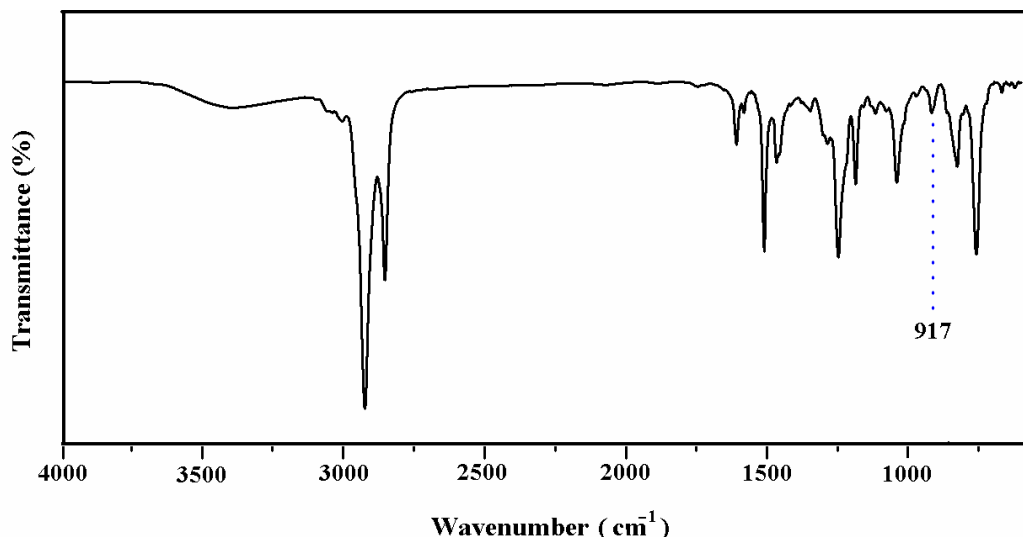


**Scheme 5.1: Synthesis of diglycidyl ether of 1,1-bis(4-hydroxyphenyl)-3-pentadecyl cyclohexane**

The diglycidyl ether of 1,1-bis(4-hydroxyphenyl)-3-pentadecylcyclohexane was characterized by FTIR, <sup>1</sup>H-NMR and <sup>13</sup>C-NMR spectroscopy.

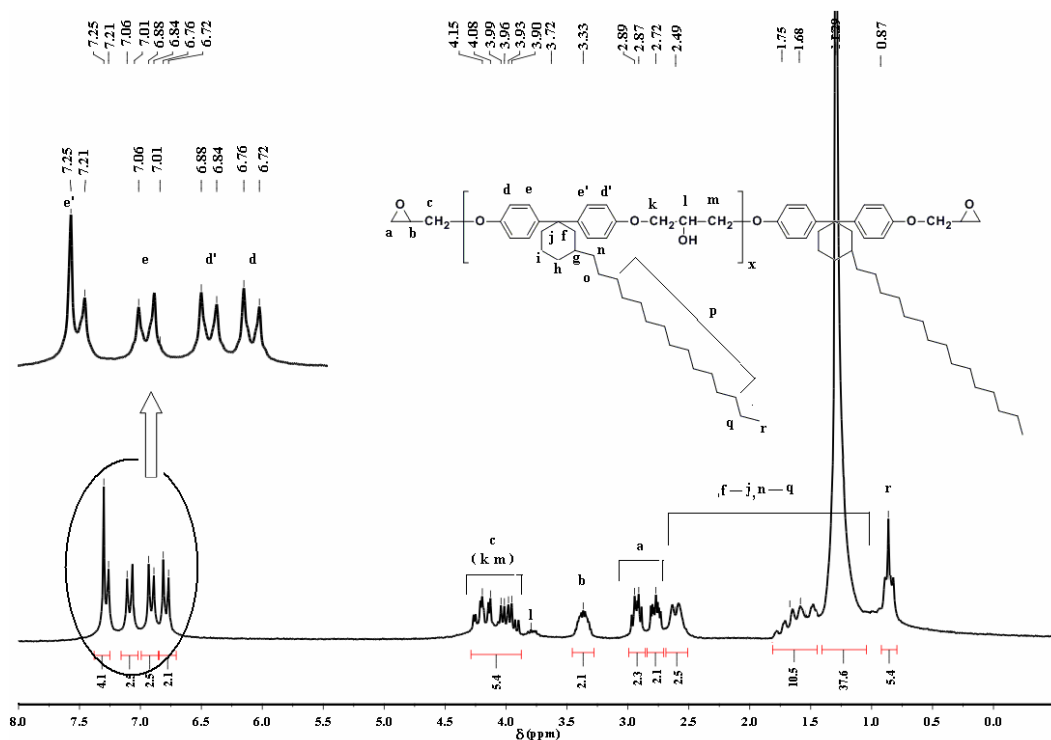
**Figure 5.2** represents IR spectrum of DGEBCP15. The characteristic oxirane ring deformation was observed at 917 cm<sup>-1</sup>.





**Figure 5.2 : IR spectrum of diglycidyl ether of 1,1-bis(4-hydroxyphenyl)-3-pentadecyl cyclohexane**

**Figure 5.3** represents  $^1\text{H-NMR}$  spectrum of DGEBC15. The aromatic protons (d, d', e and e') appeared as a set of four doublets due to the presence of magnetically non-equivalent phenyl rings. The substitution of pentadecyl chain at cyclohexyl ring restricts the ring flipping thereby making the phenyl rings magnetically non-equivalent. Aromatic protons *ortho* to epoxide group; d and d' displayed a doublet at 6.74 (axial phenyl ring) and 6.86 (equatorial phenyl ring) ppm, respectively. Aromatic protons labeled as e, e' (*meta* to epoxide group) exhibited doublets at 7.03 (axial phenyl ring) and 7.23 ppm (equatorial phenyl ring). The protons (marked as c) of methylene group adjacent to ether linkage appeared as a multiplet in the range 3.90 - 4.15 ppm. The characteristic methine proton (labeled as b) of oxirane ring displayed a multiplet in the range 3.30 - 3.36 ppm while methylene protons (designated as a) of oxirane ring showed multiplets in the region 2.72 - 2.89 ppm. The peaks due to methine and methylene protons of cyclohexyl ring and pentadecyl chain were observed in the range 1.27 - 2.49 ppm. The triplet at 0.87 ppm could be assigned to proton (r) of methyl group.



**Figure 5.3:**  $^1\text{H}$ -NMR spectrum of diglycidyl ether of 1,1-bis(4-hydroxyphenyl)-3-pentadecyl-cyclohexane ( $\text{CDCl}_3$ )

$^{13}\text{C}$  NMR spectrum of DGEBC15 alongwith peak assignments is reproduced in **Figure 5.4**. The peaks corresponding to the aromatic carbons (labeled as d, d') attached to epoxide group appeared at 155.90 ppm (axial phenyl ring) and 155.95 ppm (equatorial phenyl ring). Aromatic carbons (e, e') *ortho* to epoxide group showed peaks at 113.83 ppm (axial phenyl ring) and 114.19 ppm (equatorial phenyl ring). The signals at 138.23 ppm and 144.82 ppm could be due to aromatic carbons g (*para* to epoxide group, axial phenyl ring) and g' (*para* to epoxide group, equatorial phenyl ring), respectively. Aromatic carbons (f, f') *meta* to epoxide group exhibited signals at 127.04 ppm (axial phenyl ring) and 128.83 ppm (equatorial phenyl ring). The signals corresponding to the methylene carbons of epoxide group (labeled as c) and repeat unit (labeled as o, q) appeared in the range 68.51 - 68.18  $\delta$  ppm. The methine carbon 'p' attached to hydroxyl group (repeat unit) was observed as a weak signal at 69.65 ppm. The assignment was confirmed from DEPT spectrum (**Figure 5.5**) by the appearance in negative phase. The methine carbon 'b' of oxirane ring was observed at 50.04 ppm which was also confirmed by DEPT spectrum. The carbons labeled as h, i, j, k, l, and m were observed at 45.39, 44.20, 33.39, 26.68, 22.61 and 37.19 ppm. The assignments of 'h' and 'j' were confirmed by DEPT spectrum. The signals at 29.28, 29.63, 29.97, 31.84, and 33.18 ppm could be assigned to methylene carbons of pentadecyl chain. The peaks corresponding to the methyl carbon 'n' of pentadecyl chain appeared at 14.06 ppm.

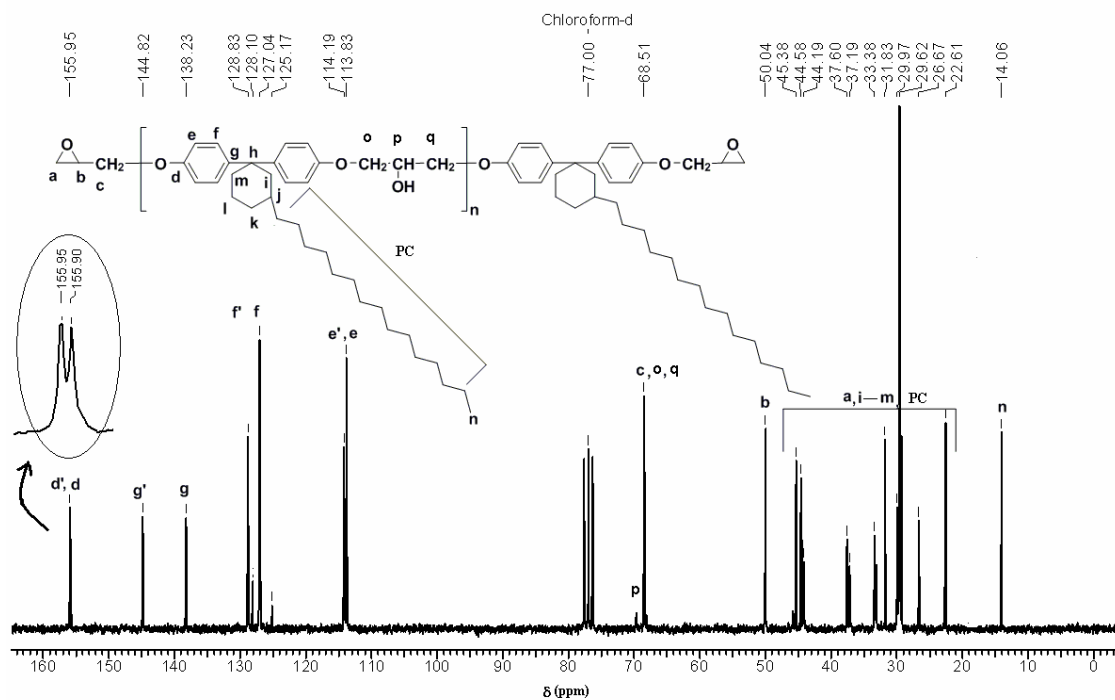


Figure 5.4 :  $^{13}\text{C}$ -NMR spectrum of diglycidyl ether of 1,1-bis(4-hydroxyphenyl)-3-pentadecyl cyclohexane ( $\text{CDCl}_3$ )

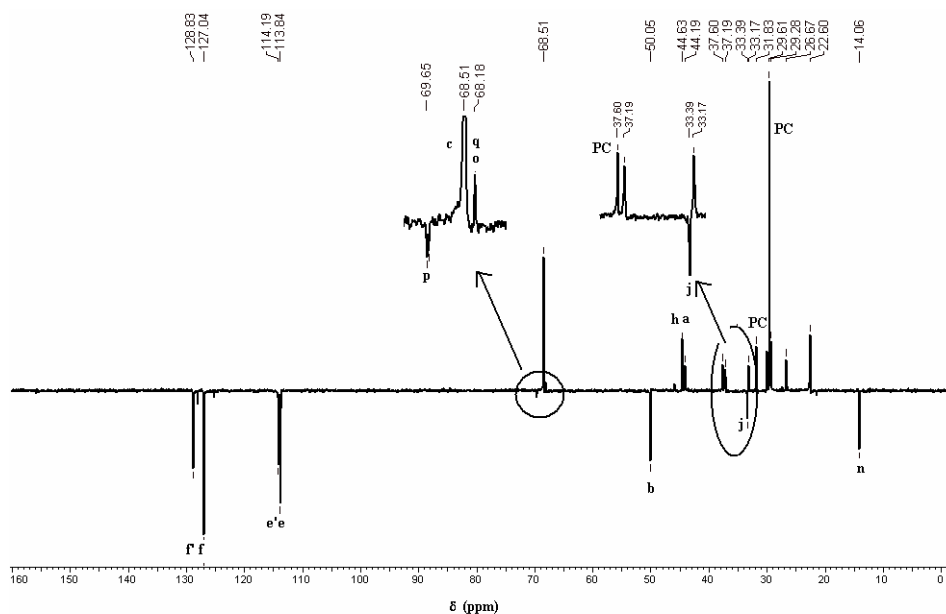
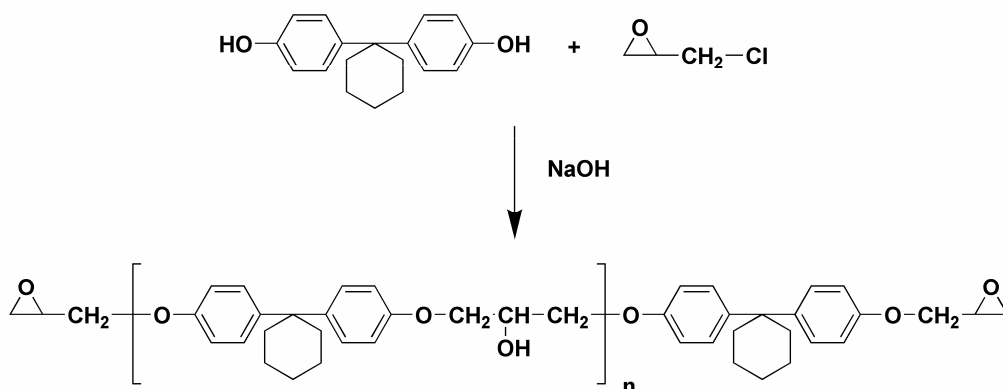


Figure 5.5 :  $^{13}\text{C}$ -DEPT NMR spectrum of diglycidyl ether of 1,1-bis(4-hydroxyphenyl)-3-pentadecylcyclohexane ( $\text{CDCl}_3$ )

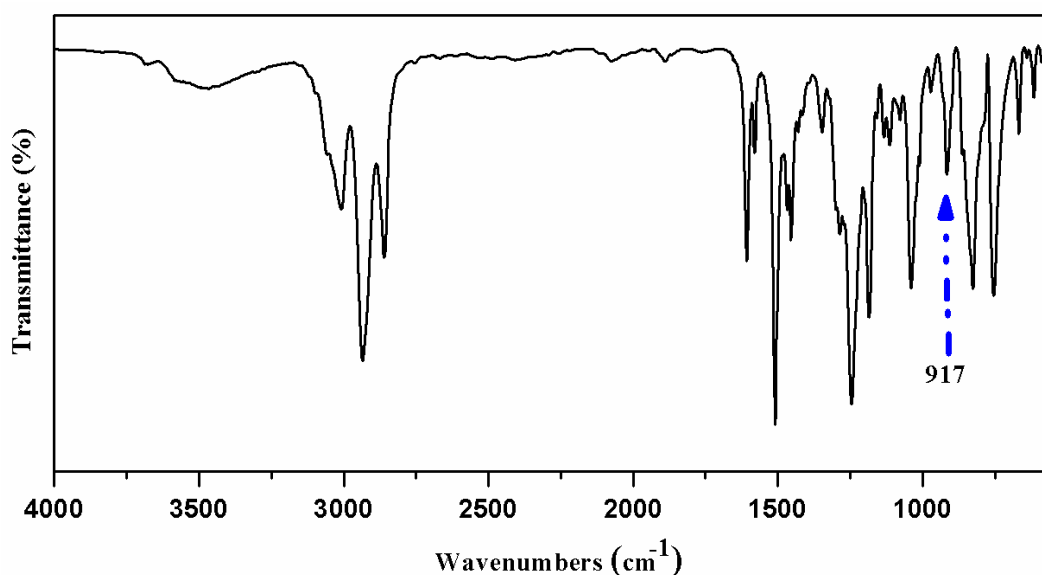
The epoxy equivalent weight of DGEBPC15 was found to be 333 g/ equiv.

In order to understand structure-property relationship, epoxy resin containing cyclohexyl moiety was also synthesized starting from 1,1-bis(4-hydroxyphenyl)cyclohexane (**Scheme 5.2**).



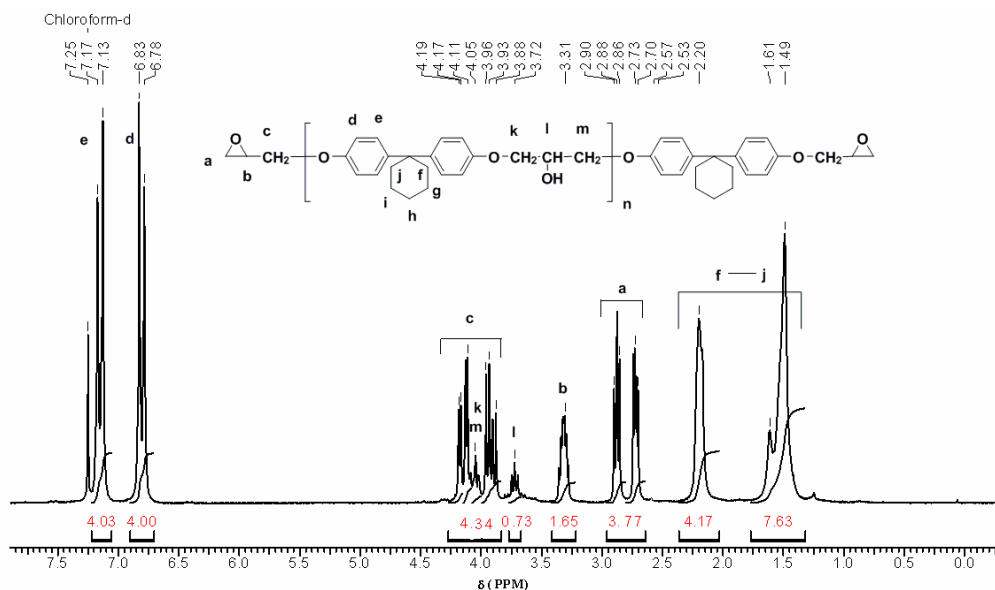
**Scheme 5. 2: Synthesis of diglycidyl ether of 1,1-bis(4-hydroxyphenyl) cyclohexane**

DGEBCPZ was characterized by IR,  $^1\text{H-NMR}$  and  $^{13}\text{C-NMR}$  spectroscopy. **Figure 5.6** represents IR spectrum of DGEBCPZ. The characteristic oxirane ring deformation was observed at  $917\text{ cm}^{-1}$ .



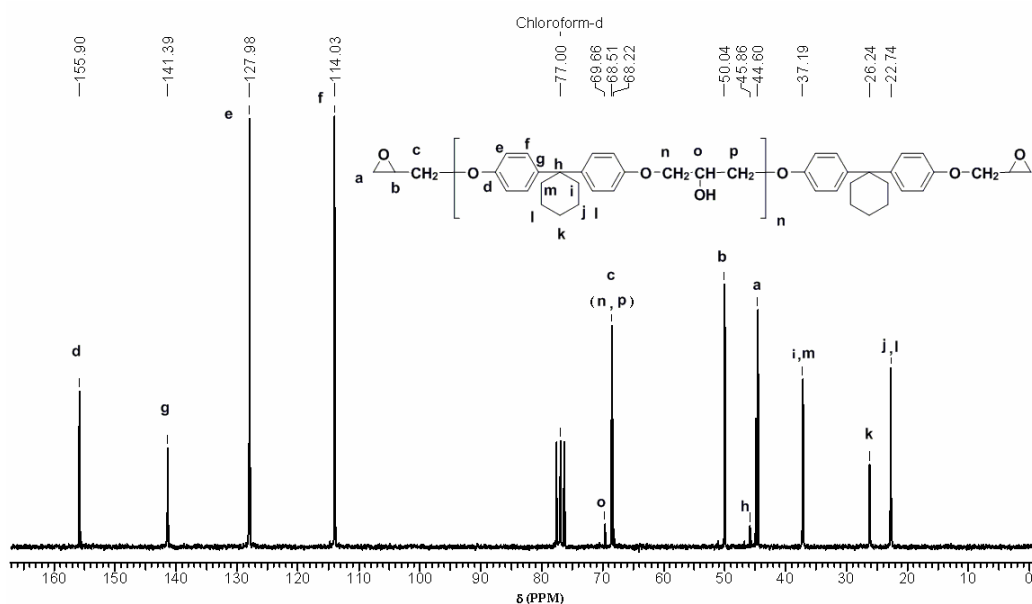
**Figure 5.6 : IR spectrum of diglycidyl ether of 1,1-bis(4-hydroxyphenyl)cyclohexane**

$^1\text{H-NMR}$  spectrum of DGEBCPZ is reproduced in **Figure 5.7**. Aromatic protons 'd' (*ortho* to epoxide group) and 'e' (*meta* to epoxide group) appeared as doublet at 6.80 and 7.15 ppm, respectively. The protons (labeled as c) of methylene group adjacent to ether linkage exhibited a multiplet in the range 3.72 - 4.19 ppm. The proton (marked as b) of oxirane ring showed a multiplet in the range 3.28 - 3.34 ppm while protons (labeled as a) of methylene group displayed a multiplet in the range 2.53 - 2.90 ppm. The peaks observed in the range 1.49 - 2.20 ppm could be due the protons (f, g, h, i and j) of cyclohexyl ring.

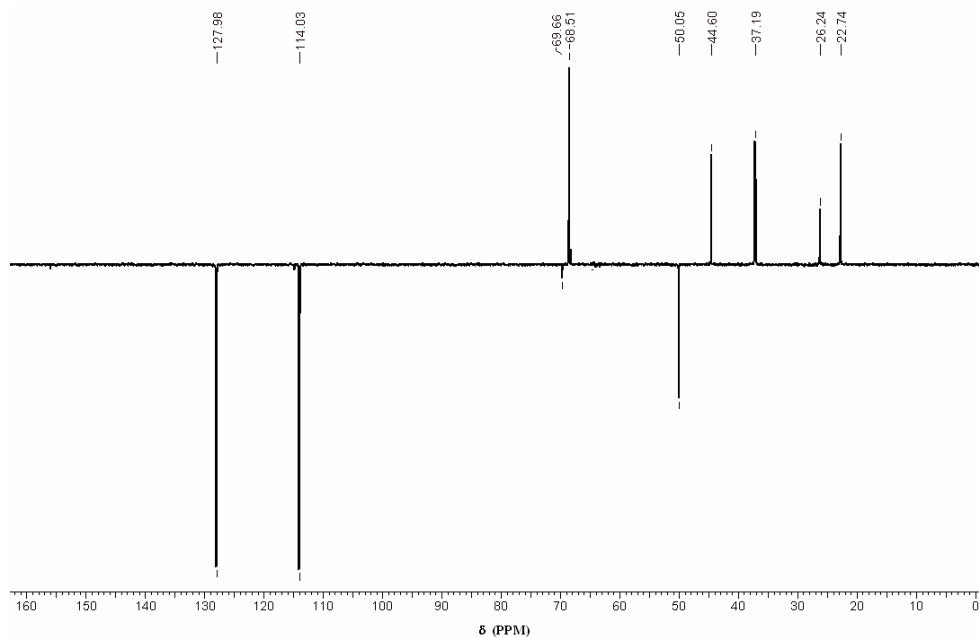


**Figure 5.7:**  $^1\text{H-NMR}$  spectrum of diglycidyl ether of 1,1-bis(4-hydroxyphenyl)cyclohexane ( $\text{CDCl}_3$ )

**Figure 5.8** represents  $^{13}\text{C-NMR}$  spectrum of DGEBPZ. Aromatic carbons labeled as d, e, f and g appeared at 155.90, 127.98, 114.03 and 141.39, respectively. The methylene carbons of epoxide group and repeat unit (c, n, p) appeared in the range 68.22 - 68.51 ppm. The methine carbon 'o' attached to hydroxyl group (repeat unit) was observed as a weak signal at 69.66 ppm. The assignments were confirmed by DEPT spectrum (**Figure 5.9**) by the appearance of peak in negative phase. The signal due to the methylene carbon 'b' of epoxide ring was observed at 50.04 ppm which was confirmed by DEPT spectrum. The methylene carbon 'a' of epoxide ring exhibited a signal at 44.60 ppm. The carbons of cyclohexyl ring showed peaks at 45.86 (h), 37.19 (i, m), 26.24 (k), and 22.74 (j, l) ppm.



**Figure 5.8:**  $^{13}\text{C-NMR}$  spectrum of diglycidyl ether of 1,1-bis(4-hydroxyphenyl)cyclohexane ( $\text{CDCl}_3$ )

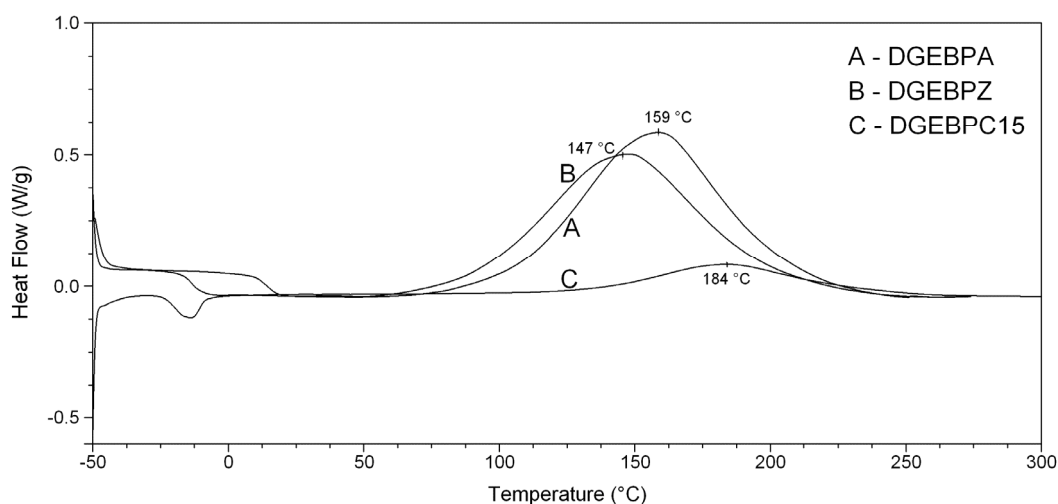


**Figure 5.9:**  $^{13}\text{C}$ -NMR DEPT spectrum of diglycidyl ether of 1,1-bis(4-hydroxyphenyl) cyclohexane ( $\text{CDCl}_3$ ).

The epoxy equivalent weight of DGEBPZ was found to be 221 g/ equiv.

### 5.3.2 Non-isothermal curing kinetics of epoxy resins

Curing kinetics of epoxy-amine system has been studied by several authors<sup>22-30</sup>. The curing kinetics of DGEBPZ, DGEBPZ and DGEBPA with MDA were examined by DSC in the present study. The DSC curves are represented in **Figure 5.10**.



**Figure 5.10:** DSC thermograms of epoxy resins (curing agent 4,4'-methylenedianiline)

The higher  $T_g$  of DGEBPZ in uncured stage ( $T_{g0}$ ) (14 °C) could be due to rigid cardo group while due to flexible C-15 alkyl chain, DGEBPZ has lower  $T_{g0}$  (-19 °C) than DGEBPA (-13.0 °C). In case of DGEBPZ, it was observed that the curing agent i.e. MDA needed comparatively

longer time for homogeneous mixing with DGEBC15 (section 5.2.4). The curing reaction which takes place during the mixing remains undetected by DSC and hence the DSC cure characteristics of DGEBC15 were not compared with DGEBCPA and DGEBCPZ system. The curing of DGEBCPA and DGEBCPZ proceeds with the calorific value ( $\Delta H$ ) 48 and 52 kJ/mol, respectively which are in agreement with the reported values.<sup>22-30</sup> The DSC cure characteristics of epoxies under study are collected in **Table 5.2**.

**Table 5.2: Curing characteristics of epoxy resins**

Epoxy Resin	T <sub>g0</sub>	T <sub>i</sub> (°C)	T <sub>p</sub> (°C)	T <sub>f</sub> (°C)	Δ H (kJ /mol)
DGEBCPA	-13.0	63	159	254	48
DGEBCPZ	14.0	54	147	257	52
DGEBC15	-19.0	67	184	295	17

### 5.3.2.1 Kinetics of curing

The kinetics of curing of epoxy resins has been established to follow a classical  $n^{\text{th}}$  order model as:

$$d\alpha/dt = k_f(1-\alpha)^n \quad (4)$$

Under nonisothermal conditions, this rate expression takes the form:

$$d\alpha/dT = (A/\phi)e^{-E/RT}(1-\alpha)^n \quad (5)$$

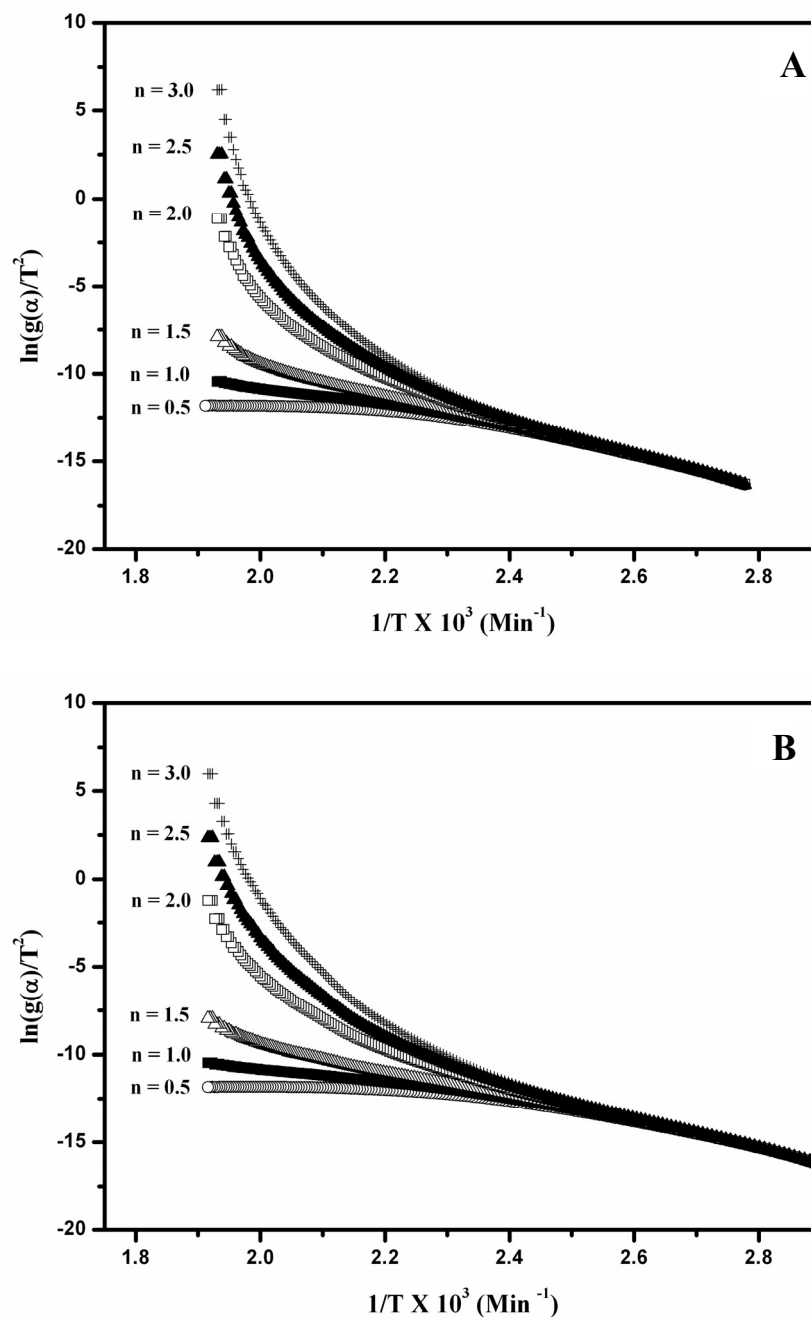
where,  $\alpha$  is the fractional conversion at temperature  $T$ , following a heating rate  $\phi$ .  $E$  is the activation energy and  $A$  the Arrhenius frequency factor. The order of reaction is  $n$ .

In present study, activation parameters were calculated using Coats-Redfern equation (Equation 6)<sup>31</sup>:

$$\ln\{g(\alpha)/T^2\} = \ln\{(AR/\phi E)(1-2RT/E)\} - E/RT \quad (6)$$

where  $g(\alpha) = [1-(1-\alpha)^{1-n}] / (1-n)$ ; for  $n = 1$ ,  $g(\alpha) = -\ln(1-\alpha)$ ;  $R$  is the gas constant.

The order of the reaction was found from the best fit plots of  $\ln(g(\alpha)/T^2)$  vs.  $1/T$  for different values of  $n$ . The kinetic plots for the determination of  $n$  for both the systems under study are shown in **Figure 5.11**.



**Figure 5.11: Coats-Redfern plot for determination of order of reaction for A) DGE BPA-MDA  
B) DGE BPZ-MDA**

The value of  $n$  for both epoxy systems was found to be very close to 1.5 within most of the conversion range. The kinetic parameters ( $E$  and  $A$ ) were determined from the linear plots of  $\ln(g(\alpha)/T^2)$  vs  $1/T$  (for  $n = 1.5$ ). The computed activation parameters are collected in **Table 5.3**.

The activation energy of DGE BPA and DGE BPZ are almost in the same range.

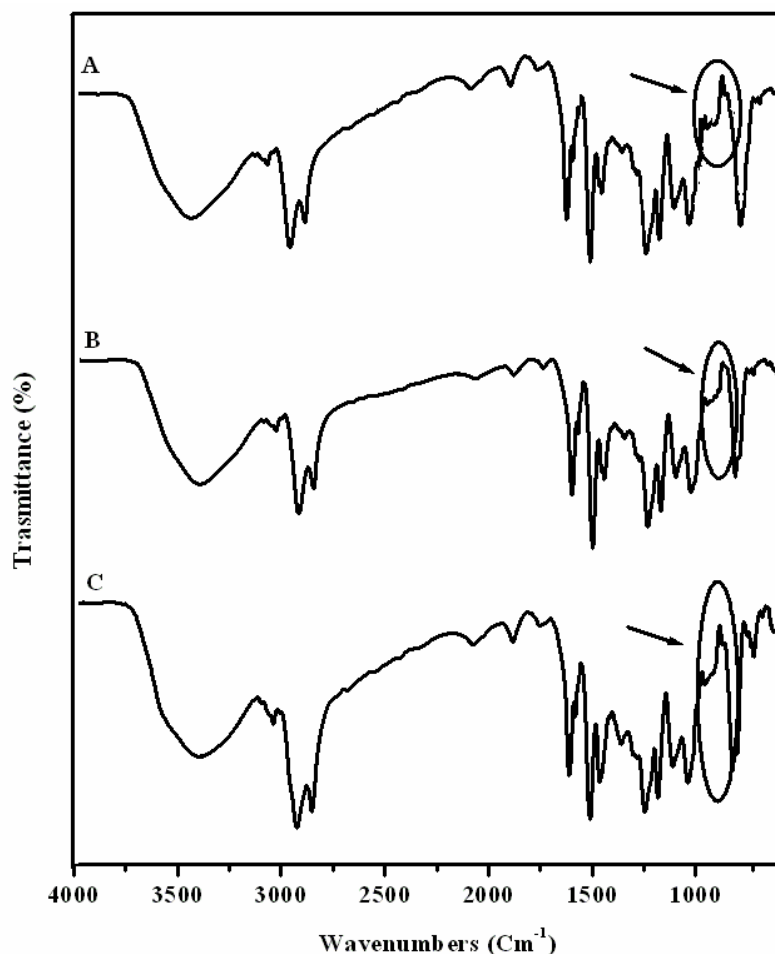


**Table 5.3 : Activation parameters of epoxy curing by Coats-Redfern method**

Monomer	Activation Energy Ea (kJ/mol)	Frequency Factor ln A (s <sup>-1</sup> )
DGEBA	70	8.28
DGEBAZ	62	5.64

### 5.3.3 Characterization of cured network

Uncured epoxy resins are characterized by characteristic epoxide ring deformation at around 915 cm<sup>-1</sup> in IR spectroscopy<sup>23</sup>. The absence of this peak in the spectrum of cured resin confirms the conversion of epoxy into a crosslinked network. IR spectra of cured DGEBA, DGEBAZ and DGEBAZ15 are shown in **Figure 5.12**. The absorption around 915 cm<sup>-1</sup> was not detected in IR spectra of cured epoxy resins of DGEBA, DGEBAZ and DGEBAZ15.



**Figure 5.12 : IR spectra of cured epoxy resins; A) DGEBA resin, B) DGEBAZ resin C) DGEBAZ15 resin.**

### 5.3.3.1 Dynamic mechanical thermal analysis

Dynamic mechanical measurements were performed to analyze the storage modulus ( $E'$ ) and measuring glass transition of cured epoxy resins. **Figure 5.13** represents storage modulus of cured DGEBPZ, DGEBPZ and DGEBPC15 network. As can be seen from the figure, the storage modulus (at 35 °C) of DGEBPC15 resin is less than that of DGEBPA and DGEBPZ resin. In case of DGEBPC15 network, the presence of long alkyl pentadecyl chain impedes tight packing of network which confers comparatively lower storage modulus. This can also be understood by lower crosslink density of the network.

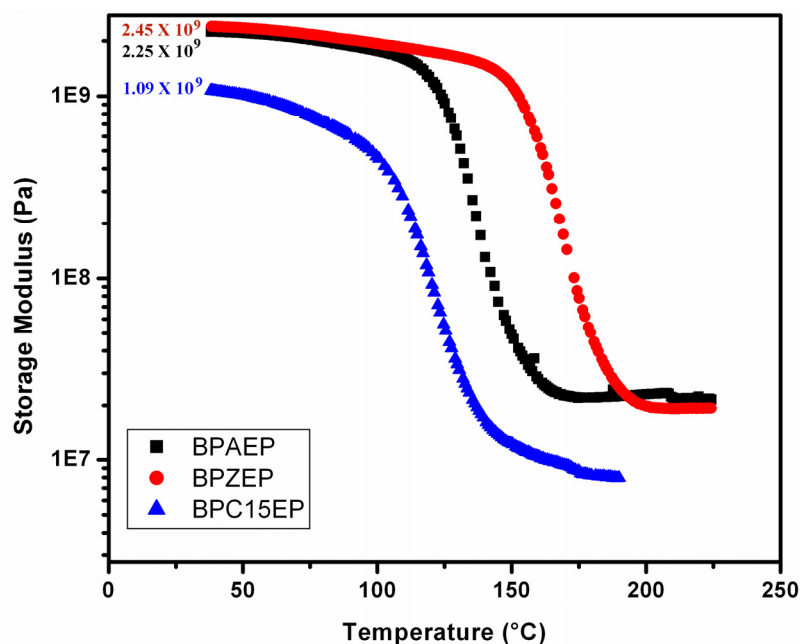
From the theory of rubber elasticity, the crosslink density of a cured polymer network can be determined by the following equation<sup>32,33</sup>;

$$G = E'/3 = \phi \nu RT \quad (7)$$

where  $G$  is the shear modulus,  $E'$  is the storage modulus of the cured network in the rubbery plateau region above  $T_g$  ( $T_g + 40$  °C),  $\phi$  is the front factor,  $R$  is the gas constant,  $T$  is the absolute temperature in Kelvin and  $\nu$  is crosslink density also known as concentration of network chains (number of network chains per unit volume of the cured polymer). For most crosslinked polymers, the value of  $\phi$  is assumed to be unity<sup>34-36</sup>. This equation holds good only for networks with low degrees of crosslinking. For highly crosslinked systems such as epoxies, another semiempirical equation (**equation 8**) results with better agreement between theory and experiment.<sup>37,38</sup>

$$\log_{10} G = 7 + 293 \nu \quad (8)$$

where  $G$  is in dynes/cm<sup>2</sup>. The crosslink densities calculated by using **equation 8** are collected in **Table 5.4**.



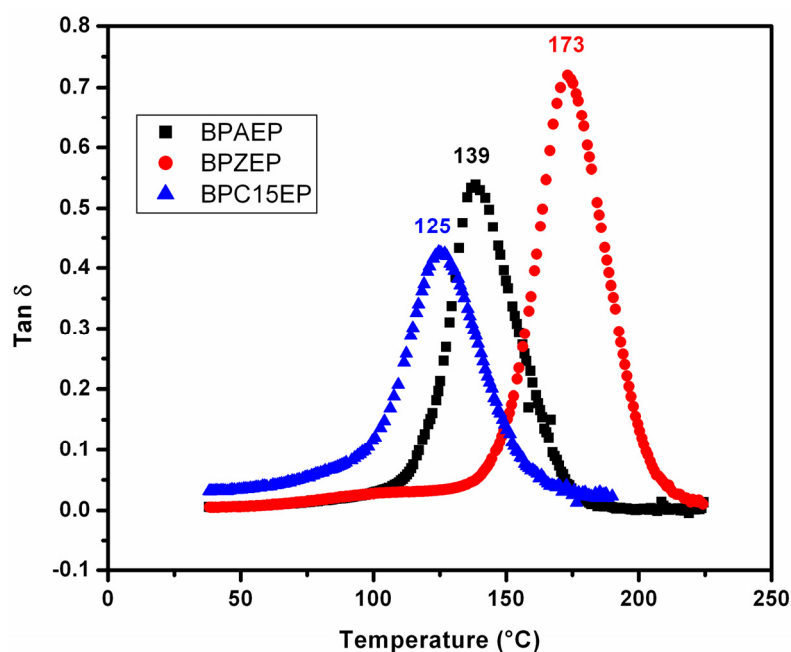
**Figure 5.13: Storage modulus of cured epoxy resins**

**Table 5.4: Dynamic mechanical properties of cured epoxy resins**

Epoxy resin	Storage modulus at 35 °C (Pa)	Glass transition temperature <sup>#</sup> (°C)	Storage modulus at T <sub>g</sub> + 40 °C (dynes/cm <sup>2</sup> )	Crosslink density (mol / cm <sup>3</sup> )
DGEBPA	2.25 x 10 <sup>9</sup>	139	5.03 x 10 <sup>8</sup>	4.2 x 10 <sup>-3</sup>
DGEBPZ	2.45 x 10 <sup>9</sup>	173	1.92 x 10 <sup>8</sup>	2.8 x 10 <sup>-3</sup>
DGEBPC15	1.09 x 10 <sup>9</sup>	125	0.97 x 10 <sup>8</sup>	1.7 x 10 <sup>-3</sup>

# from tan  $\delta$  curve

The glass transition temperatures of thermosetting resins are strongly influenced by backbone rigidity of epoxy monomer, crosslink density and free volume. The introduction of rigid backbone such as cardo moiety into epoxy backbone increases glass transition temperature. Increase in free volume results into lowering of glass transition<sup>39</sup>. In the present study, T<sub>g</sub> of cured network is measured from tan  $\delta$  peak value (**Figure 5.14**).

**Figure 5.14: Tan  $\delta$  curves of cured epoxy resins**

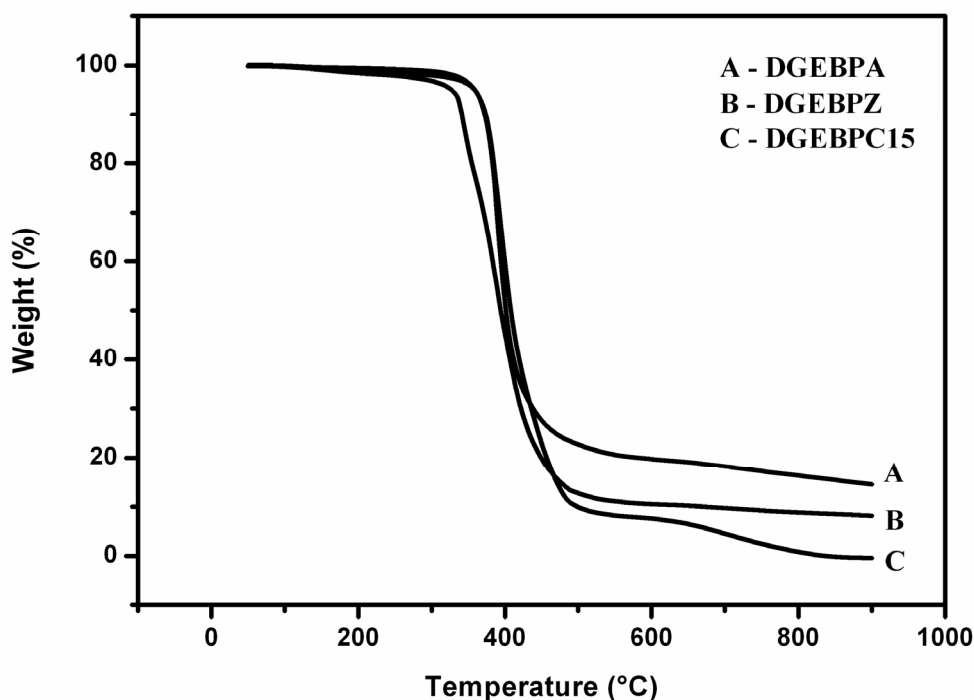
Due to higher segmental mobility and more number of relaxing species, the network of DGEBPC15 exhibits lower T<sub>g</sub> than cured DGEBPA and DGEBPZ.

### 5.3.3.2 Thermal Properties

The thermo-oxidative stability of epoxy resins has been studied by many researchers<sup>13, 40-45</sup>. Lee<sup>40</sup> found water, phenol (largest component), isopropynyl phenol (major component), and isopropyl phenol (major component) as the initial degradation products of DGEBPA cured with MDA.

**Figure 5.15** represents the weight loss of cured resins of DGEBPA, DGEBPZ, and DGEBPC15 when heated at 10 °C / min in nitrogen. The relative thermal stabilities of the cured

resins were compared by the temperature of 10 % weight loss and char yield at 800 °C. The temperature of 10 % weight loss and the char yield at 800 °C are tabulated in **Table 5.5**.



**Figure 5.15:** TGA curves of cured epoxy resins

**Table 5.5:** Thermal properties of cured epoxy resins

Epoxy resin	T <sub>10</sub> (°C)	Char Yield at 800 °C (%)
DGE BPA	374	16.3
DGE BPZ	372	8.8
DGE BPC15	341	0.8

Cured DGE BPC15 performed substantially worse than DGE BPZ and DGE BPA, with higher weight loss rates at temperatures from 350 °C to around 450 °C. The temperature of 10 % loss was found to be 374 °C, 372 °C and 341 °C respectively for DGE BPA, DGE BPZ, and DGE BPC15 cured epoxy network. The char yield at 800 °C in case of cured DGE BPC15 was observed to be 0.8 % which is lower than that of cured DGE BPZ (8.8 %) and cured DGE BPA (16.3 %). The decreased thermal stability of cured DGE BPC15 could be due to higher aliphatic content. The data shows that thermal stability of resins gets hampered after incorporation of cycloaliphatic moiety.

### 5.3.3.3 Moisture absorption

The moisture absorption seriously damages dielectric properties of a resin by the contribution of water molecules to polarization and energy dissipation<sup>46</sup>. In case of cyanate ester resins, it was observed that incorporation of cycloaliphatic “cardo” group into a cyanate ester monomer resulted into polycyanurates with lower moisture absorption. In case of epoxy resins also, it was observed that after incorporation of cycloaliphatic “cardo” group, the percentage moisture absorption of cured epoxy resin decreases. **Table 5.6** summarizes percentage moisture absorption of cured DGEBA, DGEBPZ and DGEBPC15 resins after 24 h exposure to boiling water. The weight gain during exposure for cured DGEBPC15 is only about 50 % of that observed in cured DGEBA resin.

**Table 5.6: Percentage moisture absorption of cured epoxy resins**

Epoxy resins	Moisture Absorption (%)
DGEBA	3.2
DGEBPZ	2.6
DGEBPC15	1.8

#### 5.4 Conclusions:

1. Diglycidyl ether of 1,1-bis(4-hydroxyphenyl)-3-pentadecylcyclohexane and diglycidyl ether of 1,1-bis(4-hydroxyphenyl)cyclohexane containing cycloaliphatic “cardo” group were successfully synthesized from corresponding bisphenols by the reaction with epichlorohydrin and were characterized by IR and NMR spectroscopy.
2. The diglycidyl ether of 1,1-bis(4-hydroxyphenyl)-3-pentadecylcyclohexane showed the presence of magnetically non-equivalent distereotopic phenyl rings in the NMR spectra.
3. The epoxies in the present study were cured employing 4,4'-methylenedianiline as a curing agent and the properties of cured epoxy network were studied by DMTA, TGA and percent moisture absorption measurement.
4. The activation energy of curing of epoxies calculated by Coats-Redfern method in nonisothermal mode was in the range 48-52 kJ/mol.
5. Both the storage modulus and T<sub>g</sub> of cured epoxy resin of diglycidyl ether of 1,1-bis(4-hydroxyphenyl)cyclohexane were higher than that of cured network of diglycidyl ether of bisphenol-A and diglycidyl ether of 1,1-bis(4-hydroxyphenyl)-3-pentadecylcyclohexane due to the presence of rigid cycloaliphatic “cardo” group.
6. The thermal degradation of cured epoxy resins under study, as analyzed by TGA, followed a single step degradation with T<sub>10</sub> values in the range 340 – 375 °C.
7. The cured network of diglycidyl ether of 1,1-bis(4-hydroxyphenyl)-3-pentadecylcyclohexane exhibited lower % moisture absorption than that of cured network of diglycidyl ether of bisphenol-A and diglycidyl ether of 1,1-bis(4-hydroxyphenyl)cyclohexane which could be ascribed to higher aliphatic content in the former.

## References:

1. Lee, H; Neville, K. In *Handbook of Epoxy Resins*, **1967**, McGraw Hill, New York.
2. May, C.; Tanaka, Y. Eds. *Epoxy Resins Chemistry and Technology*, **1988**, 2<sup>nd</sup> ed, Marcel Dekker, Inc, New York.
3. Bosch, A. *Epoxy Resins*, In *Polymeric Materials Encyclopedia*, Salamone J.C. Ed., **1996**, CRC Press, Boca Rathon, Vol 3, p 2246.
4. Pham, H; Marks, M. *Epoxy Resins*, In *Encyclopedia of Polymer Science and Technology*, **2004**, 3<sup>rd</sup> Ed., Wiley Interscience, New Jersey, Vol 9, p 678.
5. Serra, A; Cadiz, V; Martinez, PA; Mantecon, A. *Angew. Makromol. Chem.* **1986**, 140, 113.
6. Mantecon, A.; Cadiz, V.; Serra, A.; Martinez, P. A. *Eur. Polym. J.* **1987**, 23, 481.
7. Bucknall, C.B.; Gilbert, A.H. *Polymer* **1989**, 30, 213.
8. Mormann, W.; Brocher, M. *Macromol. Chem. Phys.* **1998**, 119, 1935
9. Batog, A.E.; Petko, I.P.; Penczek, P. *Adv. Polym. Sci.* **1999**, 144, 49.
10. Erich, W.; Bodnar, M.J. *J. Appl. Polym. Sci.* **1960**, 3, 296.
11. Korshak, V.V.; Soloveva, L.K.; Kamenskh, I.V. *Vysokomol Soedin A.* **1971**, 13, 150.
12. Lin, S.C.; Pearce, E.M. *J. Polym. Sci.: Polym. Chem.* **1979**, 17, 3095.
13. Lin, S.C.; Bulkin, B.J.; Pearce, E.M. *J. Polym. Sci.: Polym. Chem.* **1979**, 17, 3121.
14. Chen, C.S.; Bulkin, B.J.; Pearce, E.M. *J. Appl. Polym. Sci.* **1982**, 27, 1177.
15. Chen, C.S.; Bulkin, B.J.; Pearce, E.M. *J. Appl. Polym. Sci.* **1982**, 27, 3289.
16. Dai, Z; Li, Y; Yang, S; Zong, C; Lu, X; Xu, J. *J. Appl. Polym. Sci.* **2007**, 106, 1476.
17. Muller, HP; Franke, J. (Bayer AG), *European Patent* 0377909 A1, **1990**.
18. Xu, K.; Chen, M.; Zhang, K.; Hu, J. *Polymer* **2004**, 45, 1133.
19. Su, X.; Jing, X. *J. Appl. Polym. Sci.* **2007**, 106, 737.
20. Wang, T.; Wan, P.Y.; Yu, Q.P; Yu, M. *Polym. Bull.* **2008**, 59, 787.
21. Sorenson W. R.; Campbell T. W. *Preparative Methods of Polymer Chemistry*, **1961**, 2<sup>nd</sup> Ed, Interscience Inc., New York, p 309.
22. Kamal, M.R. *Polym. Eng. Sci.*, **1974**, 14, 231.
23. Pang, K.P.; Gillham, J.K. *J. Appl. Polym. Sci.*, **1989**, 37, 1969.
24. Min, B.G.; Stachurski, Z.H.; Hodgkin, J.H. *Polymer*, **1993**, 34, 4908.
25. Vyazovkin, S.; Sbirrazzuoli, N. *Macromolecules*, **1996**, 29, 1867.
26. Pichaud, S.; Duteurtre, X.; Fit, A.; Stephan, F.; Maazouz, A.; Pascault, J.P. *Polym. Int.* **1999**, 48, 1205.
27. Perrin, F, -X.; Nguyen, T.M.H; Vernet, J.-L. *Macromol. Chem. Phys.*, **2007**, 208, 718.
28. Liu, W.; Qiu, Q; Wang, J.; Huo, Z.; Sun, H. *Polymer* **2008**, 49, 4399.
29. Dai, Z.; Li, Y.; Yang, S.; Zhao, N.; Zhang, X.; Xu, J. *Eur. Polym. J.*, **2009**, 45, 1941.
30. Marks, M.J.; Snelgrove, R.V. *ACS Appl. Mater. Interaces.*, **2009**, 1, 921.
31. Coats, A.W.; Redfern, J.P. *Nature* **1964**, 201, 68
32. Tobolsky, A. V.; Carlson, D. W.; Indicator, N. *J. Polym. Sci.* **1961**, 54, 175.
33. Ferry, J. D. *Visoelastic Proerties of Polymers* **1980**, Wiley, New York.
34. Tobolsky, A. V.; Katz, D.; Thach, R.; Schaffhauser, R. *J. Polym. Sci.* **1962**, 62, S176.
35. Takahama, T.; Geil, P.H. *J. Polym. Sci. Polym. Lett. Ed.* **1982**, 20, 453.
36. Hasegawa, G.; Fukuda, A.; Tonogi, S. *J. Appl. Polym. Sci.*, **1989**, 37, 3423.
37. Nielsen, L.E. *Mechanical Properties of Polymers and Composites*, **1974**, Marcel Dekker, New York, Vol.1.
38. Ward, I. M.; Hadley, D.W. *An Introduction to the Mechanical Properties of Solid Polymers*, **1993**, Wiley, New York.
39. Prime R. B. In *Thermal Characterization of Polymeric Materials*. Turi, E.A. Ed. **1981**, Academic, New York, chapter 2 and chapter 5.
40. Lee, L.H. *J. Polym. Sci. A.*, **1965**, 3, 859.
41. Keeman, M.A.; Smith, D. A. *J. Appl. Polym. Sci.* **1967**, 11, 1009.
42. Cerceo, E. *Ind. Eng. Chem. Prod. Res. Dev.*, **1970**, 9, 96.
43. Bishop, D.P. ; Smith, D. A. *J. Appl. Polym. Sci.* **1970**, 14, 205.
44. Theocaris, P.S.; Paipetis, A. S.; Tasngaris, J.M. *Polymer* **1974**, 15, 441.
45. Patterson-Jones, J. C. *J. Appl. Polym. Sci.* **1974**, 19, 1539.
46. Snow, A.W.; Buckley L.J. In *Handbook of Low and High Dielectric Constant Materials and Their Applications*. Nalwa, H.S. Ed. **1999**, Academic Press; New York, Vol. 1, Chap 4.

# Chapter **6**

Synthesis, Characterization and  
Curing Studies of Bismaleimides



## 6.1 Introduction

Bismaleimides (BMIs) represent a class of addition-type polyimides comprising thermally curable monomers or oligomers and cured resins.<sup>1,2</sup> The cured BMIs find applications in multilayered printed wiring boards for large scale computers, in carbon fiber composites for the aerospace industry, etc.<sup>3-8</sup> One of the main reasons for the intense interest in BMIs is the ability to fabricate them with epoxy like processing conditions without evolution of void forming volatiles. The cured BMIs exhibit high glass transition temperature coupled with high modulus.<sup>2,9,10</sup>

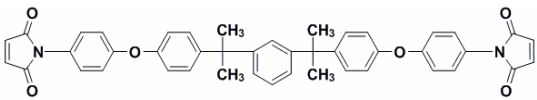
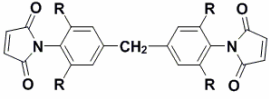
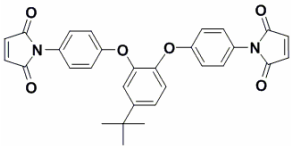
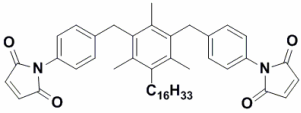
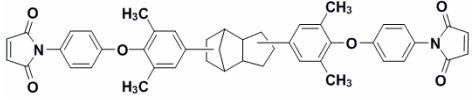
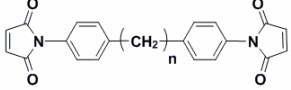
However, the higher melting points (greater than 150 °C) of BMI monomers, poor solubility of BMI monomers in common organic solvents and inherent brittleness of the cured resins limit their widespread applications to a great extent.<sup>11,12</sup> The higher melting points (> 150 °C) close to the onset temperature of curing induces a short gel time or short potlife of the melt making the processing difficult.

To overcome these problems, various approaches such as developing new BMI monomers containing flexible units<sup>13-19</sup>, modification of BMI resins by using comonomers, etc., were attempted.<sup>20-22</sup> It was observed that introduction of flexible spacers into BMI backbone lowers melting point of monomer and improves solubility in common organic solvents.<sup>23-33</sup> Barton *et. al.*<sup>28</sup> synthesized a series of BMI monomers having lower melting points (<100 °C). The authors observed that the purity of BMI monomers has marked effects on the thermal cure characteristics. Goldfrab *et. al.*<sup>17</sup> synthesized a series of bismaleimides containing flexible units of variable length with different pendent groups and found that the breadth of cure window can be controlled by varying oxyalkylene linkage between reacting imide end groups without adversely affecting thermal properties of the cured network. Hsiao *et.al.*<sup>18,30</sup> reported a series of BMI monomers containing ether bridges in order to study the effect of structure on the thermal properties of cured resins. The authors observed that increasing molecular weight between reactive end groups lowered melting points of BMIs leading to a sufficient temperature gap between melting point and cure onset. The introduction of ether linkage decreased T<sub>g</sub>, and improved toughness of cured resins without compromising thermal stability to a large extent. Grenier-Loustalot *et.al.*<sup>29</sup> studied the effect of BMI backbone on reactivity and observed that alkyl / bulky substitution at *ortho* position to maleimide ring decreases reactivity due to steric hindrance. The researchers also observed increase in melting point with increase in steric hindrance. Feng *et. al.*<sup>33</sup> observed a decrease in melting point of BMI monomer with the introduction of alkylene spacer. **Table 6.1** lists BMI monomers containing alkylene chain / ether unit and common BMIs with their melting points.

Table 6.1 : List of bismaleimide monomers containing alkylene chain / ether units

Sr. No.	Bismaleimide	Melting Point (°C)	Reference
1		155-157	23
		157-158	24
		160 (Purity: 95 %) 163 (Purity: 99.3 %)	25
2		173-174	23
		176-178	26
3		205	18
4		90-100	27
		93-100	28
5		130-132 (n = 2) 98-100 (n = 4)	17
6		53-54 (n = 2) 48-49 (n = 3) 46-47 (n = 4)	17
7		135	18
8		85	18
9		90	18
10		131	18

Table 6.1 continued.....

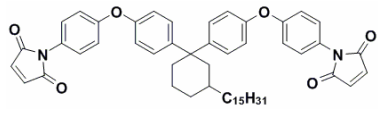
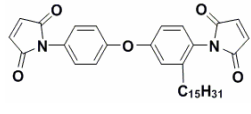
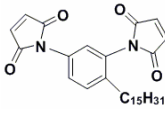
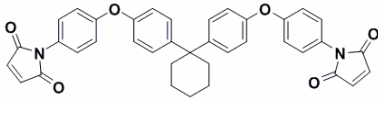
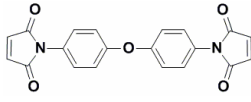
11		90	18
12	 R = -CH <sub>3</sub> , -C <sub>2</sub> H <sub>5</sub> , -CH(CH <sub>3</sub> ) <sub>2</sub>	210 (R = -CH <sub>3</sub> ) 162 (R = -C <sub>2</sub> H <sub>5</sub> ) 221 (R = CH(CH <sub>3</sub> ) <sub>2</sub> )	29
13		136	30
14		45	31
15		137	32
16	 n = 5, 6, 7, 8	101-103 (n = 5) 138-142 (n = 6) 75-78 (n = 7) 123-126 (n = 8)	33

The objective of the present work was to synthesize new BMI monomers exhibiting lower melting point and solubility in common organic solvents. One of the approaches to improve solubility and processability of high temperature / high performance polymers is the introduction of flexible chains as pendant groups.<sup>34-38</sup> The introduction of pendant groups disturbs structural regularity and hence impedes close packing of molecules which thus results into lowering of melting point. Thus, our synthetic research efforts were directed towards designing BMI monomers with asymmetry. The approach involved making use of 3-pentadecyl phenol, which in turn is obtainable from cashew nut shell liquid (CNSL) – a renewable resource material. Considering the special structural features of 3-pentadecyl phenol, different strategies were developed to design and synthesize new bismaleimides. (**Table 6.2, Sr. No. 1-3**)

The present work deals with the design and synthesis of three new BMI monomers (**Table 6.2, Sr. No. 1-3**) containing flexible pendant pentadecyl chain, characterization of BMI

monomers by FTIR, and NMR ( $^1\text{H}$  and  $^{13}\text{C}$  NMR) spectroscopic techniques. The curing kinetics of new BMIs was studied by using DSC and thermal properties of cured resins were evaluated by TGA. To understand the effect of incorporation of flexible pendent pentadecyl chain into BMI structure, reference BMI monomers (Table 6.2, Sr. No. 4, 5) were also synthesized.

**Table 6.2: List of bismaleimide monomers synthesized in the present study.**

Sr. No	Bismaleimide Monomer	Name
1		1,1-Bis[4-(4-maleimidophenoxy)phenyl]-3-pentadecyl cyclohexane
2		4,4'-Bis(maleimido)-3-pentadecyldiphenylether
3		1,3-Bis(maleimido)-4-pentadecylbenzene
4		1,1-Bis[4-(4-maleimidophenoxy)phenyl] cyclohexane
5.		4,4'-Bis(maleimido)diphenylether

## 6.2 Experimental

### 6.2.1 Materials

1,1-Bis(4-hydroxyphenyl)cyclohexane (BPZ) and 1,1-bis(4-hydroxyphenyl)-3-pentadecyl cyclohexane (BPC15) were synthesized as described in Chapter 3.

Palladium-on-carbon (10 wt %), 3-pentadecyl phenol, and 4,4'-bis(amino)diphenyl ether (4,4'-oxydianiline), were purchased from Sigma-Aldrich Inc. USA. Acetone, chloroform, dichloromethane, ethylacetate, toluene, phenol, acetic acid, hydrochloric acid, nitric acid, sulfuric acid, potassium hydroxide, triethylamine, sodium bicarbonate, sodium chloride, sodium dithionite, sodium nitrite, sodium sulfate, and silica gel were procured from Merck India. Sulfanilic acid (Fluka), 1-chloro-4-nitrobenzene, hydrazine hydrate (80%), maleic anhydride, methanesulfonyl chloride, N,N-dimethylformamide, potassium carbonate,

magnesium metal, and sodium acetate (Loba Chemie, India) were used as received. Absolute ethanol (Cympran Gludt BV, Belgium) was used as received.

## 6.2.2 Characterization

Melting points were determined by open capillary method and are uncorrected.

Infrared spectra were recorded on Perkin-Elmer, spectrum GX model at a resolution of  $4\text{ cm}^{-1}$ . The spectra were recorded by depositing samples as solvent-cast thin films on sodium chloride cells.

NMR spectra were recorded on Bruker NMR spectrophotometer (200 or 400 MHz) using  $\text{CDCl}_3$  or  $\text{DMSO-d}_6$  as a solvent.

DSC measurements were performed on TA Instrument (Q10) supported by TA Universal Analysis software for data acquisition. The samples (5-7 mg) were sealed in hermetic aluminum pans and experiments were performed under a nitrogen flow of 50 mL / min. The samples were subjected to a dynamic DSC scan at the heating rate of  $10\text{ }^\circ\text{C}/\text{min}$ . The enthalpy of curing  $\Delta H$  was determined from the area under the exothermic curve. The cure onset temperature ( $T_0$ ) was considered as the intersect of slope of baseline and tangent of curve leading to peak of transition. The fractional conversion ( $\alpha$ ) of each sample at a given temperature under nonisothermal conditions was calculated from the relation<sup>39</sup>:

$$\alpha_T = \Delta H_f / \Delta H_T \quad (1)$$

where  $\Delta H_f$  is the fractional enthalpy at that temperature and  $\Delta H_T$ , the total heat of reaction under nonisothermal mode.

Thermogravimetric analysis (TGA) data was obtained using a TA instrument, (model Q 5000) at a heating rate of  $10\text{ }^\circ\text{C} / \text{min}$  under nitrogen atmosphere.

## 6.3 Preparations

### 6.3.1 Synthesis of 1,1-bis[4-(4- maleimidophenoxy)phenyl] -3-pentadecylcyclohexane

#### 6.3.1.1 Synthesis of 1,1-bis-[4-(4-nitrophenoxy)phenyl]-3-pentadecylcyclohexane

Into a 500 mL two necked round bottom flask equipped with a nitrogen inlet, a reflux condenser and a magnetic stirring bar were placed 1,1-bis-(4-hydroxyphenyl)-3-pentadecylcyclohexane (9.56 g, 0.02 mol), 1-chloro-4-nitrobenzene (7.88 g, 0.05 mol), and DMF (150 mL). To the reaction mixture, potassium carbonate (8.28 g, 0.06 mol) was added and the reaction mixture was refluxed for 12 h under nitrogen atmosphere. The reaction mixture was cooled to room temperature and poured into water (500 mL). The crude product obtained

was filtered and the filtrate was washed with water (3 x 50 mL). The pale yellow solid was recrystallized using DMF.

Yield: 10.82 g (75 %),

MP: 79 - 80°C

### 6.3.1.2 Synthesis of 1,1-bis-[4-(4-aminophenoxy)phenyl]-3-pentadecylcyclohexane.

Into a 250 mL three necked round bottom flask equipped with a magnetic stirring bar, a nitrogen inlet, a reflux condenser and a dropping funnel were added 1,1-bis[4-(4-nitrophenoxy)phenyl]-3-pentadecylcyclohexane (7.21 g, 0.01 mol), palladium-on-carbon (10 wt %) (0.14 g, 2 wt % based on dinitro compound) and absolute ethanol (50 mL). To the reaction mixture, hydrazine hydrate (80 %) (4 mL diluted with 5 mL of ethanol) was added dropwise over a period of 30 min at reflux temperature under nitrogen atmosphere. After the completion of addition, the reaction mixture was refluxed for 4 h. The reaction mixture was filtered while hot to remove palladium-on-carbon and the filtrate was cooled to room temperature. The colorless solid obtained was isolated by filtration and recrystallized using ethanol.

Yield: 5.3 g (80 %),

MP: 71°C.

### 6.3.1.3 Synthesis of 1,1-bis[4-(4-maleimidophenoxy)phenyl]-3-pentadecylcyclohexane.

Into a 100 mL two necked round bottom flask equipped with a magnetic stirring bar, a nitrogen inlet and a reflux condenser were placed 1,1-bis[4-(4-aminophenoxy) phenyl] -3-pentadecylcyclohexane (2.52 g, 3.8 mmol), maleic anhydride (0.78 g, 8 mmol) and acetone (10 mL). The reaction mixture was stirred at room temperature for 4 h and then refluxed for 1h. To the reaction mixture, were added acetic anhydride (3 mL) and sodium acetate (0.66 g, 8 mmol) and the mixture was refluxed for 6 h. The reaction mixture was cooled to room temperature, poured into water (75 mL) and extracted with ethyl acetate. The ethyl acetate layer was successively washed with aqueous solution of sodium bicarbonate (3 x 25 mL), brine water (2 x 25 mL) and water (2 x 25 mL). The ethyl acetate layer was dried over sodium sulfate, filtered, and evaporated on rotary evaporator to afford a viscous product which was purified by column chromatography (Eluent: pet ether / ethyl acetate: 90 : 10, v/v).

Yield: 1.52 g (50%).

## 6.3.2 Synthesis of 4,4'-bis(maleimido)-3-pentadecyldiphenylether

### 6.3.2.1 Synthesis of 4-amino-3-pentadecyl phenol

Into a 500 mL three necked round bottom flask equipped with a reflux condenser, a thermowell, and a magnetic stirring bar were placed 3-pentadecyl phenol (30.4 g, 0.10 mol),

potassium hydroxide (28.0 g, 0.50 mol), and ethanol (200 mL). To the reaction mixture was added diazonium chloride (synthesized as described below) at  $-5\text{ }^{\circ}\text{C}$ . The resulting red dye solution was stirred for 2 h and then the temperature was raised to  $75\text{ }^{\circ}\text{C}$ . To the reaction mixture, a saturated solution of sodium dithionite (53.0 g, 0.30 mol) was added over a period of 10 min and the reaction mixture was stirred for 30 min (color of reaction mixture changed from dark red to orange). To the reaction mixture, was then added acetic acid (18.0 g, 0.3 mol) diluted with water (20 mL) and the reaction mixture was refluxed for 1 h (color changed to pale tan). The reaction mixture was poured into water (2 L). The precipitated product was filtered and dried under reduced pressure at  $50\text{ }^{\circ}\text{C}$ . The crude product was purified by recrystallisation using toluene.

[To prepare diazonium chloride of sulphanilic acid, sodium carbonate (11.7 g, 0.11 mol,) and sulphanilic acid dihydrate (21.0 g, 0.10 mol) were dissolved in water (100 mL). To the reaction mixture, sodium nitrite (6.9 g, 0.10 mol) dissolved in water (20 mL) was added at  $15\text{ }^{\circ}\text{C}$ . After the complete addition, the reaction mixture was poured on ice cold hydrochloric acid (36 %), (30 mL) and the resulting precipitate was allowed to settle down and filtered.]

Yield: 25.0 g (79 %).

MP:  $104\text{ }^{\circ}\text{C}$  (Lit.:  $105\text{-}106\text{ }^{\circ}\text{C}$ ).<sup>40</sup>

IR ( $\text{CHCl}_3$ ,  $\text{cm}^{-1}$ ): 3460 and 3355 ( $-\text{NH}$  stretching), 3260 ( $-\text{OH}$  stretching).

$^1\text{H-NMR}$  ( $\text{CDCl}_3$ ,  $\delta$  ppm): 6.53 - 6.60 (m, 3H, Ar-H), 3.65 (broad s, 2H,  $-\text{NH}_2$ ), 2.43 (t, 2H, benzylic  $-\text{CH}_2$ ), 1.54 - 1.60 (m, 2H,  $-\text{CH}_2$   $\beta$  to aromatic ring), 1.22 - 1.26 (m, 24H,  $-\text{CH}_2$ ), 0.87 (t, 3H,  $-\text{CH}_3$ ).

### 6.3.2.2 Synthesis of 4-(4'-nitrophenoxy)-2-pentadecylbenzenamine

Into a 500 mL three necked round bottom flask equipped with a nitrogen gas inlet, a reflux condenser and a magnetic stirring bar were placed 4-amino-3-pentadecyl phenol (20.0 g, 62 mmol), 1-chloro-4-nitrobenzene (9.87 g, 62 mmol), potassium carbonate (9.53 g, 68 mmol) and DMF (100 mL). The reaction mixture was refluxed for 3 h under nitrogen atmosphere. The reaction mixture was cooled to room temperature and poured into water (1L). The precipitated product was filtered, dried and recrystallised using ethanol.

Yield: 18.9 g (90 %).

MP:  $66\text{-}67\text{ }^{\circ}\text{C}$  (Lit.:  $67\text{ }^{\circ}\text{C}$ ).<sup>40</sup>

IR ( $\text{CHCl}_3$ ,  $\text{cm}^{-1}$ ): 3350 ( $-\text{NH}$  stretching), 1535 ( $-\text{NO}_2$  asymmetric stretching), 1340 ( $-\text{NO}_2$  symmetric stretching), 1250 ( $-\text{C-O-C-}$  stretching).

$^1\text{H-NMR}$  ( $\text{CDCl}_3$ ,  $\delta$  ppm): 8.15 (d, 2H, Ar-H, *ortho* to  $-\text{NO}_2$ ), 6.94 (d, 2H, Ar-H, *meta* to  $-\text{NO}_2$ ), 6.66 - 6.81 (m, 3H, Ar-H, pentadecyl substituted ring), 3.62 (s, 2H,  $-\text{NH}_2$ ), 2.45 (t, 2H,

benzylic -CH<sub>2</sub>), 1.56 – 1.64 (m, 2H, -CH<sub>2</sub> β to aromatic ring), 1.22 - 1.26 (m, 24H, -CH<sub>2</sub>), 0.86 (t, 3H, -CH<sub>3</sub>).

### 6.3.2.3 Synthesis of 4-(4'-aminophenoxy)-2-pentadecylbenzenamine

Into a 250 mL three necked round bottom flask equipped with a dropping funnel, a reflux condenser, and magnetic stirring bar were placed 4-(4'-nitrophenoxy)-2-pentadecyl benzenamine (10.0 g, 22 mmol), palladium-on-carbon (10 wt %) (0.2 g, 2 wt % based on nitro compound) and absolute ethanol (100 mL). To the reaction mixture, hydrazine hydrate (35 mL, diluted with 35 mL of absolute ethanol) was added dropwise over a period of 1 h at 80 °C. After the completion of addition, the reaction mixture was refluxed for 4 h. The reaction mixture was filtered while hot to remove palladium-on-carbon. The product precipitated on cooling and was isolated by filtration and recrystallised using ethanol.

Yield: 8.38 g (90%).

MP: 81 °C (Lit.: 81 °C).<sup>40</sup>

IR (CHCl<sub>3</sub>, cm<sup>-1</sup>): 3465 and 3370 (-NH stretching), 1235 (-C-O-C- stretching).

<sup>1</sup>H-NMR (CDCl<sub>3</sub>, δ ppm): 6.72 – 6.82 (m, 4H, Ar-H), 6.63 (d, 3H, Ar-H, *ortho* to -NH<sub>2</sub>), 3.12 (s, 4H, -NH<sub>2</sub>), 2.43 (t, 2H, benzylic -CH<sub>2</sub>), 1.54 – 1.61 (m, 2H, -CH<sub>2</sub> β to aromatic ring), 1.22 - 1.26 (m, 24H, -CH<sub>2</sub>), 0.87 (t, 3H, -CH<sub>3</sub>).

### 6.3.2.4 Synthesis of 4,4'-bis(maleimido)-3-pentadecyldiphenylether

Into a 100 mL two necked round bottom flask equipped with a magnetic stirring bar, a nitrogen inlet and a reflux condenser were placed 4-(4'-aminophenoxy)-2-pentadecylbenzenamine (2.05 g, 5 mmol), maleic anhydride (1.03 g, 10.5 mmol) and acetone (25 mL). The reaction mixture was stirred at room temperature for 4 h and then refluxed for 1h. To the reaction mixture were added acetic anhydride (6 mL) and sodium acetate (0.87 g, 11 mmol) and the mixture was refluxed for 6 h. The reaction mixture was cooled to room temperature and poured into water (150 mL). The solid obtained was washed with water (3 x 10 mL) and then with methanol (2 x 10 mL). The crude product was purified by column chromatography (Eluent: pet ether / ethyl acetate: 80 : 20, v/v).

Yield: 2.13 g (52 %).

MP: 69 - 70 °C.

### 6.3.3 Synthesis of 1,3-bis(maleimido)-4-pentadecylbenzene

#### 6.3.3.1 Synthesis of 1-methane sulfonyloxy-3-pentadecyl benzene

Into a 500 mL two necked round bottom flask equipped with dropping funnel and an air condenser were added 3-pentadecylphenol (10 g, 32.8 mmol), triethyl amine (3.6 g, 36 mmol)



and dichloromethane (100 mL). To the reaction mixture, methanesulfonyl chloride (4.12 g, 36 mmol) was added dropwise at 0 °C. After complete addition of methanesulfonyl chloride, the reaction mixture was stirred for 48 h. The reaction mixture was filtered and the organic layer was washed with saturated aqueous sodium chloride solution (2 x 50 mL) followed by washing with water (3 x 50 mL). The organic layer was dried over sodium sulfate and filtered. The evaporation of solvent on rotary evaporator afforded 1-methane sulfonyloxy-3-pentadecyl benzene.

Yield: 9 g (96 %).

MP: 58 °C (Lit .: 58 °C).<sup>40</sup>

IR (CHCl<sub>3</sub>, cm<sup>-1</sup>): 1370 (-SO<sub>2</sub> asymmetric stretching), 1125 (-SO<sub>2</sub> symmetric stretching)

<sup>1</sup>H-NMR (CDCl<sub>3</sub>, δ ppm): 7.34 (t, 1H, Ar-H, *meta* to mesyl), 7.05 – 7.16 (m, 3H, Ar-H), 3.12 (s, 3H, -CH<sub>3</sub>, methyl of mesyl ester group), 2.62 (t, 2H, benzylic -CH<sub>2</sub>), 1.56 – 1.62 (m, 2H, -CH<sub>2</sub> β to aromatic ring), 1.21 - 1.28 (m, 24H, -CH<sub>2</sub> ), 0.87 (t, 3H, -CH<sub>3</sub>).

### 6.3.3.2 Synthesis of pentadecyl benzene

Into a 250 mL two necked round bottom flask equipped with an air condenser and a magnetic stirring bar were placed 1-methane sulfonyloxy-3-pentadecyl benzene (5 g, 13.6 mmol), palladium-on-carbon (0.5 g), magnesium metal (0.39 g, 16.3 mmol), ammonium acetate (14.7 g, 191 mmol) and methanol (50 mL) and the reaction mixture was degassed by three vacuum / N<sub>2</sub> cycles. The reaction mixture was stirred under nitrogen atmosphere at room temperature for 1 h. After completion of the reaction, the reaction mixture was filtered and the filtrate was partitioned between dichloromethane (250 mL) and water (250 mL). The aqueous layer was extracted with dichloromethane (3 x 100 mL). The combined dichloromethane layer was washed with saturated aqueous sodium chloride solution (2 x 100 mL), followed by water (3 x 100 mL). The organic layer was dried over sodium sulfate and filtered. Evaporation of solvent on rotary evaporator afforded pentadecyl benzene as a yellow liquid. The product was purified by column chromatography (Eluent: pet ether).

Yield: 2.3 g (62 %)

IR (CHCl<sub>3</sub>, cm<sup>-1</sup>): 2925 and 2850 (aliphatic C-H stretching), 1600 (aromatic C=C stretching)

<sup>1</sup>H-NMR (CDCl<sub>3</sub>, δ ppm): 7.15 - 7.26 (m, 5H, Ar-H ), 2.59 (t, 2H, benzylic -CH<sub>2</sub>), 1.24 - 1.38 (m, 26H, -CH<sub>2</sub>), 0.87 (t, 3H, -CH<sub>3</sub>).

### 6.3.3.3 Synthesis of 1,3-dinitro-4-pentadecylbenzene

Into a 100 mL two necked round bottom flask equipped with a dropping funnel, a magnetic stirring bar and an air condenser were placed pentadecylbenzene (2.02 g, 7 mmol). A mixture of fuming nitric acid (3 mL) and sulphuric acid (2 mL) was added drop-wise over a period of

10 min and the mixture was gently heated over a flame for 2 min. The reaction mixture was cooled and poured on ice-water. The solid obtained was filtered and washed with water (4 x 20 mL). The filtrate was dried under vacuum and recrystallized using methanol.

Yield : 2.12 g (80%).

MP: 51 °C (Lit. : 51 °C).<sup>41</sup>

IR (CHCl<sub>3</sub>, cm<sup>-1</sup>): 1590 (aromatic C=C stretching), 1530 (-NO<sub>2</sub> asymmetric stretching), 1345 (-NO<sub>2</sub> symmetric stretching).

<sup>1</sup>H NMR (CDCl<sub>3</sub>, δ ppm): 8.72 (d, 1H, Ar-H), 8.33 (d, 1H, Ar-H), 7.54 (d, 1H, Ar-H), 2.97 (t, 2H, benzylic -CH<sub>2</sub>), 1.25–1.38 (m, 26H, -CH<sub>2</sub>), 0.87 (t, 3H, -CH<sub>3</sub>).

#### 6.3.3.4 Synthesis of 4-pentadecylbenzene-1,3-diamine

Into a 100 mL three necked round bottom flask equipped with a dropping funnel and a reflux condenser were added 1,3-dinitro-4-pentadecylbenzene (1.89 g, 5 mmol), palladium-on-carbon (10 wt %) (0.04 g, 2 wt % based on dinitro compound) and absolute ethanol (20 mL). The reaction mixture was heated to 70 °C and hydrazine hydrate (4 mL, diluted with 5 mL of absolute ethanol) was added drop-wise over a period of 15 min and refluxed for 6 h. The reaction mixture was filtered while hot. The product precipitated on cooling and was isolated by filtration and recrystallised using ethanol.

Yield : 1.35 g (85 %).

MP: 75 °C. (Lit.: 75 °C).<sup>41</sup>

IR (CHCl<sub>3</sub>, cm<sup>-1</sup>): 3405, 3319 and 3209 (-N-H stretching), 1600 (aromatic C-C stretching).

<sup>1</sup>H NMR (CDCl<sub>3</sub>, δ ppm): 6.79 (d, 1H, Ar-H), 6.12 (d, 1H, Ar-H), 6.06 (d, 1H, Ar-H), 3.30 (broad s, 4H, -NH<sub>2</sub>) 2.38 (t, 2H, benzylic -CH<sub>2</sub>), 1.25 – 1.38 (m, 26H, -CH<sub>2</sub>), 0.88 (t, 3H, -CH<sub>3</sub>).

#### 6.3.3.5 Synthesis of 1,3-bis(maleimido)-4-pentadecylbenzene

Into a 100 mL two necked round bottom flask equipped with a magnetic stirring bar, a nitrogen inlet and a reflux condenser were placed 4-pentadecylbenzene-1,3-diamine (0.95 g, 3 mmol), maleic anhydride (0.59 g, 6 mmol) and acetone (10 mL). The reaction mixture was stirred at room temperature for 4 h and then refluxed for 1h. To the reaction mixture, were added acetic anhydride (4 mL) and sodium acetate (0.49 g, 6 mmol) and the reaction mixture was refluxed for 6 h. The reaction mixture was cooled to room temperature and poured into water (100 mL). The solid precipitated was washed with water (3 x 10 mL) followed by methanol (2 x 10 mL). The product was purified by column chromatography (Eluent: pet ether : ethyl acetate: 80:20, v/v).

Yield: 0.80 g (56 %).

MP: 96 - 98 °C

### 6.3.4 Synthesis of 1,1-bis[4-(4-maleimidophenoxy)phenyl] cyclohexane

#### 6.3.4.1 Synthesis of 1,1-bis-[4-(4-nitrophenoxy)phenyl] cyclohexane

Into a 500 mL two necked round bottom flask equipped with a nitrogen inlet, a reflux condenser and a magnetic stirring bar were placed 1,1-bis-(4-hydroxyphenyl)cyclohexane (10.7 g, 0.04 mol), 1-chloro-4-nitrobenzene (14.2 g, 0.09 mol), and DMF (200 mL). To the reaction mixture, potassium carbonate (16.6 g, 0.12 mol) was added and the mixture was refluxed for 12 h under nitrogen atmosphere. The reaction mixture was cooled to room temperature and poured into water (700 mL). The product obtained was washed with water (4 x 25 mL). The pale yellow solid was recrystallized using DMF.

Yield: 15.9 g (78 %).

MP: 133-134 °C (Lit.: 133.8 - 134.1 °C).<sup>42</sup>

IR (CHCl<sub>3</sub>, cm<sup>-1</sup>): 1515 (-NO<sub>2</sub> asymmetric stretching), 1345 (-NO<sub>2</sub> symmetric stretching), 1235 (C–O–C stretching).

<sup>1</sup>H-NMR (CDCl<sub>3</sub>, δ ppm): 8.20 (d, 4H, Ar-H, *ortho* to –NO<sub>2</sub>), 7.35 (d, 4H, Ar-H), 7.01 (d, 8H, Ar-H, *ortho* to –O– linkage), 2.26 - 2.33 (m, 4H, –CH<sub>2</sub>), 1.48 - 1.68 (m, 6H, –CH<sub>2</sub>).

#### 6.3.4.2 Synthesis of 1,1-bis-[4-(4-aminophenoxy)phenyl]cyclohexane.

Into a 250 mL three necked round bottom flask equipped with a magnetic stirring bar, a nitrogen inlet, a reflux condenser and a dropping funnel were added 1,1-bis[4-(4-nitrophenoxy)phenyl] cyclohexane (10.2 g, 0.02 mol), palladium-on-carbon (10 wt %) (0.204 g, 2 wt % based on dinitro compound) and absolute ethanol (100 mL). To the reaction mixture, hydrazine hydrate (80%) (6 mL diluted with 10 mL of ethanol) was added dropwise over a period of 30 min at reflux temperature under nitrogen atmosphere. After the completion of addition, the reaction mixture was refluxed for 4 h. The reaction mixture was filtered while hot to remove palladium-on-carbon and the filtrate was cooled to room temperature. The colorless needles obtained were isolated by filtration and recrystallized using ethanol.

Yield: 7.2 g (80 %),

MP: 154-155 °C. (Lit.: 155 - 155.5 °C).<sup>42</sup>

IR (CHCl<sub>3</sub>, cm<sup>-1</sup>): 3450, 3375 (-NH stretching), 1230 (C–O–C stretching).

<sup>1</sup>H-NMR (CDCl<sub>3</sub>, δ ppm): 7.15 (d, 4H, Ar-H), 7.35 (d, 4H, Ar-H), 6.84 (d, 8H, Ar-H, *ortho* to –O– linkage), 6.66 (d, 4H, Ar-H, *ortho* to –NH<sub>2</sub>), 3.35 (broad s, 4H, –NH<sub>2</sub>), 2.16 - 2.23 (m, 4H, –CH<sub>2</sub>), 1.40 - 1.60 (m, 6H, –CH<sub>2</sub>).

#### 6.3.4.3 Synthesis of 1,1-bis[4-(4-maleimidophenoxy)phenyl]cyclohexane.

Into a 100 mL three necked round bottom flask equipped with a magnetic stirring bar, a nitrogen inlet, a reflux condenser and a dropping funnel were placed 1,1-bis[4-(4-aminophenoxy) phenyl] cyclohexane (2.5 g, 5.6 mmol), maleic anhydride (1.18 g, 12 mmol) and acetone (20 mL). The reaction mixture was stirred at room temperature for 4 h and then refluxed for 1 h. To the reaction mixture were added acetic anhydride (5 mL) and sodium acetate (0.98 g, 12 mmol). The reaction mixture was refluxed for 6 h, cooled to room temperature and poured into water (150 mL). The product obtained was washed with water (3 x 10 mL) and then with methanol (2 x 10 mL). The crude product was purified by recrystallization using methanol.

Yield: 2.32 g (62 %).

MP: 91 - 92 °C.

#### 6.3.5 Synthesis of 4,4'-bis(maleimido)diphenylether

Into a 100 mL two necked round bottom flask equipped with a magnetic stirring bar, a nitrogen inlet and a reflux condenser were placed 4,4'- bis(amino)diphenylether (2.00 g, 10 mmol), maleic anhydride (1.96 g, 20 mmol) and acetone (25 mL). The reaction mixture was stirred at room temperature for 4 h and then refluxed for 1h. To the reaction mixture were added acetic anhydride (10 mL) and sodium acetate (1.64 g, 20 mmol) and the mixture was refluxed for 6 h. The reaction mixture was cooled to room temperature and poured into water (100 mL). The solid obtained was washed with water (4 x 10 mL) and then with methanol (2 x 10 mL).The product was recrystallized using methanol.

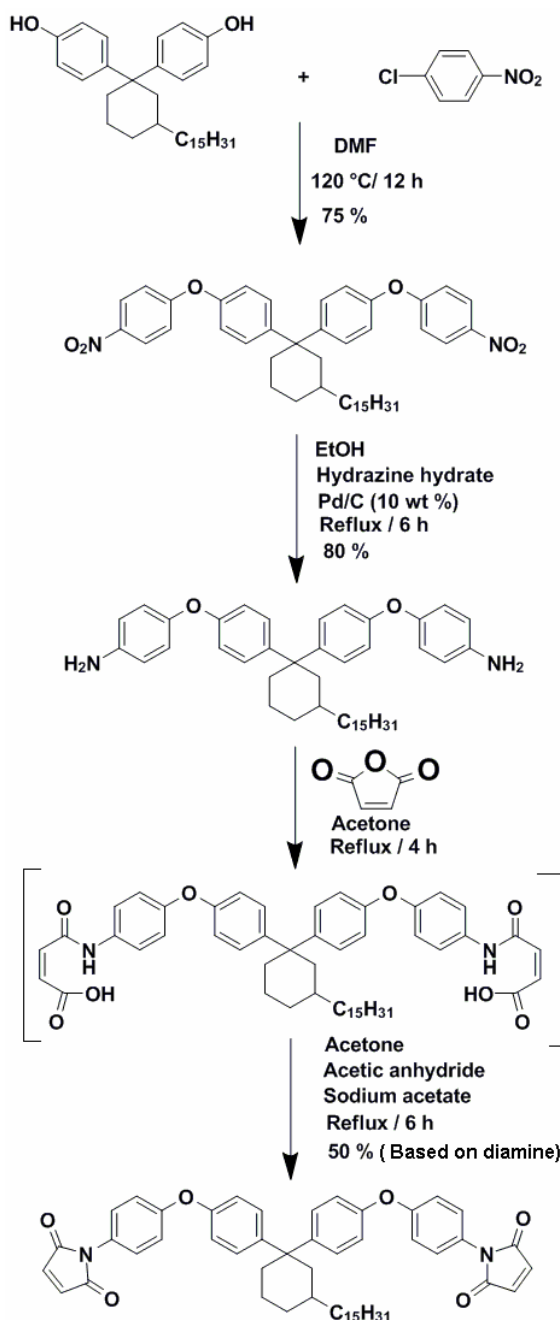
Yield: 2.1 g (60 %).

MP: 177 °C (Lit. 176 – 178 °C).<sup>26</sup>

### 6.4 Results and Discussion

#### 6.4.1 Synthesis of 1,1-bis[4-(4- maleimidophenoxy)phenyl]-3-pentadecyl cyclohexane

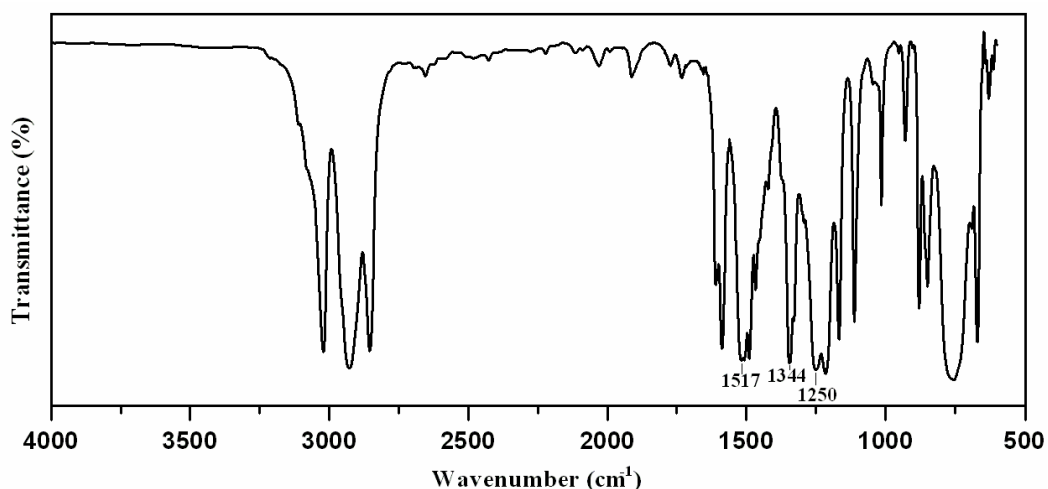
A new bismaleimide monomer, containing flexible pendent pentadecyl chain was synthesized (**Scheme 6.1**) starting from a bisphenol *viz*; 1,1-bis[4-hydroxyphenyl]-3-pentadecylcyclohexane [BPC15] which was in turn was synthesized starting from 3-pentadecylphenol as described in **chapter 3, section 3.3.1**).



### Scheme 6.1: Synthesis of 1,1-bis[4-(4-maleimidophenoxy)phenyl]-3-pentadecyl cyclohexane

Starting from bisphenol BPC15, a dinitro compound; 1, 1-bis-[4-(4-nitrophenoxy)phenyl]-3-pentadecylcyclohexane (DNBPC15) was synthesized as detailed in section 6.3.1.1. The product was characterized by FTIR, and NMR ( $^1\text{H}$  and  $^{13}\text{C}$ ) spectroscopy.

IR spectrum (**Figure 6.1**) of 1,1-bis-[4-(4-nitrophenoxy)phenyl]-3-pentadecyl cyclohexane displayed bands at 1517, 1344 and 1250  $\text{cm}^{-1}$  corresponding to  $-\text{NO}_2$  asymmetric,  $-\text{NO}_2$  symmetric and Ar-O-Ar stretchings, respectively.



**Figure 6.1:** IR spectrum of 1,1-bis-[4-(4-nitrophenoxy)phenyl]-3-pentadecyl cyclohexane

**Figure 6.2** represents  $^1\text{H-NMR}$  spectrum of DNBPC15 alongwith peak assignments. The peaks corresponding to the aromatic protons (a and a') *ortho* to nitro group appeared in the range 8.16 - 8.24 ppm. The protons labeled as d and d' observed as doublets at 7.24 and 7.43 ppm. The peaks due to aromatic protons b, b', c and c' were observed in the range 6.93 – 7.09 ppm. The methylene and methine protons of cyclohexyl ring and pentadecyl chain exhibited peaks in the range 1.25 – 2.70 ppm. A triplet observed at 0.87 ppm was assigned to the methyl protons of pentadecyl chain.

**Figure 6.3** represents  $^{13}\text{C-NMR}$  of DNBPC15. The peaks corresponding to the quaternary aromatic carbons were observed at 163.14, 163.31 (d, d'), 152.25, 152.43 (e, e'), 148.61, 142.56 (h, h') and 142.49, 142.60 (a, a') ppm. The aromatic carbons b, b' (*ortho* to nitro group) displayed peaks at 116.95 (axial phenyl ring) and 117.13 (equatorial phenyl ring) ppm while the aromatic carbons c, c' (*meta* to nitro group) showed peaks at 125.79 (axial phenyl ring) and 125.81 (equatorial phenyl ring) ppm. The peaks observed at 119.94, 120.19, 127.92 and 129.73 ppm could be assigned to the aromatic carbons labeled as f, f', g and g', respectively. The methylene and methine carbons of cyclohexyl ring and pentadecyl chain showed signals in the range 22.62 – 46.17 ppm. The terminal methyl carbon exhibited a peak at 14.06 ppm.

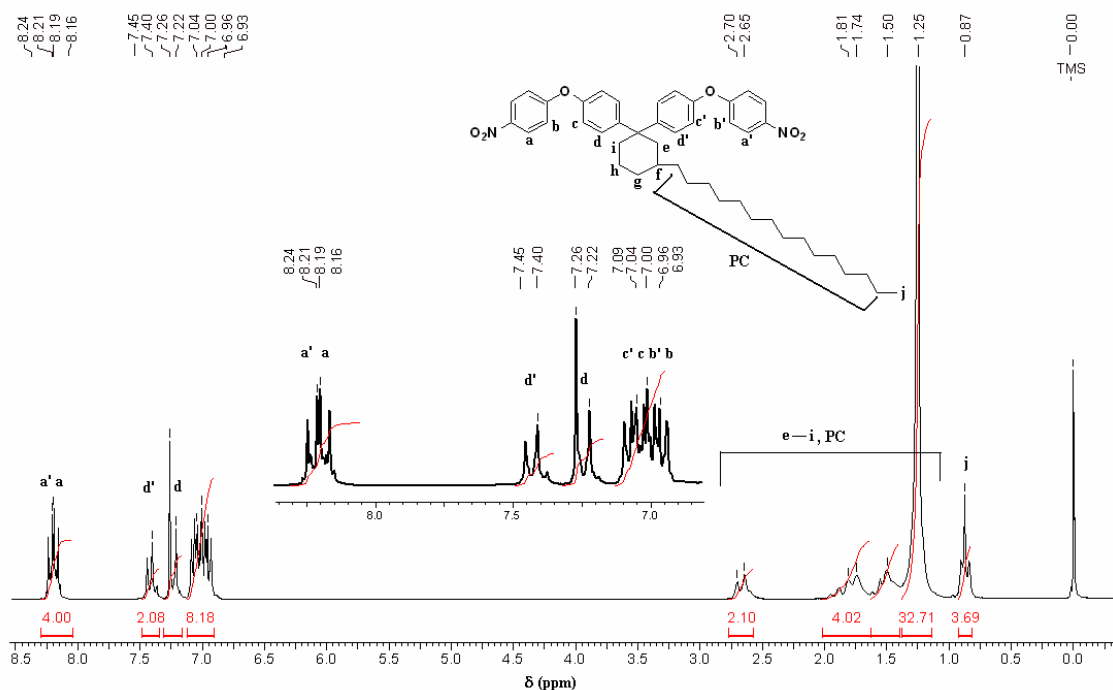


Figure 6.2:  $^1\text{H-NMR}$  spectrum of **1, 1-bis-[4-(4-nitrophenoxy) phenyl]-3-pentadecyl cyclohexane** ( $\text{CDCl}_3$ ).

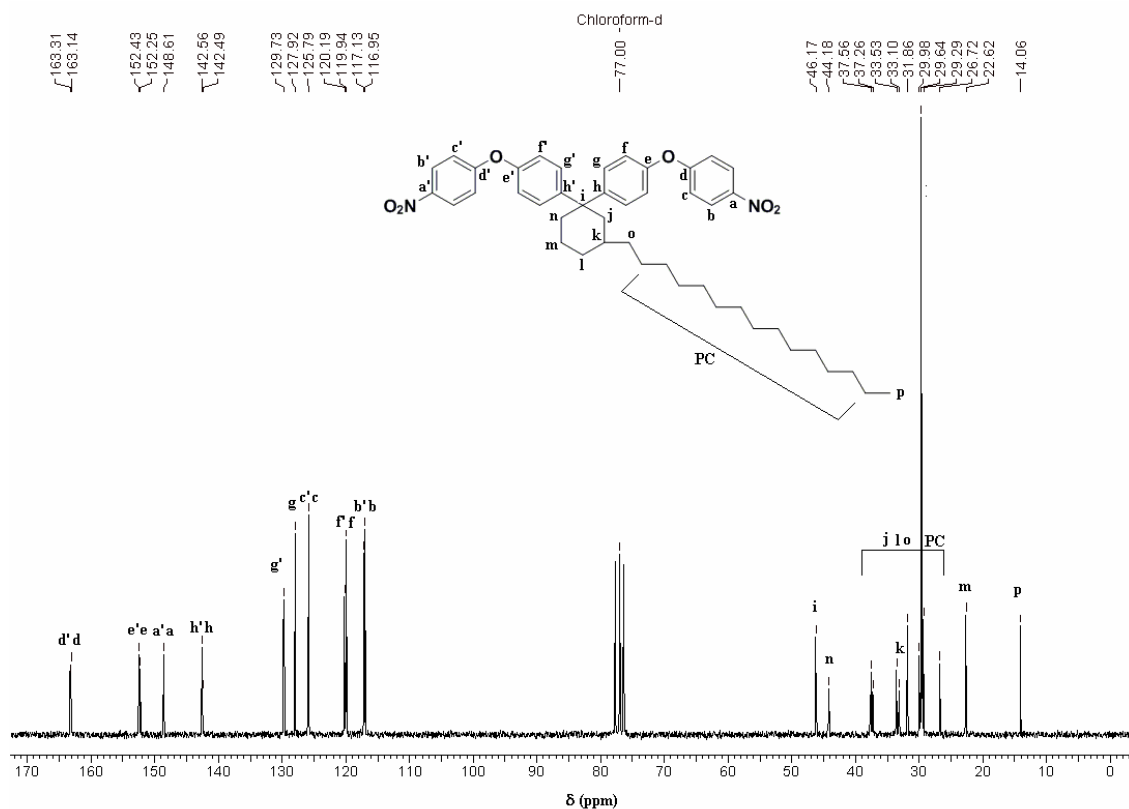
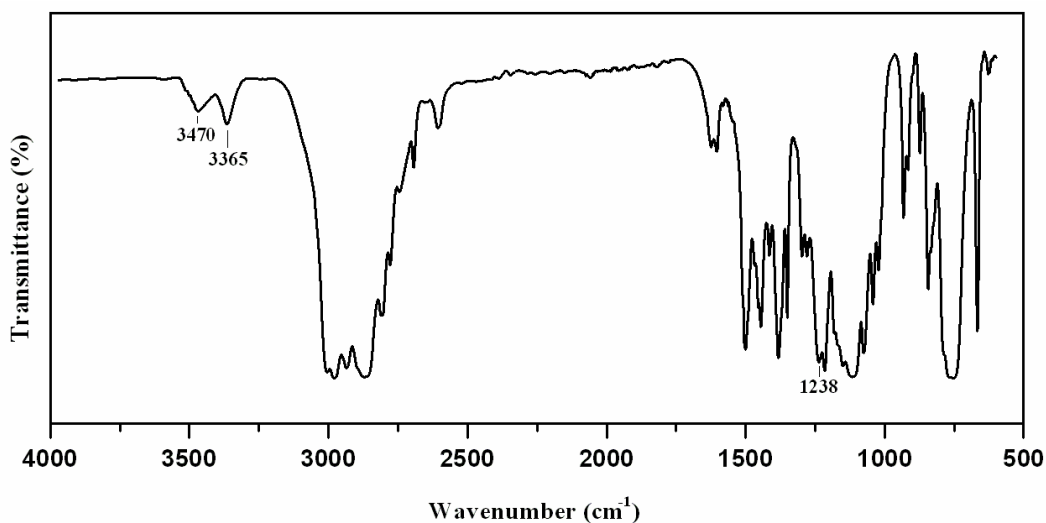


Figure 6.3:  $^{13}\text{C-NMR}$  spectrum of **1, 1-bis-[4-(4-nitrophenoxy) phenyl]-3-pentadecyl cyclohexane** ( $\text{CDCl}_3$ ).

DNBPC15 was converted into the corresponding diamine *viz*; 1, 1-bis-[4-(4-aminophenoxy) phenyl]-3-pentadecylcyclohexane (DABPC15) using hydrazine hydrate and palladium-on-carbon as a catalyst.

The diamine DABPC15 was characterized by FTIR,  $^1\text{H-NMR}$  and  $^{13}\text{C-NMR}$  spectroscopy.

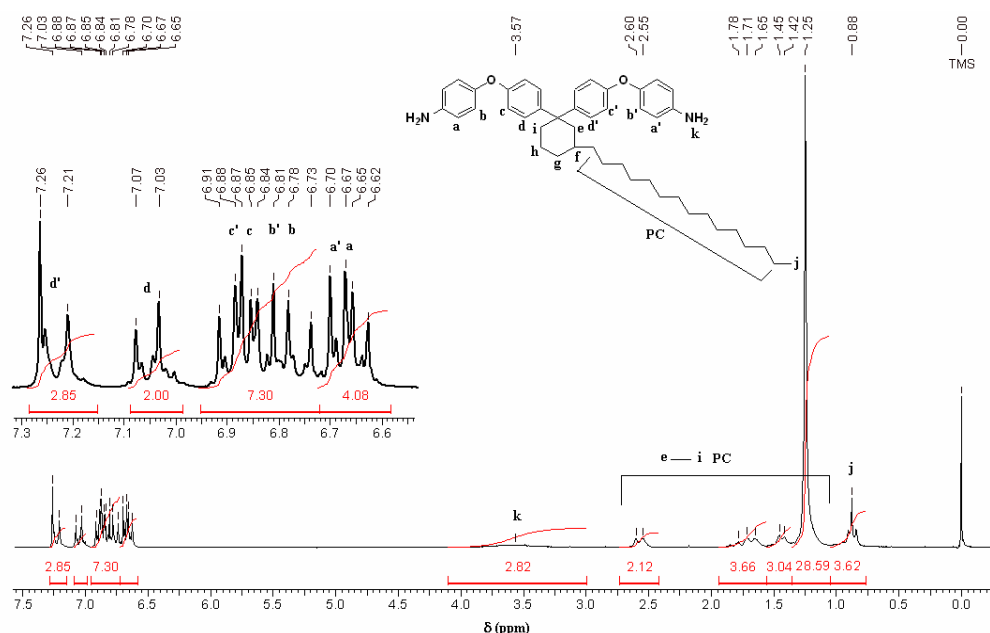
**Figure 6.4** represents IR spectrum of DABPC15. The peaks due to  $-\text{NH}$  stretchings were observed at 3470 and 3365  $\text{cm}^{-1}$ . The peak due to C-O-C stretching was observed at 1238  $\text{cm}^{-1}$ .



**Figure 6.4:** IR spectrum of 1,1-bis-[4-(4-aminophenoxy)phenyl]-3-pentadecyl cyclohexane.

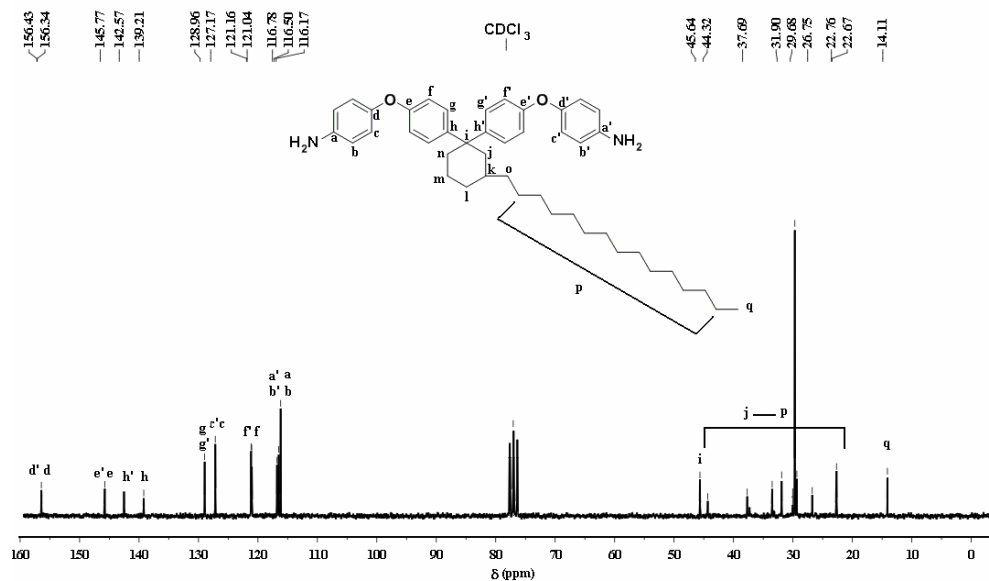
**Figure 6.5** illustrates  $^1\text{H-NMR}$  spectrum of DABPC15 alongwith peak assignments. The protons (a, a') *ortho* to amino group (which were observed in the range 8.16 – 8.24 ppm in the dinitro precursor DNBPC15) shifted upfield (6.62 – 6.70 ppm) due to the shielding effect of  $-\text{NH}_2$  group. The peaks observed in the range 6.73 – 6.91 ppm could be due to the aromatic protons labeled as b, b' and c, c'. The aromatic protons marked as d, d' exhibited doublet at 7.05 ppm (axial phenyl ring) and 7.23 ppm (equatorial phenyl ring). The broad singlet observed at 3.57 could be assigned to the protons (k) of amino group. The methylene and methine protons of cyclohexyl ring and pentadecyl chain were observed in the range 1.25 – 2.60 ppm. The protons of terminal methyl group displayed a triplet at 0.88 ppm.





**Figure 6.5:**  $^1\text{H-NMR}$  spectrum of 1,1-bis-[4-(4-aminophenoxy)phenyl]-3-pentadecyl cyclohexane ( $\text{CDCl}_3$ ).

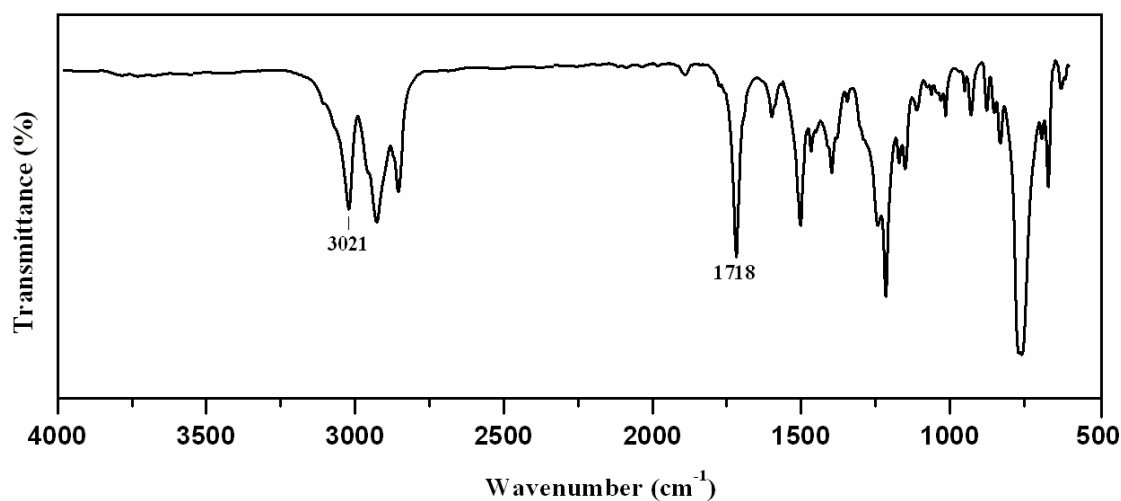
$^{13}\text{C-NMR}$  spectrum of DABPC15 is represented in **Figure 6.6** along with peak assignments. The quaternary aromatic carbon labeled as a', a (attached to amino group) displayed signals at 116.50 and 116.78 ppm. The peaks due to quaternary aromatic carbons marked as d', d, e', e and h' h were observed at 156.43, 156.54, 145.77, 142.77 and 139.21 ppm. The peaks due to methylene carbons and quaternary carbons of cyclohexyl ring and pentadecyl chain were observed in the range 22.67 – 45.64 ppm. The terminal methyl carbon of pentadecyl chain exhibited a signal at 14.11 ppm.



**Figure 6.6:**  $^{13}\text{C-NMR}$  spectrum of 1,1-bis-[4-(4-aminophenoxy)phenyl]-3-pentadecyl cyclohexane ( $\text{CDCl}_3$ ).

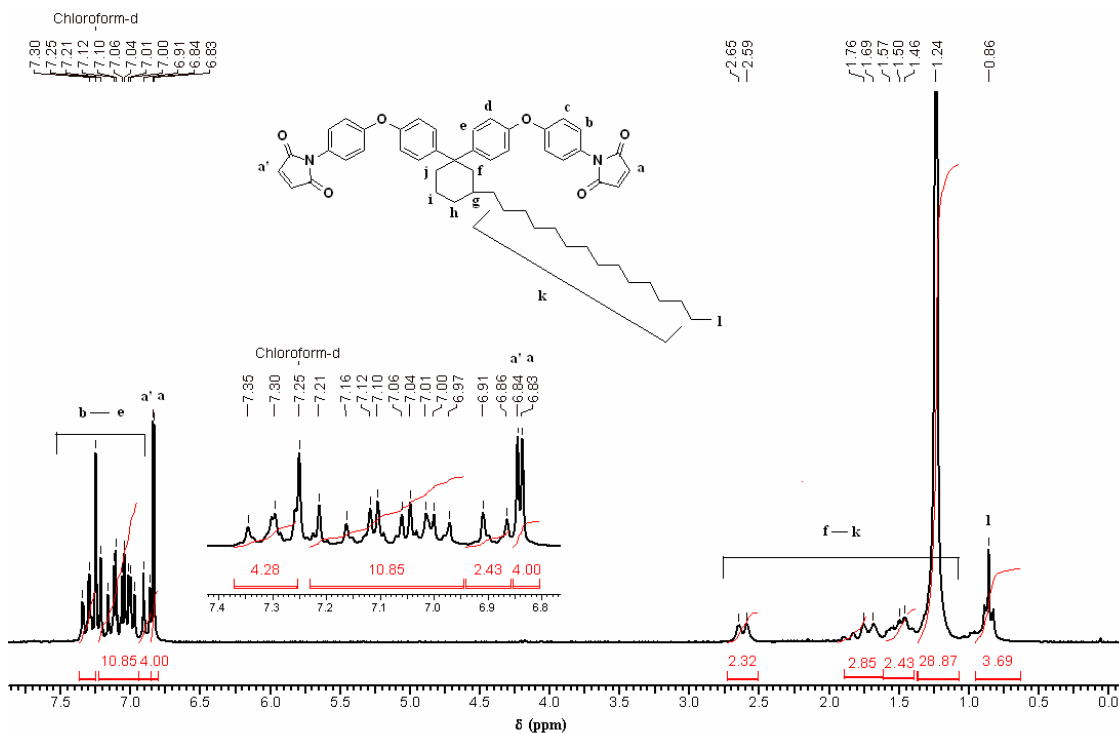
The diamine DABPC15 was converted into 1,1-bis[4-(4- maleimidophenoxy) phenyl]-3-pentadecyl cyclohexane (BPC15BMI) by following the procedure developed by Searl.<sup>43</sup> Initially, the diamine DABPC15 was reacted with maleic anhydride to give bismaleamic acid. The reaction was exothermic and proceeded with immediate precipitation of bismaleamic acid. The bismaleamic acid was cyclodehydrated *in situ* using acetic anhydride and sodium acetate to yield BPC15BMI.

IR spectrum (**Figure 6.7**) of BPC15BMI showed a strong absorption at  $1718\text{ cm}^{-1}$  due to C=O stretching of imide ring.



**Figure 6.7:** IR spectrum of 1,1-bis[4-(4- maleimidophenoxy)phenyl]-3-pentadecyl cyclohexane.

The bismaleimide was further characterized by NMR spectroscopy. **Figure 6.8** represents  $^1\text{H-NMR}$  spectrum of BPC15BMI. The peaks corresponding to the protons (a, a') of imide ring were observed at 6.83 and 6.84 ppm as two separate singlets due to the presence of two magnetically non-equivalent phenyl rings. Aromatic protons *ortho* to imide rings (labeled as b and b') exhibited signals in the range 7.30 – 7.35 ppm. The peaks corresponding to the protons marked as c, d, and e, were observed in the range 6.86 - 7.21 ppm. The methylene and methine protons of cyclohexyl ring and pentadecyl chain appeared in the range 1.24 – 2.65 ppm. The protons of terminal methyl group displayed a triplet at 0.86 ppm.



**Figure 6.8:**  $^1\text{H-NMR}$  spectrum of 1,1-bis[4-(4-maleimidophenoxy)phenyl]-3-pentadecyl cyclohexane ( $\text{CDCl}_3$ )

$^{13}\text{C-NMR}$  spectrum of BPC15BMI is reproduced in **Figure 6.9**. The peaks corresponding to  $\text{C}=\text{C}$  of imide ring were observed at 134.10 ppm while carbonyl carbon of imide ring showed a signal at 169.54 ppm. The quaternary aromatic carbons (c and c') attached to imide ring displayed peaks at 125.64 and 125.79 ppm while the peaks corresponding to the quaternary aromatic carbons attached to oxygen (marked as f, f' and g, g') were observed at 153.93, 154.12 and 156.92, 157.08 ppm, respectively. The peaks appeared in the region 118.75 – 119.02 ppm could be due to aromatic carbons e, e', h and h'. The peaks observed at 140.98 and 147.30 ppm were assigned to the aromatic carbons j (axial phenyl ring) and j' (equatorial phenyl ring) attached to cyclohexyl ring. The quaternary carbon 'k' (attached to two aromatic rings) showed a signal at 45.89 ppm. The peaks observed at 44.23, 37.63, 37.25, 33.16, 31.86, 30.03, 29.63, 29.29, 26.74 and 22.62 ppm could be assigned to methylene carbons l, n, o, p of cyclohexyl ring and of methylene carbons of pentadecyl chain.

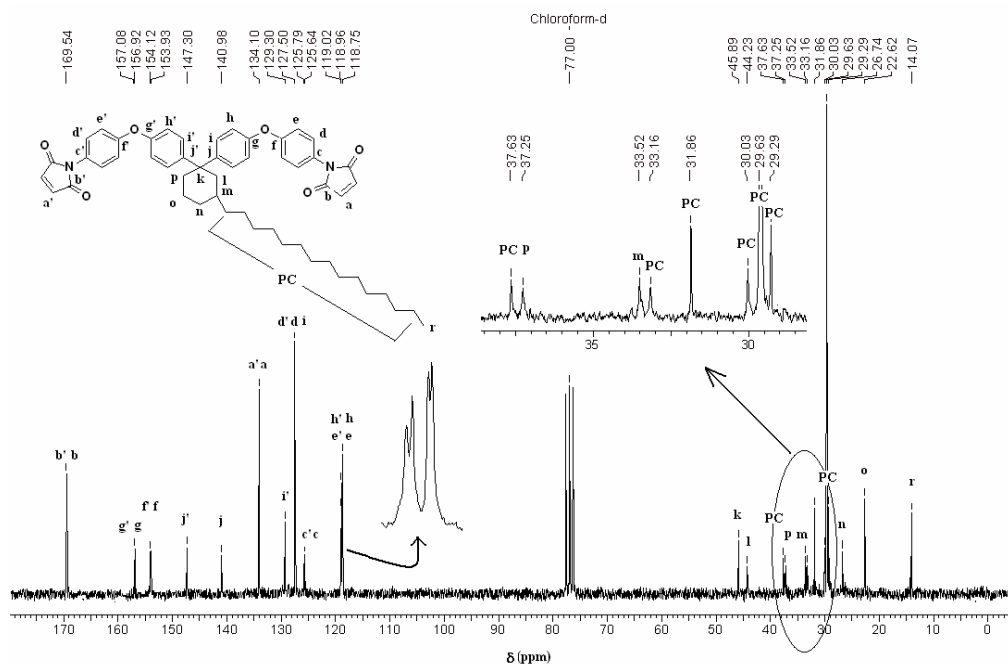


Figure 6.9: <sup>13</sup>C-NMR spectrum of 1,1-bis[4-(4-maleimidophenoxy)phenyl]-3-pentadecylcyclohexane (CDCl<sub>3</sub>)

The assignment of aromatic carbons was confirmed from <sup>13</sup>C-DEPT spectrum (Figure 6.11). Figure 6.10 illustrates overlay of aromatic region of <sup>13</sup>C and <sup>13</sup>C-DEPT spectrum. The peaks corresponding to aromatic quaternary carbons b, c, f, g, j, and k were absent in DEPT spectrum while peaks due to tertiary carbons (a, d, e, h, i and m) and methyl carbon ‘r’ appeared in negative phase.

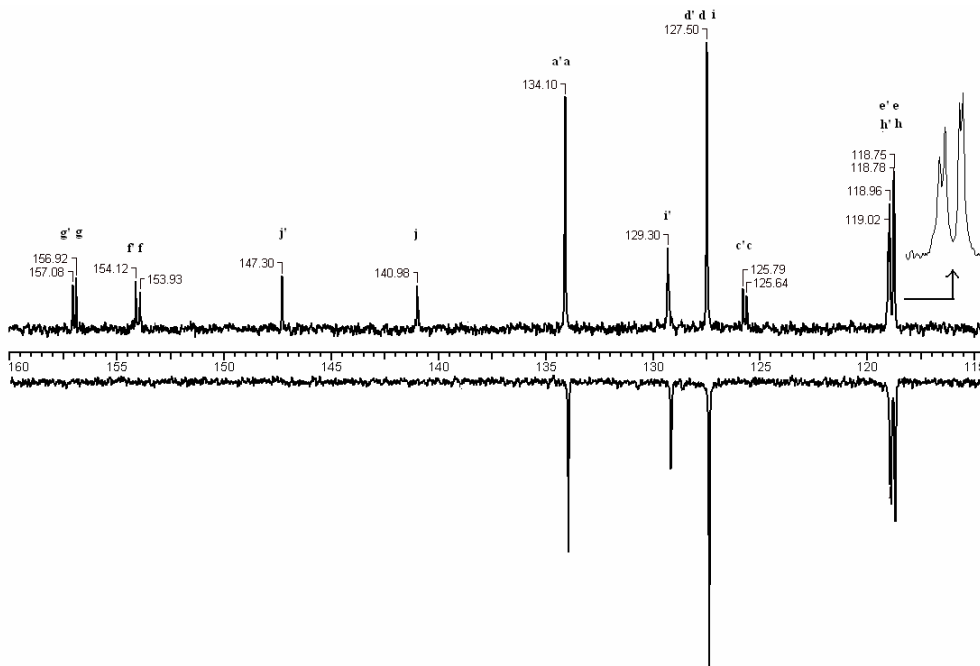
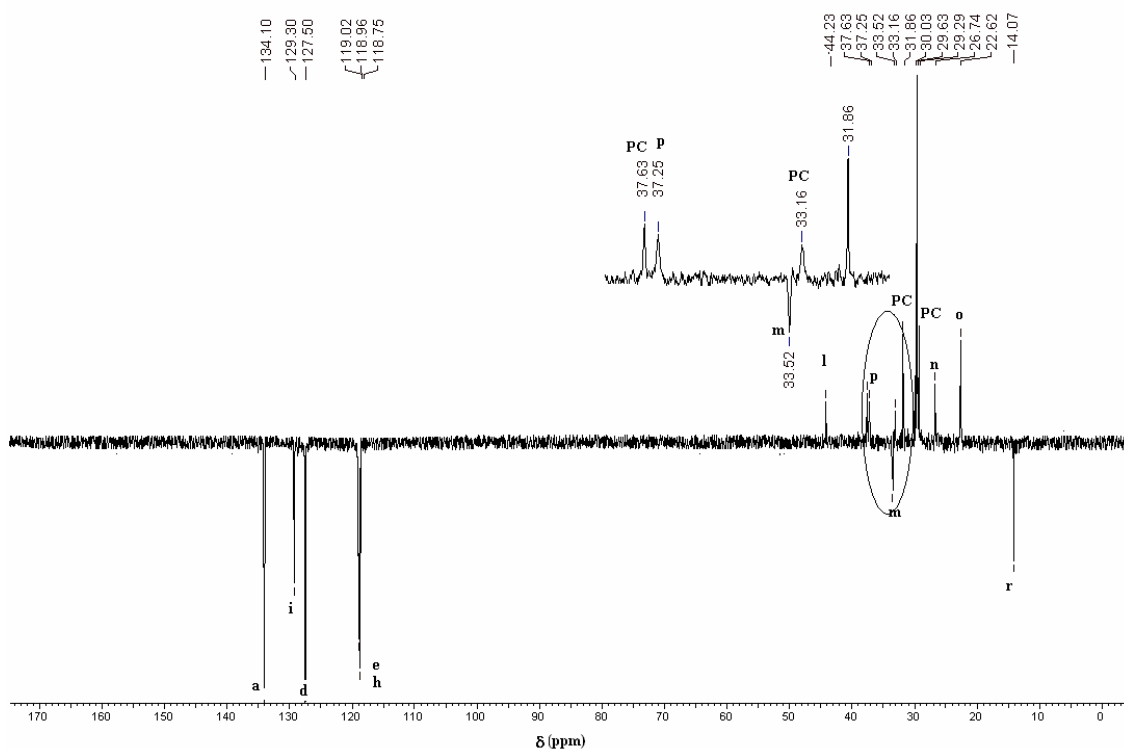


Figure 6.10: Stacked partial <sup>13</sup>C and <sup>13</sup>C-DEPT NMR spectrum of 1,1-bis[4-(4-maleimido phenoxy)phenyl]-3-pentadecylcyclohexane (Aromatic region)



**Figure 6.11:**  $^{13}\text{C}$ -DEPT NMR spectrum of 1,1-bis[4-(4-maleimidophenoxy) phenyl]-3-pentadecylcyclohexane ( $\text{CDCl}_3$ )

#### 6.4.2 Synthesis of 4,4'-bis(maleimido)-3-pentadecyldiphenylether

**Scheme 6.2** depicts route for the synthesis of 4, 4'-bis(maleimido)-3-pentadecyldiphenylether which comprised of four steps; diazotization, condensation, reduction and condensation. The diamino precursor *viz*; 4-(4'-aminophenoxy)-2-pentadecylbenzenamine was synthesized starting from 3-pentadecylphenol by following the procedure reported from our laboratory.<sup>44</sup>

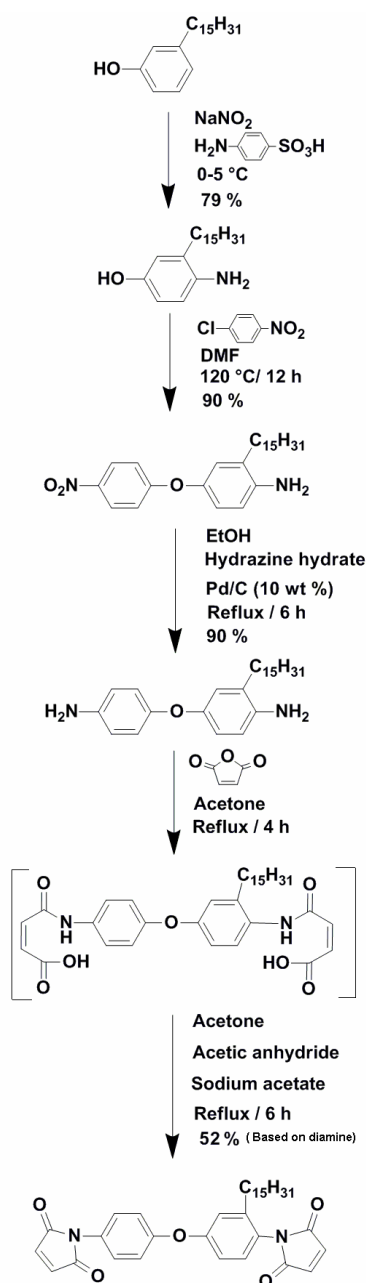
In the first step, 4-amino-3-pentadecyl phenol was obtained by reaction of 3-pentadecylphenol with diazotized sulfanilic acid and sodium dithionite. The structure of 4-amino-3-pentadecylphenol was confirmed by FTIR, and  $^1\text{H}$ -NMR spectroscopy (**section 6.3.2.1**).

The second step involved condensation of 4-amino-3-pentadecyl phenol with 1-chloro-4-nitrobenzene in the presence of potassium carbonate to yield 4-(4'-nitrophenoxy)-2-pentadecylbenzenamine. The product was purified by recrystallization using ethanol. The formation of 4-(4'-nitrophenoxy)-2-pentadecylbenzenamine was confirmed by FTIR, and  $^1\text{H}$ -NMR spectroscopy (**section 6.3.2.2**).

In the next step, the conversion of 4-(4'-nitrophenoxy)-2-pentadecylbenzenamine into 4-(4'-aminophenoxy)-2-pentadecylbenzenamine was accomplished using hydrazine hydrate

and palladium-on-carbon. The synthesized diamine was characterized by FTIR, and  $^1\text{H-NMR}$  spectroscopy (section 6.3.2.3).

The condensation of diamine with maleic anhydride resulted instantaneous precipitation yielding bismaleamic acid which was *in situ* cyclodehydrated using acetic anhydride and sodium acetate to obtain 4, 4'-bis(maleimido)-3-pentadecyldiphenylether (ODAC15BMI).



**Scheme 6.2 : Synthesis of 4,4'-bis(maleimido)-3-pentadecyldiphenylether**

The bismaleimide ODAC15 BMI was characterized by FT-IR and NMR spectroscopy.

**Figure 6.12** displays FTIR spectrum of ODAC15BMI. The absorption at  $1717\text{ cm}^{-1}$

corresponding to C=O stretching of imide ring was observed. The absorption due to C-O-C stretching was observed at  $1213\text{ cm}^{-1}$ .

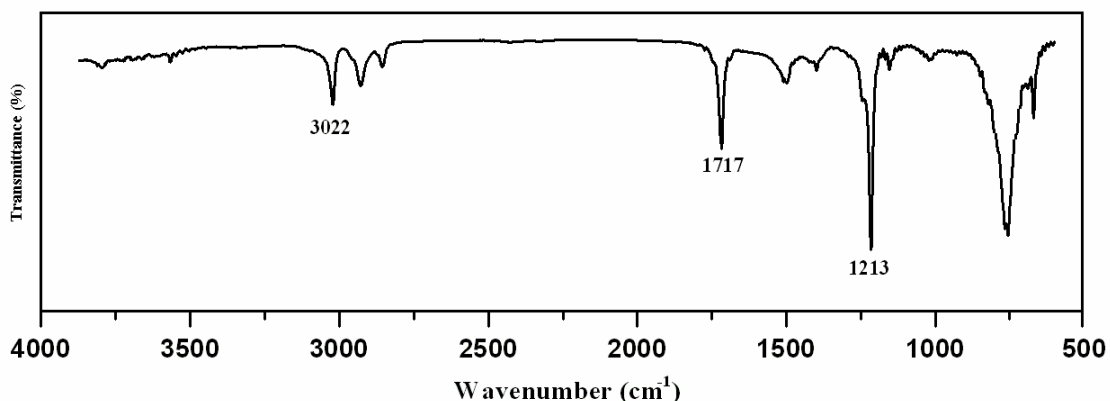


Figure 6.12: IR spectrum of 4,4'-bis(maleimido)-3-pentadecyldiphenylether

In  $^1\text{H-NMR}$  spectrum of ODAC15BMI (Figure 6.13), two singlets observed at 6.79 and 6.80 ppm could be due to the protons (a and a') of imide ring. The peaks corresponding to the proton 'f', *ortho* to imide ring appeared in the region 7.23 – 7.27 ppm while peaks due to aromatic protons labeled as b, c, and e were observed in the region 6.96 – 7.08 ppm. The aromatic proton marked as d, *meta* to imido group (from aromatic ring with pentadecyl chain) exhibited peaks in the region 6.82 – 6.87 ppm. A triplet at 2.30 ppm was assigned to benzylic –  $\text{CH}_2$  of pentadecyl group. The methylene protons  $\beta$  to aromatic ring exhibited a multiplet in the range 1.36 – 1.44 ppm while peaks due to remaining methylene protons of pentadecyl group appeared in the range 1.15 – 1.17 ppm. The methyl protons of pentadecyl chain displayed a triplet at 0.80 ppm.

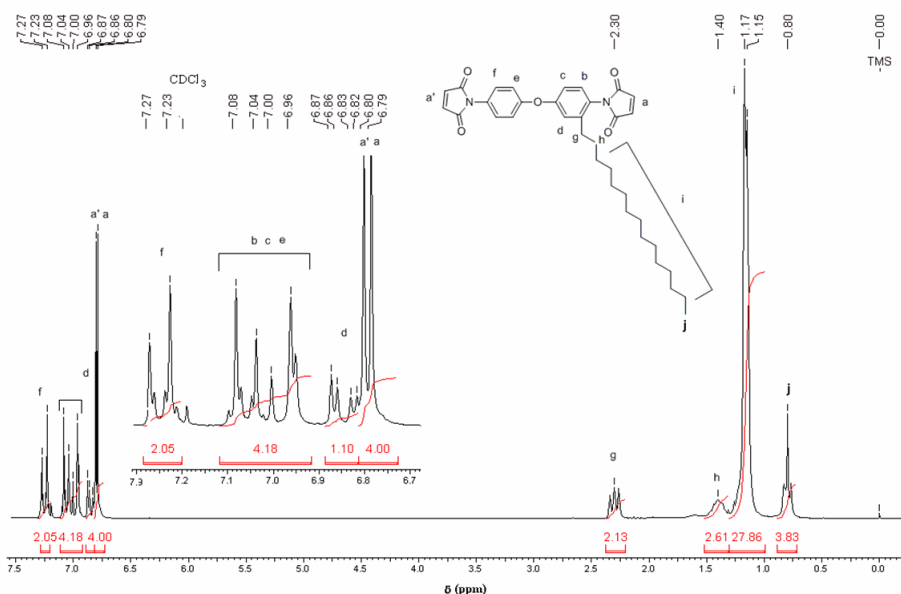
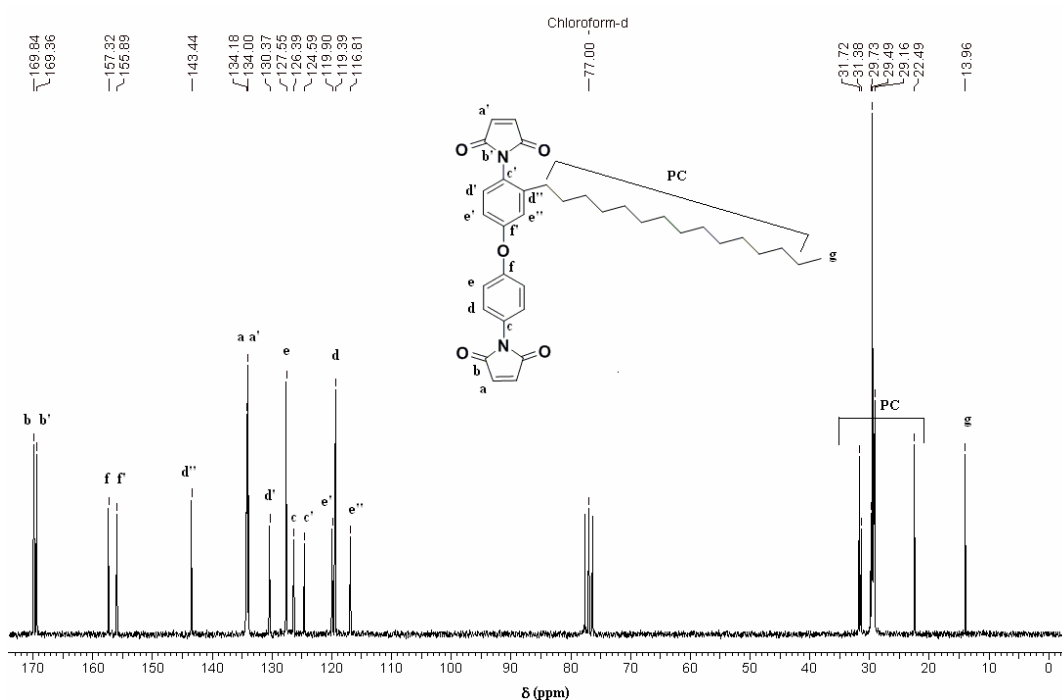


Figure 6.13:  $^1\text{H-NMR}$  spectrum of 4,4'-bis(maleimido)-3-pentadecyldiphenylether ( $\text{CDCl}_3$ )

$^{13}\text{C}$ -NMR spectrum of ODAC15BMI alongwith assignments is reproduced in **Figure 6.14** and is in accordance with the structure. The carbonyl carbons (b and b'), of imide ring exhibited peaks at 169.36 and 169.84 ppm while peaks due to olefinic carbon (a and a'), appeared at 134.0 and 134.18 ppm. The quaternary aromatic carbons c, c' (attached to imide ring) displayed peaks at 124.59 and 126.39 ppm while the carbons f, f' (attached to oxygen) exhibited signals at 155.89 and 157.32 ppm. The peak at 143.44 ppm could be assigned to the aromatic carbon marked as d''. The peaks observed at 130.37, 127.55, 119.90, 119.39 and 116.81 ppm could be assigned to aromatic carbons marked as d', e, e', d, and e'', respectively. The methylene carbons of pentadecyl chain displayed peaks in the region 22.49 – 31.72 ppm while the terminal methyl carbon exhibited a signal at 13.96 ppm.



**Figure 6.14:**  $^{13}\text{C}$ -NMR spectrum of 4,4'-bis(maleimido)-3-pentadecyldiphenylether ( $\text{CDCl}_3$ )

The assignments of aromatic carbons were further confirmed from  $^{13}\text{C}$ -DEPT spectrum. (**Figures 6.15 and 6.16**). The peaks corresponding to tertiary and methyl carbons appeared in negative phase, peaks due to methylene carbons appeared in positive phase while peaks corresponding to quaternary carbons were absent.



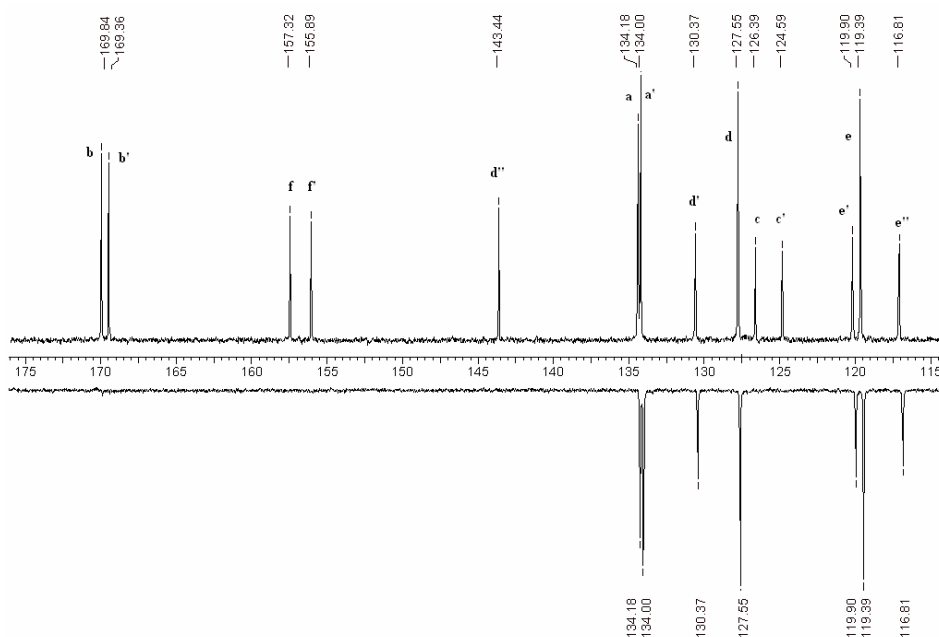


Figure 6.15: Stacked partial  $^{13}\text{C}$  and  $^{13}\text{C}$ -DEPT NMR spectrum of 4, 4'-bis(maleimido)-3-pentadecyldiphenylether (Aromatic region).

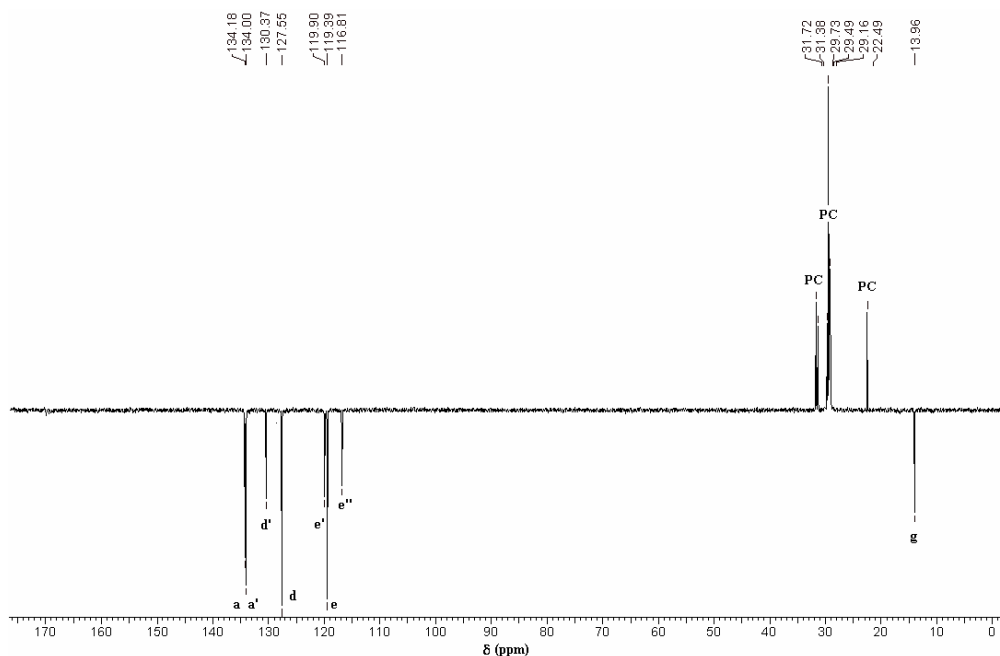


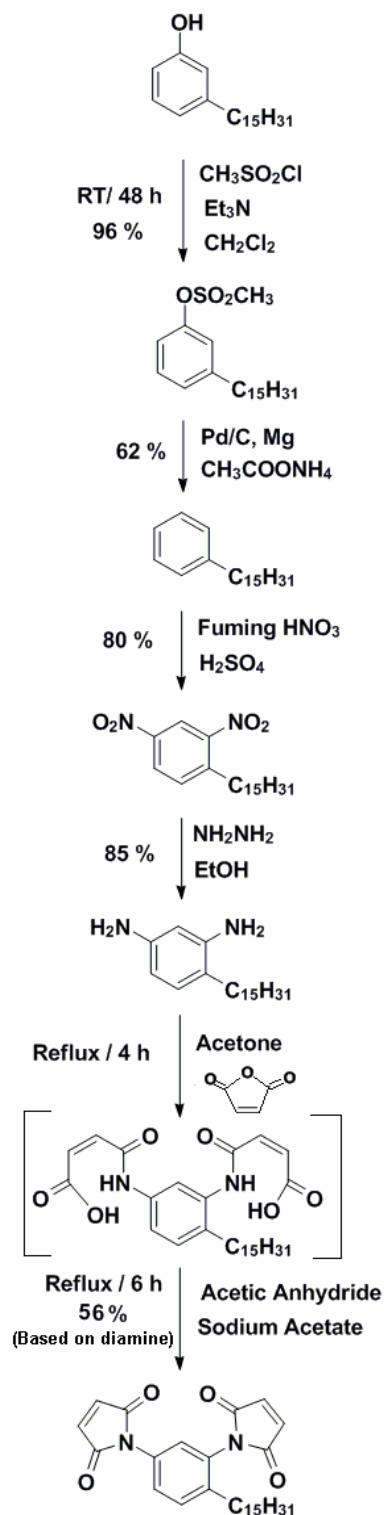
Figure 6.16:  $^{13}\text{C}$ -DEPT NMR spectrum of 4,4'-bis(maleimido)-3-pentadecyldiphenylether ( $\text{CDCl}_3$ )

### 6.4.3 Synthesis of 1,3-bis(maleimido)-4-pentadecylbenzene (MPDAC15BMI)

Starting from 3-pentadecyl phenol, a new bismaleimide monomer; 1,3-bis(maleimido)-4-pentadecylbenzene was synthesized in five steps. (**Scheme 6.3**).

In the first step, 3-pentadecylphenol was converted into 1-methyl sulfonyloxy-3-pentadecylbenzene using methansulfonyl chloride. The product was characterized by IR and <sup>1</sup>H-NMR spectroscopy. 1-Methyl sulfonyloxy-3-pentadecylbenzene was converted into pentadecyl benzene using ammonium acetate, palladium-on-carbon and magnesium metal as reported earlier from our laboratory.<sup>41</sup> The structure of pentadecylbenzene was confirmed by IR and <sup>1</sup>H-NMR spectroscopy (**section 6.3.3.2**). Pentadecylbenzene was nitrated to obtain 1,3-dinitro-4-pentadecylbenzene using the mixture of sulfuric acid and fuming nitric acid. The product was recrystallized using methanol. The reduction of 1,3-dinitro-4-pentadecyl benzene into 4-pentadecylbenzene-1,3-diamine was achieved using hydrazine hydrate and palladium-on-carbon as a catalyst. The synthesized diamine was characterized by IR, <sup>1</sup>H-NMR spectroscopy (**section 6.3.3.4**).

The conversion of diamine into bismaleimide; 1,3-bis(maleimido)-4-pentadecyl benzene (MPDAC15BMI) was accomplished by following the procedure developed by Searl.<sup>43</sup>



**Scheme 6.3: Synthesis of 1,3-bis(maleimido)-4-pentadecylbenzene**

The bismaleimide MPDAC15BMI was characterized by FT-IR and NMR spectroscopy. **Figure 6.17** represents IR spectrum of MPDAC15 BMI. The intense peak at  $1722\text{ cm}^{-1}$  due to C=O stretching of imide ring was observed.

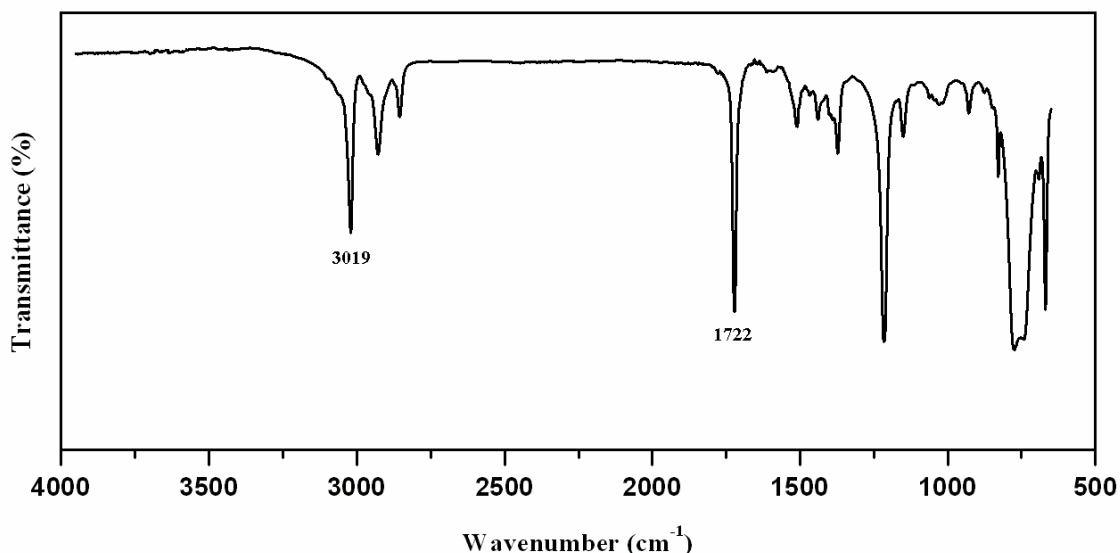


Figure 6.17: IR spectrum of 1,3-bis(maleimido)-4-pentadecylbenzene.

Figure 6.18 illustrates  $^1\text{H-NMR}$  spectrum of MPDAC15BMI alongwith peak assignments. The peak appeared at 7.44 ppm corresponds to aromatic protons marked as b and c. The aromatic proton labeled as d displayed a peak at 7.21 ppm. The protons of imide rings exhibited two separate singlets at 6.86 and 6.82 ppm. A triplet observed at 2.30 ppm could be due to benzylic  $-\text{CH}_2-$  of pentadecyl chain (marked as e). The peaks corresponding to methylene protons of pentadecyl chain appeared in the range 1.24 – 1.62 ppm. The protons of terminal methyl group of pentadecyl chain displayed a triplet at 0.86 ppm.

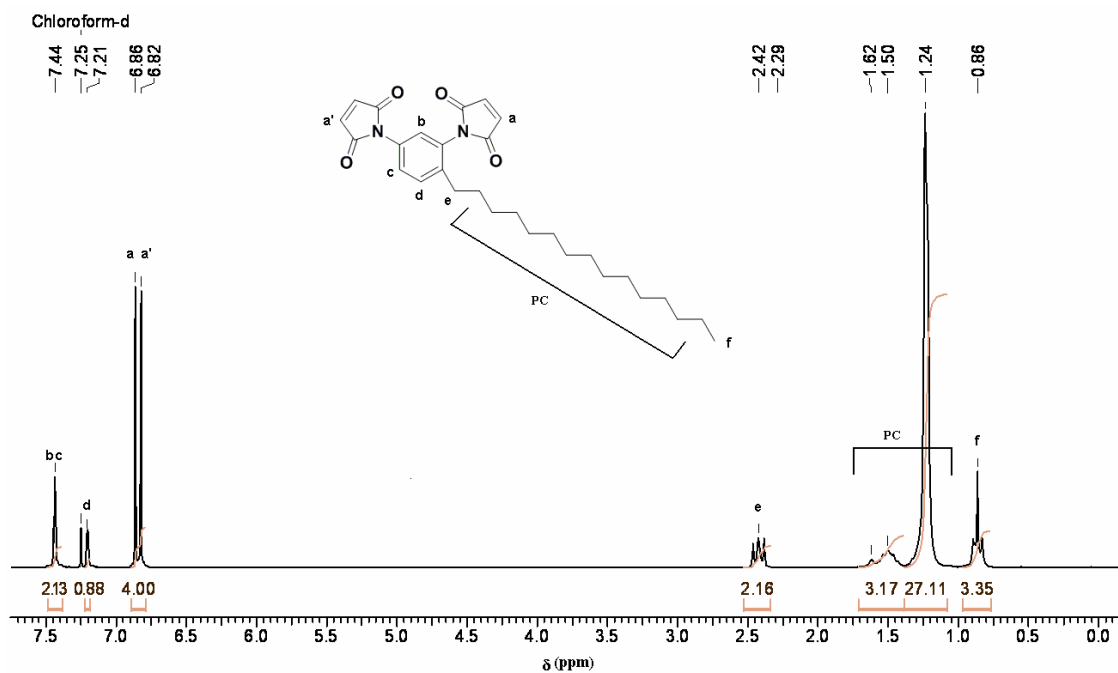
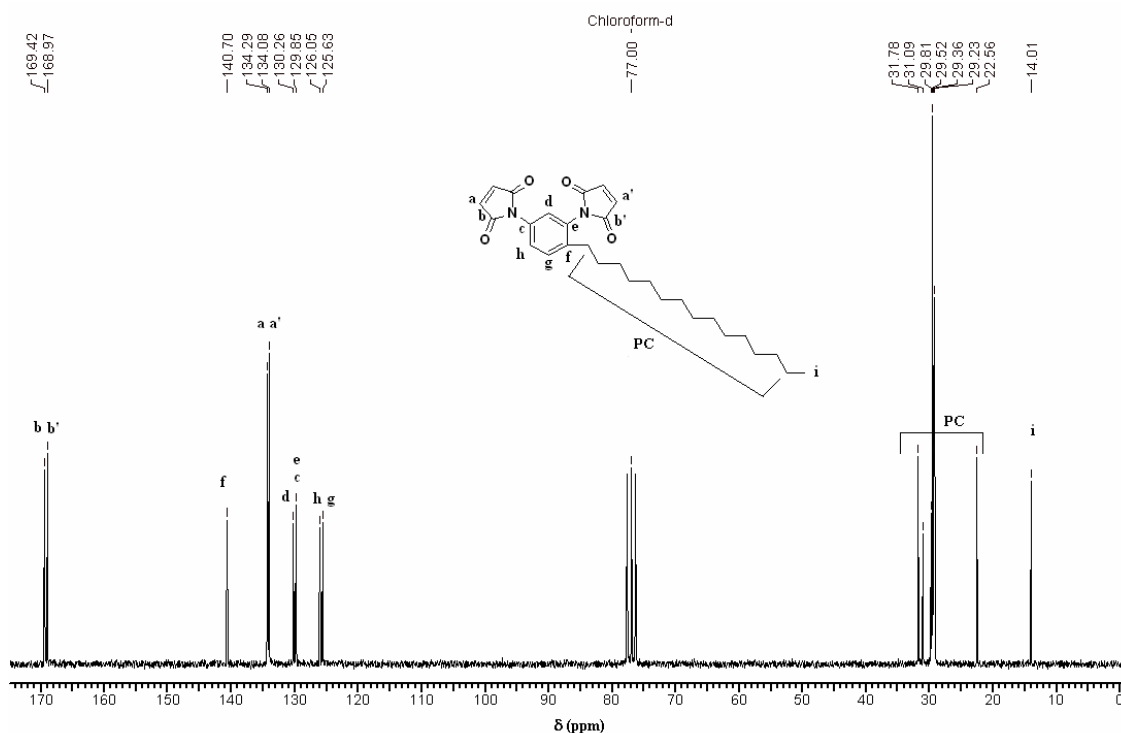


Figure 6.18:  $^1\text{H-NMR}$  spectrum of 1,3-bis(maleimido)-4-pentadecylbenzene ( $\text{CDCl}_3$ )

$^{13}\text{C}$ -NMR spectrum of MPDAC15BMI is represented in **Figure 6.19**. The peak corresponding to carbonyl carbon (marked as b, and b') of imide rings appeared at 168.97 and 169.42 ppm while olefinic carbons (a and a') of imide rings exhibited peaks at 134.08 and 134.29 ppm. The quaternary aromatic carbons (c and e) attached to imide rings showed a peak at 129.55 ppm while the signal corresponding to quaternary aromatic carbon (f) attached to pendent pentadecyl chain appeared at 140.70 ppm. The aromatic carbons labeled as h and g displayed signals at 126.05 and 125.63 ppm, respectively. The peaks appeared in the range 22.56 – 31.78 ppm were due to methylene carbons of pentadecyl chain. The peak observed at 14.01 ppm could be assigned to the terminal methyl carbon.

The peak assignments were supported by  $^{13}\text{C}$ -DEPT spectrum (**Figure 6.20 and 6.21**) wherein the signals corresponding to methylene carbons appeared in positive phase while the peaks due to tertiary and methyl carbons appeared in negative phase. The signals due to quaternary carbons were absent.



**Figure 6.19:**  $^{13}\text{C}$ -NMR spectrum of 1,3-bis(maleimido)-4-pentadecylbenzene (CDCl<sub>3</sub>)

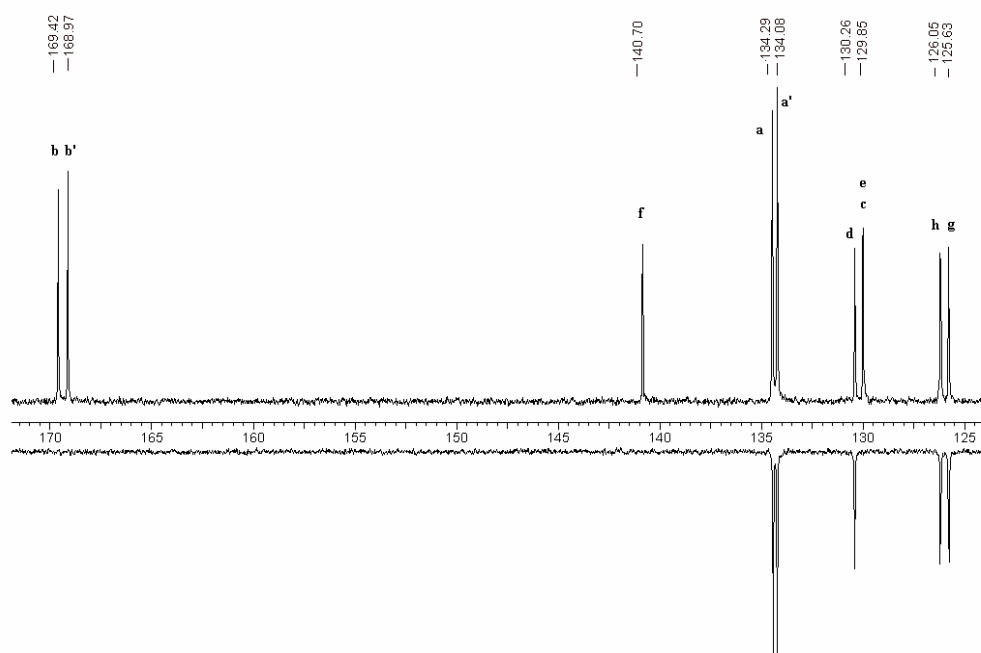


Figure 6.20: Stacked partial  $^{13}\text{C}$  and  $^{13}\text{C}$ -DEPT NMR spectrum of 1,3-bis(maleimido)-4-pentadecylbenzene (Aromatic region)

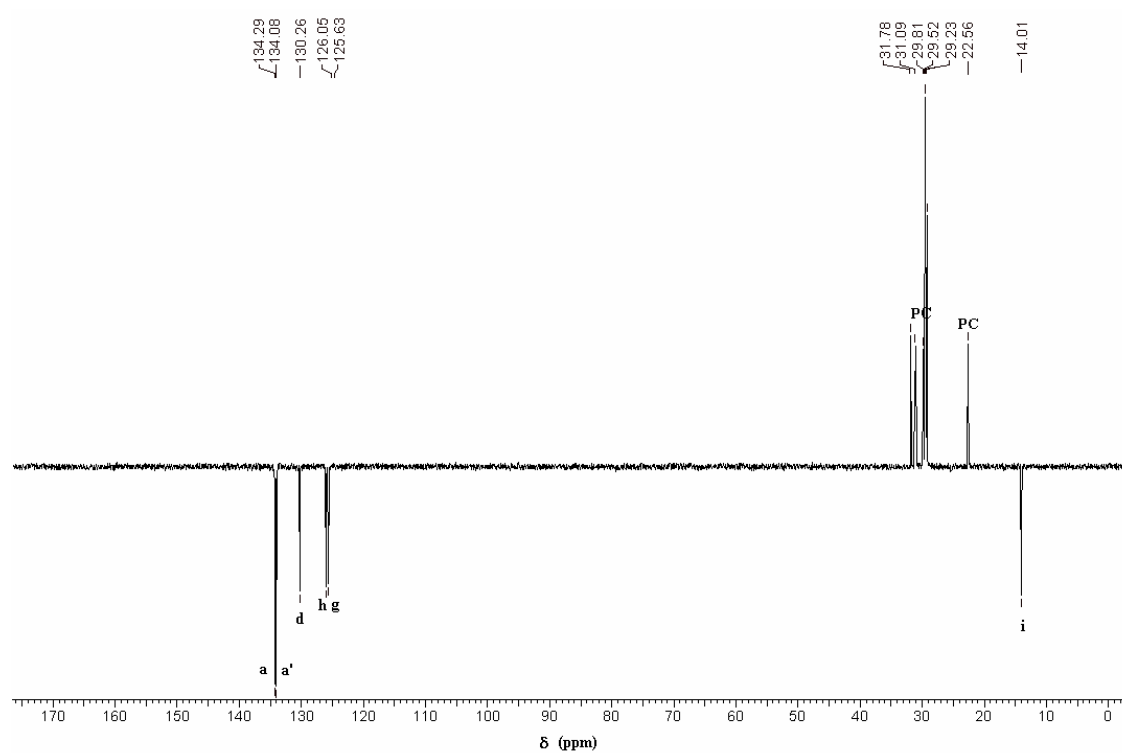
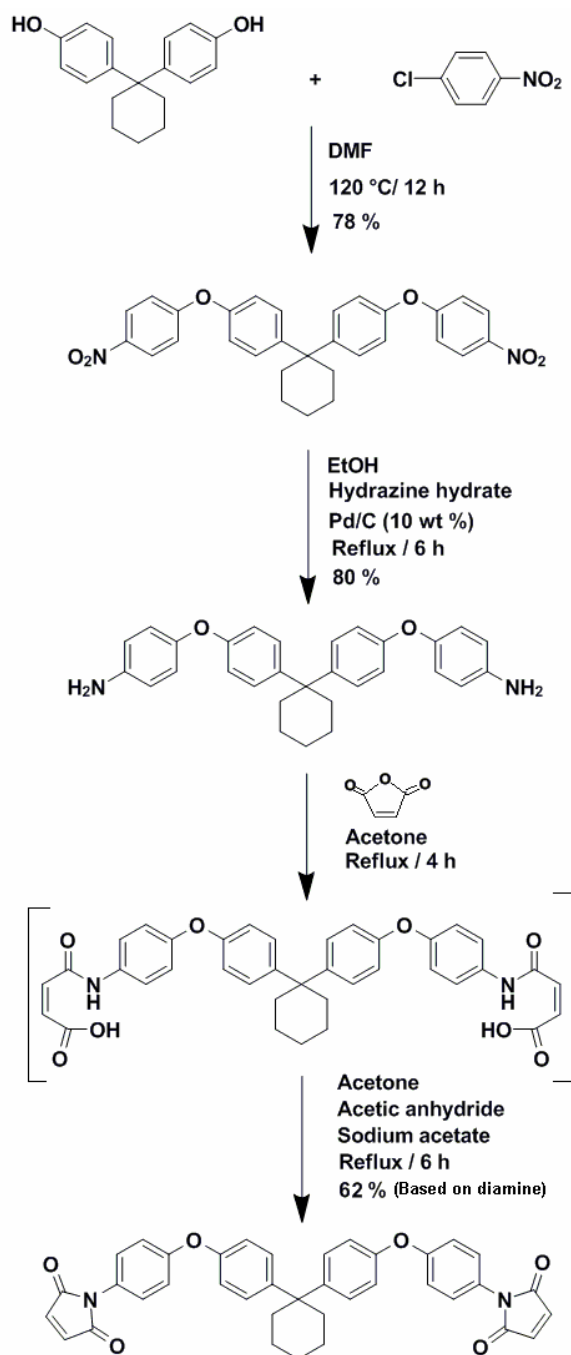


Figure 6.21:  $^{13}\text{C}$ -DEPT NMR spectrum of 1,3-bis(maleimido)-4-pentadecylbenzene ( $\text{CDCl}_3$ )

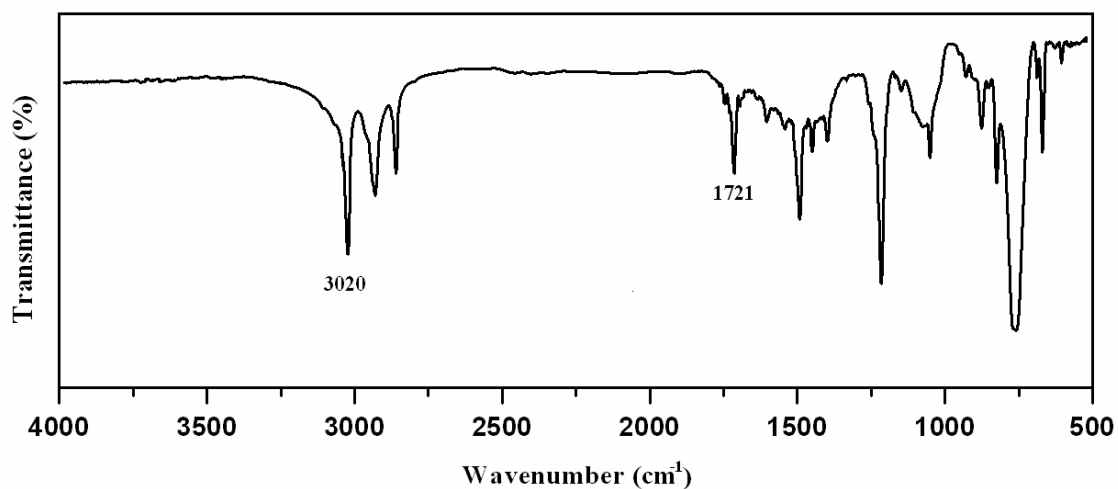
#### 6.4.4 Synthesis of 1,1-bis[4-(4- maleimidophenoxy)phenyl]cyclohexane

In order to study the structure-property relationship, a bismaleimide containing cyclohexyl ring was synthesized using 1,1-bis(4-hydroxyphenyl)cyclohexane (which was in turn synthesized from cyclohexanone as described in chapter 3, section 3.3.8) by performing etherification, reduction and condensation reactions as depicted in **Scheme 6.4**.



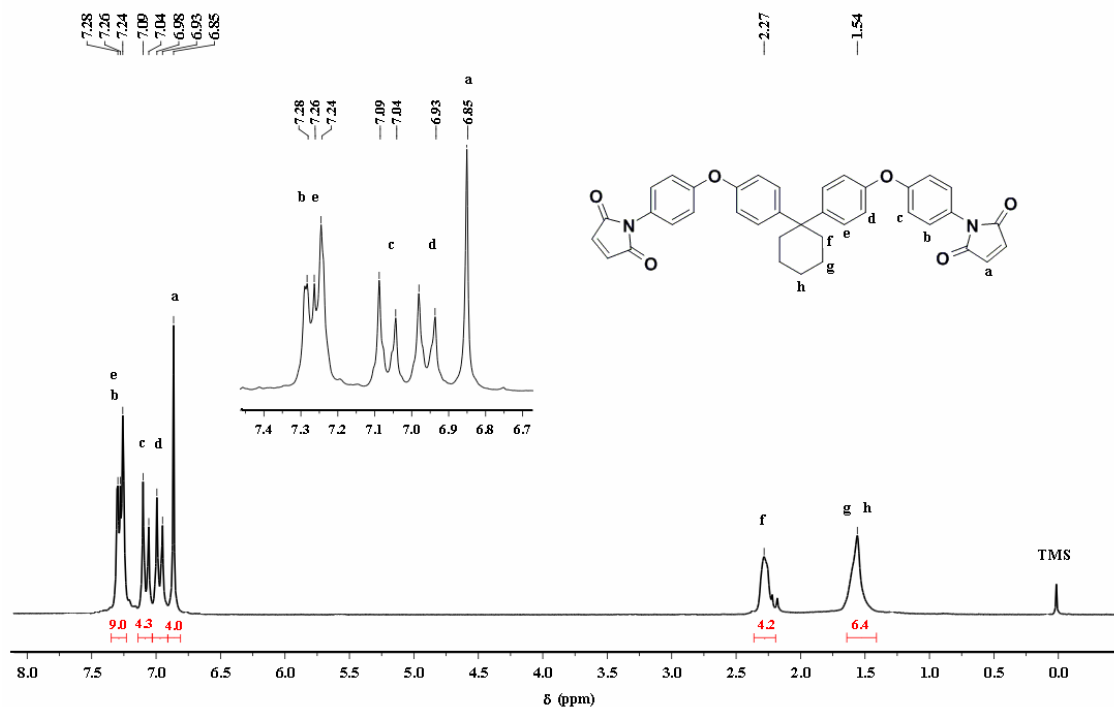
**Scheme 6.4 :** Synthesis of 1,1-bis[4-(4- maleimidophenoxy)phenyl]cyclohexane

The bismaleimide 1,1-bis[4-(4- maleimidophenoxy)phenyl]cyclohexane (BPZBMI) was characterized by FTIR, and NMR spectroscopy. IR spectrum (**Figure 6.22**) of BPZBMI showed a band at  $1721\text{ cm}^{-1}$  corresponding to the stretching of C=O group (imide ring).



**Figure 6.22:** IR spectrum of 1,1-bis[4-(4- maleimidophenoxy)phenyl]cyclohexane

**Figures 6.23, 6.24, and 6.25**, respectively represent  $^1\text{H-NMR}$ ,  $^{13}\text{C-NMR}$  and  $^{13}\text{C}$  (DEPT) NMR spectra alongwith peak assignmetns. All the assignments are in good agreement with the structure.



**Figure 6.23:**  $^1\text{H-NMR}$  spectrum of 1,1-bis[4-(4- maleimidophenoxy)phenyl]cyclohexane ( $\text{CDCl}_3$ )



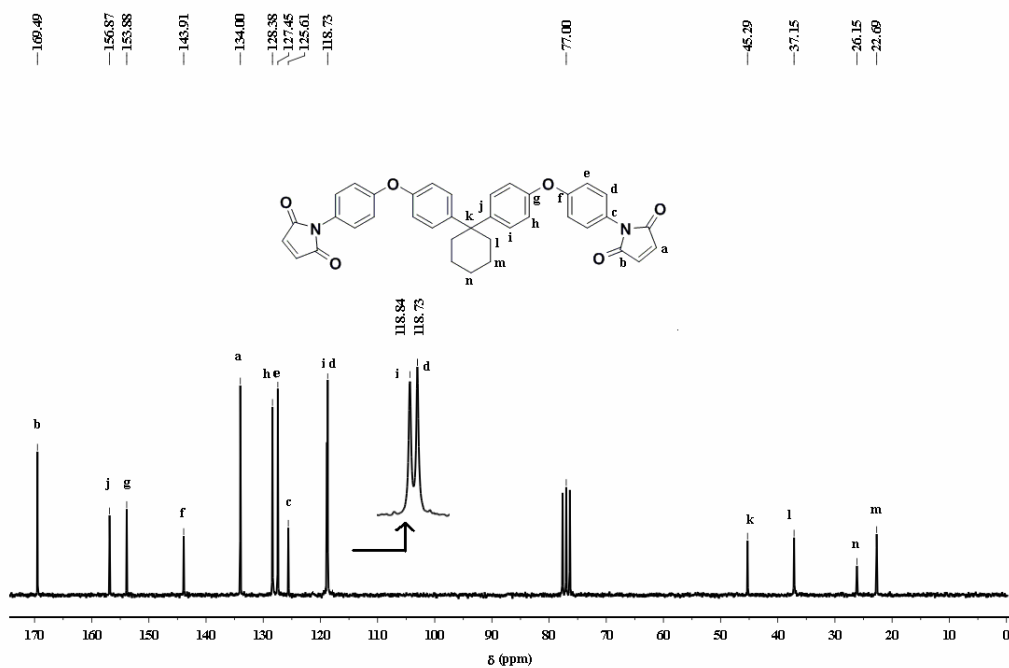


Figure 6.24:  $^{13}\text{C}$ -NMR spectrum of 1,1-bis[4-(4-maleimidophenoxy)phenyl]cyclohexane ( $\text{CDCl}_3$ )

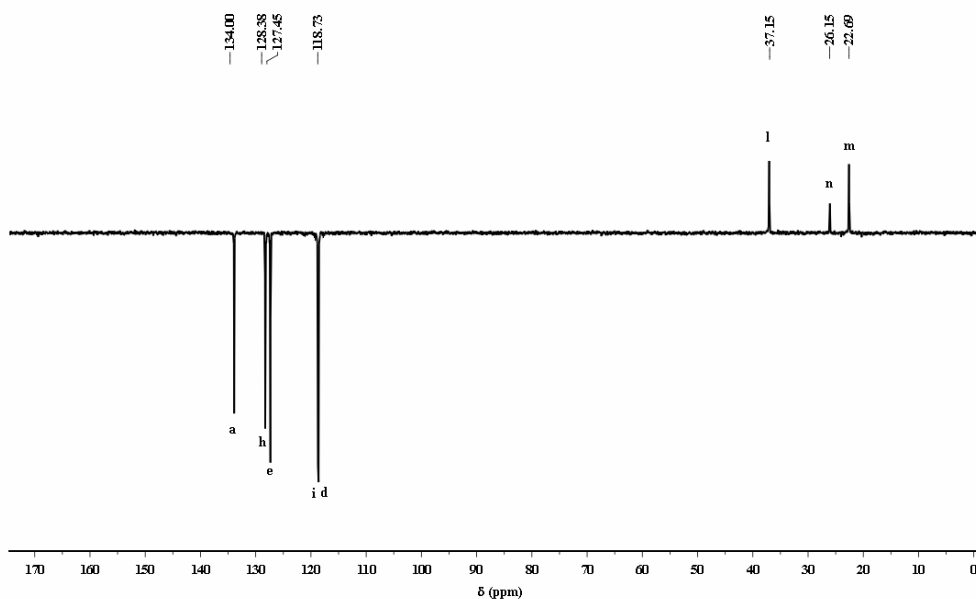
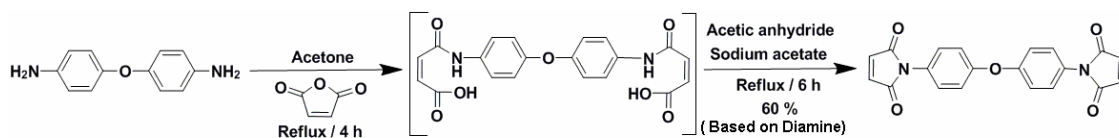


Figure 6.25:  $^{13}\text{C}$ -DEPT NMR spectrum of 1,1-bis[4-(4-maleimidophenoxy)phenyl]cyclohexane ( $\text{CDCl}_3$ ).

#### 6.4.5 Synthesis of 4, 4'-bis(maleimido)diphenylether

Starting from commercially available 4, 4'-bis(amino)diphenylether, the bismaleimide *viz.*; 4, 4'-bis(maleimido) diphenylether (ODABMI) was synthesized in order to understand the effect of pentadecyl chain on curing and thermal properties of cured network of ODAC15BMI. (Scheme 6.5).



Scheme 6.5 : Synthesis of 4, 4'-bis(maleimido)diphenylether

The bismaleimide ODABMI was characterized by FTIR, and NMR spectroscopy (Figure 6. 26 - 6. 28). The spectroscopic data was in good agreement with the reported data<sup>23,30</sup>.

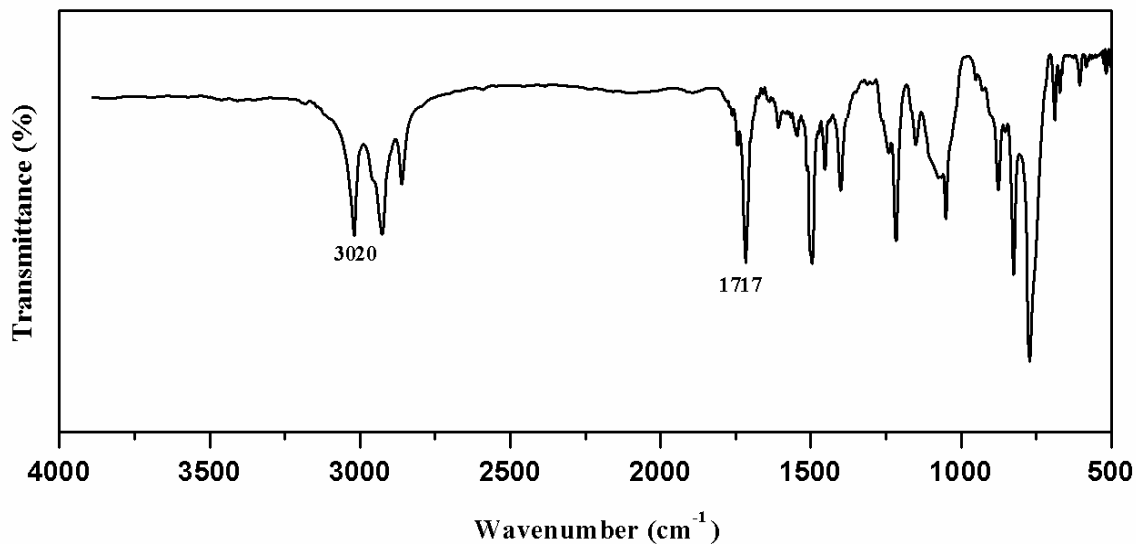
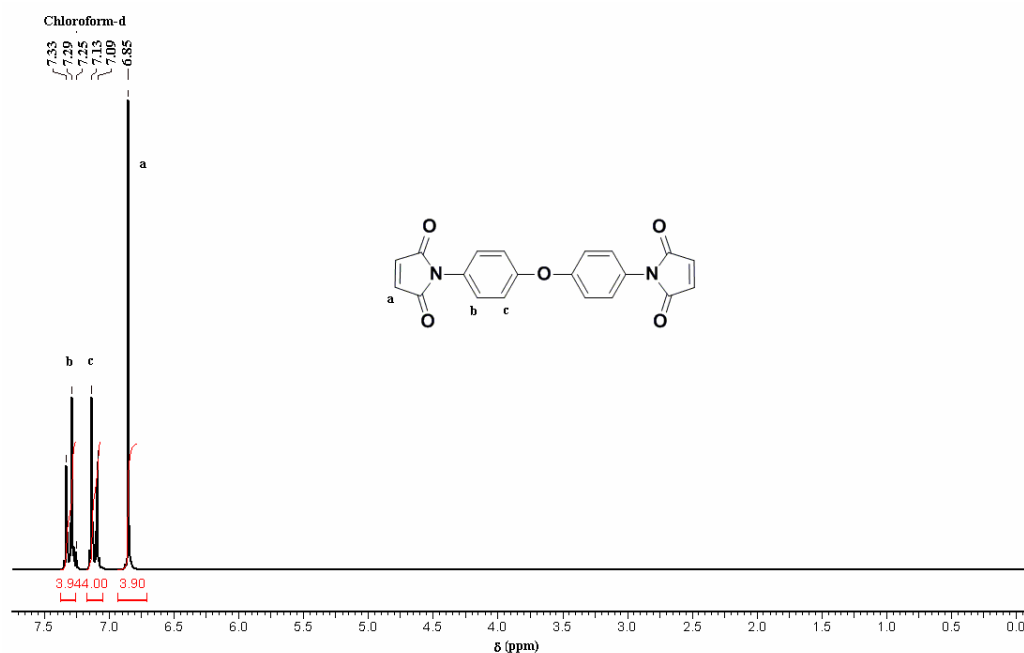


Figure 6.26: IR spectrum of 4, 4'-bis(maleimido)diphenylether

Figure 6.27: <sup>1</sup>H-NMR spectrum of 4, 4'-bis(maleimido)diphenylether (CDCl<sub>3</sub>)

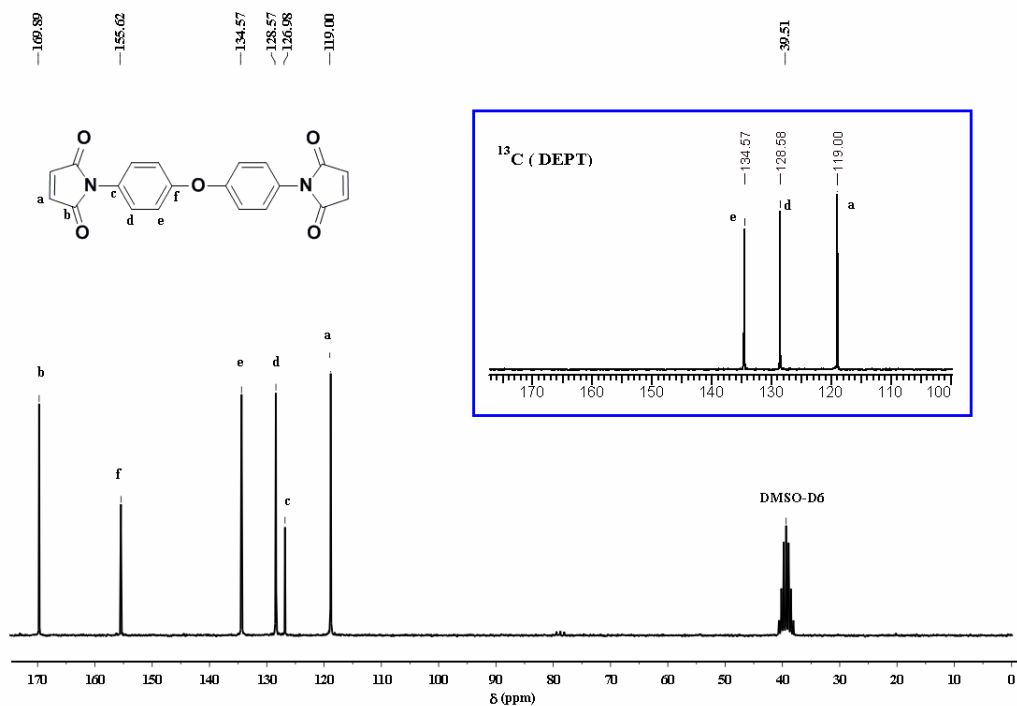


Figure 6.28:  $^{13}\text{C}$ -NMR spectrum of 4, 4'-bis(maleimido)diphenylether (DMSO- $d_6$ )

#### 6.4.6 Solubility of bismaleimides

The solubility of synthesized BMIs was tested in various organic solvents *viz*; chloroform, dichloromethane, DMSO, and DMF at 5 wt % concentration and the results are collected in Table 6.3.

Table 6.3 : Solubility of bismaleimide monomers at 5 wt % concentration.

Sr. No.	Monomer	Monomer Structure	Solvents			
			$\text{CHCl}_3$	$\text{CH}_2\text{Cl}_2$	DMSO	DMF
1	ODABMI		-	-	+	+
2	ODAC15BMI		+	+	+	+
3	BPZBMI		+	+	+	+
4	BPC15BMI		+	+	+	+
5	MPDAC15BMI		+	+	+	+

+: Soluble at room temperature.

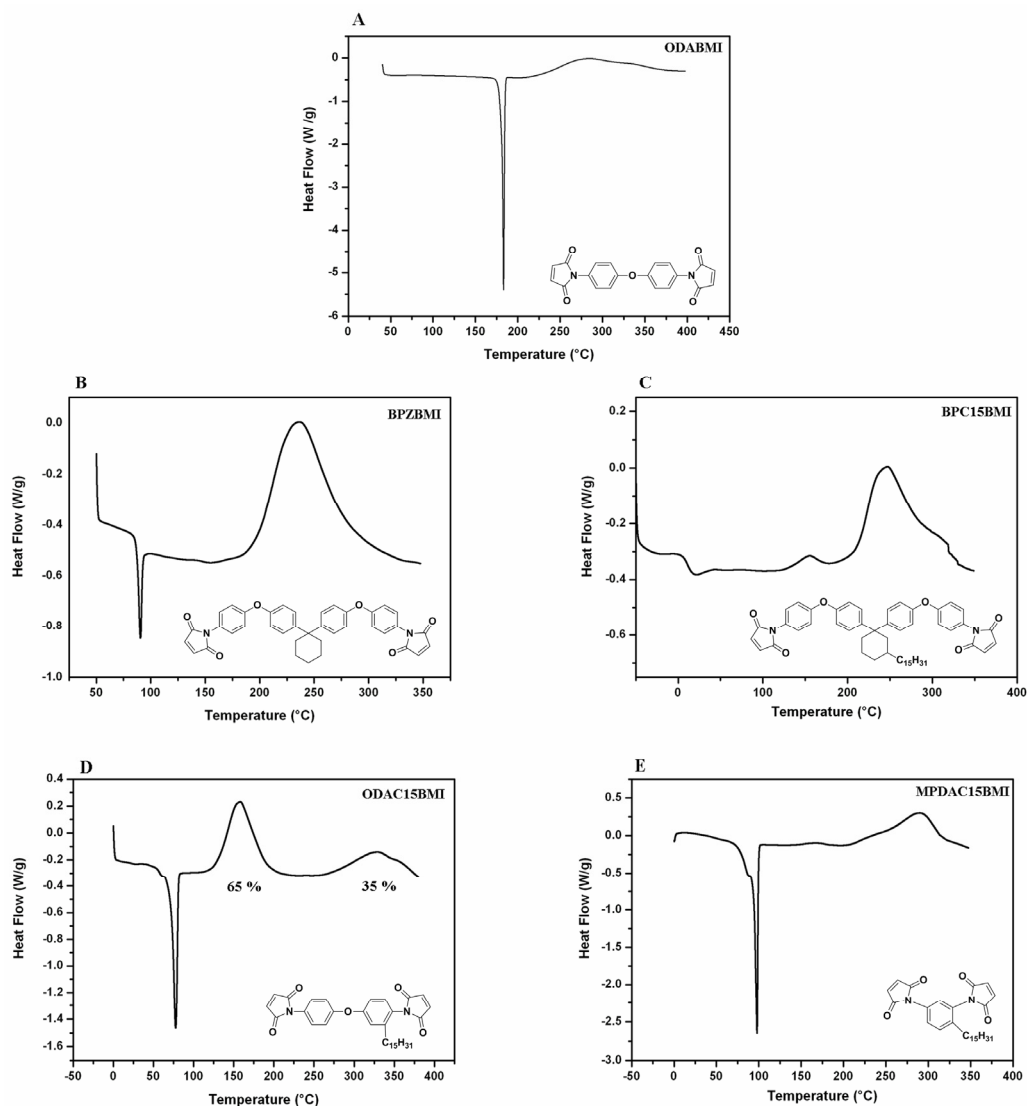
- : Insoluble at room temperature.

As compared to ODABMI, the pendent flexible pentadecyl chain containing analogue ODAC15BMI was observed to be soluble in common organic solvents such as chloroform, dichloromethane, etc., at 5 wt % concentration. Other BMI monomers *viz*; BPC15BMI, MPDAC15BMI were also soluble in chloroform, dichloromethane, etc.,. The presence of C15 alkyl chain interfered the tight packing of molecules as well as provided additional ‘handle’ for interaction with solvents.

#### 6.4.7 Kinetics of curing

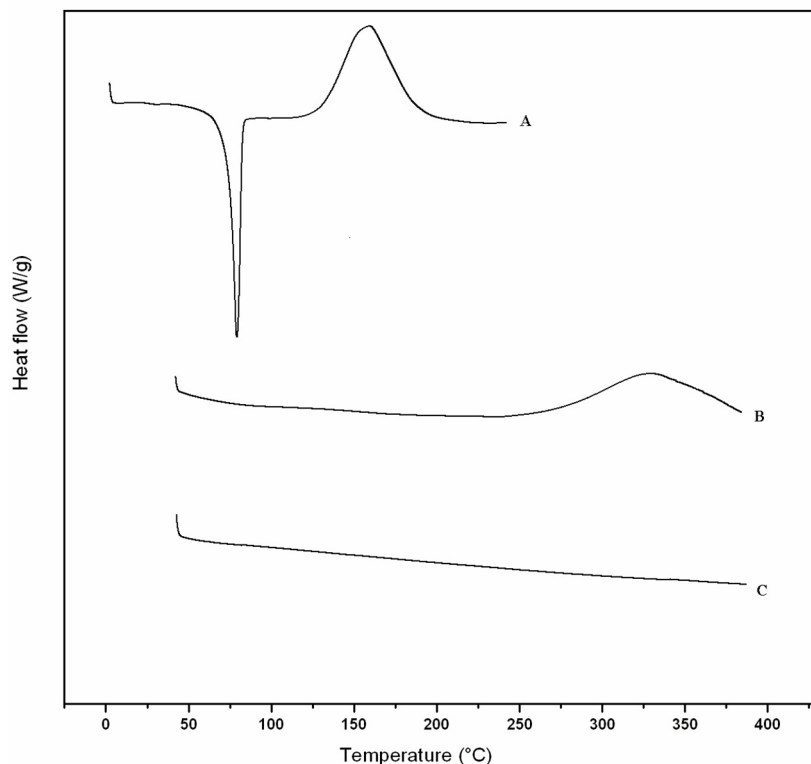
Due to the electron withdrawing nature of the two adjacent carbonyl groups, the double bond of imide group is susceptible towards homo- and copolymerization. The homopolymerization (curing) may be induced thermally or by free radicals / anions to give a network with high cross-link density *via* addition reaction.<sup>2,45</sup> The cure process of bismaleimides follows autocatalytic first order kinetics. Different techniques *viz*; IR,<sup>45, 46</sup> DSC,<sup>25,47-53</sup> NMR,<sup>29,54</sup> etc., are reported in the literature to study the curing process.

In the present study, the kinetics of BMI curing was studied using DSC. The DSC thermograms of bismaleimides under study are shown in **Figure 6. 29**



**Figure 6.29 : DSC thermograms of bismaleimides. (A) ODABMI (B) BPZBMI (C) BPC15BMI (D) ODAC15BMI (E) MPDAC15BMI.**

**Figure 6.29 (A)** represents the DSC thermogram of curing process of ODABMI. The scan shows a sharp endotherm peak at 183 °C corresponding the melting point (176 - 177 °C observed by open capillary) followed by a curing exotherm with a peak maxima at 282 °C and heat of polymerization ( $\Delta H$ ) 73 kJ / mol. **Figure 6.29 (D)** shows DSC scan of ODAC15BMI; the analogue of ODABMI with pentadecyl chain. The examination of DSC scan shows melting endotherm with a peak maxima at 78 °C (69 – 70 °C by open capillary). The thermogram shows two exotherms for curing wherein, the first exotherm shows the onset of curing (stage-I) at 128 °C and the curing then ceases at about 232 °C and then there is a considerable gap (around 30 °C) before the second curing (stage-II) onsets at 269 °C. Based on heat of polymerization data, the former curing exotherm contributes for about 65 % conversion while the latter corresponds to 35% conversion.



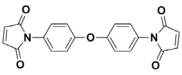
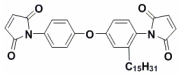
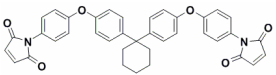
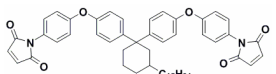
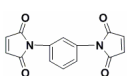
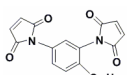
**Figure 6. 30 : DSC thermograms of ODAC15BMI (A) 0 – 240 °C @ 10 °C/min, (B) quenched A and rescanned from 40 – 385 °C @ 10 °C/min, (C) quenched B and rescanned from 40 – 385 °C @ 10 °C/min**

This observation was confirmed by rescanning the sample from 40 °C to 385 °C after the first exotherm was over (240 °C). (**Figure 6.30 B**). The rescan B does not show melting endotherm and exotherm due to curing (stage-I), and shows the exotherm due to curing stage-II. The third scan (40 - 385 °C) (**Figure 6.30 C**) shows no process. Moreover, the resinous nature of sample after curing stage-I was also confirmed by its insolubility in solvents (chloroform, dimethylsulfoxide) at room temperature and after heating as well, against the uncured monomer which was soluble in both the solvents at room temperature. Similar observations were reported by Barton *et.al.*<sup>28, 52</sup> for different BMI monomers where the authors extensively studied such behavior.

**Figure 6.29 B and C** represents DSC thermograms of BPZBMI and BPC15BMI curing, respectively. The cure process of BPC15BMI proceeds with two peaks, the former commencing at 130 °C comprises for about 1% conversion based on the values of heat of polymerization.

The cure characteristics of all BMI monomers under study are collected in **Table 6.4**.

**Table 6.4 : Cure profile of bismaleimides**

Sr. No.	Bismaleimide	Melting Point (°C) <sup>a</sup>	Processing Window (°C)	DSC Profile			$\Delta H$ (kJ/mol)
				To (°C)	Tp (°C)	Tf (°C)	
1.	 (ODABMI)	183	42	225	282	340	73
2.	 (ODAC15BMI)	78	50	128 (I) 269 (II)	158 (I) 329 (II)	232 (I) 383 (II)	119
3.	 (BPZBMI)	91	103	194	236	345	128
4.	 (BPC15BMI)	Viscous Liquid	> 100	(130) 208	247	340	134
5.	 (MPDABMI)	205 <sup>b</sup>	40	245 <sup>b</sup>	253 <sup>b</sup>	350 <sup>b</sup>	71 <sup>b</sup>
6.	 (MPDAC15BMI)	98	132	230	290	348	85

To – cure onset (initiation) temperature

Tp – Maximum cure (peak) temperature

Tf – Final cure temperature

a - From DSC melting endotherm

b - Data taken from reference 18.

The melting points of BMI monomers (ODAC15BMI, BPC15BMI and MPDAC15BMI) as can be seen from **Table 6.4**, are lower than that of corresponding BMI monomers without pentadecyl chain (ODABMI, BPZBMI and MPDABMI). This could be due the presence of pendent flexible pentadecyl chain which impedes the close packing of molecules. This lowering of melting points increased the range of processing window (between melting point and cure onset temperature) from ~ 40 °C (ODABMI, MPDABMI) to around 100 °C (BPZBMI, BPC15BMI, MPDAC15BMI) with the exception of ODAC15BMI.

The data for  $\Delta H$  of BMI curing in the present case lies in the range of 73 – 134 kJ/mol. At this point of time, no explanation can be put forth for the observed variation of  $\Delta H$  with the structure of BMI monomer, however, the range is in accordance with the reported values for other BMI monomers.<sup>18,28,30,48,49,52</sup>

#### 6.4.7.1 Nonisothermal cure kinetics

In nonisothermal conditions, the rate of reaction can be expressed by equation 2:

$$\frac{d\alpha}{dT} = (A/\phi)e^{-E/RT}(1-\alpha)^n \quad (2)$$

where  $\alpha$  is fractional conversion at temperature  $T$ ,  $\phi$  is heating rate,  $E$  is activation energy,  $A$  is Arrhenius frequency factor,  $R$  is gas constant, and  $n$  is the order of reaction.

In the present case, cure kinetics was studied by employing Coats-Redfern equation<sup>55</sup> which is expressed as:

$$\ln\{g(\alpha)/T^2\} = \ln\{AR/\phi E(1-2RT/E)\} - E/RT \quad (3)$$

where  $g(\alpha) = [1-(1-\alpha)^{1-n}] / (1-n)$ ; for  $n = 1$ ,  $g(\alpha) = -\ln(1-\alpha)$ .

To calculate kinetic parameters, fractional conversion ' $\alpha$ ' was calculated from fractional enthalpy of reaction using equation 1. Kinetic plots of  $\ln\{g(\alpha)/T^2\}$  against  $1/T$  assuming different order of reaction ( $n = 0.5, 1, 1.5, 2, 2.5$  and  $3$ ) were drawn using the Coats-Redfern equation and the best fit furnished the order of reaction ' $n$ '. In all the cases, best fit was observed for  $n = 1$ . **Figure 6.31** shows plots of determination of order of reaction and curing parameters. The curing parameters (activation energy and Arrhenius frequency factor) were computed from slope and intersect of the plot with best fitting value of ' $n$ '. In case of ODAC15BMI two activations energies were calculated for stage-I and stage-II from plots D-I and D-II, (**Figure 6.30**), respectively. The activation energy of BPC15BMI was calculated for the conversion range  $> 1\%$  (shown by dotted lines, **Figure 6.31 C**). The kinetic parameters of the bismaleimide curing calculated from these curves are collected in **Table 6.5**.



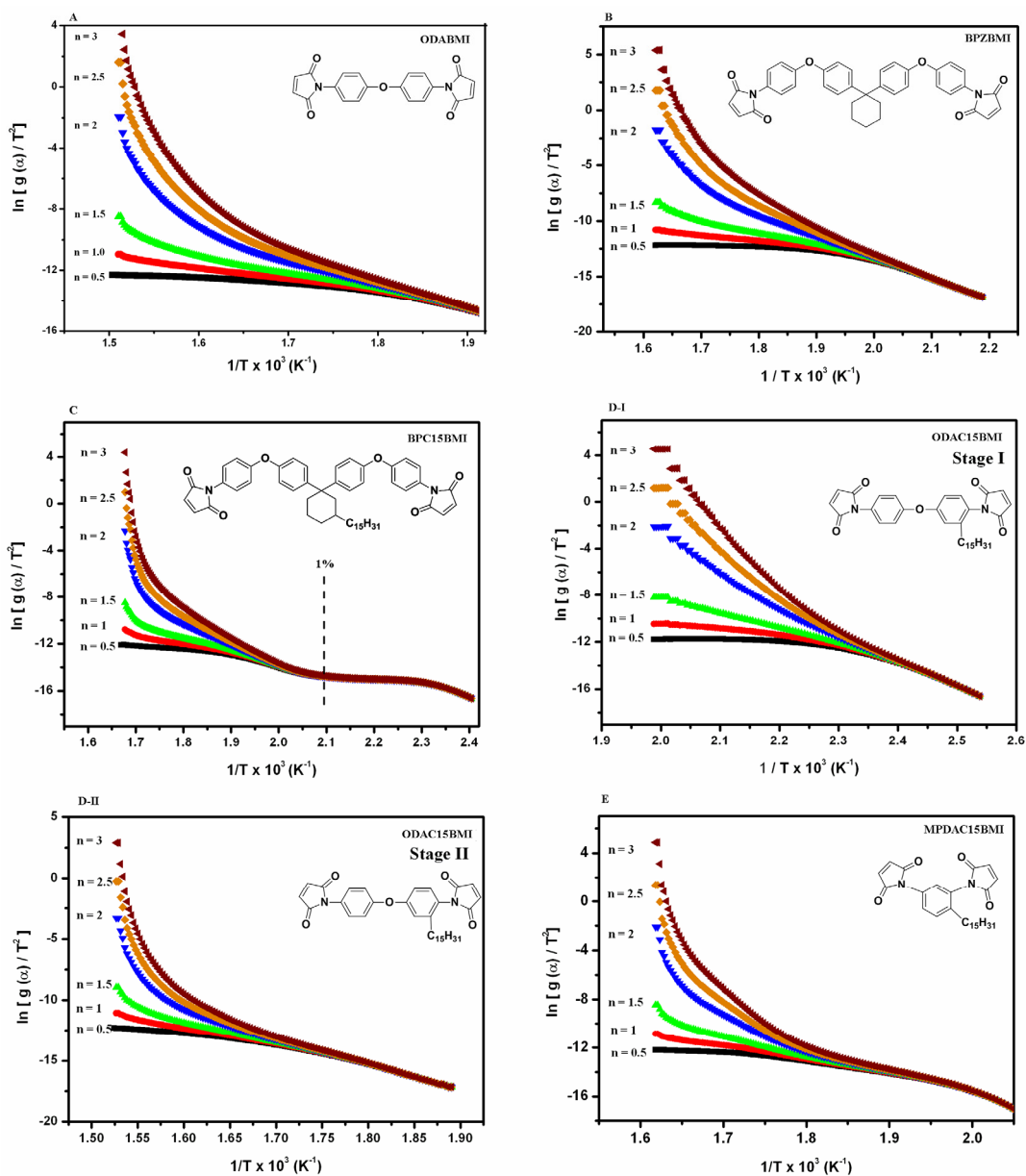
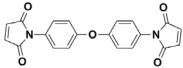
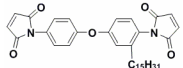
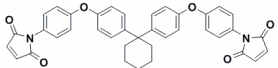
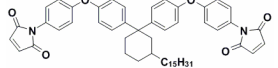
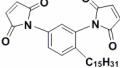


Figure 6. 31: Determination of order of bismaleimide curing reaction by Coats-Redfern equation.

**Table 6.5: Kinetic parameters of bismaleimide curing**

Sr. No	Monomer	Kinetic Parameters	
		Ea (kJ/mol)	ln A (s <sup>-1</sup> )
1.		110 (137 <sup>a</sup> , 120 <sup>b</sup> )	10.3
2.		121 (stage-I) 131 (stage-II)	21.2 (stage-I) 12.9 (stage-II)
3.		110	12.7
4.		76	4.4
5.		103	9.3

a - Reference 49

b - Reference 48

#### 6.4.8 Thermal stability of cured network

The thermal degradation of cured BMIs is a function of the structure of the bridge between the succinimide rings formed during cure process. Stenzenberger *et.al.*<sup>56</sup> studied the degradation pattern of cured BMIs with aliphatic and aromatic backbone and observed that the degradation proceeds preferably by cleavage of bond between nitrogen and aromatic carbon to yield amines, isocyanates, phenol, carbon monoxide, water, etc.

**Figure 6.32** shows the weight loss of cured ODABMI, BPZBMI, BPC15BMI, ODAC15BMI, and MPDAC15BMI heated at 10 ° C / min in nitrogen. The relative thermal stabilities of the cured BMIs were compared by the temperature of 10 % weight loss and char yield at 800 °C. The temperature of 10 % weight loss and the char yield at 800 °C are summarized in **Table 6.6**.

All the cured BMIs showed a single stage decomposition. The temperature at 10% weight loss was in the range 390- 485 °C indicating good thermal stability of cured BMIs. The stability of cured BMIs was observed in the order; ODABMI > MPDAC15BMI > ODAC15BMI > BPZBMI > BPC15BMI. Amongst the series, cured BPC15BMI showed comparatively higher weight loss rate at temperatures from 400 °C to around 600 °C. The char yield at 800 °C in case of cured BPC15BMI was observed to be 25 % which is the lowest in the

series. The decreased thermal stability of cured BPC15BMI can be correlated to the higher aliphatic content.

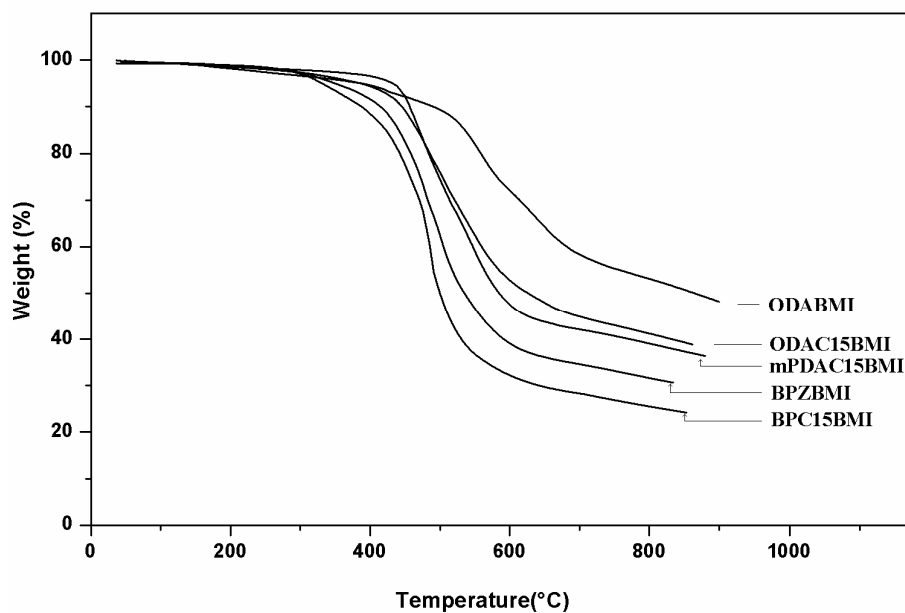


Figure 6.32 : TG curves of bismaleimides

Table 6.6: Thermal properties of cured bismaleimides.

Sr. No	Cured Bismaleimide	Monomer Structure	T <sub>10</sub> (°C)	Char Yield at 800 °C (%)
1.	ODABMI <sup>a</sup>		485	53
4.	ODAC15BMI <sup>b</sup>		440	41
2.	BPZBMI <sup>b</sup>		415	32
3.	BPC15BMI <sup>b</sup>		390	25
5.	MPDAC15BMI <sup>b</sup>		455	39
6.	PDAC15BMI <sup>c</sup>		500 <sup>c</sup>	46.5 <sup>c</sup>

a - cured at 180 °C/1h, 200 °C/1h, 250 °C/3 h.

b - cured at 100 °C/1h, 180°C/1h, 250 °C/3 h.

c - data taken from reference 18.

## 6.5 Conclusions:

1. Three new bismaleimide monomers containing flexible pendent pentadecyl chain *viz*; 4,4'-bis(maleimido)-3-pentadecyldiphenylether, 1,1-bis[4-(4-maleimidophenoxy)phenyl]-3-pentadecylcyclohexane and 1,3-bis(maleimido)-4-pentadecylbenzene were synthesized by the ring opening addition reaction of corresponding diamines with maleic anhydride followed by cyclodehydration of *N,N*-bismaleamic acids using acetic anhydride and sodium acetate and were characterized by IR, <sup>1</sup>H-NMR and <sup>13</sup>C-NMR spectroscopy.
2. The melting points of bismaleimide monomers containing pendent pentadecyl chain *viz*; 4,4'-bis(maleimido)-3-pentadecyldiphenylether (78 °C) and 1,3-bis(maleimido)-4-pentadecylbenzene (98 °C) were lower than that of 4,4'-bis(maleimido)diphenylether (183 °C) and 1,3-bis(maleimido)benzene (205 °C), respectively.
3. Due to lower melting points, the bismaleimide monomers containing pendent pentadecyl chain *viz*; 4,4'-bis(maleimido)-3-pentadecyldiphenylether, 1,1-bis[4-(4-maleimidophenoxy)phenyl]-3-pentadecylcyclohexane and 1,3-bis(maleimido)-4-pentadecylbenzene exhibited larger processing window (> 100 °C) than bismaleimide monomers *viz*; 4,4'-bis(maleimido)diphenylether and 1,3-bis(maleimido)benzene.
4. 4,4'-Bis(maleimido)-3-pentadecyldiphenylether exhibited improved solubility pattern in common organic solvents such as chloroform, dichloromethane, etc., as compared to 4,4'-bis(maleimido)diphenylether.
5. The nonisothermal cure kinetics of five bismaleimides *viz*; 4,4'-bis(maleimido)diphenylether, 4,4'-bis(maleimido)-3-pentadecyldiphenylether, 1,1-bis[4-(4-maleimidophenoxy)phenyl]cyclohexane, 1,1-bis[4-(4-maleimidophenoxy)phenyl]-3-pentadecylcyclohexane and 1,3-bis(maleimido)-4-pentadecylbenzene was studied using DSC and the kinetic parameters were calculated using Coats-Redfern method.
6. The cured network of all the bismaleimides under study showed a single stage decomposition with T<sub>10</sub> values in the range of 390 – 485 °C indicating their good thermal stability.

## References:

1. Crivello, J. V. *J. Polym. Sci.* **1973**, 11, 1185.
2. Stenzenberger, H. D. *Appl. Polym. Symp.* **1973**, 22, 77.
3. Pappalardo, L. T. *J. Appl. Polym. Sci.*, **1977**, 21, 809.
4. Gotro, J.T.; Appelt, B. K. *IBM J. Res. Dev.*, **1988**, 32, 616.
5. Takahasshi, A.; Nagai, A.; Mukoh, A.; Tsukanishi, K. *IEEE Trans. Comp. Hybrids Manuf. Technol.*, **1990**, 13, 1115.
6. Stenzenberger, H. D. *Adv. Polym. Sci.*, **1994**, 117, 165.
7. Brown, A. S. *Aerospace Am.*, **1989**, 27, 18.
8. Xiang, Z.D.; Jomes, F. R. *Composites Sci. Technol.*, **1993**, 47, 209.
9. Nagai, A.; Takahashi, A.; Wajima, M.; Tsukanishi, K. *Polym. J.* **1988**, 20, 125.9
10. Wilson, D.; Stenzenberger, H. D.; Hergenrother, P. M. Eds., *Polyimides*, **1990**, Blackie, Glasgow and London.
11. Stenzenberger, H. D.; Herzog, M.; Romer, W.; Scheiblich, R.; Reeves, J. *Br. Polym J.* **1983**, 15, 1
12. Chandra, R.; Rajabi, L. *J. Macromol.Sci.Pure Appl. Chem.* **1997**, 37, 61.
13. Nishikawa, A.; Shidara, M. Era, S.; Fukushima, T.; Suzuki, H.; Kougame, H. *Jpn.Pat. 56-103162*, **1981**.
14. Harvey, J.A.; Chartoff, R.P.; Butler, J.M. *ANTEC*, **1986**, 1311.
15. Takeda, S.; Akiyama, H.; Kakiuchi, H. *J. Appl. Polym. Sci.* **1988**, 35, 1381.
16. Nagai, A.; Takahasshi, A.; Suzuki, M.; Mukoh, A. *J. Appl. Polym. Sci.* **1992**, 44, 159.
17. Goldfarb, I.J.; Feld, W.A.; Saikumar, J. *Polymer* **1993**, 34, 813
18. Hsiao, S-H.; Chang, C-F. *J. Polym. Res.*, **1996**, 3, 31
19. Wang, C-S.; Leu, T.-S. *J. Appl. Polym. Sci.* **1999**, 73, 833.
20. King, J.J.; Chaudhari, M.A.; Zahir, S. *29th International SAMPE Symposium* **1984**, 29, 392.
21. Stenzenberger, H.D.; Konig, P.; Herzhog, M.; Romer, W.; Pierce, S.; Fear, K.; Canning, M.S. *32nd International Symposium*, **1987**, 372.
22. Davidson, G.; Soutar, I.; Preston, P.N.; Shah, V.K.; Simpson, S.W.; Stewart, N.J. *Polymer*, **1994**, 35, 653.
23. Stenzenberger, H.; Heinen, K.-U.; Hummel, D. O. *J. Polym. Sci., Polym. Chem. Edn.* **1976**, 14, 2911
24. Kovacic, P.; Hein, R.W. *J. Am. Chem. Soc.* **1959**, 81, 1187.
25. Series, A.; Mechin, F.; Pascult, J.P. *J. Appl. Polym. Sci.*, **1993**, 48, 257.
26. Kole, N.D.; Gruber, W.F. *U.S. Patent* 3127414, **1964**.
27. Domeier, L.A.; Gardner, H.C. *Eur. Pat. Appl.* 0148534, **1985**.
28. Barton, J.M.; Hamerton, I.; Rose, J. B.; Warner, D. *Polymer*, **1991**, 32, 358
29. Grenier-Loustalot, M-F.; Cunha L.D. *Eur. Polym. J.*, **1998**, 34, 95.
30. Hsiao, S-H.; Yang, C-P.; Chen, S-H. *J. Polym. Res.*, **1999**, 6, 141
31. Dumont, F.; Visseaus, M.; Barbier-Baudry, D.; Dormond, A. *Polymer* **2000**, 41, 6043.
32. Hwang, H.-J.; Li, C.-H.; Wang, C.-S. *Polym. Int.* **2006**, 55, 1341
33. Feng, J.L.; Yue, C.Y.; Chian, K.S. *e-Polymers* **2006**, 044.
34. Critchley, J. P.; Knight, G. J.; Wright, W. W. *Heat Resistant Polymers: Technologically Useful Materials*; **1983**, Plenum Press: New York.
35. Hergenrother, P. M.; Havens, S. J. *Macromolecules* **1994**, 27, 4659
36. Shifrina, Z. B.; Rusanov, A. L. *Russ. Chem. Rev.* **1996**, 65, 599.
37. Spiliopoulos, I.K.; Mikroyannidis, J.A. *Macromolecules* **1998**, 31, 1236.
38. de Abajo, J.; de la Campa, J. G. *Adv. Polym. Sci.*, **1999**, 140, 23.
39. Prime R. B. In *Thermal Characterization of Polymeric Materials*. Turi, E.A. ED **1981**, Academic, New York, p 435.
40. More, A.S. *Ph.D. Thesis*, University of Pune, India, **2009**.
41. Sadavarte, N.V.; Halhalli, M.R.; Avadhani, C.V.; Wadgaonkar, P.P. *Eur. Polym. J.* **2009**, 45, 582.

42. Murata, S.; Nakayama, M.; Furukawa, K.; Kobayashi, R. (Chisso Corp.) *Eur. Pat. Appl. EP 368604*, **1990**, and *Chem. Abstr.* **1990**, 113, 190882m.
43. Searle, N.E. (Du pont) *U.S. Patent*, 2444536, **1948**. and *Chem. Abstr.* **1948**, 42, 7340.
44. More, A. S.; Sane, P. S.; Patil, A.S.; Wadgaonkar, P.P. *Polym. Degrad. Stab.* **2010**, Communicated.
45. Hummel, D. O.; Heinen, K.-U.; Stenzenberger, H.; Siesler, H. *J. Appl. Polym. Sci.*, **1974**, 18, 2015.
46. Tungare, A.V. ; Martin, C.G. *J. Appl. Polym. Sci.*, **1992**, 46, 1125
47. Galanti, A. V. *J. Appl. Polym. Sci.*, **1984**, 29, 1611.
48. Ninan, K.N.; Krishnan, K.; Mathew, J. *J. Appl. Polym. Sci.*, **1986**, 32,6033.
49. Varma, I.K.; Sharma, S. *Polymer* **1985**, 26, 1561.
50. Acevedo, M.; de Abajo, J.; de la Campa J. G. *Polymer* **1990**, 31, 1955.
51. Nagai, A.; Takahashi, A.; Suzuki, M.; Katagiri, J.; Mukoh, A. *J. Appl. Polym. Sci.*, **1990**, 41, 2241.
52. Barton, J.M; Hamerton, I.; Rose, J. B.; Warner, D. *Polymer*, **1991**, 32, 2482.
53. Chun-Shan, W.; Tsu-Shang, L. *Polymer* **1999**, 40, 5407
54. Grenier-Loustalot, M-F.; Cunha L.D. *Polymer* **1998**, 39, 1833
55. Coats, A.W.; Redfern, J.P. *Nature* **1964**, 201, 68.
56. Stenzenberger, H.; Heinen, K.-U.; Hummel, D. O. *J. Polym. Sci.* **1976**, 14, 2911.

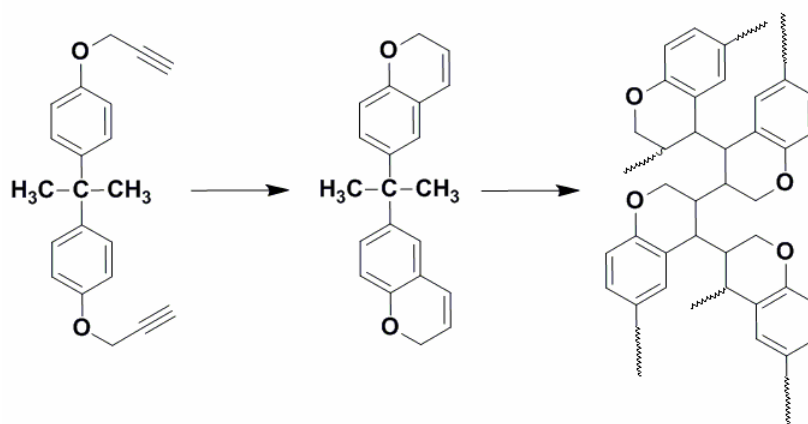
# Chapter

7

Synthesis, Characterization and  
Curing Studies of Bispropargyl Ethers

## 7.1 Introduction

Propargyl ether functional phenolic resins (also popularly known as propargyl-terminated resins) were developed as a potential hydrophobic substitute for epoxies in advanced composites, electronics, adhesives and coatings.<sup>1-4</sup> The structural similarity of bispropargyl ether monomer to epoxies is useful for their preparation, processing and development of thermally stable polymers.<sup>1,2</sup> One of the key features of these systems is their ability to undergo curing through addition reaction of the acetylene groups, either linearly or *via* cyclization. The curing *via* cyclization involves initial Claisen rearrangement to 2-*H*-1-benzopyran (chromene) groups which subsequently polymerize<sup>5-8</sup> yielding a network with high thermal stability (**Scheme 7.1**).



**Scheme 7.1 : Polymerization of bispropargyl ethers**

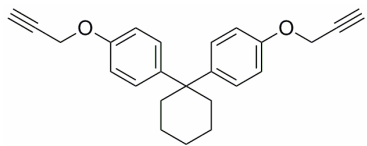
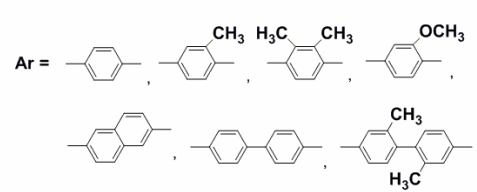
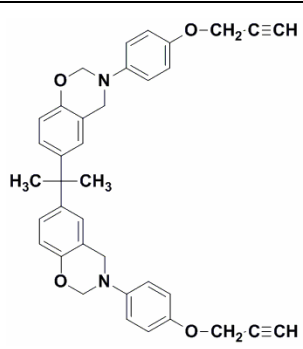
The good attributes of cured bispropargyl ethers include; good thermal stability, low water absorption, good dielectric properties, low monomer sensitivity to boiling water, good solvent resistance and excellent physico-mechanical properties.

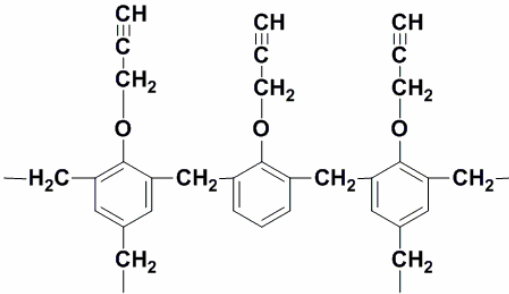
The synthetic method of bispropargyl ethers makes it possible to tailor the properties by varying the structure of monomer. Bispropargyl ethers with various structural features have been reported.<sup>1-4, 9-15</sup> The bispropargyl ether of bisphenol-A (BPAPT) remains to be the most widely studied monomer in this category. Dirlikov<sup>2</sup> discussed the properties of cured resin based on bisphenol A in detail. The cured network exhibited high T<sub>g</sub> (300 °C for cured samples and 360 °C for post-cured samples), high thermal stability (no weight loss when heated upto 380°C), low moisture absorption (1.2 wt %), low dielectric constant (2.77 at 10 MHz) and good mechanical properties. Apart from bisphenol-A based monomer, bispropargyl ethers with various functional groups such as, carbonyl, ether, fluoroaliphatic, sulfone, etc., were also reported<sup>2,9</sup>. (**Table 7.1**) Nair *et. al.*<sup>10</sup> investigated the kinetics of cure reaction of bispropargyl ethers based on bisphenol-A, 1,1-bis(4-hydroxyphenyl) methanone (BPKPT) and 1,1-bis(4-hydroxyphenyl) sulfone (BPSPT). The thermal properties of cured resins of BPKPT and BPSPT were reported to be better than that of BPAPT. The cure temperature and activation energy for reaction was observed in the order BPAPT



< BPKPT < BPSPT. Toda<sup>11</sup> reported synthesis of bispropargyl ether based on 1,1-bis(4-hydroxyphenyl)cyclohexane, however, the curing and properties of cured network were not reported. Benicewicz *et.al.*<sup>12</sup> synthesized a series of rigid rod bispropargyl ethers based on aromatic ester rigid cores and studied the effect of liquid crystallinity on cure behavior. Agag *et. al.*<sup>13,14</sup> synthesized propargyl-terminated monomers with benzoxazine backbone. The researchers synthesized linear polybenzoxazine *via* click reaction<sup>14</sup>.

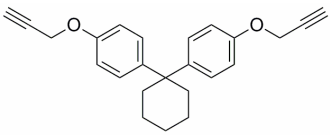
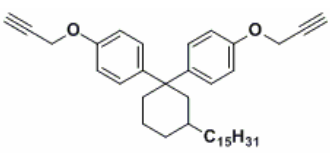
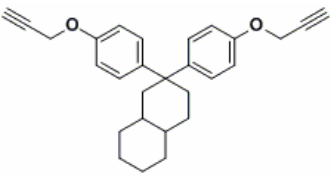
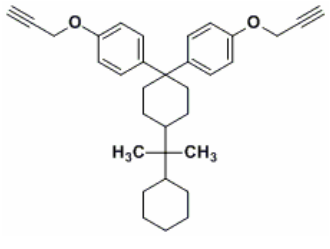
**Table 7.1 : Literature examples of bispropargyl ethers**

Sr.No.	Monomer	Reference
1.	$\text{HC}\equiv\text{C}-\text{CH}_2-\text{O}-\text{C}_6\text{H}_4-\text{R}-\text{C}_6\text{H}_4-\text{O}-\text{CH}_2-\text{C}\equiv\text{CH}$ <p style="text-align: center;">R = C(CH<sub>3</sub>)<sub>2</sub>, C(CF<sub>3</sub>)<sub>2</sub>, O, S, C=O, SO<sub>2</sub>, etc.</p>	2, 9
		10 (R = C=O, SO <sub>2</sub> )
2.		11
3.	$\text{HC}\equiv\text{C}-\text{H}_2\text{C}-\text{O}-\text{C}_6\text{H}_4-\text{C}(=\text{O})-\text{O}-\text{Ar}-\text{O}-\text{C}(=\text{O})-\text{C}_6\text{H}_4-\text{O}-\text{CH}_2-\text{C}\equiv\text{CH}$ <p style="text-align: center;">Ar = </p>	12
4.		13, 14

5.		15
----	--	----

The objective of the present work was to synthesize new bispropargyl ethers containing cycloaliphatic “cardo” group based on corresponding bisphenols and to study the effect of cycloaliphatic “cardo” group on the curing behavior of bispropargyl ethers. Thus, three new bispropargyl ethers (**Table 7.2**) were synthesized and characterized by FT-IR, <sup>1</sup>H-NMR and <sup>13</sup>C-NMR spectroscopy. The curing kinetics of the synthesized bispropargyl ethers was studied by DSC in nonisothermal mode and the thermal stability of the cured network was investigated by TGA.

**Table 7.2 : Bispropargyl ether monomers synthesized in the present work.**

Monomer	Name
	1,1-Bis[4-(2-propynyloxy) phenyl] cyclohexane (BPZPT)
	1,1-Bis[4-(2-propynyloxy) phenyl]-3-pentadecyl cyclohexane (BPC15PT)
	1,1-Bis[4-(2-propynyloxy) phenyl] decahydronaphthalene (BPDCPT)
	1,1-Bis[4-(2-propynyloxy) phenyl]-4-perhydrocumyl-cyclohexane (BPPCPPT)

## 7.2 Experimental

### 7.2.1 Materials

Propargyl bromide (80 % w/w solution in toluene) was purchased from Sigma-Aldrich Inc.USA. Acetone, diethylether, methanol, potassium carbonate, and sodium sulfate were procured from Merck India. 2,2-Bis(4-hydroxyphenyl)propane (BPA) was generously gifted by GE, Bangalore, India. 1,1-Bis(4-hydroxyphenyl)cyclohexane (BPZ), 1,1-bis(4-hydroxyphenyl)-3-pentadecylcyclohexane (BPC15), 1,1-bis(4-hydroxyphenyl)decahydro naphthalene (BPDC) and 1,1-bis(4-hydroxyphenyl)-4-perhydrocumylcyclohexane (BPPCP) were synthesized as described in chapter 3 (section 3.3). The solvents were of reagent grade quality and were used as received.

### 7.2.2 Characterization

Melting points were determined by open capillary method and are uncorrected.

Infrared spectra were recorded on Perkin-Elmer, spectrum GX model at a resolution of 4  $\text{cm}^{-1}$ . The spectra were recorded by depositing samples as solvent-cast thin films on sodium chloride cells.

NMR spectra were recorded on Bruker NMR spectrophotometer (200 or 400 MHz) using  $\text{CDCl}_3$  as a solvent.

DSC measurements were performed on TA Instruments (Q10) supported by TA Universal Analysis software for data acquisition. The samples (5-7 mg) were sealed in hermetic aluminum pans and experiments were performed under a nitrogen flow of 50 mL / min. The samples were subjected to a dynamic DSC scan at the heating rates of 10 , 20, 30 and 40  $^{\circ}\text{C}/\text{min}$ . The enthalpy of curing  $\Delta H$  was determined from the area under the exothermic curve. The cure onset temperature ( $T_0$ ) was considered as the intersect of slope of baseline and tangent of curve leading to peak of transition. The fractional conversion ( $\alpha$ ) of each sample at a given temperature under nonisothermal conditions was calculated from the relation<sup>16</sup>:

$$\alpha_T = \Delta H_f / \Delta H_T \quad (1)$$

where  $\Delta H_f$  is the fractional enthalpy at that temperature and  $\Delta H_T$ , the total heat of reaction under nonisothermal mode.

Thermogravimetric analysis (TGA) data were obtained using a TA instrument, (model Q 5000) at a heating rate of 10 $^{\circ}\text{C}$  / min under nitrogen atmosphere.

### 7.3 Preparations

A representative procedure for the preparation of 1,1-bis(4-hydroxyphenyl)-3-pentadecyl cyclohexane is described below

Into a 100 mL single-necked round bottom flask equipped with a magnetic stirring bar and a pressure equalizing dropping funnel were added 1,1-bis(4-hydroxyphenyl)-3-pentadecyl cyclohexane (1 g, 2.1 mmol), potassium carbonate (0.86 g, 6.3 mmol) and acetone (20 mL). The reaction mixture was stirred at room temperature for 30 min. To the reaction mixture, propargyl bromide (0.64 mL, 4.3 mmol) diluted with acetone (5 mL) was added dropwise over the period of 10 minutes. After completion of the addition, the reaction mixture was stirred for 12 h at room temperature and filtered. The residue was washed with acetone (5 mL). The filtrate was concentrated on rotary evaporator under reduced pressure and then dissolved in diethylether (15 mL), washed with water (2 x 5 mL) and dried over sodium sulfate and filtered. Diethylether was evaporated on a rotary evaporator and viscous liquid obtained was purified by filtration column. (Eluent: Chloroform)

Yield: 1.07 g (92 %).

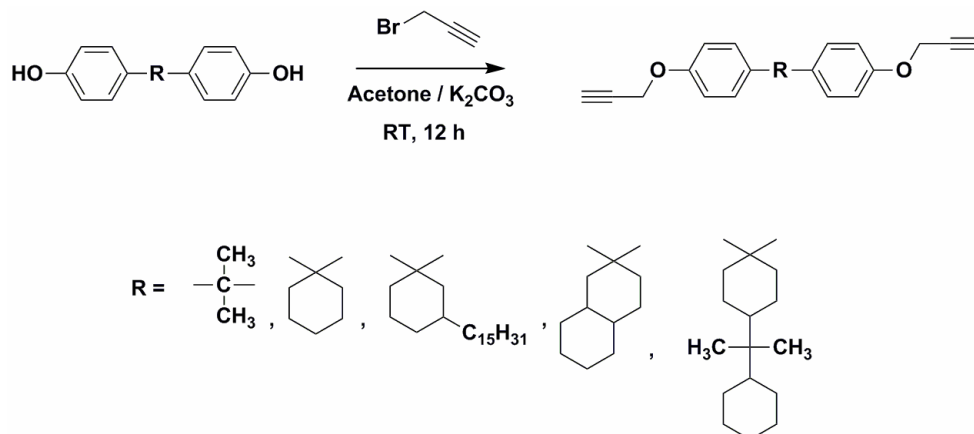
A similar procedure was followed for the preparation of other bispropargyl ethers. The purification of crude bispropargyl ethers was achieved either by filtration column chromatography (Eluent : Chloroform) or by recrystallization using methanol.

### 7.4 Results and Discussion

The synthesis of bispropargyl ethers of dihydric phenols was reported by Hay *et.al.*<sup>17,18</sup> The propargylation could be achieved using propargyl halide (*e.g.* propargyl chloride or propargyl bromide), in the presence of  $K_2CO_3$  or aqueous sodium hydroxide.<sup>1, 2, 17-19</sup> The use of phase transfer catalyst such as tetrabutylammonium bromide has been reported to facilitate the reaction.<sup>20</sup>

In the present study, all the bispropargyl ethers (**Table 7.2**) were synthesized starting from corresponding bisphenols and propargyl bromide in the presence of  $K_2CO_3$ .

**Scheme 7.2** depicts the route followed for the synthesis of bispropargyl ethers.



Scheme 7.2: General scheme for the synthesis of bispropargyl ethers.

#### 7.4.1 Synthesis and characterization of 1,1-bis[4-(2-propynyloxy)phenyl] cyclohexane (BPZPT)

Propargylation of BPZ was carried out by following the protocol developed by Dirlikov<sup>1</sup>. The product BPZPT was obtained with 94 % yield and was characterized by FTIR, <sup>1</sup>H-NMR, and <sup>13</sup>C-NMR spectroscopy.

**Figure 7.1** represents IR spectrum of BPZPT. IR spectrum indicated complete conversion of bisphenol into bispropargyl ether as the O-H stretching band at 3290 cm<sup>-1</sup> was absent. The characteristic ≡C-H absorption was observed at 3307 cm<sup>-1</sup>. The absorption owing to -C≡C- was observed at 2125 cm<sup>-1</sup> as a weak band. The -C-O-C- stretching was observed at 1225 cm<sup>-1</sup>.

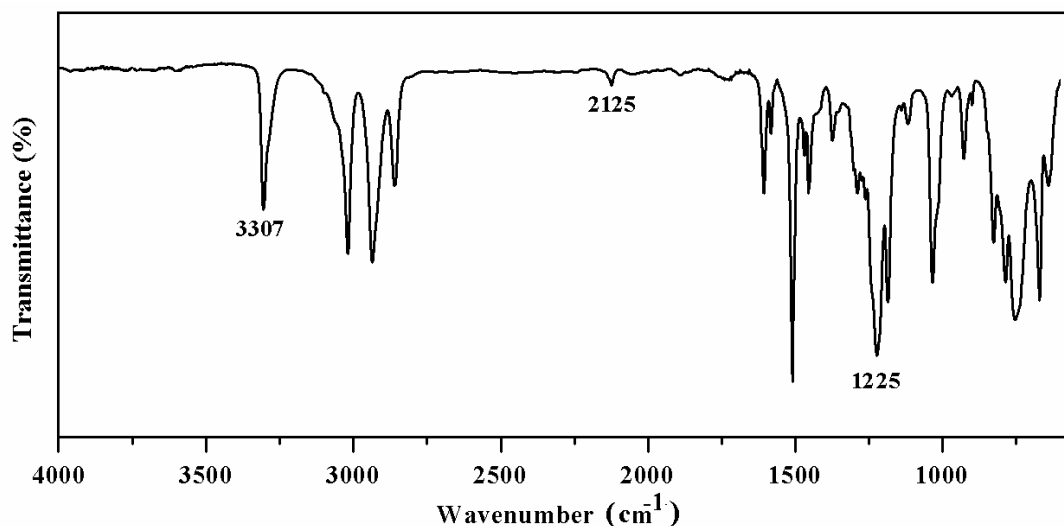
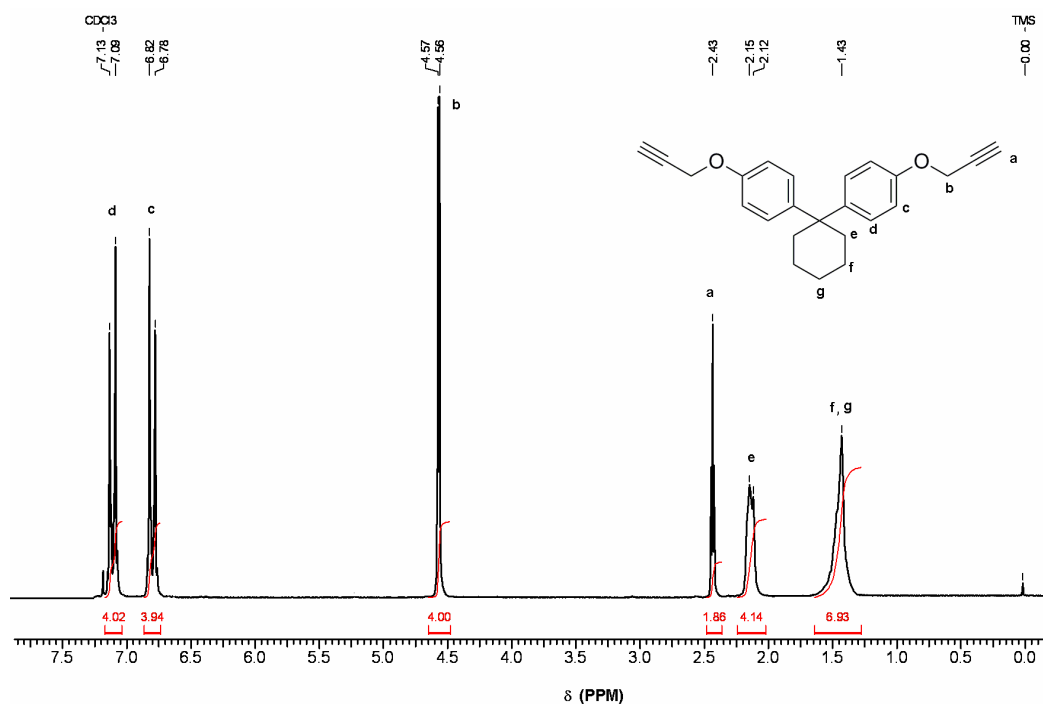


Figure 7.1 : IR spectrum of 1,1-bis[4-(2-propynyloxy)phenyl] cyclohexane

The structure of BPZPT was also confirmed by NMR spectroscopy (both  $^1\text{H}$  and  $^{13}\text{C}$  spectra). **Figure 7.2** represents  $^1\text{H}$ -NMR spectrum of BPZPT. Aromatic protons *ortho* to propynyloxy group appeared as a doublet at 6.80 ppm while protons *meta* to propynyloxy group displayed a doublet at 7.11 ppm. The methylene protons (labeled as b) were observed as a doublet at 4.56 ppm while protons corresponding to acetylene group exhibited a singlet at 2.43 ppm. The protons of cyclohexyl ring displayed peaks in the range 1.43-2.15 ppm.



**Figure 7.2 :**  $^1\text{H}$ -NMR spectrum of 1,1-bis[4-(2-propynyloxy)phenyl] cyclohexane ( $\text{CDCl}_3$ )

**Figure 7.3** represents  $^{13}\text{C}$  NMR spectrum of BPZPT alongwith peak assignments. Aromatic carbon 'd' attached to oxygen of propynyloxy group appeared at 155.17 ppm while a carbon 'g' attached to cyclohexyl ring displayed a signal at 141.78 ppm. The peaks at 114.36 and 128.05 ppm refer to aromatic carbons 'f' and 'e', respectively. The quaternary carbon 'b' exhibited a signal at 78.77 ppm while the terminal methine carbon 'a' displayed a peak at 75.31 ppm. The methylene carbon marked as 'c' appeared at 55.69 ppm. Aliphatic carbons of cyclohexyl ring displayed peaks in the range 22.81 – 45.03 ppm. The assignments were also supported by  $^{13}\text{C}$ -DEPT spectrum (**Figure 7.4**) wherein the methine carbons labeled as a, f and e exhibited signals in positive phase while the peaks due to methine carbon marked as a and methylene carbons labeled as c, i, j and k appeared in negative phase\*.

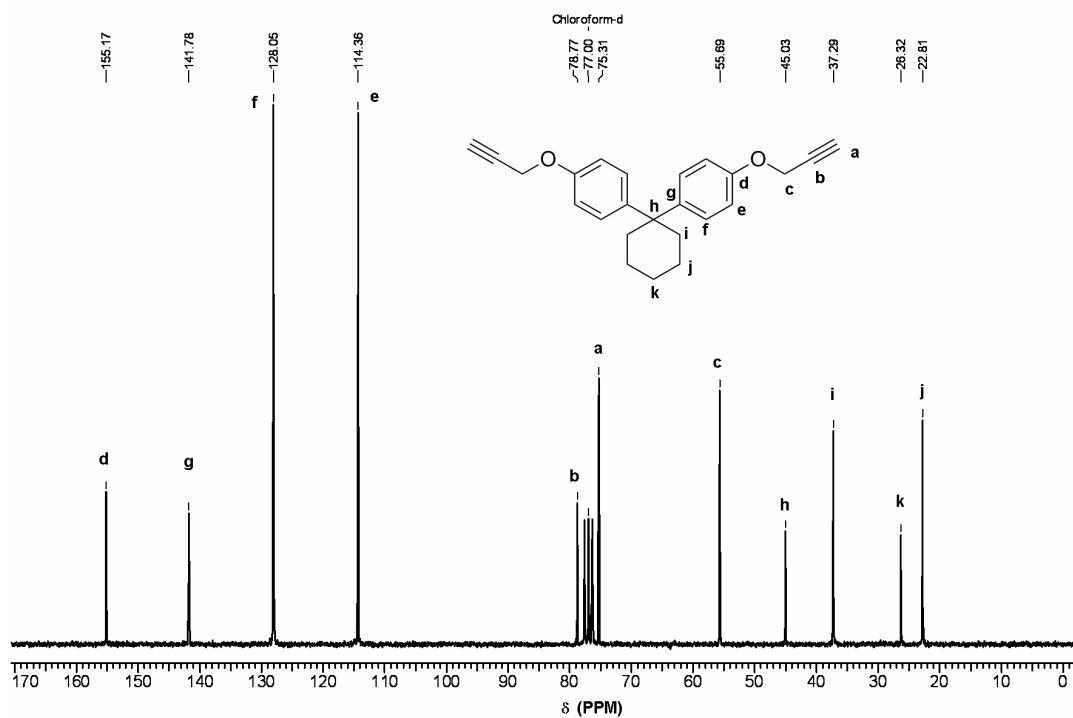


Figure 7.3:  $^{13}\text{C}$ -NMR spectrum of 1,1-bis[4-(2-propynyloxy)phenyl] cyclohexane ( $\text{CDCl}_3$ )

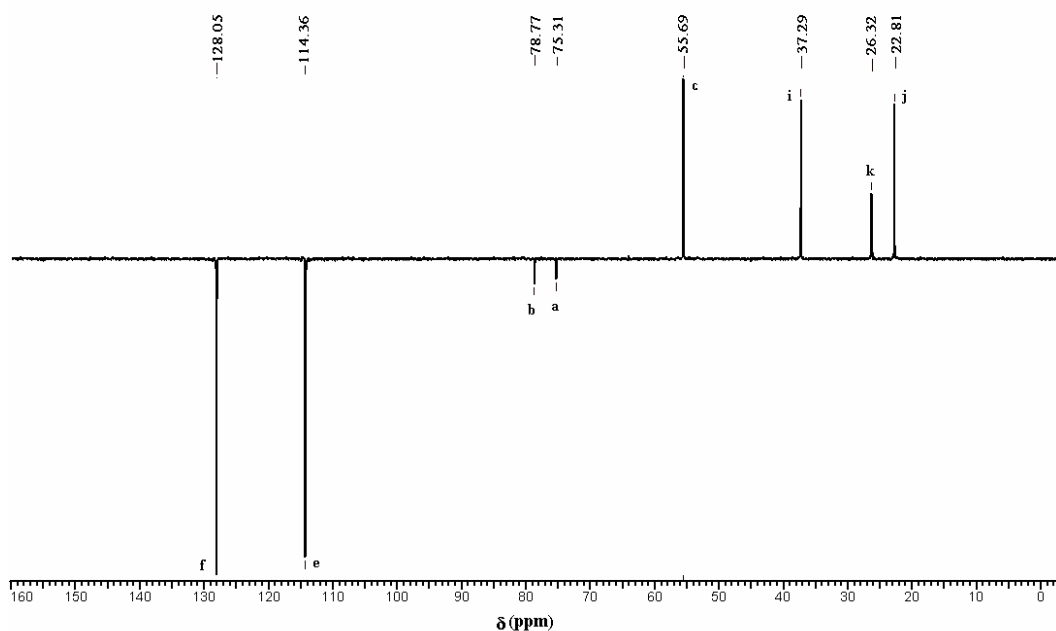


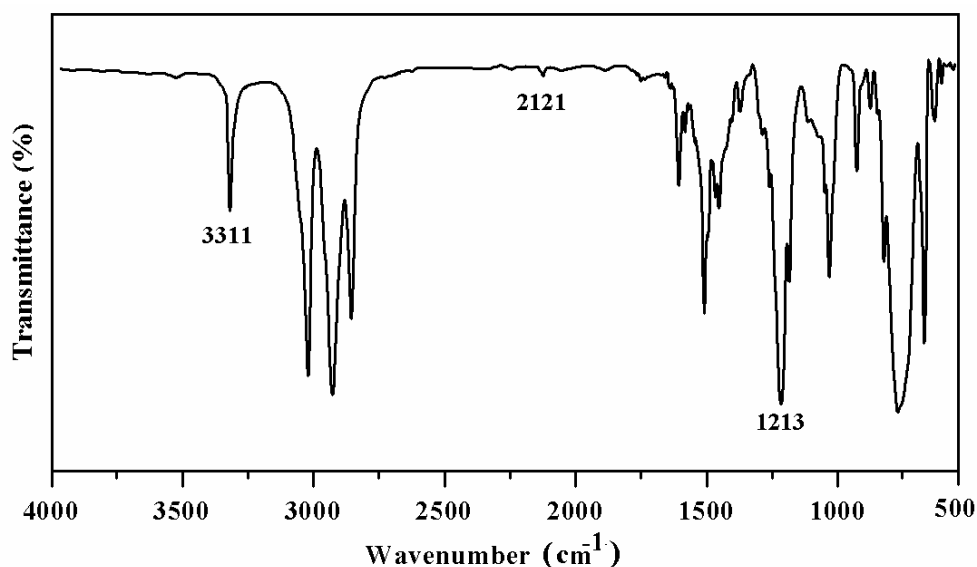
Figure 7.4:  $^{13}\text{C}$ -DEPT NMR spectrum of 1,1-bis[4-(2-propynyloxy)phenyl] cyclohexane. ( $\text{CDCl}_3$ )

\*Note: An unanticipated appearance of quaternary carbon labeled as b in DEPT spectrum could be due to comparatively higher coupling constant of  $-\text{C}-\text{CH}$  than  $-\text{C}=\text{CH}_2$  and  $-\text{C}-\text{CH}_3$ . The  $J_{\text{C}-\text{CH}}$  value is in the order of 50 Hz while  $J_{\text{C}=\text{CH}_2}$  and  $J_{\text{C}-\text{CH}_3}$  are in the order of 5 Hz. The similar observations were observed in all the bispropargyl ethers studied in the present work.

#### 7.4.2 Synthesis and characterization of 1,1-bis[4-(2-propynyloxy)phenyl]-3-pentadecylcyclohexane (BPC15PT)

1,1-Bis[4-(2-propynyloxy)phenyl]-3-pentadecylcyclohexane was synthesized by the reaction of 1,1-bis(4-hydroxyphenyl)-3-pentadecylcyclohexane and propargyl bromide using  $K_2CO_3$  as depicted in **Scheme 7.2**. BPC15PT was characterized by FTIR,  $^1H$ -NMR, and  $^{13}C$ -NMR spectroscopy.

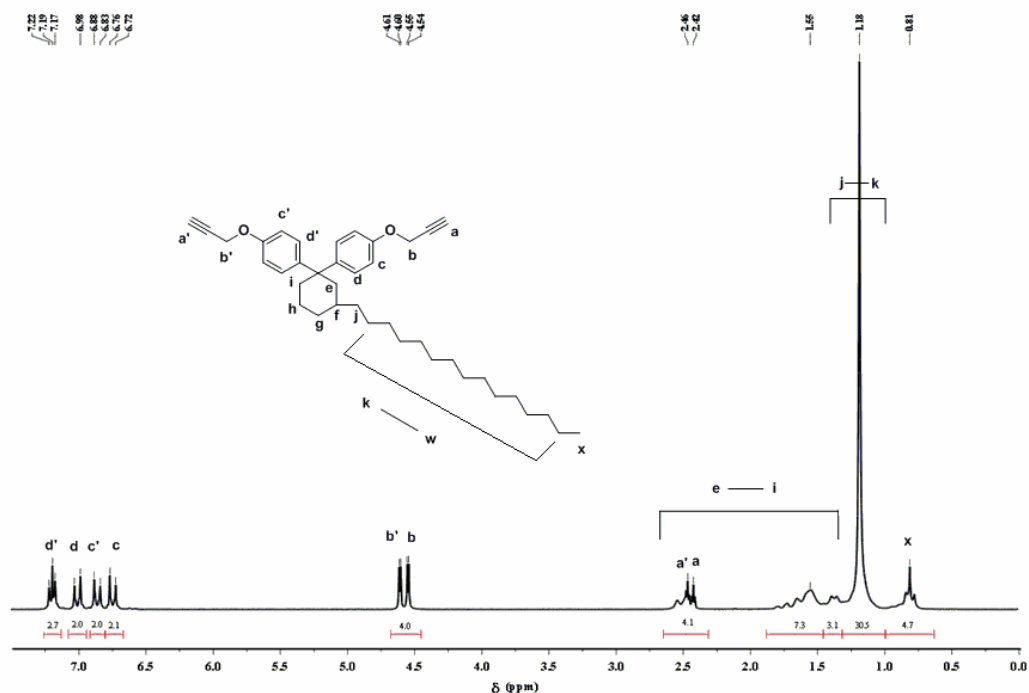
**Figure 7.5** represents IR spectrum of BPC15PT. The characteristic  $\equiv C-H$  stretching was observed at  $3311\text{ cm}^{-1}$ . The absorption corresponding to  $-C\equiv C-$  was observed at  $2121\text{ cm}^{-1}$  as a weak band. The absorption corresponding to  $-C-O-C$  stretching was observed at  $1213\text{ cm}^{-1}$ .



**Figure 7.5 : IR spectrum of 1,1-bis[4-(2-propynyloxy)phenyl]-3-pentadecylcyclohexane**

BPC15PT was further characterized by NMR spectroscopy. **Figure 7.6** represents  $^1H$  NMR spectrum of BPC15PT. As explained earlier in chapter 3 (section 3.4.1.1), the pentadecyl chain substituted at cyclohexyl ring brings asymmetry to the cyclohexyl ring making the distinction between axial and equatorial phenyl rings. Therefore, aromatic protons *c* and *c'* (*ortho* to propynyloxy group) appeared as two separate doublets at 6.74 ppm (axial ring) and 6.84 ppm (equatorial ring). The protons *d* and *d'* (*meta* to propynyloxy group) displayed doublets at 6.98 ppm (axial ring) and 7.20 ppm (equatorial ring). The methylene protons (*b* and *b'*) were observed at 4.54 (attached to axial phenyl ring) and 4.61 (attached to equatorial phenyl ring) ppm while protons *a* and *a'* corresponding to acetylene group exhibited singlets at 2.42 and 2.46 ppm. The protons of cyclohexyl ring and pentadecyl chain displayed signals in the range 1.18 - 2.54 ppm. A triplet at 0.81 ppm is due to protons of methyl group.





**Figure 7.6:**  $^1\text{H}$ -NMR spectrum of 1,1-bis[4-(2-propynyloxy)phenyl]-3-pentadecylcyclohexane ( $\text{CDCl}_3$ )

**Figure 7.7** represents  $^{13}\text{C}$ -NMR spectrum of BPC15PT. Aromatic carbons marked as d, d', e, e', f, f', g and g' appeared in two sets of four aromatic carbons confirming the presence of magnetically nonequivalent axial and equatorial phenyl rings. Aromatic carbons (d, d') attached to propynyloxy group appeared at 155.23 (axial ring) and 155.35 (equatorial ring) ppm. Aromatic carbons (e, e') *ortho* to propynyloxy group appeared at 114.02 (axial ring) and 114.80 (equatorial ring) ppm while aromatic carbons (f, f') *meta* to propynyloxy group were observed at 126.93 (axial ring) and 129.01 (equatorial ring) ppm. Aromatic carbons (g, g') *para* to propynyloxy group were observed at 138.61 (axial ring) and 145.05 (equatorial ring) ppm. Carbons a, a' and b, b' of propynyloxy group were observed in the range 75.41 - 78.89 ppm. The terminal carbons (a, a') of acetylene group exhibited peaks at 75.41 (axial ring) and 75.47 (equatorial ring) ppm while carbons b, b' displayed peaks at 78.87 (axial ring) and 78.89 (equatorial ring) ppm. The peak corresponding to methylene carbon of propynyloxy group appeared at 55.63 ppm. The carbons (-C-, -CH- and -CH<sub>2</sub>-) of cyclohexyl ring and pentadecyl chain displayed signals in the range 22.86 - 45.75 ppm. The peak corresponding to the terminal methyl carbon of pentadecyl chain appeared at 14.23 ppm.

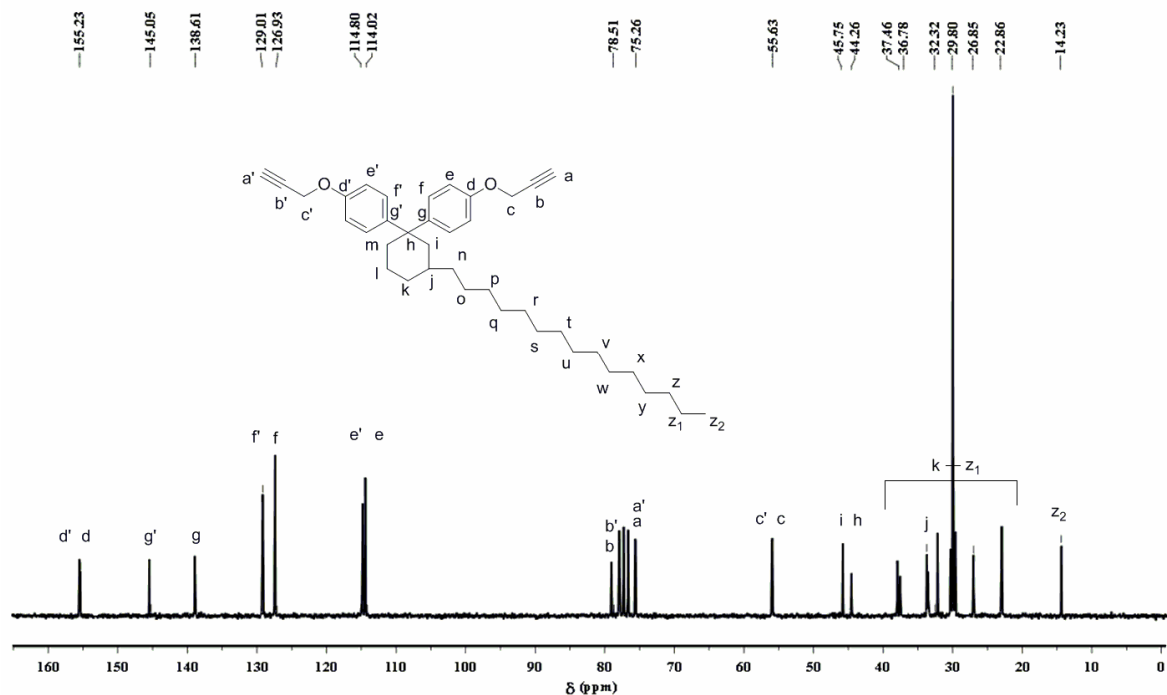


Figure 7.7:  $^{13}\text{C}$ -NMR spectrum of 1,1-bis[4-(2-propynyloxy)phenyl]-3-pentadecylcyclohexane ( $\text{CDCl}_3$ )

The  $^{13}\text{C}$ -DEPT spectrum of BPC15PT is represented in Figure 7.8. The peaks corresponding to methine carbons marked as a, a', e, e', f, f', j and z<sub>2</sub> appeared in negative phase while the peaks corresponding to methylene carbons c, c', i, k-z<sub>1</sub> were observed in positive phase.

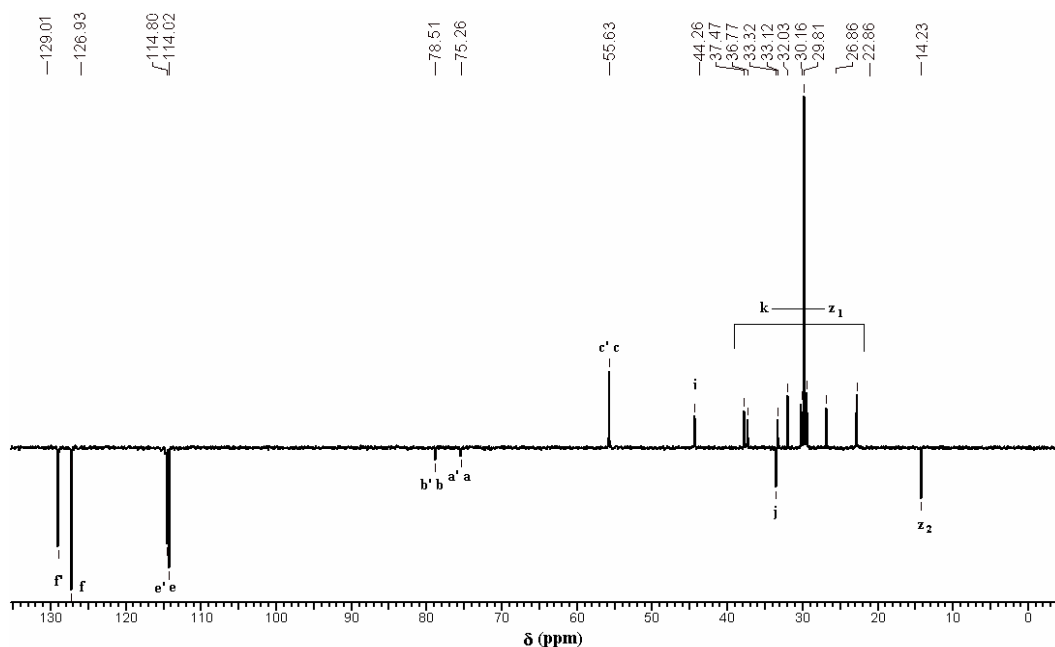
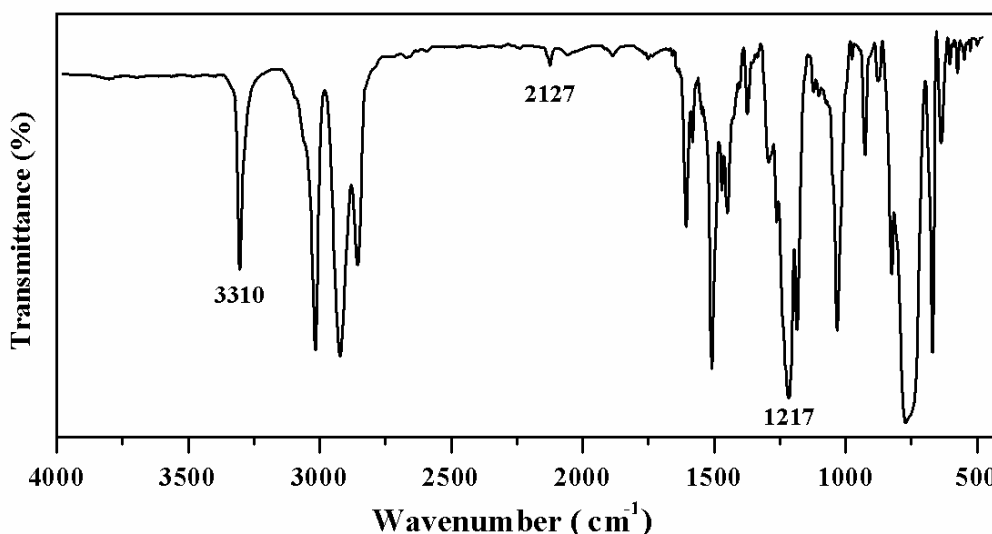


Figure 7.8:  $^{13}\text{C}$ -DEPT NMR spectrum of 1,1-bis[4-(2-propynyloxy)phenyl]-3-pentadecylcyclohexane ( $\text{CDCl}_3$ ).

### 7.4.3 Synthesis and characterization of 1,1-bis[4-(2-propynyloxy)phenyl] decahydro naphthalene (BPDCPT)

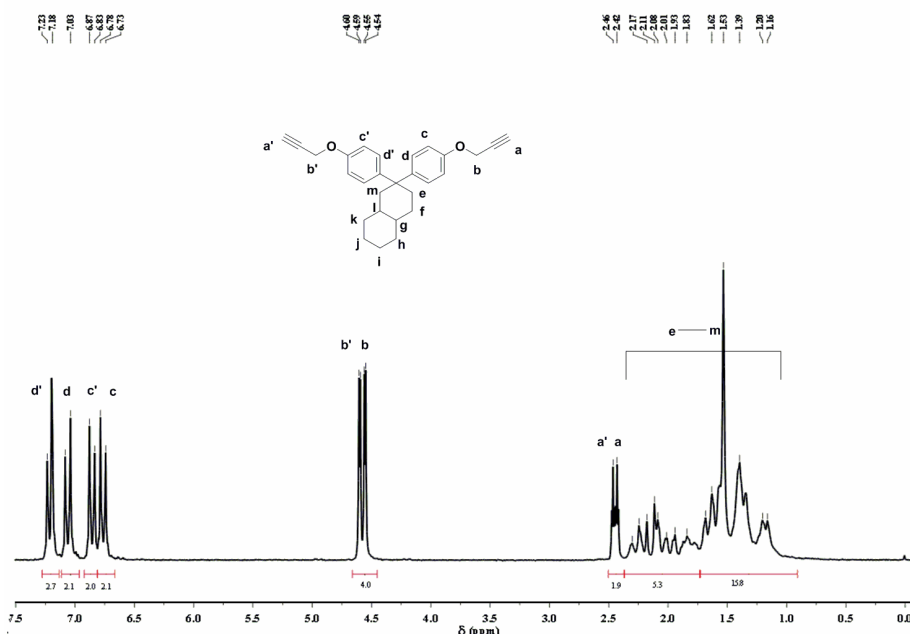
Starting from 1,1-bis(4-hydroxyphenyl) decahydronaphthalene (BPDC), 1,1-bis[4-(2-propynyloxy) phenyl] decahydronaphthalene (BPDCPT) was synthesized (yield = 92%) as described in section 7.3. The product was characterized by FTIR,  $^1\text{H-NMR}$ , and  $^{13}\text{C-NMR}$  spectroscopy.

IR spectrum of BPDCPT is reproduced in **Figure 7.9**. The  $\equiv\text{C-H}$ ,  $-\text{C}\equiv\text{C}-$  and  $-\text{C-O-C}-$  stretching were observed at 3310, 2127, and 1217  $\text{cm}^{-1}$ , respectively.



**Figure 7.9:** IR spectrum of 1,1-bis[4-(2-propynyloxy)phenyl] decahydronaphthalene

**Figure 7.10** represents  $^1\text{H-NMR}$  spectrum of BPDCPT alongwith peak assignments. As observed for BPDC; the precursor bisphenol, the two phenyl rings are magnetically non-equivalent. Aromatic protons (c, c', d and d') therefore appeared as four sets of doublet. Aromatic protons c, c' (*ortho* to propynyloxy group) displayed a doublet at 6.76 (axial phenyl ring) and 6.85 ppm (equatorial phenyl ring), respectively. The doublets corresponding to aromatic protons d, d' (*meta* to propynyloxy group) were observed at 7.05 (axial phenyl ring) and 7.20 ppm (equatorial phenyl ring). The protons b and b' appeared as two doublets at 4.55 and 4.60 ppm while protons a and a' corresponding to acetylene group exhibited singlets at 2.42 (axial ring) and 2.46 (equatorial ring) ppm. The peaks observed in the range 1.16-2.17 ppm are assignable to methine and methylene protons of decahydronaphthalene ring.



**Figure 7.10 :**  $^1\text{H-NMR}$  spectrum of 1,1-bis[4-(2-propynyloxy)phenyl] decahydronaphthalene ( $\text{CDCl}_3$ )

**Figure 7.11** represents  $^{13}\text{C-NMR}$  spectrum of BPDCPT alongwith peak assignments. The formation of BPDCPT was confirmed by the characteristic peak at 55.65 and 55.69 ppm corresponding to methylene carbons (labeled as c and c') of propynyloxy group. The peaks corresponding to aromatic carbons d, d' (attached to propynyloxy group) appeared at 155.23 (axial ring) and 155.34 ppm (equatorial ring). Aromatic carbons e, e' (*ortho* to propynyloxy group) displayed signals at 114.32 (axial phenyl ring) and 114.62 ppm (equatorial phenyl ring) while carbons *meta* to propynyloxy group (marked as f, f') displayed signals at 127.16 (axial phenyl ring) and 128.82 (equatorial phenyl ring) ppm. The peaks observed at 138.66 and 145.24 ppm could be assigned to aromatic carbons (g, g') *para* to propynyloxy group. The carbons designated as a, a' and b, b' exhibited signals in the range 75.45 -78.91 ppm. The peaks due to methine and methylene carbons of decahydronaphthalene moiety appeared in the range 21.14 - 36.61 ppm.

$^{13}\text{C-DEPT}$  spectrum (**Figure 7.12**) further confirmed the assignments. The signals corresponding to methine carbons a, a', e, e' f, f' k and p appeared in negative phase while the signals corresponding to methylene carbons c, c' i, j, l, m, n, o, and q appeared in positive phase.

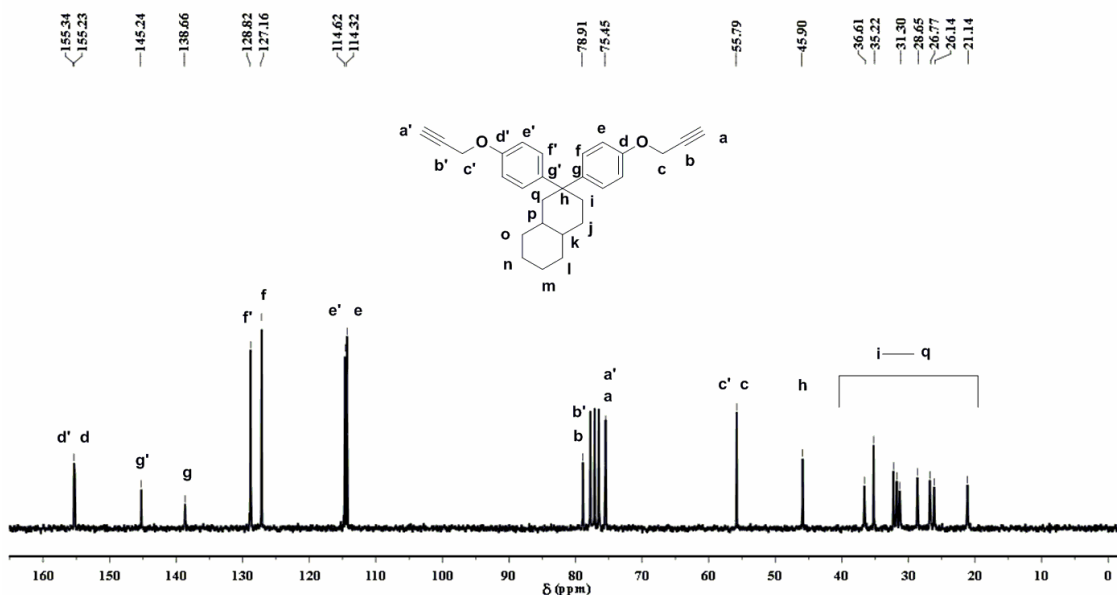


Figure 7.11 :  $^{13}\text{C}$ -NMR spectrum of 1,1-bis[4-(2-propynyloxy)phenyl] decahydronaphthalene ( $\text{CDCl}_3$ )

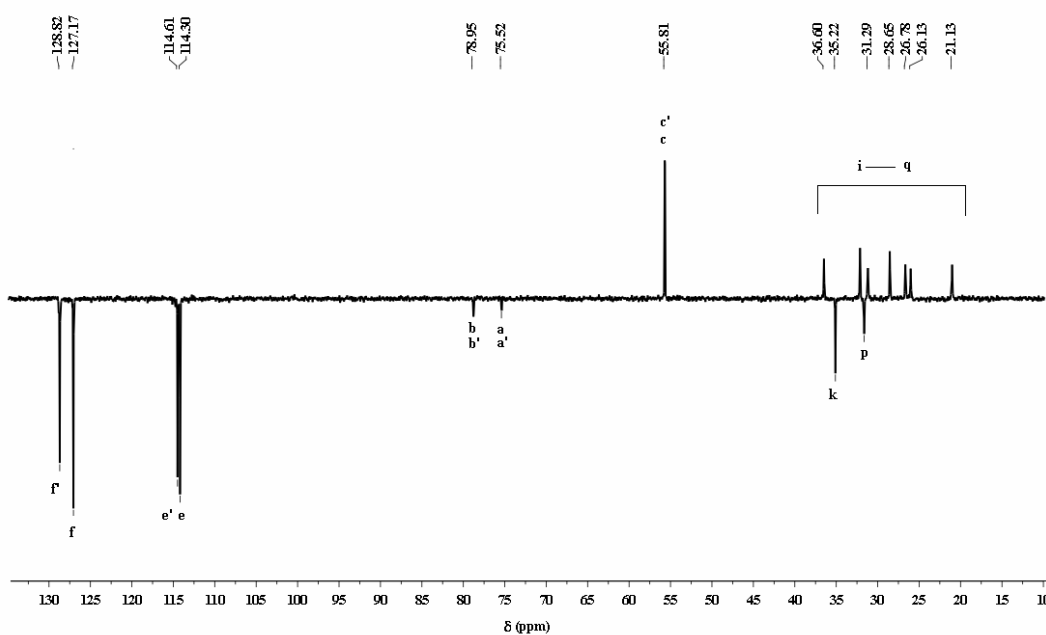


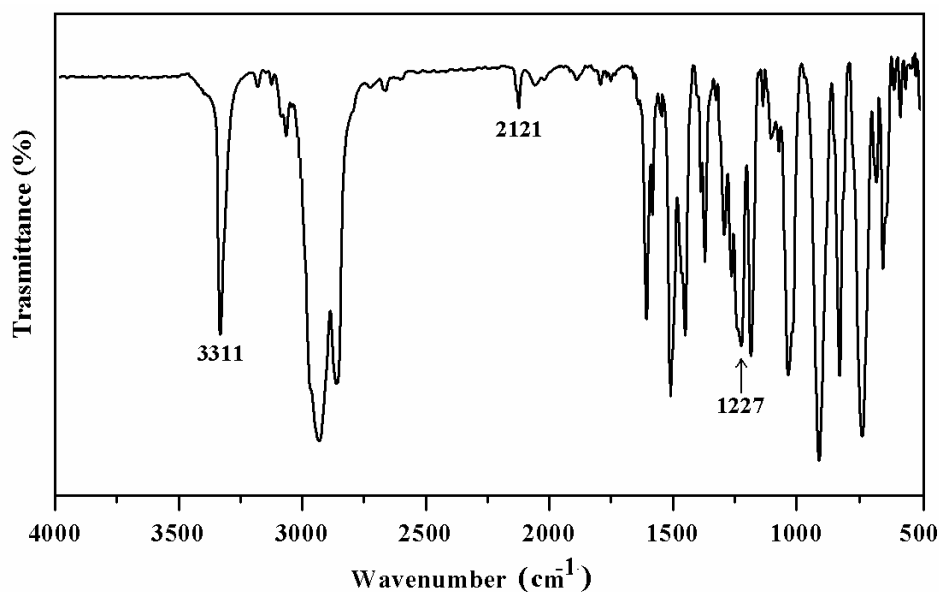
Figure 7.12 :  $^{13}\text{C}$ -NMR spectrum of 1,1-bis[4-(2-propynyloxy)phenyl] decahydronaphthalene ( $\text{CDCl}_3$ )

#### 7.4.4 Synthesis and characterization of 1,1-bis[4-(2-propynyloxy)phenyl]-4-perhydrocumyl cyclohexane (BPPCPPT).

1,1-Bis(4-hydroxyphenyl)-4-perhydrocumylcyclohexane (BPPCP), was propargylated as described in section 7.3 using propargyl bromide to afford 1,1-bis[4-(2-propynyloxy) phenyl]-4-perhydrocumylcyclohexane (BPPCPPT) in high yield (94 %)

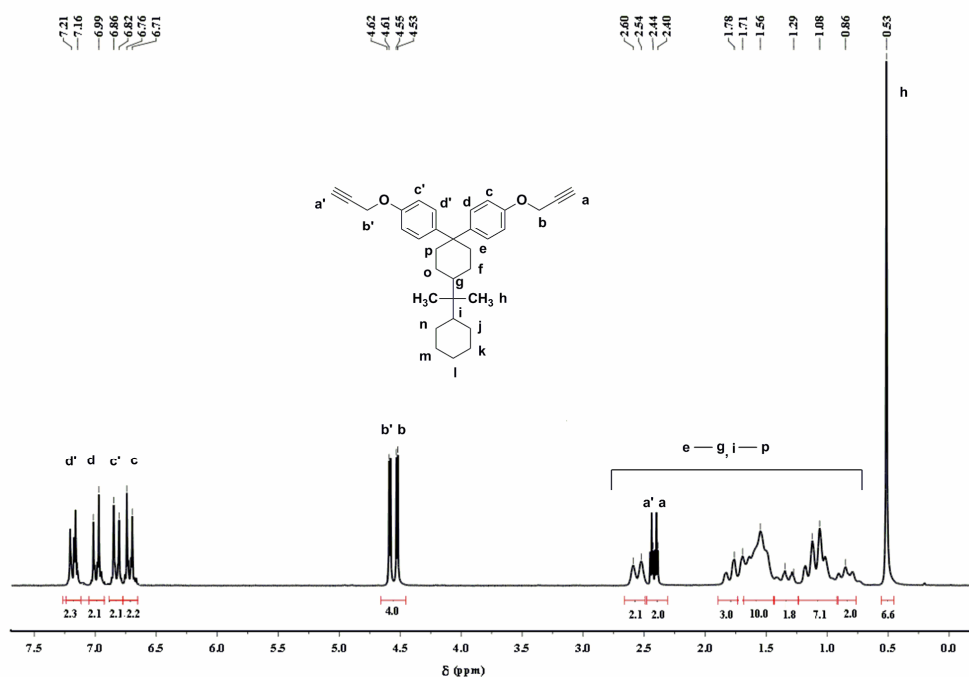
The product BPPCPPT was characterized by FTIR,  $^1\text{H}$ -NMR, and  $^{13}\text{C}$ -NMR spectroscopy.

**Figure 7.13** represents IR spectrum of BPPCPPT. The  $\equiv\text{C-H}$  and  $-\text{C}\equiv\text{C}-$  stretching vibrations were observed at  $3311$  and  $2121\text{ cm}^{-1}$ , respectively. The stretching corresponding to  $-\text{C-O-C}-$  vibration was observed at  $1217\text{ cm}^{-1}$ .



**Figure 7.13 :** IR spectrum of 1,1-bis[4-(2-propynyloxy)phenyl]-4-perhydrocumyl cyclohexane

**Figure 7.15** represents  $^1\text{H-NMR}$  spectrum of BPPCPPT. Aromatic protons (c, c', d and d') being magnetically nonequivalent, appeared in four sets of doublets. Aromatic protons c and c' (*ortho* to propynyloxy group) displayed doublets at 6.74 (axial phenyl ring) and 6.84 ppm (equatorial phenyl ring). Aromatic protons d and d' (*meta* to propynyloxy group) appeared as doublets at 7.01 (axial phenyl ring) and 7.19 ppm (equatorial phenyl ring). The protons of methylene group (labeled as b and b') exhibited doublets at 4.54 (axial phenyl ring) and 4.62 ppm (equatorial phenyl ring) while protons a and a' corresponding to acetylene group exhibited singlets at 2.40 (attached to axial phenyl ring) and 2.44 ppm (attached to equatorial phenyl ring) ppm. The methylene and methine protons of cyclohexyl ring displayed peaks in the range 0.86 – 2.60 ppm. A singlet observed at 0.53 ppm is assignable to methyl protons.



**Figure 7.14 :**  $^1\text{H-NMR}$  spectrum of 1,1-bis[4-(2-propynyloxy)phenyl]-4-perhydrocumyl cyclohexane ( $\text{CDCl}_3$ )

$^{13}\text{C-NMR}$  spectrum of BPPCPT along with peak assignments is reproduced in **Figure 7.15**. The peaks appeared at 155.21, and 155.31 ppm could be assigned to aromatic carbons d, d' (attached to propynyloxy group). The signals corresponding to aromatic carbons e, e' (*ortho* to propynyloxy group) were observed at 114.29 (axial phenyl ring) and 115.02 ppm (equatorial phenyl ring). Aromatic carbons marked as f, f' (*meta* to propynyloxy group) displayed peaks at 127.43 (axial phenyl ring) and 129.05 ppm (equatorial phenyl ring). The peaks observed at 138.48 and 145.27 ppm could be due to aromatic carbons g, g' (*para* to propynyloxy group). The carbons a, and a' of terminal acetylene group exhibited peaks at 75.28 (attached to axial phenyl ring) and 75.32 (attached to equatorial phenyl ring) ppm while carbons b, b' displayed peak at 78.91 ppm. The carbons c and c' displayed signals at 55.81 (attached to axial phenyl ring) and 55.88 ppm (attached to equatorial phenyl ring). The signals appeared in the range 23.28 - 44.89 ppm could be due to carbons (-C, -CH and -CH<sub>2</sub>) of perhydrocumylcyclohexyl moiety. The peak corresponding to methyl group appeared at 20.59 ppm.

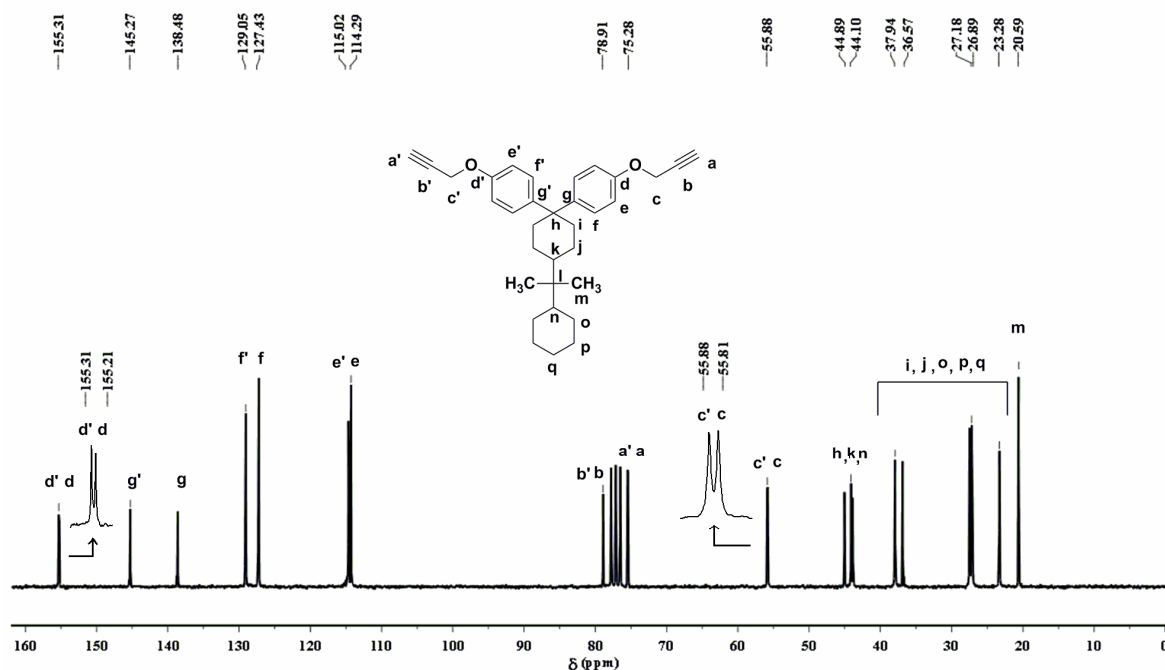


Figure 7.15 :  $^{13}\text{C}$ -NMR spectrum of 1,1-bis[4-(2-propynyloxy)phenyl]-4-perhydrocumyl cyclohexane ( $\text{CDCl}_3$ )

The structure of BPPCPPT was also supported by  $^{13}\text{C}$ -DEPT NMR spectrum (Figure 7.16). The appearance of peaks corresponding to methine carbons a, a', e, e', f, f', k and n and methyl carbon m in negative phase confirmed the assignments. The signals corresponding to methylene carbons c, c', i, j, o, p and q were observed in positive phase.

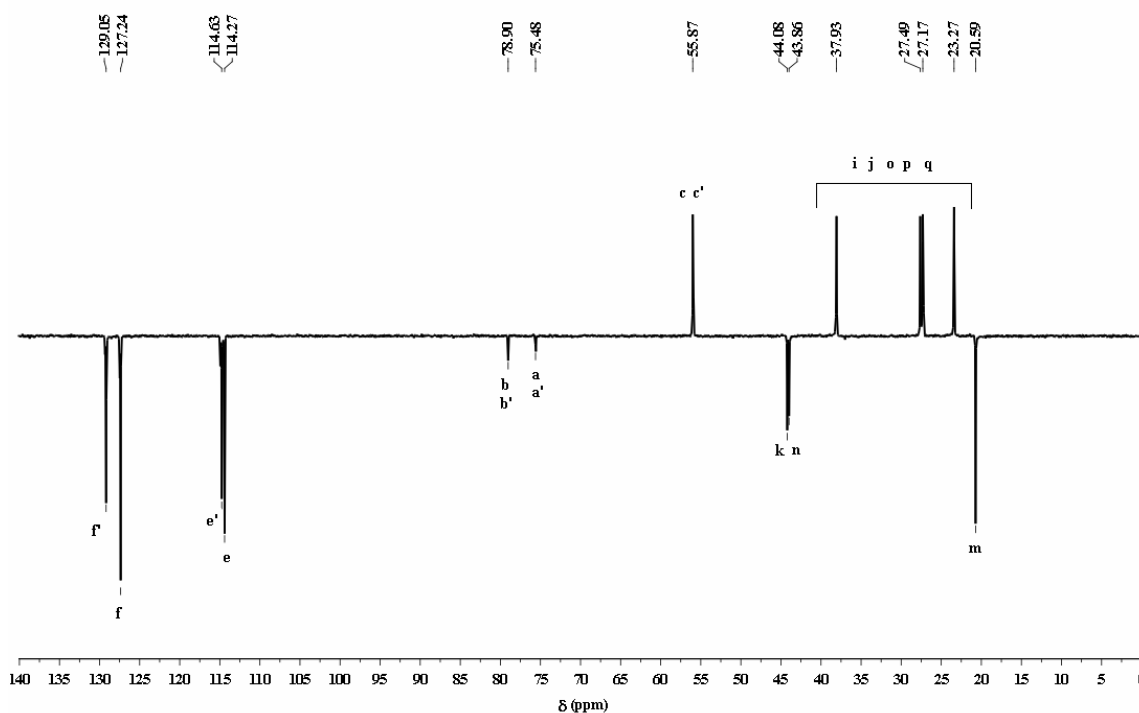


Figure 7.16 :  $^{13}\text{C}$ -DEPT NMR spectrum of 1,1-bis[4-(2-propynyloxy)phenyl]-4-perhydrocumyl cyclohexane ( $\text{CDCl}_3$ )



## 7.4.5 Synthesis of 2,2-bis[4-(2-propynyloxy) phenyl]propane (BPAPT)

As a reference for studying structure-property relationship, a bispropargyl ether of bisphenol-A was synthesized. The product BPAPT was characterized by FTIR,  $^1\text{H-NMR}$ , and  $^{13}\text{C-NMR}$  spectroscopy. **Figure 7.17** represents IR spectrum of BPAPT while  $^1\text{H-NMR}$ , and  $^{13}\text{C-NMR}$  spectra are reproduced in **Figure 7.18** and **7.19**, respectively alongwith peak assignments. All the assignments are in good agreement with the reported data<sup>2</sup>.

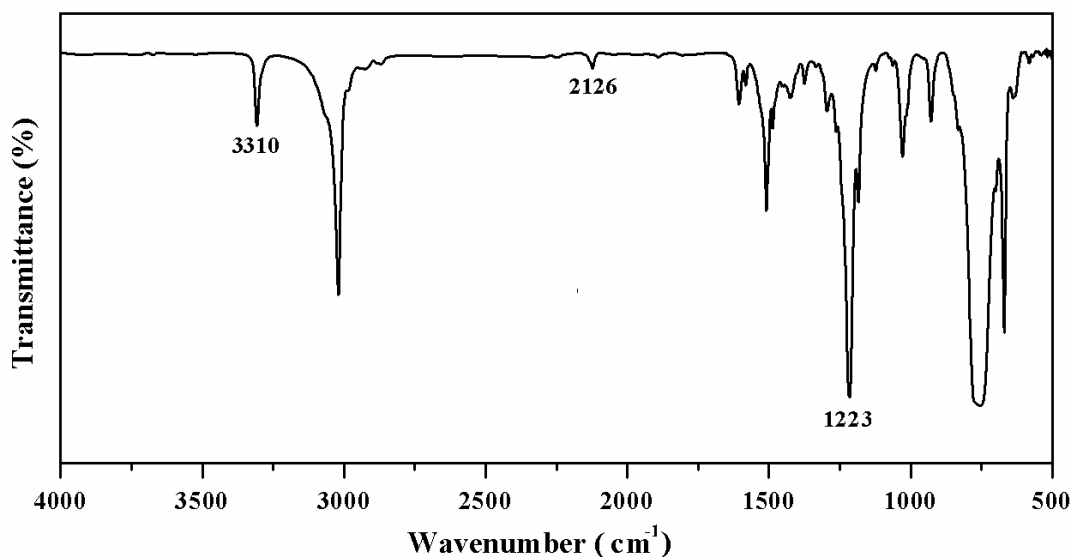
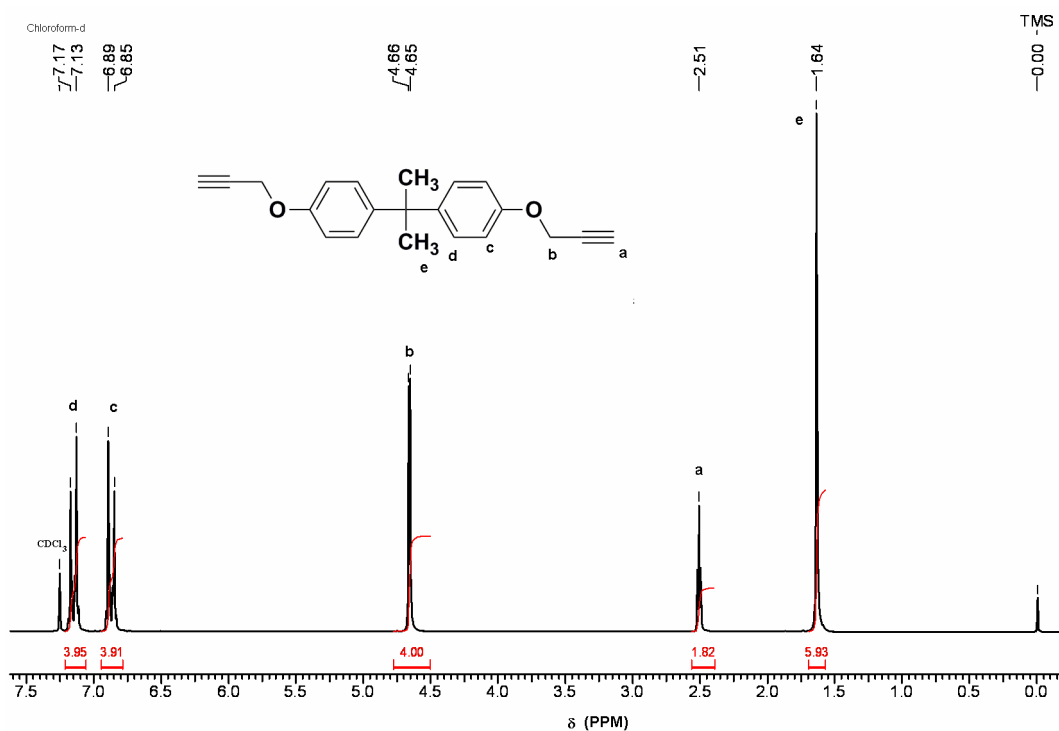


Figure 7.17 : IR spectrum of 2,2-bis[4-(2-propynyloxy) phenyl]propane

Figure 7.18:  $^1\text{H-NMR}$  spectrum of 2,2-bis[4-(2-propynyloxy) phenyl]propane ( $\text{CDCl}_3$ )

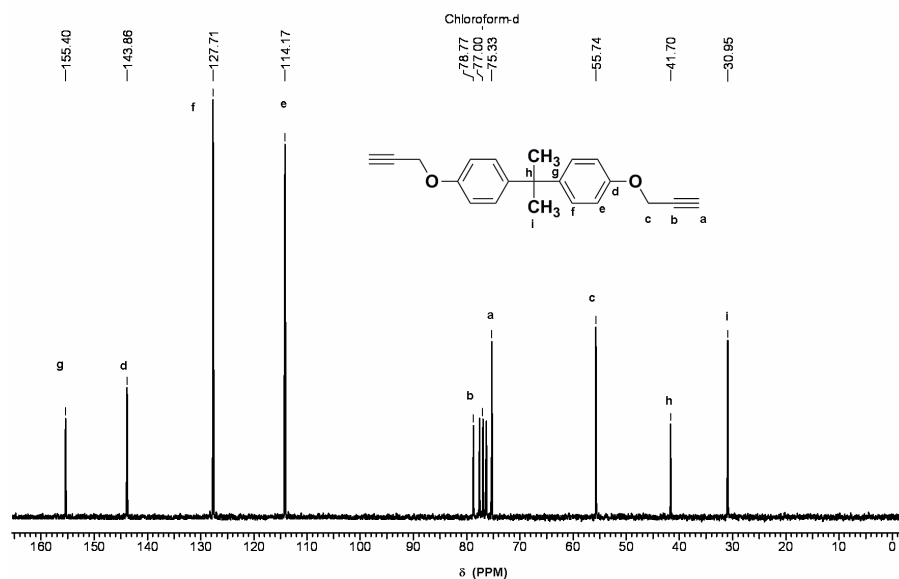


Figure 7.19 :  $^{13}\text{C}$ -NMR spectrum of 2,2-bis[4-(2-propynyloxy)phenyl]propane ( $\text{CDCl}_3$ )

#### 7.4.6 Cure kinetics of bispropargyl ethers

The cure characterization of the bispropargyl ethers was studied by DSC analysis in nonisothermal mode. The DSC curves of bispropargyl ethers are represented in **Figure 7.20**.

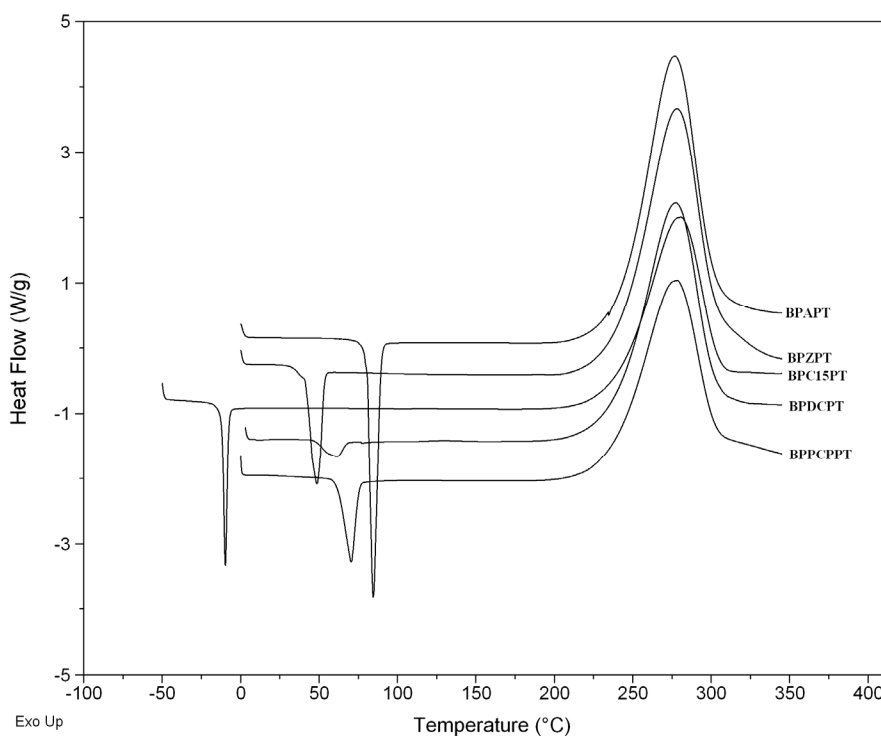


Figure 7.20 : DSC thermograms of bispropargyl ethers containing cardo / (cyclo)aliphatic moiety.

*Nair et.al*<sup>10</sup> studied the cure kinetics of bispropargyl ethers in catalyzed and uncatalyzed mode. The authors reported that in uncatalysed conditions, both the Claisen rearrangement and the subsequent curing reaction (**Scheme 7.1**) occur within a single exotherm in the range 200-350 °C.

Under catalytic conditions ( $\text{AgBF}_4$ ) the authors observed two separate exotherms for these two types of reactions. The exotherm representing Claisen rearrangement reaction occurred at around  $125^\circ\text{C}$  and the second exotherm corresponding to curing started around  $225^\circ\text{C}$ .

In the present case, the cure kinetics was studied in uncatalyzed conditions. From the DSC curves (**Figure 7.20**), it was observed that the cure onsets above  $230^\circ\text{C}$  and reaches to completion around  $350^\circ\text{C}$  with the total heat of curing in the range  $410 - 465\text{ kJ/mol}$ . The melting point and the details of cure profiles of bispropargyl ethers BPAPT, BPZPT, BPC15PT, BPDCPT and BPPCPPT are collected in **Table 7.3**.

**Table 7.3 : Melting point and cure profile of bispropargyl ethers**

Sr. No.	Monomers	Melting Point ( $^\circ\text{C}$ )		DSC Profile			$\Delta\text{H}$ (kJ/mol)
		A	B	To ( $^\circ\text{C}$ )	Tp ( $^\circ\text{C}$ )	Tf ( $^\circ\text{C}$ )	
1		88	84-85	242	276	330	413
2		52	49-50	240	278	346	415
3		-10	Not measured	240	280	313	454
4		62	Not measured	240	277	325	435
5		72	71-72	237	277	348	464

To – cure onset (initiation) temperature

A - From DSC

Tp – Maximum cure (peak) temperature

B - By open capillary method

Tf – Final cure temperature

The activation parameters were calculated by two different methods *viz*; Kissinger method and Coats-Redfern method.

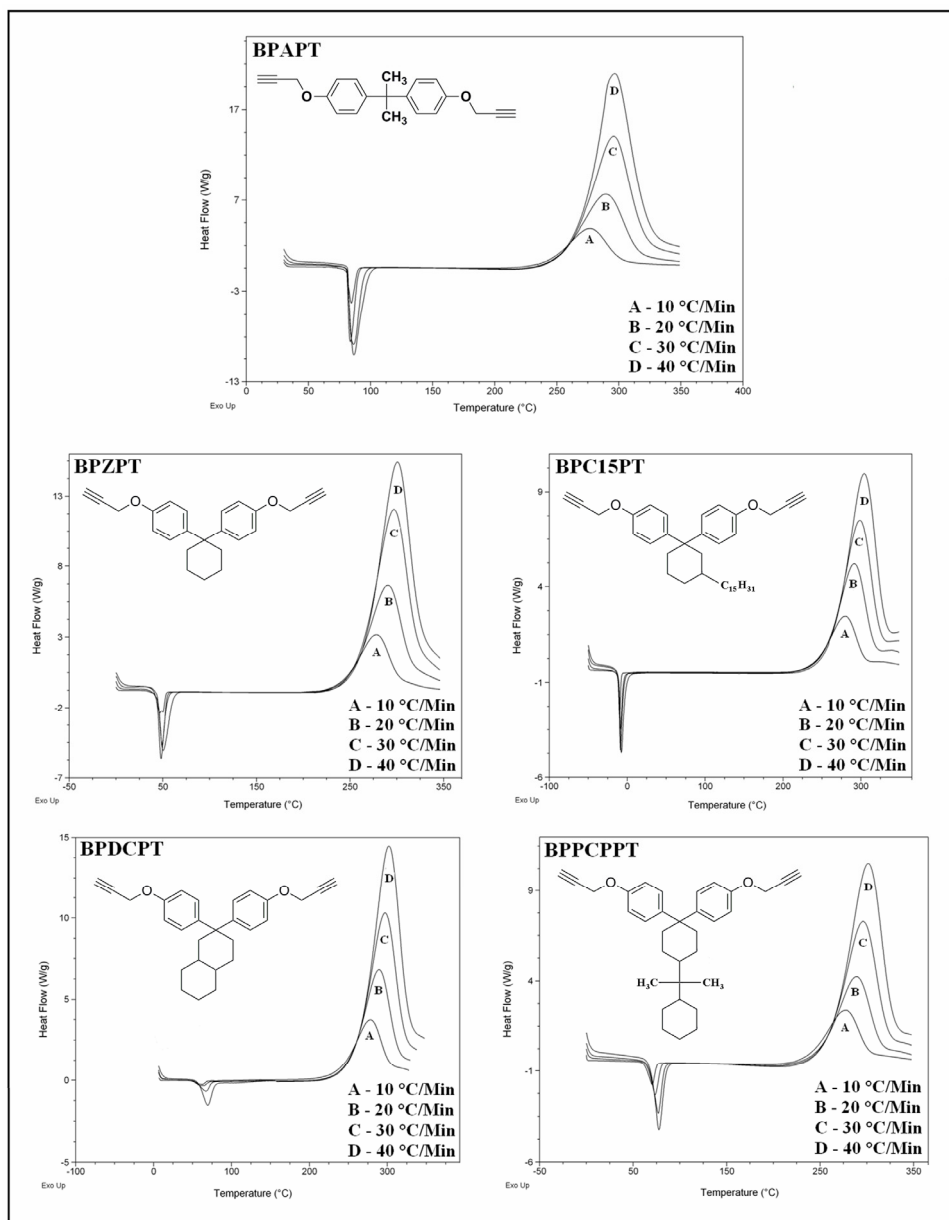
#### 7.4.6.1. Activation parameters using Kissinger method<sup>21</sup>

This method is based on shift in maximum peak temperature and independent of the order of reaction. The activation parameters can be calculated using equation 2:

$$\frac{d[\ln(\phi/T_p^2)]}{d[1/T_p]} = -\frac{E}{R} \quad (2)$$

where  $T_p$  is the maximum (peak) temperature of curing exotherm (in Kelvin),  $\phi$  is heating rate,  $E$  is the activation energy and  $R$  is the gas constant.

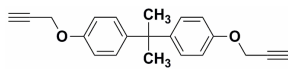
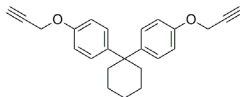
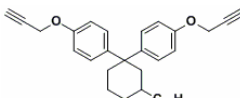
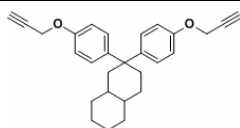
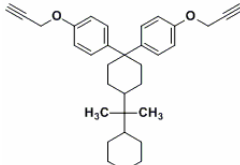
**Figure 7.21** represents DSC thermograms of bispropargyl ethers under study at four heating rates *viz*; 10, 20, 30 and 40 °C / min.



**Figure 7.21 :** DSC thermograms of bispropargyl ethers BPAPT, BPZPT, BPC15PT, BPDCPT and BPPCPPT at different heating rates.

Peak temperatures of curing of bispropargyl ethers at different heating rates are collected in **Table 7.4**.

**Table 7.4: Peak temperatures of curing of bispropargyl ethers under study.**

Sr. No	Monomer	Structure	Peak Temperature (°C) At Heating Rate (°C / Min)			
			10	20	30	40
1.	BPAPT		276	289	295	297
2.	BPZPT		278	290	297	300
3.	BPC15PT		280	292	299	303
4.	BPDCPT		277	288	296	301
5.	BPPCPPT		277	289	296	301

Activation energy  $E$  was calculated from the slope of the linear plot of  $\ln [\phi / T_p^2]$  against  $1/T_p$ . The Kissinger plots for various bispropargyl ethers are represented in **Figure 7.22** and activation energy and frequency factor calculated from the plot for bispropargyl ethers are collected in **Table 7.5**.

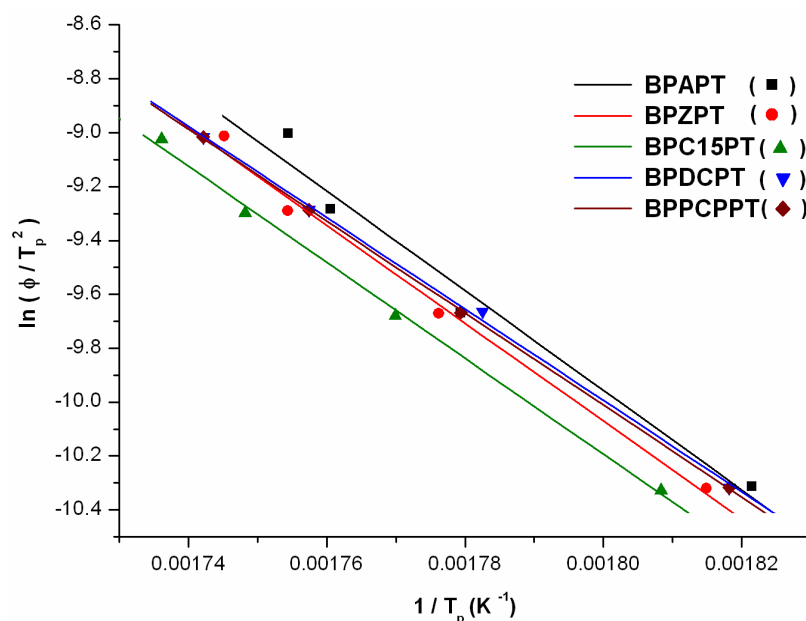


Figure 7.22 : Kissinger plots for the determination of kinetic constants

#### 7.4.6.2 Activation parameters using Coats-Redfern method<sup>22</sup>

Under nonisothermal conditions, the rate of reaction can be expressed by equation 3:

$$\frac{d\alpha}{dT} = (A/\phi)e^{-E/RT}(1-\alpha)^n \quad (3)$$

where  $\alpha$  is fractional conversion at temperature  $T$ ,  $\phi$  is heating rate,  $E$  is activation energy,  $A$  is Arrhenius frequency factor,  $R$  is gas constant, and  $n$  is the order of reaction.

In the present study, Coats-Redfern equation<sup>22</sup> (equation 4) was used to calculate the activation parameters.

$$\ln\{g(\alpha)/T^2\} = \ln\{AR/\phi E(1-2RT/E)\} - E/RT \quad (4)$$

where  $g(\alpha) = [1-(1-\alpha)^{1-n}]/(1-n)$ ; for  $n = 1$ ,  $g(\alpha) = -\ln(1-\alpha)$ .

To calculate kinetic parameters, fractional conversion ' $\alpha$ ' was calculated from fractional enthalpy of reaction using equation 1. The kinetic plots assuming different order of reaction ( $n = 0.5, 1, 1.5, 2, 2.5$  and  $3$ ) were constructed using the Coats-Redfern equation and the best fit furnished the order of reaction ' $n$ '. **Figure 7.23** represents plots for the determination of order curing reaction of bispropargyl ethers under study.

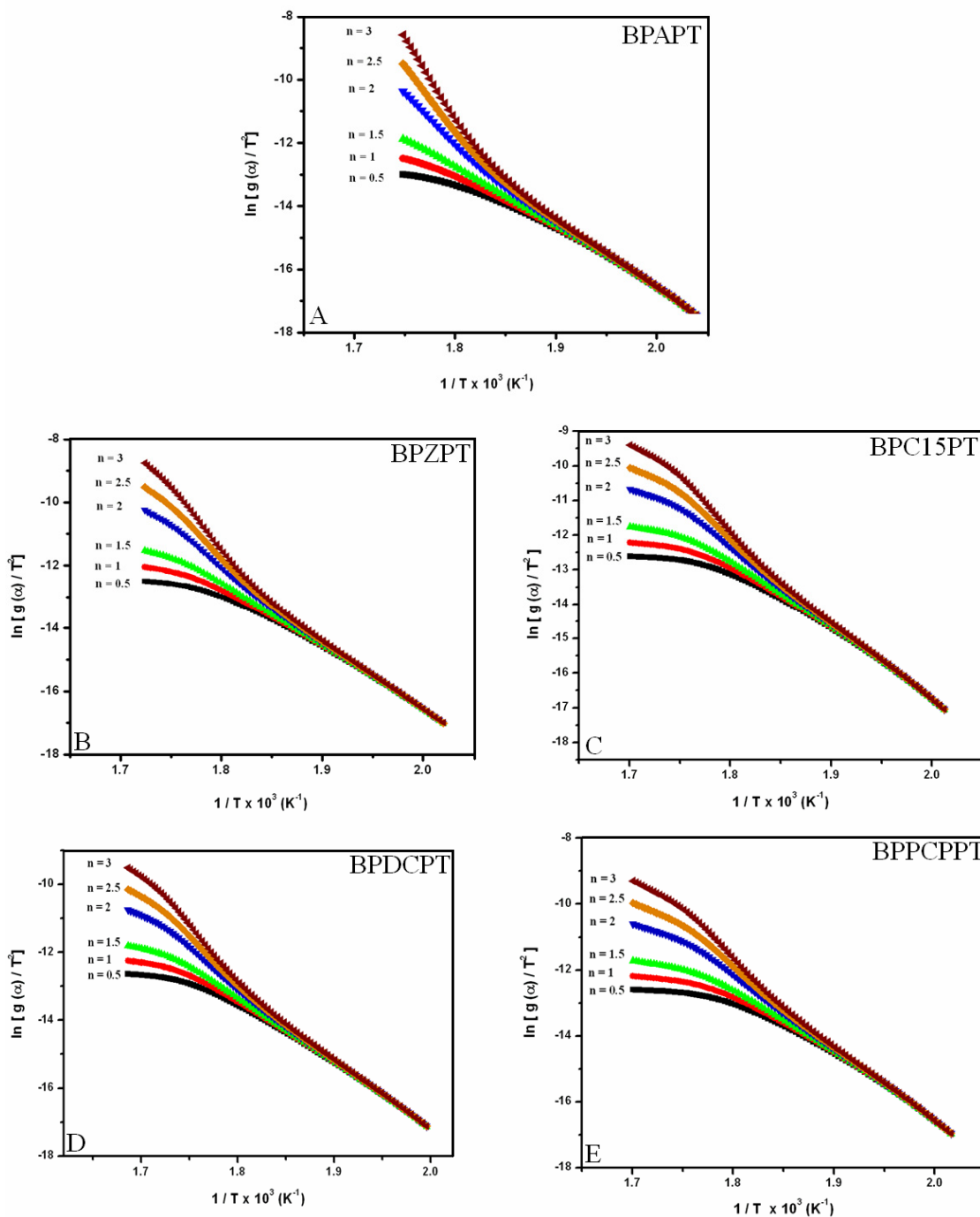
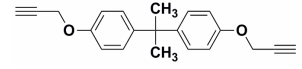
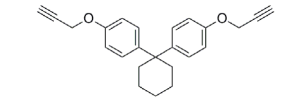
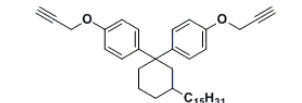
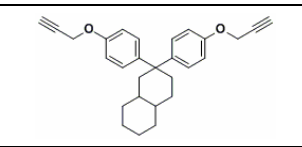
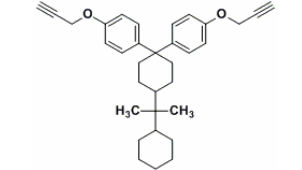


Figure 7.23: Determination of order of curing reaction of bispropargyl ethers by Coats-Redfern equation.

The kinetic constants of curing of bispropargyl ethers under study calculated from these curves are summarized in **Table 7.5**.

**Table 7.5: Kinetic parameters of bispropargyl ether curing**

Sr. No	Monomer	Structure	Kissinger Method		Coats-Redfern Method	
			Ea (kJ/mol)	ln A (s <sup>-1</sup> )	Ea (kJ/mol)	ln A (s <sup>-1</sup> )
1.	BPAPT		154	23.33	182	26.81
2.	BPZPT		151	22.69	176	25.78
3.	BPC15PT		148	21.88	177	26.12
4.	BPDCPT		141	20.55	171	24.54
5.	BPPCPPT		142	20.75	175	25.52

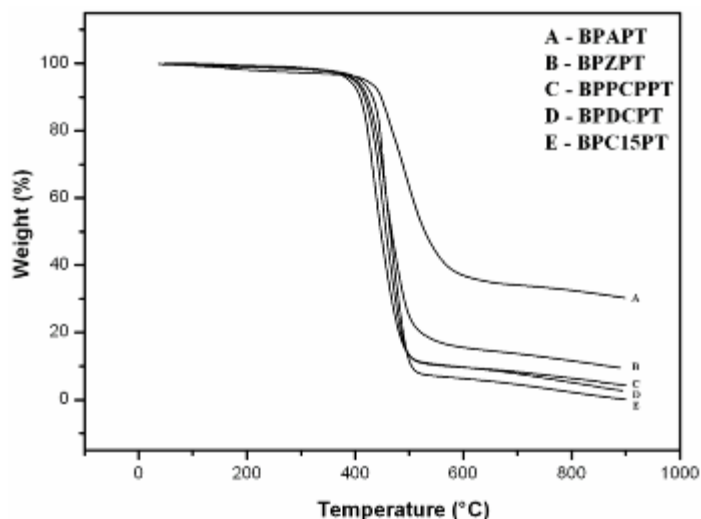
The frequency parameters obtained from Kissinger method and Coats-Redfern method are in the same range for all the bispropargyl ethers under study and the difference is practically negligible. The values for activation energy computed using Coats-Redfern equation are normally higher than Kissinger method due to the variance in the assumptions in both the methods. The introduction of cycloaliphatic “cardo” group into bispropargyl ether practically does not alter the kinetics of cure (as compared to the kinetics of bispropargyl ether based on bisphenol-A).

#### 7.4.7 Thermal stability of cured network

The cured resins of bispropargyl ether in general, possess good thermal stability. The stability has been reported to depend on the backbone (bisphenol)<sup>1,10</sup>.

In the present case, the relative thermal stabilities of the cured resins were compared by comparison of the temperature of 10 % weight loss and char yield at 800 °C. **Figure 7.24** represents weight loss of propargyl-terminated resins with respect to temperature. All the resins showed single stage decomposition. The temperature at 10 % weight loss was observed the range 410 - 448 °C indicating their good thermal stability.

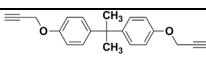
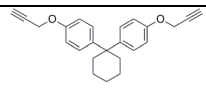
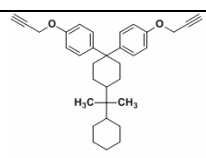
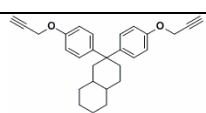
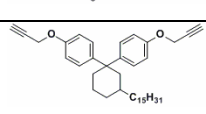




**Figure 7.24 : TG curves of propargyl terminated resins**

Amongst the series, the degradation of cured BPC15PT resin follows with higher weight loss rate in the temperature range from 450 °C to around 500 °C. The char yield at 800 °C in case of cured BPC15PT was observed to be 3 % which is lower than other resins. The lower thermal stability of cured bispropargyl ethers containing cycloaliphatic moiety than that of bisphenol A based resins could be due to higher aliphatic content. The data indicates that incorporation of cycloaliphatic “cardo” group into bispropargyl backbone hampers the thermal stability of their cured resins. The temperature of 10 % mass loss and the char yield at 800 °C are summarized in **Table 7.6**.

**Table 7.6: Thermal characterization of propargyl terminated resins**

Sr. No	Resin	Monomer Structure	T <sub>10</sub> (°C)	Char Yield at 800 °C (%)
1.	BPAPT		448	32
2.	BPZPT		433	12
3.	BPPCPPT		424	7
4.	BPDCPT		417	6
5.	BPC15PT		410	3

## 7.5 Conclusions:

1. Three new bispropargyl ethers *viz*;

i) 1,1-Bis[4-(2-propynyloxy) phenyl]-3-pentadecylcyclohexane,

ii) 1,1-Bis[4-(2-propynyloxy) phenyl]decahydronaphthalene, and

iii) 1,1-Bis[4-(2-propynyloxy) phenyl]-4-perhydrocumylcyclohexane

containing cycloaliphatic “cardo” group were synthesized by reacting corresponding bisphenols with propargyl bromide in the presence of potassium carbonate using acetone as a solvent.

2. The curing of all the bispropargyl ethers under present study occurred within a single exotherm in the temperature range 237 – 350 °C.

3. The activation energy of the cure kinetics studied in uncatalysed nonisothermal mode using DSC was in the range of 141-154 kJ/mol by Kissinger method and 171-182 kJ/mol by Coats-Redfern method for all bispropargyl ethers under study. The study indicated that the incorporation of cycloaliphatic “cardo” group into bispropargyl ether backbone practically does not affect the cure kinetics.

4.  $T_{10}$  values of cured bispropargyl ethers containing cycloaliphatic “cardo” group were in the range 410 - 435 °C indicating good thermal stability of the cured network. However, the weight residue at 800 °C of cured bispropargyl ethers containing cycloaliphatic “cardo” groups was lower than that of cured network of bispropargyl ether based on bisphenol-A due to higher aliphatic content.

**References:**

1. Dirlikov, S. K.; Feng, Y. *Polym. Mater. Sci. Eng.* **1988**, 59, 990.
2. Dirlikov, S. K. *High Perform. Polym.*, **1990**, 2, 67.
3. Dirlikov, S. K. *Polym. Mater. Sci. Eng.* **1990**, 62, 603
4. Nair, C.P.R. *Prog. Polym. Sci.*, **2004**, 29, 401
5. Douglas, W. E.; Overend, A.S. *31<sup>st</sup> IUPAC Macromolecular Symposium*, **1987 (June/July)**, Paper I/SL/46, Merseburg, Germany.
6. Douglas, W. E.; Overend, A.S. *Eur. Polym. J.* **1991**, 27, 1279.
7. Dirlikov, S. K.; Feng, Y. *Polym. Prepr.*, **1991**, 32, 363.
8. Grenier-Loustalot, M. F.; Sanglar, C. *High Perform. Polym.* **1996**, 8, 341.
9. Dirlikov, S. K.; Feng, Y. *Polym. Prep.* **1990**, 31, 322.
10. Nair, C.P.R.; Bindu, R.L.; Krishnan, K.; Ninan, K. N. *Eur. Polym. J.* **1999**, 35, 235.
11. Toda, A. (Mitsubishi Chemical Industries) *Japan Kokai Tokkyo Koho JP10291952 A2* **1998**.
12. Langlois, D.A.; Benicewicz, B.C.; Douglas, E.P. *Chem. Mater.* **1998**, 10, 3393.
13. Agag, T.; Takeichi, T. *Macromolecules* **2001**, 34, 7257.
14. Chernykh, A.; Agag, T.; Ishida, H. *Polymer*, **2009**, 50, 382.
15. Bindu, R. L.; Nair, C.P.R.; Ninan, K.N. *Polym. Int.* **2001**, 50, 651.
16. Prime R. B. In *Thermal Characterization of Polymeric Materials*. Turi, E.A. ED **1981**, Academic, New York, p 435.
17. Hay, A. S.; Bolon, D. A.; Leimer, K. R.; Clark, R. F. *Polym. Lett.*, **1970**, 8, 97.
18. Hay, A. S. *U.S.Patent* 3,594,175 **1971**.
19. Picklesimer, L. G. *U.S.Patent* 4,226,800 **1980**.
20. Inbasekaran, M. N.; Dirlikov, S. K. *U.S.Patent* 4,885,403 **1989**
21. Kissinger, H. E. *J. Res. Nat. Bur. Stand.*, **1956**, 57, 217.
22. Coats, A.W.; Redfern, J.P. *Nature*, **1964**, 201, 68.

# Chapter 8

Summary and Conclusions

## 8.1 Summary and Conclusions

Thermosetting resins *viz*; cyanate ester resins, epoxy resins, bismaleimides, propargyl-terminated resins, polybenzoxazines, etc., have been useful in many industries including aerospace, communication, construction, leisure goods and transportation. The properties such as excellent mechanical strength, high glass transition temperature, low dielectric constant, excellent metal adhesion, and compatibility with carbon fiber reinforcements make these thermosets useful in these applications. These properties can be further tuned *via* tailoring / proper selection of the precursor bisphenols.

The major objective of the current research was to design and synthesize new cyanate ester (CE) monomers containing cycloaliphatic “cardo” group and/or flexible alkyl chain based on corresponding bisphenols. The new CE monomers were designed in order to result into polycyanurates with lower percentage moisture absorption by virtue of the presence of cycloaliphatic “cardo” group. The synthetic efforts were thus directed towards structural modifications by introducing i) cycloaliphatic “cardo” group, ii) methyl groups *ortho* to cyanate functionality, and iii) alkylene spacer.

One of the approaches for pursuing the goal involved making use of 3-pentadecyl phenol, which in turn is obtainable from cashew nut shell liquid (CNSL) -a renewable resource material. The dual phenolic/ alkenyl nature of CNSL makes it an useful raw material for the synthesis of water-resistant resins and polymers. The other approaches involved the use of commercially available *p*-cumyl phenol and  $\beta$ -naphthol as a starting materials to introduce cycloaliphatic “cardo” group and adipic acid to incorporate alkylene spacer.

Starting from these raw materials, a variety of bisphenols containing cycloaliphatic “cardo” group and/or alkyl chain were synthesized using simple organic transformations. These bisphenols were then reacted with cyanogen bromide in the presence of triethylamine to yield corresponding CE monomers.

Thus, cycloaliphatic “cardo” group containing CE monomers *viz*;

1,1-Bis(4-cyanatophenyl)cyclohexane (BPZCN),

1,1-Bis(4-cyanatophenyl)-3-pentadecylcyclohexane (BPC15CN),

1,1-Bis(4-cyanatophenyl)decahydronaphthalene (BPDCCN),

1,1-Bis(4-cyanato-3-methylphenyl)decahydronaphthalene (DMBPDCCN),

1,1-Bis(4-cyanato-3,5-dimethylphenyl)decahydronaphthalene (TMBPDCCN),

1,1-Bis(4-cyanatophenyl)-4-perhydrocumylcyclohexane (BPPCPCN),

1,1-Bis(4-cyanato-3-methylphenyl)-4-perhydrocumylcyclohexane (DMBPPCPCN) and

1,1-Bis(4-cyanato-3,5-dimethylphenyl)-4-perhydrocumylcyclohexane (TMBPPCPCN)

were synthesized.

A new CE monomer containing alkylene spacer *viz*; 2,7-bis(4-cyanatophenyl)-2,7-dimethyloctane (BPC6CN) was synthesized *via* corresponding bisphenol starting from adipic acid.

Thus, total nine CE monomers were designed and synthesized. All the CE monomers except BPZCN, were synthesized for the first time.

The CE monomers and the intermediates involved in their synthesis were characterized by IR,  $^1\text{H-NMR}$ , and  $^{13}\text{C-NMR}$  spectroscopy. The melting point of BPC15CN was lower than that of BPZCN due to the presence of pendent flexible pentadecyl chain. The melting points of CE monomers containing “cardo” decahydronaphthalene moiety *viz*; BPDCCN, DMBPDCCN and TMBPDCCN and “cardo” perhydrocumyl moiety *viz*; BPPCPCN, DMBPPCPCN, and TMBPPCPCN increased with the substitution of methyl group(s) at *-ortho* position to cyanate functionality. As compared to bisphenol-A based CE monomer; 2,2-bis(4-cyanatophenyl)propane, (BPACN), the melting point of BPC6CN was lower due to the incorporation of aliphatic spacer.

The CE monomers containing substituted “cardo” group *viz*: BPC15CN, BPDCCN, DMBPDCCN, TMBPDCCN, BPPCPCN, DMBPPCPCN and TMBPPCPCN showed the presence of magnetically non-equivalent distereotopic phenyl rings in the NMR spectra.

The kinetics of curing of five cyanate esters *viz*; BPZCN, BPC15CN, BPDCCN, BPPCPCN and BPC6CN was studied under nonisothermal and isothermal mode employing copper acetylacetonate-nonylphenol catalytic system using DSC. The results obtained were compared with the cure kinetics of BPACN. The heat of catalyzed cure reaction of cyanate ester monomers under study was observed in the range 190 – 230 kJ/mol which is in accordance with the reported values for BPACN (195 – 238 kJ/mol). The activation energy of catalyzed curing of cyanate ester monomers containing “cardo” group *viz*; BPZCN, BPC15CN, BPDCCN, and BPPCPCN under nonisothermal mode was lower (65 – 85 kJ/mol) than that of BPC6CN (119 kJ/mol) and BPACN (116 kJ/mol) while the activation energy for catalyzed curing of CE monomers in isothermal mode was in the range of 53 – 60 kJ/mol.

The storage modulus of cured BPZCN, BPC15CN and BPACN was  $1.59 \times 10^9$ ,  $1.07 \times 10^9$  and  $1.39 \times 10^9$  Pa, respectively. The higher storage modulus of cured BPZCN than that of cured BPC15CN and BPACN could be due to the presence of rigid cycloaliphatic “cardo” moiety.

The glass transition temperature, as analyzed by DMTA, of cured resins followed the order BPZCN > BPACN > BPC15CN (302, 288 and 160 °C, respectively). The lower T<sub>g</sub> of cured BPC15CN could be due to the presence of flexible pentadecyl chain. The glass transition temperature of BPDCCN, BPPCPCN and BPC6BN followed the order BPDCCN > BPPCPCN > BPC6CN. The lower T<sub>g</sub> of cured BPC6CN could be due to the presence of aliphatic spacer.

The T<sub>10</sub> values, as analyzed by TGA, of the cured network of cyanate ester monomers under study were in the range 410 – 435 °C indicating their good thermal stability.

The percentage moisture absorption of polycyanurates followed the order BPC15CN < BPZCN < BPACN (0.7, 1.1, 1.5 %, respectively). The lower % moisture absorption of the cured network of BPC15CN was due to comparatively higher hydrophobic content.

Encouraged by the results of cyanate ester resins, it was of further interest to synthesize epoxy resins based on bisphenols containing cycloaliphatic “cardo” group. Thus, the diglycidyl ether of 1,1-bis(4-hydroxyphenyl)cyclohexane (DGEBPZ) and 1,1-bis(4-hydroxy phenyl)-3-pentadecylcyclohexane (DGEBPC15) were synthesized by the reaction of corresponding bisphenols with epichlorohydrin in the presence of sodium hydroxide *via* coupling reaction. The synthesized epoxies were viscous in nature. The epoxy, DGEBPC15 was synthesized for the first time. The epoxy equivalent weights of DGEBPZ and DGEBPC15, as determined by pyridine-HCl method, were 221 and 333 g/equiv., respectively.

The activation energy of epoxy curing calculated by Coats-Redfern method under nonisothermal mode employing 4,4'-methylenedianiline as a curing agent was in the range of 48-52 kJ/mol.

The storage modulus and the T<sub>g</sub> of cured epoxy resins followed the order DGEBPZ > DGEBPA > DGEBPC15. The higher storage modulus and the T<sub>g</sub> of cured DGEBPZ than that of cured network of DGEBPC15 and DGEBPA could be due to the presence of rigid “cardo” group.

The percentage moisture absorption of cured epoxy resins followed the order DGEBPC15 < DGEBPZ < DGEBPA (1.8, 2.6, and 3.2 %, respectively). The lower % moisture absorption of cured DGEBPC15 resin was due to comparatively higher hydrophobic content.

The synthesis of new bismaleimide (BMI) monomers was pursued in order to synthesize BMI monomers with lower melting points (< 150 °C) and improved solubility in common organic solvents such as chloroform, dichloromethane, etc. Considering the special structural features, the approach involved making use of 3-pentadecylphenol. The presence of pendent flexible pentadecyl chain was expected to bring asymmetry to BMI monomers and to provide additional ‘handle’ for interaction with solvents.

Thus, new bismaleimide monomers *viz*; 1,1-bis[4-(4- maleimidophenoxy)phenyl]-3-pentadecyl cyclohexane, (BPC15BMI), 4,4'-bis(maleimido)-3-pentadecyldiphenylether (ODAC15BMI) and 1,3-bis(maleimido)-4-pentadecylbenzene (MPDAC15BMI) were designed and synthesized by the ring opening addition reaction of corresponding diamines with maleic anhydride followed by cyclodehydration of *N,N*-bismaleamic acids using acetic anhydride and sodium acetate. To ascertain the effect of incorporation of pendent flexible pentadecyl chain into BMI monomer, the reference BMI monomers *viz*; 1,1-bis[4-(4- maleimidophenoxy)phenyl]cyclohexane, (BPZBMI) and 4,4'-bis(maleimido)diphenylether (ODABMI) were also synthesized. The BMIs *viz*; BPC15BMI, ODAC15BMI and MPDAC15BMI have been synthesized for the first time. The characterization of

BMI monomers and the intermediates involved in their synthesis was carried out by FTIR, and  $^1\text{H}$  NMR spectroscopic techniques.

The melting points of new BMIs *viz*; 4,4'-bis(maleimido)-3-pentadecyldiphenylether (69-70 °C) and 1,3-bis(maleimido)-4-pentadecylbenzene (96-98 °C) were lower than that of 4,4'-bis(maleimido)diphenylether (177 °C) and 1,3-bis (maleimido)benzene (MPDABMI) (205), respectively due to the presence of pendent flexible pentadecyl chain.

The BMIs *viz*; BPZBMI, BPC15BMI, ODAC15BMI, and MPDAC15BMI were soluble in common organic solvents such as chloroform and dichloromethane, while ODABMI was insoluble in these solvents at 5 wt % concentration.

The curing kinetics of BMIs was studied by using DSC under nonisothermal mode using Coats-Redfern method. The curing of BPZBMI, BPC15BMI and MPDAC15BMI exhibited comparatively broader processing window ( $> 100$  °C) than that of ODABMI and MPDABMI ( $\sim 40$  °C). The activation energy of BMI curing was observed in the range 103 – 131 kJ/mol for BPZBMI, ODAC15BMI, ODABMI and MPDAC15BMI.

The cured network of all the BMIs under study showed a single stage decomposition with  $T_{10}$  values in the range 390 – 485 °C indicating their good thermal stability.

Bispropargyl ethers containing cycloaliphatic “cardo” group were synthesized by the reaction of corresponding bisphenols with propargyl bromide in the presence of potassium carbonate using acetone as a solvent in order to study the effect of cycloaliphatic “cardo” group on the curing behavior of bispropargyl ethers. Thus, five bispropargyl ethers *viz*; 1,1-bis[4-(2-propynyloxy) phenyl] cyclohexane (BPZPT), 1,1-bis[4-(2-propynyloxy) phenyl]-3-pentadecylcyclohexane (BPC15PT), 1,1-bis[4-(2-propynyloxy) phenyl]decahydronaphthalene, (BPDCPT), 1,1-bis[4-(2-propynyloxy) phenyl]-4-perhydrocumylcyclohexane (BPPCPPT), and 2,2-bis[4-(2-propynyloxy) phenyl]propane (BPAPT) were synthesized and were characterized by IR and NMR spectroscopy. BPAPT was synthesized as a reference monomer using bisphenol-A.

The activation energy of the curing reaction studied under uncatalysed nonisothermal mode using DSC was in the range 141-154 kJ/mol by Kissinger method and 171-182 kJ/mol by Coats-Redfern method for all bispropargyl ethers under study. The study indicated that the bispropargyl ether monomers possessing cycloaliphatic “cardo” group followed similar cure kinetics as that of bisphenol-A based bispropargyl ether.

The  $T_{10}$  values of cured bispropargyl ethers containing cycloaliphatic “cardo” group were in the range 410 - 435 °C indicating good thermal stability of the cured network. However, the weight residue at 800 °C of cured bispropargyl ethers containing cycloaliphatic “cardo” group was lower (3-12 %) than that of cured network of BPAPT (32 %) due to higher aliphatic content.



Overall, several new thermosetting resins such as cyanate ester resins, epoxy resins, bismaleimides and bispropargyl ethers containing cycloaliphatic “cardo” groups were designed and synthesized. The incorporation of hydrophobic cycloaliphatic “cardo” group into cyanate ester monomer or epoxy resin resulted into corresponding cured network with lower percentage moisture absorption albeit sacrificing thermal stability. The introduction of pendent flexible pentadecyl chain into bismaleimide monomer lowered their melting points hence aiding processing characteristics with broad processing window. The presence of cycloaliphatic “cardo” group in bispropargyl ether monomer did not practically alter the cure kinetics compared to bisphenol-A based bispropargyl ether.

## 8.2 Perspectives

Thermosetting resins such as cyanate ester resins, epoxy resins, bismaleimides, propargyl-terminated resins, etc., are of great interest in view of their excellent versatility in various applications. In this context, an understanding of the structure-property relationship is of significant contemporary interest. There is a continuing need to examine approaches to address the issues related to their impact resistance, dielectric constant, moisture absorption, etc. The present work on the synthesis and characterization of new thermosetting resins based on some bisphenols has opened up new avenues for the future work.

- The primary focus of the current research was on the synthesis of new thermosetting resins such as cyanate ester resin, epoxy resins, bismaleimides and bispropargyl ethers. Detailed studies on blends of these systems with commercially available monomers and polymers and investigation of mechanical properties of their blends would yield useful information regarding the effect of cycloaliphatic “cardo” group or pendent flexible pentadecyl chain on mechanical properties.
- The evaluation of dielectric properties of polycyanurates and epoxy resins containing cycloaliphatic “cardo” group along with pendent flexible pentadecyl chain prepared in the present study would be of prime importance.
- A series of cyanate ester monomers by systematic variation of alkylene spacer could be synthesized starting from commercially available diacids such as octanedioic acid (suberic acid), decanedioic acid (sebacic acid), dodecanedioic acid, etc., to understand the effect of alkylene spacer on the properties such as mechanical, dielectric, thermal etc., of polycyanurates obtained therefrom.

- The rheological study of bismaleimide monomers synthesized in the present work would lead to better understanding of the effects of pendent flexible pentadecyl chain on the melt viscosity of monomers and their processing characteristics.
- Bispropargyl ethers synthesized in present work serve as potentially useful monomers for the synthesis of polytriazoles containing cycloaliphatic “cardo” group *via* “click reaction” with the diazido monomers.

# Synopsis

## Synopsis of the Thesis Entitled

### “New Thermosetting Resins Based on Some Bisphenols”

---

#### **Introduction:**

Advanced thermosetting polymers find an undisputed place in the design of polymer matrix composites (PMCs). High strength, light weight composite materials have helped in transforming many creative ideas into technical realities. The application of these materials has helped to boost many industries including transportation, communication, construction and leisure goods. An area that has immensely benefited from the boom in PMC technology is aerospace where the impact of these materials can be seen in the space program, rocket motors, stealth military aircraft, commercial transport, and so forth. PMCs constitute several vital components of satellites and launch vehicles ranging from motor cases and nozzle components in rocketry to systems like honeycomb structures, equipment panels, cylindrical support structures, pressurant bottles, solar array substrates, antennas, etc. Composites for specific applications with desired properties are realizable through correct choice of the resin, reinforcement, and their perfect processing. The bulk of the aerospace composite materials centers on epoxies in combination with graphite/glass and to a limited extent, with organic reinforcements like aramid. Their attractive features include ease of processing and handling convenience, good mechanical properties due to excellent adhesion to a variety of reinforcements, toughness, and low cost. Depending upon the end application, different varieties of epoxy resins are in use<sup>1-4</sup>. However, the use of a conventional epoxy system has drawbacks due to excessive water absorption and residual stress, resulting in the propensity to microcrack when thermally cycled. Epoxy resins are also not generally recommended for application in severe conditions due to poor hot/wet performance and high moisture sensitivity<sup>5</sup>. For electrical/electronic applications, an alternate resin system with better dielectric properties and reduced moisture absorptivity will be preferred.

Polyimides, with their service temperatures ranging from 200 °C to 280 °C, offer improved high temperature properties compared to epoxy systems. A number of polyimide systems that are well suited for use as matrix resins, adhesives, and coatings for high performance applications in the aerospace and electronics industries have been developed<sup>6-8</sup>. Condensation polyimides are formed by a two-step process involving formation of a polyamic acid intermediate followed by its imidization. Thus, the processing times are much longer and require the application of high pressure for consolidation, due to evolution of water or

alcohol as condensation by-product. Major disadvantages of these systems include poor shelf-life and processing difficulties<sup>9</sup>. The matrix systems encompassing both processability and good thermo-mechanical profile are the addition-type polyimide systems. These are low molar mass, multifunctional monomers or prepolymers that carry additional curable terminal functions and imide functions in their backbone<sup>10-12</sup>. Bismaleimides (BMIs), bisitaconimides, and bisnadimides are the versatile ones in this category. Of these, bismaleimides dominate the high temperature polymer scenario for aerospace applications. However, these polymers are extremely brittle. Tough compositions need blending with elastomers and/or chain extension using diamines. A recent development for tough BMI compositions is based on the blends with diamines, diallyl phenols, and with other bismaleimides<sup>13-15</sup>. Several modified versions of BMIs are currently in use in the aerospace industry<sup>16</sup>. Variations of such addition type polyimides with nadic<sup>16</sup>, paracyclophane<sup>17</sup>, acetylene<sup>18</sup>, and cyclobutene<sup>19</sup> terminals have also been reported. However, such systems also possess inherent difficulty in processing and need a solvent medium for impregnation and the curing (through a condensation reaction) requires high temperature. The release of volatiles during condensation cure of composites is not very desirable as it can result in blistering and void formation, leading to inferior laminates.

Although phenolics cannot be substitutes for epoxies and polyimides, their composites still find a major market in non-structural components, particularly in thermo-structural application in the aerospace industry. Good heat and flame resistance, ablative characteristics, and low cost are the hallmarks of phenolics which find numerous applications including aircraft interiors, automotive components, rocket nozzles, appliance moldings, etc<sup>20-22</sup>. However, brittleness, poor shelf-life, and need for high pressure curing are the major shortcomings of phenolic resins in processing and for structural composite applications. Research attention is now focused on addition-curable phenolics<sup>23</sup>, which are alternatives to condensation type phenolics, avoiding the need for high-pressure cure. To mention a few, polybenzoxazines and propargyl ether resins (also known as propargyl terminated resins) are newly emerged systems which possess much higher T<sub>g</sub> than cure temperature, low water absorption, high char yield, low coefficient of thermal expansion and good mechanical properties. However, most of them require high cure temperature, posing processing difficulties.

Against these backdrops, cyanate ester (CE) resins were developed as a compromise system<sup>24-26</sup>. These thermoset resins encompass the processability of epoxy resins, thermal characteristics of bismaleimides, and the heat and fire resistance of phenolic resins. The importance of cyanate ester systems can be understood from the increasing research interest in this area which is evident in terms of a large number of publications and patents<sup>24-26</sup>. The

highly desirable properties like built-in toughness, good dielectric properties, radar transparency, and low moisture absorption make them the resin of choice for aforementioned applications<sup>24-26</sup>. These distinctive features can further be enhanced by altering the CE backbone. The synthesis of new cyanate esters allows enormous diversity in the structure of the starting material and essentially allows the structure to be tailored at the molecular level. Although a large variety of CE monomers with various backbone structures and properties have been reported<sup>27-34</sup>, scanty information is available on CE monomers containing cardo/cycloaliphatic moiety. CE monomer developed by Dow chemicals with trade name XU71787<sup>35</sup> and dicyclopentadiene based CE monomer (DCPDCY) reported by Wang et al.<sup>36</sup> are the two notable examples. For thermoplastics, the incorporation of cardo moiety in the polymer backbone has been demonstrated to enhance Tg, mechanical properties, etc.<sup>37-39</sup>

The objective of the present study was to design and synthesize cyanate ester monomers containing cardo moiety and to study thermal, thermomechanical and moisture absorption behavior of polycyanurates derived therefrom.

Another objective of the study was to explore bisphenols containing cardo moiety to synthesize other types of thermosetting resins viz; epoxy resins, bismaleimides and propargyl ether resins (propargyl-terminated resins).

With above objectives in mind, the following specific work was chosen for the thesis:

**Objectives of the present thesis:**

- ◆ Design and synthesis of cyanate ester monomers containing cardo / (cyclo)aliphatic moiety
- ◆ To investigate cure kinetics of cyanate esters containing cardo / (cyclo)aliphatic moiety by DSC
- ◆ Processing of CE monomers and characterization of cured polycyanurate network.
- ◆ Synthesis, characterization and processing of epoxy resins.
- ◆ Synthesis, characterization and curing studies of bismaleimides.
- ◆ Synthesis, characterization and curing studies of bispropargyl ethers.

The thesis has been divided into the following eight chapters.

---

**Chapter 1: Introduction and Literature Survey**

---

This chapter deals with comprehensive review of literature on thermosetting resins with particular emphasis on cyanate ester resins, epoxy resins, bismaleimides and propargyl-terminated resins covering methods of synthesis, curing/processing, structure-property relationship, etc.

---

**Chapter 2: Scope and Objectives**

---

This chapter discusses scope and objectives of the thesis.

---

**Chapter 3: Synthesis and Characterization of Cyanate Ester Monomers**

---

This chapter describes:

Synthesis of cyanate ester monomers containing cardo / (cyclo)aliphatic moiety (as listed in Table 1. )

**Table 1 : Cyanate Ester Monomers**

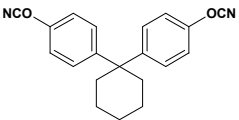
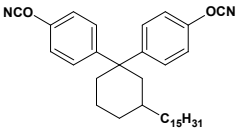
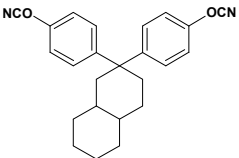
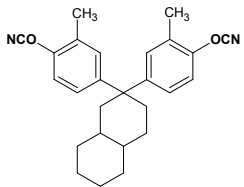
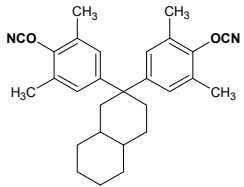
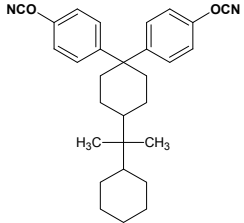
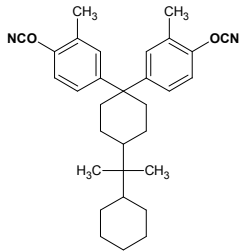
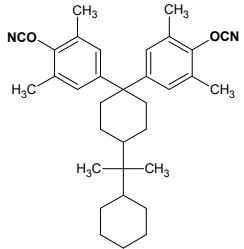
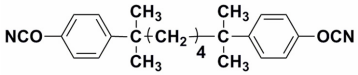
Sr.No	Monomer	Structure
1	1,1-Bis(4-cyanatophenyl)cyclohexane	
2	1,1-Bis(4-cyanatophenyl)-3-pentadecyl cyclohexane	
3	1,1-Bis(4-cyanatophenyl)decahydronaphthalene	

Table 1 continued.....

4	1,1-Bis(4-cyanato-3-methylphenyl)decahydronaphthalene	
5	1,1-Bis(4-cyanato-3,5-dimethylphenyl) decahydro naphthalene	
6	1,1-Bis(4-cyanatophenyl)-4-perhydrocumylcyclohexane	
7	1,1-Bis(4-cyanatophenyl-3-methyl)-4-perhydrocumyl cyclohexane	
8	1,1-Bis(4-cyanatophenyl-3,5-dimethyl)-4-perhydrocumyl cyclohexane	
9	2,7-Bis(4-cyanatophenyl)-2,7-dimethyloctane	

The monomers and the intermediates involved in their synthesis were characterized by IR,  $^1\text{H-NMR}$ , and  $^{13}\text{C-NMR}$  spectroscopy.



---

## Chapter 4: Curing Kinetics and Processing of Cyanate Esters

---

This chapter is divided into two sections;

### Chapter 4 A: Curing Kinetics of Cyanate Ester Monomers

This section focuses on the studies dealing with curing kinetics of cyanate ester monomers containing cardo / (cyclo)aliphatic moiety *viz*;

- a) 1,1-Bis(4-cyanatophenyl)cyclohexane
- b) 1,1-Bis(4-cyanato phenyl)-3-pentadecylcyclohexane
- c) 1,1-Bis(4-cyanatophenyl)decahydronaphthalene, and
- d) 1,1-Bis(4-cyanatophenyl)-4-perhydrocumylcyclohexane

The kinetic parameters such as activation energy and Arrhenius frequency factor were computed under both nonisothermal and isothermal mode using differential scanning calorimetry (DSC).

### Chapter 4 B: Processing of Cyanate Ester Monomers

In this section, processing of CE monomers and characterization of polycyanurates derived therefrom is discussed. The following CE monomers were polymerized;

- a) 1,1-Bis(4-cyanatophenyl)cyclohexane
- b) 1,1-Bis(4-cyanato phenyl)-3-pentadecylcyclohexane
- c) 1,1-Bis(4-cyanatophenyl)decahydronaphthalene, and
- d) 1,1-Bis(4-cyanatophenyl)-4-perhydrocumylcyclohexane.

Thermal and dynamic mechanical properties of polycyanurates of 1,1-bis(4-cyanatophenyl) cyclohexane and 1,1-bis(4-cyanatophenyl)-3-pentadecylcyclohexane were discussed and compared with that of polycyanurate of 2,2-bis(4-cyanatophenyl)propane.

---

## Chapter 5: Synthesis, Characterization and Curing of Epoxy Resins

---

This chapter describes

- I. Synthesis of epoxy resins starting from bisphenols containing cardo moiety *viz*;  
1,1-bis (4-hydroxyphenyl)cyclohexane and 1,1-bis(4-hydroxyphenyl)-3-pentadecyl cyclohexane.

- II. Curing/processing of these epoxies employing methylenedianiline as a curing agent and characterization of cured network by (DSC), thermogravimetric analysis and dynamic mechanical analysis.

---

## Chapter 6: Synthesis, Characterization and Curing Studies of Bismaleimides

---

This chapter deals with

- I) Synthesis and characterization of bismaleimides (as listed in **Table 2**)

**Table 2 : Bismaleimides**

Sr. No	Monomer	Structure
1	1,1-Bis[4-(4- maleimidophenoxy)phenyl] cyclohexane	
2	1,1-Bis[4-(4- maleimidophenoxy)phenyl]-3-pentadecylcyclohexane	
3	4,4'-Bis(maleimido)-3-pentadecyldiphenylether	
4	1,3-Bis(maleimido)-4 -pentadecylbenzene	

The monomers were characterized by IR, <sup>1</sup>H-NMR, and <sup>13</sup>C-NMR spectroscopy.

- II) Curing studies of these BMIs using DSC and studies on thermal stability of cured networks using TGA.

---

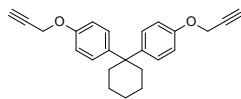
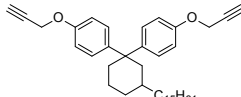
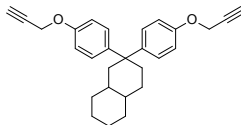
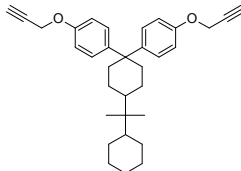
## Chapter 7: Synthesis, Characterization and Curing Studies of Bispropargyl Ethers

---

This chapter deals with

- I) Synthesis and characterization of bispropargyl ethers containing cardo moiety (listed in **Table 3**)

**Table 3 : Bispropargyl Ethers**

Sr. No	Monomer	Structure
1	1,1-Bis[4-(2-propynyloxy)phenyl] cyclohexane	
2	1,1-Bis[4-(2-propynyloxy)phenyl]-3-pentadecylcyclohexane	
3	1,1-Bis[4-(2-propynyloxy)phenyl] decahydronaphthalene	
4	1,1-Bis[4-(2-propynyloxy)phenyl]-4-perhydrocumyl cyclohexane	

The monomers were characterized by IR,  $^1\text{H-NMR}$ , and  $^{13}\text{C-NMR}$  spectroscopy.

- II) Curing studies of these monomers and studies on the thermal stability of cured network using TGA.

---

## Chapter 8: Summary and Conclusions

---

This chapter summarizes the results and describes salient conclusions of the investigations reported in the thesis.

## References:

- 1 Lee, H; Neville, K. In *Handbook of Epoxy Resins*, **1967**, McGraw Hill, New York.
- 2 May, C; Tanaka, Y. Eds. *Epoxy Resins: Chemistry and Technology*, **1988**, 2<sup>nd</sup> Ed, Marcel Dekker, Inc, New York.
- 3 Bosch, A. *Epoxy Resins*, In *Polymeric Materials Encyclopedia*, Salamone J.C. Ed., **1996**, CRC Press, Boca Raton vol 3, p 2246.
- 4 Pham, H; Marks, M. *Epoxy Resins*, In *Encyclopedia of Polymer Science and Technology*, **2004**, 3<sup>rd</sup> Ed, Wiley Interscience, New Jersey, Vol 9, p 678.
- 5 Bauer, R; Filippove, A; Schlaudt, L; Breitigam, W. *SAMPE*, **1987**, 32, 1104.
- 6 Mittal, K.L; (ed) *Polyimides: Synthesis, Characterization and Applications*, **1985**, Plenum Press, New York.
- 7 Feger, C; Khojasteh, M; McGrath J. (ed) *Polyimides: Materials, Chemistry and Characterization*, **1989**, Elsevier, Amsterdam.
- 8 Takekoshi, T; *Adv. Polym. Sci.* **1990**, 94, 1.
- 9 Volksen, W. *Recent Advances in Polyimides and Other High Performance Polymers*, **1990**, Workshop sponsored by American Chemical Society, Polymer Division.
- 10 Lin, S; Pearce, E. In *High Performance Thermosets: Chemistry, Property and Applications*, **1993**, Hanser, Munich.
- 11 Stenzenberger H. *Adv. Polym. Sci.* **1994**, 117,163.
- 12 Misson, P; Sillon, B. *Adv. Polym. Sci.* **1998**, 140,137.
- 13 Crivello, J. *J. Polym. Sci., Polym. Chem. Ed.* **1973**, 11,1185.
- 14 Morgan, R; Jurek, R; Yen, A; Donnellan, T. *Polymer*, **1993**, 34, 835
- 15 Lin, K; Lin, J; Cheng, C. *Polymer*, **1996**, 37, 4729.
- 16 Pilato, L; Michael, J. In *Advanced Composite Materials*, **1994**, Springer, Berlin Heidelberg New York, Chap 2.
- 17 Gorham W. *J.Polym.Sci., Part A-1:Polym.Chem.* **1966**, 4, 3027.
- 18 Katsman, H; Mallon, J; Barry, W. *Adv. Mater.* **1995**, 26, 21
- 19 Cava, M; Mitchell, M. In *Cyclobutadiene and Related Compounds*, **1967**, Academic Press, New York, Chap 6.
- 20 Knop, A; Pilato, L. *Phenolic Resins: Chemistry, Applications and Performance, Future Directions*. 1985, Springer, Berlin Heidelberg New York,
- 21 Kopf, P; Little, A. *Phenolic Resins* In *Encyclopedia of Polymer Science and Engineering*, Mark, H; Bikales, N; Overberger, C; Menges, G. Ed. **1988**, 2<sup>nd</sup> Ed, Wiley, Vol 11, P 45.
- 22 Fukuda, A. *Phenolic Resins* In *Polymeric Materials Encyclopedia*, Salamone, J. Ed, **1996**, CRC Press, Florida, Vol 7, P 5035
- 23 Nair, C.P.R. *Prog.Polym.Sci.* **2004**, 29, 401
- 24 Hamerton, I. Ed *Chemistry and Technology of Cyanate Ester Resins*,. **1994**, Chapman and Hall, Glassow.
- 25 Fang, T; Shimp, DA. *Prog. Polym. Sci.* **1995**, 20, 61
- 26 Nair, CPR; Mathew, D; Ninan, KN. *Adv. Polym. Sci.* 2001, 155, 1.
- 27 Snow, AW. In *Chemistry and Technology of Cyanate Ester Resins*. Hamerton, I. ED **1994**, Chapman and Hall, Glasgow, Chap 2.
- 28 Abed, J.; Mercier, R.; McGrath, J.E. *J.Polym.Sci., Part A:Polym.Chem.* **1997**, 35, 977.
- 29 Marcos-Fernandez, A; Posadas, P; Rodriguez, A; Gonzalez, L. *J. Polym. Sci. Part. A: Polym. Chem.* **1999**, 37, 3155.
- 30 Maya, E.M.; Snow, A.W.; Buckely, L.J. *J.Polym.Sci., Part A:Polym.Chem.* **2003**, 41, 60.
- 31 Laskoski, M; Dominguez, DD; Keller, TM. *Polymer*, **2006**, 47, 3727.
- 32 Guenther, AJ; Yandek, GR; Wright, ME, Petteys, BJ; Quintana, R; Connor, D; Gilardi, RD; Marchant, D. *Macromolecules*, **2006**, 39, 6046.
- 33 Anuradha, G.; Sarojadevi, M. *J. Appl. Polym. Sci.* **2008**, 110, 938.
- 34 Zhang, B; Wang, Z; Zhang, X. *Polymer*, **2009**, 50, 817.
- 35 Woo, EP; Dellar, DV. (Dow Chemicals) *U.S.Patent* 4,528,336, **1985**.

- 36 Hwang, HJ; Li, CH; Wang, CS. *J. Appl. Polym. Sci.* **2005**, 96, 2079.
- 37 Hougham, G.; Tesoro, G.; Viehbeck, A. *Macromolecules* **1996**, 29, 3453.
- 38 Vibhute, SS; Joshi, MD; Wadgaonkar, PP; Patil, AS; Maldar, NN. *J. Polym. Sci., Part A: Polym. Chem.* **1997**, 35, 3227.
- 39 Sagar, AD; Shingte, RD; Wadgaonkar, PP; Salunkhe, MM. *Eur. Polym. J.* **2001**, 37, 1493.

Arun D. Kulkarni  
(Student )

Prakash P. Wadgaonkar  
(Research Guide)

## List of Publications and Presentations

### Publications

- 1 K. S. Santhosh Kumar,; C. P. Reghunadhan Nair,; K. N. Ninan,; **A. D. Kulkarni**,; P. P. Wadgaonkar. "Synthesis and properties of new polybenzoxazines containing (substituted) cyclohexyl moieties." *Polym. Adv. Technol.* **2009**, 20, 1107-1113.
- 2 Anjana Sarkar,; Mahadeo R. Halhalli,; **Arun D. Kulkarni**,; Prakash P. Wadgaonkar. "Polyimides based on aromatic diisocyanates containing pendent flexible alkoxy chains and aromatic dianhydrides: Synthesis, characterization, and liquid-crystal alignment properties." *J. Appl. Polym. Sci.* **2009**, 112, 461-472.
- 3 Cyanate ester resins containing (substituted) cyclohexyl moiety: Synthesis and structure-property relationship. (*To be communicated*).
- 4 Cyanate ester resins containing (substituted) cyclohexyl moiety: Nonisothermal and isothermal curing kinetics. (*To be communicated*).
- 5 Cyanate ester resins containing cardo perhydrocumyl moiety: Synthesis and cure kinetics (*To be communicated*).
- 6 Cyanate ester resins containing cardo decahydronaphthalene moiety : Synthesis and cure kinetics (*To be communicated*).
- 7 Cyanate ester resins containing alkylene spacer: Synthesis and cure kinetics (*To be communicated*).
- 8 Epoxy resins containing (substituted) cyclohexyl moiety: Synthesis and structure-property relationship. (*To be communicated*).
- 9 Synthesis, characterization and cure kinetics of new bismaleimides containing pendent flexible pentadecyl chain. (*Manuscript under preparation*).
- 10 Propargyl terminated resins containing (substituted) cyclohexyl moiety: Synthesis, characterization and cure kinetics. (*Manuscript under preparation*).

### Presnetations

- 1 Presented poster entitled "Synthesis characterization and cure kinetics of new cyanate ester monomer" during MACRO 2006, held at National Chemical Laboratory, Pune, in December 2006.
- 2 Presented poster entitled "Cyanate ester resins containing (substituted) cyclohexyl moiety" during MACRO 2009, held at Indian Institute of Technology, Chennai, in March 2009.